

Open Research Online

The Open University's repository of research publications and other research outputs

Gut Patterning In Development And Evolution: A Comparative Differential Transcriptomics Approach

Thesis

How to cite:

Cuomo, Claudia (2017). Gut Patterning In Development And Evolution: A Comparative Differential Transcriptomics Approach. PhD thesis The Open University.

For guidance on citations see [FAQs](#).

© 2017 The Author



<https://creativecommons.org/licenses/by-nc-nd/4.0/>

Version: Version of Record

Link(s) to article on publisher's website:

<http://dx.doi.org/doi:10.21954/ou.ro.0000c461>

Copyright and Moral Rights for the articles on this site are retained by the individual authors and/or other copyright owners. For more information on Open Research Online's data [policy](#) on reuse of materials please consult the policies page.

oro.open.ac.uk

**GUT PATTERNING IN DEVELOPMENT AND
EVOLUTION: A COMPARATIVE
DIFFERENTIAL TRANSCRIPTOMICS
APPROACH**

CLAUDIA CUOMO

**Diploma Degree in Biology
University of Napoli Federico II**

DOCTOR OF PHILOSOPHY

**Affiliated Research Centre (ARC):
STAZIONE ZOOLOGICA ANTON DOHRN DI
NAPOLI, ITALY
THE OPEN UNIVERSITY OF LONDON**

FEBRUARY 2017

**GUT PATTERNING IN DEVELOPMENT AND
EVOLUTION: A COMPARATIVE
DIFFERENTIAL TRANSCRIPTOMICS
APPROACH**

A thesis submitted to the
Open University of London for the degree of
DOCTOR OF PHILOSOPHY

by
Claudia Cuomo
Diploma Degree in Biology
University of Napoli Federico II

Affiliated Research Center (ARC)
STAZIONE ZOOLOGICA ANTON DOHRN
Naples, Italy

February 2017

This thesis work has been carried out in the laboratory of
Dr. Maria I. Arnone at the Stazione Zoologica Anton Dohrn Naples, Italy

Director of Studies: Dr. M.I. Arnone, Stazione Zoologica di Napoli, Italy

External Supervisor: Prof. Peter W.H.Holland, University of Oxford, United
Kingdom

To my grandmother Vittoria,
example of determination, hardwork and love for family

ABSTRACT

All bilaterians share a common kit of transcription factors and cis-regulatory elements that compose the Gene Regulatory Network (GRN) essential for the development of the body plan. Modifications within the elements of the GRN determine the evolution of animal forms. In this study, the GRN for embryonic gut specification in two echinoderm species, the sea urchin *Strongylocentrotus purpuratus* and the sea star *Patiria miniata*, has been studied with the purpose of acquiring further knowledge on the process of gut patterning in the sea urchin larva and to compare it with the sea star embryo, focusing on the role that Xlox and Cdx transcription factors have in this process in both echinoderm species. In fact, despite the fact the GRN for endomesoderm specification in *S. purpuratus* has been well studied, however, the molecular mechanisms leading a primitive undifferentiated gut to become a highly specialized structure are still partially unknown for both *S. purpuratus* and *P. miniata*; for the latter the GRN is mostly unrevealed. Taking advantage of genome-wide approaches and modern high-throughput technologies, a partial reconstruction of the sea urchin GRN around Xlox and Cdx transcription factors, known for their key role to start the gut specification process, has been achieved leading to describe the putative interactions of the TFs in the network. An important novel node of the sea urchin GRN featuring the interaction between *Sp-Meis*, an homeobox gene, and Sp-Lox protein has been revealed and the occupancy of Sp-Lox protein on *Sp-Meis* regulatory region has been demonstrated by ChIP-PCR. The comparison of the differentially expressed genes after Xlox and Cdx perturbation in both sea urchin and sea star embryos has revealed that, although the absence of these two proteins

affects some digestive functions and developmental processes related to its specification, however many of the regulatory genes involved in these mechanisms are not the same in the two species. This result suggests a phenomenon of rewiring of the gut GRN in *S. purpuratus* and *P. miniata* that, although belonging to the same phylum Echinodermata, are distant million years in term of evolutionary time, as recorded by fossil records.

Further studies aimed to reconstructing the sea star gut GRN will lead to a best comprehension of the gut specification mechanisms also in this animal. A comparative/divergence analysis with the reconstructed sea urchin gut GRN will help to identify the kernel elements that did not change during evolution with a key role in gut formation and patterning, as well as the intrinsic differences in the GRN accumulated during the evolution of both lineages.

TABLE OF CONTENTS

ABSTRACT	I
TABLE OF CONTENTS	III
LIST OF FIGURES	VI
LIST OF TABLES	IX
LIST OF ABBREVIATIONS	X
CHAPTER 1	1
INTRODUCTION	1
1.1. The approach: gene regulatory network	1
1.1.1 Gene Regulatory Networks and their evolution	1
1.1.2 Building a Gene Regulatory Network	6
1.2. The experimental animal system: Echinoderms	10
1.2.1 Deuterostomes: the phylum of Echinodermata	10
1.2.2 Sea urchin development	13
1.2.3 Sea urchin GRN for specification of endomesoderm	17
1.2.4 Sea star development	19
1.2.5 Sea star endomesoderm specification	22
1.3. The biological process: gut development	25
1.3.1 Gastrulation: the first step for gut development	25
1.3.2 Gut development in Bilateria	27
1.3.3 ParaHox gene family	29
1.3.4 Parahox and gut shape in sea urchin and sea star embryos	32
1.4. Aim of the thesis	38
CHAPTER 2	40
MATERIALS AND METHODS	40
2.1 Animal handling and culture of sea urchin and starfish embryos	40
2.2 Microinjection procedure	42
2.2.1 Preparation of materials	42

2.2.2 Microinjection procedure	43
2.2.3 Injection of morpholinos	44
2.3 RNA-Seq	44
2.3.1 Total RNA purification	44
2.3.2 RNA quality check and sequencing	45
2.3.3 RNA-Seq filtration and mapping	46
2.4 Real Time Quantitative PCR	46
2.4.1 Reverse transcription	46
2.4.2 Quantitative PCR	47
2.5 Whole Mount in Situ Hybridizations (WMISH)	48
2.6 Basic molecular biology procedures	50
2.6.1 PCR amplification	50
2.6.2 DNA sequencing	50
2.6.2 DNA gel electrophoresis	50
2.7 Chromatin Immuno Precipitation procedures	51
2.7.1 Chromatin isolation of cross-linked cells	51
2.7.2 Chromatin shearing by sonication	51
2.7.2 Immunoprecipitation	52
2.8 Assay for Transposase-Accessible Chromatin (ATAC)	53
2.9 Primer and morpholino antisense oligonucleotides used	55
CHAPTER 3	58
A genome wide comparison downstream of Xlox and Cdx in sea urchins and sea stars	58
3.1 Introduction: differential RNA-Seq approach	58
3.2 Results and discussion	60
3.2.1 Choice of the sea urchin and the sea star developmental stages for the RNA-Seq	60
3.2.2 RNA-Sequencing (RNA-Seq)	62
3.2.3 Gene Ontology annotation analysis for <i>S. purpuratus</i> and <i>P. miniata</i>	

differential RNA-Seq data sets	69
3.2.4 Orthology analysis	79
3.2.5 Differential expression analysis	82
3.3Conclusions	97
CHAPTER 4	98
Partial reconstruction of the posterior gut GRN downstream of Sp-Lox and Sp-Cdx with the combination of RNA-Seq, ATAC-Seq and ChIP-PCR approaches	98
4.1 Introduction	98
4.2 Results and Discussion	99
4.2.1 ATAC-Seq analysis	99
4.2.2 Genome-wide analysis of DNA-protein interactions involved in regulation of gene expression during gut differentiation in the sea urchin embryo	111
4.2.3 The <i>Meis</i> gene	115
4.2.4 <i>Sp-Meis</i> temporal and spatial expression.	116
4.2.5 Sp-Meis functional characterization	118
4.2.6 Validation in trans of <i>Sp-Meis</i> node: ChIP analysis	122
4.3 Conclusions	125
CHAPTER 5	126
DISCUSSION	126
5.1 Conservation and divergence between the sea urchin and sea star gut GRNs	126
5.2 The reconstruction of the <i>S. purpuratus</i> gut GRN reveals a key role of the homeobox gene <i>Sp-Meis</i>	132
5.3 A novel, powerful method for building GRNs through the integration of omics approaches	135
5.4 Conclusions and future perspectives	139
BIBLIOGRAPHY	142
APPENDIX I - RNA-SEQ DATA SETS	157
APPENDIX II - PUBLISHED PAPERS	228

LIST OF FIGURES

Fig. 1.1. Network components and changes in the GRN	5
Fig. 1.2. Sea urchin development	16
Fig. 1.3. Biotapestry diagram summarizing the gene regulatory interactions occurring during endomesoderm specification in <i>S. purpuratus</i>	18
Fig. 1.4. Sea star development	21
Fig. 1.5. Evolution of ParaHox gene cluster and relative expression domains in bilateral animals	31
Fig. 1.6 Morphological phenotype caused by Xlox and Cdx protein depletion	36
Fig. 1.6bis. Progression of <i>Xlox</i> and <i>Cdx</i> expression during gut formation in sea urchins and sea stars	37
Fig. 3.1. Bioanalyzer results of the total RNA samples generated for differential RNA-Seq	63
Fig. 3.2. Gene ontology analysis for DE genes downstream of Sp-Lox at 48 hpf	70
Fig. 3.3. Gene ontology analysis for DE genes downstream of Sp-Lox at 72 hpf	72
Fig. 3.4. Gene ontology analysis for DE genes downstream of Sp-Cdx	74
Fig. 3.5. Gene ontology analysis for DE genes downstream of Pm-Lox	77
Fig. 3.6. Gene ontology analysis for DE genes downstream of Pm-Cdx	78
Fig. 3.7. Gene ortholog relationship between <i>S. purpuratus</i> (SPU), <i>P. miniata</i> (PMI), and <i>X. tropicalis</i> (XEN)	80
Fig. 3.8. Sea urchin misexpressed genes	83
Fig. 4.1. ATAC-Seq analysis around the <i>Sp-Lox</i> gene locus	101
Fig. 4.2. ATAC-Seq analysis around the <i>Sp-Cdx</i> gene locus	101
Fig. 4.3. ATAC-Seq analysis around the <i>Sp-Meis</i> gene locus	103

Fig. 4.4. ATAC-Seq analysis around the <i>Sp-FoxA</i> gene locus	104
Fig. 4.5. ATAC-Seq analysis around the <i>Sp-Hox11/13b</i> gene locus	106
Fig.4.6. ATAC-Seq analysis around the <i>Sp-Nr1m3</i> gene locus	108
Fig.4.7. ATAC-Seq analysis around the <i>Sp-Ets4</i> gene locus	109
Fig. 4.8. ATAC-Seq analysis around the <i>Sp-Bra</i> gene locus	110
Fig. 4.9. Schematic representation using Biotapestry (http://www.biotapestry.org/) of the main identified TF inputs of the TFs at sea urchin 48 hpf and 72 hpf	113
Fig. 4.10. Temporal expression profile of <i>Sp-Meis</i> gene	116
Fig. 4.11. WMISH experiment using <i>Sp-Meis</i> antisense and sense riboprobes	118
Fig. 4.12. <i>Sp-Meis</i> knocked-down embryos	119
Fig. 4.13. Q-PCR analysis of gene expression in <i>Sp-Meis</i> morphants	121

Fig. 4.14. Sheared chromatin of 48 hpf sea urchin embryos	100
Fig 4.15. Sequence of Sp-Lox binding site in the <i>Sp-Meis</i> intron and primers position	101
Fig. 4.16. Histogram of fold enrichments of <i>Sp-Meis</i> gene after immunoprecipitation with anti Sp-Lox antibody and pre-immune serum	102
Fig. 5.1. General scheme for constructing a GRNs from omics data	110
Fig. 5.2. Xlox and Cdx TFBS alignments	113

LIST OF TABLES

Table 2.1. Sequences of the morpholinos used in microinjection experiments	55
Table 2.2. Primers used to clone Sp-Meis in different regions of the gene	55
Table 2.3. Primers used in QPCR experiments	57
Table 2.4. Primers used in ChIP-QPCR experiments	57
Table 3.1. Data sets obtained by differential RNA-Seq	68
Table 3.2. Homology of differential expressed transcripts	81
Table 3.3 Summary of sea star affected genes	84
Table 3.4. Transcription factors downstream of Sp-Lox	88
Table 3.5. Transcription factors downstream of Sp-Cdx	91
Table 3.6. Transcription factors downstream of Pm-Lox	94
Table 3.7. Transcription factors downstream of Pm-Cdx	95
Table 4.1. List of the TFs inputs in the sea urchin gut at 48hpf and 72 hpf	114

LIST OF ABBREVIATIONS

AP	Alkaline phosphatase
ASW	Artificial seawater
ATP	Adenosine triphosphate
BCIP	5-bromo-4-chloroindole-3-indolyl phosphate
bp	base pair
BSA	Bovine serum albumine
ChIP	Chromatin Immuno Precipitation
DNA	Complementary DNA
CRM	Cis regulatory module
DIG	Digoxigenin
DNA	Deoxyribonucleic Acid
DNase	Deoxyribonuclease
dNTP	Deoxyribonucleoside triphosphate
EDTA	Ethylenediaminetetraacetic acid
FLUO	Fluorescein
GRN	Gene regulatory network
hpf	Hour post fertilization
IP	Immunoprecipitation
MASO/MO	Morpholino antisense oligonucleotide
M	Molar
min.	minute
ml	milliliter

mM	millimolar
MOPS	3-(N-Morpholino) propanesulfonic acid 4 Morpholinepropanesulfonic acid
MFSW	Millipore Filtered Sea Water
mRNA	messenger RNA
NBT	Nitrobluetetrazolium
NSM	Non skeletogenic mesoderm
ON	Over night
PABA	Para aminobenzoic acid
<i>Pm</i>	<i>Patiria miniata</i>
PBS	Phosphate buffered saline
PCR	Polymerase chain reaction
PIPES	1,4-piperazinediethanesulfonic acid
PMC	Primary mesenchyme cell
QPCR	Quantitative PCR
RA	Retinoic acid
RNA-Seq	RNA-Sequencing
rpm	Rotations per minute
RT	Room temperature
SDS	Sodium dodecyl sulphate
SMC	Secondary mesenchyme cell
SSC	Standard saline citrate

<i>Sp</i>	<i>Strongylocentrotus purpuratus</i>
SSC	Standard saline citrate
SW	Seawater
TF	Transcription factor
TFBS	Transcription factor binding site
Tris-HCl	Tris-(hydroxymethyl)aminoethane
WMISH	Whole Mount <i>in Situ</i> Hybridization
<i>X.tropicalis</i> /XEN	<i>Xenopus tropicalis</i>
μg	microgram
μl	microliter
μM	micromolar

CHAPTER 1

INTRODUCTION

This thesis focuses on the evolution and developmental mechanisms underlying body plan change. To acquire knowledge on these processes, a comparative study of the gene regulatory networks controlling development of the digestive tract in two echinoderms, the sea urchin *Strongylocentrotus purpuratus* and the sea star *Patiria miniata* was performed. This introductory chapter describes the systems-level approach, the experimental animal system and the biological process studied to perform this thesis work.

1.1. The approach: gene regulatory network

1.1.1 Gene Regulatory Networks and their evolution

The Cambrian explosion, occurred 540-515 millions ago according to fossil evidence, has been considered the most important moment of animal evolution during which the major branches of the tree of life appeared for the first time. According to many studies (Erwin et al. 2011) (Valentine 2004) this large expansion permitted to pass from a two dimensional world mostly inhabited by microbial fauna to a three dimensional world with the evolution of animal body

plan capable of active and directed locomotion, active burrowing and feeding in sediments with the formation of muscle and a gut with a distinct anus, and a centralized nervous system with anterior brain and sense organ. This has been considered as possible cause of the development of the bilaterian class, a group of animals characterized by antero posterior axis (head to tail), a dorsoventral axis (top to the bottom) and a left-right axis (P. W. H. Holland 2015). How this sudden explosion of animal diversity occurred in such a short evolutionary period lasting over 10 million years has been a debated topic in animal evolution for more than one century (Darwin 2004) (Walcott and Resser 1916) (G. A. Wray, Levinton, and Shapiro 1996). Nowadays, the most accepted theories about Cambrian burst state that evolutionary changes already happened at the dawn of the Cambrian and were caused by multiple factors (M. P. Smith and Harper 2013). According to a post-genomic era point of view, starting from a pre-existing genomic toolkit there was a rearrangement of this material to adapt it to new ways of control and regulation of biological pathways during development, resulting in inherited genomic regulatory program, the gene regulatory network (GRN). The mechanism to explain changes in the body shape of the organisms and the formation of new living forms may lie in the structure and evolution of these GRNs (Eric H. Davidson and Erwin 2006) (Erwin and Davidson 2009) (Eric H. Davidson and Erwin 2010) (Peter and Davidson 2011b). The GRN is responsible of the development of all the organisms. It consists of genes products, represented as nodes, and interactions among the genes, represented as edge. A transcription factor (TF) interacts with a cis-regulatory module (CRM), i.e. a sequence of the DNA where the TF can bind, of a target gene determining its spatial and temporal expression. The unique combination of transcription factors and interactions occurring in each cell in a given time of development determine the regulatory state of that cell. The function of the GRN is to establish specific regulatory states in the

spatial domain of developing organism, determining which gene will be active or inactive in each domain (specification) and the progression of these states lead to the development of such a body part. Since regulatory genes regulate several genes and every regulatory gene responds to multiple inputs and at the same time regulates multiple other genes, all these interactions form a network. GRNs are hierarchical so that the genes controlling the initial stages of development are at the top of the network, the portion controlling intermediate processes of spatial subdivision or the formation of future morphological pattern are in the middle and the portion controlling the detailed functions of cell differentiation and morphogenesis are at the periphery. The GRNs show a modular structure consisting of four multigenic sub circuits. Each sub circuit performs a distinct regulatory function in the process of development and changes in its structure will have different consequences for the outcome of the developmental process and for evolution (Fig. 1.1). The first evolutionarily inflexible circuit is represented by the “**kernels**”, that consists of regulatory genes required to specify the spatial domain of an embryo in which a given part will form. The “**plug ins**” sub circuit is part of many different networks where It provides inputs for a variety of regulatory apparatus. Its elements can be differently used for different purpose during development. For example, the bilaterian transforming growth factor beta (TGF), Hedgehog, Notch are used differently and in a great variety of regulatory apparatus. It follows that this sub circuit is evolutionarily very labile. The **input/output** switch sub circuit allows or disallows developmental sub circuits to function in a given context. An example of I/O switch sub circuit are Hox genes that prevents or induce the development of entire embryonic structure. The differentiation **gene battery** circuit is made up of protein coding genes involved in cell type specific function such as the formation of muscles, skin, skeleton, etc. In contrast to the kernels or plug ins, this sub circuit does not have regulatory functions. Differentiation gene

batteries undergo continuous renovation with changes in the protein coding sequences, addition or loss of new genes through modification in cis regulatory modules of transcriptional regulators to which that battery responds. Differentiation gene battery are expressed in the final stages of a developmental process and do not make body parts. Due to this modularity, modifications in the GRN structure, due to mutations, transposable elements, replication slippage, etc. can have more or less catastrophic effects on the animal body shape and diverse evolution consequences. This depends on where the affected element acts in the network: if the change occurs in the upper levels of the network (kernels) it causes much more deleterious problems downstream than if the change occurs in the lower levels (plugins, I/O switch, gene batteries). The kernels represent the most stable element and highly resistant to evolutionary change and their function and characteristics provide a molecular explanation to the conservation of the phyletic body plans since their appearance in the Cambrian (Eric H. Davidson and Erwin 2006). Interference with expression of any one kernel gene will destroy kernel function altogether and cause the catastrophic phenotype of lack of the body part. Plug ins and I/O switches can work at high or low level of the hierarchy of the GRN. They are evolutionary labile and changes in these types of sub circuits bring to novel characteristic at the class, order and family taxonomic levels. The differentiation gene batteries can only alter the function of a body part, for this reason changes occurring in this sub circuit can only produce changes in the development and evolution at the species level.

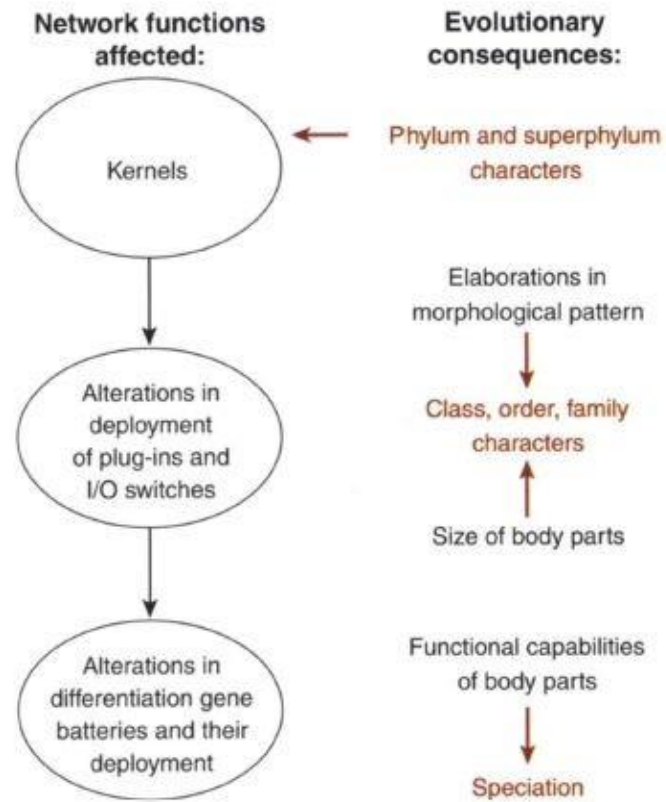


Fig.1.1. Network components and changes in the GRN. The left column shows changes in the network components. The right column show evolutionary consequences. Adapted from Davidson and Erwin, 2006.

1.1.2 Building a Gene Regulatory Network

The construction of a gene regulatory network (GRN) for a given developmental process requires knowledge of the regulatory states that progressively establish the identity of cell population during development and give them a specific function. A protocol published in 2008 (Materna and Oliveri 2008) well describe the approach to experimentally determine the complex structure of a GRN. Although the method refers to the experimental determination of the function of a specific regulatory element in the complexity of the sea urchin network, it can be extensively applied to many other organisms. A first approach to unravel a GRN is to have a general understanding of the process that has to be explained in terms of cell lineages and fate map of the embryo and to simplify the study focusing to a limited set of events in time and space. The studied set of events is then linked to the others in order to reconstruct the whole process making the formation of an entire embryo or an organ. The regulatory genes taking part to each process can be identified taking advantage of the fact that Bilateria retain a toolkit of regulatory genes that share similar sequence (Erwin and Davidson 2002). Then, the regulatory genes need to be analyzed in the temporal and spatial expression in order to characterize the regulatory state of the cells involved in the process. Approaches such as quantitative PCR (qPCR), cDNA microarray and RNA-Seq have been extensively adopted for the temporal studies, while *in situ* hybridization using labeled specific probes are used for the spatial aspect. The specific role that an element has in the network, the regulatory interactions in which it is involved and the developmental event it took part in, are analyzed with methods that measure gene expression in order to determine the effect that a missing protein has in the network and to validate its predicted interactions. In order to prevent the activity of a certain protein several are the approaches that can be used: morpholino, RNAi, CRISPR-

Cas9. However, so far morpholino injection is the most used and allowed the construction of the most complete GRN in the sea urchin embryos. The absence of the element in the network has minor or major effects that depend on its position in the hierarchy of the GRN, as described in (Erwin and Davidson 2002; Erwin and Davidson 2009). Experiments of *in situ* hybridization to detect the transcripts of a specific gene in the organism are used to observe the effects of the perturbation in the network. An increased transcripts level of a specific target gene after knock-down or knock-out experiments indicates a negative regulation of the affected element on that gene in normal conditions; at the same time if the missing protein causes a decrease of the number of the transcripts of the target gene, we can conclude that the protein is an activator of its expression or a repressor of its repressor. An important consideration to be done is that the predicted interactions are not necessarily direct and that the perturbation experiments reveal the global effects in the network. This means that the absence of a protein may affect not only one gene, its putative direct target, but also other downstream genes with a cascade event. These perturbation techniques are now being combined with next generation sequencing (NGS) to gain a global view of the mechanisms involved in development and evolution of GRNs. In order to detect the *in vivo* occupancy of a specific TF on the binding site within a gene regulatory region, a population of DNA fragments bound to a given transcription factor is pulled down in the Chromatin immunoprecipitation approach (see material and methods). The enrichment of the immunoprecipitated DNA compared to an input (not immunoprecipitated chromatin) provides evidence of a direct interactions between the trans-regulatory element and the cis-regulatory module. The presence of a TF on a transcription factor binding site (TFBS), however, does not imply its capability on driving gene expression. For this reason the function of the cis-regulatory element needs to be tested with the generation of a reporter construct in which the

putative TFBS is mutated and cloned upstream of a reporter gene. Changes in the reporter gene expression are checked to verify if there is any increase, decrease, expansion or restriction of the expression. The described approaches taken together give the most comprehensive analysis of a GRN. However, this depth of knowledge is not easy to be achieved. Among the existing animals, so far, echinoderms represent the most feasible model system for the application of this described method of GRN reconstruction.

One of the most complete cis regulatory network among the Metazoa is the endomesoderm specification of the sea urchin embryos of which a first draft was published in 2002 (Ransick et al. 2002). For its construction the expression of many regulatory genes and several signaling process were altered with a large scale perturbation analysis through antisense oligonucleotide morpholino, blockade of endomesoderm specification (β -catenin/Tcf signal), blockade of mesoderm specification (Notch signaling system), ectopic expression of regulatory proteins from mRNA injection and from genetic expression construct, dominant repressor form of transcription factors by construction of Engrailed repressor domain fusions. The effects that the perturbations had on other genes were tested measuring the gene level expression by quantitative real time PCR (qPCR) and considering significant perturbations the ones whose effects are threefold greater with respect to the control. The map of the network was built using the BioTapestry Interactive Network Viewer, and is uploaded and constantly updated on the website <http://sugp.caltech.edu/endomes/index.html>. Two models have been developed to represent the sea urchin GRN: the view from the genome and the view from the nucleus. In the view from the genome are represented all the presumed interactions occurring among the genes of the network in all cell types at all stages during a developmental process. The view from the nucleus describes the subsets of interactions shown in the view from the genome that operate at a given time and in

a given nucleus in a specific moment of development.

Since the 2002 papers, the regulatory circuitry of endomesoderm specification in the sea urchin embryo has been studied in great detail and has led to the elaboration of a GRN model that displays how endomesoderm development progresses from fertilization until 30 hours post fertilization (hpf) at 15°C, when the tissue has already been segregated into definitive endoderm and mesoderm (Ransick and Davidson 2006) (Croce and McClay 2010) (Peter and Davidson 2010) (Peter and Davidson 2011a) (Peter and Davidson 2011a; Lhomond et al. 2012) (Li, Materna, and Davidson 2012).

The approach to study GRNs in development can obviously be applied to any developmental process in any embryo that allows for high throughput gene perturbation analyses. Several studies are emerging which use this approach, for instance, and within echinoderms, the GRN which controls muscle formation in the sea urchin embryo (Andrikou et al. 2015), the network responsible for oral and aboral ectoderm differentiation and ecto-endoderm boundary formation (Su et al. 2009) (Li et al. 2014), or the network that defines the distribution of ciliary band-associated neurons in the bipinnaria larva of the sea star (Yankura et al. 2013). Other recent examples of the use of the same approaches outside echinoderms are the deciphering of the primary cardiac gene regulatory network in the invertebrate chordate *Ciona intestinalis* (Woznica et al. 2012), or the GRNs that underlies the compartmentalization of the *Ciona* central nervous system (Imai et al. 2009). GRN studies not only provide explanation of how regulatory states are established in particular cells during development and how these states eventually determine the final morphology of the embryo, but also provide a powerful tool, through comparisons of GRN architectures, to reveal the molecular evolution of developmental programs among different organisms (Hinman et al. 2003) (Hinman and Davidson 2007) (McCauley, Weideman, and Hinman 2010)

The experimental animal system: Echinoderms

1.1.3 Deuterostomes: the phylum of Echinodermata

Deuterostomes are a group of animals characterized by the formation of the anus from the blastopore and the formation of the mouth in a secondary anterior location during embryo development. Deuterostomes belong to Bilateria and are sister group of Protostomia (Ikuta 2011). Deuterostomes include two major clades, the Ambulacraria and Chordata. Ambulacraria consists of Echinodermata and Hemichordata. Echinodermata is composed of five classes: Crinoidea (e.g. sea lilies and feather sea stars), Asteroidea (e.g. sea stars), Ophiuroidea (e.g. brittle stars), Holothuroidea (e.g. sea cucumbers) and Echinoidea (e.g. sea urchins); all these animals share bilateral dipleurula larva and pentamerous adult body plan with a thin epithelium covering an internal skeleton. The skeleton consists of plates that collectively form five ambulacra and are penetrated by many holes through which tube feet extend providing the animal of movement. More than 7000 existent species of echinoderms live on earth and more than 13000 echinoderms species have been recognized in the fossil records. Pisani and colleagues (Ikuta 2011; Pisani et al. 2012) place the origin of Echinodermata in the late Precambrian, around 570 MY ago, time that corresponds to the divergence of Echinodermata from Hemichordata. This date is based on a molecular clock method and is controversial; fossil data suggests an origin in the Cambrian period. There are two different hypothesis to explain the phylogenetic relationship among all extant echinoderm classes. The first one is called “Cryptosyringida” and suggests a clade that includes ophiuroids, echinoids and holothuroids; the second one, called “Asterolzoa-Echinozoa”, proposes a close association between asteroids and ophiuroids (Mooi and David 2000). Echinoderms have an indirect development

with the formation of a larva. Species with eggs less than 150 μm develop a planktotrophic larva; while species with larger eggs have nonfeeding larva. Echinoidea, Ophiuroidea, Holothuroidea and Asteroidea give rise to small eggs and to two types of feeding larvae: the pluteus-like larvae of sea urchins and brittle stars and the auricularia-like larvae of sea cucumbers and sea stars. The same classes also include species that possess nonfeeding larvae. Crinoidea are the only echinoderm class that does not have a feeding larva. This great diversity of larval and adult forms in Echinoderms has always excited curiosity of biologists to understand the mechanisms that lay behind such body diversity. Since the mid-nineteenth century echinoderms have represented a powerful tool for developmental biology, cell biology, and genetic studies. In 1892 Hans Driesch isolated the blastomeres from sea urchin embryos at 2 and 4 cells-stage and demonstrated that each blastomere was capable of producing entire larva. This was called regulative development, meaning the capability of the embryonic cells to change their fate according to the external conditions. In 1902 Theodor Boveri, working at the Stazione Zoologica Anton Dohrn of Naples, fertilized sea urchin eggs with high concentration of sperm obtaining eggs fertilized by two spermatozoa. During the first events of segmentation each cell developed in a different and anomalous way, as consequence of the fact that each cell had different types of chromosomes. This was the first evidence showing the mechanism of inheritance according to which only when nuclei received a complete set of chromosome develop normally. In 1939 Sven Hörstadius recombined isolated micromeres, the future skeletogenic cells, with the top two animal cells tiers, normally fated to become ectoderm, with the result that the animal cells generated endoderm, demonstrating the inductive capacity of sea urchin blastomeres. The success of echinoderms as developmental model system is related to the ease collection of million gametes, the external fertilization and development of the

embryos that made possible to study the early development. The transparency of eggs and embryos makes possible to directly observe developmental processes and the application of technologies including fluorescence-based methods for monitoring gene expression, protein localization, protein–protein interactions, and biochemical activity. The physical manipulation of the embryo allows embryo dissociation, cell isolation, and cell transplantation. Several molecular approaches for gene regulation and functional studies such as expression of exogenous mRNAs, injection of reporter DNA constructs for cis-regulatory analysis, and injection of morpholino antisense oligonucleotides are also feasible with these animals. With the development of genomic-based resources, genome sequencing became available also for echinoderms. The most echinoderm species studied in development are restricted to small number. In 2006 after the first sequencing efforts concentrated on the model organisms such as *Drosophila melanogaster*, *Caenorhabditis elegans* and *Mus musculus*, the genome of the first echinoderm, the sea urchin *Strongylocentrotus purpuratus*, has been sequenced due to the extended use of sea urchin as research model system for molecular, evolutionary and cell biology (Mooi and David 2000; Ettensohn, Wessel, and Wray 2004; Sea Urchin Genome Sequencing Consortium et al. 2006). This study led to discover that sea urchin possess representatives of nearly all vertebrate gene families, including orthologues of many human disease-associated genes, and that some genes thought to be vertebrate-specific are already present in echinoderms; moreover sea urchin has a sophisticated immune system and genes associated with sensory capabilities. Moreover many genes present in more copies in vertebrate, i.e. Hox gene cluster, have a single copy in the invertebrate deuterostome. The availability of the genome and its simplicity compared to the vertebrates was fundamental for the study of developmental pathways, gene networks, and the functions of conserved gene products that are more challenging to study in vertebrates because of the

proliferation of the genes involved (Mooi and David 2000; Ettensohn, Wessel, and Wray 2004). So far, the process of endomesoderm specification in the sea urchin *Strongylocentrotus purpuratus* is the most exhaustive gene regulatory network among all the developmental systems. Other echinoid genomes are currently being sequenced such as *Paracentrotus lividus*, *Lytechinus variegatus*, *Eucidaris tribuloides*. Complete genomic and transcriptomic data are available for the first asteroid species *Patiria miniata*. (<http://www.echinobase.org/Echinobase/PmAbout>).

1.1.4 Sea urchin development

The sea urchin animals have separate sex. During the gravid period that, according to the species, can be year around, only in short period of time or with a lunar periodicity, eggs and sperm are released into the sea water and fertilization occurs externally. The majority of sea urchin species has an indirect development that produces a free-swimming larva that after metamorphosis becomes a juvenile with fivefold symmetry and grows to become an adult animal. About one-fifth of the animals, instead, possess large eggs of ~300 µm, due to the accumulation in the cytoplasm of proteins, RNAs, morphogenetic factors and protective substances that supply the embryo of energy source and directly reaches the juvenile stage bypassing the larva formation. The sea urchin egg has completed the meiotic division associated with the oogenesis when it is still in the ovary. Two envelopes surround the sea urchin egg: the inner vitelline envelope that will fuse with the plasma membrane of the spermatozoon and the outer jelly coat involved in the activation and contact of the spermatozoon. The fertilization event involves the fusion of the sperm and the egg membrane and the fusion of the male and female haploid pronuclei. During the first fusion event the sperm binds, a species-specific

protein (Vacquier and Moy 1977), interacts with specific receptors (Giusti, Hoang, and Foltz 1997); (Stears and Lennarz 1997) on the egg surface. This interaction causes the exocytosis of the sperm's acrosomal vesicle and the release of proteolytic enzymes that allow the sperm to digest the jelly coat and ingress the egg to take contact with the vitelline envelop. At this point the sperm pronucleus move towards the egg pronucleus and a diploid zygote is formed. After fertilization the zygote begins a series of cleavages that lead to the formation of the embryo (Fig. 1.2), as described in (Stears and Lennarz 1997; McClay 2011) . The segmentation in sea urchin is holoblastic, meaning that it takes the entire egg, and radial, because it occurs either parallel or perpendicular to the polar axis of the oocyte. The first two cleavages are equal and parallel to the animal-vegetal axis and divide the egg into four cells of equal size. The third cleavage is equatorial and separates four animal blastomeres from four vegetal blastomeres. The fourth cleavage divides the four animal blastomeres meridionally giving rise to eight equal-sized cells called mesomeres (the future ectoderm); the four vegetal blastomeres divide asymmetrically producing four larger cells called macromeres that will become veg2 and will give rise to the future endoderm and non skeletogenic mesoderm NSM, including pigment cells, blastocoelar cells, muscle cells and coelomic pouch cells, and four smaller cells called micromeres. Above the future veg2 tier there is a tier of cells called Veg1 that will give rise to the endoderm and some ectoderm. At the fifth cleavage the eight mesomeres divide equally and horizontally, forming two tiers of cells (an1 and an2). The four macromeres divide meridionally forming a tier of eight cells, while micromeres divide asymmetrically once more and give rise to four small micromeres (the future coelomic pouches) at the vegetal pole and four large micromeres (the future skeletogenic cells or primary mesenchyme cells PMCs) above them. At sixth cleavage all the cells divide horizontally producing the 60-cell stage embryo. From this stage the embryo hollows forming a blastocoel

cavity and now the embryo is called blastula. At mid blastula stage cilia appear on the surface of the embryo that hatches from the fertilization envelope and start to swim in the water. Gastrulation then starts and the vegetal part of the embryo thickens and flattens and the PMC ingress the blastocoel cavity in a region called blastopore that becomes the future anus of the larva. After ingression, the remaining non-skeletogenic mesoderm cells (descendants of veg2) at the vegetal pole move and fold inwards. The invaginated region is now called archenteron that elongates by recruiting endodermal cells and by movements of thin filopodia by non skeletogenic mesoderm cells to pull the archenteron toward the animal pole. As the archenteron elongates, secondary mesenchyme cells delaminate from its tip and disperse within the blastocoel where they proliferate to form non-skeletogenic mesoderm cells. Once the archenteron reaches the animal pole the tip of the archenteron makes contact with the oral epithelium that invaginates to form the stomodeum. After gastrulation other changes affect the embryo to form the pluteus larva. A ciliary band develops around the stomodeum and form the neural network. The archenteron is divided into foregut, midgut and hindgut. Two oral arms and two anal arms appear and grow from the surface of the embryo. Triradiate spicules develop into skeletal rods that extend through the body. Coelomic pouches form to both the side of the foregut. A pluteus larva is now formed.

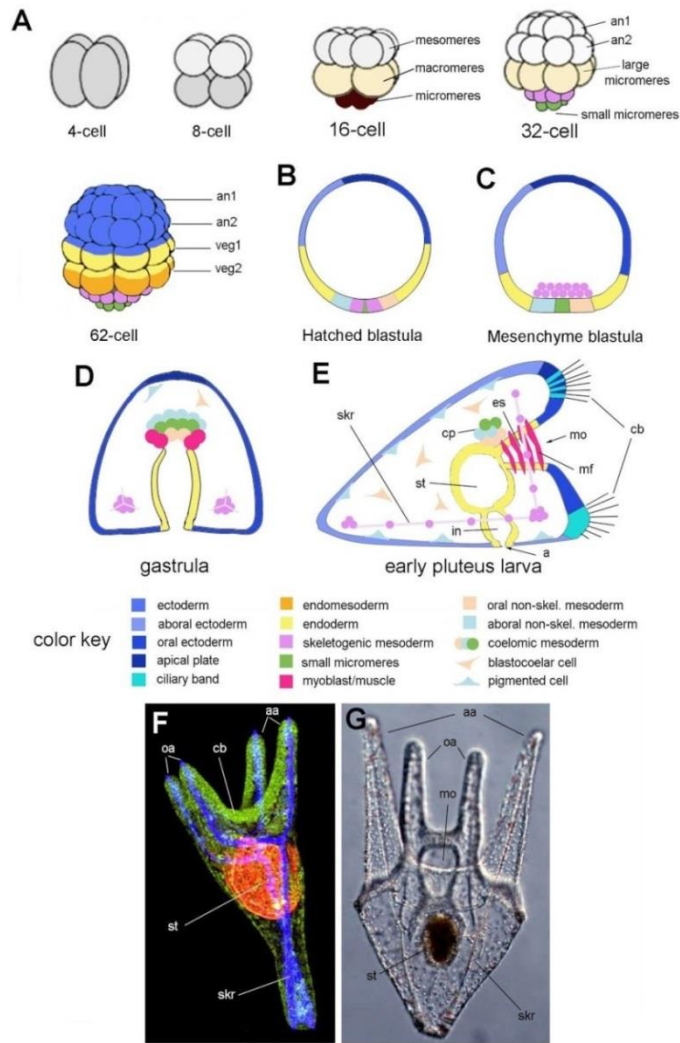


Fig. 1.2. Sea urchin development. (A) Cleavage stages seen along the animal (top)-vegetal (bottom) axis. At the 16-cell stage there are four micromeres (brown) at the vegetal pole, four central macromeres (light yellow) and eight mesomeres (grey) at the animal pole. The colors indicate when the cells begin to be specified towards ectoderm, endoderm and mesoderm (see color key). (B) Hatched blastula stage, mid-sagittal section. The ectoderm is already subdivided (as indicated by different shades

of blue) and the non-skeletogenic mesoderm (oral and aboral) has separated from the endoderm. (C) Mesenchyme blastula stage, mid-sagittal section. Primary mesenchyme cells have ingressed into the blastocoel while small micromeres stay behind. (D) Mid-sagittal section of a mid-gastrula stage, showing the gut invaginating, the skeletogenic cells beginning to synthesize the skeleton, and non-skeletogenic mesoderm at the tip of the archenteron subdividing into domains occupying different positions along the oral/aboral and animal/vegetal axis (different cell types are indicated following the color key). (E) Pluteus larva, lateral view, showing the definite structures and cell types generated during embryogenesis. (F) *Paracentrotus lividus* pluteus larva stained to show the gut (red), the skeleton (blue) and the ectoderm (green) (courtesy of David McClay). Length of larva, from posterior end to anterior tip = 120 μ m. (G) *Strongylocentrotus purpuratus* at the 4-arm stage larva. Length of larva = 200 μ m. The inset shows details of the ciliary band on one larval arm (purple). Abbreviations: a, anus; aa, anal arm; an, animal; cb, ciliary band; cp, coelomic pouch; es, esophagus; in, intestine; mf, muscle fiber; mo, mouth; oa, oral arm; skr, skeletal rod; st, stomach; veg, vegetal. Adapted from (Maria Ina Arnone, Byrne, and Martinez 2015).

1.1.5 Sea urchin GRN for specification of endomesoderm

Specification is the process by which cells obtain their developmental identity with the expression of unique set of genes, defined gene regulatory state. The process of endomesoderm specification in sea urchin embryo involves a network of regulatory genes specifying endoderm and mesoderm territories from a common cell-lineage called endomesoderm (Fig.1.3). All of the endomesoderm emerges from the vegetal plate and from distinct embryonic lineages: the micromeres (skeletogenic mesoderm) that form at the fourth cleavage and part of the veg1 (endoderm) and the veg2 (non-skeletogenic mesoderm and endoderm) which segregate from one another at sixth cleavage after fertilization. Ruffins and Ettensohn (Ruffins and Ettensohn 1996) traced the veg2 cells and established that the veg2 mesoderm cells type derive from the more central region of the vegetal plate, while the endodermal veg2 cell types from the more peripheral region. The future mesoderm express both endoderm and mesoderm GRNs with the endodermal regulatory gene *foxA* and the mesoderm regulatory gene *gcm* expressed both in an inner ring of veg2-derived cells., whereas the future endoderm express only an endoderm regulatory state with *foxA* expressed alone in the peripheral cells of the veg2 lineage (Ruffins and Ettensohn 1996; Peter and Davidson 2011a). The distinction between endoderm and mesoderm in veg2 depends on two inputs. The first one is the nuclearization of β -catenin, a cofactor of the Tcf transcription regulator, triggered initially by a maternal cytoplasmic system (Ruffins and Ettensohn 1996; Peter and Davidson 2011a; Logan et al. 1999); Weitzel *et al.*, 2004) and increased by the expression of *wnt8* (J. Smith, Theodoris, and Davidson 2007). Every cell, the progeny of which will express an endodermal or a mesodermal fate, displays elevated nuclear β -catenin at seventh cleavage. The nuclearized β -catenin together with the maternal Otx transcription factor activates the endodermal regulatory genes *blimp1b* and

hox11/13b (J. Smith et al. 2008) (Arenas-Mena, Andrew Cameron, and Davidson 2006) that activate *foxa* and *brachyury*. All these genes constitute the endodermal kernel essential for endoderm development. During the seventh to the ninth cleavage a second signal, Delta/Notch, is transmitted from the micromeres to the *veg2*, that induces the specification of these cells as mesodermal precursors. The skeletogenic micromere lineage expressing Delta ligand activates Notch receptor in the adjacent *veg2* cell initiating mesoderm specification. Only the cells directly adjacent to the micromere lineage become mesoderm and express *gcm* (Ransick and Davidson 2006), whereas more distal *veg2* derived-cells which are not exposed to Delta/Notch signal become endoderm and contribute to the foregut and midgut formation.

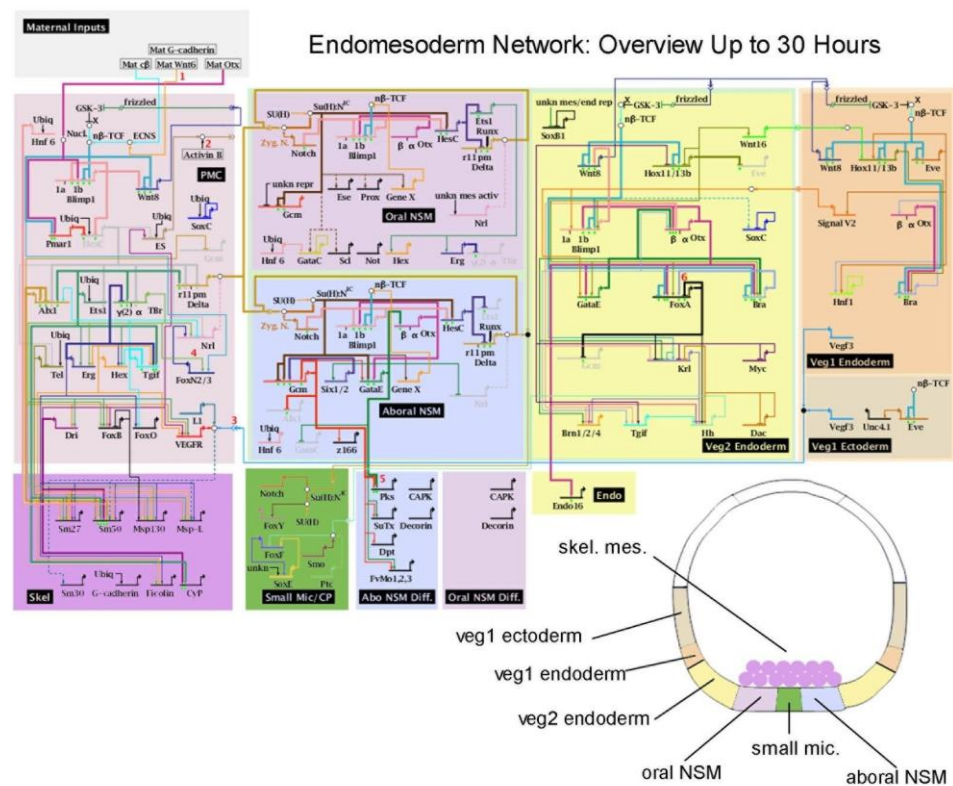


Fig. 1.3. Biotapestry diagram summarizing the gene regulatory interactions occurring during endomesoderm specification in *S. purpuratus*. The last updated diagram is schematized (11/2011). The diagram is also available on the E. H. Davidson's laboratory webpage (<http://sugp.caltech.edu/endomes>). Colors label the different embryonic territories. Connecting

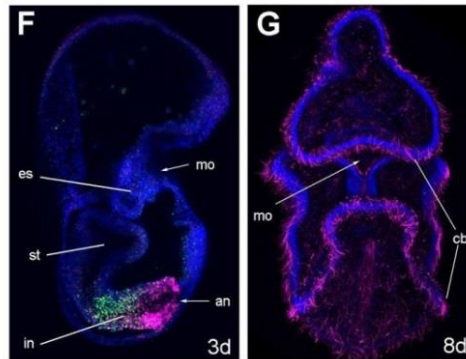
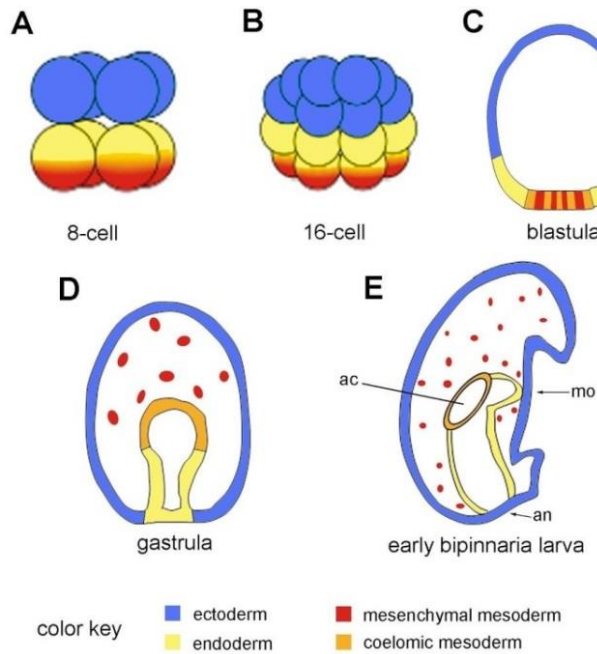
lines indicate gene interactions. Adapted from Arnone, Byrne and Martinez (2015).

The exclusion of the mesoderm GRN is based on the Tcf sites that are used to initiate the endoderm GRN in veg2 lineage and that now are used again to suppress the expression of all the endodermal regulatory genes in the mesoderm precursors. Cells receiving Notch signaling have a reduced availability of nuclear β -catenin leading to Tcf/Groucho-mediated repression that affects veg2 endoderm regulatory genes. At late blastula stage (after 24h) nuclear β -catenin reappears in the veg1 progeny that begin to express *evenskipped* gene (Ransick et al. 2002) that is the only known endoderm regulatory gene expressed in veg1 at early blastula stage. The assembly of the veg1 endoderm GRN is spatially activated by *eve* and temporally motivated by a predicted signal, which is probably *Wnt15*, activated by *Hox11/13b* in the veg2 endoderm GRN and that induce *Hox11/13b* expression in veg1 endoderm progenitors and activates *bra*. At the same time *Hox11/13b* autorepression clears its expression from veg2 endoderm. The veg1 progeny invaginate and will contribute mainly to hindgut formation. Thus, before functional and morphological differentiation of gut, specification of distinct anterior and posterior endoderm progenitors is already accomplished by parallel activation of two distinct GRNs.

1.1.6 Sea star development

For years sea urchin has been the focus of developmental studies for an extensive comprehension of the mechanisms of its development. On the other side sea star embryogenesis has been poorly studied and only now, that the genome of the sea star *Patiria miniata* has been sequenced (not yet published), is considered a developmental model organism. The development of the sea star *Patiria miniata* (Fig. 1.4), through the formation of a feeding larva, is it well described in a study of

Hinman *et al* (2003b) (Hinman, Nguyen, and Davidson 2003). As in other echinoderms the cleavage is equal and the 16-cells embryo consists of equal-sized blastomeres. Like sea urchin, starfish embryos can be conceptually divided into an1, an2, veg1 and veg2 cell lineages. Unlike sea urchin that during the 4th cleavage stage divides embryo into macromeres, mesomeres and micromeres, sea star does not form micromeres, due to the equal cleavage. By the end of blastula formation, the ectoderm is covered in cilia and the embryos start to rotate within the fertilization envelope about 1 h before hatching, at around 26h at 15°C. Prior to gastrulation, a thickened vegetal plate appears. Similar to sea urchin this is the region from which endodermal and mesodermal derived structures will develop. Gastrulation occurs by a sequential invagination of the inner to outermost cells of the vegetal plate. In a work of Kuraishi and Osanai (1992) (Kuraishi and Osanai 1992) on *Asterina pectinifera*, cell labeling experiments indicate that the early part of the invaginating archenteron, which derives from the veg2 lineage, contributes to the rounded top of the archenteron in mid to late gastrulae, and to the anterior coeloms and esophagus of the bipinnaria larva. Later invaginating veg2 cells contribute to the stomach, while the hindgut derives in part, from the still later invagination of the veg1 cells. Mesenchyme cells migrate from the top of the archenteron during gastrulation, but unlike in sea urchins, many more presumptive mesoderm cells remain associated with the archenteron and develop into prominent anterior coeloms on either side of the esophagus in the bipinnaria larvae. By the late bipinnaria (7d) larval stage, ciliated cells distributed over the ectoderm at earlier stages have coalesced into two distinct bands, a preoral and anal loop, as observed in *Astropecten auranciacus* (Hyman 1955). At this stage the mouth is fully formed and the gut tube is divided into esophagus, stomach and intestine which opens posteriorly through the anus.



involuting ectoderm of the oral plate, the anterior coeloms (orange) extend vegetally. (F) *Patiria miniata* bipinnaria larva, lateral view after 3 days of development. Regionalization of the digestive tube is evident from both morphology and ParaHox gene expression patterns: *PmLox* expression (green) marks the anterior part and *PmCdx* (magenta) the posterior part of the intestine. Length of larva = 300 μ m. (G) Fluorescence immunostaining with an antibody against acetylated tubulin (magenta) which reveals the distribution of cilia in the 8-day old bipinnaria larva; oral view. Length of larva = 400 μ m. Abbreviations: ac, anterior coelom; an, anus; cb, ciliary band; in, intestine, mo, mouth; es, esophagus; st, stomach. Adapted from Arnone Byrne and Martinez (2015).

Due to the absence of micromere cells, sea star larva does not form a skeleton and it is completely transparent for the lack of pigment cells. Similarly to sea urchin, sea star have an apical concentration of serotonergic neurons (Byrne et al. 2007) that coordinate the action of the cilia for the swim and the feeding in the water column.

Fig. 1.4. Sea star development. (A, B)

Early cleavage stages, animal pole towards the top. As in sea urchins, vegetal blastomeres give rise to endomesoderm (yellow and red), while the animal blastomeres become ectoderm (blue). Cleavage is equal in sea stars, as typical of most echinoderms, and micromeres are not formed. (C) Blastula, lateral view. A thickening at the vegetal pole, the vegetal plate, is noticeable. Unlike sea urchins, no mesoderm has ingressed before gastrulation starts. (D) Mid-gastrula, mesenchyme cells (red) migrate from the top of the archenteron. (E) Lateral view of an early bipinnaria larva; oral surface is to the right. The archenteron curves towards the

1.1.7 Sea star endomesoderm specification

Most of the studies aimed to reveal the mechanisms undergo specification of endomesoderm territories in sea star embryos are based on the comparison of the *Patiria miniata* gene interactions with specific subregions of the well known *Strongylocentrotus purpuratus* endomesoderm GRN. Studies performed in 2003 (Hinman et al. 2003) revealed an extraordinarily conserved subcircuit of five regulatory genes involved in positive feedback loops required upstream of initial endomesoderm specification in both sea urchin and sea star embryos. *krox* (ortholog of the sea urchin *blimp1b*), *bra*, *otx*, *gatae* and *foxa* sea star spatial expression is very similar to the patterns produced by their orthologs in *S. purpuratus*. The most remarkable homology is the presence of the identical three gene loop that set up a positive feedback loop between *krox* and *otxa* genes that later activate *gatae*. As in sea urchin, the sea star *gatae* is an essential endodermal driver required for the activation of *foxA* and *bra* genes. The function of *foxA* is to prevent both itself and *gatae* from being expressed in the central part of the vegetal plate fated to become mesoderm; once this repression has occurred in the late blastula period, *gatae* can have no effect on mesodermal specification, whereas in sea urchin it can assist in driving mesodermal specification. In sea star *gatae* can be used strictly as an endoderm specifier and an excluder of mesodermal state. The major difference between sea urchin and sea star endomesoderm GRN is found in the micromere specification. While in sea urchin the micromere lineage has a function in skeletogenic differentiation and pigment cells formation, the sea star does not form micromeres during embryogenesis and totally lacks a skeleton and the larva is completely transparent. Sea urchin skeletogenic cells transmit the Delta signal to the future mesodermal cells that will express *gcm* gene; since sea star lacks this cell lineage the mesoderm specification is accomplished in a different

way, as explained in (Hinman and Davidson 2007). The sea star *delta* gene is expressed within the mesodermal progenitors of the central vegetal plate and scattered in the cells of the ectoderm at the blastula stage; the first phase of delta-notch signaling that in sea urchin occurs at around 10h post fertilization and leads to the activation of *gcm*, is not observed in sea star where *gcm* is not expressed at all within the vegetal plate, displaying a spotty pattern of ectodermal expression. *Delta* is transcribed in sea star mesoderm only as in the second phase of *delta* expression of sea urchin mesoderm at around 21 h. At this stage the future endodermal cells surround and are adjacent to the delta-expressing vegetal plate mesodermal cells and the cis-regulatory target of Delta-Notch signaling is *gatae* gene, essential for endoderm specification. This shows up that while in the sea urchin Delta-Notch signaling is required for pigment cell and blastocoelar cell specification through the activation of the mesodermal *gatac* gene by *gatae*, in sea star it prevents mesoderm specification and the cells that receive the Delta-Notch signal become endoderm, the ones do not receive it become mesoderm. In sea star *gatae*, that is expressed in the archenteron barrel (future hindgut and midgut), operates an “exclusion function” repressing in the endodermal domain the mesodermal gene *gatac*. Experiments of interference of *gatae* expression by morpholino cause an upregulation of *gatac* in the archenteron barrel. This is in contrast with what has been observed in sea urchin where *gatae* expression provides a positive input into *gatac* expression. While in sea urchin the boundary between mesoderm and endodermal territories depends on the delta-notch responsiveness of *gcm* in the future mesodermal cells, in the sea star the endoderm cells are prevented from expressing mesoderm genes by foxa repression of *gatae*. The last strong difference relies on the role of *tbr* gene in the two GRNs. In the sea urchin *tbr* regulatory gene is a controller of the skeletogenic specification and is expressed exclusively in the skeletogenic micromere lineage. In contrast the sea

star *tbr* is expressed across the entire vegetal plate, i.e. the prospective mesoderm and endoderm and is necessary for the expression of endomesodermal and endodermal regulatory genes, such as *bra*, *gatae* and *foxa*, as a consequence of its positive input on *delta*. The *tbr* gene is required for the archenteron formation in the sea star embryos and is expressed under the control of *otx* and *gatae* endodermal regulators.

1.2. The biological process: gut development

1.2.1 Gastrulation: the first step for gut development

*"It is not birth, marriage, or death, but
gastrulation, which is truly the most
important time in your life."*

Lewis Wolpert (1986)

The term “gastrulation” was coined for the first time by Haeckel in his *Gastraea Theory* (Haeckel 1874) . During his studies on sponges he defined a gastrula as “an elongated rounded body, which contain an inner cavity with an external opening” (Haeckel 1872). The original concept of gastrulation referred to the infolding of surface cells of the blastula to form the archenteron, the precursor structure of the digestive tube, linking development to digestion for many years. A more recent interpretation of this process describes it as the key event of animal development during which movements of cells of a single-layered blastula reorganize the embryo in a multi layered gastrula with the out layer, the ectoderm, giving rise to the future skin and nervous tissues, the inner layer, the endoderm, giving rise to the skeleton and organs, in particular, the gut, and the mesoderm, between the endoderm and the ectoderm, giving rise to the skeleto-muscular system, connective tissues, the blood and internal organs such as the kidney and the heart (Sperber 1995). Depending on whether the animals possess mesoderm or not they are grouped as triploblasts or diploblasts, respectively. Gastrulation therefore comprises two elements: the formation of a multilayered organism and the

formation of a digestive system. A variety of cellular mechanisms exists in the different phyla of animals that lead to the formation of the archenteron during the gastrulation process.

Invagination is the mechanism of bending of an epithelial sheet of cells to form a pocket or cavity. In some cases, such as in some echinoderms (Logan and McClay 1997), the initial invagination is followed by an **involution**, as cells initially outside the lip of the invagination roll around it and move inside. Invagination occurs during gastrulation of amphibians, echinoderms, *Drosophila*, ascidians and crustaceans. **Delamination** is the mass separation of an entire layer from a preexisting layer. **Epiboly** is the movement of epithelial sheets which spread as a unit rather than individually. Epiboly is found in yolk-rich embryos and examples of this mechanism are found in the amphibian *Xenopus* and the zebrafish. **Ingression** is the migration of individual cells from the surface layers into the interior of the embryo. The ingression of the primary mesenchyme cells in echinoderm, the ingression of a large area of superficial presumptive endoderm and mesoderm from the epiblast through the primitive streak of the amniote are examples.

Gastrulation in the sea urchin (McClay, D. R., Gross, J. M., Range, R., Peterson, R. E., & Bradham, C. 2004) represents the archetypal model of deuterostome morphogenesis that is modified by chordates as an adaptive mechanism to accommodate huge amount of yolk, and/or production of extraembryonic membranes. The first evidence of gastrulation movement is represented by the epithelial-mesenchymal transition of the primary mesenchyme cells, PMCs, that leave the monolayer of cells that constitute the blastula and migrate into the blastocoel. Several hours after **ingression**, in the center of the vegetal plate a group of mesenchyme cells, the secondary mesenchyme cells (SMCs), initiate an inward fold (**invagination**). The gut then elongates by three different kinds of movements:

convergent-extension movement of epithelial cells, so that the diameter of the archenteron narrows and it elongates; **involution** movements of endodermal cells from regions lateral to the vegetal plate; stretching of the length of the archenteron by deployment of contractile filopodia of SMCs. Finally, SMCs at its tip make contact with the substrate at the animal pole and pull the archenteron to its final length. SMCs lineage subdivide in four different cell types: pigment cells, coelomic cells, muscle and blastocoel cells. The ones that become pigment cell **delaminate** from the cluster of SMCs throughout gastrulation, cross the blastocoel, invade the ectoderm and distribute throughout the aboral ectoderm. The remaining SMCs reside at the tip of the future archenteron until gastrulation is completed. In the hours leading up to these morphogenetic events there are no cell movements other than the cell divisions that characterize the cleavage stages and the expansion of the blastocoel cavity.

1.2.2 Gut development in Bilateria

The formation of a digestive system conferred to the animals the capacity to perform extracellular digestion with the development of a specialized structure. This marked the transition from Protista to Metazoa, since the multicellularity is accompanied with specific role in digestion of the cells in the inner part of the organism. The development of the gut is also the first process to establish an anterior and posterior axis in the body plan by forming an entry and an exit of the organism. In all animals the development of a functional digestive system is a multistage process starting with the formation of a primitive gut during the gastrulation movements that lead to the formation of a hollow tube, the archenteron. Within Bilateria, three principal forms of the gut exist: a sac-shaped gut with one opening to the exterior, observed in Platyhelminthes and

Gnathostomulida, a one-way gut with two openings (mouth and anus) in Deuterostomia, Nematelminthes/Ecdysozoa, Syndermata and in Spiralia, a presence of a digestive syncytium instead of an epithelially bordered intestine in Acoela. During development a one-way gut can develop in three different ways. In addition to the blastopore, a second opening of the archenteron can break through and develop either as the anus (protostomy) or as mouth (deuterostomy). The blastopore can also elongates, its margin can approach and fuse in the centre leaving an opening either end (amphystomy). The one-way gut has some advantages over the sac-shaped one. In a sac-shaped gut the passage of food can be guided in a limited way and food can pass the same region more than once. The one-way gut allows an unidirectional passage of food allowing a regionalization with a more specialized digestion. One-way guts are composed of three parts. The central part is of endodermal origin, while the ectoderm forms the anterior and posterior regions. The anterior ectodermal part is often specialized for food uptake and possess a strongly developed musculature, named “pharynx”. The central endodermal part is specialized for digestion and nutrient uptake. In most Deuterostomes during gastrulation endodermal cells are internalized by invagination through the blastopore of sea urchin and frog embryos or the primitive streak of the avian and mammalian epiblast. The first endodermal cells to exit either the blastopore or the primitive streak will contribute to the anterior definitive endoderm, whereas the later moving cells will contribute to the posterior endoderm. Besides the fact the endodermal tube does not show any morphological differentiation, several and overlapping transcription factors and signaling molecules can be detected along the whole archenteron. The interactions among these elements lead to the establishment of boundaries of gene expression subdividing the gut into distinct domains that are the precursors of digestive organs. The primitive gut is divided into foregut, midgut and hindgut, each of which will

give rise to specialized regions, such as the thyroid, lungs, liver and pancreas.

1.2.3 ParaHox gene family

Homeobox genes (Hox genes) are genes known for their conserved role in anterior-posterior patterning of animal embryos, providing a specific positional information along the main body axis of the animal. They are characterized by the presence of a variable DNA sequence, the homeobox, that, in the final protein, encodes a helix-loop-helix-turn-helix domain, called homeodomain (P. W. Holland 2001). The homeodomain mediates the interaction of the protein and a sequence-specific DNA binding that directs the expression of other genes. The homeobox gene of animal genomes can be divided in 11 classes, where each class is a set of genes that share additional motif or that fell together in an evolutionary tree (P. W. H. Holland 2013). The largest class of animal homeobox genes is represented by the ANTP that has been found only in the Metazoa and that contains most of the genes responsible of body patterning. The ANTP class contains several families of Hox genes, but also ParaHox genes, NK genes and various others. ParaHox family have aroused interest because they share a similar homeodomain sequence with Hox genes. ParaHox family consists of three genes, *Gsx*, *Xlox* and *Cdx*, whose cluster organization has been described for the first time in amphioxus (Brooke, Garcia-Fernàndez, and Holland 1998). ParaHox cluster is considered an evolutionary sister of the Hox cluster and both arose from a duplication of an ancestral “ProtoHox” gene cluster (Brooke, Garcia-Fernàndez, and Holland 1998). When this duplication occurred during animal evolution has been always source of debate. In 2012, a study on Hox and ParaHox loci in the sponge *Amphimedon queenslandica* (Mendivil Ramos, Barker, and Ferrier 2012) has suggested that Hox and Parahox cluster evolved before the origin of the Porifera, considered the earliest branching

animal lineage. However, this hypothesis is still partially unbelieved. ParaHox cluster exhibits the phenomenon of spatial and temporal collinearity. Spatial collinearity represents the order of the genes along the cluster that reflects the order of their expression domain along the antero-posterior axis during embryogenesis. Temporal collinearity is when the order of the genes along the cluster corresponds to the order in which the genes start to be expressed. However with the increase of the number of species from which ParaHox genes have been isolated, the phenomenon of collinearity and the cluster organization has not been considered a peculiarity of this gene family. In fact, in some species ParaHox are not organized in cluster and even when they are do not always show collinearity. However, temporal collinearity rather than spatial collinearity has a strong correlation with the genomic organization of the ParaHox genes (Garstang and Ferrier 2013). When the ParaHox cluster is broken, temporal collinearity is absent. This can be observed comparing the ParaHox organization in the echinoderms *S. purpuratus* and *Patiria miniata*. In *P. miniata* ParaHox are organized in cluster (Rossella Annunziata, Martinez, and Arnone 2013) and the order of expression matches that of the cluster in the chordates *Xenopus* (Illes, Winterbottom, and Isaacs 2009) and cephalochordate amphioxus (Osborne et al. 2009) with *Cdx* expressed first, followed by *Xlox* and finally *Gsx*. In *S. purpuratus*, where the cluster is broken, the first gene to be activated is *SpGsx*, followed by *SpLox* and finally *SpCdx* (Maria I. Arnone et al. 2006). The hemichordate *Ptychodera flava*, instead, possesses an intact ParaHox cluster that does not have complete spatial collinearity, but does have temporal collinearity (Ikuta et al. 2013). These examples make closer the idea to the fact that intact cluster coincides with temporal collinearity. The genomic organization of the ParaHox and their spatial expression in the sea urchin, the sea star and other bilaterian embryos is shown in Fig. 1.5.

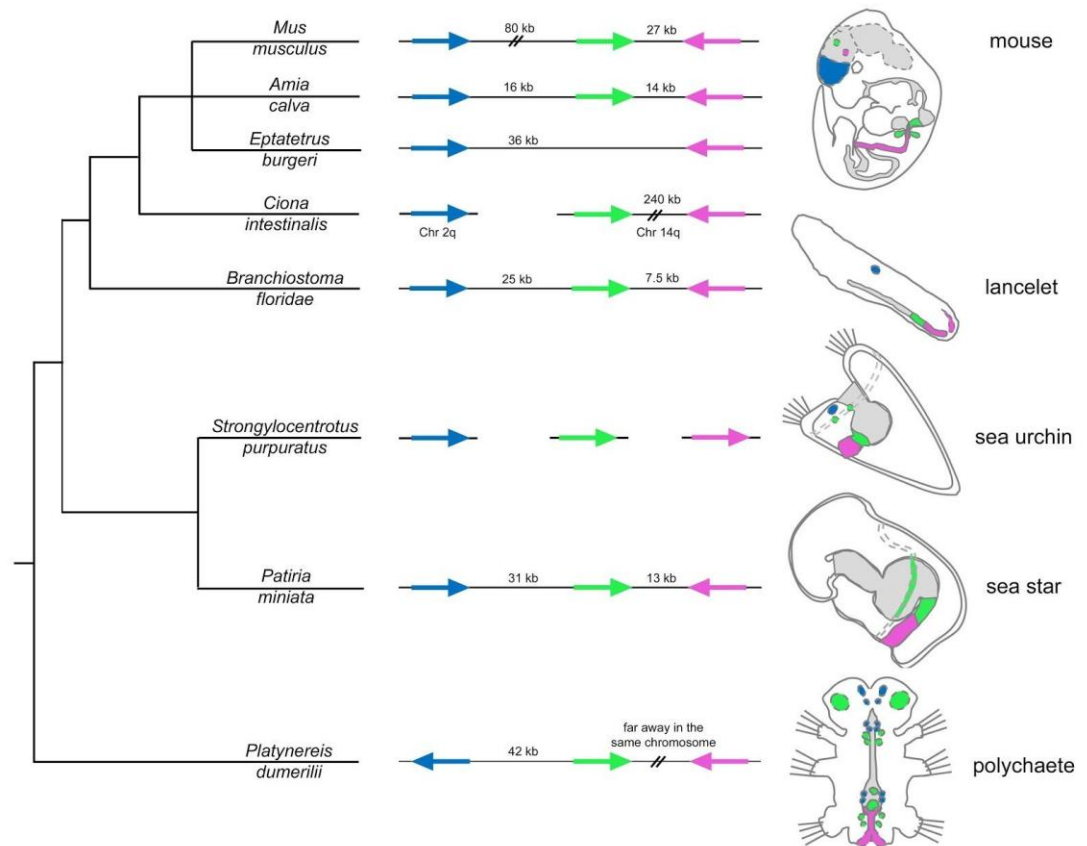


Fig. 1.5. Evolution of ParaHox gene cluster and relative expression domains in bilaterian animals. Schematic representation of ParaHox genomic organization and expression patterns in several bilateral animals: the mouse *Mus musculus*, the bowfin fish *Amia calva*, the hagfish *Eptatretus burgeri*, the lancelet *Branchiostoma floridae*, the sea urchin *Strongylocentrotus purpuratus*, the sea star *Patiria miniata*, the polychaete *Platynereis dumerilii*. Arrows indicate ParaHox genes and their orientation in the genome; a continuous line below arrows indicates an intact cluster. The cartoons on the right side of the panel schematize the domains of expression of ParaHox genes in representatives of some of the bilaterian groups. Mouse, amphioxus, sea urchin and sea star embryos are in lateral view; the polychaete embryo is in frontal view. Nervous system domains are depicted with dashed lines. Endodermal structures are in grey. Gsx expression is shown in blue, Xlox in green and Cdx in magenta. kb, kilobases; Chr, chromosome. Double-parallel lines indicate long genomic distance. Adapted from Annunziata, Martinez and Arnone (2013).

In contrast to the Hox genes that have a role in anterior-posterior patterning of ectoderm in most bilateria (Peter W.H. Holland 1996), ParaHox genes are mostly involved in CNS and endoderm (gut) patterning with Gsx being the anterior-most, Xlox the ‘middle’ gene and Cdx the posterior-most expressed ParaHox gene. Gsx is

expressed in bilaterian nervous system. The mice *Gsh1* and *Gsh2* paralogs are active in the developing brain. The amphioxus *AmphiGsx* is expressed in the neural tube and then in the cerebral vesicle. In the sea urchin embryo *SpGsx* is detected in a small ectodermal domain. In the mollusk *Gibbula varia* and in the worm *P. dumerilii* the expression is observed in the CNS and the gut. *Xlox* is lost from all insect genome; in vertebrates it is expressed in both the developing gut and CNS; in amphioxus in the gut and two cells of the neural tube; in the mollusk *Gibbula* in the middle part of the digestive tract and in some neuroectodermal cells. *Cdx* (or *caudal* in insect) has three mouse paralogs, *Cdx1*, *Cdx2*, *Cdx4* are expressed in the posterior part of the gut and in some areas of the CNS, as observed in most vertebrates. The amphioxus ortholog is also expressed in the posterior gut and in the developing neural tube. Urochordate express *Cdx* in cells of the neural plate and the posterior gut. In polychaete *Cdx* is expressed both in the gut and in the area of the CNS. The mollusk *Gibbula* expresses *Cdx* in the posterior end of the digestive tract (Samadi and Steiner 2010).

1.2.4 Parahox and gut shape in sea urchin and sea star embryos

Most sea urchin and sea star are indirect developer and pass through a bilaterally symmetrical and feeding pelagic larva, called pluteus for sea urchin and bipinnaria for sea star. The pluteus larval digestive system is tripartite and composed by muscular esophagus, a large spherical stomach and a short tubular intestine. The esophagus is divided in two regions: a narrow and ciliated zone close to the mouth and a bulbous distal half of the esophagus with less cilia and surrounded by muscle fibers. A cardiac sphincter separates the esophagus and the stomach; it is a constriction made from a myoepithelium with a “hourglass-like” shape. The stomach is made of a columnar epithelium that includes two cell types: cell-type I

are distributed throughout the organ, form the luminal surface and contain several microvilli; cell-type II are restricted to the anterior portion of the stomach, do not have cilia and contain residual algal cells in different stages of digestion. Based on their morphology, type I stomach cells are involved in secretory functions while type II are for phagocytosis and digestion of algal cells. A pyloric sphincter separates the stomach and the intestine. It is composed of type I stomach cells that contain non-striated myofilaments. The intestine is made up of squamous epithelium and the intestinal cells contain vesicles and a single cilium. The intestine terminates with the anal sphincter that is provided with intracellular basal filaments. Although the structure of the bipinnaria digestive system is less studied, it looks very similar to the pluteus one with the only exception that the stomach and the intestine are separated by a simple bending without any pyloric sphincter. The establishment of the distinct domains of the larval gut is due to the interactions of signalling molecules and transcription factors that can be detected along the digestive tract since the first stages of gut development. At the end of gastrulation when the gut is still a straight tube stomach specific markers are already expressed in the future midgut cells, such as *Macrophage mannose receptor ManrCIA* and *Chaperonin precursor ChP* (R. Annunziata and Arnone 2014) and *Endo16* (Cole et al. 2009); the muscle specific terminal differentiation gene *Myosin heavy chain MHC* (Andrikou et al. 2013) is already expressed in the cells that will form the cardiac and anal sphincters and the *Carboxypeptidase 2L Cpa2L* is expressed in few cells posterior to where the cardiac sphincter will form. However while the foregut and midgut domains are molecularly defined from late gastrula on and undergo mainly morphological changes, the hindgut domain undergoes cell specification throughout the late gastrula and prism stage. Among the transcription factors expressed during gut development, *Xlox* and *Cdx* have been demonstrated to play a central role in intestine development in sea urchin and sea star and in other

several animals.

The first description of Xlox and Cdx temporal and spatial expression pattern in *S. purpuratus* has been provided in 2006 (Maria I. Arnone et al. 2006) corroborated by a more detailed analysis a few years later (Cole et al. 2009). Xlox and Cdx are expressed during sea urchin embryogenesis in partially overlapping domains of the growing archenteron that in the late stages will give rise to a tripartite gut. From 72-96 hpf (pluteus stage) Xlox is expressed around the midgut/hindgut sphincter region, whereas Cdx marks a region posterior to the Xlox domain in the hindgut. The Cdx domain fades anteriorly where it still overlaps with the Xlox domain. These patterns resemble the endodermal expression of Xlox and Cdx in mouse's and other bilaterians' gut suggesting that they are key components of the regulatory network mediating the regionalization of gut in all these animals. Functional analysis have been performed knocking down Xlox with injection of gene specific morpholino antisense oligonucleotide in *S. purpuratus* fertilized eggs. In absence of Xlox protein, the pyloric sphincter fails to form and Cdx expression drastically disappears with the consequence of Xlox transcripts accumulation in the hindgut (Cole et al. 2009) (Fig 1.6). The absence of Cdx expression suggests that the transcription factor Xlox is involved in Cdx activation, whereas Xlox expansion is the result of the absence of Cdx that restrict Xlox expression to the midgut-hindgut boundary region. In this way Xlox is repressed in the intestinal cells and a subdivision between stomach and intestine is formed. In a more recent work (R. Annunziata and Arnone 2014) has been demonstrated that the mutual regulation between these two transcription factors is a clear example of indirect positive-feedback loop acting in a GRN. Wnt10 is the ligand involved in the signaling between Xlox and Cdx. It is active in most posterior cells of the gut and starts its activation few hours later the activation of Cdx expression, suggesting a positive input of Cdx in Wnt10 activation (also confirmed by the absence of Wnt10

transcripts in Cdx knocked down larvae). From the moment Wnt10 is expressed, Xlox transcripts become undetectable in the posterior cells of the intestine and when the gut is completely elongated all the intestinal cells are depleted from Xlox transcripts. To better resolve the gene expression analysis during gut formation, the expression of three endodermal transcription factors has been also analyzed. *Hox11/13b* and *Bra* are expressed in the very posterior cells of the gut throughout gastrulation and then are confined in the pluteus anal cells. *Brn1/2/4* is expressed in the foregut and in a few ectodermal cells. In the Xlox and Cdx positive cells also *Hox11/13b* and *Bra* are expressed suggesting that all these four genes define a regulatory state exclusive to the most posterior part of the late gastrula archenteron. When *Hox11/13b*, *Bra* and *FoxA* are knocked down, Cdx transcripts are undetectable in the intestinal cells, where Xlox transcripts accumulate, demonstrating that the three endodermally transcription factors are all required for Cdx activation together with Xlox and that Cdx has a repressive function on Xlox transcripts. In addition to the morphological effect, digestive functions are inhibited in the absence of Xlox and the expression of three stomach differentiation genes, *ChP*, *ManrC1A* and *Endo-16* is severely affected. This demonstrates that Xlox acts upstream of a cascade of regulatory events responsible for the differentiation of the larval stomach. Embryos perturbed with Cdx antisense oligonucleotide morpholino present a phenotypic alteration very similar to the one observed in SpLox knocked down conditions: the gut has a normal size but it misses the pyloric sphincter conditions (Fig. 1.6). Moreover the absence of Cdx proteins causes an ectopic expression of SpLox in the intestinal cells and a strong reduction of Wnt10 and Cdx transcripts.

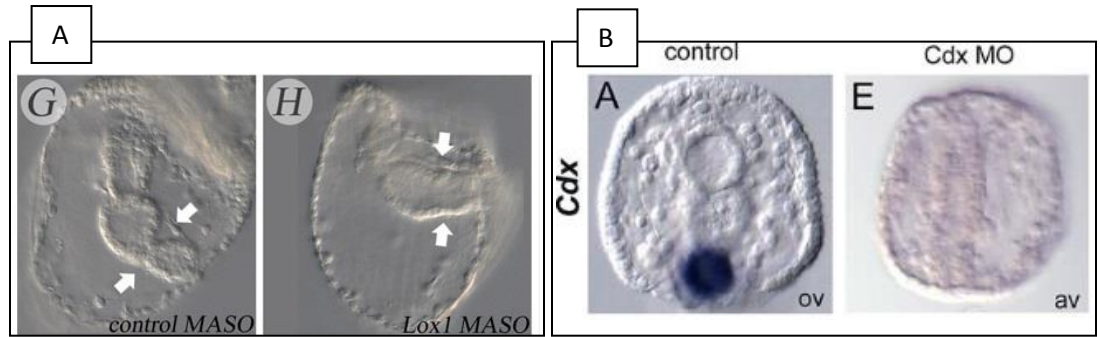


Fig. 1.6 Morphological phenotype caused by Xlox and Cdx protein depletion. Panel A: (G) Control embryos develop a tripartite gut, with a well-developed posterior constriction (white arrows). (H) Embryos perturbed with Lox-MASO develop into larvae with slightly smaller guts that lack the constriction marking the position where the posterior sphincter will form in normal embryos. Panel B: A Pluteus larvae with a tripartite gut show Cdx mRNA localization in the posterior cells of the endoderm determined by *in situ* hybridization. E Pluteus embryo perturbed with MASO against Sp-Cdx shows the absence of the pyloric sphincter between midgut and hindgut and no accumulation of Sp-Cdx transcripts. Adapted from Cole et al., 2009 and Annunziata and Arnone, 2014.

Only recently, ParaHox genes have been characterized in another non-chordate Deuterostome, the sea star *Patiria miniata* (Annunziata, Arnone and Martinez 2013). Xlox and Cdx spatial expression along the antero-posterior axis of the starfish larval gut resembles that one observed in sea urchin, with Cdx always expressed in a more posterior domain with respect to Xlox. In fact, in the 3-day sea star larva, Xlox transcripts are localized in the anterior part of the hindgut and Cdx is expressed in the posterior part extending until the blastopore. In the 4-day bipinnaria larva, the two genes extend their expression domains with Cdx occupying most of the hindgut and Xlox localizing in the boundary between midgut and hindgut. Since, except a partial overlap of expression at larval stages, no sign of overlapping between the expression domains of the two transcription factors has

been detected during gastrula stage, when both genes start to be expressed, it cannot be hypothesized any direct interaction between the two genes at the early stages of gut differentiation, unlike sea urchin. The comparison between sea star and sea urchin *Xlox* and *Cdx* genes during gut shaping from a straight tube to a tripartite structure is recapitulated in Fig. 1.6 bis.

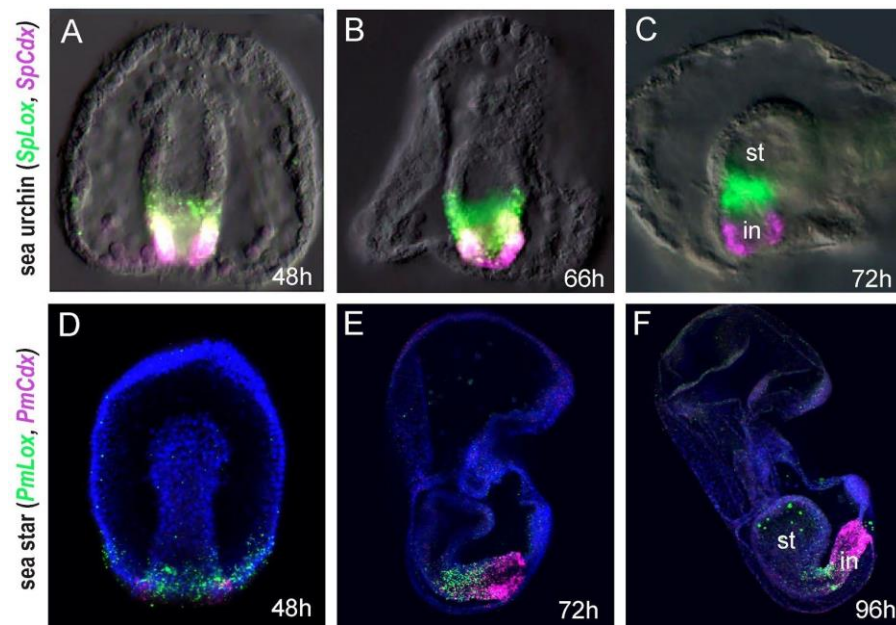


Fig. 1.6 bis. Progression of *Xlox* and *Cdx* expression during gut formation in sea urchins and sea stars. Double in situ of *SpXlox* and *PmXlox* (green) and *SpCdx* and *PmCdx* (magenta) expression domains in sea urchin (A-C) and sea star (D-F) embryos and larvae. In A and B, sea urchin gastrula and prism are shown in frontal view. In C, an early sea urchin larva is depicted in lateral view. In D, a sea star gastrula is shown in frontal view. In E and F, sea star larvae are shown in lateral view. Sea urchin images, shown as DIC photographs with the fluorescent gene expression patterns overlaid, are adapted from Cole *et al* (2009). Sea star images, shown as full projection of confocal z-series coupled with nuclei staining (blue), are adapted from Annunziata, Arnone and Martinez (2013). Developmental stages are provided in each panel (h, hour

1.3. Aim of the thesis

Since years, the sea urchin has been representing an excellent model system for developmental and evolutionary studies, due to the relative simplicity of its embryogenesis, the amenability to physical manipulation for the study of gene expression, and the possibility to apply advanced high-throughput technologies such as RNA-Seq, ChIP-Seq or ATAC-Seq. This led, in recent years, to extensive knowledge of the sea urchin endomesoderm GRN. However, something is still missing in the study of the GRN controlling the gut patterning process. This thesis work aims to acquire further knowledge on the process of gut specification in the sea urchin embryo and to compare it with the sea star embryo, focusing on the role that Xlox and Cdx transcription factors have in this process in both the echinoderm species. To this aim, a combination of -omics approaches for studying gene transcriptional regulation has been adopted to partially reconstruct the sea urchin gut GRN downstream of Sp-Lox and Sp-Cdx. In parallel, a similar approach has been applied to the sea star embryo for a comparative study aiming to reveal the differences accumulated during the evolution of both lineages. A differential RNA-Seq is generated for homologous developmental stages of sea urchin and sea star embryos after Xlox and Cdx protein depletion through injection of antisense oligonucleotide morpholinos. The genes that change their expression in the altered conditions are considered putative targets of Xlox and Cdx proteins. The integration of the sea urchin RNA-Seq data with the sea urchin ATAC-Seq, that provides information on the chromatin states of the interesting genes, allows a reconstruction of the putative gene interactions occurring at a specific developmental stage and territory of the sea urchin embryo. Functional analysis experiments with morpholino microinjection followed by qPCR and ChIP-PCR experiments have been adopted to validate some of the nodes of the reconstructed

sea urchin network. The final aim of the work is to verify the revealed sea urchin gene interactions in the sea star embryos and to establish the degree of conservation of the posterior gut GRN.

CHAPTER 2

MATERIALS AND METHODS

2.1 Animal handling and culture of sea urchin and starfish embryos

Adults *S. purpuratus* and *P. miniata* have been obtained from Patrick Leahy (Kerchoff Marine Laboratory, California Institute of Technology, Pasadena, CA, USA), housed in circulating seawater aquaria in the Stazione Zoologica Anton Dohrn of Naples and kept in large tanks of seawater at 15-16 °C. Sea urchins were fed with algae and starfishes with mussels. All the glassware and plastic used for animals and embryo cultures were preserved from any detergent and washed only with deionised H₂O, to avoid the presence of phosphates which disturb the normal development of the embryos. There is no external morphological difference between male and female sea urchins and starfishes. The sex can be determined only after gamete shedding has begun. For sea urchins, spawning was induced using three different methods: vigorous shaking, injection of 0.5 M potassium chloride; induction of gamete spawning by shaking is preferred because survival of the animals is good and only the amount of gametes needed is obtained. The sea urchin eggs were collected placing the female upside down in a beaker glass filled with millipore filtered sea water (MFSW), and were let to settle by gravity. To preserve the eggs, the temperature of the seawater was kept below 10°C placing the beaker on ice water. Then, the eggs were washed with seawater once and passed through a nitex screening of 60 µm to remove coelomic fluid (known to interfere

with the fertilization process), broken spines, and body surface debris. The starfish gametes were obtained by punching a 4mm diameter hole in the tough skin of the animal, on one side of the arm (every arm can be used twice, but it is good to go around the animal clockwise from the madreporite and use each arm only once, until all arms are used). If the animal is a female, yellow/orange ovaries will be close to the surface; in a male the gonads are white. For both male and female a piece of gonad was taken with curved tweezers; the ovary was put into calcium free artificial seawater (cfASW) in a small beaker where it was shredded with two tweezers into small pieces; oocytes and follicle cells were allowed to flow out of the ovary for 2-3 minutes and when most oocytes were in suspension and follicle cells were detached from the eggs, the cfASW was replaced by regular ASW. Oocytes were matured in 10 μ M 1-methyl-adenin MFSW for around one hour until the germinal vesicle (GV) had broken down. Immature oocytes could be maintained in MFSW on ice for at least 10 h prior to maturation and fertilization. For both sea urchins and starfishes the sperm was collected concentrated (dry sperm) and kept on ice until used for fertilization. A suitable amount of eggs were fertilized in 30 ml of seawater. To activate the sperm, it has to be diluted in sea water: about 2 μ l of dry sperm are diluted 1/1000 in MFSW to fertilize the eggs reducing the risk of polyspermy. Fertilization was monitored by the elevation of the vitelline membrane.

After fertilization, the embryos were washed twice in sea water to remove the excess of sperm. The embryos were cultured at 15 °C in MFSW diluted 9:1 with deionized H₂O. Antibiotics, penicillin and streptomycin, at a final concentration of 20 U/ml and 50 μ g/ml respectively, were added to prevent bacterial growth.

2.2 Microinjection procedure

Dejellied sea urchin or starfish eggs were fixed to protamine sulphate (PS) coated plastic Petri dishes and injected using a glass micropipette. The main difference in the microinjection procedure between sea urchin and starfish is the following: while sea urchin eggs are dejellied and attached to the PS-coated dish before fertilization, starfish eggs are fertilized prior dejellying, let developing for around 20 minutes at 15°C, and finally transferred to the PS-coated dish for microinjection. Details of the protocol are given below.

2.2.1 Preparation of materials

Protamine plate preparation: 60 mm plastic Petri-dish lids (Falcon) were filled for 1 minute with a 1% protamine sulfate solution (in dH₂O). Following protamine coating, dishes were washed thoroughly with distilled water to remove unadhered protamine sulfate solution, and air-dried. The protamine sulfate solution was kept in the refrigerator and reused several times. Before rowing eggs, a 1-inch scratch was made in the center of the dish, using a broken Pasteur pipette or razor blade, and then the dish was rinsed in clean filtered seawater.

Microinjection needle preparation: needles for microinjection were prepared from 1.0 mm outside diameter, 0.75 mm inside diameter, borosilicate glass supplied by Sutter Instrument Co. Novato, CA (No. B100-75-10). Fine-tipped microinjection needles were pulled on a Sutter P-97 micropipette puller (P=300; H=560; Pu=140; V=80; T=200) and, just prior to injection, were touched against the scratch in the microinjection dish to break open the tip to a diameter of ~0.4-0.9 µm.

Preparation of glass pipettes for egg transfer: glass Pasteur pipettes were drawn out in a Bunsen flame and broken off at the end. The internal diameter of a “rowing” pipette should be roughly the same as the egg diameter to warranty optimal rowing

of eggs. Due to the differences in egg diameters (80 μm for *S. purpuratus*; 175 μm for *P. miniata*) different pipettes have been prepared.

Preparation of solutions for microinjection: all solutions to be microinjected have been filtered through 0.2 μm filters and centrifuged for 15 minutes in a microfuge.

Sea urchin egg preparation: once the eggs have settled under gravity, they were washed twice through 550 μm Nitex filter to remove adhering matter, then dejellied by swirling in pH 5 MFSW (50 ml MFSW + 175 μl 1M citric acid) for less than one minute in a Petri dish until the egg membranes touch one another. The eggs were washed by transferring to a new Petri dish containing MFSW using a Pasteur pipette. The eggs were allowed to settle again and finally transferred as above to a Petri dish coated with 1% agarose and containing MFSW.

S. purpuratus eggs, could be also dejellied by filtering them once or twice through a 66 μm Nitex filter directly in the agarose plate.

Starfish egg preparation: fertilized starfish eggs were incubated at 15°C for 25 minutes and then dejellied by swirling in pH 4-4.5 MFSW for 2-3 minutes; after that the eggs were filtered slowly back and forth through 200 μm Nitex for 2-3 more minutes and then dumped into a large volume of normal pH MFSW. Starfish dejellied zygotes need to be rowed immediately (within max 15 minutes) because they rapidly secrete new jelly and do not stick to the dish anymore.

2.2.2 Microinjection procedure

Dejellied eggs were placed in groups of hundreds in a line on a protamine sulfate-coated dish in 10 ml of 4°C MFSW containing penicillin (20 units/ml), streptomycin (50 $\mu\text{g/ml}$), and, only for sea urchin, 2mM para-aminobenzoic acid (PABA; PS-SW + PABA) using a mouth-controlled pulled Pasteur pipette. The injection plate was positioned at the top of the row of eggs and 2-3 drops of freshly diluted sperm suspension were added. The needle was quickly moved, with the

solution flowing, in and out of the egg. The procedure was repeated for the next egg in line until the entire plate was injected.

2.2.3 Injection of morpholinos

The MASOs against SpLox, SpCdx, PmLox and PmCdx were already available in the laboratory where I performed the PhD work. SpMeis morpholino has been newly designed. As a control experiment, a Standard Morpholino Control oligo end modified with 3'-Carboxyfluorescein (control-fluo MASO, Gene Tools) was injected in parallel at the same concentration as the corresponding experiments. In table 2.1, sequences, characteristics and references for each morpholino are summarized.

Morpholino oligos were resuspended in water to a concentration of 500 μ M for sea urchin and 2mM for starfish. A working solution of 100 μ M- 1 mM of morpholino oligos in 0.2 M KCl was injected into fertilized eggs (2 to 4 pl). In all experiments with anti Cdx morpholinos, as a negative control, embryos were injected with 100 μ M of the standard control morpholino, at equal or greater concentration, and compared side-by-side with uninjected and MASO embryos. The newly designed morpholinos were acquired from Gene Tools (Corvallis, OR).

2.3 RNA-Seq

2.3.1 Total RNA purification

To eliminate RNAase contaminations all the procedures were carried out in a dust free environment, using clean gloves and RNAase free plastic instruments. Embryos at the right developmental stage were collected in a tube and centrifuged at 2000 rpm for 5 minutes. The pellet of embryos was washed once in ASW, and

centrifuged again to remove all the water. Total RNA purification was carried out using RNAqueous- Micro Kit (Ambion), that allow to extract RNA from a small amount of embryos. About 600 perturbed sea urchin embryos and 50 perturbed sea star embryos were resuspended in the Lysis solution of RNAqueous- Micro Kit (Ambion) and homogenized with a 1 minute vortex step at maximum speed. One half volume of 100% ethanol was added to the lysate and the mix was vortexed briefly but thoroughly. The lysate/ethanol mix was loaded onto a Micro Filter Cartridge Assembly and centrifuged for 1 minute at maximum speed; the RNA bound to the filter was washed with the two washing solutions provided in the kit and then eluted in RNase free water. A DNase step was performed according to the manufacturer's instructions.

2.3.2 RNA quality check and sequencing

Integrity and quantification of RNA has been checked before the sequencing using the Agilent Bioanalyzer 2100 with the RNA 6000 Pico kit for total eukaryotic RNA. cDNA libraries have been prepared with 1 µg of starting total RNA and using the Illumina TruSeq RNA Sample Preparation Kit (Illumina), according to TruSeq protocol. Each library has been diluted to 2 nM and denatured; 8 pM of each library has been loaded onto cBot (Illumina) for cluster generation with cBot Paired End Cluster Generation Kit (Illumina) and sequenced using the Illumina HiSeq 1500 with 100 bp paired-end reads in triplicate, obtaining ~31-38 million reads for replicate. The sequencing service has been provided by the Laboratory of Molecular Medicine and Genomics (<http://www.labmedmolge.unisa.it>) at the University of Salerno, Italy. All computational analyses have been conducted on the high performance-computing cluster at Michigan State University.

2.3.3 RNA-Seq filtration and mapping

The bioinformatic analysis to assemble and annotate the transcriptomes and to identify the differentially expressed transcripts were performed by the post-doc of the lab, Dr. Elijah Lowe. The first step after the generation of an RNA-Seq dataset is to make it feasible to the analysis of the differential expressed genes. Since the RNA-Seq is based on fragmenting cDNA used to produce libraries that are sequenced and the read fragments are mapped onto a reference or assembled, the sequencing data need to be cleaned in order to avoid misassembly and consequently misleading results in downstream analysis. The fragments obtained by sequencing the sea urchin and the sea star samples have been filtered removing low quality reads, adaptors, over abundant or contaminated sequences of microbial and viral metagenome. To do that, softwares such as fastqc for visualization and trimmomatic, Tag Cleaner or fastx for trimming and filtering have been adopted. After filtration, *S. purpuratus* reads have been mapped to genome sequence (V3.1) and *P. miniata* reads to the genome sequence (V1.0) Scaffolds

2.4 Real Time Quantitative PCR

2.4.1 Reverse transcription

First-strand cDNA was synthesized in a 20 µl reaction from 1 µg of total RNA using the SuperScript VILO cDNA synthesis kit (Invitrogen). The synthesis of the cDNA was performed in the PCR machine, with the following programme: 25°C for 10min, 42°C for 60 min, 85°C for 5min. The cDNA was stored at -20 °C until use.

2.4.2 Quantitative PCR

Abundance of transcripts after morpholino microinjection has been monitored using real-time quantitative polymerase chain reaction (QPCR). Specific primer sets (Table 2.3) for each gene were designed using the Primer3 program (Rozen and Skaletsky, 2000) (<http://primer3.ut.ee/>). Primer sets were chosen to amplify products of 100–200 bp in length. Blast searches were used to ensure that primers were specific for each individual gene. Reactions were performed in duplicate or triplicate using the ViiA 7 REAL TIME PCR with SYBR Green chemistry (Applied Biosystems). All primer pairs were validated by QPCR against a positive (genomic DNA) and negative (water) control. Each 10 µl reaction contained 5 µl of SYBR Green reagent, 4 µl of forward and reverse primer mix (0,75 µM each) and 1 µl of cDNA (diluted to a concentration of 1 embryo/µl). Thermal cycling parameters were 95 °C for 15 s, 60 °C for 1 min, 40 cycles, followed by a denaturation step to verify the presence of a single product.

A QPCR experiment measures the number of cycles needed to attain a threshold concentration of QPCR product (Ct). The number of cycles needed for the standard to reach a specified Ct can be compared to the Ct for an unknown. A higher Ct for the unknown implies a lower initial concentration in the sample, and vice versa. The threshold value is chosen to fall within the exponential amplification phase, before limiting reagents become a factor in the efficiency of each cycle. For duplicate or triplicate samples, Ct is calculated as the average among the replicates. For sea urchin embryos, data for each gene were normalized against ubiquitin mRNA, which is known to be expressed at constant levels during the first 72 h of development (Nemer et al., 1991).

2.5 Whole Mount in Situ Hybridizations (WMISH)

Embryos fixing and storage

Embryos at the right developmental stage were collected by gentle centrifugation and fixed overnight at 4°C in the Fixing solution (4% formaldehyde, 0.1M MOPS pH 7, 0.5M NaCl). The embryos were washed five times in MOPS buffer (0.1M MOPS pH7, 0.5M NaCl, 0.1% Tween-20 in nuclease free water) and used immediately or stepped in 70% ethanol and stored at -20°C.

Riboprobessynthesis

Sp-Meis riboprobes have been newly cloned, amplifying four different fragments from the *S. purpuratus* genome that include both the coding and the non coding regions of the gene. Each reverse primer contains the Sp6 polymerase binding sequence at its 5' region to skip the cloning in a vector. The sequences of the four sets of primers used to perform the cloning PCR are listed in the table 2.2.

DIG and FLUO-labelled probe synthesis

For all the fragments both antisense- and sense-digoxigenin (DIG)-labelled RNA probes were obtained using a DIG-RNA labelling kit (Roche, Indianapolis, IN), following the manufacturer's instructions and using 500 ng of purified PCR product amplified (using as template the miniprep). Riboprobe synthesis reactions were conducted at 37 °C for 2 hours. DNase I RNase free was added (1U/μl), to remove the DNA template. The mix was incubated for another 20 minutes at 37 °C and the reaction was stopped by adding 0.5 M EDTA pH 8 (25mM). To remove the unincorporated nucleotides the RNA probes were purified using the Mini Quick Spin RNA Columns G-50 Sephadex (Roche), following manufacturer's instructions. For the synthesis of fluorescein (FLUO)-labelled RNA probes, the same kit was used but the Fluorescein-labelled dNTPs mix was used (Roche).

Probes were stored at -80 °C.

WMISH procedure

The fixed embryos/larvae were rehydrated by three washes in MOPS wash buffer, 15 minutes each. After, they were pre hybridized for 3 hours in the prehybridization buffer (containing 70% formamide, 100 mM MOPS pH 7, 500 mM NaCl, 0.1% Tween 20, 1 mg/ml BSA) at 50 °C. Hybridization was initiated with the exchange of hybridization buffer containing 0.1 ng/μl RNA probe(s), and was allowed to proceed for 1 week at 50°C. The volume of the hybridization was at least ten times more than the volume of the embryos used. To remove the probe not bound, the embryos were washed in the prehybridization buffer for 3 h at 50 °C replacing the buffer twice. After the post hybridization washes, the embryos were washed three times with MOPS buffer at room temperature. The embryos were incubated in MOPS buffer containing 10 mg/ml BSA (Blocking solution I) for 20 min at room temperature, followed by additional incubation in the MOPS buffer containing 10% sheep serum and 1 mg/ml BSA (Blocking solution II) for 30 min at 37 °C. DIG epitope detection was done in the MOPS buffer containing 1% sheep serum, 0.1 mg/ml BSA, and 0.5 U/ml Anti-DIG AP Fab fragments (Roche), overnight at 4°C. To remove antibody excess, the embryos/larvae were washed six times with MOPS buffer 1 h each at room temperature, with rocking. The detection of the antibody was carried out in alkaline conditions. First the embryos/larvae were washed twice with AP buffer (100 mM Tris-HCl pH 9.5, 50mM MgCl₂, 100 mM NaCl, and 1 mM Levamisole) for 30 minutes at room temperature. The staining reaction was done in the AP buffer containing 10% dimethyl formamide and NBT/BCIP until colour was developed. The reaction was stopped by dilution in MOPS buffer. For control experiments, the embryos/larvae were hybridized with the same labelling-sense-strand probes. The embryos were mounted and examined with DIC microscope.

2.6 Basic molecular biology procedures

2.6.1 PCR amplification

Polymerase chain reaction (PCR) is a method that allows logarithmic amplification of short DNA sequences within a longer double stranded DNA molecule. Each amplification reaction was conducted in a volume of 50 or 100 µl containing: 100 ng DNA template, 1X synthesis buffer; 0.2 mM dNTP mix, 50 pmol/µl of each primer, 1U/µl Taq DNA polymerase (Roche) and H₂O. The amplification cycles were conducted by means of Thermal cycler Perkin-Elmer-Cetus. After denaturation at 95 °C minutes, 30 amplification cycles were structured as follows: denaturation at 94 °C for 30 seconds, annealing at 55-65 °C for 30 s, extension at 72 °C for 0.5-2 minutes (considered 1 minute to synthesize 1 kb). An extension cycle was carried out at 72 °C for 10 minutes to complete all the strands. To purify the amplified DNA from the excess of Buffer and dNTPs, the Invitrogen PCR Purification kit was used according to the manufacturer's instructions.

2.6.2 DNA sequencing

The DNA sequences were obtained using the Automated Capillary Electrophoresis Sequencer 3730 DNA Analyzer (Applied Biosystems, Foster City, CA) by the Molecular Biology Service of the Stazione Zoologica "Anton Dohrn" in Naples.

2.6.2 DNA gel electrophoresis

To check the length of DNA from PCR amplification, 1 to 15 µl of DNA solution and Gel Loading Buffer 1X (Gel Loading Buffer (6X) 0.25% (w/v) Bromophenol Blue, 15% (v/v) Ficoll 400, 120 mM EDTA, 0.25% (w/v) Xylene Cyanol FF)

were run on an agarose gel (1 to 2%) in 0.5X TBE buffer and Ethidium Bromide final concentration of 0.5 µg/ml (TBE Buffer 1X, 89 mM Boric Acid, 2 mM EDTA pH 8.0 and 89 mM Tris).

2.7 Chromatin Immuno Precipitation procedures

2.7.1 Chromatin isolation of cross-linked cells

Approximately 10^5 48h sea urchin embryos have been collected by smooth centrifugation, washed with artificial seawater and cross-linked in 1% formaldehyde for 10 min at room temperature. The fixation reaction has been stopped adding 0.125 M glycine pH 8.0. The embryos have been then collected by smooth centrifugation and washed three times with cold 1X PBS. Afterwards, the embryos have been resuspended in lysis buffer containing 5 mM PIPES pH 8.0, 85 mM KCl, 0.5% NP-40, complete protease inhibitors (Roche Diagnostics) and kept on ice for 10 min. The lysate has been centrifuged to collect the pellet that has been lysed on ice for 10 min in 50 mM Tris pH 8.0, 10 mM EDTA, 1% SDS, protease inhibitors (Roche Diagnostics). The crude nuclear preparation has been then centrifuged and the nuclei resuspended in RIPA buffer containing 1X PBS, 1% NP-40, 0.5% sodium deoxycholate, 0.1 % SDS, protease inhibitors (Roche Diagnostics) for the chromatin sonication.

2.7.2 Chromatin shearing by sonication

Before sonication, the lysate has been centrifuged at maximum speed for 10 min at 4°C in order to pellet the debris. Sonication has been carried out with a Covaris Sonicator (S2) with the following settings: intensity 5 with 20% duty, cycles/burst 200 with 240 sec duration and sweeping mode frequency. To check the sonication

efficiency, RNA and protein have been removed from a 50 µl sheared chromatin aliquot by digestion with 1% SDS, 100 mM NaCl, 50 mg/mL RNase A for 30 min at 55°C and 200 mg/mL Proteinase K, for 1,5 h at 65°C respectively. DNA has been extracted by phenol-chloroform, precipitated and purified using DNA purification columns (QIAGEN). The DNA concentration in the shared chromatin has been determined with the use of photospectrometry (nanodrop) and 1 µg has been loaded on a 1.7% agarose gel to check the fragment sizes. The protein concentration has been measured with the Bradford assay. Finally the samples have been aliquoted as 200 µl in 1.5mL DNA low binding Eppendorf tubes (Eppendorf).

2.7.2 Immunoprecipitation

Depending on the protein concentration, samples have been aliquoted in a way that each tube contained a maximum amount of 300-500 mg of protein and approx. 20 mg of DNA. Chromatin has been then diluted in ChIP dilution buffer containing 1,1% Triton X-100, 1,2 mM EDTA, 16,7 mM tris pH 8.0, 167 mM NaCl, 0,01% SDS. To reduce unspecific binding in the immunoprecipitation, a pre-clearing has been performed with 30 µl of pre-blocked Protein A agarose beads (Roche) for each tube, incubated at 4°C for 1h. After, the chromatin has been centrifuged at 8000 rpm for 4 minute at 4°C and an aliquot of 50 µl has been saved for input fraction. After the pre-clearing, chromatin has been subjected to immunoprecipitation with 30 µl of anti Sp-Lox specific antibody, followed by the addition of 30 µl of beads and five washes in a buffer containing 100 mM Tris-HCl pH 8.0, 500 mM LiCl, 1% NP-40, 1% deoxycholate and once TE containing 10 mM Tris-HCl pH 8.0, 1 mM EDTA. After washes the bound DNA has been eluted by heating the beads twice to 65°C in elution buffer containing 0.1 M sodium hydrogen carbonate and 1% SDS. As above and after reverse-crosslinking, protein digestion and DNA isolation,

fragments have been purified with DNA purification columns (QIAGEN) and tested by qPCR.

2.8 Assay for Transposase-Accessible Chromatin(ATAC)

Assay for Transposase-Accessible Chromatin approach has been described for the first time by Buenrostro and colleagues in 2013 (ref.). It allows epigenomic analysis revealing the interplay between genomic locations of open chromatin, DNA-binding proteins, individual nucleosomes and chromatin compaction at nucleotide resolution, taking advantage of the high-throughput sequencing technology (ATAC-Seq). Using a simple two-step protocol with only 500–50,000 cells ATAC-Seq captures open chromatin sites revealing all the accessible genomic region for the binding of regulatory proteins. The simplicity of the protocol, compared to the multistep protocols of other epigenomic assays such as the DNase-seq and formaldehyde-assisted isolation of regulatory elements with sequencing (FAIRE-seq), and the necessity of a very low amount of starting material makes ATAC-Seq a powerful approach to study genome wide the chromatin states.

Transposition Reaction of sea urchin embryos

A total number of 400 wild type and SpLox perturbed late gastrula sea urchin embryos, and from 50 to 150 sea star embryos at different developmental stages have been centrifuged at 4°C for 5 min at 500 g in order to collect 50.000 cells. The supernatant has been removed and the embryo pellet washed (one or more times if necessary) with in ice cold 1X PBS. The pellet has been resuspended in 50 ul of lysis buffer (10 mM Tris-HCl, pH 7.4, 10 mM NaCl, 3 mM MgCl₂, 0.1% NP40) and pipet up and down to lyse the cells and obtain the nuclei. Few microliters of nuclear pellet have been used to count the number of nuclei with Hoechst fluorescent dye under the fluorescent microscope. The remaining cells have been

centrifuged at 500 g 10 min at 4°C. The lysis buffer has been removed and the nuclear pellet resuspend in 50 ul of Transposition Reaction and gently pipette up and down to resuspend nuclei. The Transposition Reaction mix has been made combining the following reagents:

25 µL 2x TD Buffer (Illumina Cat #FC-121- 1030)

2.5 µL Tn5 Transposes (Illumina Cat #FC-121- 1030)

22.5 µL Nuclease Free H₂O

The transposition reaction has been incubated 30 min at 37°C. Immediately following transposition, the transposed DNA has been purified using DNA purification columns (QIAGEN). The transposed DNA has been eluted in 10 µL Elution Buffer (10mM Tris buffer, pH 8.0). Purified DNA has been stored at -20°C until use.

PCR Amplification

Library generation

To amplify transposed DNA fragments, the following reagents have been combined in a PCR tube:

10 µL Transposed DNA

10 µL Nuclease Free H₂O

2.5 µL Nextera PCR Primer 1*

2.5 µL Nextera PCR Primer 2* [Barcode]

25 µL NEBNext High-Fidelity 2x PCR Master Mix (New England Labs Cat #M0541)

for a total volume of 50 µL

* Complete list of primers available in Supp. Table 1 Buenrostro *et al.* Nat. Methods 2013 (stock concentration of primers is 10uM)

The PCR reaction has been set with the following program:

- (1) 72°C, 5 min
- (2) 98°C, 30 sec
- (3) 98°C, 10 sec
- (4) 63°C, 30 sec
- (5) 72°C, 1 min
- (6) Repeat steps 3-5, 13x
- (7) Hold at 4°C

The amplified library has been purified using Qiagen PCR Cleanup Kit and eluted in 20 µL of Elution Buffer (10mM Tris Buffer, pH 8). The sea urchin library preparation has been performed at the CABD Institute of the Universidad Pablo de Olavide in Seville thanks to a collaboration with the Dr. Luis Gomez-Skarmeta.

Gel Electrophoresis

2-5 ul of the amplified library have been run on 2% Agarose gel in order to observe bands of different lengths corresponding to the different nucleosomes localization in the chromatin.

2.8 Primer and morpholino antisense oligonucleotides used

Table 2.1. Sequences of the morpholinos used in microinjection experiments

MASO	Sequence	Type	Reference
Sp-Lox	AGTACGCGGGATTGTTCCCTTCCAT	translation	Cole et al., 2009
Sp-Cdx	TAGCTTTTGGTTAAATACCTGTTT	splicing	unpublished
Sp-Meis	TCATCGTAACCCCTCTGTGCCATG	translation	unpublished
Pm-Lox	CCAGGGTCATCATGTTTCATGTTGGT	translation	unpublished
Pm-Cdx	TTGACCTGTAGTTGAAATATGAGAA	splicing	unpublished

Translation: MASO targeted against the translation initiation site

Splicing: MASO targeted against a splicing site

Table 2.2. Primers used to clone *Sp-Meis* in different regions of the gene

Gene	Primer Forward	Primer Reverse
Sp-Meis 1	TTCGACTCTGCGTGGTTGTA	TTTCACGATGCACTCCACAC
Sp-Meis 2	CGCTCAACCTCACATGAACC	ACATGTCGCTAGCTCGCACT
Sp-Meis 3	ATTACGGAACCTTGGACG	AATAAGGCAGTGTTTTGATTAGG
Sp-Meis 4	ACCCGACAATTTGCACACTC	ACCATCAGATGCCAACCAGA
Sp6 pol.	ATTAGGTGACACTATAG	

Sp6 pol.: sequence of the Sp6 polymerase binding site added to the 5'-end of each reverse primer

Table 2.3. Primers used in QPCR experiments

Gene	Primer Forward	Primer Reverse
Sp-FoxA	CCAACCGACTCCGTATCATC	CGTAGCTGCTCATGCTGTGT
Sp-GataE	CTGGCTCAAACGAGAAGGA	CCTCTTCCGAGTCTGAAATGC
Sp-Ets4	CTCCAGCCCAACTCCTACAG	GATGGAGCGAGAGAGCTTGT
Sp-Cdx	AAGGACAAGTATCGCGTCGT	CTTTCCGAGAGGCCAGAG
Sp-Hox11/13b	CACAGGCTCTCGACCTAACC	GGTGGATGAGGTGGTAGATGA
Sp-Lox	GTGCGACGGACTCCCTATAA	TTCAGACGCCATGGTGTAAA
Sp-Bra	CTTGTTCCGAAACCCTCACC	TTGCCAATAGCCACTGACATC
Sp-Nr1m3	GACGAGGCTTCTGGGATACA	CTCGCAGTGTCCTTCCTTCT
Sp-Meis	GTCAACCGAAACTTCTCCGG	TGCAATCTACGGGTACAGCA
Sp-Ubiq	CACAGGCAAGACCATCACAC	GAGAGAGTGCGACCATCCTC

Table 2.4. Primers used in ChIP-QPCR experiments

Gene	Primer Forward	Primer Reverse
Sp-Meis	GTCAACCGAAACTTCTCCGG	TGCAATCTACGGGTACAGCA
Sp-Interg	ATGGAGGGTGGCAAACATAG	GATTACATGGTTCGCCGTTT

CHAPTER 3

A genome wide comparison downstream of Xlox and Cdx in sea urchins and sea stars

3.1 Introduction: differential RNA-Seq approach

In the new genomic and transcriptomic era the advances of sequencing technologies are driving the study of animal development from an organismal to a transcriptomic level. This facilitates the ability to examine organism on a more genomic scale. The RNA-Seq approach uses deep-sequencing technologies for transcriptome profiling allowing the description of the complete set of transcripts in a cell and its quantity at a given development time point, in a defined tissue or territory of the embryo, and/or in a wild-type condition versus a treatment. RNA-seq has many advantages, the number of genes covered, the fact that no prior information is needed, the possibility of detecting splice variants and sequence variations (for example, SNPs) in the transcribed regions, and the number of downstream analyses that can be performed. RNA-Seq represents a powerful tool also for organisms without available genome, since the transcriptome can be assembled de novo or aligning the RNA-seq reads to a closely related species. It allows to produce a genome-scale transcription map that consists of both the transcriptional structure and/or level of expression for each gene (Wang, Gerstein, and Snyder 2009). Among the challenges of the RNA-Seq technology there is the

development of an efficient method to store, retrieve and process such large amounts of data for an unbiased interpretation of the data. This can be partially overcome with more targeted approaches such as tissue specific, or single-cell RNA-seq. The statistical power of an RNA-Seq experiment and so its reliability strongly depends on the number of biological replicas. In general, having a low number of replicates make it more difficult to identify a bad replicate, while having a higher number of replicates increase the statistical power and accounts for a bad replicate. For this reason in most of the cases three biological replicas are the minimum acceptable number. RNA-Seq approach allows different types of analysis: identification of TFs, analysis of gene pathway that groups genes according to the biological process, co-expression analysis that allows genes to be grouped by expression patterns. Moreover, very interesting and informative is the comparison of the transcriptome profile before and after perturbation experiments (differential RNA-Seq), that allows to identify differentially expressed gene involved in a specific biological process. RNA-Seq comparison among different organisms allows to verify the conservation of regulatory elements of the genome that have been preserved during evolution for their important functions in driving gene expression as well as changes in some gene sequences that define the origin of phenotypic features and their developmental programs.

In this chapter, I describe the analysis and the comparison of five differential RNA-Seq datasets obtained by various gene perturbations at different developmental stages of the sea urchin and the sea star embryos. The effects of perturbation have been reached by knocking down Xlox and Cdx proteins into sea urchin and sea star zygotes in order to identify the target genes of these proteins. The comparison of the RNA-Seq between the two species allows to verify the effects of the evolution in the genome of two close related species.

3.2 Results and discussion

3.2.1 *Choice of the sea urchin and the sea star developmental stages for the RNA-Seq*

In order to identify the genes that change their expression after Xlox and Cdx perturbation and that, consequently, could act downstream of these proteins in gut formation I have generated differential RNA-Seq for both sea urchin and sea star. To this aim morpholinos against Xlox and Cdx transcripts have been microinjected into sea urchin and sea star zygotes (see table 2.1 for sequences), the embryos have been cultured in FSW at 15°C until the desired stages of development and the RNAs have been extracted to generate a complete transcriptome from both the perturbed and the wild type embryos. As negative control, a standard control morpholino has been microinjected to verify that changes in gene expression are only a consequence of the absence of the functional protein and is not caused by the technique of microinjection. The sea urchin differential RNA-Seq has been performed at late gastrula (48 hpf) and pluteus of Sp-Lox knocked-down, wild type and negative control. One RNA-Seq replica for both the developmental stages was already available in the lab. I have generated the two missing replicas for 48 hpf, in order to have three biological replicas for this time point. The sea urchin differential RNA-Seq of Cdx perturbed, wild type and negative control embryos has been performed at prism stage (66hpf). For the sea star, embryos at late gastrula (66 hpf) and embryos at early bipinnaria larva (90 hpf) have been collected for differential RNA-Seq after Xlox and Cdx microinjection, respectively, and for their respective wild type and negative control embryos. *P. miniata* late gastrula and bipinnaria larva are homologous stages to those of *S. purpuratus*. For each RNA-Seq, three biological replicas and three technical replicas have been

performed. To understand the choice of these developmental stages we have to give a look to the gut morphology and *Xlox* and *Cdx* temporal expression in both the animals (see also Fig 1.5).

Sp-Lox expression starts at mid-gastrula stage (40 hpf) in few cells on one side of the blastopore, and as gastrulation proceeds it becomes expressed in all cells surrounding the blastopore and in the posterior most part of the endodermal tube. After the end of the gastrulation, at prism stage (66 hpf), the entire posterior endodermal tube expresses Sp-Lox gene and in the pluteus larva the expression is exclusively restricted in the pyloric sphincter. Sp-Cdx expression starts at late gastrula stage in cells surrounding the blastopore and continues in later stages up to the larval stage with high levels of expression in the hindgut region until the blastopore (Maria I. Arnone et al. 2006) (Cole et al. 2009).

Pm-Lox expression starts from 24 hpf when a slow accumulation of messages is detectable. From 48 hpf, Pm-Lox levels of expression strongly increase reaching a maximum at 72 hpf. After this stage and until six day larva transcript levels decrease continuously but some expression of the gene is still detectable. The Pm-Cdx mRNA is not present in eggs. After the first 20 hours of embryonic development the levels of Pm-Cdx transcripts increase progressively reaching maximum accumulation at 24 hpf. After this time the levels start to drop, and they do so for the next 24 hours, until 48 hpf. During the next three days, until day five post fertilization, a second wave of expression of Pm-Cdx is detectable. The expression levels increase again reaching a maximum (at five days post fertilization (dpf) that is less than half of what was detected at 24 hpf. Subsequently, up until day six, the levels of Pm-Cdx mRNA seem to decrease although the transcription of the gene is still ongoing (Rossella Annunziata, Martinez, and Arnone 2013).

Analyzing the Q-PCR expression trends, the time corresponding to the midpoint of *Xlox* and *Cdx* expression, i.e. when the number of transcripts reached half of their

maximum accumulation, has been chosen for the generation of differential RNA-Seq in both sea urchin and sea star.

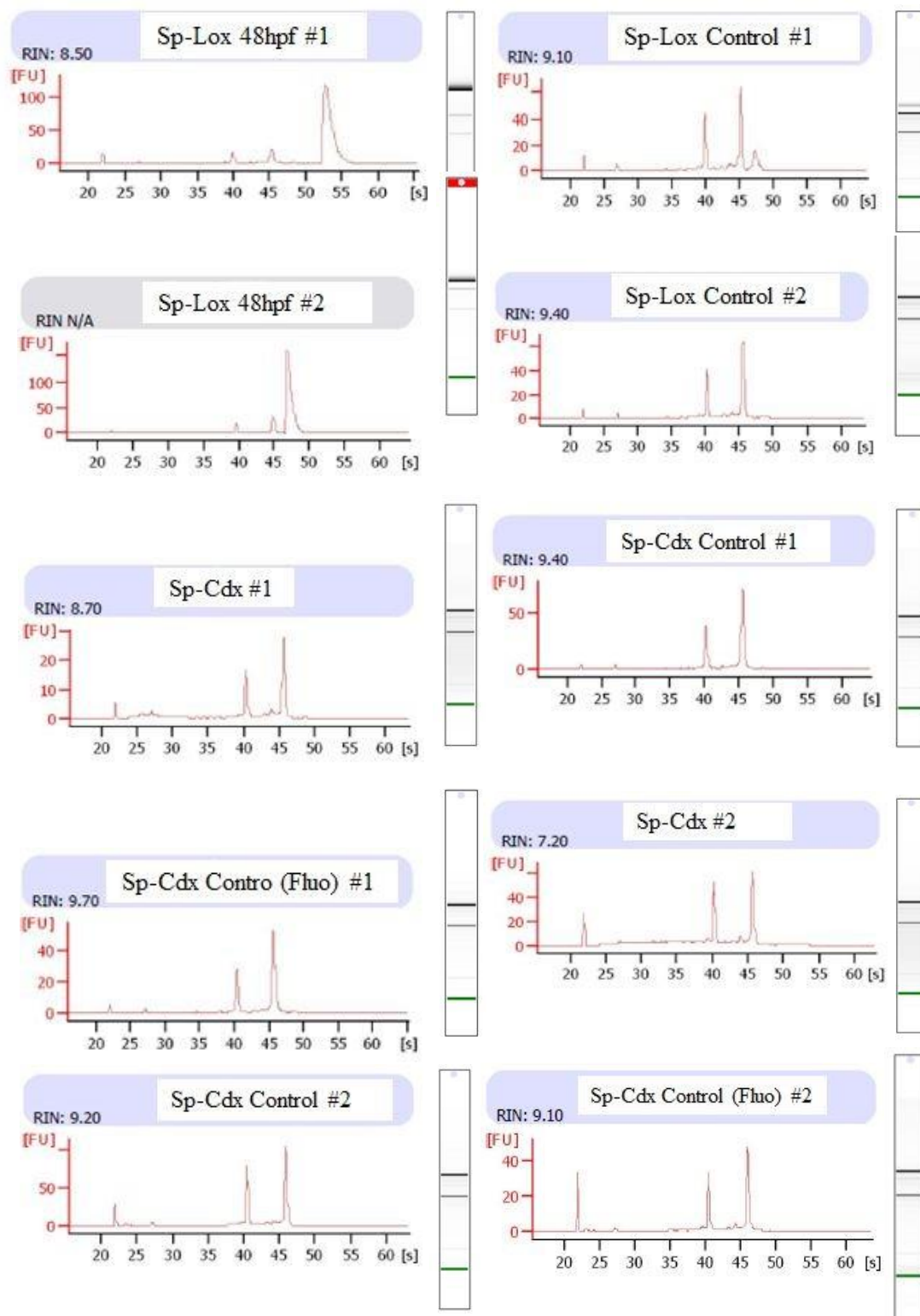
Looking at the morphology of the embryos, the sea urchin and the sea star late gastrula represents the stage when the gastrulation is close to the end and the gut almost reached its maximum extension but is still undifferentiated without any constrictions. However the genes required for the differentiation of foregut, midgut and hindgut are already detectable along the whole archenteron. The sea urchin prism and the sea star early bipinnaria larva, instead, corresponds to the moment when the gut has a tripartite shape, but the formation of the sphincters that separate the three compartments is not complete (this is completely true for the sea urchin, while the sea star never forms a pyloric sphincter). The pluteus larva is an extra point we chose for the sea urchin in which the gut is now completely formed with its cardiac and pyloric sphincter visible. Choosing these developmental stages we are looking at the time of sea urchin and sea star development during which Xlox and Cdx proteins are already active in the gut gene network and are still on for some hours later. Moreover we are considering the developmental stages that allow us to analyze the gene network at the beginning of the gut specification and in the late moments of its regionalization.

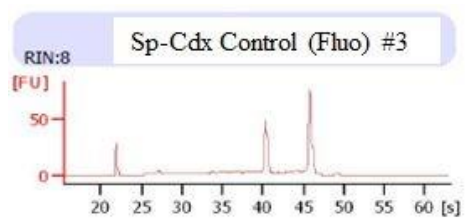
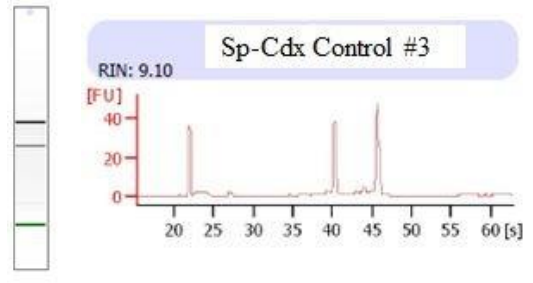
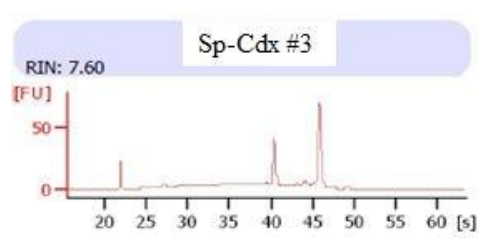
3.2.2 RNA-Sequencing (RNA-Seq)

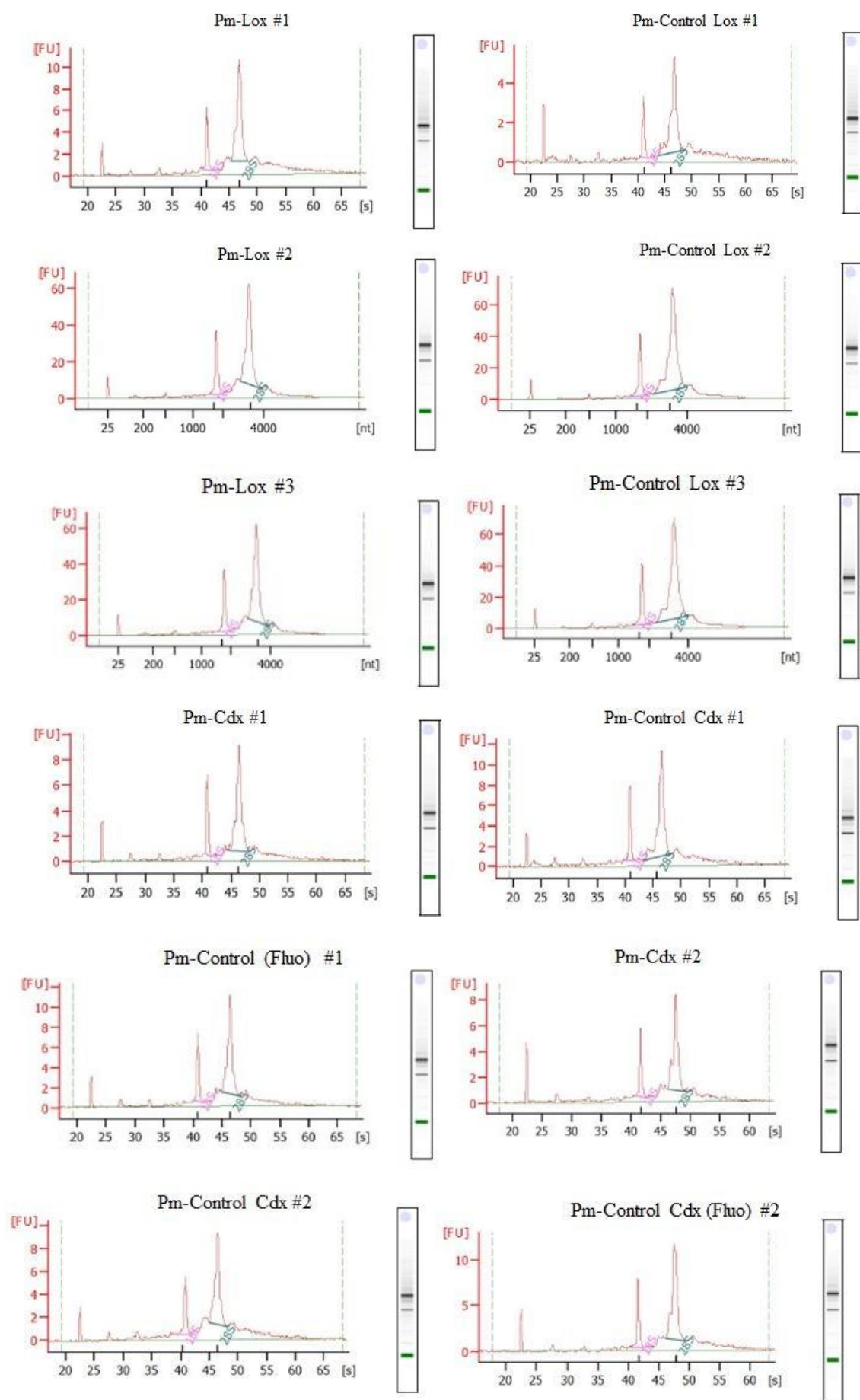
RNA quality check

A good quality RNA has a high RNA integrity number ($RIN \geq 7$) that is calculated by the ratio of the two ribosomal bands in the electrophoretic trace of the total RNA or based on the height of the two peaks in the electropherogram. Bands and peaks correspond to the 18s and 28s ribosomal subunits. The RNA samples generated for differential RNA-Seq which have shown an acceptable quality were

selected for sequencing and are shown in Fig. 3.1.







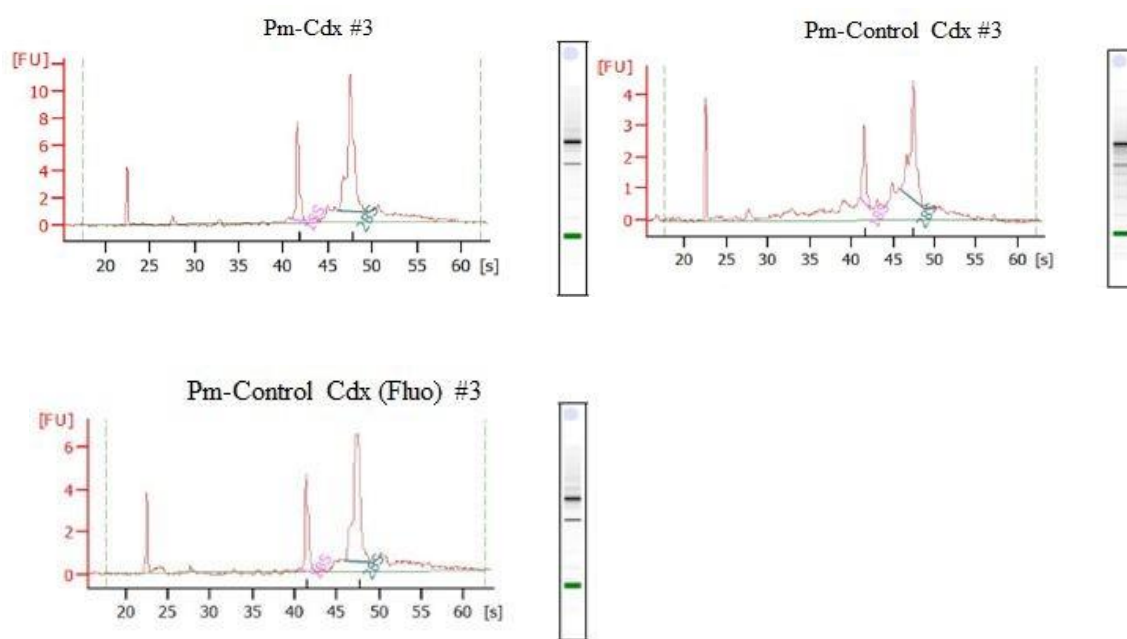


Fig. 3.1. Bioanalyzer results of the total RNA samples generated for differential RNA-Seq. RNA samples were extracted and purified as described in section 2.3.1 from 3 independent batches of embryos (3 biological replicas) as described in section 2.2.

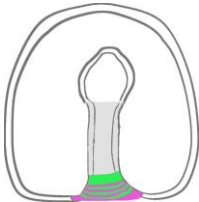
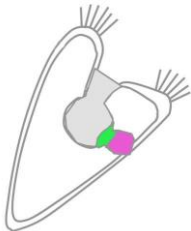
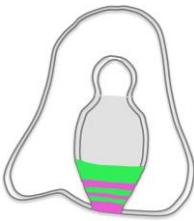

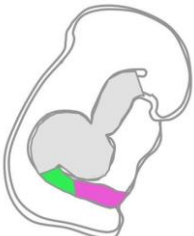
Sequencing, filtering and generation of differential RNA-Seq data sets

Sea urchin and sea star cDNA libraries have been prepared with 1 µg of starting total RNA and using the Illumina TruSeq RNA Sample Preparation Kit (Illumina), according to TruSeq protocol. The cDNA samples have been sequenced using the Illumina HiSeq 1500 with 100 bp paired-end reads in triplicate, obtaining ~31-38 million reads for replicate. The sequencing service has been provided by the Laboratory of Molecular Medicine and Genomics (<http://www.labmedmolge.unisa.it>) at the University of Salerno, Italy. Reads have been first trimmed using Trimmomatic (v0.33) to efficiently remove erroneous reads while maximizing the information within the reads. *S. purpuratus* reads have been mapped to Genome sequence (V3.1) and *P. miniata* reads have been mapped to the genome sequence (V1.0) Scaffolds. After mapping, reads have been sorted using SamTools (v1.2)

and counts have been extracted using HTSeq (v0.6.1). The differential expressed transcripts have been identified using DESeq2 with a threshold of $\log_2fc > \pm 0.5$ and adjusted p-value of < 0.05 . The bioinformatics analyses to assemble and annotate the transcriptome and to identify the differentially expressed transcripts has been performed by the postdoc of the lab., Dr. Elijah Lowe.

The complete raw data of the sea urchin and sea star RNA-Seq are reported in Appendix I. The generated RNA-Seq datasets are summarized in table 3.1. As notable, the number of biological replicas used to generate Sp-Lox MASO data set at 72hpf is only one compared to the three biological replicas used to generate all the other sea urchin and sea star datasets. The explanation of this lays in the fact that at the beginning of this work the sea urchin pluteus stage (72hpf) was not meant to be included in the analysis of the posterior gut GRN. However, the SpLox MASO 72h dataset, previously generated in the lab, has been used for a comparative analysis with the new generated sea urchin RNA-Seq. datasets. A less number of biological replicas available for the SpLox MASO 72h dataset makes it less reliable for the analysis of the genes that change their expression in the perturbed condition at pluteus stage.

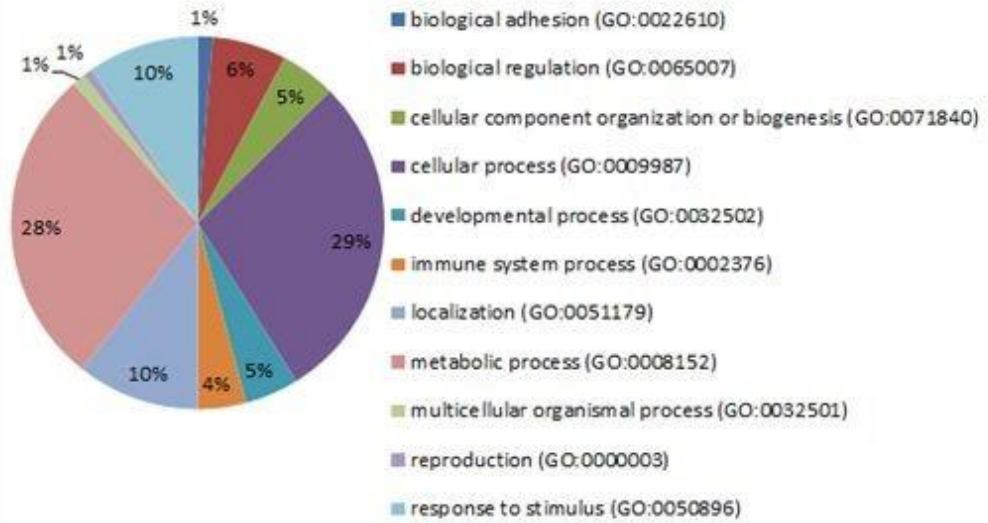
Table 3.1. Data sets obtained by differential RNA-Seq. Total numbers of differentially expressed (DE) genes are reported per each data-set along with information about species, stage and perturbation used.

data set name	species	developmental stage (time) with Xlox and Cdx gut expression	perturbation used	number of biological replicas	total number of DE genes
SpLox48h	<i>S. purpuratus</i>		SpLox MASO injection	3	294
SpLox72h	<i>S. purpuratus</i>		SpLox MASO injection	1 with 3 technical replicas	2384
SpCdx66h	<i>S. purpuratus</i>		SpCdx MASO injection	3	723
PmLox48h	<i>P. miniata</i>		PmLox MASO injection	3	108
PmCdx90h	<i>P. miniata</i>		PmCdx MASO injection	3	693

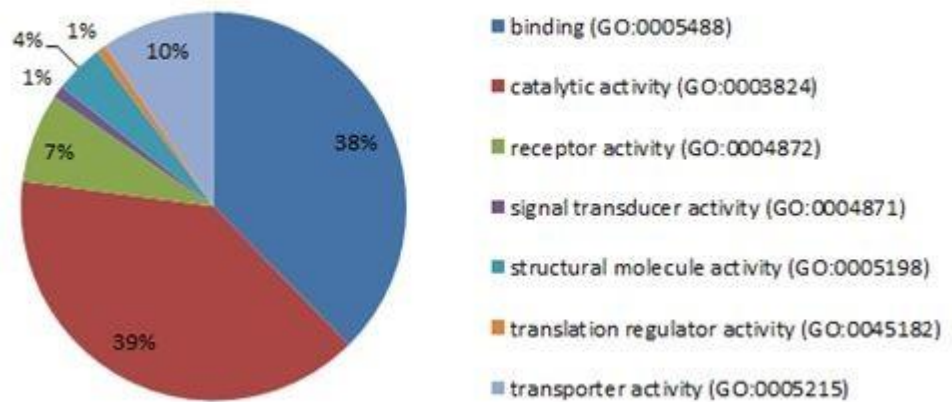
3.2.3 Gene Ontology annotation analysis for *S. purpuratus* and *P. miniata* differential RNA-Seq data sets

For all the RNA-Seq datasets I have performed an enrichment analysis to identify the class of proteins encoded by genes misexpressed after Xlox and Cdx knockdown and to verify the biological process they participate to and their molecular function. To do that, IDs of *S. purpuratus* and *P. miniata* differential RNA-Seq have been uploaded into PANTHER (Protein ANalysis THrough Evolutionary Relationships) software <http://www.pantherdb.org/> to classify proteins (and their genes) according to their family, subfamily, molecular function, biological process and pathway. PANTHER contains the complete sets of protein coding genes for 104 organisms, obtained from the definitive [Reference Proteomes project](#) at UniProt, however the *P. miniata* proteins dataset is still missing. For this reason, the *P. miniata* IDs have been converted thank to the collaboration of the post doc of the lab into *S. purpuratus* IDs based on the protein homology and used for the classification. For each classification, a pie chart has been produced to sum up the data. However, since the quality of the genome annotation is not the same for both species, it occurred that there was not always a correspondence 1:1 of *P. miniata* and *S. purpuratus* genes. However, this should not have affected so deeply the analysis of the data. Starting from the SpLox 48hpf MO RNA-Seq (see Fig. 3.2), a high number of affected protein is involved in the binding to the DNA or to proteins, in the catalytic activity mediated by kinase or methyltransferase for the activation/repression of proteins and modification of chromatin organization, respectively, and in the enzyme activities linked to G-coupled receptors or nuclear hormone receptors.

SpLox 48hpf MO RNA-Seq biological process



SpLox 48hpf MO RNA-Seq molecular function



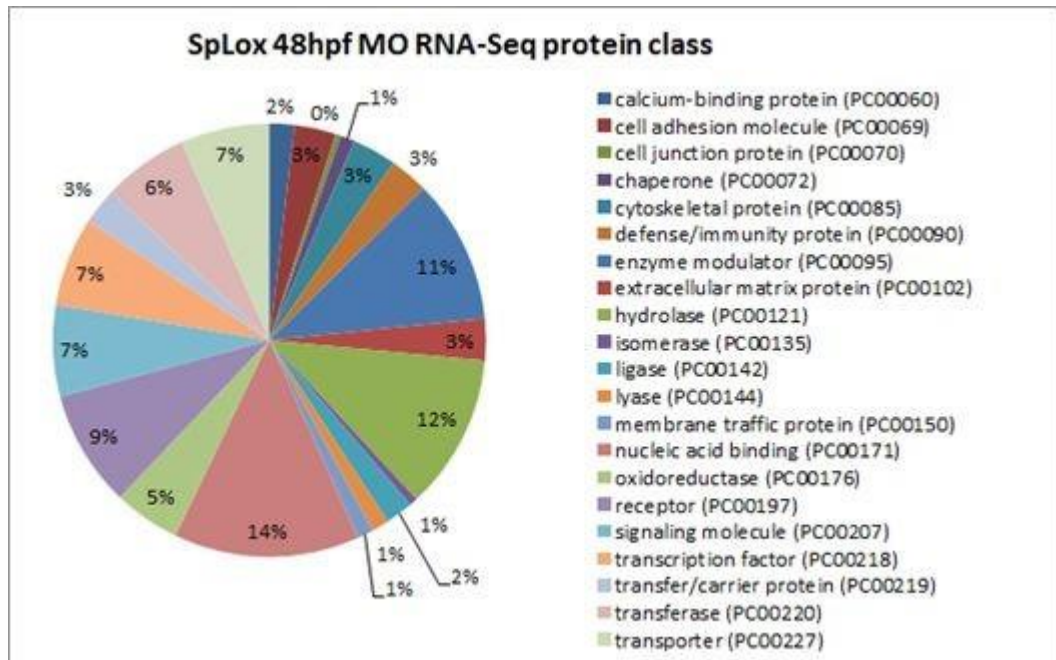


Fig. 3.2. Gene ontology analysis for DE genes downstream of SpLox at 48 hpf.

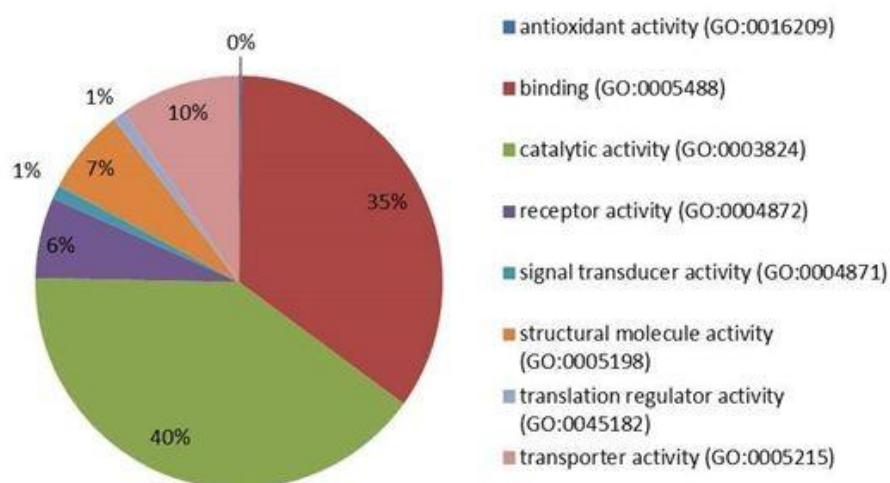
The injection of the Sp-Lox morpholino has perturbed some biological processes in the late gastrula sea urchin embryos such as metabolic process that includes protein, lipid and carbohydrates metabolism, cellular process of the signal transduction mechanism, cell-cell communication, cell cycle, protein localization and transport, and developmental processes linked to mesoderm and ectoderm formation, as well as nervous system development. This last process may be due to the absence of Lox protein in few cells of the ectoderm where it is normally localized. As expected after microinjection, there is an high alteration of the process of response to stress. Among the proteins misexpressed in the Sp-Lox knocked-down embryos there are several transcription factors among which transcription cofactors, zinc-finger transcription factor, homeobox transcription factors, basic helix loop helix transcription factors.

The enrichment analysis of the Sp-Lox 72 hpf MO RNA-Seq (Fig.3.3) revealed a situation very similar to that one observed at late gastrula with the binding and the

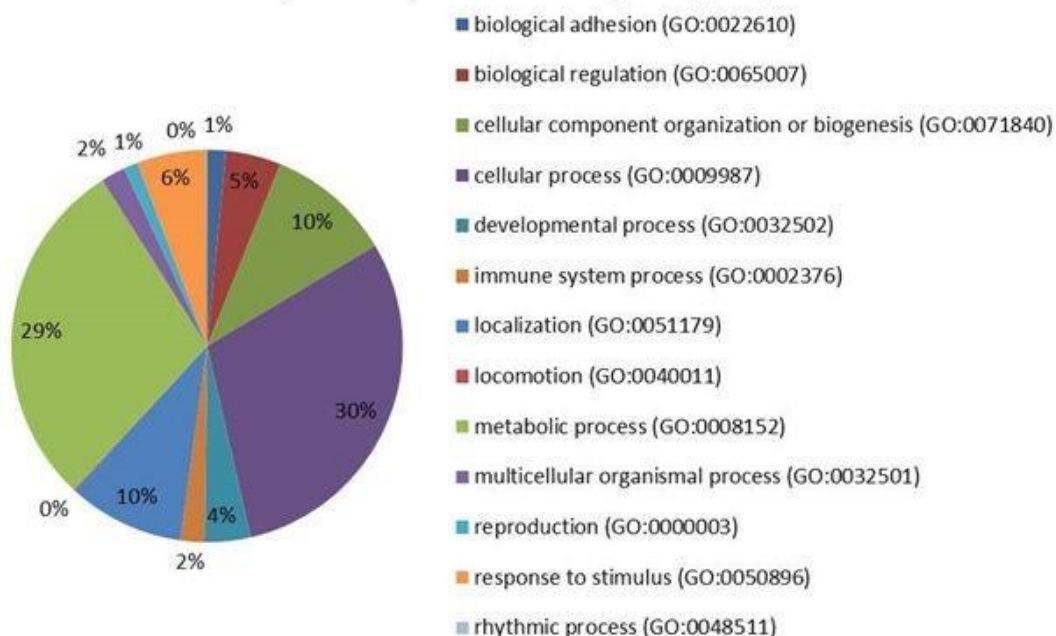
catalytic activities being the most affected molecular functions, and the metabolic and cellular processes the most affected biological process. However the number of misexpressed genes is much higher, with the number of affected transcription factors that increases from

32 to 96; this increase has a consequence on the nucleic acid binding, with 344 misexpressed proteins involved in this process, compared to the 67 observed at 48 hpf.

SpLox 72hpf MO RNA-Seq molecular function



SpLox 72hpf MO RNA-Seq biological process



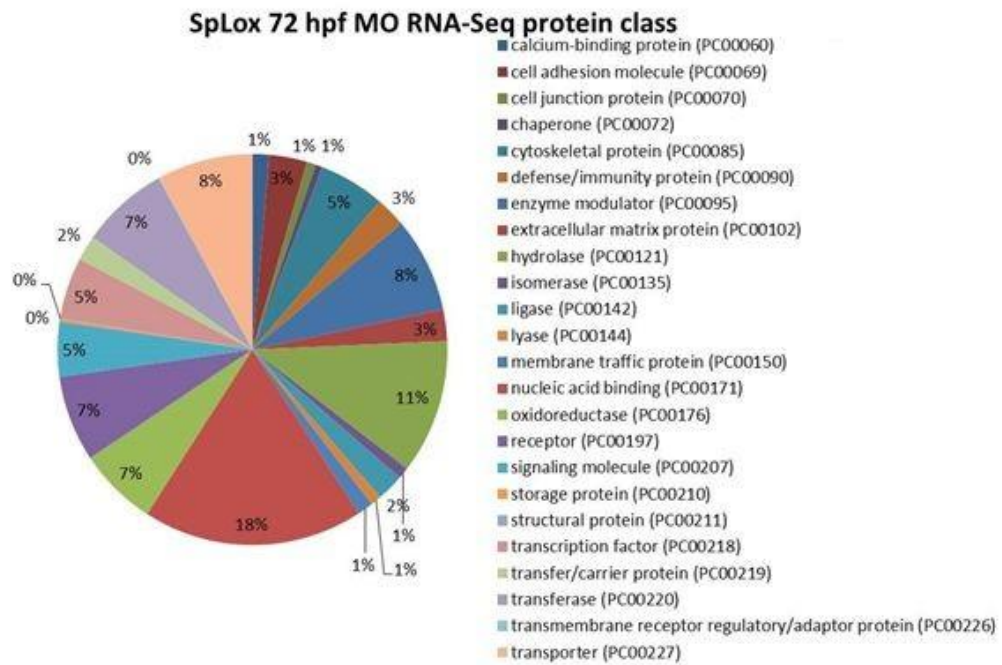
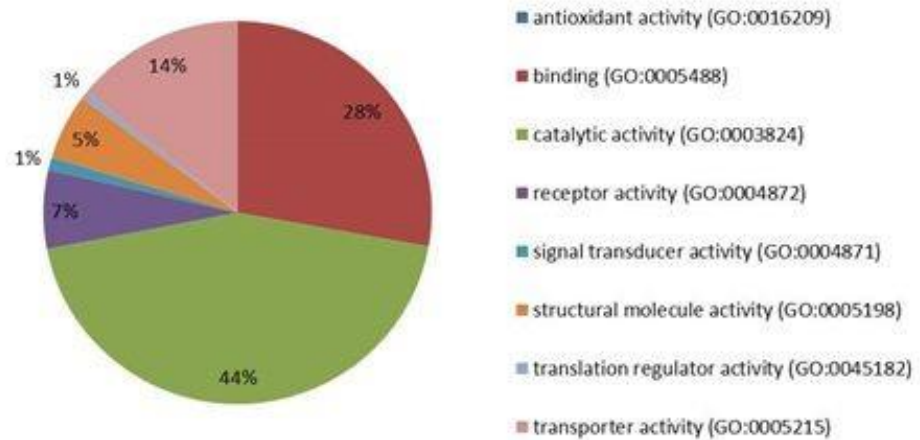


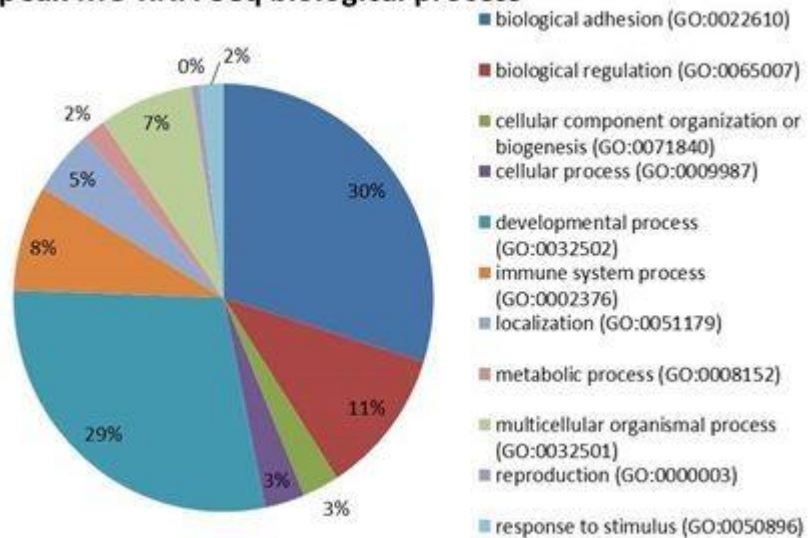
Fig. 3.3. Gene ontology analysis for DE genes downstream of SpLox at 72 hpf.

The enrichment analysis of the Sp-Cdx MO RNA-Seq (Fig.3.4) also verifies the binding and the catalytic activities as the most affected molecular functions by the perturbation experiment with Cdx morpholino. Together with these functions, the transporter activity of lipids or ions through the cell membrane are also altered. Among the biological processes, the primary metabolic process including protein, lipid and carbohydrates metabolism and the cellular process including cell communication and cell cycle result as the most affected. Besides, although there is a big variety of affected protein class, the most interesting affected protein classes are the transcription factors, signaling molecules and nucleic acid binding.

SpCdx MO RNA-Seq molecular function



SpCdx MO RNA-Seq biological process



SpCdx MO RNA-Seq molecular function

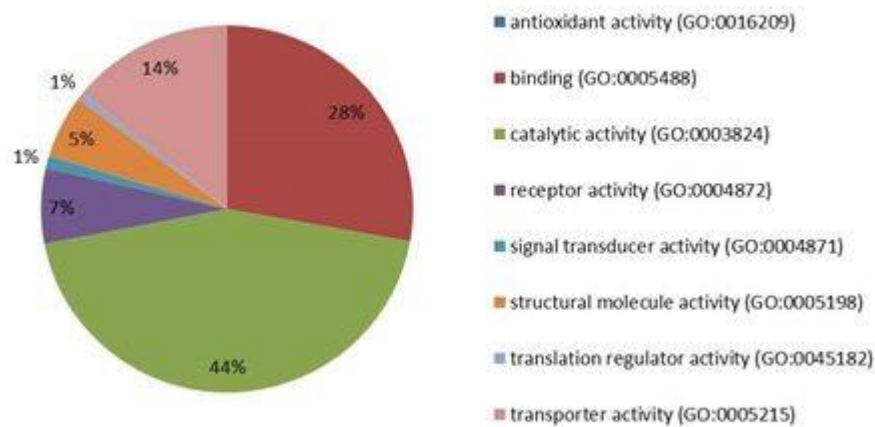


Fig. 3.4. Gene ontology analysis for DE genes downstream of Sp-Cdx.

The same enrichment analysis has been also performed for PmLox and PmCdx MO RNA-Seq datasets and has been compared with the sea urchin's one. The microinjection of Pm-Lox morpholino affects less molecular functions compared to the SpLox, but the catalytic activity always represents the most abundant affected function together with the binding activity and the transmembrane transporter activity.

The biological processes changed by the Pm-Lox knockdown (Fig. 3.5) regards the metabolic process related to lipid, protein and carbohydrate metabolism, cellular process as cell communication and cell cycle, suggesting that Lox protein may have a similar function in both the species, since its absence is responsible of the alteration of the same type of cellular processes. The major affected protein classes are the ATP binding cassette transporters that mediate translocation of various substrates across membranes, either for uptake or for export utilizing the energy of adenosine triphosphate (ATP), the kinases, that phosphorylate protein, lipid, or carbohydrate, changing their ability to bind other molecules, the hydrolases

such as deaminase, glucosidase and lipase involved in carbohydrates, proteins and lipids metabolism, DNA and RNA binding proteins, and three families of transcription factors: HMG box transcription factor, nuclear hormone receptor, basic helix-loop-helix transcription factor.

The microinjection of Pm-Cdx morpholino (Fig. 3.6) affects the same molecular functions observed in Pm-Lox MO RNA-Seq and some more activities such as enzyme activity related to glutamate receptor and translation activity. The most changing biological processes are again the cell communication, cell cycle, primary metabolic process, and the transport mediated by ATP-binding cassette transporter, carbohydrate transporter or amino acid transporter. Many hydrolase proteins are affected such as deaminase, esterase, glucosidase, lipase, phosphatase, phosphodiesterase, pyrophosphatase, protease. Compared to Pm-Lox knockdown, there is only one family of transcription factor, the basic helix-loop-helix transcription factor, that result affected.

Despite the diversity and the number of biological activities that change after injection of Xlox and Cdx morpholino in both sea urchin and sea star embryos, there are some important processes relevant for gut development and function that are always affected in all the analyzed RNA-Seqs. There are many proteins involved in the metabolism of lipids, carbohydrates and proteins that change their expression in the perturbed conditions suggesting that the knocked down proteins alter the normal gut development and its digestive activity. Moreover, genes involved in the cell signalling or in DNA binding are also affected in their expression.

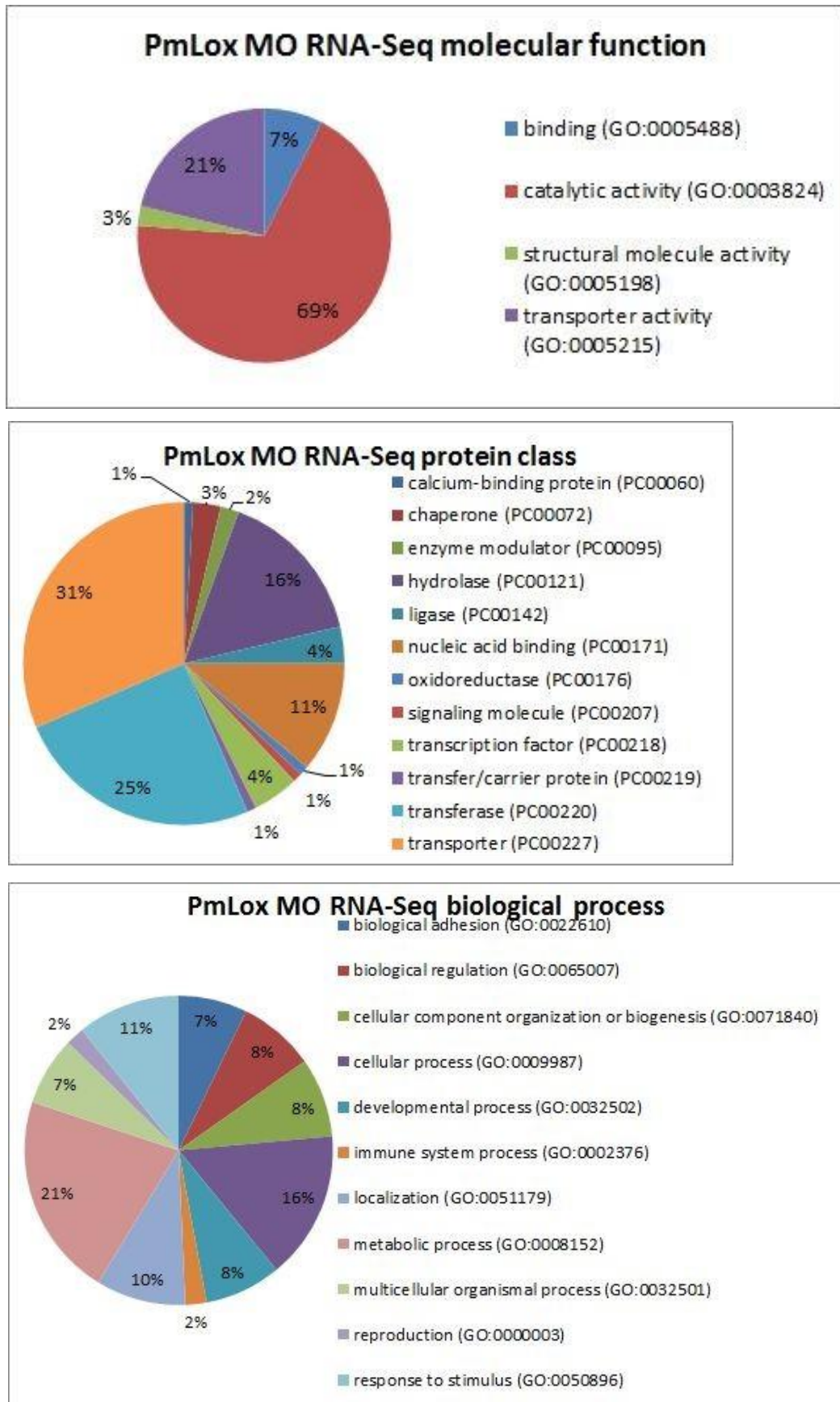


Fig. 3.5. Gene ontology analysis for DE genes downstream of Pm-Lox.

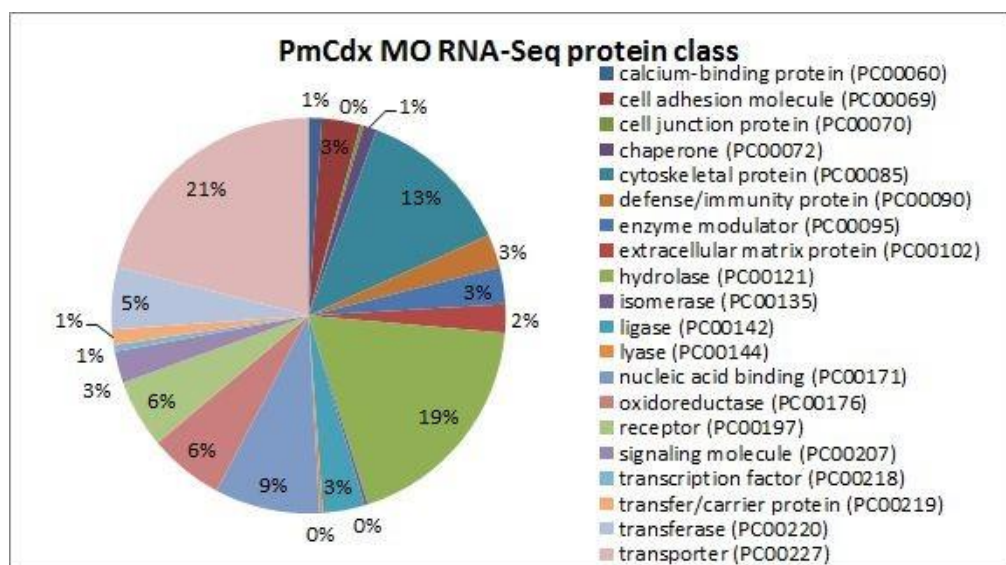
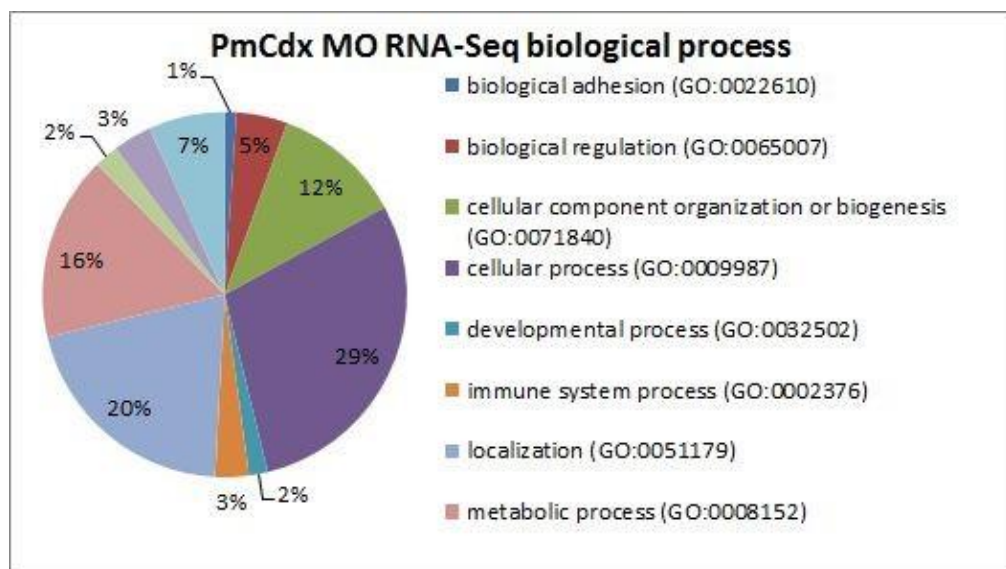
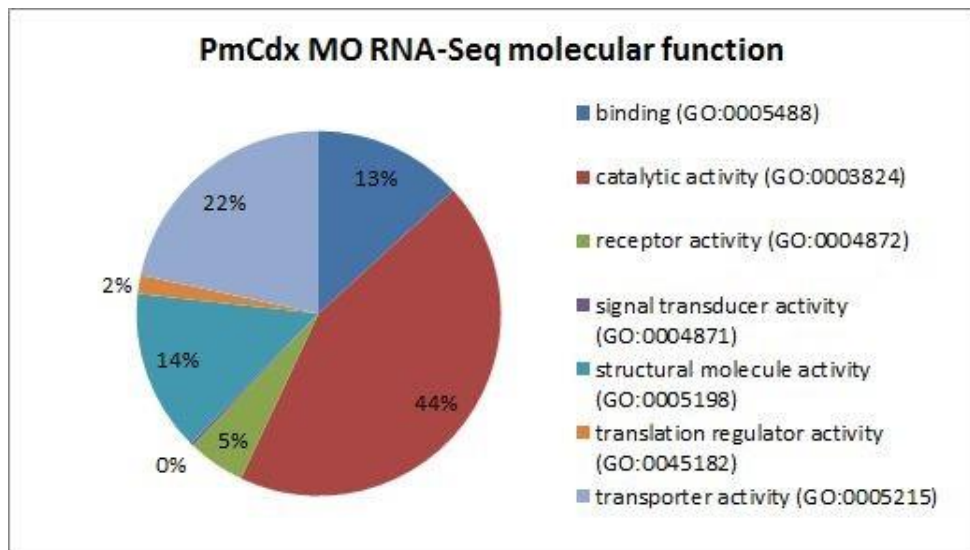


Fig. 3.6. Gene ontology analysis for DE genes downstream of Pm-Cdx.

Taken together these results show that the microinjection of Xlox and Cdx morpholinos has similar effects in both sea urchin and sea star embryos with the alteration of the activity of transcription factors, fundamental for gene regulation, cell communication, indispensable for the mechanisms of cell specification and differentiation, metabolic process linked to lipid, carbohydrates and protein, that are part of the digestive function, suggesting that Xlox and Cdx are key elements for the development and the activity of the gut in these animals. When the embryos reach the late stage of pluteus, the number of proteins involved in these activities and that are altered by SpLox morpholino microinjection considerably increases suggesting an important role for SpLox as upstream regulator of a cascade of events leading to gut development.

3.2.4 Orthology analysis

Before identifying the differentially expressed genes, the homology relationship between the two echinoderms has been assessed in order to establish the number of proteins that are conserved among the two organisms and a third species, the vertebrate *Xenopus tropicalis*. To this aim, the proteomes from *S. purpuratus*, *P. miniata* and *X. tropicalis* have been analyzed to construct homologous groups of proteins. The 22,576 *S. purpuratus* proteins have been clustered in 10,480 groups, 22,252 *P. miniata* proteins in 10,724 and 20,813 *X. tropicalis* proteins in 8,386 groups. The three proteomes share 6,034 protein groups, with echinoderms showing the largest number of orthologs with 2,545 orthologous groups. *X. tropicalis* shares instead only 283 homologous groups uniquely with *P. miniata* and 628 uniquely with *S. purpuratus* (Fig. 3.7).

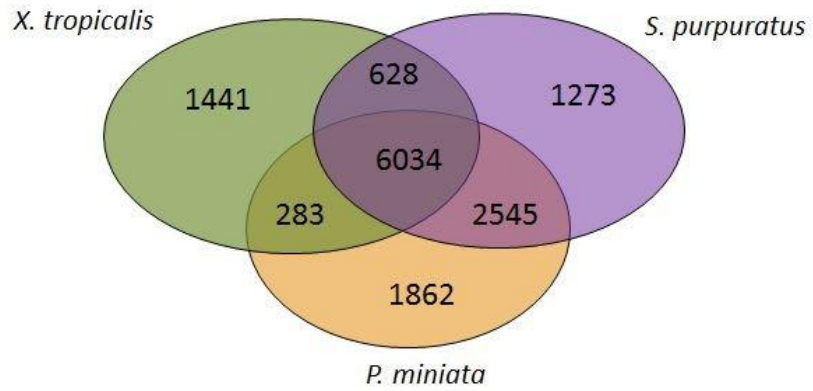


Fig. 3.7. Gene orthology relationship between *S. purpuratus* (SPU), *P. miniata* (PMI), and *X. tropicalis* (XEN). Each circle represents one of the species and their overlap represents the orthologous groups that are in common. The numbers represent the protein groups of *S. purpuratus*, *P. miniata* and *X. tropicalis*.

When analyzed the homology of the differential expressed transcripts among all species, at least 450 transcripts (observed in the Pm-Cdx MO experiments) corresponding to the 65% of the total number were clustered into homologous groups, while the remaining 35% of the transcripts from each experiment are species specific (table 3.2).

Table 3.2. Homology of differential expressed transcripts. In parenthesis is the number of differentially expressed genes for the given MASO RNA-seq experiment. Orthologous groups refers to the number of groups the total number of proteins were clustered into, while “Total proteins” refers to the total number of proteins that were clustered into orthologous groups. Proteins in core are the number of proteins found in *S. purpuratus*, *P. miniata* and *X. tropicalis*. SCO in all are the number of single copy orthologous found in *S. purpuratus*, *P. miniata* and *X. tropicalis*, while SCO in echinoderm are the number of single copy orthologs found in only *S. purpuratus*, and *P. miniata*.

	Splox 48h (294)	Splox 72h (2384)	Spcdx 66h (723)	Pmlox 66h (108)	Pmcdx 90h (693)
Orthologous groups	183	1457	470	70	404
Proteins in core	97 (33%)	929 (39%)	289 (40%)	39 (36%)	270 (39%)
SCO in all	16 (5%)	145 (6%)	39 (5%)	5 (5%)	34 (5%)
SCO in echinoderms	23 (8%)	150 (6%)	48 (7%)	10 (9%)	31 (4%)
Total proteins	207 (70%)	1659 (70%)	529 (73%)	78 (72%)	450 (65%)

The Cdx MO RNA-Seq shows the largest overlap between *P. miniata* and *S. purpuratus* with 129 shared transcripts, 91 of which are present in all the examined organisms. The Xlox MO RNA-Seq has only 10 common genes between sea urchin and sea star when the comparison occurs between the sea urchin 48 hpf and the sea star 66 hpf late gastrula. However, when compared the 72 hpf sea urchin pluteus with the 66 hpf sea star late gastrula, the shared genes increase to 25, despite the fact these stages are less morphologically similar. The explanation can lay either in a temporal shift in the sea star embryos of the set of events occurring earlier in the sea urchin animal or in a redeployment of the gene interactions that involve the same actors that, instead, work inside different connections.

3.2.5 Differential expression analysis

Differentially expressed genes have been identified using DESeq2 and a threshold of $\log_2fc > \pm 0.5$ and adjusted p-value of <0.05 . A small adjusted p-value indicates that the difference in gene expression observed between two different conditions is not due to chance and there is a small probability of getting data if no real difference exists. The fold change (fc) represents the quantity change in gene expression before and after perturbation and is calculated as ratio between the perturbed and the control gene expression that can be expressed with the logarithmic formula \log_2fc . A $\log_2fc > \pm 0.5$ includes all the genes that have a fc bigger than 1.5 (upregulated genes) and smaller than -1,5 (downregulated genes). The sea urchin 48 hpf RNA-Seq dataset shows 294 transcripts affected by Sp-Lox MASO, 32 of which downregulated (11%) and 262 upregulated (89%), compared to 2384 at 72 hpf with 1326 genes downregulated (55,6%) and 1059 upregulated (44,4%). This result indicates that in *S. purpuratus*, as time progressed, the knocked down protein has a larger effects of more transcripts. This can be easily explained with the central role that Xlox has as upstream regulator of a cascade of regulatory events responsible for the differentiation of the middle larval gut (R. Annunziata and Arnone 2014). Later in development since gut differentiation is induced by SpLox expression, more genes are directly or indirectly affected by the absence of this protein. Moreover, 167 of transcripts affected by Sp-Lox MASO at 48 hpf are also affected at 72 hpf, showing similarities in the GRN transitions from a tube like structure to a tripartite gut. The sea urchin 66 hpf RNA-Seq, instead, shows 723 transcripts affected by Sp-Cdx MASO at 66 hpf with 306 genes downregulated (42,3%) and 418 upregulated (57,8%). The number of affected genes after MASO experiments and the common genes in the Sp-Lox MASO datasets are summarized in Fig. 3.7.

	SpLox MASO 48hpf	SpLox MASO 72hpf	SpCdx MASO 66hpf
n. affected genes ($\pm 0,5 \log_2\text{foldchange}$)	294	2384	723



Fig. 3.8. Sea urchin misexpressed genes. Table and Eulero-Venn diagram showing the number of misexpressed transcripts having $\pm 0,5 \log_2\text{foldchange}$ at late gastrula (48hpf), prism (66hpf) and pluteus (72hpf) after SpLox and SpCdx morpholinos microinjection.

Examining the *P. miniata* 66 hpf RNA-Seq only 109 transcripts have been affected by Pm-Lox MASO with 55 (50,46%) genes downregulated and 54 genes upregulated (49,54%), while many more genes, 693, 393 (56,7%) of which downregulated and 300 upregulated (43,3%), have changed their expression after Pm-Cdx morpholino, and 450 of them are homologous to the *S. purpuratus*. The larger number of transcripts affected by Pm-Cdx MASO compared to Pm-Lox can be due to the dual activity of Cdx during sea star development, since it is activated at both blastula and gastrula stages, resembling the vertebrate expression of its ortholog. The number of the sea star affected genes under Pm-Lox and Pm-Cdx perturbation is summarized in table 3.3.

Table 3.3 Summary of sea star affected genes. Shown are number of affected genes showing $\pm 0,5$ log2foldchange at late gastrula (66hpf) and early bipinnaria larva (90hpf) after microinjection of PmLox and PmCdx morpholinos.

	PmLox MASO 66hpf	PmCdx MASO 90hpf
n. affected genes ($\pm 0,5$ log2foldchange)	109	693

Differentially expressed transcription factors

Transcription factors (TF) are proteins that bind to the enhancer or promoter regions regulating gene expression in time and space (cell type). Each enhancer can be bound by more than one factor and it can lay at a large distance from the promoter, so that multiple signals are required to determine the transcription of the gene. Most transcription factors can bind to specific DNA sequences, the CRMs, and can be grouped together in families based on similarities in structure. Alteration in the interaction between the TF and the CRM, due to either a modification in the regulatory sequence or to changes in the protein structure, is source of evolutionary change. Modification of the expression of a specific gene can, in fact, cause changes in the regulatory state of a specific cell, having effects on all the downstream gene-protein interactions. Given this, knowing which are the TFs altered in the Xlox and Cdx perturbed embryos are of extreme importance to understand the gene interactions in which they are involved and the ones they can affect in absence of their proteins. For this reason, from all the sea urchin and the sea star differential RNA-Seq datasets the TFs genes have been selected and analyzed to determine the TF family they belong to and the spatial expression in the sea urchin or sea star embryos (if known). Before showing this analysis, a brief description of the most important TF families is necessary and is described

below.

Homeodomain family. The hox proteins are critical for specifying the antero-posterior body axes throughout the animal kingdom. As already described in the introduction of this thesis, the homeodomain consists of 60 amino acids arranged in helix-turn-helix, with the third helix contacting the major groove of the DNA and the N-terminal portion of the homeodomain contacting the minor groove. The homeodomain was first observed in proteins that specify segment identity in *Drosophila* and mutation of these proteins caused one body segment to be transformed into another.

POU family. The POU domain common to these factors constitutes the DNA binding domain of the protein and consists of a POU specific domain of approximately 150–160 amino acids which is unique to these factors and a POU homeodomain which is related to that found in the homeobox proteins. These two major subdomains are joined together by a short linker region. The initial comes from the four proteins first seen to have such domains: Pit-1, a pituitary specific factor that activates the gene encoding growth hormone, prolactin and other pituitary proteins; Oct-1, a ubiquitous protein, that recognizes a certain eight-base-pair sequence called the octa box, and Oct-2, the B-cell-specific protein that recognized the octa box and activates immunoglobulin genes; and unc-86, a nematode gene product involved in determining neuronal cell fates. These four genes play a critical role in regulating gene expression, particularly in cells of the nervous system (Latchman 1999).

Basic helix-loop-helix transcription factors. The bHLH proteins bind to DNA through a region of basic amino acids (typically 10-13 residues) that precedes the first α -helix. homodimers between two identical bHLH proteins do not bind well to DNA. in most cells there is an ubiquitous bHLH protein that can form dimers with either a positive regulator or a negative regulator. when the positive regulator

dimerizes with the ubiquitous protein, it forms an activator complex that stimulates transcription from the gene it recognizes. when the negative regulator dimerizes with the bHLH protein, it forms an inhibitory complex that represses transcription from those same genes (Jones 1990). Examples of this kind of proteins are the muscle-specific transcription factors MyoD and myogenin and the genes that determine the sex of *Drosophila*, such as *Sex-lethal (Sxl)*, *Transformer (Tra)*, and *Transformer-2 (Tra-2)*.

Basic leucine zipper transcription factors. Leucine zippers (Landschulz, Johnson, and McKnight 1988) are a dimerization domain of the bZIP (Basic-region leucine zipper) class of eukaryotic transcription factors. The structure of basic leucine zipper (bZip) transcription factors is very similar to that of the bHLH proteins. The bZip proteins are dimers, each of whose subunits contains a basic DNA-binding domain, followed by an α -helix containing several leucine residues. these leucine are placed in the helix such that they interact with similarly spaced leucine residues on other bZip proteins to form a “leucine zipper” between them, causing dimers to form. These proteins include the yeast GCN4 transcriptional activator, the Jun, Fos and Myc oncoproteins, and the C/EBP enhancer binding protein (involved in adipogenesis and liver-specific gene expression).

Zinc finger transcription factors. Zinc finger transcription factors (Gommans, Haisma, and Rots 2005) are transcription factors composed of two or more zinc finger-binding domains, α -helical domains whose central amino acids tend to be basic. These domains are linked together in tandem and are each stabilized by a centrally located zinc ion coordinated by two cysteines at the base of the helix and two internal histidines. Zinc finger proteins can function in binding RNA and also participate in protein–protein interactions, but their major role is the recognition of DNA. Members of this protein family are the *Xenopus* 5S rRNA transcription factor TFIIIA, Krox 20 that regulates gene expression in developing hindbrain,

Kruppel that specifies abdominal cells in *Drosophila*, and numerous steroid binding transcription factors.

Nuclear hormone receptors. This family includes nuclear hormone receptors (NHRs) (Kumar and Thompson 1999) and orphan nuclear receptors. NHRs are receptors for which hormonal ligands have been identified, whereas orphan receptors are so named because their ligands are unknown. Nuclear hormone receptors recognize steroid hormone such as estrogen, progesterone, testosterone, cortisone, and nonsteroid lipids such as retinoic acid, thyroxin and vitamin D. The DNA sequences capable of binding nuclear hormone receptors are called hormone-responsive elements, and they can be either enhancers or promoters. The nuclear hormone receptors contain three functional domains: a hormone binding domain, a DNA binding domain that recognizes the hormone responsive element and a *trans*-activation domain which is involved in mediating the signal of the hormone to initiate transcription. For transcriptional activation, the receptor has to enter the nucleus and dimerize with a similar hormone-binding protein. The binding of the receptor protein to the hormone responsive enhancer element is accomplished by a zinc finger region in the DNA binding domain.

Differentially expressed TFs have been identified with a $\log_2\text{fc} > \pm 0.5$ and adjusted p-value of <0.05 . A complete list of the TFs from both the sea urchin and the sea star RNA-Seq datasets is summarized in the tables below. For each TF I have indicated the identity number (SPU_ID), the common name (gene symbol), the gene family (gene description), the gene superfamily, the \log_2 fold change ($\log_2\text{FC}$), the spatial expression in the sea urchin or the sea star embryos (if known) and the references. According to the changes in gene expression, the $\log_2\text{FC}$ values are highlighted in red and green scales, with the most red and the most green the genes with the lowest and highest $\log_2\text{FC}$, respectively.

Table 3.4 Transcription factors downstream of Sp-Lox. Description of the identified TFs ($\log_2fc > \pm 0.5$ and adjusted p-value of <0.05) in the Sp-Lox MO 48hpf RNA-Seq dataset.

SPU ID	Gene symbol	Gene description	Superfamily	log2FC	Spatial expression in Sp	References
SPU_011202	Sp-Meis	none	homeobox-atypical	-0.567	Unknown	-
SPU_008752	Sp-Nfe2_1	none	basic-zipper	0.516	Unknown	-
SPU_014684	Sp-Z94	none	zf-C2H2	0.517	Unknown	-
SPU_022816	Sp-Alx4	none	homeobox-paired	0.547	Gastrula: PMCs. Later stages: NSM cells in the coelomic pouches	Rafiq, K., et al., 2012
SPU_011174	Sp-Nfe2	none	basic-zipper	0.569	Unknown	-
SPU_008528	Sp-Ets4	PDEF	Ets	0.588	Gastrula: hindgut. Pluteus:hindgut, midgut	Unpublished data from Arnone lab
SPU_002631	Sp-Hox11/13b	none	Hox	0.611	Gastrula: blastopore. Pluteus: hindgut.	Arenas-Mena, C. et al., 2006
SPU_028093	Sp-Scl	none	bHLH	0.721	Gastrula:blastocoelar cells and tip of the archenteron	Sharma, T., et al, 2011
SPU_008920	Sp-Hypp_1813	hypothetical protein-1813	bZIP_1 superfamily	0.735	Unknown	-
SPU_006032	Sp-Hypp_1626	hypothetical protein-1626	bZIP_1 superfamily	0.735	Unknown	-

SPU_002320	Sp-FoxN1/4	none	Forkhead	0.766	Maternal expression	Tu, Q et al., 2006
SPU_008559	Sp-Hypp_3068	hypothetical protein-3068	none	0.778	Unknown	-
SPU_006917	Sp-Runt1	SpRunt-1, SpRunt	Runx	0.829	Gastrula:endomesoderm and oral ectoderm. Pluteus: foregut and ciliary band ectoderm	Robertson, A.J., et al., 2002
SPU_001657	Sp-Cebpa	CCAAT/enhancer binding protein alpha,	bZIP_1 superfamily	0.838	Unknown	-
SPU_017837	Sp-Nkx3.2	nkx3.2	homeobox	0.939	Gastrula: oral animal pole ectoderm and foregut	Wei, Z et al., 2011
SPU_024903	Sp-Ese	Ehf	Ets	0.968	Gastrula:SMC	Rizzo, F. et al., 2006
SPU_011246	Sp-IrxB	none	homeobox-atypical	0.982	Unknown	-
SPU_025584	Sp-Tbr	none	T-box	0.983	Blastula:SMC. Gastrula:PMC.	Croce, J. et al, 2001
SPU_020411	none	none	none	1.058	Unknown	-
SPU_010403	Sp-FoxY	forkhead C-like	Forkhead	1.083	Gastrula: tip of the archenteron. Pluteus: coelomic pouches	Ransick et al., 2002
SPU_020311	Sp-Klf2/4	z85	zf-C2H2	1.165	Blastula:oral ectoderm	Materna, S. et al, 2006
SPU_022573	Sp-Nk7	none	Homeobox-nk	1.287	PMCs	Rafiq, K. et al., 2014.
SPU_026877	Sp-Irf4	none	misc	1.324	Unknown	-
SPU_012469	Sp-Elk	Net Sap	Ets	1.504	Gastrula: endoderm-proximal to oral ectoderm, tip of archenteron, apical plate	Squarzone et al., 2006
SPU_021172	Sp-Fra2	none	bZIP	1.550	Unknown	-
SPU_013178	Sp-Nr1m3	none	nuclear receptor	1.572	Unknown	-

SPU_021173	Sp-Fos	fos-related antigen-2, c-Fos protein, ATF3	none	2.614	PMCs	Rafiq, K. et al., 2012.
------------	--------	--	------	-------	------	-------------------------

The analysis of the sea urchin misexpressed TFs after Splox knockdown revealed 27 affected genes at 48 hpf, 26 of which downregulated and 1 upregulated compared to 93 misexpressed genes at 72hpf, 55 of which upregulated and 38 downregulated (TF list not shown). The increase of the number of TFs at pluteus stage is explained with the fact that this stage is more advanced in development compared to the late gastrula stage, so the number of genes already active in the gut and affected by the absence of Sp-Lox protein is higher; moreover, terminal differentiation genes that are expressed at the end of the gut specification process are also affected at this time point. The genes that have been found misexpressed also in the standard control morpholino dataset, such as *Sp-Irf4*, have been excluded from any analysis because changes in their expression is highly related to the microinjection procedure and not to the specific morpholino. *Sp-Meis*, belonging to the homeobox family, is the only gene that is repressed by the absence of SpLox protein. Moreover, it is not affected in the Sp-Cdx knocked down conditions. Given to this, *Sp-Meis* is a putative target of SpLox and can be activated before Sp-Cdx. Among the upregulated genes there is *Sp-Nr1m3*, a nuclear hormone receptor, that can be involved in the retinoic acid signalling pathway. Retinoic acid has been demonstrated to regulate ParaHox expression in zebrafish, *Xenopus*, chicken, mouse and amphioxus *Branchiostoma floridae* (Stafford and Prince 2002) (Chen et al. 2004) (Bayha et al. 2009) (Gaunt, Drage, and Cockley 2003) (Osborne et al. 2009). The absence of SpLox can be responsible of the alteration of the retinoic acid pathway response through modification of the expression of its cellular receptor. Finally, most of the upregulated TF and that are

normally repressed during sea urchin development at late gastrula stage belong to regulatory states that induce skeleton or anterior gut formation in the sea urchin. This can be interpreted as an exclusion mechanism of SpLox protein that, in wild type conditions, clarifies the posterior gut from all the genes that specify other territories of the sea urchin embryos.

Table 3.5 Transcription factors downstream of Sp-Cdx. Description of the identified TFs ($\log_2fc > \pm 0.5$ and adjusted p-value of <0.05) in the Sp-Cdx MO 66 hpf RNA-Seq dataset.

SPU ID	Gene symbol	Gene description	Superfamily	log2FC	Spatial expression in Sp	References
SPU_020921	Sp-Hypp_1005	hypothetical protein-1005	none	-1.588	Unknown	-
SPU_025632	Sp-Pou4f2	Brn3b	POU domain protein	-1.548	retinal ganglion cells	Xiang et al., 1995
SPU_020346	Sp-Tbx6	none	tbx	-1.531	Unknown	-
SPU_020345	Sp-Tbx6/16	Tbx6, Tbx16	T-box	-1.531	Gastrula: tip of the archenteron, PMC Pluteus:cardiac sphincter	Andrikou, C. et al, 2013
SPU_021963	none	none	none	-1.531	Unknown	-
SPU_018393	Sp-Scratch	z213	zf-C2H2	-1.391	Unknown	-
SPU_000276	Sp-PaxC	none	homeobox-paired	-1.357	Unknown	-
SPU_003488	Sp-Wdhd1_2	WD repeat and HMG-box DNA binding protein 1-2	WD40 superfamily, HMG-box superfamily	-1.300	Unknown	-
SPU_027491	Sp-Z133_1	none	zf-C2H2	-1.060	Gastrula:apical ectoderm	Materna, S. C. et al., 2006
SPU_019089	Sp-Z133	none	zf-C2H2	-1.060	-	-
SPU_013962	Sp-Sim_1	none	bHLH-PAS	-1.018	Unknown	-

SPU_003488	Sp-Wdhd1_2	WD repeat and HMG-box DNA binding protein 1-2	WD40 superfamily, HMG-box superfamily	-0.988	Unknown	-
SPU_021560	none	none	none	-0.931	Unknown	-
SPU_006462	Sp-Gcm	Glial Cells Missing	GCM	0.774	Gastrula:SMC Pluteus:pigment cells	Ransick, A., et al., 2001; Ransick, A., et al., 2006
SPU_008979	Sp-P53L	p53-family transcription factor	p53	0.784	Unknown	-
SPU_020722	Sp-Smad1/5/8_1	none	smad	0.787	mesenchyme blastula:aboral ectoderm	Chen, J. H., et al., 2011
SPU_013439	Sp-Hypp_91	hypothetical protein-91	HLH superfamily	0.897	Unknown	-
SPU_006093	Sp-Ubtf	upstream binding transcription factor, RNA polymerase I; nucleolar transcription factor UBF	HMG-box superfamily	0.901	Unknown	-
SPU_006803	Sp-Creb313	none	basic-zipper	0.910	Unknown	-
SPU_022018	Sp-Hypp_1036	hypothetical protein-1036	none	1.008	Unknown	-
SPU_022017	Sp-Hypp_180	hypothetical protein-180	none	1.008	Unknown	-
SPU_011174	Sp-Nfe2	none	basic-zipper	1.022	Ubiquitous	Materna, S. C. et al., 2006
SPU_013579	Sp-Moka_1	modulator of KLF7	F-box	1.040	Unknown	-
SPU_007778	Sp-Moka	modulator of KLF7	F-box	1.040	Unknown	-
SPU_012772	Sp-Klf7	z86	zf-C2H2	1.041	Blastula:aboral or oral ectoderm	Materna, S. C. et al., 2006

SPU_022540	Sp-Deaf1L	deformed	SAND	1.120	Unknown	-
		epidermal autoregulatory factor 1-like; suppressin-like	superfamily			-
SPU_008559	Sp-Hypp_3068	hypothetical protein-3068	none	1.123	Unknown	-
SPU_026877	Sp-Irf4	none	misc	1.139	Unknown	-
SPU_020411	none	none	none	1.146	Unknown	-
SPU_017837	Sp-Nkx3.2	nkx3.2	homeobox	1.274	Gastrula:oral animal pole ectoderm and foregut	Wei, Z et al., 2011
SPU_026947	none	none	none	1.307	Unknown	-
SPU_014802	Sp-Hlx	none	homeobox-nk	1.410	Gastrula:oral ectoderm, archenteron	Dobias, S.L. et al., 1996
SPU_001657	Sp-Cebpa	CCAAT/enhancer binding protein alpha, C/EBP alpha	bZIP_1 superfamily	1.515	Unknown	-
SPU_008556	Sp-Znf622	zinc finger protein 622	none	1.519	Unknown	-
SPU_002320	Sp-FoxN1/4	none	Forkhead	1.594	Ubiquitous	-
SPU_025584	Sp-Tbr	none	T-box	1.881	Gastrula:PMC	Croce, J. et al., 2001
SPU_010403	Sp-FoxY	forkhead C-like	Forkhead	1.900	Gastrula:tip of the archenteron	Ransick, A., et al., 2001; Materna, S. C et al., 2013
SPU_009474	Sp-Z364	none	zf-C2H2	2.022	Unknown	-
SPU_008920	Sp-Hypp_1813	hypothetical protein-1813	bZIP_1 superfamily	2.027	Unknown	-
SPU_006032	Sp-Hypp_1626	hypothetical protein-1626	bZIP_1 superfamily	2.027	Unknown	-

The number of affected TFs at 66 hpf are 40 in Cdx knocked-down conditions, 27 of which upregulated and 13 downregulated. Compared to Sp-Lox knocked-down conditions there are more repressed genes in the datasets that are active in wild type conditions, given to the fact that SpLox has the major role in initiating the mid-hindgut specification process. Sp-Cdx, instead, is involved in SpLox regulation and activation of all the hindgut genes. Sp-Cebpa, Sp-FoxN1/4 and Sp-Irf4 genes are also affected in the standard control morpholino. This means that changes in their expression is probably due to the microinjection procedure and not to the specific activity of the morpholino. The same TFs have been excluded from all the interpretation analyses of both the SpLox and Sp-Cdx MO datasets.

Table 3.6 Transcription factors downstream of Pm-Lox. Description of the identified TFs ($\log_2fc > \pm 0.5$ and adjusted p-value of <0.05) in the Pm-Lox MO 66 hpf RNA-Seq dataset.

PMI ID	Gene symbol	Gene family	\log_2FC	Spatial expression in <i>P. miniata</i>
PMI_003594	PMI_003594	Unclassified	-0.895	Unknown
PMI_027346	Pm-Nfe2	Transcription Factor_ leucine zipper	0.859	Unknown
PMI_019393	Pm-Hypp_1626	hypothetical protein-1626	1.009	Unknown
PMI_027023	Pm-Nr1h6c	nuclear orphan receptor	1.088	Unknown
PMI_005790	PMI_005790	Unclassified	1.089	Unknown
PMI_015902	Pm-Fra2	Signaling_TGFB_SmadInteract	1.114	Unknown
PMI_015901	Pm-Fos	TranscriptionFactor_bzip	1.616	Unknown
PMI_024682	Pm-Usf	TranscriptionFactor_bHLH	1.636	Unknown
PMI_009520	Pm-Usf	TranscriptionFactor_bHLH	1.801	Unknown
PMI_002316	Pm-Nurr1	nuclear orphan receptor, NR4A,RNR-1, NOT	1.873	Unknown
PMI_022566	Pm-Hgf	hypothetical protein-1329	1.957	Unknown

PMI_015900	-	-	2.596	Unknown
------------	---	---	-------	---------

The analysis of the sea star MASO RNA-Seq datasets is more complicated because of the few information available about the genes belonging to this species. However I give a try for its analysis and interpretation. In the sea star RNA-Seq datasets, the number of affected TFs are lower, with 12 misexpressed genes in the Lox knocked-down, 1 of which downregulated and 11 upregulated. Among the upregulated genes there is Pm-Nr1h6c, a nuclear orphan receptor, that can be involved in the RA signaling pathway. The misexpression of nuclear hormone receptors in both SpLox and Pm-Lox MO datasets endorses the hypothesis that also in echinoderm, as in vertebrates and amphioxus, ParaHox expression is related to the RA signal.

Table 3.7 Transcription factors downstream of Pm-Cdx. Description of the identified TFs (log2fc > ± 0.5 and adjusted p-value of <0.05) in the Pm-Cdx MO 90 hpf RNA-Seq dataset.

PMI ID	Gene symbol	Gene Family	log2FC	Spatial expression in P. m	Reference
PMI_020940	Pm-Pou4f2	POU domain protein	-2.525	Unknown	-
PMI_025688	Pm-SoxC	-	1.230	Ectoderm	Yankura, K. A et al., 2013
PMI_027346	Pm-Nfe2	bZIP TF	1.300	Unknown	-
PMI_025115		leucine zipper	1.335	Unknown	-
PMI_015902	Pm-Fra2	-	1.568	Unknown	-
PMI_004263	Pm-Znf622	-	1.634	Unknown	-
PMI_018030	Pm-Znf622	zinc finger protein 622	1.795	Unknown	-
PMI_002049	Pm-Gatad1	zinc finger	1.855	Unknown	-

PMI_019393	Pm-Hypp_1626	-	2.048	Unknown
PMI_015900	-	-	2.233	Unknown
PMI_022566		hypothetical protein-1329	3.078	Unknown
PMI_015901	Pm-Fos	leucine zipper	3.209	Unknown
PMI_010266	Pm-Arxl	drg11, paired related homeobox like, prx	3.230	Unknown

In the Pm-Cdx MASO 90 hpf RNA-Seq datasets there are 13 misexpressed genes, 1 of which downregulated and 12 upregulated. The only downregulated genes is Pm-Pou4f2, that is also strongly repressed in the Sp-Cdx knocked-down conditions. However this gene changes after standard control morpholino microinjection and can not be considered for the analysis of the sea star genes. The number of affected genes in the dataset generated after injection of the standard control morpholino is very high. Many of the transcription factors affected by Sp-Lox and Sp-Cdx morpholino microinjection have been observed misexpressed also in the standard control morpholino dataset and for this reason change in their expression can not be considered reliable.

3.3 Conclusions

The gene ontology and the differential expression analyses have revealed many sea urchin and sea star common genes that change their expression after Xlox and Cdx perturbation. The highest number of affected genes in both the animals is observed after Cdx knock-down when more genes are active in the control of the specification mechanism of the embryonic gut. Among the sea urchin affected genes has been possible to identify a putative Sp-Lox target, *Sp-Meis*, that is the only TF activated by Sp-Lox during the normal gut development. All the other TFs, which resulted upregulated under perturbed condition, are repressed by Sp-Lox. Among these proteins there are factors involved in the specification of the skeletogenic mesenchyme cells and the anterior region of the gut. This has suggested the key role of Sp-Lox as upstream regulator of the mid-posterior gut specification, as already predicted in previous works. The analysis of the sea star RNA-Seq datasets has been more difficult due to the lack of information related to its genes, but it has been possible to find common genes with the sea urchin embryo, that are affected under morpholino condition. Among these, *Pm-Nr1h6c*, a putative gene of the RA pathway has been identified in the Pm-Lox MASO RNA-Seq, suggesting a possible role of RA in regulating ParaHox expression also in echinoderms species, as already observed in vertebrates.

CHAPTER 4

Partial reconstruction of the posterior gut GRN downstream of Sp-Lox and Sp-Cdx with the combination of RNA-Seq, ATAC-Seq and ChIP- PCR approaches

4.1 Introduction

Behind the expression of each gene, there is a functional interaction between a *cis*-regulatory region and a *trans*-element, the transcription factor, that controls its expression. Knowing which are the elements involved in this interaction, i.e. the protein(s) and the bound DNA region, allow to describe the activity of the specific gene, when and where it is expressed. The interaction between the *trans* and the *cis* elements only occurs when the chromatin is not wrapped around the nucleosome, but has been modified by the activity of specific proteins and pass from an heterochromatic to euchromatic state. The chromatin organization of the DNA around a single gene is constantly modified during development limiting its transcriptional regulation to a specific set of proteins and during a precise moment of development. Characterizing chromatin changes at specific genome locus occurring over the development of an organism permits to predict which genes are active at a certain developmental stage and the inputs that drive their expression.

Assay for Transposase-Accessible Chromatin (ATAC-Seq) technique takes advantage of a transposase enzyme to study chromatin accessibility. A mutated hyperactive bacteria enzyme, the Tn5 transposase, cuts nucleosome-free region of chromatin and ligates specific sequences, called adapters. Adapter-ligated DNA fragments are then isolated, amplified by PCR and used for next generation sequencing. The millions of next generation sequencing reads are mapped on the reference genome and generate an ATAC-Seq peak profile. Regions of the genome where DNA was accessible to the activity of the Tn5 during the experiment, because free of the nucleosome occupancy, contains significantly more sequencing reads and form peaks in the ATAC-seq signal. According to their distance from the transcription start site (TSS) or data from experiments, these regions can be categorized as promoter, enhancer, insulator regions. This kind of approach has been adopted for this work in order to reveal the free chromatin regions around and inside the gene body of the TFs selected by differential RNA-Seq analysis in order to identify the interactions with the proteins that drive their expression. To the combination of the RNA-Seq and ATAC-Seq approaches follows a partial reconstruction of the sea urchin gut GRN, describing all the putative gene-TF interactions occurring in the gut at 48 hpf and 72 hpf, the characterization of *Sp-Meis* gene, considered as central element of the *Sp-Lox/Sp-Cdx* positive-negative feedback loop, and the validation of the *Sp-Lox/Sp-Meis* node.

4.2 Results and Discussion

4.2.1 ATAC-Seq analysis

Sea urchin ATAC-Seq data obtained by 24 hpf, 48hpf and 72 hpf sea urchin embryos and generously provided by Gomez-Skarmeta lab have been integrated

with the generated differential RNA-seq data in order to study the regulatory state of the sea urchin gut at late gastrula stage and to verify how it changes in the altered conditions after morpholino microinjection. The 48hpf and 72 hpf sea urchin ATAC-Seq peak profiles have been analyzed to explore a 10kb upstream and 10 kb downstream region around the TSS of all the TFs that appear affected in the differential RNA-Seq datasets and that are known to be expressed in the sea urchin mid-hindgut. The mentioned TFs correspond to SpLox, Sp-Cdx, Sp-Meis, Sp-Ets4, Sp-Nr1m3, Sp-FoxA, Sp-Bra, Sp-Hox11/13b, SpHlx. Although Sp-Bra does not appear in any differential RNA-Seq dataset, it has been included in this analysis due to its important role in gastrulation and archenteron formation during *S. purpuratus* development (Rast et al. 2002). The identified regions have been checked for the presence of known binding motifs for transcription factors, putative regulators of the expression of the altered genes. The complete analysis of the ATAC-Seq data is described below and the binding motifs are found mostly based on the similarities with the ones for vertebrate transcription factors, that are the most abundant in literature.

The analysis of the ATAC-Seq profile for Sp-Lox (Fig.4.1) has revealed the presence of three transcription factors binding sites inside the first exon of the gene. The binding motifs belong to three vertebrate proteins, Pdx1, Hoxa9, Cdx2, orthologs of the sea urchin Sp-Lox, Sp-Hox11/13b and Sp-Cdx. This analysis suggests an autoregulatory loop of Sp-Lox and an interaction with Sp-Hox11/13b and Sp-Cdx proteins.

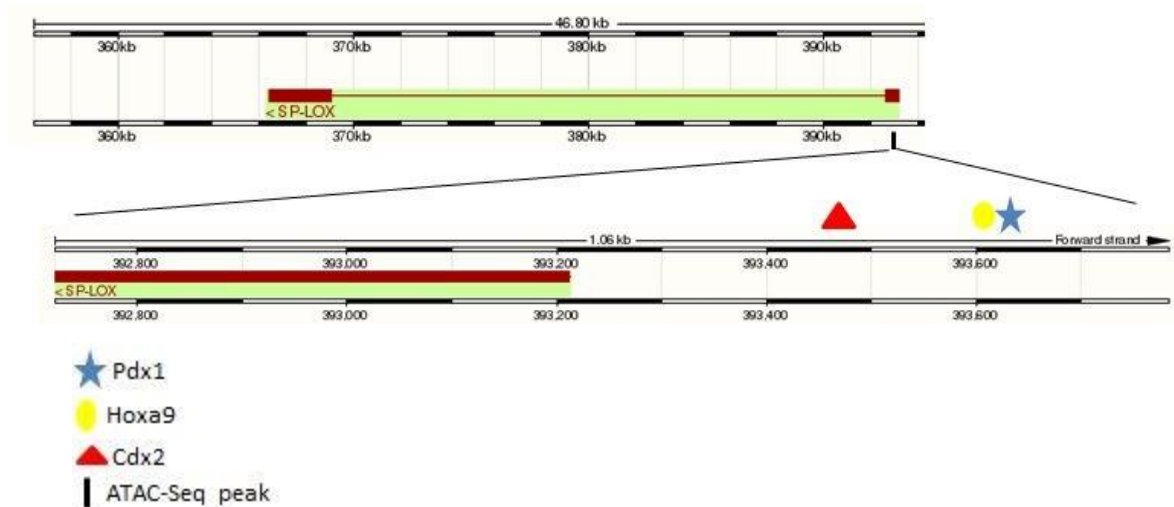


Fig.4.1 ATAC-Seq analysis around the *Sp-Lox* gene locus. Graphic representation of the in silico prediction of the transcription factor binding sites falling in the ATAC-Seq peak (1061 bp) at a distance of 321 bp from the TSS of the *Sp-Lox* gene. The vertical black line indicates the position of the ATAC-Seq peak referred to the gene locus. The colored symbols indicate the position of the predicted binding motifs for Sp-Cdx (red triangle), Sp-Hox11/13b (yellow circle) and Sp-Lox (blue star) within the 1061-long sequence corresponding to the ATAC peak.

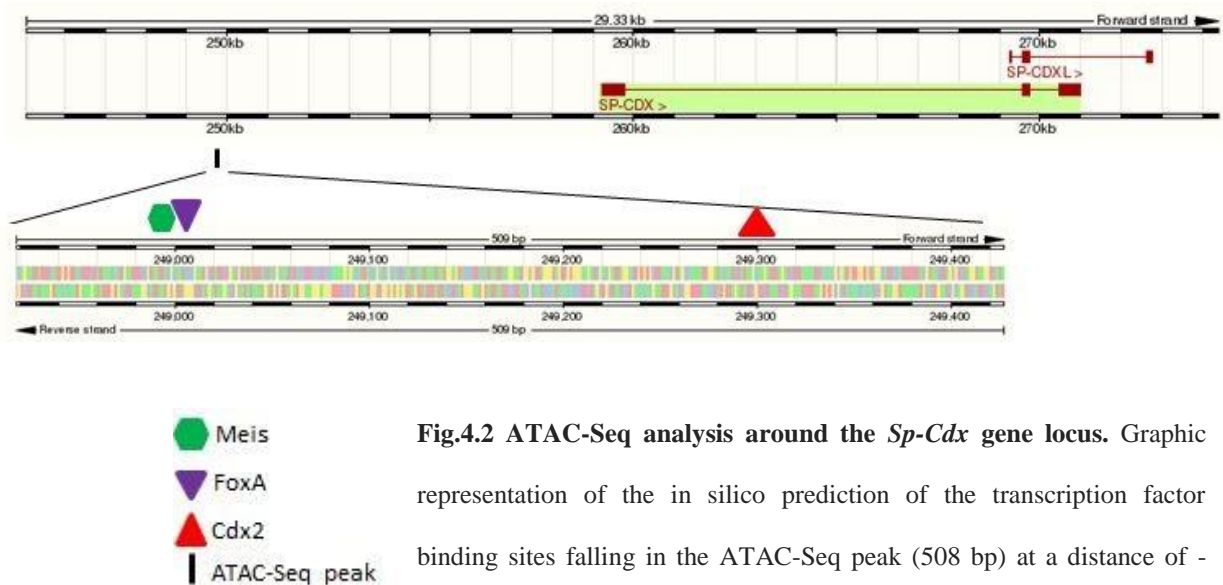


Fig.4.2 ATAC-Seq analysis around the *Sp-Cdx* gene locus. Graphic representation of the in silico prediction of the transcription factor binding sites falling in the ATAC-Seq peak (508 bp) at a distance of -9744 bp from the TSS of the *Sp-Cdx* gene. The small black line indicates the position of the ATAC-Seq peak referred to the gene. The colored symbols correspond to the binding motifs for specific proteins.

The ATAC-Seq analysis of the region around *Sp-Cdx* gene (Fig.4.2) revealed the presence of binding sites for Meis, FoxA and Cdx itself transcription factors. All

the sites fall quite far from the promoter site and within an intergenic region close to the 5'-end of the gene. The revealed binding motif for Cdx suggests the possibility of an autoregulation of its expression.

The ATAC-Seq profile analysis for *Sp-Meis* gene (Fig. 4.3) has revealed the presence of three different peaks, two before and inside the first exon and one in the intergenic region close to the 5'-end of the gene. As already observed for *Sp-Lox* and *Sp-Cdx*, *Sp-Meis* also possesses a putative autoregulatory activity due to the presence of the binding site for its own protein falling in the outside region of the gene. Two regions of 180 and 301 bp in the area before and inside the first exon, respectively, present specific sequences for Sp-Hox11/13b and Sp-Lox proteins. The putative interaction with Sp-Lox suggests the existence of a regulatory module including SpLox, Sp-Meis and Sp-Cdx, in which SpLox interacts with Sp-Meis that has an effect on *Sp-Cdx* expression. A positive-negative feedback loop between Sp-Lox and Sp-Cdx has been already demonstrated in the work of (R. Annunziata and Arnone 2014), but it has never demonstrated if it was direct or indirect. This ATAC-Seq analysis strongly suggests an indirect effect of Sp-Lox protein on *Sp-Cdx* gene mediated by Sp-Meis that represents the connective gene between these two.

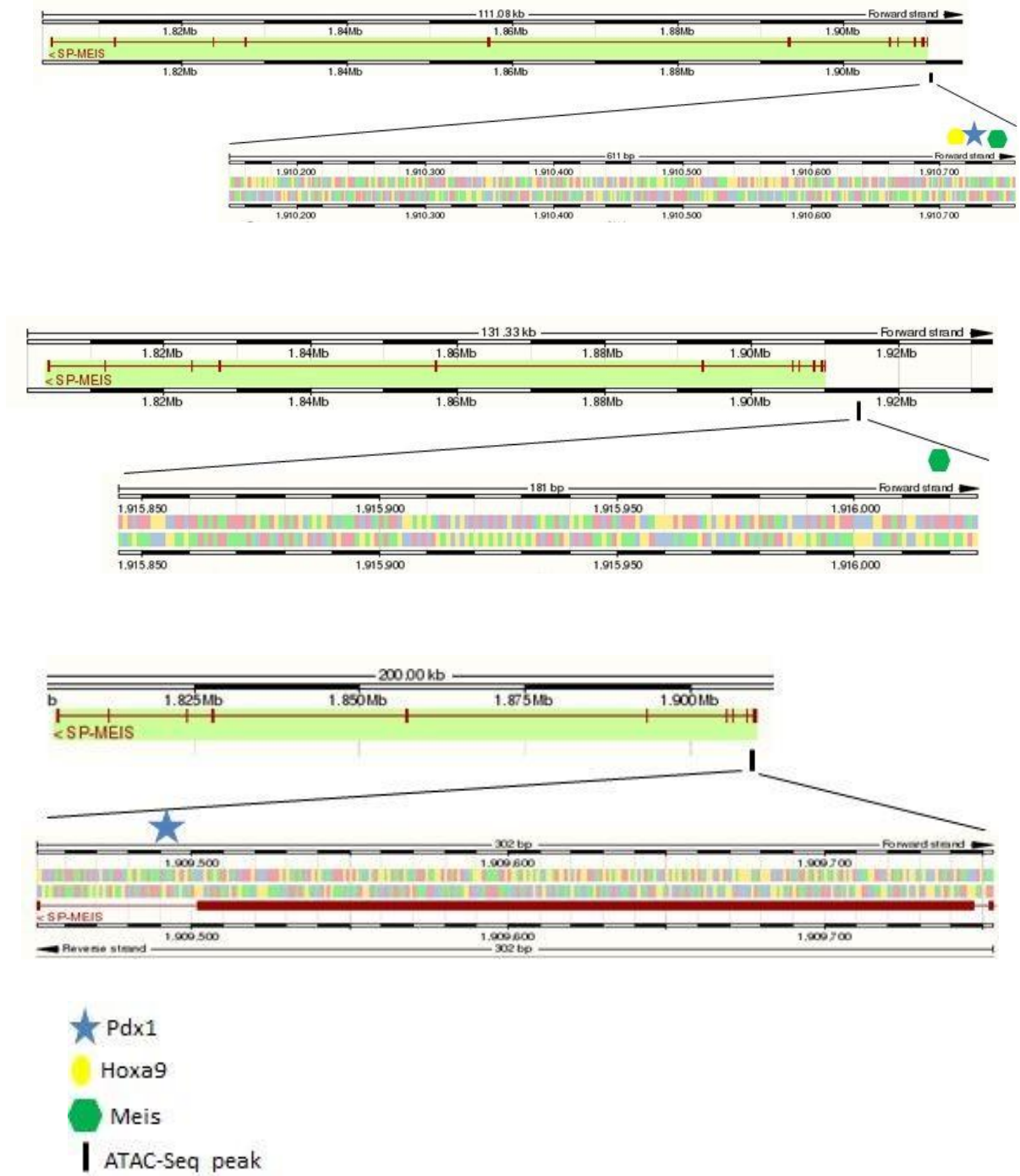
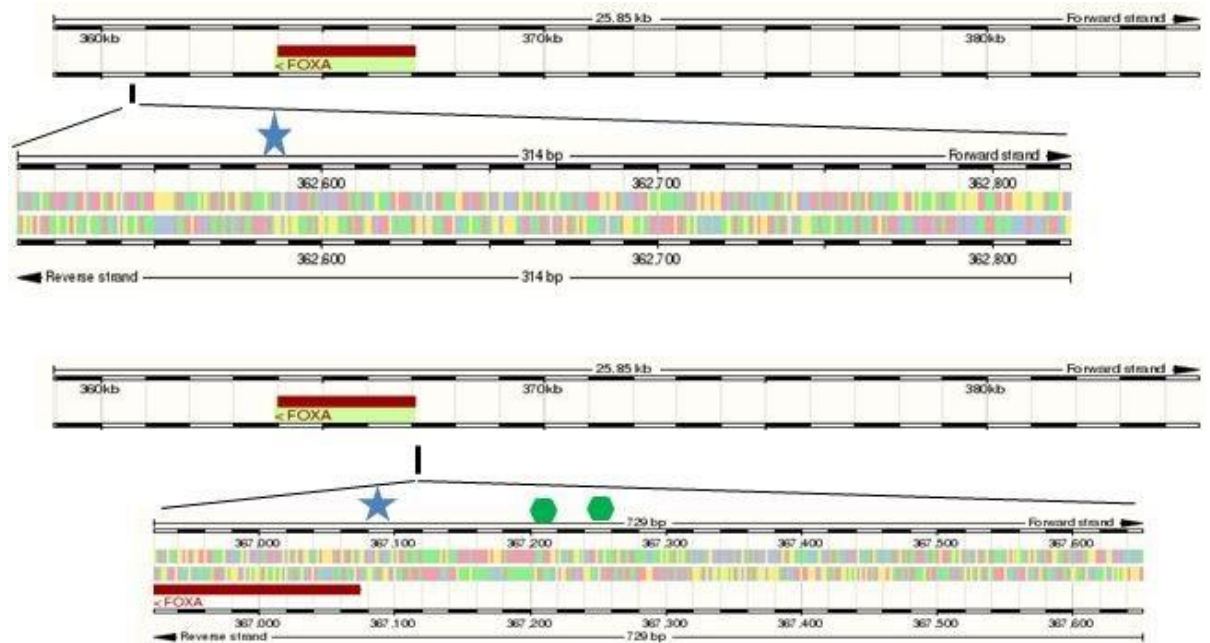


Fig.4.3 ATAC-Seq analysis around the *Sp-Meis* gene locus. Graphic representation of the in silico prediction of the transcription factor binding sites falling in the ATAC-Seq peak (610 bp, 180bp and 301 bp) at a distance of -5236 bp, -247 bp and -1098 bp from the TSS of *Sp-Meis* gene. The small black line indicates the position of the ATAC-Seq peak referred to the gene. The colored symbols correspond to the binding motifs for Sp-Hox11/13b (yellow circle), Sp-Lox (blue star) and Sp-Meis (green hexagon) proteins.

Analyzing the ATAC-Seq profile around *Sp-FoxA* gene (Fig.4.4) many peaks have been identified that contain Sp-Bra, Sp-Meis, Sp-FoxA, SpLox binding sites. In particular two peaks belong to the area of the intergenic region before the 5'-end of the gene: the first peak of 176 bp length contains Sp-FoxA binding site suggesting also for this gene an autoregulation; the second peak of 243 bp length contains Sp-Meis binding domain. A third peak of 696 bp length included in the promoter region of the gene shows the binding motifs for Sp-Lox, Sp-Meis and Sp-Bra. The latter has two binding sites very close each other suggesting the possibility that two Bra proteins co-interact for the binding to the Sp-FoxA promoter. An extra peak of 313 bp lays in the 3'-end of Sp-FoxA gene and contain a single binding site for Sp-Lox. A last peak of 728 bp overlaps the first exon of the gene and its region at the 5'-end. It contains a specific binding region for Sp-Lox and two binding sites for Sp-Meis.



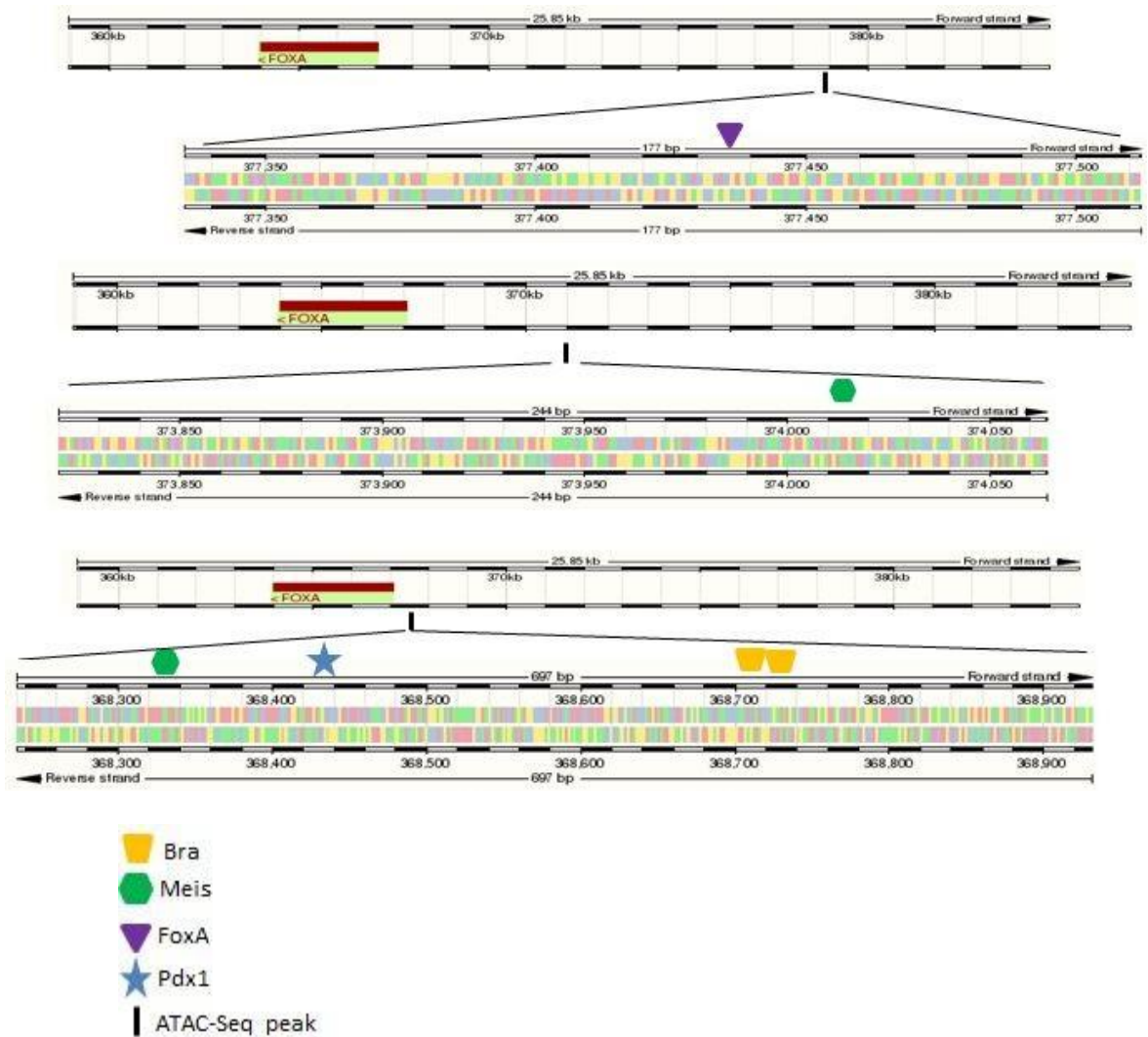


Fig.4.4 ATAC-Seq analysis around the *Sp-FoxA* gene locus. Graphic representation of the in silico prediction of the transcription factor binding sites falling in the ATAC-Seq peak (176 bp, 243 bp, 696 bp, 313 bp, 728 bp length) at a distance of -9673 bp, -6191 bp, -832 bp, 464 bp, 5085 bp from the TSS of *Sp-FoxA* gene. The small black line indicates the position of the ATAC-Seq peak referred to the gene. The colored symbols correspond to the binding motifs for Sp-Bra (yellow trapezoid), Sp-Meis (green hexagon), Sp-FoxA (violet diamond) and Sp-Lox (blue star) proteins.

The ATAC-Seq peaks for *Sp-Hox11/13b* (Fig. 4.5) are either included in the promoter region or in the unique intron of the gene. The first analyzed peak of 868 bp contains two binding motifs for Sp-Hox11/13b and two for Sp-Cdx. The autoregulation of *Sp-Hox11/13b* and its interaction with Sp-Cdx have been already predicted by (Rossella Annunziata et al. 2014) and are now confirmed by the ATAC analysis. Two peaks of 492 bp and 113 bp falling within close regions of

the intron contain specific sequences for two Sp-Meis and one Sp-Lox binding in first peak and one Sp-Meis binding in the second peak.



Fig. 4.5 ATAC-Seq analysis around the *Sp-Hox11/13b* gene locus. Graphic representation of the in silico prediction of the transcription factor binding sites falling in the ATAC-Seq peak (868 bp, 492 bp, 113 bp length) at a distance of -75 bp, 5093 bp, 6450 bp from the TSS of *Sp-Hox11/13b* gene. The small black line indicates the position of the ATAC-Seq peak referred to the gene. The colored symbols correspond to the binding motifs for Sp-Hox11/13b (yellow circle), Sp-Cdx (red triangle), Sp-Meis (green hexagon) and Sp-FoxA (violet diamond) proteins.

The analysis of the ATAC-profile for *Sp-Nr1m3* (Fig. 4.6) gene has allowed to reveal specific binding regions for Sp-Hox11/13b, Sp-Lox and Sp-Cdx proteins. Both the identified peaks belong to the intergenic region before the 5' end of the

gene and have a length of 192 bp and 706 bp. The biggest peak contains a 10 bp sequence that is recognized by both Sp-Lox and Sp-Hox11/13b proteins. This overlap can be interpreted as a competition between Sp-Lox and Sp-Hox11/13b in the binding of *Sp-Nr1m3*, according to which if Sp-Lox already occupies the specific region Sp-Hox11/13b can not bind to it and viceversa. Another explanation can be due to a mistake in the prediction of the TF binding motifs, since most of the sequences specific for TFs have been validated in vertebrate species and considered conserved outside the vertebrate for the important role that the protein has in the interaction with the target gene. However, as already explained, each TF has modularity, so it can act as gene transcriptional regulator using a secondary binding motif, less conserved among species and alternative to the primary motif, for the DNA binding. In this case, Hox11/13b can possess a secondary motif in the Sp-Nr1m3 without competing with Sp-Lox for its regulation. The second peak that is closer to the gene shows the same situation: a binding region of 12 bp can be bound by both Sp-Hox11/13b and Sp-Cdx. The interactions among Sp-Lox, Sp-Cdx and Sp-Hox11/13b, all homeodomain proteins, with *Sp-Nr1m3*, that codifies for a nuclear hormone receptor, does not surprise. In fact, it has been already demonstrated by several studies in other species that nuclear hormone receptors and Hox and ParaHox genes are often partners in regulating gene expression during development (Yussa et al. 2001) (Srinivasan et al. 2010) (Wightman et al. 2005) (Osborne et al. 2009). Maybe the most plausible interpretation of the presence of one binding motif for two different TFs in both the identified peaks is related to the nuclear receptor Sp-Nr1m3 that first interacts with one homeobox protein (for example Sp-Cdx, Sp-Lox or Sp Hox-11/13b) and the complex nuclear receptor-homeobox protein increases the specificity of the binding to another homeobox gene to regulate its expression.

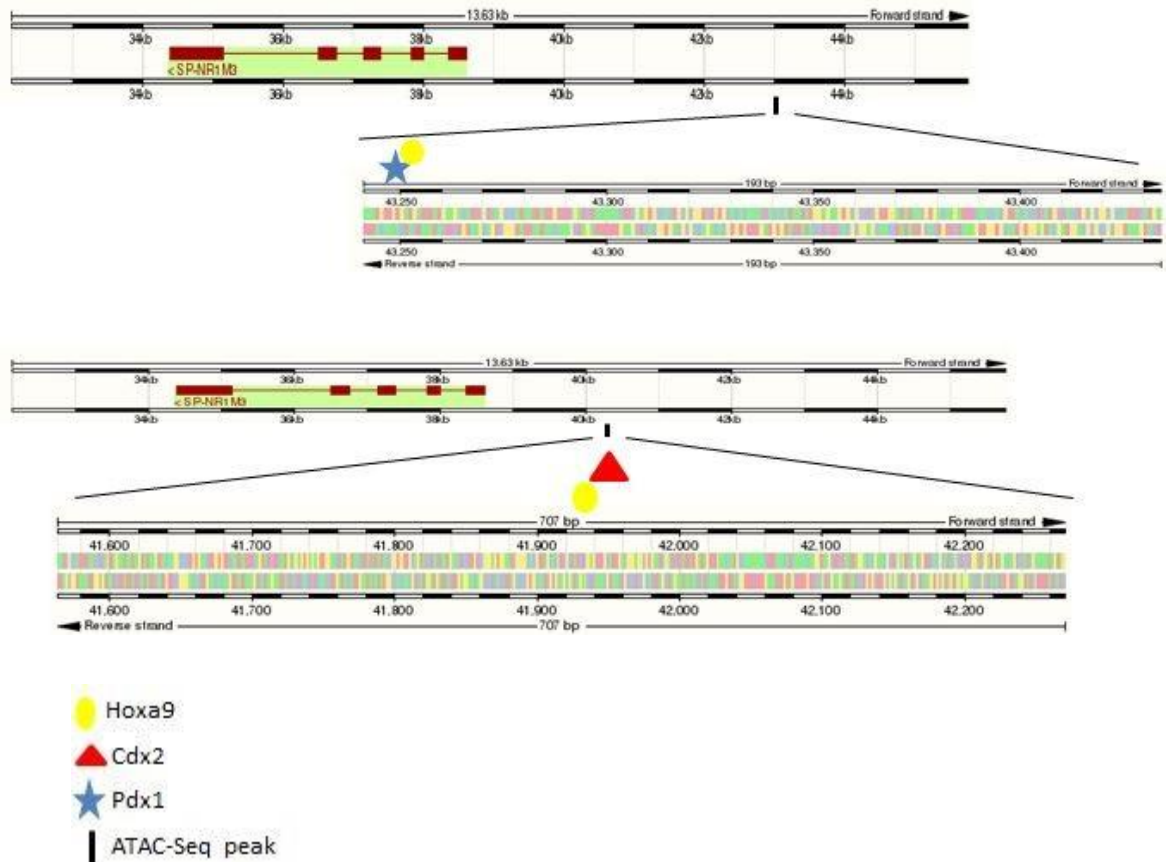


Fig.4.6 ATAC-Seq analysis around the *Sp-Nr1m3* gene locus. In silico prediction of the transcription factor binding sites falling in the ATAC-Seq peaks (192 bp and 706 bp) at a distance of -4560 and -3139 bp from the TSS of the *Sp-Nr1m3* gene. The vertical black line indicates the position of the ATAC-Seq peak referred to the gene locus. The colored symbols indicate the position of the predicted binding motifs for Sp-Cdx (red triangle), Sp-Hox11/13b (yellow circle) and Sp-Lox (blue star) within the 192 and 706-long sequence corresponding to the ATAC peaks.

The ATAC-Seq analysis for *Sp-Ets4* gene (Fig.4.7) revealed only one peak of 690 bp falling in the promoter region of the gene. The peak contains two distant binding sites for Sp-Lox and two consecutive binding sites for Sp-FoxA. These latter suggest the possibility for Sp-Lox to work as dimers for the binding to *Sp-Ets4* or the necessity of two Sp-Lox proteins to reinforce the regulation of the gene expression.

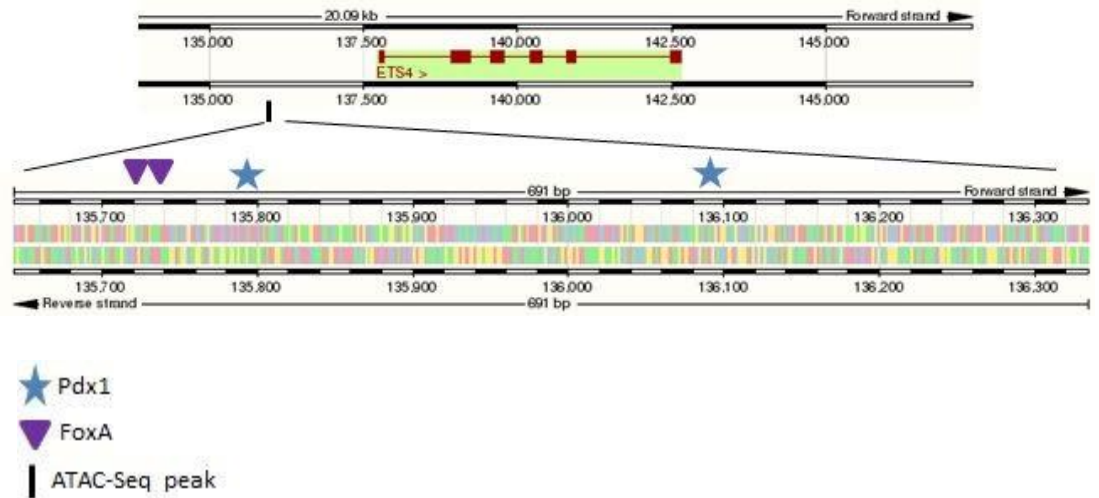


Fig.4.7 ATAC-Seq analysis around the *Sp-Ets4* gene locus. In silico prediction of the transcription factor binding sites falling in the ATAC-Seq peak (690 bp) at a distance of -189 bp from the TSS of the *Sp-Ets4* gene. The vertical black line indicates the position of the ATAC Seq peak referred to the gene locus. The colored symbols indicate the position of the predicted binding motifs for Sp-Lox (blue star) and Sp-FoxA (violet diamond) within the 690 bp-long sequence corresponding to the ATAC peak.

Analyzing ATAC profile for *Sp-Bra* gene (Fig. 4.8) two peaks, one in the promoter region and one in the third region of the gene, have been found with a length of 889 bp and 410 bp, respectively. The peak included in the regulatory region of the gene contains binding sites for Sp-Lox and for Sp-FoxA. The peak inside the intron, instead, contains two distant binding site for Sp-Cdx, one of which overlap with the one for Sp-Hox11/13b. Since enhancers for transcriptional gene regulation can lay other in the proximity of the promoter or far from it at both 5'-end and 3'-end, as well as in exon or intron of adjacent genes, the binding motifs within *Sp-Bra* intron do not necessary belong to *Sp-Bra* regulatory complex, but can also be necessary to the regulation of gene expression of a close gene.

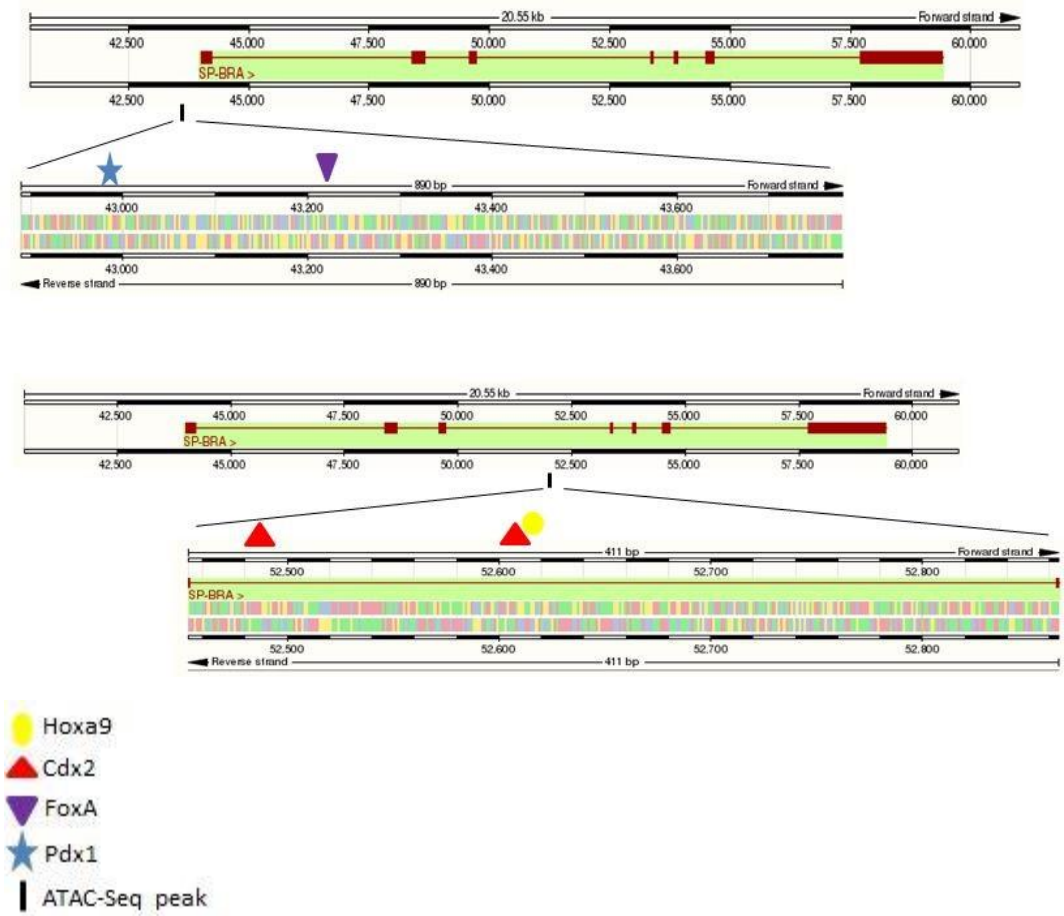


Fig.4.8 ATAC-Seq analysis around the *Sp-Bra* gene locus. In silico prediction of the transcription factor binding sites falling in the ATAC-Seq peaks (889 bp and 410 bp) at a distance of 35 bp and 9360 bp from the TSS of the *Sp-Bra* gene. The vertical black line indicates the position of the ATAC-Seq peak referred to the gene locus. The colored symbols indicate the position of the predicted binding motifs for Sp-Lox (blue star), Sp-FoxA (violet diamond), Sp-Cdx (red triangle) and Sp-Hox11/13b (yellow circle) within the 889 and 410 bp-long sequences corresponding to the ATAC peaks.

The ATAC-Seq approach has allowed to identify the putative TFs binding motifs of the misexpressed genes identified in the RNA-Seqs looking at the entire region inside and around the gene body. Before this analysis, experiments with morpholinos microinjection (R. Annunziata and Arnone 2014) (Cole et al. 2009) predicted some of the nodes in which Sp-Lox and Sp-Cdx proteins are involved in the GRN gut differentiation, without, however, having the possibility to analyze whether they are direct or indirect. ATAC-Seq permits to make a truthful prediction

of the direct and indirect interactions based on the finding of TF binding sites inside the regulatory regions of the genes. The combination of the data coming from the ATAC-Seq and the Sp-Lox and Sp-Cdx putative target genes revealed by the RNA-Seq data has allowed to depict a preliminary GRN around these two transcription factors for the late gastrula and pluteus sea urchin embryos, as described in the next paragraph.

4.2.2 Genome-wide analysis of DNA-protein interactions involved in regulation of gene expression during gut differentiation in the sea urchin embryo

The generation of differential transcriptomics for late gastrula, prism and pluteus stages after Sp-Lox and Sp-Cdx perturbation experiments defined the complete set of genes under the direct or indirect control of these proteins. Among the affected elements, I could identify the TFs that I have taken into account for the reconstruction of the sea urchin GRN. However, the RNA-Seq approach alone does not tell much about the physical gene-protein interactions occurring during the gut differentiation, but only provides a list of the actors of this process. For a further understanding of the mechanism of gut specification, a second approach is required that reveals all the regulatory inputs and outputs of the genes network starting from the pool of TFs selected by RNA-Seq. The prediction of the TFs occupancy in the sea urchin chromatin at late gastrula stage and pluteus stage by analysis of the ATAC-Seq profile for the TF genes affected by Sp-Lox and Sp-Cdx knockdown led me to define the active proteins and chromatin region under transcriptional regulation activity during sea urchin development. The combination of the two methods has allowed me to describe the gene connections around and involving Sp-Lox and Sp-Cdx defining for each gene the inputs coming from a specific protein

and the type of effect they produce, if they activate or repress the gene expression (based on the RNA-Seq analysis of this work or experimental data found in literature) and the opened chromatin regions that the protein are able to bind (predicted by ATAC-Seq).

Some gene-protein interactions have been already predicted by other studies, as the positive input of Sp-Hox11/13b on *Sp-Bra* gene and its autoregulation (Peter and Davidson 2010) or the autoregulation of *Sp-Lox* (Cole et al. 2009), helping to confirm the effectiveness of the adopted method to predict the GRN. The rest of the regulatory inputs comes out from this work integrating RNA-Seq and ATAC-Seq analysis. One of the most interesting module is the one involving Sp-Lox, Sp-Meis and Sp-Cdx. So far, functional experiments using morpholino against Sp-Lox and Sp-Cdx have only demonstrated the important role of Sp-Lox in driving *Sp-Cdx* expression and Sp-Cdx to restrict Sp-Lox transcripts to the area of the pyloric sphincter clarifying its expression from the hindgut (R. Annunziata and Arnone 2014). However, how this positive-negative feedback loop works has not been described. With this study I can add a third element to this module marking the presence of Sp-Meis as possible mediator of Sp-Lox activity on *Sp-Cdx*. ATAC-Seq analysis have in fact demonstrated that there is any Sp-Lox binding domain in the *Sp-Cdx* peak profile, while there is one Sp-Cdx binding site in the *Sp-Lox* gene body. These results strongly suggest that the activation of *Sp-Cdx* by Sp-Lox is not direct but mediated by Sp-Meis whose binding motif has been found in the region close to the 5'-end of *Sp-Cdx* gene. At the same time, Sp-Cdx repression activity on *Sp-Lox* transcription can be putatively due to the presence of Sp-Cdx binding sites on *Sp-Lox* regulative region and to the absence of any other TF, besides Sp-Lox itself, that shows a negative input on *Sp-Lox* at the analyzed developmental stage. The Sp-Cdx input on *Sp-Cdx* gene at 72 hpf also requires to be mentioned. I can speculate that at pluteus stage (72 hpf) when Sp-Lox is now restricted to the pyloric

sphincter region, *Sp-Cdx* occupies the entire hindgut and the transcription of its gene by Sp-Cdx protein is necessary to maintain its expression in absence of Sp-Lox and Sp-Meis activity in the same region.

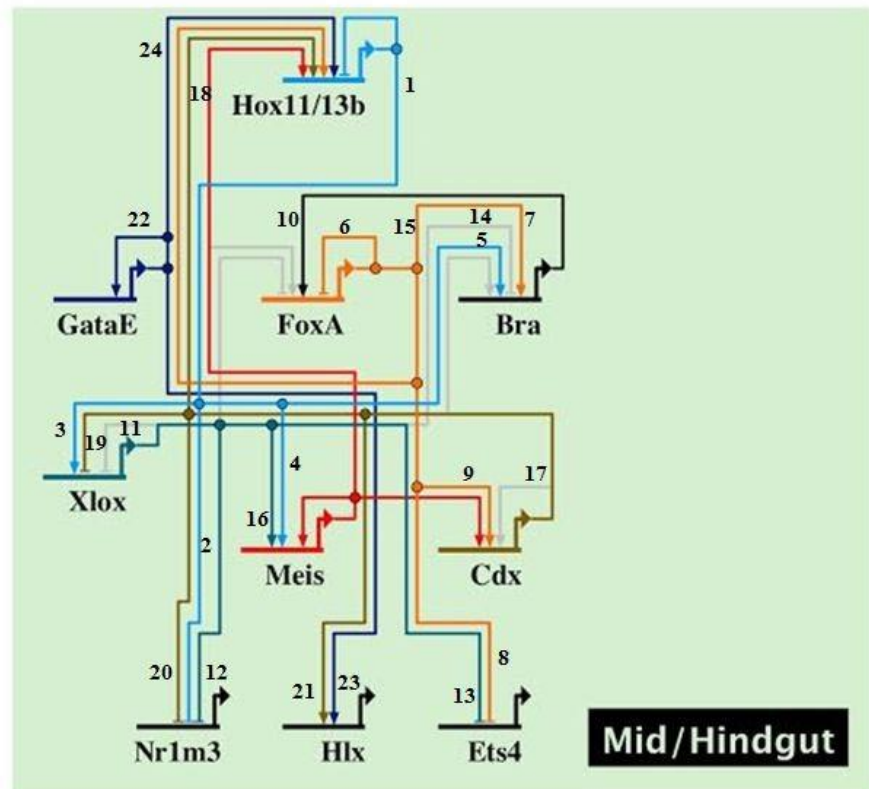


Fig. 4.9. Schematic representation using Biotapestry (<http://www.biotapestry.org/>) of the main identified TF inputs of the TFs at sea urchin 48 hpf and 72 hpf. Inputs coming from the same gene are shown with one colored line. The arrow at the end of the line indicates a positive input. The horizontal bar at the end of the line indicates a negative input. The grey line indicates inputs active at 72 hpf. Each interaction is numbered and specified how it was predicted in the Table4.1.

Although demonstrating the efficiency of the RNA-Seq/ATAC-Seq combinatory method to confirm known gene-protein interactions and to reveal new nodes of the GRN, however for all the predicted interactions validation experiments, such as knockdown functional experiments and *cys*-regulatory analysis, and spatial and temporal characterization, are required.

Table 4.1. List of the TFs inputs in the sea urchin gut at 48hpf and 72 hpf. The TFs inputs identified by RNA-Seq, ATAC-Seq, ChIP-PCR and functional analysis experiments. are summarized. The numbers in parenthesis refer to the gene connection illustrated in the Fig.4.9.

Gene	TF input	Experiment	Reference
Hox11/13b (1)	Hox11/13b	MASO functional experiment	Peter. & Davidson (2010)
Nr1m3(2), Lox (3), Meis (4)	Hox11/13b	Differential RNA-Seq/ ATAC-Seq	This work
Bra (5)	Hox11/13b	MASO functional experiment	Peter & Davidson 2010
FoxA (6)	FoxA	MASO functional experiment/cis-regulation	Oliveri <i>et al.</i> , (2006)
Bra (7), Ets4 (8)	FoxA	Differential RNA-Seq/ATAC-Seq	This work
Cdx (9)	FoxA	MASO functional experiment	Annunziata & Arnone. (2014)
FoxA (10)	Bra	MASO functional experiment/ChIP-Seq	de-Leon and Davidson, 2010; Andrikou and Arnone, unpublished
Xlox (11)	Xlox	MASO functional experiment	Cole <i>et al.</i> , (2009)
Nr1m3 (12), Ets4 (13), Bra (14), FoxA (15)	Xlox	Differential RNA-Seq/ATAC-Seq	This work
Meis (16)	Xlox	Differential RNA-Seq/ATAC-Seq/ChIP-Seq	This work
Cdx (17), Hox11/13b (18), Xlox (19)	Cdx	MASO functional experiment	Annunziata& Arnone (2014)
Nr1m3 (20), Hlx (21)	Cdx	Differential RNA-Seq/ATAC-Seq	This work
GataE (22), Hlx (23), Hox11/13b (24)	GataE	Differential RNA-Seq/ATAC-Seq	This work
Meis (25), Cdx (26)	Meis	MASO functional experiment	This work

4.2.3 The *Meis* gene

Meis gene (myeloid ecotropic viral integration site homologue) (Moskow et al. 1995) is an homeodomain transcription factor able to form heterodimers and heterotrimers with different Hox genes. In fact, Hox proteins usually do not bind alone to enhancers or promoter regions, but the specificity of the binding to the DNA is frequently dependent on interactions with other DNA-binding proteins which act as Hox cofactors. These include the PBC and MEIS classes of TALE (Three Amino acid Loop Extension) homeodomain proteins (Rezsohazy et al. 2015). Hox-TALE complexes are also found in the sea anemone *Nematostella* (Ferrier 2014) which does indicate an ancient role for these TALE proteins. Assembly of the Hox-TALE complex typically involves one TALE protein—a PBC/Pbx protein—binding to a hexapeptide motif (HX) in the Hox protein. It has been shown that the four murine *Meis* gene together with the *Drosophila homothorax* gene and the murine *Prep-1* (*Pbx regulating protein-1*) directly bind the PBC proteins. In *Drosophila Exd* (*extradenticle*), the single representative of the PBC class in *Drosophila*, is required for proper Hox protein activity (Peifer and Wieschaus 1990). In mouse, the genomic distribution of *Meis* proteins overlaps with those of *Hoxc9* and *Hoxa2* (Penkov et al. 2013). A *Hoxb1*-Pbx-*Meis* complex plays a role in controlling *Hoxb1a* transcription in zebrafish (Choe et al. 2009). *Meis* gene is involved in many processes of animal development. It controls patterning and cell differentiation in the developing nervous system of vertebrates (Shim et al. 2006) (Sánchez-Guardado et al. 2010), as well as in *Drosophila* (Kurant et al. 1998) and *C. elegans* (Potts, Wang, and Cameron 2009). Expression of *Meis* is also associated to morphogenesis and specification of the developing eye (Hisa et al. 2004) (Bumsted-O'Brien et al. 2007), and the developing inner ear (Sánchez-Guardado et al. 2010). In addition, *Meis* expression influences early

patterning in several organs, such as liver, lungs, and kidney (Hisa et al. 2004). Finally, *Meis* has been implicated in the development of murine myeloid leukaemia (Knoepfler et al. 1997; Moskow et al. 1995) and neuroblastoma.

4.2.4 *Sp-Meis* temporal and spatial expression.

The important role that *Meis* has in many biological processes of several organisms as well as its important role as Hox-cofactor has led me to investigate the role of *Sp-Meis* in the sea urchin gut and its activity as putative cofactor of *Sp-Lox*, a gene of the ParaHox family, considered evolutionarily related to the Hox family. In order to characterize *Sp-Meis* gene, I have first checked its temporal expression during sea urchin development. Looking at the transcriptome data available on the echinoderm genomic database (<http://www.echinobase.org/Echinobase/>) and here represented by chart (Fig. 4.10) *Sp-Meis* maternal transcripts are stable in the sea urchin zygote until early blastula (18 hpf). At blastula stage (24 hpf), *Sp-Meis* starts to be actively transcribed by the embryo and the number of transcripts progressively accumulates until pluteus stage (72 hpf), reaching their maximum concentration at late gastrula stage (48 hpf).



Fig. 4.10. Temporal expression profile of *Sp-Meis* gene. Transcripts accumulation expressed as number of transcripts/embryo of *Sp-Meis* gene during sea urchin development (hpf).

For a further characterization of *Sp-Meis* gene I have checked the territories where its transcripts are expressed at late gastrula and prism stages (the same stages chosen for the RNA_Seq experiments) by performing whole mount *in situ* hybridization (WMISH) experiments. In order to clone *Sp-Meis* gene from the sea urchin genome I have designed four different sets of primers (sequences in material and methods) amplifying the coding and a small piece of non coding region of the gene. The inclusion of the non coding region has helped to amplify fragments of the right size for the riboprobe synthesis. The cloned fragments have been used to generate four DIG/FLUO labeled antisense riboprobes directed against different regions of the *Sp-Meis* transcripts. All the riboprobes have been hybridized together to the *Sp-Meis* transcripts, in order to increase the sensitivity of the signal, due to the low expression of *Sp-Meis* in the sea urchin embryo. The embryos have been contemporary hybridized with the same riboprobes transcribed as sense compared to the RNA of the gene, in order to demonstrate the specificity of the antisense riboprobes. The results of the WMISH experiment (Fig.4.11) show an ubiquitous expression of *Sp-Meis* transcripts at all the analyzed developmental stages. The missed detection of a specific territory of expression of *Sp-Meis* can be related to a low sensitivity of the adopted method. At all the chosen developmental stages the number of transcripts is very low compared to the number of cells that constitute the entire embryo. Late gastrula, in fact, is made up of around 1000 cells and prism even more, and the number of *Sp-Meis* transcripts at these stages is 253 and around 251, respectively. This means that if *Sp-Meis* is expressed in more cells of the gut, the number of transcripts for each cell might be not enough to be detected by hybridization with a labeled riboprobe. The sense riboprobes, instead, have not been able to bind any transcripts and the embryos look without any staining.

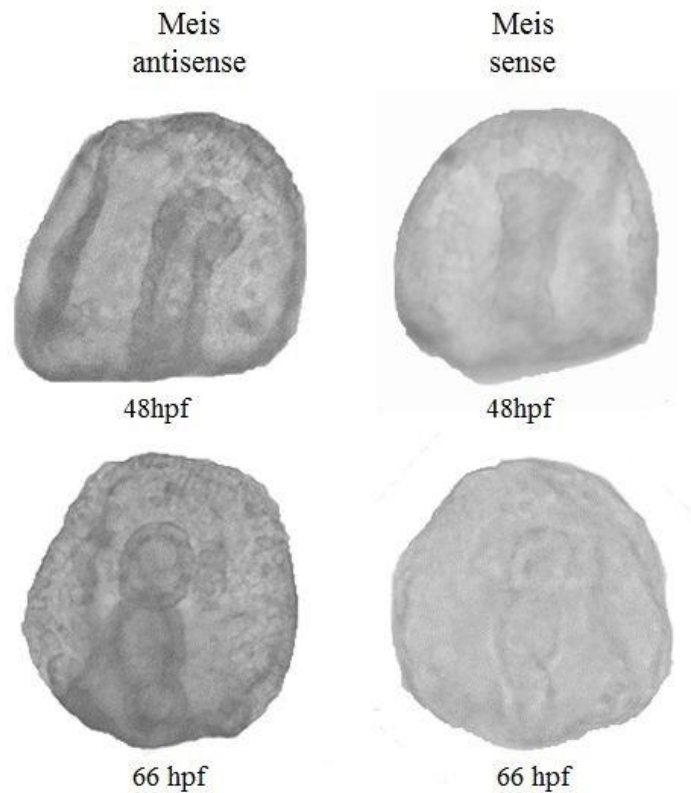


Fig. 4.11. WMISH experiment using *Sp-Meis* antisense and sense riboprobes. Late gastrula and prism sea urchin embryos hybridized with four different antisense riboprobes show ubiquitous localization of *Sp-Meis* transcripts. The same embryos hybridized with four antisense riboprobes appear clear.

4.2.5 Sp-Meis functional characterization

The combination of the RNA-Seq and ATAC-Seq analyses has revealed the activity of *Sp-Meis* as putative activator of *Sp-Cdx* expression under *Sp-Lox* control. In order to verify this connection and its general role in the sea urchin gut specification process, I have perturbed embryos with antisense nucleotide morpholino (MASO) designed against the translation start site of *Sp-Meis*, in order to prevent the synthesis of its protein by steric

hindrance. Sea urchin zygotes have been injected with 300 μ M of Sp-Meis MASO, the embryos have been led to develop until late gastrula keeping the temperature at 15°C and the phenotype observed under optical microscope. The MASO perturbation has shown a severe effect on the embryo gastrulation, since the cells have invaginated through the blastopore, but the archenteron could not elongate (Fig. 4.12).

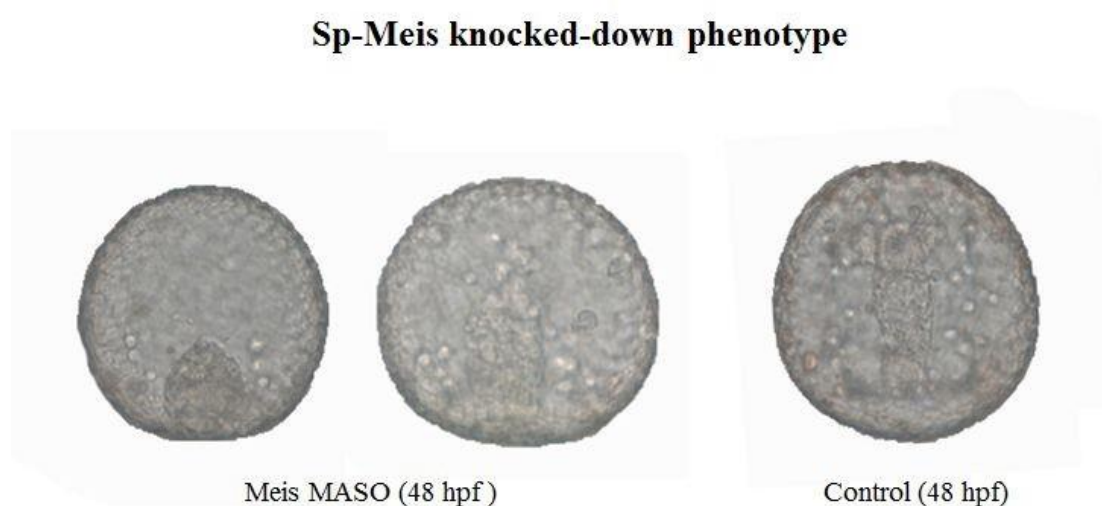


Fig. 4.12. *Sp-Meis* knocked-down embryos. Comparison of the phenotype of the sea urchin late gastrula (48 hpf) *Sp-Meis* knocked down embryos and wild type. In the perturbed embryos the archenteron does not elongate. All the embryos have been snapped in frontal view.

The effects of *Sp-Meis* morpholino have been examined at the molecular level by checking the expression of the genes of the predicted gut gene network by quantitative real time PCR (Q-PCR) (Fig. 4.13). Two independent injection experiments have been performed and several late gastrula embryos have been collected for RNA extraction and cDNA synthesis. For each gene tested, results are indicated as fold-differences in the transcript levels between experimental and control embryos. The strongest evidence is the dramatic reduction of *Sp-Cdx* expression after *Sp-Meis* knock-down. This result clearly supports our prediction of

Sp-Cdx activation by *Sp-Meis* regulatory activity. Besides, the regulation of *Sp-Meis* transcription under *Sp-Meis* protein, that has been predicted by ATAC-Seq, is also confirmed by Q-PCR observing a reduction of *Sp-Meis* transcripts under the effects of the morpholino. At the same time, *Sp-Lox* weakly reduces its expression as consequence of *Sp-Cdx* downregulation. I would expect that at later stages, when *Sp-Cdx* transcripts are normally highly expressed in the wild type embryos, *Sp-Lox* transcripts undergo a stronger reduction due to the major effects that *Sp-Cdx* missed protein has on the regulation of its gene. The remaining genes *Sp-FoxA*, *Sp-Nr1m3*, *Sp-Hox11/13b*, *Sp-GataE*, *Sp-Ets4* and *Sp-Bra* do not show significant changes in their expression in the perturbed conditions.

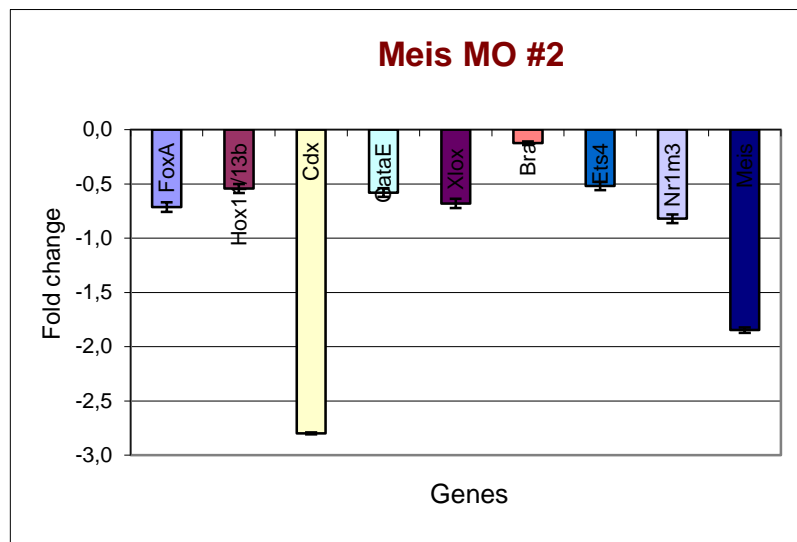
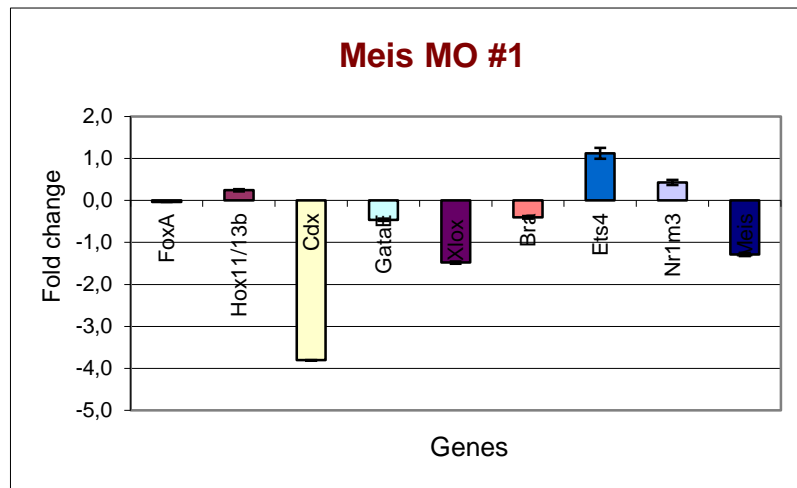


Fig. 4.13. Q-PCR analysis of gene expression in Sp-Meis morphants. Graphical representation of Q-PCR results, columns represent average values calculated between all the results of three technical replicas. Error bars indicate standard deviations.

4.2.6 Validation in trans of *Sp-Meis* node: ChIP analysis

The only prediction by ATAC-Seq of the presence of Sp-Lox binding sites in the regulatory region of *Sp-Meis* gene does not demonstrate the real occupancy of the TF on the chromatin region. In order to verify the physical binding of Sp-Lox protein to the DNA region I have taken advantage of the Chromatin immunoprecipitation (ChIP) approach to immunoprecipitate sea urchin chromatin with specific antibody designed against Sp-Lox protein that was already available in the lab. Approximately 100,000 embryos dissociated in cells and fixed smoothly have been sonicated generating DNA fragments averaging 200 bp in length (150-350 bp) (Fig. 4.14).

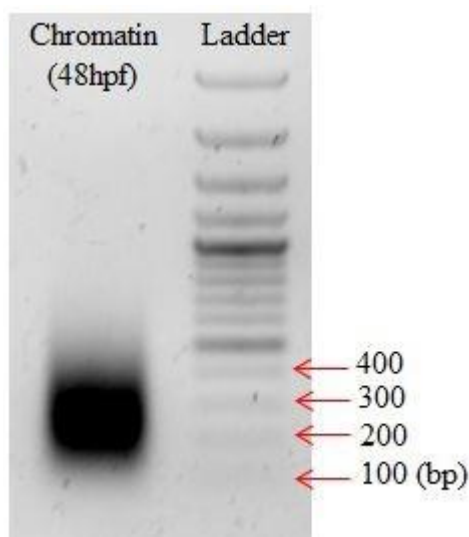


Fig. 4.14. Sheared chromatin of 48 hpf sea urchin embryos. Chromatin after sonication showing a fragment range between 150-350bp. Ladder used: 100-1500bp.

Immunoprecipitations (IPs) have been then performed, in late gastrula stage embryos, by adding 30 μ l of Sp-Lox antibody and 30 μ l of pre-immune serum, as negative control. The pre-immune serum possesses all the IgG normally present in the immune system of the animal before its immunization with Sp-Lox protein, so it is not enriched with antibodies against Sp-Lox. Input chromatin has been used as

positive control since it has not been immunoprecipitated with any antibody. Input chromatin contains certain trace amount of DNA retrieved from ChIP assay, which may or may not be correlated with the analyzed regulatory region.

In order to validate the IP efficiency, the DNA of Sp-Lox immunoprecipitated chromatin (IP Lox), pre-immune serum immunoprecipitated chromatin (IP pre-immune serum) and Input have been analyzed by Q-PCR. To this aim, specific primers for Sp-Lox binding site in the *Sp-Meis* intron (Fig.4.14) and some random intergenic ones to be used as a negative control have been designed. The QPCR results show no change in the amount of DNA amplifying the Input with both Meis and Intergenic primers. However, a difference in the Ct (number of cycles required for the fluorescent signal to cross the threshold), has been observed when I amplify IP Lox with the same two sets of primers. The amplification of IP Lox with Meis primers shows a higher concentration of DNA compared to the amplification with Intergenic primers. This demonstrates that when I do immunoprecipitate chromatin with anti Sp-Lox specific antibody there is an enrichment of *Sp-Meis* gene region.

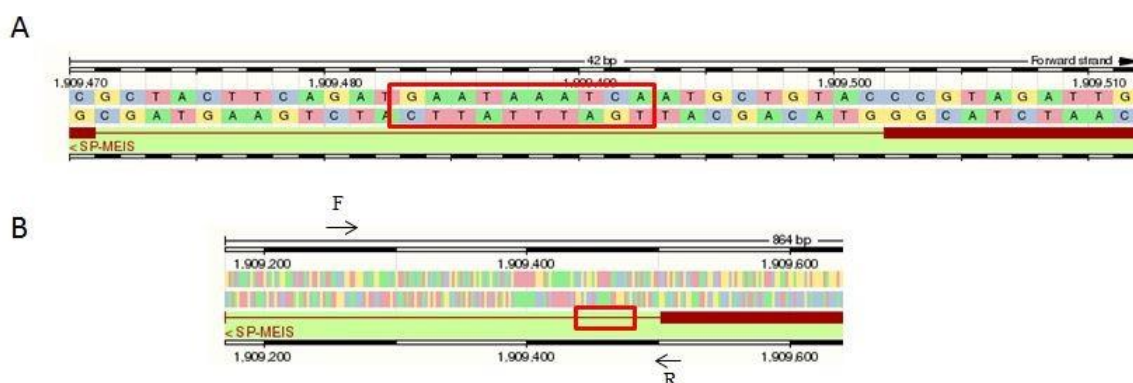


Fig 4.15. Sequence of Sp-Lox binding site in the Sp-Meis intron and primers position. **A** Sp-Meis gene sequence downloaded from <http://metazoa.ensembl.org/index.html> showing Sp-Lox binding site (red rectangle) in the first intron of the gene. **B** Forward (F) and reverse (R) primers position, indicated with black arrows, within Sp-Meis gene body amplifying a region of 191 bp that includes Sp-Lox binding site.

The Ct values obtained from the Q-PCR experiments have been also used to calculate the fold difference between IP_{Lox} and IP pre-immune serum. Q-PCR analysis has revealed a 16,34 fold enrichment of *Sp-Meis* gene immunoprecipitated with Sp-Lox compared to the one immunoprecipitated with Pre-immune serum. The enrichment obtained by pre-immune serum IP is due to the nonspecific binding of the IgG to Sp-Lox protein, also related to the high amount of serum used for the IP. However, the considerable fold difference between IP-Lox and IP-pre immune serum suggests the presence of Sp-Lox protein on *Sp-Meis* gene, revealed by specific binding of anti Sp-Lox antibody.

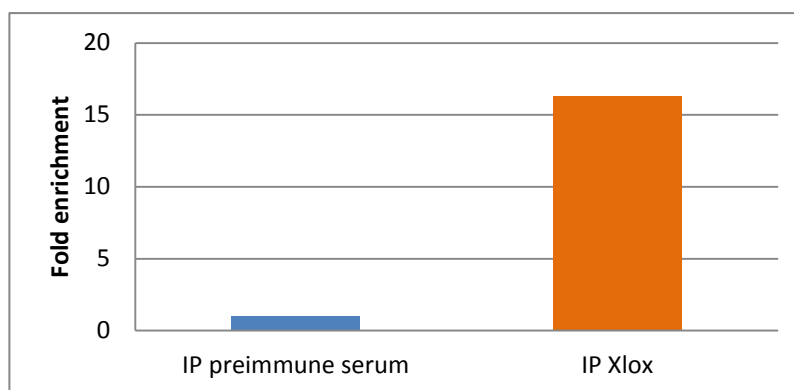


Fig. 4.16 Histogram of fold enrichments of *Sp-Meis* gene after immunoprecipitation with anti *Sp-Lox* antibody and pre-immune serum.

4.3 Conclusions

The generation of the RNA-Seq datasets has allowed to identify putative target genes acting downstream of Sp-Lox and Sp-Cdx, without, however, giving any information about how they interact in the sea urchin gut. Approaching to the ATAC-Seq technique has been useful to predict the occupancy of the predicted TFs on the regulatory regions of the genes of the network. This has led me to partially reconstruct the gene-proteins interactions occurring at late gastrula and pluteus stages of the sea urchin gut, taking into account the most affected transcription factors under Sp-Lox and Sp-Cdx knock-down revealed by the RNA-Seq. In this way, some of the interactions already predicted and, in some cases, validated by previous works have been confirmed and new ones have been revealed, demonstrating the efficiency of the combinatorial RNA-Seq/ATAC-Seq method. Moreover, a new important gene of the network, *Sp-Meis*, has been discovered as key element mediating the regulatory activity of Sp-Lox on the *Sp-Cdx* gene. Given the importance of *Sp-Meis* in this central node, its expression in the gut has been assessed and its functional activity in the network has been analyzed. Functional knock-down experiments followed by Q-PCR analysis have demonstrated its fundamental role in regulating *Sp-Cdx* expression and, consequently, *Sp-Lox*, besides having an autoregulatory activity. Finally, the validation of the interaction between Sp-Lox protein and *Sp-Meis* gene has been achieved with ChIP analysis, demonstrating a physical binding of the protein to the DNA region.

All the generated data have allowed to reach further information on the mechanism of the gut specification, permitting to identify the key transcription factors of the network and the putative interactions occurring in the sea urchin gut.

CHAPTER 5

DISCUSSION

5.1 Conservation and divergence between the sea urchin and sea stargut GRNs

Since Darwin's theory on natural selection and Haeckel assumption that ontogeny recapitulates phylogeny, evolutionary biologists have always been trying to explain the origin of animal diversity. How organisms, passing through the same embryonic developmental processes starting with a zygote formation, can differentiate in different body plans has always been the central biological question in the evolutionary field. Nowadays, it is clear that the key to understand such animal diversity lays in the study of the molecular mechanisms underlying animal development, because alteration of their organization causes changes in body shape and, consequently, evolution of new animal forms. At the beginning of the 19th century, Evolutionary Developmental Biology has arose with the purpose to shed light on the basic mechanisms driving body formation, studying the changes occurred in animal structure over evolutionary time. The main task of this field is to answer the question of how embryonic development is controlled at the molecular level and how the evolution of developmental processes affects the phenotype. One way to attempt this is to analyze the GRN that establishes specific regulatory states in the spatial domain of the developing organism, studying the genes involved in

the developmental mechanisms and their functions to understand what makes one organism different from another. It has been widely demonstrated, in fact, that random mutations in the genes composing the network can have drastic effects on the animal development and consequently causes evolution (Eric H. Davidson and Erwin 2006) (Erwin and Davidson 2009) (Erwin and Davidson 2009; Eric H. Davidson and Erwin 2010). Based on this, conservation of morphological features implies retention of ancestral developmental GRN features. Among the mechanisms that contribute to the adaptive radiation, through which organisms diversify rapidly from an ancestral species into a multitude of new forms, there is the phenomenon of co-option (True and Carroll 2002). Genes can be co-opted to generate developmental and physiological novelties by changing their patterns of regulation, the functions of the proteins they encode or both. This can be easily achieved within a GRN which is made of regulatory subcircuits. The modularity of the network makes possible to adapt a single gene or one entire subcircuit to a new background producing new phenotype. The evolution of a GRN (Peter and Davidson 2011b) can occur through changes in the protein regulators and by changes to the sequence of the regulatory DNA, but *cis*-regulatory DNA changes are more prevalent and occur more rapidly, as reviewed in (Gregory A. Wray 2007). However to understand the phenomenon of co-option and how it creates novelty is necessary to have a clear knowledge of the specification, differentiation and morphogenesis mechanisms that a network of genes drive in a cell territory (Levine and Davidson 2005) in order to understand how they change during evolution. The comparison of the GRN among different species has resulted efficient for this type of studies. Evolutionary developmental biology tackles the problem of understanding evolution from development by comparing the development of one organism to another, through the analysis of GRNs, and looking at the ancestral relationship between them. Echinoderms have been

demonstrated to be a powerful model system for comparative evo-devo studies, as reviewed in (Hinman and Cheate Jarvela 2014), for their morphological diversity and the possibility to perform regulatory analysis to construct GRNs (Hinman et al. 2003) (Röttinger, Dahlin, and Martindale 2012) (E. H. Davidson 2002) (Oliveri, Tu, and Davidson 2008) (Peter and Davidson 2010) (Rafiq, Cheers, and Ettensohn 2011). Moreover, the conserved patterns of early development and the few distinct evolutionary differences and novelties make them a more simple tool for the study of the GRN evolution. This potential has been already well illustrated by the comparison of the GRNs controlling endomesoderm specification in sea urchins and sea stars (Hinman et al. 2003) (Hinman and Davidson 2007) (Hinman, Nguyen, and Davidson 2007). Besides, the concept of rewiring of GRN has been demonstrated with several studies using echinoderms as model system, as reviewed in (Maria Ina Arnone, Andrikou, and Annunziata 2016). Two examples are also here described. A recent study has demonstrated that major differences in GRN architecture for larval skeletogenesis exist between sea urchins and brittle stars, the only two echinoderm classes which display an elaborated larval skeleton. In the *Amphiura filiformis*, the initiation of the specification network subcircuit with the *pmar1/hesc* double negative gate, that operates in sea urchin, undergoes major changes and the expression of late regulatory genes *foxb* and *dri* is completely missed (Dylus et al. 2016). This study suggested that the GRN controlling specification of the skeletogenic lineage underwent extensive rewiring through mechanisms of gene duplication, protein function diversification, and *cis* regulatory element evolution. Another example of gene wiring plasticity is the GRN leading sea urchin esophageal muscle differentiation. This GRN involves members of TF families, such as MRFs, Six, Sox, Fox, and signaling molecules, as FGF, with known myogenic roles in vertebrates. However, no putative kernel has been so far discovered for myogenesis and the relative position of the genes often

differs within the GRNs. This study suggests that, besides the ancestral function of the elements of the sea urchin esophageal muscle GRN in muscle development, novel animal specific genes have been placed at the apex of the myogenic cascade (Andrikou et al. 2015). These examples highlight a frequent rewiring of developmental GRNs during evolution, through reorganization of the regulatory modules of which they are composed.

This thesis work has taken advantage of the potential that echinoderm systems have to answer key questions in evolution and development, in order to acquire further knowledge on the process of gut specification in the sea urchin larva and to compare it with the sea star embryo, focusing on the role that *Xlox* and *Cdx* transcription factors have in this process in both the echinoderm species. It has been already demonstrated that the gut GRN of sea urchins and sea stars highlighted differences and similarities with respect to vertebrate (Rossella Annunziata, Martinez, and Arnone 2013) with *Cdx* repressive function on *Xlox* in the intestine cells of both sea urchin and mouse embryos, *Cdx* early activation in the sea star and mouse, but not in the sea urchin, *Xlox* pancreas development and function in vertebrate and stomach differentiation function in the sea urchin, and *Xlox* role in pyloric sphincter morphogenesis in both. Moreover, the conservation of their relative expression along the antero-posterior axis of the gut in most bilaterians supports an ancestral role in gut patterning. However, the specific regulatory subcircuit in which both *Xlox* and *Cdx* are involved, how *Xlox* explicates its regulative function on *Cdx* and which are the targets of their proteins is still partially unknown in both the sea urchin and the sea star. Within this thesis work, using a differential RNA-Seq approach, I have been able to identify the complete set of genes that require *Xlox* and *Cdx* activity in the network of the sea urchin and sea star gut from when the archenteron reaches its maximum extension until the formation of a tripartite shaped gut. The ontology analysis of the complete pool of

genes that arose from the five RNA-Seq datasets (Sp-Lox MASO 48 hpf, Sp-Lox MASO 72 hpf, Sp-Cdx MASO 66 hpf, Pm-Lox MASO 66 hpf, Pm-Cdx MASO 90 hpf) reveals a common digestive function and gut development for Xlox and Cdx in both the echinoderms. In fact, the analysis of the datasets shows that the most affected processes after Xlox and Cdx repression are the lipid, protein and carbohydrate metabolism, part of the digestive activities, and the cell-cell communication process, the signal transduction mechanism, the cell cycle, the protein localization and transport, all required for embryo development. When performed the homology relationship between the two echinoderms and a third species, the vertebrate *Xenopus tropicalis*, in order to establish the number of proteins conserved, at least 450 proteins (observed in the Pm-Cdx MO experiments) corresponding to the 65% of the total number are clustered into homologous groups, while the remaining 35% of the transcripts from each experiment are species specific. All these data suggest a strong conservation of the genes coding for proteins involved in development and function of the digestive system of echinoderms, suggesting that a common toolkit of genes, shared also with vertebrates, exists and specifies the gut and its function in the two species. The ontology analysis also reveals a high number of affected TFs in both sea urchin and sea star. For the fundamental role that TFs have in gene transcriptional regulation and for their importance in the gene regulatory network, affected TFs that show a significant fold change ($\log_2 Fc > \pm 0.5$) with adjusted p-value of < 0.05 in the RNA-Seq datasets have been analyzed in more detail. While for the sea urchin is more easy to analyze the selected genes, for many of which ortholog/homologue are known helping to establish their putative role in the embryo development and for some the temporal and spatial expression profiles are also available, for the sea star the work is harder, due to the recent assembly of the genome that requires some improvements and the very few information available for the genes of this species.

The comparison of the TFs found in sea urchin and sea star identifies not so many common genes that change their expression after Xlox and Cdx knock-down. Of particular interest is the case of the comparison of the data sets obtained after Xlox perturbation in sea urchin and sea star. In fact, when comparing the homologous late gastrula stages, the number of common genes between the two datasets is very low, but when the comparison is performed using sea urchin pluteus and sea star late gastrula data sets, the number of shared affected genes increases, suggesting that while the genes of the GRN are partially conserved, their interaction are not. This leads to the hypothesis that, although the ultimate effects of the absence of these proteins is reflected in alteration of the gut development and digestive activity (as also demonstrated in (Cole et al. 2009)), however the mechanism through which the gut is specified and formed in the two species involved similar genes that are involved in different interactions, being in one case targets of Xlox and Cdx proteins, and in the other case acting upstream of their expression. The results obtained from this work can be considered as a preliminary demonstration of another, as compared to the cases above described, rewiring mechanism involving in this case the evolution of the regulatory subcircuits around Xlox and Cdx controlling sea urchin and sea star gut patterning. The next step will be to reconstruct the GRNs around Xlox and Cdx and to compare them between the sea urchin and the sea star to identify the kernel elements that didn't change during evolution and that have a key role in gut formation and patterning in these animals, as well as the intrinsic differences in the GRN accumulated during the evolution of both lineages.

5.2 The reconstruction of the *S. purpuratus* gut GRN reveals a key role of the homeobox gene *Sp-Meis*

Hox genes encode a family of transcription factors discovered for the first time in *Drosophila* (Bridges, Morgan, and Washington 1923), that are involved in the allocation of segmental identity along animal body axes. They are evolutionary conserved across distant animal phyla possessing the key information to specify diverse developmental programs. The regulation of Hox expression occurs through different inputs represented by transcriptional regulation from earlier segmentation genes (Irish, Martinez-Arias, and Akam 1989), the action of Polycomb (PcG)/trithorax (trxG) group proteins, firstly identified in *Drosophila* and known for silencing Hox genes through modulation of chromatin structure (Puro and Nygrén 1975), and cross-regulatory interactions among the Hox genes themselves (Morata and Kerridge 1982). A rigorous analysis of gene interactions and Hox expression patterns during early *Drosophila* development revealed that Hox genes are able to repress the expression of more anterior genes, a process termed ‘posterior prevalence’ (Akam 1987) (Akam 1987; Duboule and Morata 1994). A key property of Hox genes in most bilateria is their genomic arrangement in cluster, and the position of the genes within the cluster reflects their relative domain of expression along the body axis (spatial collinearity). In some taxa, an additional regulatory step keeps Hox genes globally silent and progressively activate them during development following a temporal sequence that respect gene’s position within the cluster, according to a property called “temporal collinearity” (Garstang and Ferrier 2013). Since their conservation among different taxa and their key role in specifying diverse developmental programs, Hox genes represent a valid tool to understand how the same set of developmental genes can be involved in the generation of widely diverse developmental programs.

In this thesis work, the combinatorial RNA-Seq/ATAC-Seq approach permits to establish, by prediction of protein occupancy on the DNA regulatory sequence, the putative interactions that the sea urchin TFs make during gut development. The reconstruction of the network has been performed taking into account the transcription factors of the RNA-Seq that show significant \log_2FC and that are known to be expressed in the mid-posterior gut of the sea urchin embryos. The genes for which any spatial information is available have been included in the analysis with the exception of hypothetical proteins and zinc finger genes, for which the analysis requires a much big effort. The depiction of the network has led to confirm some already studied gene-protein interactions, such as Sp-Cdx input on *Sp-Lox* gene or Sp-Bra input on *FoxA*, but also to identify new interactions and a new element of the network, the Hox gene *Sp-Meis*. Functional analysis experiments by MASO microinjection, together with Q-PCR analysis on the expression of the TFs of the depicted gut GRN, reveal the role of Sp-Meis in the transcriptional regulation of *Sp-Cdx*. The lack of Sp-Meis protein, in fact, causes a dramatic reduction of the *Sp-Cdx* transcripts. Moreover, *Meis* is known for its role as Hox co-factor, as responsible factor to increase the specificity of the binding of Hox proteins to the regulatory element of the target genes. ChIP experiments performed on late gastrula sea urchin embryos demonstrate that a physical binding of Sp-Lox protein to *Sp-Meis* gene occurs at this developmental stage, suggesting a putative role for Sp-Meis to direct Sp-Lox input on *Sp-Cdx* gene. The absence of *Meis* among the genes affected by Pm-Lox and Pm-Cdx knock-down suggests that this element takes part to a species-specific subcircuit of the sea urchin gut GRN. Again, these results suggest a rearrangement of the gene interactions, with the putative exclusion of some genes, in the sea urchin and sea star networks. Moreover, given the prevalence of usage of the *Meis* gene during development of nervous system in vertebrate (Shim et al. 2006) (Sánchez-Guardado et al. 2010) as

well as *Drosophila* (Kurant et al. 1998) and *C. elegans* embryos (Potts, Wang, and Cameron 2009), the key role of the *Meis* gene in the formation of the sea urchin gut unraveled by this study could be interpreted as a co-option from the nervous system to endoderm formation. However, more studies on *Meis* function in non-chordate deuterostomes is necessary to support this hypothesis.

5.3 A novel, powerful method for building GRNs through the integration of omics approaches

Over the last decades, new high-throughput technologies have made the collection of several different types of data in database repertoires, helping researchers in reproducing and validating the analysis of other labs and to analyze data in novel ways and/or with different methodologies (Gomez-Cabrero et al. 2014). For example, the availability of gene expression datasets generated by perturbation experiments of TFs has made possible to reconstruct GRNs. However, identifying all the components that make up a complex organism and understanding the interactions among them still constitutes a challenge in systems biology. The understanding of a system, in fact, can not be limited to the collection of biological data, but requires integration of these data to describe the relationships between the components of the organism. For years, the analysis of the genome-wide data has been focusing on the independent analysis of datasets generated by a single experiment. This missed a fully exploitation of the information that next-generation sequencing data provide due to a limited availability of multi-omics data integration tools. However, in the last decade, new works have been published demonstrating that integration of different omics-data permits a deeper understanding of the cell functionality and organism development not only in vertebrates (Cheng et al. 2011) (Ackermann et al. 2016) but also in invertebrate deuterostomes (Cary et al, 2017).

This thesis work provides an excellent example of how integration of different -omics approaches permits to reach a deeper comprehension of the molecular mechanisms of embryo development. A new method, that combines the well known RNA-Seq, ATAC-Seq and ChIP-PCR techniques, is developed with the purpose of constructing a gene regulatory network and is summarized in Fig. 5.1.

The first step of the method always requires the assessment of the quality of the raw sequencing data, removing low quality reads or over abundant or contaminated sequences. Then, for species without an assembled genome, in many cases de novo assembly is required before a GRN can be reconstructed. The RNA-Seq approach is then adopted to determine the expression of genes at a given development time point and in a given territory of the embryo, under and/or in a wild-type condition versus a treatment. For this thesis work, the RNA-Seq for both the sea urchin and the sea star is performed after perturbation of *Xlox* and *Cdx* genes at different developmental stages. It reveals all the differential genes under perturbed condition that are used for the ontology analysis to describe the most affected cellular and molecular processes and provides information about the affected TFs for which an orthology analysis is possible to identify the conserved proteins among the two echinoderm species and a vertebrate one.

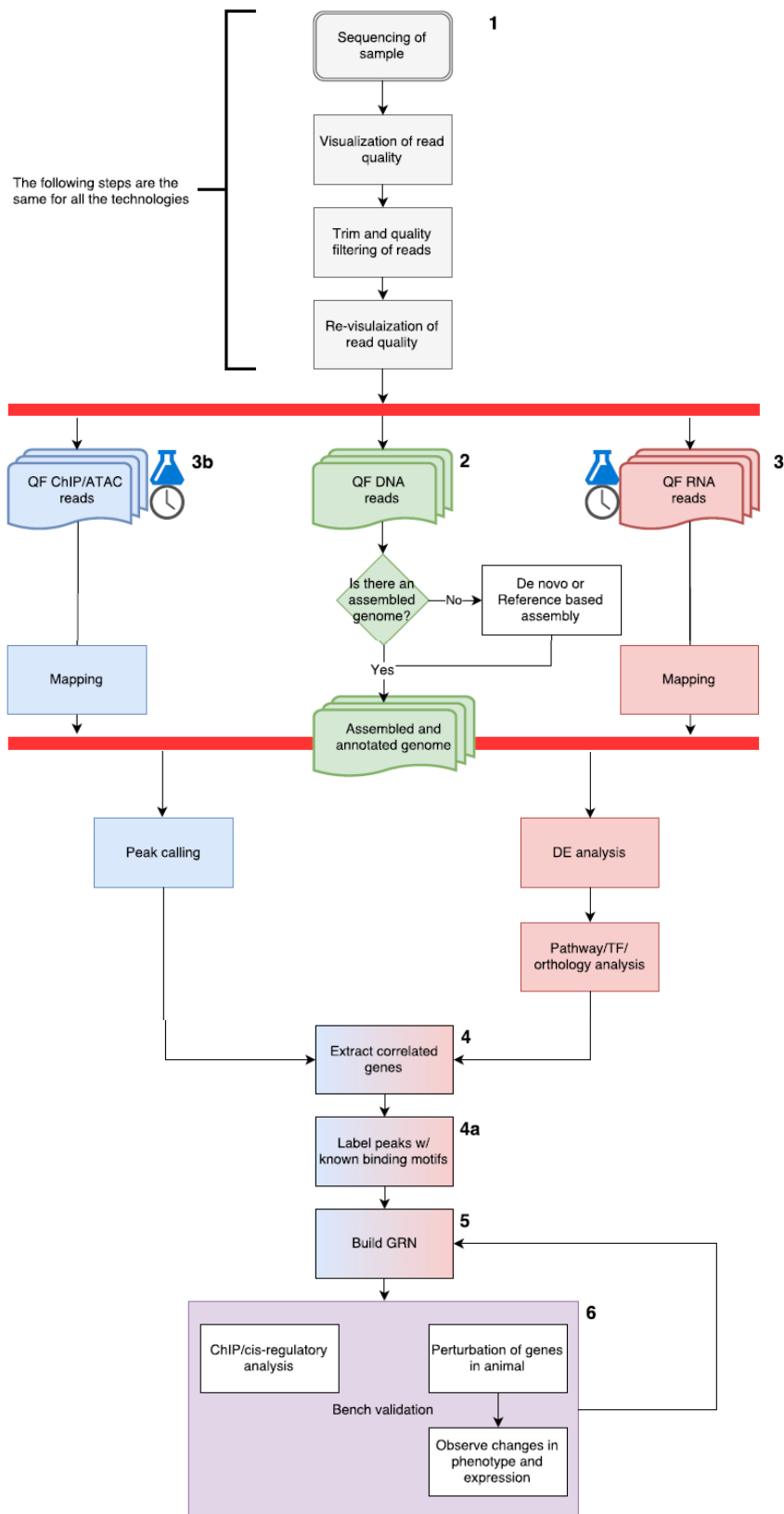


Fig. 5.1. General scheme for constructing a GRNs from omics data

The complex of these analyses reveals a multitude of information, some fundamental for the construction of a GRN. ATAC-Seq approach is then applied to identify accessible region of chromatin where proteins are able to bind and to label them with binding motifs. The combination of the differential RNA-Seq and ATAC-Seq gives the possibility to restrict the ATAC-Seq analysis to the genes of interest that change the expression after perturbation experiments.

For this thesis work, only the TFs showing a significant fold change in the RNA-Seq datasets and that are potentially expressed in the mid-posterior sea urchin gut have been analyzed by ATAC-Seq revealing all their putative interactions in the network. However, ATAC-seq alone cannot demonstrate whether these interactions are real nor if they are effective. ChIP-PCR partially fills this gap showing the physical binding between the TF and the regulatory region of the gene. The ultimate demonstration occurs when a combination of functional data, such as the Sp-Meis MASO experiments performed in this work, and/or *cis*-regulatory analyses, as described in the following paragraph, are used to validate predicted nodes. Using a combination of perturbation experiments and ChIP-PCR approach, in fact I reveal a key node of the network demonstrating that the *Sp-Meis* gene is a direct target of Sp-Lox, which is considered the upstream regulator of the cascade of events driving the sea urchin gut differentiation, and is necessary for the activation of downstream Sp-Cdx gene. Finally, the combination of these methods allows a partial reconstruction of the gut network revealing the TFs that belong to it and how they may interact each other. It is worth noting that the role of *Sp-Meis* in endoderm formation unraveled by the use of omics approach in this study was so far obscured due to the low level of expression of this gene during sea urchin development and the limitations of candidate gene approach so far used in reconstructing the sea urchin endomesoderm GRN, thus highlighting once more the power of this approach.

The method applied in this thesis work and under review in a review paper, written in collaboration with my Director of Studies and the bioinformatician post-doc of the lab, demonstrates that the integration of omics approaches is a powerful tool to study gene regulatory interactions during development.

5.4 Conclusions and future perspectives

In the new genomic and transcriptomic era, the advances of sequencing technologies are driving the study of animal development from an organismal to a transcriptomic level. In this way, the genes that are expressed at a given time of development and the way their expression changes in altered conditions are revealed, leading researchers to a deeper knowledge of the regulatory mechanisms underneath/behind developmental processes. RNA-Seq, ATAC-Seq and ChIP-PCR system-level approaches have been chosen for a better understanding of the molecular mechanisms driving gut formation in two classes of Echinoderms: Echinozoa and Asterozoa. With this approaches I have reconstructed a preliminary network around Sp-Lox and Sp-Cdx sea urchin proteins highlighting the potential role of *Meis*, an homeobox gene, as mediator of Sp-Lox input on *Sp-Cdx* gene. On the contrary, a less comprehensive knowledge of the *P. miniata* system, that has been poorly studied compared to *S. purpuratus* and for which the genome has been annotated only recently, did not allow me to describe the gene network for its gut formation. One of the first aims to be accomplished for the study of the sea star gut GRN is to validate the observed sea urchin *Xlox* and *Cdx* interactions in this system to start to lay the foundations for the reconstruction of the gut regulatory network also in this animal. To this end, the generation of *P. miniata* wild type ATAC-Seq for several developmental stages starting from blastula until bipinnaria larva has been set up within this thesis work and is

currently underway in the lab where I am performing my studies. Regarding *S. purpuratus*, for which a GRN has been already designed, all the predicted nodes of the network need to be validated by functional analysis experiments through MASO microinjection that verifies the transcriptional regulation activity of a protein on a specific gene, and/or ChIP-PCR to reveal the Sp-Lox/Sp-Cdx direct targets, and/or *cys*-regulatory analysis, to experimentally demonstrate the functionality of a TF binding on a predicted gene regulatory region. In order to analyze the actual capability of a TF binding site (TFBS) to drive gene expression, CRM reporter gene constructs that contains wild type and mutated forms of each TFBS are created and tested in developing embryos by measuring both qualitative and quantitative changes in gene expression. For this purpose I will take advantage of the method described in (Nam et al. 2010) that uses a 13-vectors *cys*-regulatory system to analyze contemporary 13 different CRMs. In this way, the analysis of the TFBS results easy and fast. An alignment of the Xlox and Cdx TFBS falling close or inside the analyzed genes of the network has been already performed to verify the similarities of the sequences of their binding sites in the different regions of the genome (Fig. 5.2).

Nearest gene	Pdx1/Xlox binding site
Nr1m3	TGATTTATGA
FoxA	CCATCTCTCA
	TGACAGATTA
	TGATGGATTA
Ets4	TGCTTAATTA
	CAATTTATCA
Bra	TCATTTATTA
Meis	CCGTCAATCA
	GAATAAATCA
Xlox	TCATCAATTA
Cdx	TGACAGATTA

CLUSTAL O(1.2.4) multiple sequence alignment	
Xlox7	TCATTTATTA
Xlox10	TCATCAATTA
Xlox1	TGATTTATGA
Xlox3	TGACAGATTA
Xlox11	TGACAGATTA
Xlox4	TGATGGATTA
Xlox5	TGCTTAATTA
Xlox2	CCATCTCTCA
Xlox8	CCGTCAATCA
Xlox6	CAATTTATCA
Xlox9	GAATAAATCA
	* *

Nearest Gene	Cdx2 binding site
Nr1m3	GTTTTATGGT
Bra	GCCATAAATT
	ATAATAAAAA
	GTAATAAAAC
	GTCATAAAAA
Xlox	GCAATAAAAA
Cdx	ATTTTATGAC
	GTTTATTAT

CLUSTAL O(1.2.4) multiple sequence alignment	
Cdx2	GCCATAAATT
Cdx6	GCAATAAAAA
Cdx5	GTCATAAAAA
Cdx3	ATAATAAAAA
Cdx4	GTAATAAAAC
Cdx8	GTTTATTAT
Cdx1	GTTTATGGT
Cdx7	ATTTTATGAC
	**

Fig. 5.2. Xlox and Cdx TFBS alignments. The sequences have been aligned using Clustal Omega program (<http://www.ebi.ac.uk/Tools/msa/clustalo/>). The asterisk indicates conservation of the nucleic acid and its position among the aligned sequences.

The alignment shows the conservation of only two invariant positions among the sequences analyzed for both Xlox and Cdx. However, except for the one already tested within the *Sp-Meis* gene, these are only predicted binding sites, which need validation through functional analysis. The combinatorial method of genome wide approaches, together with the validation experiments applied to both the sea urchins and the sea stars, drive this thesis study to establish an experimentally verified GRN based on predictions of omics approaches. Once the sea urchin and sea star gut GRN around Xlox and Cdx proteins will be fully reconstructed, a thorough comparison can be performed to highlight all the differences and similarities within the gut GRN, which will allow to put forward a theory for its evolution/conservation among the two echinoderm species.

BIBLIOGRAPHY

- Ackermann, Amanda M., Zhiping Wang, Jonathan Schug, Ali Naji, and Klaus H. Kaestner. 2016. "Integration of ATAC-Seq and RNA-Seq Identifies Human Alpha Cell and Beta Cell Signature Genes." *Molecular Metabolism* 5 (3): 233–44.
- Akam, Michael. 1987. "The Molecular Basis for Metameric Pattern in the *Drosophila* Embryo." *Development* 101 (1): 1–22.
- Andrikou, Carmen, Edmondo Iovene, Francesca Rizzo, Paola Oliveri, and Maria Ina Arnone. 2013. "Myogenesis in the Sea Urchin Embryo: The Molecular Fingerprint of the Myoblast Precursors." *EvoDevo* 4 (1): 33.
- Andrikou, Carmen, Chih-Yu Pai, Yi-Hsien Su, and Maria Ina Arnone. 2015. "Logics and Properties of a Genetic Regulatory Program That Drives Embryonic Muscle Development in an Echinoderm." *eLife* 4. doi:10.7554/elife.07343.
- Annunziata, Rossella, and Maria Ina Arnone. 2014. "A Dynamic Regulatory Network Explains ParaHox Gene Control of Gut Patterning in the Sea Urchin." *Development* 141 (12): 2462–72.
- Annunziata, Rossella, Pedro Martinez, and Maria Arnone. 2013. "Intact Cluster and Chordate-like Expression of ParaHox Genes in a Sea Star." *BMC Biology* 11 (1): 68.
- Annunziata, Rossella, Margherita Perillo, Carmen Andrikou, Alison G. Cole, Pedro Martinez, and Maria I. Arnone. 2014. "Pattern and Process during Sea Urchin Gut Morphogenesis: The Regulatory Landscape." *Genesis* 52 (3): 251–68.
- Arenas-Mena, Cesar, R. Andrew Cameron, and Eric H. Davidson. 2006. "Hindgut Specification and Cell-Adhesion Functions of Sphox11/13b in the Endoderm of the Sea Urchin Embryo." *Development, Growth & Differentiation* 48 (7): 463–72.

- Arnone, Maria Ina, Carmen Andrikou, and Rossella Annunziata. 2016. "Echinoderm Systems for Gene Regulatory Studies in Evolution and Development." *Current Opinion in Genetics & Development* 39: 129–37.
- Arnone, Maria Ina, Maria Byrne, and Pedro Martinez. 2015. "Echinodermata." In *Evolutionary Developmental Biology of Invertebrates* 6, 1–58.
- Arnone, Maria I., Francesca Rizzo, Rosella Annunziata, R. Andrew Cameron, Kevin J. Peterson, and Pedro Martínez. 2006. "Genetic Organization and Embryonic Expression of the ParaHox Genes in the Sea Urchin *S. Purpuratus*: Insights into the Relationship between Clustering and Colinearity." *Developmental Biology* 300 (1): 63–73.
- Bayha, Elke, Mette C. Jørgensen, Palle Serup, and Anne Grapin-Botton. 2009. "Retinoic Acid Signaling Organizes Endodermal Organ Specification along the Entire Antero-Posterior Axis." *PloS One* 4 (6): e5845.
- Bridges, Calvin Blackman, Thomas Hunt Morgan, and Carnegie Institution of Washington. 1923. *The Third-Chromosome Group of Mutant Characters of Drosophila Melanogaster*.
- Brooke, Nina M., Jordi Garcia-Fernández, and Peter W. H. Holland. 1998. "The ParaHox Gene Cluster Is an Evolutionary Sister of the Hox Gene Cluster." *Nature* 392 (6679): 920–22.
- Bumsted-O'Brien, Keely M., Anita Hendrickson, Silke Haverkamp, Ruth Ashery-Padan, and Dorothea Schulte. 2007. "Expression of the Homeodomain Transcription Factor Meis2 in the Embryonic and Postnatal Retina." *The Journal of Comparative Neurology* 505 (1): 58–72.
- Byrne, Maria, Yoko Nakajima, Francis C. Chee, and Robert D. Burke. 2007. "Apical Organs in Echinoderm Larvae: Insights into Larval Evolution in the Ambulacraria." *Evolution & Development* 9 (5): 432–45.
- Cary, G. A., Jarvela, A. M. C., Francolini, R. D., & Hinman, V. F. 2017. Genome-

wide use of high-and low-affinity Tbrain transcription factor binding sites during echinoderm development. *Proceedings of the National Academy of Sciences*, 114(23), 5854-5861.

Cheng, Chao, Koon-Kiu Yan, Woonchang Hwang, Jiang Qian, Nitin Bhardwaj, Joel Rozowsky, Zhi John Lu, et al. 2011. “Construction and Analysis of aIntegrated Regulatory Network Derived from High-Throughput Sequencing Data.” *PLoS Computational Biology* 7 (11). Public Library of Science: e1002190.

Chen, Yonglong, Fong Cheng Pan, Nadia Brandes, Solomon Afelik, Marion Sölter, and Tomas Pieler. 2004. “Retinoic Acid Signaling Is Essential for Pancreas Development and Promotes Endocrine at the Expense of Exocrine Cell Differentiation in *Xenopus*.” *Developmental Biology* 271 (1): 144–60.

Choe, Seong-Kyu, Peiyuan Lu, Mako Nakamura, Jinhyup Lee, and Charles G. Sagerström. 2009. “Meis Cofactors Control HDAC and CBP Accessibility at Hox-Regulated Promoters during Zebrafish Embryogenesis.” *Developmental Cell* 17 (4): 561–67.

Cole, Alison G., Francesca Rizzo, Pedro Martinez, Montserrat Fernandez-Serra, and Maria I. Arnone. 2009. “Two ParaHox Genes, SpLox and SpCdx, Interact to Partition the Posterior Endoderm in the Formation of a Functional Gut.” *Development* 136 (4): 541–49.

Croce, Jenifer C., and David R. McClay. 2010. “Dynamics of Delta/Notch Signaling on Endomesoderm Segregation in the Sea Urchin Embryo.” *Development* 137 (1): 83–91.

Darwin, Charles. 2004. *On the Origin of Species*, 1859. Routledge.

Davidson, Eric H. 2002. “A Genomic Regulatory Network for Development.” *Science* 295 (5560): 1669–78.

Davidson, Eric H., and Douglas H. Erwin. 2006. “Gene Regulatory Networks and the Evolution of Animal Body Plans.” *Science* 311 (5762): 796–800.

- Davidson, Eric H., and Douglas H. Erwin. 2010. "Evolutionary Innovation and Stability in Animal Gene Networks." *Journal of Experimental Zoology. Part B, Molecular and Developmental Evolution* 314 (3): 182–86.
- Duboule, Denis, and Gines Morata. 1994. "Colinearity and Functional Hierarchy among Genes of the Homeotic Complexes." *Trends in Genetics: TIG* 10 (10): 358–64.
- Dylus, David Viktor, Anna Czarkwiani, Josefine Stångberg, Olga Ortega-Martinez, Sam Dupont, and Paola Oliveri. 2016. "Large-Scale Gene Expression Study in the Ophiuroid *Amphiura Filiformis* Provides Insights into Evolution of Gene Regulatory Networks." *EvoDevo* 7 (1). doi:10.1186/s13227-015-0039-x.
- Erwin, Douglas H., and Eric H. Davidson. 2002. "The Last Common Bilaterian Ancestor." *Development* 129 (13): 3021–32.
- Erwin, Douglas H., and Eric H. Davidson. 2009. "The Evolution of Hierarchical Gene Regulatory Networks." *Nature Reviews. Genetics* 10 (2): 141–48.
- Erwin, Douglas H., Marc Laflamme, Sarah M. Tweedt, Erik A. Sperling, Davide Pisani, and Kevin J. Peterson. 2011. "The Cambrian Conundrum: Early Divergence and Later Ecological Success in the Early History of Animals." *Science* 334 (6059): 1091–97.
- Ettensohn, Charles A., Gary M. Wessel, and Gregory A. Wray. 2004. "The Invertebrate Deuterostomes: An Introduction to Their Phylogeny, Reproduction, Development, and Genomics." *Methods in Cell Biology* 74: 1–13.
- Ferrier, David E. K. 2014. "The Hox-TALE Has Been Wagging for a Long Time." *eLife* 3. doi:10.7554/elife.02515.
- Garstang, Myles, and David E. K. Ferrier. 2013. "Time Is of the Essence for ParaHox Homeobox Gene Clustering." *BMC Biology* 11 (June): 72.
- Gaunt, Stephen J., Deborah Drage, and Adam Cockley. 2003. "Vertebrate Caudal

- Gene Expression Gradients Investigated by Use of Chick Cdx-A/lacZ and Mouse Cdx-1/lacZ Reporters in Transgenic Mouse Embryos: Evidence for an Intron Enhancer.” *Mechanisms of Development* 120 (5): 573–86.
- Giusti, Andrew F., Kenneth M. Hoang, and Kathy R. Foltz. 1997. “Surface Localization of the Sea Urchin Egg Receptor for Sperm.” *Developmental Biology* 184 (1): 10–24.
- Gomez-Cabrero, David, Imad Abugessaisa, Dieter Maier, Andrew Teschendorff, Matthias Merckenschlager, Andreas Gisel, Esteban Ballestar, Erik Bongcam-Rudloff, Ana Conesa, and Jesper Tegnér. 2014. “Data Integration in the Era of Omics: Current and Future Challenges.” *BMC Systems Biology* 8 Suppl 2 (March): I1.
- Gommans, Willemijn M., Hidde J. Haisma, and Marianne G. Rots. 2005. “Engineering Zinc Finger Protein Transcription Factors: The Therapeutic Relevance of Switching Endogenous Gene Expression On or Off at Command.” *Journal of Molecular Biology* 354 (3): 507–19.
- Haeckel, Ernst. 1872. *Die Kalkschwämme. Eine Monographie.* Edited by Berlin Verlag von Georg Reimer.
- Haeckel, Ernst. 1874. “Die Gastraea-Theorie, Die Phylogenetische Classification Des Thierreichs Und Die Homologie Der Keimblätter.” *Jenaische Zeitschrift Fur Medicin Und Naturwissenschaft*, 81–55.
- Hinman, Veronica F., and Alys M. Cheatle Jarvela. 2014. “Developmental Gene Regulatory Network Evolution: Insights from Comparative Studies in Echinoderms.” *Genesis* 52 (3): 193–207.
- Hinman, Veronica F., and Eric H. Davidson. 2007. “Evolutionary Plasticity of Developmental Gene Regulatory Network Architecture.” *Proceedings of the National Academy of Sciences of the United States of America* 104 (49): 19404–9.

- Hinman, Veronica F., Albert Nguyen, and Eric H. Davidson. 2007. "Caught in the Evolutionary Act: Precise Cis-Regulatory Basis of Difference in the Organization of Gene Networks of Sea Stars and Sea Urchins." *Developmental Biology* 312 (2): 584–95.
- Hinman, Veronica F., Albert T. Nguyen, R. Andrew Cameron, and Eric H. Davidson. 2003. "Developmental Gene Regulatory Network Architecture across 500 Million Years of Echinoderm Evolution." *Proceedings of the National Academy of Sciences of the United States of America* 100 (23): 13356–61.
- Hinman, Veronica F., Albert T. Nguyen, and Eric H. Davidson. 2003. "Expression and Function of a Starfish Otx Ortholog, AmOtx: A Conserved Role for Otx Proteins in Endoderm Development That Predates Divergence of the Eleutherozoa." *Mechanisms of Development* 120 (10): 1165–76.
- Hisa, Tomoyuki, Sally E. Spence, Rivka A. Rachel, Masami Fujita, Takuro Nakamura, Jerrold M. Ward, Deborah E. Devor-Henneman, et al. 2004. "Hematopoietic, Angiogenic and Eye Defects in Meis1 Mutant Animals." *The EMBO Journal* 23 (2): 450–59.
- Holland, Peter W. H. 2013. "Evolution of Homeobox Genes." *Wiley Interdisciplinary Reviews. Developmental Biology* 2 (1): 31–45.
- Holland, Peter W. H. 2015. "Did Homeobox Gene Duplications Contribute to the Cambrian Explosion?" *Zoological Letters* 1 (January): 1.
- Holland, Peter W. H. 2001. "Beyond the Hox: How Widespread Is Homeobox Gene Clustering?" *Journal of Anatomy* 199 (Pt 1-2): 13–23.
- Hyman, L. H. 1955. "Echinodermata." In *The Invertebrates*, edited by Macgraw-Hill: New York., 4.:763 pp.
- Ikuta, Tetsuro. 2011. "Evolution of Invertebrate Deuterostomes and Hox/ParaHox Genes." *Genomics, Proteomics & Bioinformatics* 9 (3): 77–96.

- Ikuta, Tetsuro, Yi-Chih Chen, Rossella Annunziata, Hsiu-Chi Ting, Che-Huang Tung, Ryo Koyanagi, Kunifumi Tagawa, et al. 2013. "Identification of an Intact ParaHox Cluster with Temporal Colinearity but Altered Spatial Colinearity in the Hemichordate *Ptychodera Flava*." *BMC Evolutionary Biology* 13 (1): 129.
- Illes, Jean C., Emily Winterbottom, and Harry V. Isaacs. 2009. "Cloning and Expression Analysis of the Anterior Parahox Genes, Gsh1 and Gsh2 from *Xenopus Tropicalis*." *Developmental Dynamics: An Official Publication of the American Association of Anatomists* 238 (1): 194–203.
- Imai, Kaoru S., Alberto Stolfi, Michael Levine, and Yutaka Satou. 2009. "Gene Regulatory Networks Underlying the Compartmentalization of the Ciona Central Nervous System." *Development* 136 (2): 285–93.
- Irish, Vivian F., Alfonso Martinez-Arias, and Michael Akam. 1989. "Spatial Regulation of the Antennapedia and Ultrabithorax Homeotic Genes during *Drosophila* Early Development." *The EMBO Journal* 8 (5): 1527–37.
- Jones, Nic. 1990. "Transcriptional Regulation by Dimerization: Two Sides to an Incestuous Relationship." *Cell* 61 (1): 9–11.
- Knoepfler, Paul S., Katherine R. Calvo, Haiming Chen, Stylianos E. Antonarakis, and Mark P. Kamps. 1997. "Meis1 and pKnox1 Bind DNA Cooperatively with Pbx1 Utilizing an Interaction Surface Disrupted in Oncoprotein E2a-Pbx1." *Proceedings of the National Academy of Sciences* 94 (26): 14553–58.
- Kumar, Raj, and E. Brad Thompson. 1999. "The Structure of the Nuclear Hormone Receptors." *Steroids* 64 (5): 310–19.
- Kuraishi, Ritsu, and Kenzi Osanai. 1992. "Cell Movements during Gastrulation of Starfish Larvae." *The Biological Bulletin* 183 (2): 258–68.
- Kurant, Estee, C. Y. Pai, Rakefet Sharf, Naomi Halachmi, Y. Henry Sun, and Adi Salzberg. 1998. "Dorsotons/homothorax, the *Drosophila* Homologue of

- meis1, Interacts with Extradenticle in Patterning of the Embryonic PNS.” *Development* 125 (6): 1037–48.
- Landschulz, William H., Peter F. Johnson, and Steven L. McKnight. 1988. “The Leucine Zipper: A Hypothetical Structure Common to a New Class of DNA Binding Proteins.” *Science* 240 (4860): 1759–64.
- Latchman, David S. 1999. “POU Family Transcription Factors in the Nervous System.” *Journal of Cellular Physiology* 179 (2): 126–33.
- Levine, Michael, and Eric H. Davidson. 2005. “Gene Regulatory Networks for Development.” *Proceedings of the National Academy of Sciences* 102 (14): 4936–42.
- Lhomond, Guy, David R. McClay, Christian Gache, and Jenifer C. Croce. 2012. “Frizzled1/2/7 signaling directs β -catenin nuclearisation and initiates endoderm specification in macromeres during sea urchin embryogenesis.” *Development* 139 (4): 816–25.
- Li, Enhui, Miao Cui, Isabelle S. Peter, and Eric H. Davidson. 2014. “Encoding Regulatory State Boundaries in the Pregastrular Oral Ectoderm of the Sea Urchin Embryo.” *Proceedings of the National Academy of Sciences of the United States of America* 111 (10): E906–13.
- Li, Enhui, Stefan C. Materna, and Eric H. Davidson. 2012. “Direct and Indirect Control of Oral Ectoderm Regulatory Gene Expression by Nodal Signaling in the Sea Urchin Embryo.” *Developmental Biology* 369 (2): 377–85.
- Logan, Catriona Y., and David R. McClay. 1997. “The Allocation of Early Blastomeres to the Ectoderm and Endoderm Is Variable in the Sea Urchin Embryo.” *Development* 124 (11): 2213–23.
- Logan, Catriona Y., Jeffrey R. Miller, Michael J. Ferkowicz, and David R. McClay. 1999. “Nuclear Beta-Catenin Is Required to Specify Vegetal Cell Fates in the Sea Urchin Embryo.” *Development* 126 (2): 345–57.

- Materna, Stefan C., and Paola Oliveri. 2008. "A Protocol for Unraveling Gene Regulatory Networks." *Nature Protocols* 3 (12): 1876–87.
- McCauley, Brenna S., Erin P. Weideman, and Veronica F. Hinman. 2010. "A Conserved Gene Regulatory Network Subcircuit Drives Different Developmental Fates in the Vegetal Pole of Highly Divergent Echinoderm Embryos." *Developmental Biology* 340 (2): 200–208.
- McClay, David R. 2011. "Evolutionary Crossroads in Developmental Biology: Sea Urchins." *Development* 138 (13): 2639–48.
- McClay, D. R., Gross, J. M., Range, R., Peterson, R. E., & Bradham, C. 2004. *Sea Urchin Gastrulation. Gastrulation: From Cells to Embryo*. Edited by Cold Spring Harbor Laboratory. Vol. 123–37. Cold Spring Harbor.
- Mendivil Ramos, Olivia, Daniel Barker, and David E. K. Ferrier. 2012. "Ghost Loci Imply Hox and ParaHox Existence in the Last Common Ancestor of Animals." *Current Biology: CB* 22 (20): 1951–56.
- Mooi, Rich, and Bruno David. 2000. "What a New Model of Skeletal Homologies Tells Us About Asteroid Evolution¹." *American Zoologist* 40 (3): 326–39.
- Morata, Gines, and Stephen Kerridge. 1982. "The Role of Position in Determining Homoeotic Gene Function in *Drosophila*." *Nature* 300 (5888): 191–92.
- Moskow, John J., Florencia Bullrich, Kay Huebner, Ira O. Daar, and Arthur M. Buchberg. 1995. "Meis1, a PBX1-Related Homeobox Gene Involved in Myeloid Leukemia in BXH-2 Mice." *Molecular and Cellular Biology* 15 (10): 5434–43.
- Nam, Jongmin, Ping Dong, Ryan Tarpine, Sorin Istrail, and Eric H. Davidson. 2010. "Functional Cis-Regulatory Genomics for Systems Biology." *Proceedings of the National Academy of Sciences of the United States of America* 107 (8): 3930–35.
- Oliveri, Paola, Qiang Tu, and Eric H. Davidson. 2008. "Global Regulatory Logic

- for Specification of an Embryonic Cell Lineage.” *Proceedings of the National Academy of Sciences* 105 (16): 5955–62.
- Osborne, Peter W., Gérard Benoit, Vincent Laudet, Michael Schubert, and David E. K. Ferrier. 2009. “Differential Regulation of ParaHox Genes by Retinoic Acid in the Invertebrate Chordate *Amphioxus* (*Branchiostoma Floridae*).” *Developmental Biology* 327 (1): 252–62.
- Peifer, Mark, and Eric Wieschaus. 1990. “Mutations in the *Drosophila* Gene *Extradenticle* Affect the Way Specific Homeo Domain Proteins Regulate Segmental Identity.” *Genes & Development* 4 (7): 1209–23.
- Penkov, Dmitry, Daniel Mateos San Martín, Luis C. Fernandez-Díaz, Catalina A. Rosselló, Carlos Torroja, Fátima Sánchez-Cabo, H. J. Warnatz, et al. 2013. “Analysis of the DNA-Binding Profile and Function of TALE Homeoproteins Reveals Their Specialization and Specific Interactions with Hox Genes/Proteins.” *Cell Reports* 3 (4): 1321–33.
- Peter, Isabelle S., and Eric H. Davidson. 2010. “The Endoderm Gene Regulatory Network in Sea Urchin Embryos up to Mid-Blastula Stage.” *Developmental Biology* 340 (2): 188–99.
- Peter, Isabelle S., and Eric H. Davidson. 2011a. “A Gene Regulatory Network Controlling the Embryonic Specification of Endoderm.” *Nature* 474 (7353): 635–39.
- Peter, Isabelle S., and Eric H. Davidson. 2011b. “Evolution of Gene Regulatory Networks Controlling Body Plan Development.” *Cell* 144 (6): 970–85.
- Peter W.H. Holland, Jordi Garcia-Fernàndez. 1996. “HoxGenes and Chordate Evolution.” *Developmental Biology* 173 (2): 382–95.
- Pisani, Davide, Roberto Feuda, Kevin J. Peterson, and Andrew B. Smith. 2012. “Resolving Phylogenetic Signal from Noise When Divergence Is Rapid: A New

- Look at the Old Problem of Echinoderm Class Relationships.” *Molecular Phylogenetics and Evolution* 62 (1): 27–34.
- Potts, Malia B., David P. Wang, and Scott Cameron. 2009. “Trithorax, Hox, and TALE-Class Homeodomain Proteins Ensure Cell Survival through Repression of the BH3-Only Gene Egl-1.” *Developmental Biology* 329 (2): 374–85.
- Puro, Jaakko, and Tuire Nygrén. 1975. “Mode of Action of a Homoeotic Gene in *Drosophila Melanogaster*. Localization and Dosage Effects of Polycomb.” *Hereditas* 81 (2): 237–48.
- Rafiq, Kiran, Melani S. Cheers, and Charles A. Ettensohn. 2011. “The Genomic Regulatory Control of Skeletal Morphogenesis in the Sea Urchin.” *Development* 139 (3): 579–90.
- Ransick, Andrew, and Eric H. Davidson. 2006. “Cis-Regulatory Processing of Notch Signaling Input to the Sea Urchin Glial Cells Missing Gene during Mesoderm Specification.” *Developmental Biology* 297 (2): 587–602.
- Ransick, Andrew, Jonathan P. Rast, Takuya Minokawa, Cristina Calestani, and Eric H. Davidson. 2002. “New Early Zygotic Regulators Expressed in Endomesoderm of Sea Urchin Embryos Discovered by Differential Array Hybridization.” *Developmental Biology* 246 (1): 132–47.
- Rast, Jonathan P., R. Andrew Cameron, Albert J. Poustka, and Eric H. Davidson. 2002. “Brachyury Target Genes in the Early Sea Urchin Embryo Isolated by Differential Macroarray Screening.” *Developmental Biology* 246 (1): 191–208.
- Rezsohazy, René, Andrew J. Saurin, Corinne Maurel-Zaffran, and Yacine Graba. 2015. “Cellular and Molecular Insights into Hox Protein Action.” *Development* 142 (7): 1212–27.
- Röttinger, Eric, Paul Dahlin, and Mark Q. Martindale. 2012. “A Framework for the Establishment of a Cnidarian Gene Regulatory Network for ‘Endomesoderm’ Specification: The Inputs of β -Catenin/TCF

- Signaling.” *PLoS Genetics* 8(12): e1003164.
- Ruffins, Seth W., and Charles A. Ettensohn. 1996. “A Fate Map of the Vegetal Plate of the Sea Urchin (*Lytechinus Variegatus*) Mesenchyme Blastula.” *Development* 122 (1): 253–63.
- Samadi, Leyli, and Gerhard Steiner. 2010. “Conservation of ParaHox Genes’ Function in Patterning of the Digestive Tract of the Marine Gastropod *Gibbula Varia*.” *BMC Developmental Biology* 10 (July): 74.
- Sánchez-Guardado, Luis Óscar, José Luis Ferran, Lucía Rodríguez-Gallardo, Luis Puellas, and Matías Hidalgo-Sánchez. 2010. “Meis Gene Expression Patterns in the Developing Chicken Inner Ear.” *The Journal of Comparative Neurology* 519 (1): 125–47.
- Sea Urchin Genome Sequencing Consortium, Erica Sodergren, George M. Weinstock, Eric H. Davidson, R. Andrew Cameron, Richard A. Gibbs, Robert C. Angerer, et al. 2006. “The Genome of the Sea Urchin *Strongylocentrotus Purpuratus*.” *Science* 314(5801): 941–52.
- Shim, Sungbo, Yujin Kim, Jongdae Shin, Jieun Kim, and Soochul Park. 2006. “Regulation of EphA8 Gene Expression by TALE Homeobox Transcription Factors during Development of the Mesencephalon.” *Molecular and Cellular Biology* 27 (5): 1614–30.
- Smith, Joel, Ebba Kraemer, Hongdau Liu, Christina Theodoris, and Eric Davidson. 2008. “A Spatially Dynamic Cohort of Regulatory Genes in the Endomesodermal Gene Network of the Sea Urchin Embryo.” *Developmental Biology* 313 (2): 863–75.
- Smith, Joel, Christina Theodoris, and Eric H. Davidson. 2007. “A Gene Regulatory Network Subcircuit Drives a Dynamic Pattern of Gene Expression.” *Science* 318 (5851): 794–97.
- Smith, M. Paul, and David A. T. Harper. 2013. “Earth Science. Causes of the

- Cambrian Explosion.” *Science* 341 (6152): 1355–56.
- Sperber, G. H. 1995. “Developmental Biology, 4th Edition. By Scott F. Gilbert, Sinauer Associates, Inc., Sunderland, Massachusetts, and W.H. Freeman, U.K., 1994.” *American Journal of Medical Genetics* 57 (4): 1096–8628.
- Srinivasan, R. Sathish, Xin Geng, Ying Yang, Yingdi Wang, Suraj Mukatira, Michèle Studer, Marianna P. R. Porto, Oleg Lagutin, and Guillermo Oliver. 2010. “The Nuclear Hormone Receptor Coup-TFII Is Required for the Initiation and Early Maintenance of Prox1 Expression in Lymphatic Endothelial Cells.” *Genes & Development* 24 (7): 696–707.
- Stafford, David, and Victoria E. Prince. 2002. “Retinoic Acid Signaling Is Required for a Critical Early Step in Zebrafish Pancreatic Development.” *Current Biology: CB* 12 (14): 1215–20.
- Stears, Robin L., and William J. Lennarz. 1997. “Mapping Sperm Binding Domains on the Sea Urchin Egg Receptor for Sperm.” *Developmental Biology* 187 (2): 200–208.
- Su, Yi-Hsien, Enhu Li, Gary K. Geiss, William J. R. Longabaugh, Alexander Krämer, and Eric H. Davidson. 2009. “A Perturbation Model of the Gene Regulatory Network for Oral and Aboral Ectoderm Specification in the Sea Urchin Embryo.” *Developmental Biology* 329 (2): 410–21.
- True, John R., and Sean B. Carroll. 2002. “Gene Co-Option in Physiological and Morphological Evolution.” *Annual Review of Cell and Developmental Biology* 18 (April): 53–80.
- Vacquier, Victor D., and Gary W. Moy. 1977. “Isolation of Bindin: The Protein Responsible for Adhesion of Sperm to Sea Urchin Eggs.” *Proceedings of the National Academy of Sciences of the United States of America* 74 (6): 2456–60.
- Valentine, James W. 2004. *On the Origin of Phyla*. University of Chicago Press.

- Walcott, Charles Doolittle, and Charles Elmer Resser. 1916. *Cambrian Geology and Paleontology ...: Cambrian and Ozarkian Trilobites*. 1925. (Pub.2823).
- Wang, Zhong, Mark Gerstein, and Michael Snyder. 2009. "RNA-Seq: A Revolutionary Tool for Transcriptomics." *Nature Reviews. Genetics* 10 (1): 57–63.
- Wightman, Bruce, Bryan Ebert, Nicole Carmean, Katherine Weber, and Sheila Clever. 2005. "The C. Elegans Nuclear Receptor Gene Fax-1 and Homeobox Gene Unc-42 Coordinate Interneuron Identity by Regulating the Expression of Glutamate Receptor Subunits and Other Neuron-Specific Genes." *Developmental Biology* 287 (1): 74–85.
- Woznica, Arielle, Maximilian Haeussler, Ella Starobinska, Jessica Jemmett, Younan Li, David Mount, and Brad Davidson. 2012. "Initial Deployment of the Cardiogenic Gene Regulatory Network in the Basal Chordate, Ciona Intestinalis." *Developmental Biology* 368 (1): 127–39.
- Wray, Gregory A., Jeffrey S. Levinton, and Leo H. Shapiro. 1996. "Molecular Evidence for Deep Precambrian Divergences Among Metazoan Phyla." *Science* 274 (5287): 568–73.
- Wray, Gregory A. 2007. "The Evolutionary Significance of Cis-Regulatory Mutations." *Nature Reviews. Genetics* 8 (3): 206–16.
- Yankura, Kristen A., Claire S. Koechlein, Abigail F. Cryan, Alys Cheatle, and Veronica F. Hinman. 2013. "Gene Regulatory Network for Neurogenesis in a Sea Star Embryo Connects Broad Neural Specification and Localized Patterning." *Proceedings of the National Academy of Sciences* 110 (21): 8591–96.
- Yussa, Miyuki, Ulrike Löhr, Kai Su, and Leslie Pick. 2001. "The Nuclear Receptor Ftz-F1 and Homeodomain Protein Ftz Interact through Evolutionarily Conserved Protein Domains." *Mechanisms of Development* 107 (1-2): 39–53.

APPENDIX I - RNA-SEQ DATA SETS

This appendix contains the raw data of the sea urchin and sea star differential RNA-Seq data-sets containing the list of genes that change the expression after XLox and Cdx perturbation.

	baseMean	log2FoldCha	lfcSE	stat	pvalue	padj
WHL22.3470	130.925713	3.43027377	0.25024296	206.485444	8.03E-47	9.73E-45
WHL22.4989	435.170397	2.84043454	0.12808527	509.838063	6.88E-113	1.73E-110
WHL22.2205	237.167599	2.77031975	0.16848628	281.602238	3.36E-63	4.96E-61
WHL22.4989	646.645748	2.67552895	0.10340069	686.866185	2.15E-151	9.71E-149
WHL22.6197	180.72785	2.58674962	0.18881355	193.398711	5.76E-44	6.63E-42
WHL22.5384	407.082842	2.46407108	0.12504566	396.906337	2.60E-88	5.34E-86
WHL22.4344	2027.3014	2.45145545	0.06055407	1638.1645	0	0
WHL22.5674	111.986154	2.19128915	0.23353859	88.808581	4.35E-21	2.78E-19
WHL22.5330	273.807275	2.15851524	0.14986023	209.012008	2.26E-47	2.78E-45
WHL22.3119	182.196508	2.1464522	0.18287011	138.851198	4.75E-32	4.18E-30
WHL22.5761	882.697854	2.1383266	0.08410634	649.956592	2.28E-143	8.15E-141
WHL22.1621	491.811887	1.76569378	0.11037297	255.389357	1.74E-57	2.40E-55
WHL22.1588	544.09051	1.68508659	0.10237343	270.933258	7.10E-61	1.03E-58
WHL22.1771	713.321846	1.67510036	0.09004426	345.707941	3.65E-77	6.19E-75
WHL22.3065	167.519027	1.63084122	0.18142549	80.8597577	2.42E-19	1.47E-17
WHL22.6375	1914.66874	1.61851448	0.05689321	805.06329	4.28E-177	2.23E-174
WHL22.3940	330.900322	1.61168033	0.13107281	150.963726	1.07E-34	9.66E-33
WHL22.5674	1258.12852	1.5941993	0.06860792	538.173642	4.71E-119	1.39E-116
WHL22.2103	2091.69044	1.56488501	0.05485047	808.812524	6.55E-178	3.70E-175
WHL22.5385	560.104867	1.53985185	0.10273707	223.705636	1.41E-50	1.77E-48
WHL22.4375	858.408113	1.53110673	0.08233363	344.753203	5.88E-77	9.74E-75
WHL22.3692	446.516916	1.52666105	0.11086268	189.589276	3.91E-43	4.30E-41
WHL22.3562	917.284717	1.49309363	0.07951608	351.428874	2.07E-78	3.60E-76
WHL22.6269	2109.40336	1.48678082	0.05364189	764.36268	3.02E-168	1.47E-165
WHL22.5778	4128.3821	1.47637494	0.04051512	1315.75251	4.27E-288	7.24E-285
WHL22.1237	1152.33004	1.44986724	0.07104914	414.910908	3.13E-92	7.32E-90
WHL22.6503	161.187192	1.44894208	0.18393976	61.9416601	3.54E-15	1.63E-13
WHL22.7561	756.161273	1.38505374	0.08615538	257.770276	5.25E-58	7.43E-56
WHL22.1078	202.97044	1.36213327	0.16173011	70.8851403	3.79E-17	1.99E-15
WHL22.2247	1250.4723	1.33333299	0.06836725	378.729769	2.35E-84	4.70E-82
WHL22.4940	129.910822	1.32731145	0.20354613	42.4169998	7.37E-11	2.50E-09
WHL22.5674	169.905753	1.31780868	0.18107486	52.7201249	3.85E-13	1.57E-11
WHL22.2862	633.710512	1.31493435	0.09365565	196.593305	1.16E-44	1.35E-42
WHL22.5909	598.170012	1.31210714	0.09517714	189.737068	3.63E-43	4.10E-41
WHL22.6915	633.012959	1.28115781	0.0929468	189.579315	3.93E-43	4.30E-41
WHL22.5207	173.375682	1.27774563	0.17505753	53.179329	3.04E-13	1.26E-11
WHL22.4718	567.703233	1.24443381	0.09724329	163.479233	1.97E-37	1.85E-35
WHL22.4227	11471.9175	1.20071863	0.02911483	1676.93819	0	0
WHL22.7561	8983.13517	1.18280034	0.03090356	1447.60416	9.507478639	2.150591668

WHL22.6149	98.4416177	1.1807733	0.23107372	26.0415906	3.34E-07	7.11E-06
WHL22.5466	572.351564	1.16570198	0.0965872	145.388646	1.77E-33	1.58E-31

WHL22.1943	3477.64891	1.16116643	0.04447351	676.408017	4.04E-149	1.61E-146
WHL22.4837	4493.43422	1.157856	0.03863747	891.677897	6.32E-196	4.77E-193
WHL22.4614	264.829474	1.1512838	0.1468815	61.1048099	5.41E-15	2.45E-13
WHL22.5466	1003.85262	1.14638795	0.07480716	234.064338	7.74E-53	1.01E-50
WHL22.5148	304.82069	1.14020925	0.13539952	70.6051029	4.36E-17	2.28E-15
WHL22.2277	187.452864	1.13068968	0.16594372	46.373654	9.77E-12	3.62E-10
WHL22.2974	1923.16833	1.12348479	0.05880514	362.409468	8.41E-81	1.59E-78
WHL22.4606	200.368502	1.12292347	0.16222046	47.8060275	4.71E-12	1.79E-10
WHL22.2763	119.644661	1.11726749	0.208868	28.5524239	9.12E-08	2.11E-06
WHL22.3070	745.038005	1.11328826	0.08458357	172.909584	1.71E-39	1.73E-37
WHL22.7331	881.050978	1.10307341	0.07830593	197.985923	5.75E-45	6.84E-43
WHL22.9177	827.93784	1.08495128	0.0825849	171.973579	2.74E-39	2.70E-37
WHL22.1926	2841.10912	1.08199895	0.04628391	543.936446	2.62E-120	8.10E-118
WHL22.2247	146.836308	1.07482168	0.18803392	32.6140281	1.12E-08	3.00E-07
WHL22.1751	274.188823	1.07114674	0.13903555	59.2140717	1.41E-14	6.23E-13
WHL22.5737	400.196528	1.06181207	0.11899931	79.2722774	5.41E-19	3.19E-17
WHL22.4188	432.364361	1.0558716	0.36008059	8.20071617	0.00418739	0.03084721
WHL22.2225	468.878875	1.05247344	0.10626668	97.8921081	4.42E-23	2.97E-21
WHL22.2068	604.471286	1.05194564	0.09423042	124.342525	7.09E-29	5.87E-27
WHL22.1119	1514.68005	1.04806974	0.06102315	294.049473	6.52E-66	1.03E-63
WHL22.6576	934.572847	1.0390277	0.0760731	186.115806	2.24E-42	2.37E-40
WHL22.1437	553.13685	1.03825611	0.10013168	107.150436	4.13E-25	3.01E-23
WHL22.2036	1339.70077	1.01642295	0.0641161	250.65739	1.87E-56	2.48E-54
WHL22.4968	147.634085	0.98686096	0.18557139	28.2443072	1.07E-07	2.45E-06
WHL22.5468	399.174692	0.98680158	0.11382719	75.0462116	4.60E-18	2.56E-16
WHL22.4617	411.722926	0.98580846	0.11864588	68.6917284	1.15E-16	5.83E-15
WHL22.5002	444.404776	0.9845627	0.1083048	82.5066324	1.05E-19	6.50E-18
WHL22.5036	230.65253	0.97998212	0.15165476	41.6461246	1.09E-10	3.67E-09
WHL22.2274	456.14653	0.97297593	0.10849478	80.2246635	3.34E-19	1.99E-17
WHL22.5087	571.05013	0.96671238	0.09679532	99.5198958	1.94E-23	1.33E-21
WHL22.3881	135.100153	0.96658713	0.1961352	24.2247213	8.57E-07	1.75E-05
WHL22.6082	3596.84336	0.96508275	0.04264039	509.589329	7.79E-113	1.89E-110
WHL22.2429	103.006305	0.96475224	0.22870954	17.6898367	2.60E-05	0.00039123
WHL22.4832	161.748441	0.96393372	0.18975844	25.5844513	4.23E-07	8.84E-06
WHL22.2620	220.411542	0.96223626	0.15394171	38.9828208	4.28E-10	1.32E-08
WHL22.1105	996.822326	0.96165491	0.07369025	169.916318	7.72E-39	7.48E-37
WHL22.7518	662.454425	0.95646345	0.09072889	110.843555	6.40E-26	4.83E-24
WHL22.7128	239.517526	0.94711937	0.14792639	40.8994138	1.60E-10	5.28E-09
WHL22.1321	119.520134	0.93576467	0.2132564	19.1466361	1.21E-05	0.0001989
WHL22.5229	125.562952	0.93080083	0.21545386	18.4828783	1.71E-05	0.00027182
WHL22.3393	209.597506	0.9292486	0.15924799	33.9453447	5.67E-09	1.56E-07
WHL22.6426	466.409792	0.92882538	0.10636013	76.1073525	2.69E-18	1.51E-16

WHL22.5864	102.959336	0.91333926	0.22705111	16.1037351	6.00E-05	0.00082709
WHL22.4874	1564.02039	0.91020539	0.06014194	228.392935	1.34E-51	1.71E-49
WHL22.6713	109.515639	0.90868208	0.22309897	16.4916539	4.89E-05	0.00069227
WHL22.1816	106.295888	0.90577134	0.22058788	16.8088257	4.13E-05	0.00059436
WHL22.4511	229.161572	0.9020337	0.14952385	36.3348678	1.66E-09	4.92E-08
WHL22.6982	276.882101	0.87995189	0.13771437	40.7364574	1.74E-10	5.68E-09
WHL22.4966	276.129451	0.87695192	0.1385017	39.986408	2.56E-10	8.15E-09
WHL22.4729	156.515401	0.87391629	0.18122887	23.2050508	1.46E-06	2.87E-05
WHL22.2222	135.166136	0.86737128	0.19885615	18.937689	1.35E-05	0.00022031
WHL22.2360	120.094188	0.86568432	0.21930195	15.4312737	8.56E-05	0.00112741
WHL22.7482	145.901761	0.85825952	0.18652795	21.1404455	4.27E-06	7.81E-05
WHL22.4395	551.428308	0.85384327	0.10005918	72.6104997	1.58E-17	8.51E-16
WHL22.7363	4999.98057	0.85349528	0.03728559	521.414217	2.08E-115	5.66E-113
WHL22.3010	114.312949	0.84558086	0.20955903	16.2624788	5.51E-05	0.00076527
WHL22.5900	347.849421	0.84293347	0.12446612	45.7359534	1.35E-11	4.96E-10
WHL22.1458	737.627691	0.84099398	0.08688306	93.432059	4.20E-22	2.74E-20
WHL22.3706	1257.95593	0.84001915	0.06623204	160.48277	8.88E-37	8.25E-35
WHL22.7559	7200.50857	0.83590461	0.03245508	659.709526	1.73E-145	6.51E-143
WHL22.3027	221.615224	0.83417717	0.15074589	30.5886487	3.19E-08	8.05E-07
WHL22.3101	422.788087	0.8325749	0.11514904	52.0897911	5.30E-13	2.15E-11
WHL22.2555	7659.21169	0.83168384	0.03184305	678.305737	1.56E-149	6.62E-147
WHL22.6309	264.127797	0.82772774	0.14134029	34.2077904	4.95E-09	1.38E-07
WHL22.2143	211.801142	0.81662408	0.15532631	27.5955118	1.50E-07	3.36E-06
WHL22.4253	1438.66928	0.81554886	0.06197851	172.762523	1.84E-39	1.84E-37
WHL22.6944	591.128381	0.81117207	0.09401751	74.3204734	6.64E-18	3.63E-16
WHL22.6309	286.588052	0.81007221	0.13679225	34.9671294	3.35E-09	9.72E-08
WHL22.4530	503.667365	0.80558762	0.10128867	63.164092	1.90E-15	8.90E-14
WHL22.2767	4233.20974	0.80328726	0.04138782	374.836864	1.66E-83	3.21E-81
WHL22.9120	252.649946	0.80216652	0.14148874	32.1039699	1.46E-08	3.86E-07
WHL22.4147	165.542203	0.79721744	0.17528201	20.6506402	5.51E-06	9.79E-05
WHL22.5979	320.476981	0.78806329	0.13275419	35.0860949	3.15E-09	9.19E-08
WHL22.6787	973.954158	0.78438036	0.07388995	112.498483	2.78E-26	2.12E-24
WHL22.4040	378.845459	0.78389254	0.12084353	41.9395716	9.41E-11	3.18E-09
WHL22.7163	100.590062	0.7776608	0.2291009	11.4680936	0.00070801	0.00705518
WHL22.6506	559.492326	0.77280452	0.09645663	64.0940402	1.19E-15	5.71E-14
WHL22.6830	784.386165	0.77040807	0.08454919	82.8073092	9.05E-20	5.63E-18
WHL22.8976	148.504321	0.76165528	0.183513	17.2089425	3.35E-05	0.00049506
WHL22.6045	824.662248	0.76160693	0.08642289	77.3344492	1.44E-18	8.30E-17
WHL22.2898	3371.76927	0.75218035	0.04297089	305.463178	2.13E-68	3.44E-66
WHL22.5125	455.788568	0.75052357	0.10666837	49.4316293	2.05E-12	7.97E-11
WHL22.4118	289.338181	0.74673101	0.13237432	31.7842343	1.72E-08	4.50E-07
WHL22.5899	156.685197	0.74575207	0.18014168	17.109523	3.53E-05	0.00051716

WHL22.6993	546.809487	0.74489068	0.1015117	53.6795969	2.36E-13	9.83E-12
WHL22.4154	17995.0234	0.73922595	0.02570262	821.553771	1.11E-180	7.54E-178
WHL22.3243	601.557875	0.73432004	0.09469609	60.0029323	9.47E-15	4.26E-13
WHL22.6991	7954.89093	0.7285244	0.03215161	510.93983	3.96E-113	1.03E-110
WHL22.3639	100.100515	0.72543647	0.23131773	9.78066965	0.00176356	0.01518721
WHL22.4503	5519.64747	0.72455909	0.03585148	406.870128	1.76E-90	3.85E-88
WHL22.7248	503.292497	0.72212028	0.10121033	50.8376668	1.00E-12	4.00E-11
WHL22.2898	415.805656	0.7198646	0.11186371	41.3439467	1.28E-10	4.23E-09
WHL22.2252	624.287445	0.71922439	0.09146764	61.7389937	3.92E-15	1.80E-13
WHL22.4507	139.301587	0.71862569	0.19763125	13.1505957	0.00028743	0.00325216
WHL22.3997	430.401167	0.71361381	0.1087785	42.9881274	5.51E-11	1.89E-09
WHL22.4204	740.988629	0.71106418	0.0861754	67.9327954	1.69E-16	8.44E-15
WHL22.7035	654.914619	0.70736877	0.08875056	63.4488501	1.65E-15	7.76E-14
WHL22.7180	236.674871	0.70151143	0.14705492	22.7195525	1.87E-06	3.67E-05
WHL22.1451	158.81204	0.69733578	0.17691204	15.5240424	8.15E-05	0.00108181
WHL22.7366	108.299319	0.6920937	0.21950712	9.90316067	0.00164995	0.01435458
WHL22.2445	276.8468	0.68650036	0.13538139	25.6812423	4.03E-07	8.43E-06
WHL22.6096	312.201804	0.67935303	0.12704074	28.567545	9.05E-08	2.10E-06
WHL22.3242	291.716262	0.67797164	0.13251673	26.1371854	3.18E-07	6.85E-06
WHL22.2234	169.220109	0.67769216	0.17190656	15.5245541	8.14E-05	0.00108181
WHL22.1447	110.427992	0.67579974	0.21185353	10.1666854	0.00143001	0.01265196
WHL22.5837	870.016172	0.67307881	0.08021349	70.2550019	5.21E-17	2.70E-15
WHL22.3686	108.227396	0.66523951	0.21651701	9.42047372	0.00214576	0.01800824
WHL22.1578	236.302579	0.66516998	0.14847733	20.0263816	7.64E-06	0.00013256
WHL22.1502	182.684967	0.6612053	0.16834335	15.3933326	8.73E-05	0.00114582
WHL22.2277	199.464849	0.66054052	0.16120048	16.7530688	4.26E-05	0.0006095
WHL22.2502	30403.5205	0.65752323	0.0229531	815.494673	2.31E-179	1.42E-176
WHL22.5490	954.476895	0.65702421	0.07522139	76.1687918	2.60E-18	1.47E-16
WHL22.5199	13713.5653	0.6554471	0.02683432	593.791802	3.75E-131	1.27E-128
WHL22.3890	1027.4237	0.6528978	0.07652809	72.5704019	1.61E-17	8.61E-16
WHL22.2654	95.6013205	0.64914496	0.22918379	8.0080335	0.00465703	0.03361978
WHL22.2359	177.289668	0.64701065	0.17429886	13.7247043	0.00021165	0.00248061
WHL22.2637	357.225551	0.64696804	0.1201584	28.9486254	7.43E-08	1.76E-06
WHL22.2153	219.447325	0.64449931	0.15704545	16.7828413	4.19E-05	0.00060128
WHL22.5815	4464.69955	0.64448613	0.03825979	283.001266	1.67E-63	2.51E-61
WHL22.7360	398.768413	0.64404944	0.11380095	31.9845273	1.55E-08	4.09E-07
WHL22.2252	126.287224	0.63641582	0.20177594	9.92230436	0.00163288	0.01426089
WHL22.5036	413.173493	0.6291493	0.11382004	30.490739	3.35E-08	8.37E-07
WHL22.3859	159.691141	0.62243176	0.17833759	12.1603191	0.00048817	0.00512805
WHL22.4563	408.529628	0.62205647	0.1121812	30.7116971	2.99E-08	7.64E-07
WHL22.4725	3008.36061	0.6204738	0.04644368	178.016478	1.31E-40	1.35E-38
WHL22.7380	201.348367	0.61894549	0.16011507	14.9122757	0.00011263	0.00142592

WHL22.3180	8908.80142	0.61745593	0.03068642	403.400119	1.00E-89	2.12E-87
WHL22.3731	117.580835	0.61610448	0.20494946	9.02996437	0.0026559	0.02145585
WHL22.4137	111.443642	0.61593218	0.2282724	7.2086924	0.00725513	0.04874588
WHL22.6062	469.647137	0.61580064	0.10494159	34.3900017	4.51E-09	1.27E-07
WHL22.4310	248.702209	0.61490539	0.14468009	18.0281246	2.18E-05	0.00033646
WHL22.6660	201.705818	0.60960786	0.16150752	14.20866	0.00016362	0.00196513
WHL22.7318	566.532752	0.60799465	0.09553257	40.4573054	2.01E-10	6.49E-09
WHL22.7352	339.976272	0.60798884	0.1225713	24.5749535	7.15E-07	1.47E-05
WHL22.1155	17166.3413	0.60750577	0.02641482	526.443349	1.68E-116	4.74E-114
WHL22.4838	208.971521	0.60601382	0.15554554	15.1594698	9.88E-05	0.00128442
WHL22.1378	179.573257	0.60563811	0.16724901	13.0975028	0.00029569	0.0033221
WHL22.9118	163.147786	0.60493248	0.17621679	11.7651195	0.00060351	0.0061217
WHL22.6301	741.579411	0.60341831	0.08513494	50.159569	1.42E-12	5.59E-11
WHL22.3751	656.607329	0.60168182	0.08928165	45.3596175	1.64E-11	5.95E-10
WHL22.4923	449.031915	0.6006549	0.10851613	30.5870411	3.19E-08	8.05E-07
WHL22.7483	184.864147	0.5950184	0.16898811	12.3609951	0.0004384	0.00467761
WHL22.2804	1251.72598	0.59442339	0.06625485	80.3721256	3.10E-19	1.86E-17
WHL22.2701	3239.25349	0.59298384	0.04380415	182.873397	1.14E-41	1.19E-39
WHL22.3018	233.065645	0.59101921	0.14647577	16.2660861	5.50E-05	0.00076527
WHL22.2344	131.431612	0.59045737	0.20009347	8.67777897	0.00322113	0.02506721
WHL22.4188	19504.7331	0.58733138	0.02471214	562.404531	2.52E-124	8.15E-122
WHL22.3731	372.301896	0.58588998	0.11683359	25.1212622	5.38E-07	1.12E-05
WHL22.6519	587.547643	0.58469425	0.09371052	38.8882463	4.49E-10	1.38E-08
WHL22.7382	232.998741	0.57993595	0.15109784	14.6915686	0.00012661	0.00158814
WHL22.4884	119.704387	0.57847709	0.20621525	7.85251213	0.00507501	0.03598646
WHL22.5326	238.076084	0.57253626	0.14612698	15.3311609	9.02E-05	0.00117732
WHL22.6130	5276.56182	0.57201879	0.03587943	253.585024	4.29E-57	5.83E-55
WHL22.7006	862.639892	0.56840954	0.07945051	51.1061672	8.75E-13	3.51E-11
WHL22.5786	997.223834	0.56457838	0.07364291	58.6953798	1.84E-14	8.06E-13
WHL22.3615	840.208308	0.55274082	0.08377002	43.4308788	4.39E-11	1.53E-09
WHL22.4923	153.340893	0.55153987	0.17988267	9.39308322	0.00217806	0.01813532
WHL22.4008	194.520458	0.55065567	0.16254352	11.455859	0.00071269	0.00708098
WHL22.2619	382.757411	0.54976192	0.11664584	22.1805253	2.48E-06	4.72E-05
WHL22.3392	295.320079	0.54751861	0.13015747	17.6818497	2.61E-05	0.00039201
WHL22.7565	638.059407	0.54688781	0.09297205	34.536445	4.18E-09	1.19E-07
WHL22.1155	13721.8873	0.54503782	0.02673711	414.178135	4.52E-92	1.02E-89
WHL22.6214	525.414564	0.5433658	0.09960809	29.7220114	4.99E-08	1.23E-06
WHL22.1435	1097.15827	0.53996817	0.0698502	59.6914825	1.11E-14	4.92E-13
WHL22.4313	184.283862	0.53915914	0.16402365	10.7969343	0.00101668	0.0095293
WHL22.1222	130.035654	0.53783382	0.19799648	7.36292536	0.00665824	0.04568534
WHL22.4691	138.984153	0.5374177	0.188855	8.09110723	0.0044483	0.03231922
WHL22.4580	129.138395	0.53521582	0.19824562	7.27404639	0.0069958	0.04747351

WHL22.3823	242.114323	0.53211644	0.143779	13.6849878	0.00021618	0.00252926
WHL22.3500	275.958263	0.53009197	0.13636001	15.0917505	0.00010241	0.0013162
WHL22.5229	202.893207	0.52960812	0.15822792	11.1874011	0.00082355	0.00801805
WHL22.1101	828.658837	0.52921863	0.081966	41.619004	1.11E-10	3.71E-09
WHL22.3578	1379.5814	0.52893461	0.06991825	57.0528882	4.24E-14	1.80E-12
WHL22.5906	160.80149	0.52837564	0.18153896	8.44246522	0.00366559	0.02788643
WHL22.6157	435.306667	0.52705354	0.10780135	23.8843575	1.02E-06	2.05E-05
WHL22.7355	179.486746	0.52640988	0.1662043	10.0242745	0.00154491	0.01352739
WHL22.7421	538.886144	0.52640009	0.0977426	28.9764448	7.33E-08	1.75E-06
WHL22.3844	1040.54187	0.52611798	0.07214886	53.11069	3.15E-13	1.30E-11
WHL22.4758	424.043428	0.5258081	0.11263912	21.7494617	3.11E-06	5.82E-05
WHL22.2231	488.446971	0.5255697	0.10228552	26.3779033	2.81E-07	6.10E-06
WHL22.6397	1400.49013	0.52511814	0.0631211	69.1177681	9.28E-17	4.77E-15
WHL22.1140	264.959339	0.52425515	0.13766814	14.488657	0.00014101	0.00174611
WHL22.3802	156.861501	0.52416212	0.18432955	8.05604767	0.0045352	0.03284512
WHL22.5285	195.576047	0.52368042	0.16161297	10.4825792	0.00120505	0.01090333
WHL22.9020	218.409263	0.52343008	0.15064632	12.064798	0.00051383	0.00535613
WHL22.3253	221.98737	0.52237272	0.15018295	12.0870793	0.00050772	0.00530064
WHL22.4530	204.443307	0.52087219	0.15644621	11.0744349	0.00087526	0.00845805
WHL22.7311	148.105929	0.52078256	0.18537714	7.87704026	0.00500664	0.03565061
WHL22.2718	403.181772	0.51794282	0.11199098	21.3724876	3.78E-06	7.01E-05
WHL22.5917	1403.41447	0.51715465	0.06238132	68.6505365	1.18E-16	5.91E-15
WHL22.6697	384.321452	0.51490556	0.1168165	19.4004094	1.06E-05	0.00017802
WHL22.5688	482.398868	0.5139485	0.10339701	24.6821312	6.76E-07	1.39E-05
WHL22.4834	150.350698	0.51325879	0.1843664	7.73441682	0.00541781	0.03805925
WHL22.1674	808.904225	0.50843378	0.08525306	35.4849842	2.57E-09	7.55E-08
SPU_008752	289.99692	0.50841353	0.13397281	14.3775892	0.00014957	0.00182882
WHL22.9998	2820.36424	0.50833478	0.04748791	114.380215	1.08E-26	8.30E-25
WHL22.7565	852.458234	0.50799433	0.07966577	40.6096483	1.86E-10	6.04E-09
WHL22.5479	2382.42749	0.50776409	0.04969974	104.232756	1.80E-24	1.28E-22
WHL22.5804	4963.63123	0.50596211	0.03673064	189.40583	4.29E-43	4.62E-41
WHL22.6865	373.110436	0.5050204	0.12178666	17.1510328	3.45E-05	0.00050928
WHL22.7506	162.48639	-0.5027236	0.17955721	7.82224231	0.00516071	0.03651783
WHL22.4439	178.487665	-0.5121083	0.17792494	8.24375552	0.00408924	0.03042003
WHL22.5869	256.932634	-0.5121932	0.1423865	12.9239737	0.0003244	0.00360292
WHL22.5761	235.896766	-0.5233243	0.14543779	12.9458753	0.00032063	0.00356685
WHL22.4727	186.349824	-0.5246299	0.16894086	9.62081774	0.00192384	0.01640098
WHL22.1983	207.439985	-0.527499	0.15525008	11.5424484	0.00068025	0.00680852
WHL22.1362	168.658308	-0.5277643	0.17290961	9.31017306	0.00227885	0.01888786
WHL22.2247	213.707092	-0.5319506	0.1542377	11.886518	0.00056542	0.00576981
WHL22.2608	440.490368	-0.5328002	0.10965538	23.5856491	1.19E-06	2.37E-05
WHL22.4750	351.373884	-0.5329507	0.12333447	18.6466058	1.57E-05	0.0002527

WHL22.3897	145.761969	-0.5365291	0.18788092	8.14147327	0.00432641	0.03160283
WHL22.6879	138.652711	-0.5391882	0.19992396	7.23468602	0.00715083	0.04818823
WHL22.6216	2647.0539	-0.5409532	0.04716255	131.42039	2.00E-30	1.70E-28
WHL22.3202	162.015736	-0.5596458	0.17948479	9.70253615	0.00184014	0.01578658
WHL22.2236	136.833278	-0.5670869	0.19125951	8.78658385	0.00303454	0.02394464
WHL22.2276	135.983194	-0.5678711	0.19248547	8.69707986	0.0031872	0.02489085
WHL22.1610	9302.64442	-0.5693862	0.03031648	351.698293	1.81E-78	3.23E-76
WHL22.6936	735.410499	-0.5824329	0.08577772	46.059943	1.15E-11	4.23E-10
WHL22.5119	126.551522	-0.5868378	0.20385018	8.26408739	0.0040437	0.03015444
WHL22.6630	591.054528	-0.5965701	0.09329631	40.8740214	1.62E-10	5.32E-09
WHL22.6801	180.441292	-0.5971763	0.17018505	12.2904785	0.00045528	0.00483379
WHL22.4216	118.344421	-0.6154509	0.20551367	8.96403945	0.00275345	0.02208622
WHL22.6628	188.574294	-0.6313093	0.16284031	15.0282006	0.00010592	0.0013587
WHL22.5980	338354.677	-0.6404106	0.01923958	1099.29442	4.70E-241	6.38E-238
WHL22.1599	217.683215	-0.6474734	0.15256473	18.0036555	2.20E-05	0.00034004
WHL22.5566	464.71325	-0.6606416	0.10538293	39.280043	3.67E-10	1.14E-08
WHL22.1993	105.073079	-0.6790304	0.21834464	9.66712329	0.00187595	0.01607347
WHL22.3616	434.043442	-0.6952839	0.11009611	39.8441044	2.75E-10	8.66E-09
WHL22.7526	128.805998	-0.6956225	0.19969184	12.1155522	0.00050003	0.00523643
WHL22.3501	98.004979	-0.7123951	0.22698216	9.84226543	0.00170547	0.01481362
WHL22.6819	231.570221	-0.7298387	0.15053587	23.4687962	1.27E-06	2.51E-05
WHL22.7134	119.145665	-0.7408747	0.20786872	12.6807743	0.00036943	0.00403052
WHL22.7445	121.666234	-0.7647695	0.20492287	13.9110764	0.00019167	0.00225806
WHL22.5441	6269.25916	-1.1714572	0.03696697	993.191604	5.42E-218	5.26E-215
WHL22.7206	522.499106	-1.1964393	0.10339002	133.695416	6.37E-31	5.54E-29
WHL22.9990	276.357408	-1.2222839	0.13837322	78.0609696	9.99E-19	5.79E-17
WHL22.1194	3042.05059	-1.4211507	0.04606664	946.452035	7.83E-208	6.65E-205
WHL22.1319	1205.74193	-2.4249404	0.07451634	1079.62674	8.85E-237	1.00E-233

	baseMean	log2FoldCha	lfcSE	stat	pvalue	padj
WHL22.3245	38.3067891	6.37903986	0.89837961	112.374436	2.96E-26	1.07E-24
WHL22.3119	302.635998	5.51809306	0.37382355	194.217517	3.82E-44	2.49E-42
WHL22.5414	19.4089927	5.37598047	0.95510308	51.1853538	8.40E-13	1.53E-11
WHL22.3452	26.1525504	5.29773977	1.17399671	17.1495678	3.45E-05	0.00025811
WHL22.2249	29.52429	4.54102736	0.64455184	62.8257692	2.26E-15	4.94E-14
WHL22.2526	13.1844141	4.12362012	0.87457838	26.3416623	2.86E-07	2.91E-06
WHL22.4125	228.954374	4.10475826	0.21249935	436.977148	4.92E-97	7.16E-95
WHL22.3470	72.3625897	4.03420005	0.37164275	136.397385	1.63E-31	7.22E-30
WHL22.7557	31.3304237	3.79392099	0.53115949	58.2742948	2.28E-14	4.72E-13
WHL22.7595	426.361579	3.59163922	0.14566612	653.420618	4.03E-144	1.14E-141
WHL22.1694	664.950103	3.57079052	0.11161899	1133.00913	2.21E-248	1.35E-245
WHL22.2683	15.2898279	3.54687094	0.74597842	24.2541892	8.44E-07	8.03E-06
WHL22.4287	43.819104	3.52833485	0.60959568	30.3433958	3.62E-08	4.08E-07
WHL22.2985	11.7355018	3.46219133	0.85026269	17.6370125	2.67E-05	0.00020451
WHL22.3649	48.7815547	3.44636609	0.4068771	77.846295	1.11E-18	2.89E-17
WHL22.1816	109.847311	3.3043281	0.27805343	146.414452	1.05E-33	5.01E-32
WHL22.6401	108.568801	3.30094243	0.26303867	170.368376	6.15E-39	3.34E-37
WHL22.1269	12.569418	3.26525073	0.77386263	18.8345765	1.43E-05	0.00011455
WHL22.3995	48.0096731	3.25822497	0.39199033	74.4523338	6.21E-18	1.57E-16
WHL22.2106	31.1305136	3.20408376	0.48585689	46.3925319	9.68E-12	1.59E-10
WHL22.5326	17.3166063	3.12506679	0.64176478	25.2294103	5.09E-07	4.99E-06
WHL22.1729	13.252603	3.12505645	0.73728062	18.9420747	1.35E-05	0.00010869
WHL22.1588	575.692427	3.11047128	0.22160683	174.629695	7.21E-40	4.03E-38
WHL22.5468	415.289264	3.09816578	0.13126293	589.405673	3.37E-130	7.08E-128
WHL22.6993	1418.09964	3.09757517	0.07318536	1866.037	0	0
WHL22.4150	3281.61156	3.04684461	0.04939339	3891.8644	0	0
WHL22.4154	12920.2726	3.04631351	0.02661147	13058.0947	0	0
WHL22.3562	1846.98674	3.0437451	0.06384746	2355.74337	0	0
WHL22.7106	443.936589	3.028608	0.18456922	250.412218	2.11E-56	1.80E-54
WHL22.6201	900.496668	3.01700976	0.09273981	1086.18092	3.33E-238	1.69E-235
WHL22.6201	290.502059	2.92773058	0.15519808	369.55295	2.34E-82	2.79E-80
SPU_012384	37.0448729	2.89647708	0.43733225	44.9432367	2.03E-11	3.20E-10
WHL22.5229	122.629339	2.89301432	0.23391205	159.789379	1.26E-36	6.57E-35
WHL22.5460	167.017383	2.88503922	0.20729091	198.83339	3.75E-45	2.53E-43
WHL22.7098	21.3185366	2.88209688	0.56828091	26.4001614	2.78E-07	2.83E-06
WHL22.2246	292.176004	2.87799273	0.1512679	377.688736	3.96E-84	4.89E-82
WHL22.4729	151.956757	2.83283514	0.21038632	187.845654	9.39E-43	5.92E-41
WHL22.2525	107.286979	2.83205458	0.38269491	50.2601214	1.35E-12	2.40E-11
WHL22.7205	291.51307	2.79060792	0.15496114	331.709228	4.08E-74	4.28E-72

WHL22.7658	70.3551906	2.77782129	0.30827571	83.8185863	5.42E-20	1.51E-18
WHL22.6197	1244.59905	2.75365325	0.07496338	1376.71959	2.41E-301	1.77E-298

WHL22.3468	16.870076	2.73498583	0.63874796	18.282012	1.90E-05	0.00015027
WHL22.5778	3236.58984	2.72942185	0.04805576	3248.88835	0	0
WHL22.6886	87.9257061	2.70913261	0.27038336	103.561005	2.52E-24	8.46E-23
WHL22.7252	21.4544504	2.6877204	0.55019165	24.3719757	7.94E-07	7.59E-06
WHL22.6201	1348.97581	2.61660884	0.07108701	1373.1727	1.42E-300	9.92E-298
WHL22.6123	102.164012	2.61072649	0.24773784	114.048338	1.27E-26	4.67E-25
WHL22.6681	31.7201533	2.57592302	0.44336197	34.6171373	4.01E-09	5.11E-08
WHL22.4379	70.1124177	2.50847087	0.29610435	73.3017768	1.11E-17	2.78E-16
WHL22.1599	303.721557	2.50751079	0.14489954	304.228319	3.95E-68	3.92E-66
WHL22.6738	32.7491665	2.44756665	0.43770845	31.525494	1.97E-08	2.31E-07
WHL22.6359	11.6972581	2.41288363	0.73929338	10.4733271	0.0012111	0.00657751
WHL22.3215	41.1114394	2.38101631	0.38945026	37.6173172	8.61E-10	1.16E-08
WHL22.6192	64.0447986	2.3574405	0.3040166	61.14861	5.29E-15	1.13E-13
WHL22.6576	1010.41812	2.34507958	0.07866895	896.192956	6.60E-197	2.69E-194
WHL22.5337	11.8622174	2.33544275	0.70408369	11.1904763	0.00082218	0.00464395
WHL22.3024	23.6276173	2.33019888	0.49908223	22.1538248	2.52E-06	2.27E-05
WHL22.5447	92.6495966	2.316186	0.26218982	78.1039605	9.78E-19	2.55E-17
WHL22.1712	37.0711216	2.31035416	0.39742607	34.3136515	4.69E-09	5.93E-08
WHL22.1446	1624.59207	2.30006079	0.06254226	1358.40551	2.30E-297	1.47E-294
WHL22.2360	31.4279039	2.29772884	0.43134961	28.7588064	8.20E-08	8.87E-07
WHL22.4085	44.9053267	2.25075497	0.37220658	36.5786063	1.47E-09	1.94E-08
WHL22.3849	13.7931014	2.23082553	0.64838453	11.9821539	0.00053712	0.00316032
WHL22.9177	672.806355	2.22410256	0.09474133	554.697379	1.20E-122	2.41E-120
WHL22.4333	40.2551051	2.20827846	0.39965346	30.0873717	4.13E-08	4.61E-07
WHL22.6193	16.0898032	2.20821936	0.59974813	13.7488093	0.00020895	0.00135787
WHL22.4334	18.2910186	2.1823468	0.56552773	14.890726	0.00011392	0.00077821
WHL22.9502	105.208549	2.1715168	0.25730964	69.8671789	6.34E-17	1.52E-15
WHL22.4203	13.0813253	2.15145831	0.65868428	10.7691839	0.00103204	0.0056892
WHL22.3393	106.717512	2.1380066	0.23616384	82.191397	1.24E-19	3.37E-18
WHL22.6085	36.0266317	2.12777342	0.39990188	28.4347856	9.69E-08	1.04E-06
WHL22.6990	16.7858609	2.11902878	0.59401815	12.6243993	0.00038074	0.00233083
WHL22.5375	11.5998995	2.09919847	0.73423451	7.8601132	0.00505372	0.02298285
WHL22.3023	29.4187747	2.09847146	0.44170358	22.6478951	1.95E-06	1.78E-05
WHL22.7104	54.6926179	2.09704078	0.3288629	40.6830783	1.79E-10	2.57E-09
WHL22.1321	156.58133	2.07943665	0.19399363	115.124356	7.39E-27	2.75E-25
WHL22.2105	121.722587	2.07052602	0.21824672	90.297119	2.05E-21	6.14E-20
WHL22.1307	41.3877299	2.0659437	0.39566307	26.6164752	2.48E-07	2.54E-06
WHL22.4968	144.270131	2.06524879	0.20040174	106.568723	5.53E-25	1.90E-23
WHL22.1136	35.3256253	2.05996884	0.40589419	25.6953086	4.00E-07	3.97E-06
WHL22.5324	63.5960034	2.05535479	0.30156215	46.5499646	8.93E-12	1.46E-10
WHL22.1049	94.3843373	2.04347178	0.24842193	67.7428073	1.86E-16	4.29E-15
WHL22.5481	334.720938	2.03805368	0.13287934	235.475708	3.81E-53	3.03E-51

WHL22.5140	95.1333438	2.03255176	0.24664478	68.0595101	1.59E-16	3.67E-15
WHL22.4530	573.441664	2.03214324	0.10262088	391.840706	3.29E-87	4.16E-85
WHL22.4679	26.0851513	2.02968633	0.46255127	19.3726872	1.08E-05	8.79E-05
WHL22.9950	23.1473523	2.02137296	0.49796064	16.4151722	5.09E-05	0.00036864
WHL22.8445	15.1096545	2.02021758	0.61605466	10.6809022	0.00108247	0.00594489
WHL22.1599	69.0785301	2.01120514	0.28664454	49.3951143	2.09E-12	3.69E-11
WHL22.2429	371.129765	1.96843591	0.12421688	251.612588	1.16E-56	9.98E-55
WHL22.1447	89.6561414	1.96239444	0.3792226	25.1662834	5.26E-07	5.15E-06
WHL22.5899	281.37574	1.96085904	0.14140805	192.922135	7.32E-44	4.71E-42
WHL22.5740	25.3457035	1.94968646	0.47980217	16.3090398	5.38E-05	0.00038777
WHL22.2225	336.433135	1.93575535	0.12902488	225.74662	5.05E-51	3.84E-49
WHL22.2266	17.3488104	1.92899787	0.56425115	11.6907839	0.0006281	0.00363015
WHL22.4376	15.0848304	1.92424646	0.60310817	10.2093985	0.00139727	0.00747245
WHL22.5900	588.143289	1.92398108	0.10008425	368.947483	3.17E-82	3.76E-80
WHL22.5036	87.9378975	1.90730315	0.25682783	54.938283	1.24E-13	2.43E-12
WHL22.4040	593.437623	1.87795356	0.0986091	362.359702	8.63E-81	9.82E-79
WHL22.6130	6158.85594	1.85012873	0.03257112	3197.03237	0	0
WHL22.2243	25.0885304	1.84471315	0.47098412	15.2510198	9.41E-05	0.00065086
WHL22.7191	74.9865175	1.83994469	0.26901538	46.9011665	7.47E-12	1.24E-10
WHL22.2360	143.335596	1.83887293	0.19828491	85.9078387	1.89E-20	5.35E-19
WHL22.4414	44.0963324	1.83674786	0.35610226	26.5183433	2.61E-07	2.66E-06
WHL22.2429	106.027264	1.83188963	0.23307902	61.5460126	4.33E-15	9.28E-14
WHL22.1853	35.126608	1.82555959	0.39153734	21.7989807	3.03E-06	2.70E-05
WHL22.1458	567.795386	1.82515889	0.09833833	345.027253	5.13E-77	5.58E-75
WHL22.6035	74.3727327	1.82377222	0.27304387	44.6302072	2.38E-11	3.71E-10
WHL22.1247	80.1179604	1.81600156	0.25980265	48.9706228	2.60E-12	4.52E-11
WHL22.5635	122.634107	1.80575451	0.21077915	73.4899305	1.01E-17	2.53E-16
WHL22.1136	135.430337	1.79546708	0.20041136	80.3620267	3.12E-19	8.41E-18
WHL22.7437	12.3927253	1.77370639	0.66401165	7.14596565	0.00751328	0.03255459
WHL22.4333	845.762417	1.74498333	0.08256482	445.222251	7.90E-99	1.17E-96
WHL22.2354	44.8800459	1.73996766	0.35716465	23.4890951	1.26E-06	1.17E-05
WHL22.1511	15.7200657	1.735527	0.586528	8.69903569	0.00318378	0.01534404
WHL22.4839	35.375512	1.73087263	0.40340825	18.1487327	2.04E-05	0.00016013
WHL22.3392	348.590707	1.73036584	0.12892909	179.263147	7.02E-41	4.07E-39
WHL22.6926	48.6193865	1.72827097	0.33691835	26.2071899	3.07E-07	3.10E-06
WHL22.7491	1661.83777	1.70288298	0.05805876	858.516727	1.02E-188	3.76E-186
WHL22.7480	30.2149996	1.70209147	0.4304773	15.5018878	8.24E-05	0.00057618
WHL22.5688	397.615941	1.6836125	0.11697277	206.996079	6.21E-47	4.43E-45
WHL22.6936	458.055079	1.67610006	0.10840569	239.004362	6.48E-54	5.26E-52
WHL22.6799	13.9844127	1.66731392	0.61341777	7.39606873	0.00653666	0.02885959
WHL22.3684	374.671828	1.65636834	0.12156137	185.196729	3.56E-42	2.16E-40
WHL22.7477	18.7818476	1.64664162	0.52803621	9.73273205	0.00181015	0.0093699

WHL22.6157	297.405323	1.6129664	0.1341584	144.399252	2.91E-33	1.36E-31
WHL22.6968	79.1870493	1.60992754	0.26651216	36.2253507	1.76E-09	2.31E-08
WHL22.7334	2716.12506	1.60807783	0.04839765	1093.79008	7.39E-240	3.87E-237
WHL22.6939	18.222238	1.59026974	0.53884397	8.66823201	0.00323805	0.0155698
WHL22.6050	26.5012245	1.57907149	0.44716677	12.4176168	0.0004253	0.00257674
WHL22.2619	110.458303	1.57722622	0.2181433	52.2409954	4.91E-13	9.10E-12
WHL22.2142	20.3846983	1.56810853	0.51502503	9.22904134	0.00238206	0.01192717
WHL22.6936	716.220547	1.56448906	0.08680707	324.167412	1.79E-72	1.84E-70
WHL22.5674	1273.018	1.5593064	0.06930362	502.193587	3.17E-111	5.67E-109
WHL22.7104	27.3077701	1.55768327	0.43916858	12.5869414	0.00038845	0.00237306
WHL22.6436	232.691908	1.55589607	0.23780058	41.2177339	1.36E-10	1.98E-09
WHL22.6160	36.8178002	1.55343573	0.38804673	15.8330149	6.92E-05	0.00048923
WHL22.7014	167.806525	1.55321033	0.17906147	75.026924	4.64E-18	1.18E-16
WHL22.1022	297.558885	1.54555624	0.13739939	125.866112	3.29E-29	1.32E-27
WHL22.6233	26.1586864	1.54523239	0.4478332	11.8985024	0.00056179	0.003287
WHL22.6375	26.2701369	1.54214093	0.47812493	10.0794307	0.00149934	0.00796031
WHL22.5502	16.4929255	1.541018	0.57914506	6.89738201	0.00863221	0.03654002
WHL22.1718	30.592772	1.5293217	0.41533324	13.4962674	0.00023904	0.00153369
WHL22.5490	491.685943	1.52641926	0.16259801	85.3791418	2.46E-20	6.98E-19
WHL22.5449	110.98614	1.52458353	0.21747323	49.0759905	2.46E-12	4.30E-11
WHL22.2359	166.361333	1.52067227	0.17756594	73.2525383	1.14E-17	2.84E-16
WHL22.7167	41.5295525	1.51160236	0.35969022	17.5420709	2.81E-05	0.00021397
WHL22.2500	55.7194007	1.49164407	0.30948641	23.1203456	1.52E-06	1.41E-05
WHL22.4414	881.725098	1.48804842	0.07797351	363.315841	5.34E-81	6.17E-79
WHL22.7421	33.4616387	1.48629365	0.43634582	11.0715193	0.00087664	0.00491936
WHL22.6681	19.3729048	1.47987598	0.51601996	8.21495256	0.00415466	0.01930687
WHL22.3401	90.4632676	1.46643011	0.24465362	35.7395548	2.26E-09	2.93E-08
WHL22.7612	23.8162329	1.46395907	0.53172529	7.13223287	0.00757104	0.03272758
WHL22.7492	187.758451	1.46262514	0.16811851	75.5006095	3.65E-18	9.34E-17
WHL22.2308	17.6813397	1.4620598	0.53911208	7.33816189	0.00675058	0.02967911
WHL22.6830	559.62174	1.45963389	0.09701226	225.936556	4.59E-51	3.51E-49
WHL22.6216	27.3659495	1.45850268	0.44594639	10.5986018	0.00113173	0.00618534
WHL22.4253	1097.1686	1.45752386	0.07205228	407.030652	1.62E-90	2.17E-88
WHL22.1119	1714.95183	1.45678569	0.05702258	649.884848	2.37E-143	6.32E-141
WHL22.7180	158.709839	1.4549595	0.18247216	63.4022323	1.69E-15	3.72E-14
WHL22.4282	180.152229	1.4541077	0.16984804	73.1871555	1.18E-17	2.93E-16
WHL22.2858	44.6126927	1.44721288	0.34741577	17.2098387	3.35E-05	0.00025081
WHL22.6426	353.732261	1.43241543	0.12513009	130.396438	3.36E-30	1.40E-28
WHL22.2142	43.9552311	1.4306019	0.35541389	15.9773769	6.41E-05	0.00045571
WHL22.5007	345.998272	1.42938616	0.12450209	131.379801	2.04E-30	8.68E-29
WHL22.5823	64.4213432	1.4288943	0.28753788	24.5597076	7.20E-07	6.95E-06
WHL22.4333	100.562544	1.4097577	0.23313204	36.3080626	1.68E-09	2.22E-08

WHL22.7421	814.327612	1.40882603	0.08304761	286.316096	3.16E-64	3.05E-62
WHL22.7310	1830.69573	1.40589161	0.05457205	661.283962	7.85E-146	2.26E-143
WHL22.1371	45.7356026	1.40254073	0.3393181	16.9911577	3.76E-05	0.00027886
WHL22.5385	465.477081	1.39926045	0.10658902	171.882873	2.87E-39	1.57E-37
WHL22.4979	33.9142841	1.39340199	0.39743148	12.1692796	0.00048583	0.00289801
WHL22.5087	250.16524	1.39179894	0.14373646	93.5964253	3.87E-22	1.20E-20
WHL22.2683	40.5935591	1.39149296	0.3596288	14.884634	0.00011429	0.00078036
WHL22.4832	89.8712211	1.3900577	0.24502248	31.9767905	1.56E-08	1.85E-07
WHL22.7621	19.1868949	1.38874973	0.51437357	7.28038933	0.00697114	0.03050264
WHL22.7261	168.32368	1.38598097	0.1838552	56.3398927	6.10E-14	1.22E-12
WHL22.2456	19.7025827	1.38460542	0.51262063	7.25970016	0.00705191	0.03076454
WHL22.3880	56.3349912	1.38222452	0.30575143	20.3285727	6.52E-06	5.53E-05
WHL22.7452	312.126927	1.3818907	0.14286866	92.3793638	7.16E-22	2.19E-20
WHL22.4176	97610.0639	1.37939402	0.01495374	8268.19209	0	0
WHL22.3359	19.7051205	1.37830618	0.51364933	7.1425563	0.00752758	0.03258809
WHL22.7200	21.5745632	1.37503722	0.49981795	7.44355968	0.00636638	0.02825228
WHL22.1906	387.553885	1.37304311	0.11965358	130.967471	2.52E-30	1.06E-28
WHL22.1668	94.3093995	1.36402254	0.23678444	33.0297478	9.08E-09	1.11E-07
WHL22.3844	1117.0915	1.35815354	0.06989168	376.123978	8.69E-84	1.06E-81
WHL22.5037	49.4481495	1.35343162	0.32446276	17.323322	3.15E-05	0.0002376
WHL22.1806	77.3079555	1.35280322	0.25776999	27.4877613	1.58E-07	1.66E-06
WHL22.4533	61.7890441	1.34985816	0.28872379	21.8020019	3.02E-06	2.69E-05
WHL22.6489	24.6110785	1.346624	0.48816099	7.36100944	0.00666534	0.02935708
WHL22.6991	9559.93982	1.32992696	0.02696337	2406.96447	0	0
WHL22.4832	353.211644	1.32914651	0.12273336	116.858408	3.08E-27	1.17E-25
WHL22.8441	1592.64494	1.32836081	0.06078012	474.524048	3.32E-105	5.60E-103
WHL22.7040	282.387823	1.32715405	0.13597905	94.9866926	1.92E-22	6.04E-21
WHL22.7472	31.2910144	1.32571269	0.4051599	10.6617625	0.00109373	0.00599999
WHL22.2234	173.581594	1.32035119	0.17238148	58.5332024	2.00E-14	4.14E-13
WHL22.4559	111.863059	1.31217428	0.21360418	37.664929	8.40E-10	1.13E-08
WHL22.4522	88.7094104	1.31189568	0.24329453	28.9394348	7.47E-08	8.14E-07
WHL22.2143	35.3648581	1.31067305	0.38101353	11.78501	0.0005971	0.00347418
WHL22.3059	180.982806	1.30101693	0.17224846	56.7817672	4.87E-14	9.85E-13
WHL22.5375	50.2977282	1.30096029	0.33249815	15.1236446	0.00010069	0.00069399
WHL22.9873	29.6916624	1.29184777	0.44041922	8.35685659	0.00384235	0.01809033
WHL22.5134	66.3550273	1.28866242	0.28117665	20.8912258	4.86E-06	4.19E-05
WHL22.2989	21.5317135	1.28513462	0.49236258	6.73550718	0.00945124	0.03931543
WHL22.2561	51.1960937	1.28271392	0.3193802	16.0420851	6.20E-05	0.00044147
WHL22.7565	585.138485	1.27542533	0.09956311	162.97777	2.53E-37	1.34E-35
WHL22.4118	151.165945	1.27484901	0.18646209	46.5564447	8.90E-12	1.46E-10
WHL22.7647	88.3452368	1.27086532	0.24379231	27.0334475	2.00E-07	2.07E-06
WHL22.6476	475.401889	1.26791798	0.10466099	146.34514	1.09E-33	5.17E-32

WHL22.3242	230.725528	1.26788359	0.14905845	72.1809434	1.96E-17	4.82E-16
WHL22.6301	558.262931	1.26639379	0.0966029	171.368102	3.72E-39	2.03E-37
WHL22.5901	41.6793467	1.26552807	0.34928082	13.0963886	0.00029587	0.00185295
WHL22.7518	605.996444	1.2640614	0.0925169	186.18577	2.16E-42	1.34E-40
WHL22.1200	46.6755788	1.26298785	0.33941561	13.6954653	0.00021497	0.00139145
WHL22.3273	88.406992	1.26229891	0.24340404	26.7669276	2.30E-07	2.36E-06
WHL22.4530	142.928384	1.26074005	0.19046137	43.6724081	3.88E-11	5.91E-10
WHL22.4889	266.765119	1.25883291	0.14507594	74.7843538	5.25E-18	1.33E-16
WHL22.1530	110.30044	1.25593902	0.21443074	34.2417874	4.87E-09	6.15E-08
WHL22.5872	1227.31165	1.25587616	0.06655936	354.572213	4.28E-79	4.76E-77
WHL22.2394	1794.26736	1.24970253	0.0545601	522.824067	1.03E-115	1.96E-113
WHL22.4392	501.480964	1.24830681	0.10142839	151.088149	1.00E-34	4.97E-33
WHL22.4936	60.7799825	1.24503019	0.29077825	18.261213	1.93E-05	0.00015184
WHL22.5030	309.971033	1.24268513	0.13116277	89.3906836	3.24E-21	9.63E-20
WHL22.5453	150.088254	1.24252673	0.18976235	42.6066863	6.69E-11	9.99E-10
WHL22.5325	230.237271	1.24059494	0.14922965	68.9367862	1.02E-16	2.38E-15
WHL22.3420	57.9850948	1.23779202	0.29633081	17.3956755	3.04E-05	0.00022943
WHL22.4376	116.219507	1.23165339	0.21056821	34.096948	5.24E-09	6.61E-08
WHL22.4675	68.3156149	1.22916235	0.27276817	20.2590637	6.76E-06	5.71E-05
WHL22.5798	21.8350917	1.22817197	0.48256047	6.43908784	0.0111636	0.04535887
WHL22.7311	102.466143	1.22715175	0.22371097	30.0007453	4.32E-08	4.81E-07
WHL22.5009	156.232278	1.22450995	0.1827058	44.7450964	2.24E-11	3.51E-10
WHL22.3358	41.4211102	1.22374635	0.34942673	12.2340878	0.00046924	0.00281048
WHL22.2502	154.883737	1.22334974	0.18364762	44.2133032	2.94E-11	4.56E-10
WHL22.5354	37.2044902	1.22314439	0.37896828	10.3454472	0.00129794	0.00699479
WHL22.3759	482.506962	1.2215973	0.1030699	140.132753	2.49E-32	1.14E-30
WHL22.7552	94.3384506	1.22008534	0.23115068	27.8063035	1.34E-07	1.41E-06
WHL22.4595	25.9168327	1.2198301	0.44872015	7.31759918	0.00682826	0.02996144
WHL22.4117	28.9733317	1.21889448	0.41943039	8.41511183	0.00372115	0.01755913
WHL22.3248	261.908992	1.21868293	0.1440758	71.1683484	3.28E-17	7.92E-16
WHL22.4871	59.9891999	1.2170846	0.29121788	17.4111582	3.01E-05	0.00022769
WHL22.5808	58.588048	1.21530476	0.29456502	16.9770284	3.78E-05	0.00028051
WHL22.5547	238.323502	1.21509065	0.14750552	67.6597191	1.94E-16	4.46E-15
WHL22.4794	114.212249	1.21469749	0.21623777	31.3717269	2.13E-08	2.48E-07
WHL22.4354	136.739533	1.21381375	0.20218645	35.7189315	2.28E-09	2.96E-08
WHL22.1479	25.7225841	1.21220612	0.45958744	6.82512767	0.00898841	0.03779717
WHL22.1664	34.6461087	1.20746759	0.38155421	9.98691611	0.00157656	0.00830426
WHL22.3045	31.0190448	1.20547117	0.40185439	8.98113476	0.00272781	0.01342866
WHL22.3974	29.9710403	1.20358302	0.42770201	7.76575161	0.00532461	0.02408051
WHL22.5622	143.553196	1.20089405	0.18923342	40.1421374	2.36E-10	3.35E-09
WHL22.4650	51.3292088	1.19993112	0.31567888	14.3901664	0.00014858	0.00099231
WHL22.7577	1510.45848	1.1995777	0.05939274	406.517124	2.10E-90	2.78E-88

WHL22.3110	39.1975967	1.19848628	0.36219394	10.8924348	0.00096558	0.00536108
WHL22.3893	152.049755	1.19627441	0.19137468	38.7571996	4.80E-10	6.62E-09
WHL22.7249	253.405516	1.19504642	0.14242913	70.1970064	5.37E-17	1.29E-15
WHL22.2804	1563.30964	1.1934256	0.05827193	418.020973	6.58E-93	8.94E-91
WHL22.6157	63.7360426	1.1927848	0.28316454	17.675802	2.62E-05	0.00020059
WHL22.7054	86.5133365	1.19247631	0.24331431	23.9356854	9.96E-07	9.41E-06
WHL22.2689	784.528731	1.18882783	0.08145395	212.387044	4.14E-48	3.01E-46
WHL22.7248	456.668582	1.18478073	0.10990787	115.58237	5.87E-27	2.21E-25
WHL22.1524	28.6259184	1.18299886	0.43748156	7.15982327	0.00745545	0.03232462
WHL22.2701	3530.76393	1.17984452	0.04039967	848.328302	1.68E-186	6.01E-184
WHL22.3174	342.718532	1.17309008	0.12366552	89.660806	2.83E-21	8.44E-20
WHL22.4313	235.721659	1.17273182	0.14867116	61.9952308	3.44E-15	7.44E-14
WHL22.1281	93.4919746	1.16999692	0.2325749	25.2414494	5.06E-07	4.97E-06
WHL22.3692	145.813516	1.16914021	0.18923416	38.0051911	7.06E-10	9.57E-09
WHL22.4837	4720.57519	1.16728556	0.03508189	1101.07314	1.93E-241	1.09E-238
WHL22.3772	25.5164585	1.16494688	0.44221031	6.92730178	0.00848897	0.03606889
WHL22.4066	139.384101	1.16306005	0.19277874	36.2643636	1.72E-09	2.26E-08
WHL22.7355	176.240819	1.15665091	0.17027427	46.0196852	1.17E-11	1.89E-10
WHL22.5946	32.6604984	1.1559416	0.40075902	8.23102615	0.00411802	0.01917304
WHL22.1853	166.440176	1.15516847	0.17467683	43.6184974	3.99E-11	6.06E-10
WHL22.5839	870.043709	1.1468546	0.07748417	218.392302	2.03E-49	1.50E-47
WHL22.6066	172.46126	1.14211491	0.17112583	44.4387519	2.62E-11	4.08E-10
WHL22.5449	244.930886	1.14154705	0.14692034	60.1166495	8.94E-15	1.87E-13
WHL22.2620	231.245326	1.13603663	0.15110943	56.2899968	6.25E-14	1.25E-12
WHL22.2999	85.292645	1.13559987	0.24230947	21.9170131	2.85E-06	2.55E-05
WHL22.5057	116.734087	1.13458458	0.2078024	29.7358229	4.95E-08	5.47E-07
WHL22.1252	103.838257	1.13445505	0.22388908	25.564049	4.28E-07	4.24E-06
WHL22.5906	114.824614	1.13341051	0.22002175	26.2935501	2.93E-07	2.98E-06
WHL22.5661	36.5824457	1.13321871	0.37935064	8.83114794	0.00296132	0.014433
WHL22.3731	44.9132343	1.13152126	0.33523079	11.3524624	0.00075348	0.00429223
WHL22.7206	125.824982	1.12926329	0.20797897	29.2733864	6.29E-08	6.90E-07
WHL22.7309	256.859098	1.12653501	0.14419096	60.7544782	6.47E-15	1.37E-13
WHL22.5021	163.834773	1.12592745	0.17553213	41.0448322	1.49E-10	2.15E-09
WHL22.1771	240.244172	1.12530899	0.14857089	57.11651	4.11E-14	8.35E-13
WHL22.1240	753.026911	1.12517958	0.08296556	183.394814	8.79E-42	5.29E-40
WHL22.1316	83.3762966	1.12349835	0.24772284	20.4867303	6.00E-06	5.12E-05
WHL22.7565	408.11841	1.1225284	0.12001797	86.8202461	1.19E-20	3.45E-19
WHL22.2452	90.3448697	1.12229858	0.24001902	21.7461116	3.11E-06	2.77E-05
WHL22.3022	28.9043506	1.1221993	0.42731631	6.80180094	0.0091066	0.03819567
WHL22.6548	264.248722	1.12163753	0.13906012	64.8729706	7.99E-16	1.79E-14
WHL22.5808	103.969608	1.12092696	0.22131961	25.5653799	4.28E-07	4.24E-06
WHL22.7360	488.39898	1.11709603	0.10305581	117.142838	2.67E-27	1.02E-25

WHL22.5133	190.536331	1.11610216	0.16256928	47.0239388	7.01E-12	1.17E-10
WHL22.4833	831.067084	1.1136216	0.07873535	199.49165	2.70E-45	1.83E-43
WHL22.4948	46.4500237	1.11082417	0.32739678	11.4889641	0.00070011	0.00401467
WHL22.1847	16724.3781	1.1079296	0.02208041	2490.91075	0	0
WHL22.1486	4860.6214	1.10775711	0.03507707	991.573114	1.22E-217	5.77E-215
WHL22.1013	68.0512515	1.1023605	0.27444926	16.0624294	6.13E-05	0.00043718
WHL22.5633	420.042892	1.10091531	0.11446474	92.0263544	8.55E-22	2.60E-20
WHL22.5213	866.158277	1.09808987	0.07991139	187.937477	8.96E-43	5.67E-41
WHL22.3023	36.7109072	1.09084232	0.37106021	8.6136079	0.00333661	0.01597567
WHL22.5688	75.2542696	1.08796359	0.25912849	17.5701944	2.77E-05	0.00021094
WHL22.4614	144.202782	1.08759714	0.19054151	32.4363821	1.23E-08	1.48E-07
WHL22.4758	244.855796	1.08549531	0.14837493	53.2514455	2.93E-13	5.57E-12
WHL22.6522	7551.24762	1.08281597	0.0288761	1397.02967	9.29E-306	7.18E-303
WHL22.8378	63.4048946	1.08196567	0.28670839	14.1439723	0.00016934	0.00112028
WHL22.7446	480.512458	1.07934335	0.10498332	105.293241	1.05E-24	3.58E-23
WHL22.2506	57.141492	1.07900555	0.29892161	12.9663705	0.00031714	0.00197269
WHL22.2993	271.920989	1.077706	0.13808581	60.7042385	6.63E-15	1.40E-13
WHL22.3094	56.9273292	1.0752165	0.30221986	12.5840533	0.00038905	0.00237574
WHL22.5244	201.875515	1.07391781	0.15858636	45.7287399	1.36E-11	2.18E-10
WHL22.1761	91.1930063	1.07116856	0.23629601	20.4716133	6.05E-06	5.15E-05
WHL22.1939	179.959729	1.06562879	0.16769062	40.2734724	2.21E-10	3.15E-09
WHL22.4927	160.167697	1.06547229	0.18106492	34.4633483	4.34E-09	5.52E-08
WHL22.4884	82.8949035	1.06532863	0.24892763	18.2308178	1.96E-05	0.00015411
WHL22.5860	424.266089	1.06452043	0.11034164	92.784214	5.83E-22	1.79E-20
WHL22.7681	449.375272	1.06372828	0.10717401	98.208763	3.77E-23	1.20E-21
WHL22.7176	428.882082	1.06198273	0.10936456	94.0272806	3.11E-22	9.66E-21
WHL22.4794	146.115667	1.06082945	0.19496586	29.3686046	5.98E-08	6.59E-07
WHL22.4242	141.297232	1.05980445	0.19099339	30.6675841	3.06E-08	3.49E-07
WHL22.1502	220.661654	1.05933761	0.1527187	47.9517918	4.37E-12	7.42E-11
WHL22.1918	67.0798404	1.05602291	0.27747596	14.4029947	0.00014757	0.00098647
WHL22.4128	44.3161746	1.05565573	0.34236267	9.42898232	0.00213583	0.01084537
WHL22.4530	402.082894	1.05283224	0.11749015	79.8653704	4.01E-19	1.07E-17
WHL22.6958	100.392676	1.04619378	0.22270571	22.020071	2.70E-06	2.42E-05
WHL22.3789	480.117968	1.04429894	0.1027845	102.964965	3.41E-24	1.14E-22
WHL22.5022	625.934014	1.04298209	0.09343664	124.040517	8.25E-29	3.28E-27
WHL22.5763	56.1756718	1.04186557	0.30216701	11.8191053	0.00058626	0.0034152
WHL22.6651	71.300968	1.04077011	0.26598608	15.257444	9.38E-05	0.00064895
WHL22.1687	67.4920498	1.03777581	0.27498509	14.1773212	0.00016636	0.00110258
WHL22.6131	30.0302202	1.0372506	0.40575609	6.52046771	0.010664	0.04352167
WHL22.4008	307.188219	1.03514995	0.12768654	65.5762515	5.59E-16	1.26E-14
WHL22.3410	126.49326	1.03348158	0.21030195	23.924746	1.00E-06	9.46E-06
WHL22.2080	62.5122112	1.032271	0.28689108	12.8708195	0.00033375	0.00206377

WHL22.6322	66.7836332	1.02747736	0.27519312	13.8866076	0.00019418	0.00126972
WHL22.4344	968.218292	1.02576853	0.07416445	190.613594	2.34E-43	1.50E-41
WHL22.6030	53.9138573	1.0244209	0.31194253	10.6971014	0.00107304	0.00589748
WHL22.1479	59.4242203	1.02331097	0.30456693	11.1431857	0.00084341	0.00474741
WHL22.5359	50.5690048	1.02133029	0.32922692	9.48217001	0.00207478	0.01057196
WHL22.5737	1686.41772	1.01926355	0.05575276	333.20467	1.93E-74	2.03E-72
WHL22.7366	87.6074988	1.01925096	0.25337006	15.9930358	6.36E-05	0.00045262
WHL22.2943	58.7785368	1.01789985	0.29202661	12.1163128	0.00049983	0.00296822
WHL22.5076	98.9358799	1.01260348	0.22853457	19.5420247	9.84E-06	8.12E-05
WHL22.4455	76.6614157	1.00914849	0.25419417	15.7288418	7.31E-05	0.00051419
WHL22.4118	239.520318	1.00686163	0.14903357	45.4266822	1.58E-11	2.52E-10
WHL22.7006	1090.44253	1.00469953	0.06954811	208.008875	3.73E-47	2.67E-45
WHL22.3660	129.965497	1.00386881	0.19747111	25.7584365	3.87E-07	3.85E-06
WHL22.3823	121.079861	1.00254709	0.20731535	23.2704672	1.41E-06	1.30E-05
WHL22.2265	95.7316359	1.00185657	0.23056091	18.8066623	1.45E-05	0.00011617
WHL22.3557	152.812454	1.00141752	0.18132132	30.421877	3.48E-08	3.93E-07
WHL22.6396	350.824954	1.00105291	0.1202281	69.1415917	9.16E-17	2.16E-15
WHL22.1278	685.672233	0.99821365	0.08724693	130.490173	3.20E-30	1.34E-28
WHL22.3050	63.0009706	0.99587242	0.28917002	11.7680956	0.00060255	0.00350173
WHL22.8923	694.043679	0.99572424	0.08807006	127.332992	1.57E-29	6.39E-28
WHL22.3241	625.883424	0.99560424	0.09333192	113.305816	1.85E-26	6.77E-25
WHL22.1269	85.065656	0.99404003	0.24267642	16.7304821	4.31E-05	0.00031591
WHL22.1071	814.376964	0.99378536	0.07985454	154.41255	1.88E-35	9.59E-34
WHL22.6147	274.945037	0.99261094	0.21309434	21.2655488	4.00E-06	3.49E-05
WHL22.3500	245.171879	0.99213942	0.14610176	45.9278103	1.23E-11	1.98E-10
WHL22.5789	702.772945	0.99199661	0.08502028	135.797455	2.21E-31	9.74E-30
WHL22.5797	195.456519	0.99127984	0.16007326	38.2576366	6.20E-10	8.45E-09
WHL22.1788	242.956187	0.9912447	0.14330623	47.739267	4.87E-12	8.22E-11
WHL22.3255	51.5620251	0.9907881	0.31644798	9.73437016	0.00180854	0.00936485
WHL22.4389	317.625609	0.98876948	0.13018839	57.4085615	3.54E-14	7.25E-13
WHL22.4397	3679.6459	0.98862956	0.04038452	596.184681	1.13E-131	2.48E-129
WHL22.6888	64.9849725	0.98624629	0.29510724	11.0034383	0.00090943	0.00508976
WHL22.4794	95.1898394	0.98578751	0.22845478	18.578031	1.63E-05	0.00013019
WHL22.6739	536.121784	0.98326381	0.10085926	94.6218166	2.30E-22	7.20E-21
WHL22.5120	198.581506	0.98310435	0.15976136	37.7570829	8.01E-10	1.08E-08
WHL22.6318	83.968822	0.98306931	0.24435066	16.1371909	5.89E-05	0.00042148
WHL22.7317	143.532264	0.9817311	0.18819871	27.1236818	1.91E-07	1.99E-06
WHL22.4698	113.324088	0.98169118	0.20936359	21.9390761	2.81E-06	2.52E-05
WHL22.3152	324.014134	0.98073065	0.12547447	60.9152964	5.96E-15	1.26E-13
WHL22.4933	75.5898166	0.98017388	0.26138651	13.9825509	0.00018452	0.00121234
WHL22.2291	633.338262	0.9800407	0.09078744	116.164958	4.37E-27	1.66E-25
WHL22.3713	65.9824098	0.97903082	0.28102441	12.0582608	0.00051563	0.00305099

WHL22.4421	560.122416	0.97770554	0.09501934	105.615907	8.95E-25	3.06E-23
WHL22.4143	303.559122	0.97447646	0.12870713	57.183563	3.97E-14	8.08E-13
WHL22.7561	698.580219	0.97382917	0.08603629	127.741841	1.28E-29	5.21E-28
WHL22.3022	43.3604772	0.96919549	0.35612532	7.27613626	0.00698767	0.03052945
WHL22.5740	285.69877	0.96861323	0.132079	53.6652508	2.38E-13	4.55E-12
WHL22.7379	47.2718296	0.96016663	0.32343479	8.7920562	0.00302545	0.01471624
WHL22.5456	205.791921	0.95873792	0.16057405	35.4753242	2.58E-09	3.34E-08
WHL22.5901	80.4215581	0.95873111	0.26430725	12.9850101	0.00031399	0.00195564
WHL22.2298	51.3188607	0.95866023	0.31032051	9.52147992	0.00203081	0.01038393
WHL22.1493	72.9819133	0.95855092	0.26512951	13.005695	0.00031055	0.00193827
WHL22.5737	298.313108	0.95835718	0.13136834	53.0482466	3.25E-13	6.16E-12
WHL22.6580	138.773817	0.95670678	0.1898144	25.3385214	4.81E-07	4.74E-06
WHL22.7652	538.501096	0.95641723	0.09739625	96.168842	1.05E-22	3.35E-21
WHL22.7252	219.208779	0.95323457	0.15050405	40.0305092	2.50E-10	3.54E-09
WHL22.6619	2700.67452	0.94872766	0.04473615	448.226155	1.75E-99	2.63E-97
WHL22.3997	413.571334	0.94583851	0.1109251	72.5095708	1.66E-17	4.11E-16
WHL22.7653	54.1871159	0.94566921	0.30473886	9.58763947	0.00195892	0.01004432
WHL22.2718	390.150595	0.94537145	0.11327974	69.4893307	7.68E-17	1.83E-15
WHL22.7977	1334.0315	0.94259654	0.06269162	225.39435	6.02E-51	4.53E-49
WHL22.3057	173.137718	0.94138787	0.16990036	30.6273702	3.13E-08	3.55E-07
WHL22.4465	466.34252	0.94058508	0.10785422	75.7238397	3.26E-18	8.37E-17
WHL22.4201	384.359044	0.9403808	0.11672416	64.6796851	8.81E-16	1.97E-14
WHL22.397.0	84.6358358	0.93689243	0.24508482	14.5528709	0.00013628	0.00091897
WHL22.4794	48.0357024	0.93502649	0.3210565	8.45957801	0.00363126	0.01720133
WHL22.4464	41.3127183	0.93451556	0.35205955	6.99134933	0.00819046	0.03498281
WHL22.4523	62.2131084	0.93272004	0.29599749	9.81090439	0.0017348	0.00903402
WHL22.7577	86.2287269	0.93121894	0.23935978	15.1046218	0.00010171	0.0006997
WHL22.7082	205.895998	0.92972497	0.15636815	35.2570455	2.89E-09	3.72E-08
WHL22.5820	97.1105333	0.927429	0.22557384	16.8682068	4.01E-05	0.00029572
WHL22.7071	40.4376233	0.92697116	0.34864153	7.0541771	0.00790806	0.03396239
WHL22.6004	42.3212314	0.92603048	0.34902175	6.98444595	0.00822211	0.03507718
WHL22.1859	152.293653	0.92387845	0.18098985	25.9930294	3.43E-07	3.44E-06
WHL22.3389	135.495688	0.92325622	0.19263657	22.9034641	1.70E-06	1.57E-05
WHL22.3848	295.011009	0.92289647	0.13555938	46.119116	1.11E-11	1.81E-10
WHL22.7326	906.764616	0.92035921	0.0751146	149.744424	1.97E-34	9.58E-33
WHL22.3575	63.2319614	0.91758275	0.28313082	10.4554944	0.00122285	0.0066315
WHL22.5113	53.1808999	0.91756228	0.30531662	9.01090487	0.00268374	0.01323832
WHL22.2787	262.930537	0.91596425	0.1384749	43.6393693	3.95E-11	6.01E-10
WHL22.5477	2096.89686	0.9157777	0.05043376	328.689472	1.85E-73	1.92E-71
WHL22.1954	380.529941	0.91559401	0.11512616	63.0951143	1.97E-15	4.33E-14
WHL22.7822	47.3164427	0.91273587	0.32482525	7.86474241	0.0050408	0.02294771
WHL22.3415	163.225929	0.91191568	0.17450928	27.2451484	1.79E-07	1.87E-06

WHL22.1629	91.9767954	0.91169827	0.23511119	14.9728699	0.00010907	0.00074714
WHL22.3644	141.450938	0.911541	0.18786148	23.4842747	1.26E-06	1.17E-05
WHL22.3931	395.517016	0.91138604	0.11472453	62.9002479	2.17E-15	4.76E-14
WHL22.3109	3079.88857	0.91069425	0.04195984	469.520336	4.08E-104	6.65E-102
WHL22.5593	73.8288527	0.90739049	0.25914042	12.2330645	0.0004695	0.00281087
WHL22.1983	110.113941	0.90456756	0.21243341	18.086928	2.11E-05	0.00016523
WHL22.6031	200.737948	0.90410284	0.15994667	31.8453896	1.67E-08	1.98E-07
WHL22.1101	46.1502244	0.90245394	0.33847518	7.02709091	0.00802857	0.03440145
WHL22.6453	205.163191	0.90134301	0.15626992	33.1875126	8.37E-09	1.03E-07
WHL22.6005	237.839696	0.9012431	0.14663565	37.6602659	8.42E-10	1.14E-08
WHL22.7363	3617.0235	0.89976956	0.04051688	490.968611	8.77E-109	1.53E-106
WHL22.6259	368.465848	0.89891329	0.11705575	58.8243493	1.72E-14	3.58E-13
WHL22.2864	1147.79614	0.8970893	0.06735179	176.912935	2.29E-40	1.31E-38
WHL22.3859	103.923789	0.89686821	0.2184645	16.8144171	4.12E-05	0.000303
WHL22.1043	74.8314729	0.89569263	0.27116182	10.7858444	0.00102279	0.00564034
WHL22.3359	1157.60669	0.89449519	0.06894833	167.677633	2.38E-38	1.28E-36
WHL22.7483	140.27483	0.89415474	0.18749941	22.6967614	1.90E-06	1.73E-05
WHL22.2958	249.464549	0.89338235	0.14280078	39.0230766	4.19E-10	5.82E-09
WHL22.5912	656.337554	0.89138628	0.08790969	102.567219	4.17E-24	1.38E-22
WHL22.6455	67.5361212	0.89130707	0.27084903	10.8035133	0.00101308	0.00559517
WHL22.3145	50.0891009	0.88962435	0.31521257	7.94183814	0.00483047	0.02213905
WHL22.3364	48.8677675	0.88743729	0.32682956	7.30172022	0.00688886	0.03020565
WHL22.6530	114.79326	0.88669291	0.20764178	18.1951824	1.99E-05	0.00015669
WHL22.5020	203.640696	0.8860813	0.1658947	28.3268073	1.02E-07	1.09E-06
WHL22.5969	77.1543915	0.8853201	0.25530233	11.9801965	0.00053769	0.00316237
WHL22.3177	292.26727	0.88272948	0.13230787	44.3778616	2.71E-11	4.20E-10
WHL22.3253	213.48091	0.88102141	0.15317471	33.000423	9.21E-09	1.12E-07
WHL22.5247	65.1194535	0.88079319	0.28401256	9.54795507	0.00200172	0.01024949
WHL22.3439	1377.17705	0.87613852	0.06202455	198.939267	3.56E-45	2.41E-43
WHL22.3253	137.516355	0.87578712	0.20412018	18.2266953	1.96E-05	0.00015436
WHL22.3574	52.8900729	0.87494528	0.30972823	7.93574034	0.00484678	0.02219299
WHL22.5710	101.216492	0.87395793	0.22778506	14.6373754	0.0001303	0.00088395
WHL22.5676	71.9722099	0.87347864	0.26798423	10.5587053	0.00115642	0.00630854
WHL22.1326	184.411783	0.87315823	0.16372667	28.383043	9.95E-08	1.06E-06
WHL22.3087	255.336711	0.87272083	0.14089121	38.2618761	6.19E-10	8.45E-09
WHL22.6317	1193.31454	0.86964929	0.06681505	168.893235	1.29E-38	6.99E-37
WHL22.1995	403.483562	0.86886051	0.11455479	57.3113884	3.72E-14	7.61E-13
WHL22.5596	182.183777	0.86828259	0.16536559	27.505503	1.57E-07	1.64E-06
WHL22.2688	46.6037982	0.86802277	0.32570995	7.08192827	0.00778652	0.03353068
WHL22.7695	119.527056	0.86756543	0.20380911	18.076633	2.12E-05	0.00016578
WHL22.7326	767.175786	0.86754144	0.08106581	114.271973	1.14E-26	4.18E-25
WHL22.4080	169.888505	0.86696767	0.17063026	25.7639736	3.86E-07	3.85E-06

WHL22.6052	2059.63118	0.86576303	0.05078377	289.794116	5.51E-65	5.36E-63
WHL22.7344	45.0976647	0.86464351	0.33499802	6.62146151	0.01007571	0.04146662
WHL22.1622	618.069107	0.86450259	0.09267996	86.7180314	1.25E-20	3.61E-19
WHL22.1561	767.23437	0.86371756	0.08126577	112.69794	2.51E-26	9.11E-25
WHL22.2668	263.079494	0.86353994	0.13849226	38.7767472	4.75E-10	6.56E-09
WHL22.6588	427.844341	0.86304102	0.11157208	59.6121426	1.16E-14	2.41E-13
WHL22.8718	332.137834	0.86284578	0.12528884	47.2702191	6.18E-12	1.03E-10
WHL22.6256	156.982353	0.85984527	0.17939001	22.9070888	1.70E-06	1.56E-05
WHL22.3360	51.468363	0.85959285	0.31134248	7.59448634	0.00585471	0.02621937
WHL22.1572	704.902508	0.85887096	0.08824656	94.3601961	2.63E-22	8.20E-21
WHL22.7342	303.106259	0.85877424	0.13048594	43.1785551	5.00E-11	7.52E-10
WHL22.1420	194.67128	0.85773251	0.15925928	28.9484897	7.43E-08	8.11E-07
WHL22.6543	60.4782759	0.8573694	0.29636746	8.28589438	0.00399542	0.01867923
WHL22.5917	959.646691	0.85734091	0.07290665	137.954374	7.46E-32	3.34E-30
WHL22.3778	293.302898	0.85673411	0.13074582	42.8396993	5.94E-11	8.88E-10
WHL22.5385	308.892667	0.85623051	0.12906572	43.8796701	3.49E-11	5.37E-10
WHL22.2101	95.7001361	0.85510104	0.23039565	13.7184997	0.00021235	0.00137631
WHL22.5805	4774.94828	0.85471985	0.03602584	560.316189	7.18E-124	1.46E-121
WHL22.5131	234.268357	0.85186815	0.14687431	33.5474098	6.95E-09	8.62E-08
WHL22.5215	2160.27793	0.85174025	0.04979918	291.667944	2.15E-65	2.11E-63
WHL22.6987	151.158679	0.85152443	0.18340079	21.4853884	3.57E-06	3.14E-05
WHL22.5693	1344.75306	0.85139089	0.06222938	186.688684	1.68E-42	1.05E-40
WHL22.5789	70.8892054	0.85009185	0.26373447	10.3649951	0.00128427	0.0069262
WHL22.5046	63.4866279	0.84980789	0.29131192	8.4237414	0.00370353	0.01748723
WHL22.9499	99.1488412	0.84952401	0.22700565	13.9454004	0.0001882	0.00123502
WHL22.2488	798.940387	0.84594701	0.08037974	110.470112	7.73E-26	2.75E-24
WHL22.3889	184.293254	0.84593339	0.16468511	26.3227111	2.89E-07	2.93E-06
WHL22.5207	208.685953	0.84269671	0.15378608	29.9677429	4.39E-08	4.89E-07
WHL22.2299	310.255077	0.84192906	0.13025749	41.6232622	1.11E-10	1.62E-09
WHL22.3264	51.3224307	0.83991868	0.31697163	6.97038124	0.00828698	0.03532315
WHL22.2600	133.946113	0.83886415	0.19262613	18.9188034	1.36E-05	0.00010979
WHL22.7312	95.531629	0.83849433	0.2295482	13.2955265	0.00026604	0.00168703
WHL22.5811	359.524381	0.83848529	0.11760523	50.7297817	1.06E-12	1.90E-11
WHL22.6746	122.346787	0.83733848	0.20100769	17.3151644	3.17E-05	0.0002385
WHL22.5429	400.195077	0.83677307	0.11255192	55.1360889	1.12E-13	2.20E-12
WHL22.5385	657.718132	0.83577167	0.08991038	86.1280365	1.69E-20	4.80E-19
WHL22.5075	297.23155	0.83478038	0.13006151	41.0962156	1.45E-10	2.09E-09
WHL22.5096	66.8276051	0.83359037	0.27513733	9.1386513	0.00250266	0.01246657
WHL22.3487	48.6225187	0.83327164	0.32658829	6.45221207	0.01108143	0.04509991
WHL22.3684	1014.68905	0.83277868	0.07145272	135.487018	2.58E-31	1.13E-29
WHL22.5798	59.200717	0.8322599	0.29024391	8.19383362	0.0042033	0.019482
WHL22.2224	228.752414	0.83185518	0.14940933	30.9047569	2.71E-08	3.11E-07

WHL22.4216	52.2500686	0.83086918	0.31265169	7.01952638	0.00806256	0.03448669
WHL22.5515	53.6192272	0.83076342	0.30754341	7.25530835	0.00706917	0.03080968
WHL22.4823	1531.0402	0.83055656	0.06054962	187.472997	1.13E-42	7.10E-41
WHL22.6702	162.967049	0.83005405	0.17656292	22.0314477	2.68E-06	2.41E-05
WHL22.5396	183.35336	0.82742488	0.16681649	24.5205273	7.35E-07	7.07E-06
WHL22.2930	68.7355086	0.82721197	0.27008073	9.34492602	0.00223604	0.01130728
WHL22.1977	47.0881811	0.82707194	0.32264218	6.55651651	0.01045007	0.04283917
WHL22.6604	338.322091	0.82574097	0.12812002	41.3296231	1.29E-10	1.87E-09
WHL22.4672	57.7939398	0.82538472	0.30086422	7.46633196	0.00628635	0.02791398
WHL22.8807	1512.81838	0.8220356	0.06089104	181.600713	2.17E-41	1.28E-39
WHL22.5917	1159.12245	0.82124317	0.06725266	148.714107	3.31E-34	1.60E-32
WHL22.4221	116.415207	0.81955347	0.20672236	15.6768795	7.51E-05	0.000527
WHL22.5002	260.1345	0.81876425	0.14562209	31.4385821	2.06E-08	2.41E-07
WHL22.4587	63.068366	0.81761417	0.27980162	8.51703792	0.00351837	0.01674218
WHL22.3878	109.033975	0.81750191	0.22011559	13.7123553	0.00021305	0.00138021
WHL22.1979	368.336429	0.81729249	0.11751426	48.2428133	3.77E-12	6.43E-11
WHL22.5967	555.452394	0.81725616	0.09826996	68.9203943	1.03E-16	2.40E-15
WHL22.1984	144.058768	0.81718448	0.18614389	19.2220642	1.16E-05	9.50E-05
WHL22.4389	870.471603	0.81643697	0.07746823	110.766033	6.66E-26	2.38E-24
WHL22.7209	49.7521162	0.81421072	0.31386253	6.71464559	0.00956243	0.03971046
WHL22.7524	60.5517595	0.81419286	0.28962882	7.86019904	0.00505348	0.02298285
WHL22.6318	77.5340764	0.81374819	0.25235903	10.3734545	0.0012784	0.00690452
WHL22.4691	71.0113001	0.81318046	0.26367739	9.48670416	0.00206966	0.0105642
WHL22.1837	164.284975	0.81266069	0.18354975	19.4655141	1.02E-05	8.40E-05
WHL22.1433	110.764695	0.8118096	0.21426935	14.2975962	0.00015606	0.00103854
WHL22.1598	235.471805	0.81178063	0.14833986	29.842733	4.69E-08	5.19E-07
WHL22.1494	78.4598887	0.80768345	0.25641026	9.86397533	0.00168547	0.00881462
WHL22.7413	674.767499	0.80527399	0.08638198	86.7179973	1.25E-20	3.61E-19
WHL22.9503	179.398545	0.8042098	0.17276616	21.5511301	3.45E-06	3.04E-05
WHL22.1808	92.3659028	0.80367823	0.24398949	10.7455735	0.00104529	0.00576008
WHL22.6396	94.3263382	0.80348832	0.22880945	12.3047834	0.0004518	0.0027211
WHL22.3957	160.474935	0.80292597	0.17513659	20.9775551	4.65E-06	4.02E-05
WHL22.2748	61.5276084	0.8026561	0.28194794	8.08913018	0.00445315	0.02057026
WHL22.5282	51.2506793	0.80180926	0.31815606	6.29975629	0.01207546	0.04856964
WHL22.2849	405.320743	0.8012691	0.11589066	47.6118938	5.20E-12	8.77E-11
WHL22.5485	177.946415	0.8005993	0.17056291	21.9461202	2.80E-06	2.51E-05
WHL22.3604	353.099286	0.80027061	0.12038081	44.0760867	3.16E-11	4.88E-10
WHL22.6289	51.4505447	0.79921159	0.31664475	6.32045417	0.01193531	0.04808186
WHL22.6278	133.598368	0.79893296	0.19198967	17.2841148	3.22E-05	0.00024218
WHL22.7302	104.959448	0.7984955	0.21929854	13.2140805	0.00027785	0.00175285
WHL22.5352	55.1152514	0.79687214	0.29770072	7.15255924	0.00748571	0.0324447
WHL22.2122	156.39303	0.79577518	0.18167385	19.1081369	1.24E-05	0.00010018

WHL22.6142	66.4959002	0.7956223	0.27860809	8.10784255	0.00440742	0.02037822
WHL22.3101	264.54163	0.79521875	0.13774353	33.2518601	8.10E-09	9.96E-08
WHL22.2416	53.9582758	0.79310096	0.30311117	6.82280932	0.00900009	0.03783542
WHL22.7437	541.901853	0.79268247	0.09615753	67.8188005	1.79E-16	4.14E-15
WHL22.5479	1626.57629	0.79122254	0.05633331	196.817951	1.03E-44	6.83E-43
WHL22.5380	811.745543	0.79086241	0.08115782	94.6698309	2.25E-22	7.06E-21
WHL22.4128	221.461861	0.78990086	0.15326712	26.4612621	2.69E-07	2.74E-06
WHL22.2062	56.1257379	0.78795851	0.2968868	7.02248313	0.00804925	0.03445991
WHL22.3041	77.5934876	0.78677685	0.25335182	9.61522475	0.00192971	0.00991534
WHL22.2487	367.199537	0.7858456	0.12079373	42.1673011	8.38E-11	1.25E-09
WHL22.6163	1618.70496	0.78028472	0.05715466	185.902114	2.49E-42	1.53E-40
WHL22.6253	60.8340008	0.77934994	0.28452555	7.4841227	0.00622454	0.02766462
WHL22.1599	149.866887	0.7778824	0.18128411	18.3772572	1.81E-05	0.00014371
WHL22.5513	107.467162	0.77442105	0.2182282	12.5388178	0.00039858	0.00242588
WHL22.2824	62.2967163	0.77420728	0.28361095	7.42182811	0.00644373	0.02853514
WHL22.6757	126.602262	0.77404813	0.20316383	14.4436003	0.00014442	0.00096763
WHL22.4346	80.0990734	0.77361557	0.26368233	8.50507948	0.00354156	0.01683074
WHL22.7308	94.9611895	0.77347159	0.23148629	11.1183178	0.00085479	0.00480596
WHL22.7801	1156.32592	0.77343538	0.06704528	132.756624	1.02E-30	4.37E-29
WHL22.6119	97.3934145	0.77339441	0.23440485	10.8089834	0.00101009	0.00558076
WHL22.4874	63.0181684	0.77000524	0.28297539	7.36999799	0.0066321	0.02922823
WHL22.1502	1926.32033	0.7697643	0.05256578	213.88455	1.95E-48	1.43E-46
WHL22.4388	243.439534	0.7683248	0.14283069	28.8774483	7.71E-08	8.38E-07
WHL22.4902	2200.64411	0.76790241	0.04881242	246.897318	1.23E-55	1.04E-53
WHL22.2210	1213.30676	0.7675913	0.06500866	139.110069	4.17E-32	1.89E-30
WHL22.3410	62.7931557	0.76703058	0.28189638	7.3785552	0.00660062	0.02910696
WHL22.4224	69.2672105	0.76694354	0.27205816	7.90226094	0.0049373	0.02255824
WHL22.4162	877.187181	0.76602012	0.08093431	89.2189961	3.53E-21	1.05E-19
WHL22.6659	53.5852631	0.76550207	0.30362051	6.33728	0.0118226	0.0477195
WHL22.7680	330.654749	0.76414541	0.12509559	37.1991725	1.07E-09	1.43E-08
WHL22.2471	453.518409	0.76363137	0.10494869	52.8394726	3.62E-13	6.79E-12
WHL22.4372	1425.23323	0.76261749	0.06282727	146.848008	8.47E-34	4.06E-32
WHL22.5411	1434.839	0.75693508	0.0610972	153.074867	3.69E-35	1.87E-33
WHL22.4999	1452.97492	0.75644655	0.05971798	160.087735	1.08E-36	5.68E-35
WHL22.1502	309.459117	0.75640645	0.12795987	34.8544614	3.55E-09	4.55E-08
WHL22.2488	75.5075483	0.75632052	0.26407333	8.14479587	0.00431849	0.01997966
WHL22.5761	573.859042	0.75620346	0.09505669	63.120067	1.94E-15	4.28E-14
WHL22.3458	64.5619926	0.75604559	0.27968875	7.27248354	0.00700189	0.0305825
WHL22.2587	160.221525	0.75428109	0.17537232	18.4630933	1.73E-05	0.00013768
WHL22.7658	770.506938	0.7529918	0.08100297	86.2326212	1.60E-20	4.56E-19
WHL22.7461	1578.62805	0.75254913	0.05719948	172.713634	1.89E-39	1.04E-37
WHL22.6046	65.1962298	0.74992934	0.28514456	6.85211009	0.00885366	0.03731605

WHL22.2761	1106.03687	0.74965261	0.07038572	113.083319	2.07E-26	7.54E-25
WHL22.2393	412.176521	0.74900856	0.11226384	44.3868785	2.69E-11	4.19E-10
WHL22.4704	103.557678	0.74890289	0.21879283	11.686426	0.00062958	0.00363723
WHL22.2557	398.848228	0.74848286	0.11294456	43.8123249	3.61E-11	5.54E-10
WHL22.6147	399.688742	0.74739645	0.11286031	43.7500277	3.73E-11	5.71E-10
WHL22.9756	108.436971	0.7472849	0.2138626	12.181345	0.0004827	0.00288166
WHL22.2862	342.114713	0.7472446	0.12008973	38.6488376	5.07E-10	6.96E-09
WHL22.4223	89.5183316	0.74679246	0.23831328	9.77604532	0.001768	0.0091841
WHL22.5909	296.917329	0.74653521	0.13081111	32.4862491	1.20E-08	1.45E-07
WHL22.7477	440.676255	0.74553131	0.10601444	49.3641998	2.13E-12	3.74E-11
WHL22.3120	301.276924	0.7445101	0.13111257	32.1466083	1.43E-08	1.71E-07
WHL22.3802	148.750326	0.7442378	0.18194477	16.7004337	4.38E-05	0.00032048
WHL22.1791	4762.53124	0.74406823	0.03459873	461.114763	2.75E-102	4.29E-100
WHL22.3180	9083.89245	0.74322852	0.02658543	778.55049	2.49E-171	8.30E-169
WHL22.7637	95.0281743	0.74311085	0.22955063	10.4493969	0.0012269	0.00665097
WHL22.5050	77.2731855	0.74300438	0.25468464	8.48036581	0.00359	0.01703335
WHL22.5100	113.804666	0.74261689	0.20934254	12.5493589	0.00039634	0.00241323
WHL22.6102	248.26595	0.74221667	0.14116871	27.5910307	1.50E-07	1.57E-06
WHL22.2265	144.276468	0.74182034	0.18698377	15.6928911	7.45E-05	0.00052331
WHL22.4877	98.653726	0.74169246	0.22418178	10.9187719	0.00095195	0.00529942
WHL22.2100	4522.45527	0.74090628	0.03556653	432.651408	4.30E-96	6.07E-94
WHL22.9505	784.654178	0.74073806	0.0813497	82.7074903	9.51E-20	2.63E-18
WHL22.1168	324.725586	0.74069012	0.12615902	34.3714308	4.55E-09	5.77E-08
WHL22.2027	8487.98868	0.73771153	0.02764701	709.232133	2.94E-156	9.18E-154
WHL22.1065	81.5840847	0.73667759	0.24458798	9.05586669	0.00261853	0.0129515
WHL22.4580	70.4469524	0.735767	0.26777608	7.51768537	0.00610961	0.02721977
WHL22.2353	2237.91376	0.73539429	0.04860716	228.359567	1.36E-51	1.07E-49
WHL22.4347	229.220046	0.73403975	0.14634452	25.1152885	5.40E-07	5.28E-06
WHL22.4776	97.1230161	0.73364085	0.22494854	10.6156452	0.00112135	0.00613316
WHL22.7455	106.1552	0.73294303	0.23383345	9.7003149	0.00184236	0.00952656
WHL22.2685	308.275106	0.7282755	0.12871435	31.9303493	1.60E-08	1.90E-07
WHL22.4054	187.5273	0.72677536	0.16423347	19.5269938	9.92E-06	8.17E-05
WHL22.1363	59.1123902	0.72496846	0.28958769	6.24927015	0.01242445	0.04971134
WHL22.7202	156.841916	0.72342004	0.17840912	16.4032097	5.12E-05	0.00037061
WHL22.6997	1003.56575	0.72319831	0.07366071	96.1099541	1.09E-22	3.45E-21
WHL22.5247	163.1081	0.72265156	0.17329155	17.3616146	3.09E-05	0.00023334
WHL22.1140	165.295899	0.72172775	0.17313393	17.3414932	3.12E-05	0.00023558
WHL22.5595	654.824037	0.71974469	0.0914632	61.7174699	3.96E-15	8.56E-14
WHL22.2231	299.94605	0.71854908	0.12846889	31.2263031	2.30E-08	2.66E-07
WHL22.1178	161.92631	0.7171383	0.17717763	16.3300112	5.32E-05	0.00038388
WHL22.1713	98.3089439	0.71587305	0.22474218	10.1184094	0.00146796	0.007805
WHL22.5433	76.3764911	0.71519465	0.26429526	7.26150326	0.00704483	0.03075174

WHL22.6031	151.210405	0.71514582	0.18206533	15.3880426	8.75E-05	0.0006105
WHL22.6290	417.280272	0.7150532	0.11118454	41.2514374	1.34E-10	1.95E-09
WHL22.7686	70.8217727	0.71293177	0.2626718	7.35386472	0.00669188	0.02944746
WHL22.7482	327.879191	0.71287893	0.12285922	33.6060435	6.75E-09	8.39E-08
WHL22.7645	65.8645287	0.71185912	0.27387043	6.73737764	0.00944133	0.0392965
WHL22.1472	91.4832994	0.71076918	0.23391115	9.20281075	0.00241644	0.01206575
WHL22.2470	195.360775	0.71073587	0.16077132	19.4923269	1.01E-05	8.30E-05
WHL22.7684	429.42015	0.70982082	0.10809269	43.0359294	5.37E-11	8.06E-10
WHL22.2442	261.45418	0.70843979	0.13824462	26.2040439	3.07E-07	3.10E-06
WHL22.1732	76.9362353	0.70579217	0.2522801	7.814244	0.0051836	0.02350797
WHL22.4560	306.335824	0.70456335	0.12663563	30.9036933	2.71E-08	3.11E-07
WHL22.4460	139.68979	0.7035008	0.18824291	13.9361205	0.00018913	0.00124058
WHL22.2865	78.9959956	0.70316502	0.24973603	7.90844783	0.00492045	0.02249522
WHL22.4766	937.403551	0.70306353	0.07777178	81.4410534	1.81E-19	4.92E-18
WHL22.2800	521.406687	0.70238241	0.097431	51.8814589	5.90E-13	1.09E-11
WHL22.6915	486.923308	0.70219877	0.10266259	46.6730759	8.39E-12	1.38E-10
WHL22.2134	99.8813832	0.70145437	0.22108799	10.0491048	0.00152422	0.0080749
WHL22.1003	547.696247	0.70139555	0.09605989	53.2064703	3.00E-13	5.69E-12
WHL22.1636	148.022693	0.70139108	0.18327075	14.6127198	0.00013202	0.00089394
WHL22.7391	873.205306	0.70124743	0.07630226	84.2971442	4.26E-20	1.20E-18
WHL22.1037	3376.484	0.70118553	0.04067215	296.435249	1.97E-66	1.94E-64
WHL22.4768	338.197357	0.70060021	0.12197286	32.9249855	9.58E-09	1.16E-07
WHL22.6441	69.9335434	0.7003617	0.26615081	6.90385397	0.00860101	0.03643951
WHL22.5238	85.3111454	0.70024491	0.24040175	8.46426572	0.00362191	0.01716813
WHL22.7349	301.514995	0.69991116	0.13040344	28.7308329	8.32E-08	8.98E-07
WHL22.6893	145.950947	0.69984226	0.18314548	14.5769166	0.00013455	0.00090967
WHL22.2377	1973.37426	0.6997582	0.05229838	178.589581	9.85E-41	5.69E-39
WHL22.4452	16080.7206	0.69920046	0.02228582	979.732305	4.57E-215	2.10E-212
WHL22.1493	406.612518	0.69736982	0.1121263	38.5887102	5.23E-10	7.17E-09
WHL22.7820	119.283297	0.69717606	0.2033501	11.7301149	0.00061497	0.00356264
WHL22.1481	196.774501	0.69657002	0.15924954	19.0887919	1.25E-05	0.00010114
WHL22.6432	1220.9319	0.69604033	0.06532516	113.282782	1.87E-26	6.83E-25
WHL22.1282	2323.96473	0.69589095	0.04871289	203.548138	3.51E-46	2.46E-44
WHL22.3540	371.236123	0.69513951	0.11549777	36.1600591	1.82E-09	2.38E-08
WHL22.7202	71.2201096	0.69369881	0.26189358	7.00360147	0.00813459	0.0347543
WHL22.5779	72.4397628	0.69013268	0.26434873	6.78399256	0.00919789	0.03845772
WHL22.5378	199.002357	0.68960301	0.15805977	18.9953825	1.31E-05	0.00010598
WHL22.2478	125.136486	0.68914352	0.19999808	11.8409782	0.00057941	0.003378
WHL22.2052	169.438997	0.68897844	0.17056125	16.2860008	5.45E-05	0.00039232
WHL22.2405	630.080494	0.68822902	0.09302308	54.5626448	1.51E-13	2.93E-12
WHL22.7399	73.57574	0.68796632	0.26346773	6.78195381	0.0092084	0.03847069
WHL22.3407	363.040417	0.68737962	0.11638797	34.8238222	3.61E-09	4.62E-08

WHL22.6652	69.1634481	0.68713766	0.26556413	6.68374088	0.00972962	0.04029079
WHL22.7301	498.851563	0.68694362	0.09974168	47.3519415	5.93E-12	9.96E-11
WHL22.3786	2924.03806	0.68656418	0.04291576	255.353494	1.77E-57	1.54E-55
WHL22.6494	397.787541	0.68625254	0.11440548	35.8841256	2.09E-09	2.73E-08
WHL22.4022	441.555959	0.68408723	0.10588111	41.6725306	1.08E-10	1.59E-09
WHL22.5015	155.600253	0.68361385	0.17945513	14.47369	0.00014213	0.00095447
WHL22.4503	4395.05806	0.68293911	0.03566272	365.806513	1.53E-81	1.80E-79
WHL22.3310	103.643353	0.68199222	0.21793246	9.772715	0.00177121	0.0091975
WHL22.5988	88.3841895	0.68184091	0.23570053	8.35067094	0.00385545	0.01813457
WHL22.5805	292.535857	0.68144022	0.13150877	26.7871127	2.27E-07	2.34E-06
WHL22.7612	96.5975325	0.68055574	0.22523838	9.11180373	0.00253965	0.01262516
WHL22.1583	226.656405	0.68035531	0.14858313	20.9205171	4.79E-06	4.13E-05
WHL22.2751	128.508556	0.68010743	0.20534673	10.8959117	0.00096377	0.00535507
WHL22.7299	256.79726	0.67974468	0.13894783	23.8879446	1.02E-06	9.63E-06
WHL22.7123	260.561196	0.67974058	0.13777117	24.2980744	8.25E-07	7.86E-06
WHL22.6264	146.527404	0.67858802	0.18402184	13.5677878	0.0002301	0.00148087
WHL22.3500	77.7166722	0.67857642	0.25160341	7.25775612	0.00705954	0.03077936
WHL22.2244	74.4358547	0.67777961	0.25552739	7.02486124	0.00803857	0.03443426
WHL22.4811	69.7454657	0.67727081	0.265854	6.47256184	0.01095525	0.04463588
WHL22.4634	81.2397957	0.67641884	0.25172103	7.18199825	0.00736386	0.0319449
WHL22.3068	499.087753	0.6763753	0.10130375	44.4778056	2.57E-11	4.00E-10
WHL22.3574	582.099222	0.67619115	0.0944869	51.0923967	8.81E-13	1.59E-11
WHL22.2444	73.1811091	0.67606681	0.26363108	6.54500849	0.01051788	0.04308106
WHL22.5297	388.682467	0.67576861	0.11323556	35.5502215	2.49E-09	3.22E-08
WHL22.7382	152.974486	0.67535535	0.18023021	14.0096375	0.00018188	0.00119675
WHL22.1622	196.026915	0.67513564	0.15879743	18.0405243	2.16E-05	0.00016877
WHL22.3037	116.249624	0.67472461	0.20825728	10.4615478	0.00121885	0.00661224
WHL22.1288	182.958685	0.67227974	0.16907006	15.749557	7.23E-05	0.00050908
WHL22.4066	93.4172613	0.67207342	0.22878957	8.6142876	0.00333536	0.01597492
WHL22.5242	223.363736	0.67176419	0.14852314	20.4217458	6.21E-06	5.28E-05
WHL22.1524	140.975577	0.67174658	0.1929383	12.0630753	0.0005143	0.00304435
WHL22.3551	104.442979	0.67133852	0.21648025	9.59963769	0.00194616	0.00999286
WHL22.2987	101.827441	0.67063419	0.22308887	9.00357485	0.00269452	0.01328259
WHL22.4730	486.928752	0.67062403	0.10242915	42.7710214	6.15E-11	9.19E-10
WHL22.5380	153.377719	0.66958229	0.18229181	13.4477427	0.0002453	0.00156907
WHL22.1457	396.71381	0.66953798	0.11160693	35.9291593	2.05E-09	2.67E-08
WHL22.6357	196.146096	0.66930024	0.15784872	17.9510135	2.27E-05	0.00017652
WHL22.2044	119.773119	0.66921848	0.20309655	10.8332223	0.00099695	0.00551233
WHL22.6444	391.97562	0.66853796	0.11464424	33.9213924	5.74E-09	7.19E-08
WHL22.7423	126.35581	0.66837265	0.20026576	11.1009942	0.00086281	0.0048492
WHL22.5774	85.2297952	0.66792418	0.23927571	7.77871775	0.00528653	0.02392302
WHL22.3315	453.946288	0.66760842	0.10499345	40.3565994	2.12E-10	3.02E-09

WHL22.2716	121.427392	0.66733076	0.20233707	10.8499246	0.000988	0.00546901
WHL22.6742	230.850461	0.6667716	0.14995093	19.7085893	9.02E-06	7.49E-05
WHL22.5753	116.949264	0.66589093	0.20855782	10.1583375	0.0014365	0.00765717
WHL22.4647	526.902736	0.66534933	0.09780616	46.1881163	1.07E-11	1.75E-10
WHL22.3420	187.539153	0.66461213	0.16826794	15.5320313	8.11E-05	0.00056787
WHL22.5348	533.665854	0.6643224	0.09677132	47.0424956	6.95E-12	1.16E-10
WHL22.5674	120.186139	0.6643149	0.21021673	9.92889391	0.00162704	0.00855173
WHL22.5324	293.538093	0.66354906	0.13434015	24.3140312	8.18E-07	7.81E-06
WHL22.1105	894.665549	0.66340426	0.07509608	77.9015503	1.08E-18	2.81E-17
WHL22.2299	1667.85621	0.6627898	0.05548527	142.426676	7.84E-33	3.63E-31
WHL22.1322	410.065904	0.66211045	0.11209941	34.800438	3.65E-09	4.67E-08
WHL22.7460	7454.28552	0.66138843	0.02907245	515.948991	3.22E-114	5.98E-112
WHL22.6354	104.388519	0.66109328	0.22249182	8.78430595	0.00303833	0.01475806
WHL22.4933	153.629239	0.66026556	0.18100726	13.2689106	0.00026984	0.0017082
WHL22.3402	88.2985187	0.65963003	0.23601474	7.79407633	0.00524178	0.02374247
WHL22.1404	444.05808	0.65939808	0.10574612	38.8178223	4.65E-10	6.43E-09
WHL22.6078	387.223952	0.65860743	0.11464616	32.9272191	9.57E-09	1.16E-07
WHL22.6396	145.727026	0.65850564	0.1854604	12.5727895	0.0003914	0.00238529
WHL22.3172	732.446675	0.65825808	0.08273497	63.1922078	1.87E-15	4.13E-14
WHL22.6486	345.659648	0.65740749	0.11932055	30.3072184	3.69E-08	4.15E-07
WHL22.2946	430.554143	0.65722426	0.10816552	36.8457731	1.28E-09	1.70E-08
WHL22.3884	671.128047	0.65638281	0.08868907	54.6380931	1.45E-13	2.82E-12
WHL22.6849	263.502327	0.65629117	0.13792587	22.5929455	2.00E-06	1.83E-05
WHL22.4700	375.657302	0.65492301	0.11610204	31.752217	1.75E-08	2.07E-07
WHL22.1416	353.275028	0.65458917	0.11901281	30.193875	3.91E-08	4.37E-07
WHL22.5876	156.93641	0.6544094	0.17898857	13.3307098	0.00026109	0.00165925
WHL22.6781	75.7481306	0.65414173	0.25430226	6.60273101	0.01018225	0.04186986
WHL22.6134	320.429718	0.65392425	0.12811444	25.9732947	3.46E-07	3.47E-06
WHL22.2891	238.077886	0.65206659	0.14543045	20.0567381	7.52E-06	6.32E-05
WHL22.1336	82.3973041	0.65180337	0.24621525	6.98566203	0.00821653	0.03506354
WHL22.5216	370.125684	0.65115136	0.11684556	30.9907684	2.59E-08	2.98E-07
WHL22.2563	533.021473	0.65087599	0.09704923	44.8973426	2.08E-11	3.26E-10
WHL22.6766	88.5217292	0.65060998	0.24040407	7.28869833	0.00693897	0.03039813
WHL22.6493	195.947548	0.64914805	0.15982987	16.4574582	4.98E-05	0.00036158
WHL22.3617	106.617636	0.64910176	0.21367623	9.21458898	0.00240094	0.01200471
WHL22.2838	688.918427	0.6485714	0.08797552	54.21153	1.80E-13	3.48E-12
WHL22.1437	99.0089407	0.64721775	0.22427391	8.3048302	0.00395398	0.01850905
WHL22.3248	6835.72479	0.64717957	0.0296863	473.971308	4.38E-105	7.31E-103
WHL22.4421	82.6688281	0.64693388	0.24762324	6.79810366	0.00912547	0.03826392
WHL22.9998	2587.36188	0.6462578	0.04701394	188.461708	6.89E-43	4.38E-41
WHL22.4310	221.096174	0.64615481	0.14869048	18.856453	1.41E-05	0.0001133
WHL22.3347	93.5069416	0.64607406	0.23010323	7.86415173	0.00504245	0.02294771

WHL22.1101	668.678547	0.64495979	0.08856814	52.905418	3.50E-13	6.59E-12
WHL22.4194	227.156393	0.64493979	0.14864869	18.7824389	1.47E-05	0.00011753
WHL22.4834	112.941725	0.64459025	0.21338317	9.08554735	0.00257637	0.01279038
WHL22.5493	6012.07231	0.64457421	0.03126372	423.981008	3.32E-94	4.60E-92
WHL22.3384	108.406696	0.64438846	0.21475156	8.9772236	0.00273366	0.01345293
WHL22.5015	111.419563	0.64412313	0.20900578	9.48351522	0.00207326	0.01057155
WHL22.5984	121.272484	0.64385235	0.20122611	10.2192823	0.0013898	0.00743872
WHL22.6328	215.978804	0.64313603	0.15276916	17.6800816	2.61E-05	0.00020024
WHL22.4667	375.940428	0.64253441	0.11439525	31.4998685	1.99E-08	2.33E-07
WHL22.3652	203.202735	0.64216346	0.15977092	16.0990095	6.01E-05	0.00042944
WHL22.5546	204.725608	0.64193566	0.15482698	17.1626587	3.43E-05	0.00025646
WHL22.2837	244.342423	0.64083313	0.14302602	20.0331497	7.61E-06	6.38E-05
WHL22.6672	4092.08649	0.64066311	0.03852995	275.691759	6.52E-62	6.06E-60
WHL22.5056	150.641087	0.6401443	0.18638561	11.745656	0.00060985	0.0035386
WHL22.6839	91.0086729	0.63871873	0.23899281	7.10201922	0.00769972	0.03320559
WHL22.4237	150.364174	0.63847867	0.18988328	11.2381319	0.00080134	0.0045437
WHL22.6004	220.98761	0.63738903	0.14923227	18.21193	1.98E-05	0.0001554
WHL22.6689	122.787123	0.63686525	0.2084371	9.28024704	0.00231638	0.01164746
WHL22.6160	204.345782	0.63536335	0.15609655	16.5362309	4.77E-05	0.00034773
WHL22.5646	548.172391	0.63368595	0.09873722	41.0784548	1.46E-10	2.11E-09
WHL22.3376	95.9015655	0.63286933	0.22656401	7.78548279	0.00526677	0.0238483
WHL22.1367	390.857609	0.6320729	0.11333657	31.0434584	2.52E-08	2.91E-07
WHL22.3387	261.059018	0.63161272	0.13687919	21.2613025	4.01E-06	3.50E-05
WHL22.2276	212.77249	0.63134698	0.15219875	17.1776236	3.40E-05	0.00025459
WHL22.5036	304.270419	0.63064554	0.12922091	23.7641987	1.09E-06	1.02E-05
WHL22.6553	1449.11756	0.6306348	0.05997432	110.356004	8.19E-26	2.91E-24
WHL22.5979	181.975285	0.63062002	0.16440911	14.6873071	0.0001269	0.00086204
WHL22.1775	158.08569	0.63053092	0.18237702	11.9008369	0.00056109	0.00328551
WHL22.7568	568.541776	0.62932538	0.09482618	43.955973	3.36E-11	5.17E-10
WHL22.4560	425.009333	0.62843776	0.10849245	33.4923042	7.15E-09	8.85E-08
WHL22.3959	103.787847	0.62830059	0.21728963	8.34518443	0.00386711	0.01817777
WHL22.2485	129.868599	0.62815348	0.20771174	9.07081894	0.00259721	0.01285902
WHL22.6150	152.655575	0.62807746	0.17934723	12.2428726	0.00046704	0.00279956
WHL22.2957	87.1080638	0.62803894	0.24510959	6.52663775	0.01062707	0.04344251
WHL22.7712	268.010337	0.62798316	0.1355144	21.4398944	3.65E-06	3.21E-05
WHL22.3486	1888.46192	0.62766287	0.052325	143.635639	4.27E-33	1.99E-31
WHL22.5592	173.425148	0.62734273	0.17177184	13.2970539	0.00026582	0.00168638
WHL22.6973	1037.97394	0.62597648	0.06975016	80.4091343	3.04E-19	8.23E-18
WHL22.6949	1253.68098	0.62565694	0.06402046	95.335618	1.61E-22	5.07E-21
WHL22.4933	160.541174	0.62550647	0.17971912	12.0680278	0.00051294	0.00303872
WHL22.5504	854.416643	0.62531862	0.07804701	64.0599764	1.21E-15	2.68E-14
WHL22.4346	276.667827	0.62296185	0.13493788	21.2679784	3.99E-06	3.49E-05

WHL22.2429	88.3600261	0.62283574	0.24003935	6.70318335	0.00962409	0.03991008
WHL22.5509	292.692081	0.62261908	0.13299045	21.8582474	2.94E-06	2.62E-05
WHL22.4903	89.4475882	0.62201398	0.24083714	6.63529314	0.00999777	0.04126155
WHL22.2456	11515.6712	0.6214767	0.02513145	609.425176	1.49E-134	3.53E-132
WHL22.7869	180.416231	0.62140087	0.16886979	13.4971867	0.00023892	0.00153361
WHL22.4560	528.39793	0.61787796	0.09807489	39.6131046	3.10E-10	4.34E-09
WHL22.3183	132.098039	0.61779917	0.19211528	10.3256192	0.00131196	0.00706515
WHL22.6124	112.310069	0.61755082	0.2090012	8.714799	0.00315637	0.01524196
WHL22.4406	922.711044	0.61733796	0.07405976	69.3668833	8.17E-17	1.94E-15
WHL22.2704	229.661862	0.61658185	0.14661969	17.6546397	2.65E-05	0.00020273
WHL22.4679	146.584128	0.61610925	0.18328091	11.2789902	0.00078389	0.00445683
WHL22.5352	438.549708	0.61539622	0.11058637	30.8749908	2.75E-08	3.16E-07
WHL22.7252	617.427316	0.61440008	0.09098738	45.509125	1.52E-11	2.43E-10
WHL22.5722	1775.88076	0.61396282	0.05387669	129.639532	4.91E-30	2.04E-28
WHL22.1451	1133.42207	0.61344132	0.06673675	84.3568681	4.13E-20	1.16E-18
WHL22.1537	8931.15408	0.61315828	0.02861966	457.418402	1.75E-101	2.71E-99
WHL22.6208	294.556513	0.61292552	0.13152292	21.6654713	3.25E-06	2.88E-05
WHL22.2546	2489.61901	0.61253558	0.04636368	174.205816	8.93E-40	4.94E-38
WHL22.5288	124.008514	0.61253239	0.20054148	9.30690686	0.00228292	0.01150076
WHL22.6855	1728.67093	0.61218006	0.05547402	121.541073	2.91E-28	1.14E-26
WHL22.2452	106.765458	0.61174286	0.21377662	8.17568488	0.00424556	0.01966084
WHL22.8655	748.249274	0.61150956	0.08213687	55.3345154	1.02E-13	2.00E-12
WHL22.4307	187.604904	0.61074535	0.16181457	14.2221184	0.00016245	0.0010781
WHL22.1494	207.71953	0.61057608	0.15377691	15.7404054	7.27E-05	0.00051131
WHL22.3642	1181.46495	0.60980136	0.06682271	83.1090352	7.76E-20	2.15E-18
WHL22.2925	84.5033719	0.60972187	0.24089507	6.39335618	0.01145483	0.0463753
WHL22.2936	2473.08275	0.60923829	0.04950172	151.044553	1.02E-34	5.07E-33
WHL22.3769	1358.56095	0.60910352	0.06139468	98.2618638	3.67E-23	1.18E-21
WHL22.4221	3319.28969	0.60850117	0.04114173	218.274832	2.15E-49	1.59E-47
WHL22.4003	1949.87891	0.60778635	0.05218135	135.40748	2.69E-31	1.17E-29
WHL22.4643	202.837465	0.60704911	0.15604435	15.1072917	0.00010157	0.00069904
WHL22.5536	3250.37367	0.6062658	0.04143489	213.631168	2.22E-48	1.62E-46
WHL22.3347	139.501834	0.6056378	0.18754677	10.4113674	0.00125242	0.00678182
WHL22.3817	253.732142	0.60551627	0.13905896	18.9320931	1.35E-05	0.0001092
WHL22.2410	1011.32963	0.60528929	0.0716614	71.2090223	3.21E-17	7.78E-16
WHL22.1992	98.706472	0.6037997	0.22701636	7.04480351	0.00794955	0.03410271
WHL22.3172	446.968637	0.60372533	0.1060881	32.3276568	1.30E-08	1.56E-07
WHL22.3219	1258.4569	0.60358115	0.06708466	80.7388823	2.58E-19	6.99E-18
WHL22.6000	569.013772	0.60344342	0.09396516	41.1724526	1.39E-10	2.02E-09
WHL22.6229	118.73062	0.60296712	0.20395565	8.72164723	0.00314454	0.01520982
WHL22.1543	1177.28541	0.6026084	0.0663356	82.3740045	1.13E-19	3.10E-18
WHL22.2127	534.795046	0.60140075	0.10432234	33.0963253	8.77E-09	1.07E-07

WHL22.3387	255.204641	0.60139341	0.14553724	17.0040889	3.73E-05	0.0002771
WHL22.6093	972.656115	0.60090068	0.07252312	68.5326833	1.25E-16	2.92E-15
WHL22.5041	9949.43037	0.60063518	0.02557735	549.938893	1.30E-121	2.54E-119
WHL22.9155	161.581359	0.59967869	0.17377873	11.8906771	0.00056416	0.00329821
WHL22.5801	604.352184	0.59941341	0.090627	43.6806369	3.87E-11	5.89E-10
WHL22.6874	197.282519	0.59878608	0.15728832	14.4722809	0.00014224	0.00095475
WHL22.5813	135.884068	0.59759989	0.19077999	9.79216238	0.00175257	0.00912009
WHL22.6434	150.907465	0.59690646	0.18347108	10.5535482	0.00115965	0.00632381
WHL22.6247	265.993602	0.59613254	0.13740691	18.7837711	1.46E-05	0.00011751
WHL22.6546	114.219561	0.5959295	0.20670839	8.29855387	0.00396767	0.01856721
WHL22.6033	121.044996	0.59581018	0.20191394	8.68910015	0.00320119	0.01541779
WHL22.3191	86.9826981	0.59571168	0.23713564	6.29964148	0.01207624	0.04856964
WHL22.4544	319.847722	0.59483846	0.12517463	22.5401546	2.06E-06	1.87E-05
WHL22.6269	1186.04895	0.59345458	0.06539647	82.220514	1.22E-19	3.33E-18
WHL22.5057	164.6018	0.59334471	0.18250134	10.5083654	0.00118835	0.00646591
WHL22.6568	1989.34237	0.59307754	0.05118506	134.027658	5.39E-31	2.33E-29
WHL22.6786	185.616002	0.59229983	0.16396198	13.0215696	0.00030792	0.00192272
WHL22.3065	189.266417	0.59189745	0.16147713	13.4123012	0.00024998	0.00159552
WHL22.2277	129.759229	0.59171392	0.1955464	9.1355529	0.0025069	0.01247923
WHL22.5325	126.344113	0.59164573	0.1988896	8.82644144	0.00296897	0.01446547
WHL22.6864	244.574163	0.59113853	0.14136766	17.4613032	2.93E-05	0.00022268
WHL22.7443	1032.97434	0.58963173	0.07057862	69.6717536	7.00E-17	1.67E-15
WHL22.1440	322.93662	0.58944833	0.12507343	22.1655431	2.50E-06	2.26E-05
WHL22.7610	351.604342	0.58877733	0.1217263	23.3339056	1.36E-06	1.26E-05
WHL22.6839	348.710508	0.58836216	0.12043518	23.8181802	1.06E-06	9.96E-06
WHL22.8710	427.277964	0.58826826	0.10953572	28.7826745	8.10E-08	8.78E-07
WHL22.7049	165.698051	0.58788103	0.17171028	11.7041915	0.00062359	0.00360692
WHL22.5175	99.115879	0.58694899	0.22368677	6.8692215	0.00876928	0.03702419
WHL22.8420	2758.3275	0.58636838	0.04430508	174.829636	6.52E-40	3.65E-38
WHL22.1060	110.580599	0.58454373	0.21169068	7.60682527	0.00581478	0.02608033
WHL22.5174	166.199671	0.58408571	0.17383934	11.2629061	0.00079071	0.00449039
WHL22.2729	119.419649	0.5838083	0.20318244	8.24116781	0.00409508	0.01907678
WHL22.6552	306.841102	0.58377091	0.12756151	20.9060599	4.82E-06	4.16E-05
WHL22.7416	155.463983	0.58334271	0.1781337	10.7044651	0.00106877	0.00587845
WHL22.7618	125.438238	0.58302566	0.19846807	8.61216404	0.00333925	0.01598312
WHL22.6269	109.808679	0.58252047	0.21232035	7.50976771	0.00613653	0.02731564
WHL22.6787	940.247004	0.58217836	0.0729613	63.5757096	1.54E-15	3.41E-14
WHL22.2948	12151.487	0.58214786	0.0238556	593.812976	3.71E-131	8.01E-129
WHL22.7136	97.5587887	0.58206199	0.22335123	6.78217123	0.00920728	0.03847069
WHL22.4294	138.41666	0.58157934	0.19015117	9.33191565	0.00225197	0.01136435
WHL22.5209	503.787127	0.58026413	0.09949671	33.9587512	5.63E-09	7.07E-08
WHL22.2286	103.756889	0.58002003	0.21661685	7.15973998	0.0074558	0.03232462

WHL22.4237	663.952859	0.57965209	0.08638421	44.9636371	2.01E-11	3.17E-10
WHL22.1702	3979.0266	0.57890748	0.03761639	236.36745	2.44E-53	1.95E-51
WHL22.4265	204.150175	0.57767109	0.15533053	13.8079035	0.00020248	0.00131933
WHL22.2456	35987.5886	0.57763611	0.0174066	1096.66045	1.76E-240	9.55E-238
WHL22.8179	3129.67933	0.57752837	0.04153221	193.015127	6.99E-44	4.52E-42
WHL22.4391	102.270259	0.57700242	0.22080846	6.81072482	0.0090612	0.03803399
WHL22.1022	1432.70832	0.57634937	0.06102863	89.0165911	3.92E-21	1.16E-19
WHL22.6581	321.847226	0.57606718	0.12399746	21.5501455	3.45E-06	3.04E-05
WHL22.7235	163.579784	0.57604033	0.17355218	10.9982392	0.00091198	0.00510211
WHL22.1989	557.102066	0.57589229	0.09890405	33.8093784	6.08E-09	7.60E-08
WHL22.6039	262.223737	0.5740184	0.14388079	15.8536403	6.84E-05	0.00048416
WHL22.5730	167.388624	0.57386769	0.17068923	11.2880208	0.00078009	0.00444036
WHL22.2863	409.567954	0.57246296	0.11227188	25.941081	3.52E-07	3.52E-06
WHL22.3747	495.335441	0.57197899	0.10221969	31.2452368	2.27E-08	2.64E-07
WHL22.1434	554.870615	0.56946896	0.09596916	35.1454947	3.06E-09	3.93E-08
WHL22.7413	337.814136	0.56943324	0.12325886	21.2945741	3.94E-06	3.44E-05
WHL22.5936	2978.05729	0.56912579	0.04292977	175.421345	4.84E-40	2.73E-38
WHL22.7314	15522.8917	0.56897411	0.02235847	645.56289	2.06E-142	5.40E-140
WHL22.1586	668.785867	0.56846069	0.08816516	41.4906674	1.18E-10	1.73E-09
WHL22.6892	116.731066	0.56843985	0.21536335	6.9193275	0.0085269	0.03619865
WHL22.4467	124.432579	0.56825877	0.20181549	7.90468533	0.00493069	0.02253504
WHL22.2120	640.952871	0.56813413	0.08839614	41.2450149	1.34E-10	1.95E-09
WHL22.7579	243.95149	0.56779144	0.14459215	15.381884	8.78E-05	0.00061191
WHL22.6537	127.829515	0.56739861	0.19721104	8.2588791	0.00405532	0.01892911
WHL22.5094	156.671868	0.56666108	0.17654905	10.2869504	0.00133974	0.00719891
WHL22.6524	187.438928	0.56522215	0.16243663	12.0859055	0.00050804	0.00301094
WHL22.3703	156.624668	0.56514839	0.17654208	10.2333533	0.00137924	0.00738949
WHL22.7381	111.165655	0.56479863	0.21465637	6.89495371	0.00864394	0.03657914
WHL22.6517	193.812495	0.56411699	0.16035311	12.3514526	0.00044064	0.00266199
WHL22.4216	154.090756	0.56406779	0.18102701	9.68282166	0.00185999	0.00960754
WHL22.7679	1091.21604	0.56404475	0.06868819	67.320539	2.31E-16	5.26E-15
WHL22.7034	108.154172	0.56370966	0.21212141	7.05191099	0.00791807	0.03398752
WHL22.4214	279.820388	0.56370285	0.13346106	17.8083092	2.44E-05	0.00018876
WHL22.6345	267.470387	0.56333158	0.14337916	15.3706925	8.83E-05	0.00061525
WHL22.4940	110.131354	0.56305957	0.21127227	7.08874414	0.00775696	0.033423
WHL22.4691	205.112981	0.56289786	0.15959442	12.3973514	0.00042994	0.00260164
WHL22.8517	614.539185	0.56261099	0.0901792	38.8653065	4.54E-10	6.30E-09
WHL22.4038	134.853466	0.56224318	0.1917865	8.5755684	0.00340704	0.01625985
WHL22.5684	857.960276	0.56191776	0.0781634	51.5815617	6.87E-13	1.26E-11
WHL22.5873	6786.65195	0.56060888	0.02975408	354.234638	5.07E-79	5.60E-77
WHL22.6345	1543.74728	0.560561	0.05884853	90.5682599	1.79E-21	5.36E-20
WHL22.6445	109.815638	0.56001751	0.2166773	6.64948682	0.00991844	0.04098021

WHL22.2178	349.954343	0.55942615	0.11885878	22.1197444	2.56E-06	2.31E-05
WHL22.2524	572.644627	0.55915685	0.09555309	34.1714056	5.05E-09	6.37E-08
WHL22.7204	114.597753	0.55878487	0.20774664	7.21900319	0.00721358	0.03136709
WHL22.2407	101.103489	0.55823887	0.21937831	6.46580832	0.01099696	0.04479339
WHL22.1126	231.671623	0.55791236	0.14709912	14.3556215	0.00015133	0.00100931
WHL22.6319	122.61037	0.55751554	0.21327152	6.77947511	0.0092212	0.0384894
WHL22.6059	248.733707	0.55749904	0.14069938	15.6772394	7.51E-05	0.000527
WHL22.6392	745.701005	0.55680937	0.0825283	45.448321	1.57E-11	2.50E-10
WHL22.1073	1038.36206	0.55623809	0.07113427	61.0325418	5.61E-15	1.19E-13
WHL22.8502	275.080399	0.55620892	0.1334916	17.3369603	3.13E-05	0.00023603
WHL22.7035	538.423428	0.55592929	0.09883047	31.5700957	1.92E-08	2.26E-07
WHL22.3947	446.042531	0.55571574	0.10573634	27.5796382	1.51E-07	1.58E-06
WHL22.6035	290.348952	0.55560398	0.13087039	17.9941519	2.22E-05	0.00017266
WHL22.7637	324.004448	0.55468309	0.12640812	19.2074525	1.17E-05	9.55E-05
WHL22.3255	250.830585	0.55459249	0.1412723	15.3824348	8.78E-05	0.00061191
WHL22.3261	277.528974	0.55449594	0.1333038	17.2765437	3.23E-05	0.00024301
WHL22.3255	157.695575	0.55418656	0.18374007	9.05407712	0.0026211	0.01295545
WHL22.1008	1043.77912	0.55383559	0.07486164	54.5746563	1.50E-13	2.91E-12
WHL22.4171	110.411907	0.55268364	0.21050026	6.88253956	0.00870418	0.03680224
WHL22.1438	208.664178	0.55244895	0.15361498	12.9136813	0.00032619	0.00202047
WHL22.2036	157.060516	0.55242347	0.17619763	9.81614039	0.00172987	0.00901473
WHL22.6506	379.162564	0.55148563	0.11831322	21.6682304	3.24E-06	2.87E-05
WHL22.2893	365.313692	0.55141024	0.11597134	22.577261	2.02E-06	1.84E-05
WHL22.5807	539.237368	0.55120579	0.09717383	32.1194668	1.45E-08	1.73E-07
WHL22.2000	3252.89373	0.55086655	0.04139688	176.745225	2.49E-40	1.42E-38
WHL22.1501	4700.17502	0.55027146	0.03466547	251.508037	1.22E-56	1.05E-54
WHL22.6253	298.284744	0.54993721	0.13082409	17.6315457	2.68E-05	0.00020496
WHL22.5211	178.801459	0.54966104	0.17078547	10.3210119	0.00131524	0.00708021
WHL22.1942	218.197925	0.5492614	0.14994049	13.3997462	0.00025166	0.00160484
WHL22.6949	275.900249	0.54907472	0.14348927	14.5694419	0.00013509	0.0009126
WHL22.1247	149.66833	0.54892786	0.18032965	9.25379451	0.00235008	0.01178653
WHL22.1636	177.181085	0.54745043	0.16708097	10.7164574	0.00106187	0.00584485
WHL22.6359	427.106567	0.54692531	0.10906899	25.0999946	5.44E-07	5.31E-06
WHL22.3137	110.562692	0.54540471	0.21543373	6.38391594	0.01151591	0.04659689
WHL22.5934	243.196819	0.54509403	0.14681013	13.7424954	0.00020966	0.00136184
WHL22.7242	189.69102	0.54489494	0.1617301	11.3304003	0.00076248	0.00434184
WHL22.1145	718.787944	0.54452188	0.08599232	40.0112164	2.53E-10	3.57E-09
WHL22.4728	3394.89301	0.54430257	0.04073859	178.177367	1.21E-40	6.98E-39
WHL22.2809	165.206034	0.54411129	0.17768043	9.34265791	0.00223881	0.01131738
WHL22.7138	131.673841	0.54340418	0.19415452	7.81764193	0.00517387	0.02347106
WHL22.3002	684.199499	0.54318005	0.08616531	39.6767346	3.00E-10	4.21E-09
WHL22.5926	216.166642	0.54267195	0.15319627	12.517827	0.00040309	0.00244922

WHL22.7025	483.474625	0.54221248	0.10107919	28.7367751	8.29E-08	8.96E-07
WHL22.6314	371.360677	0.5420461	0.11545292	22.010728	2.71E-06	2.43E-05
WHL22.4375	372.143116	0.54196666	0.11920351	20.6154753	5.61E-06	4.80E-05
WHL22.4700	7107.7401	0.54130262	0.03093801	305.339005	2.26E-68	2.26E-66
WHL22.3197	128.01083	0.54069832	0.19813293	7.42658871	0.00642671	0.02848552
WHL22.5578	177.419931	0.54067134	0.16741463	10.4094463	0.00125372	0.006784
WHL22.1243	9651.48445	0.54013968	0.02649769	414.501086	3.84E-92	5.17E-90
WHL22.5344	709.496419	0.53978496	0.08495722	40.301055	2.18E-10	3.11E-09
WHL22.3769	1613.04528	0.53932336	0.05648188	91.0425373	1.41E-21	4.25E-20
WHL22.1118	150.549767	0.53894333	0.18346229	8.60885503	0.00334533	0.01600697
WHL22.8501	840.414029	0.53865584	0.07717867	48.6445041	3.07E-12	5.31E-11
WHL22.3367	165.199645	0.53838564	0.18642968	8.27650846	0.00401613	0.01875812
WHL22.7561	140.647482	0.53739469	0.19140415	7.8550202	0.00506798	0.02304055
WHL22.1386	218.695105	0.53708457	0.15506689	11.9566796	0.00054452	0.00319869
WHL22.4360	193.732824	0.53627143	0.1586348	11.4136416	0.00072907	0.00416935
WHL22.4011	247.899926	0.53581226	0.14224101	14.1621118	0.00016771	0.00111053
WHL22.6881	124.648761	0.5354207	0.19772342	7.3226047	0.00680927	0.02989235
WHL22.7663	194.437933	0.53516911	0.15860219	11.370087	0.00074636	0.00425831
WHL22.5481	125.381613	0.53490076	0.19768303	7.30994429	0.00685741	0.0300767
WHL22.5427	575.327183	0.53479832	0.09298632	33.0324985	9.06E-09	1.11E-07
WHL22.5589	290.41877	0.53455031	0.13233077	16.2831803	5.45E-05	0.00039271
WHL22.7256	469.997485	0.53344044	0.1029742	26.7967431	2.26E-07	2.33E-06
WHL22.7454	116.541933	0.53319549	0.20414115	6.81351162	0.00904707	0.0379894
WHL22.5805	1348.17532	0.53275218	0.06197637	73.7787192	8.74E-18	2.20E-16
WHL22.7502	2719.01703	0.53254463	0.04534449	137.676212	8.58E-32	3.82E-30
WHL22.5411	364.192118	0.5322769	0.11641368	20.8769352	4.90E-06	4.22E-05
WHL22.4255	1094.79961	0.53117649	0.07108786	55.7105055	8.40E-14	1.65E-12
WHL22.3817	241.416639	0.5308399	0.14353085	13.6557514	0.00021957	0.00141806
WHL22.4237	183.499496	0.52994567	0.16502806	10.2912247	0.00133664	0.00718752
WHL22.4260	277.992693	0.52993217	0.13372794	15.6779537	7.51E-05	0.000527
WHL22.2294	913.096314	0.52986359	0.07538455	49.3212338	2.17E-12	3.81E-11
WHL22.3727	1185.51023	0.52957353	0.06876879	59.1688144	1.45E-14	3.01E-13
WHL22.5199	8717.59868	0.52870465	0.02681705	387.877484	2.40E-86	2.98E-84
WHL22.1636	160.582296	0.52832218	0.17640397	8.9500064	0.00277469	0.01364569
WHL22.6267	562.360597	0.52810229	0.09433307	31.2960819	2.22E-08	2.58E-07
WHL22.7133	1269.1725	0.52797295	0.06348859	69.0571815	9.56E-17	2.25E-15
WHL22.7703	622.183169	0.52793002	0.09444322	31.1625221	2.37E-08	2.74E-07
WHL22.1958	201.590368	0.52768716	0.15557475	11.4900867	0.00069968	0.00401382
WHL22.3714	185.659011	0.52694323	0.16274047	10.467999	0.0012146	0.00659407
WHL22.3642	568.941229	0.52675886	0.09393695	31.3990856	2.10E-08	2.45E-07
WHL22.3643	559.41669	0.52538746	0.09407857	31.1470712	2.39E-08	2.76E-07
WHL22.3149	2076.61551	0.52536749	0.05037291	108.610128	1.98E-25	6.92E-24

WHL22.6396	466.864741	0.52530168	0.1052296	24.8700686	6.13E-07	5.94E-06
WHL22.7245	253.097856	0.52460356	0.13871509	14.2858441	0.00015704	0.00104457
WHL22.4749	316.334851	0.52407991	0.13000873	16.2007692	5.70E-05	0.00040837
WHL22.1268	332.608873	0.52391917	0.12421311	17.7527459	2.52E-05	0.00019354
WHL22.6392	4874.46211	0.52225306	0.03455895	227.949684	1.67E-51	1.30E-49
WHL22.7702	1498.95795	0.52221687	0.0583111	80.0958852	3.57E-19	9.57E-18
WHL22.3771	785.291128	0.52184447	0.08042498	42.0393999	8.95E-11	1.33E-09
WHL22.4901	272.64932	0.52164984	0.13654314	14.5645799	0.00013544	0.00091454
WHL22.5797	155.041172	0.52160651	0.18312735	8.08213459	0.00447038	0.02063034
WHL22.1474	180.383317	0.52093128	0.17361957	8.95839221	0.00276198	0.01358775
WHL22.3938	167.964102	0.51978685	0.17354961	8.94780996	0.00277802	0.01365753
WHL22.3422	252.98927	0.51895961	0.14096397	13.5271126	0.00023514	0.00151133
WHL22.4911	206.967659	0.51882977	0.15569497	11.0816143	0.00087188	0.00489452
WHL22.2475	503.528882	0.51778141	0.10160148	25.9191157	3.56E-07	3.56E-06
WHL22.4795	267.424581	0.51691024	0.13806561	13.9861368	0.00018416	0.00121125
WHL22.2963	414.124393	0.51563759	0.10882247	22.4253301	2.18E-06	1.98E-05
WHL22.6938	1851.79904	0.51553248	0.05305941	94.2673994	2.76E-22	8.57E-21
WHL22.5480	160.791286	0.51549234	0.17521973	8.64084078	0.0032871	0.01576947
WHL22.6386	461.544687	0.51513738	0.10314713	24.9122504	6.00E-07	5.82E-06
WHL22.7444	2102.83161	0.51497873	0.04977762	106.88084	4.73E-25	1.63E-23
WHL22.6239	1163.4706	0.51454469	0.06573787	61.1875347	5.19E-15	1.11E-13
WHL22.5473	310.045223	0.51421448	0.12636944	16.5341107	4.78E-05	0.00034794
WHL22.7645	535.296964	0.51401927	0.09722092	27.9097341	1.27E-07	1.34E-06
WHL22.4372	190.971291	0.5140159	0.16099937	10.1755846	0.00142313	0.00758863
WHL22.1735	19279.4565	0.51269243	0.0203234	634.70973	4.73E-140	1.22E-137
WHL22.7412	1982.19203	0.51236329	0.05122945	99.8868041	1.61E-23	5.26E-22
WHL22.3091	230.508549	0.51189255	0.14882818	11.8022283	0.0005916	0.00344356
WHL22.6600	709.975896	0.51154798	0.08517321	36.0125604	1.96E-09	2.56E-08
WHL22.1129	552.759065	0.51152244	0.09552396	28.6334178	8.75E-08	9.41E-07
WHL22.6922	163.498524	0.51147934	0.17242773	8.78859519	0.0030312	0.01473442
WHL22.5447	697.434783	0.51138321	0.08591196	35.3734408	2.72E-09	3.51E-08
WHL22.6580	183.298352	0.5108839	0.1664198	9.39953709	0.0021704	0.0110095
WHL22.3760	156.611836	0.51072831	0.17842486	8.17592432	0.004245	0.01966084
WHL22.3604	154.672321	0.50850828	0.18107993	7.86400062	0.00504287	0.02294771
WHL22.7319	184.048059	0.50792869	0.17322223	8.5502809	0.00345469	0.01646586
WHL22.6813	1346.10121	0.50707026	0.06157496	67.724907	1.88E-16	4.33E-15
WHL22.5596	548.923816	0.50671902	0.09566921	28.0142411	1.20E-07	1.28E-06
WHL22.6831	412.979525	0.50646095	0.10952763	21.3529731	3.82E-06	3.35E-05
WHL22.3148	170.509864	0.50643015	0.16888192	8.98158014	0.00272715	0.01342866
WHL22.2239	1262.4275	0.50505534	0.06384171	62.4966839	2.67E-15	5.80E-14
WHL22.3948	278.628636	0.50479289	0.13293858	14.3988305	0.00014789	0.0009882
WHL22.3027	160.476481	0.50449874	0.17514024	8.28401148	0.00399957	0.01869266

WHL22.5837	692.254789	0.50374075	0.08975058	31.4217263	2.08E-08	2.42E-07
WHL22.6247	127.063718	0.50368467	0.19788216	6.46442806	0.01100551	0.04481318
WHL22.5916	125.928658	0.50341429	0.20032858	6.29577038	0.01210264	0.0486526
WHL22.1031	279.988224	0.50270182	0.13495431	13.8462012	0.0001984	0.00129616
WHL22.4350	1338.57335	0.5026138	0.06448069	60.6385121	6.86E-15	1.44E-13
WHL22.1660	566.22228	0.50218874	0.09385836	28.5910161	8.94E-08	9.61E-07
WHL22.2597	1324.52458	0.501829	0.06286826	63.6203426	1.51E-15	3.34E-14
WHL22.4809	597.345097	0.50116831	0.09402747	28.3523248	1.01E-07	1.08E-06
WHL22.1837	4049.09851	0.50070493	0.04048323	152.606778	4.67E-35	2.36E-33
WHL22.3843	1385.41395	0.50040654	0.0630968	62.7798334	2.31E-15	5.04E-14
WHL22.3345	146.272965	-0.5001679	0.18379291	7.40783466	0.00649404	0.02870642
WHL22.4805	147.685119	-0.5002298	0.18240473	7.52452596	0.00608646	0.02714956
WHL22.6624	238.836918	-0.500466	0.14507677	11.9000327	0.00056133	0.00328561
WHL22.5872	481.068451	-0.5007239	0.10150528	24.3478133	8.04E-07	7.68E-06
WHL22.1750	241.263624	-0.5007508	0.14278181	12.3069839	0.00045127	0.00271946
WHL22.2701	631.425025	-0.500758	0.08962533	31.2251903	2.30E-08	2.66E-07
WHL22.5530	265.551746	-0.500871	0.13849806	13.0750075	0.00029926	0.00187182
WHL22.5393	519.95105	-0.501153	0.09802583	26.1488554	3.16E-07	3.19E-06
WHL22.6432	149.496381	-0.5014881	0.183815	7.43840183	0.00638466	0.02831624
WHL22.7019	931.706151	-0.5026805	0.07514036	44.7506166	2.24E-11	3.51E-10
WHL22.2496	683.224434	-0.5028992	0.08680734	33.5647078	6.89E-09	8.56E-08
WHL22.2446	138.525652	-0.5032704	0.18854985	7.12724319	0.00759214	0.03279946
WHL22.2538	976.225803	-0.5038441	0.07233809	48.5268409	3.26E-12	5.61E-11
WHL22.5525	986.464481	-0.5043903	0.07179835	49.3691038	2.12E-12	3.73E-11
WHL22.1474	803.539103	-0.5046776	0.07896483	40.8671297	1.63E-10	2.35E-09
WHL22.7324	197.595007	-0.5047941	0.15755024	10.2723332	0.0013504	0.00725086
WHL22.4188	9095.5339	-0.5053454	0.02724078	343.72256	9.87E-77	1.07E-74
WHL22.2880	688.191157	-0.5058218	0.08610112	34.5194631	4.22E-09	5.37E-08
WHL22.2375	328.073678	-0.5066519	0.12308672	16.9506889	3.84E-05	0.00028414
WHL22.5949	171.323563	-0.5070895	0.17203397	8.68328509	0.00321142	0.01545185
WHL22.6448	245.823607	-0.5076139	0.14497198	12.2518048	0.00046481	0.00278847
WHL22.7049	130.225118	-0.5078128	0.19494427	6.78654803	0.00918473	0.03842978
WHL22.7592	145.948275	-0.5084916	0.18774895	7.32559848	0.00679793	0.02985152
WHL22.4013	151.181971	-0.5084957	0.18271412	7.74102035	0.00539803	0.02437498
WHL22.1262	239.963598	-0.5089085	0.14341388	12.5985567	0.00038604	0.00236131
WHL22.6220	132.277997	-0.5092246	0.19453665	6.85021289	0.00886307	0.03734404
WHL22.4750	207.117726	-0.5093939	0.15399527	10.9488742	0.00093661	0.00522591
WHL22.7547	3044.10652	-0.5113372	0.04348176	138.222329	6.52E-32	2.93E-30
WHL22.5181	928.330465	-0.5115979	0.07405539	47.740962	4.86E-12	8.22E-11
WHL22.7569	258.171265	-0.5117479	0.14407118	12.5957202	0.00038663	0.00236391
WHL22.7181	514.674943	-0.5119577	0.0988625	26.8260171	2.23E-07	2.29E-06
WHL22.3311	350.192461	-0.5123425	0.11906591	18.5248793	1.68E-05	0.00013351

WHL22.2061	159.221691	-0.5127621	0.18461532	7.68946813	0.0055544	0.02500417
WHL22.4362	385.433996	-0.512961	0.11341415	20.4676498	6.06E-06	5.16E-05
WHL22.1458	857.41244	-0.513787	0.08251657	38.7103568	4.92E-10	6.76E-09
WHL22.1403	347.446787	-0.5143933	0.12175129	17.8445002	2.40E-05	0.00018571
WHL22.5559	744.11134	-0.5150133	0.08235089	39.1269871	3.97E-10	5.53E-09
WHL22.7331	864.390546	-0.5151376	0.07821465	43.3703632	4.53E-11	6.84E-10
WHL22.3861	168.630868	-0.5151486	0.17494147	8.66233476	0.00324855	0.01561516
WHL22.5319	422.27759	-0.5161975	0.11420808	20.3965048	6.29E-06	5.34E-05
WHL22.1155	7097.93533	-0.5164026	0.02931929	309.993796	2.19E-69	2.22E-67
WHL22.6613	357.414747	-0.5173368	0.11809196	19.1991788	1.18E-05	9.59E-05
WHL22.3576	130.011919	-0.5174893	0.19541051	7.0140118	0.00808743	0.03458299
WHL22.6681	136.685283	-0.517595	0.19063916	7.37220271	0.00662397	0.02920119
WHL22.7726	355.380628	-0.5179165	0.1239069	17.4442436	2.96E-05	0.00022434
WHL22.2956	122.829273	-0.5184521	0.20263658	6.54152562	0.01053849	0.04314141
WHL22.2195	238.901088	-0.5185327	0.14438876	12.9007325	0.00032845	0.00203361
WHL22.5390	9954.27922	-0.5196278	0.02578027	405.792195	3.02E-90	3.96E-88
WHL22.6082	157.944747	-0.5196732	0.18001464	8.32524195	0.00390979	0.01834903
WHL22.4353	276.267138	-0.5208723	0.1349135	14.9069954	0.00011294	0.0007726
WHL22.6200	583.780964	-0.5209399	0.09256032	31.6909383	1.81E-08	2.13E-07
WHL22.6619	613.558673	-0.5214359	0.09154834	32.4432898	1.23E-08	1.48E-07
WHL22.3656	309.474421	-0.5216152	0.13072015	15.9060341	6.66E-05	0.00047139
WHL22.3607	416.559101	-0.521837	0.10927603	22.8161629	1.78E-06	1.64E-05
WHL22.2423	127.97403	-0.5219098	0.19636748	7.0678235	0.00784805	0.03375606
WHL22.4984	196.251936	-0.5223753	0.15907165	10.7874189	0.00102192	0.00563766
WHL22.3641	171.874061	-0.5229799	0.17572775	8.83639838	0.00295281	0.01440489
WHL22.5137	137.235383	-0.523203	0.19083154	7.5152297	0.00611795	0.02724863
WHL22.7385	461.371593	-0.5234791	0.1080112	23.4661681	1.27E-06	1.18E-05
WHL22.1202	291.27664	-0.5240632	0.13011814	16.2318957	5.60E-05	0.0004025
WHL22.2648	537.302512	-0.524773	0.09642962	29.6300322	5.23E-08	5.77E-07
WHL22.5872	171.640085	-0.52494	0.17566209	8.91126965	0.00283416	0.01389165
WHL22.7246	2323.96586	-0.5255438	0.049974	110.514977	7.56E-26	2.70E-24
WHL22.1663	310.997304	-0.5255445	0.12669761	17.2117913	3.34E-05	0.00025068
WHL22.5335	1699.1431	-0.5256854	0.05514226	90.9096318	1.50E-21	4.53E-20
WHL22.7652	850.857079	-0.5258641	0.07763103	45.8956253	1.25E-11	2.01E-10
WHL22.5845	385.092879	-0.5281246	0.11434717	21.3369715	3.85E-06	3.37E-05
WHL22.7577	623.887626	-0.5284732	0.09007983	34.4298085	4.42E-09	5.61E-08
WHL22.3358	4262.81346	-0.5285404	0.03734609	200.153561	1.93E-45	1.32E-43
WHL22.6697	415.085014	-0.5295337	0.11014391	23.1195546	1.52E-06	1.41E-05
WHL22.5336	722.951722	-0.5303522	0.08737216	36.8111609	1.30E-09	1.73E-08
WHL22.6759	724.86295	-0.53088	0.08372325	40.2200014	2.27E-10	3.23E-09
WHL22.6035	163.15515	-0.5319463	0.17523992	9.21336679	0.00240254	0.01200863
WHL22.2445	211.375441	-0.5328034	0.15503445	11.8063618	0.00059029	0.00343729

WHL22.5937	145.598823	-0.5334933	0.18594351	8.22850414	0.00412375	0.01919361
WHL22.4202	219.774608	-0.5337256	0.15298887	12.1618196	0.00048778	0.00290726
WHL22.1494	139.540963	-0.5339456	0.18946145	7.94037397	0.00483438	0.02215005
WHL22.5391	400.778338	-0.5349266	0.11224058	22.7189644	1.88E-06	1.72E-05
WHL22.2361	137.300949	-0.5352846	0.19063787	7.88344019	0.00498895	0.02277294
WHL22.5691	223.849091	-0.535388	0.1504066	12.668182	0.00037193	0.0022845
WHL22.4875	135.729834	-0.5355942	0.19144824	7.82751843	0.00514567	0.02335037
WHL22.7539	260.820545	-0.5358508	0.14104319	14.4223892	0.00014606	0.00097681
WHL22.4162	115.207697	-0.5362857	0.20830271	6.62614392	0.01004926	0.04136935
WHL22.2971	780.605814	-0.5365864	0.08133286	43.530945	4.17E-11	6.32E-10
WHL22.5846	177.298294	-0.5383988	0.16781569	10.2950121	0.0013339	0.00717541
WHL22.3018	305.901178	-0.5387978	0.13018853	17.118387	3.51E-05	0.00026198
WHL22.9035	237.477463	-0.5391335	0.1457603	13.6804077	0.0002167	0.00140141
WHL22.1585	203.389122	-0.5391459	0.16080583	11.2233078	0.00080776	0.00457484
WHL22.5141	1811.04133	-0.5395559	0.05443646	98.2342331	3.72E-23	1.19E-21
WHL22.3029	782.542769	-0.5398133	0.08320493	42.0672889	8.82E-11	1.31E-09
WHL22.5712	210.076803	-0.5399216	0.1540202	12.2921493	0.00045487	0.00273666
WHL22.7317	1418.29036	-0.5401439	0.06109525	78.1629629	9.49E-19	2.48E-17
WHL22.5102	278.762799	-0.5417399	0.13665236	15.705368	7.40E-05	0.00052037
WHL22.4660	550.685197	-0.5434624	0.09671616	31.5753637	1.92E-08	2.26E-07
WHL22.5721	218.208209	-0.5435222	0.15103194	12.9553648	0.00031901	0.00198349
WHL22.7329	565.241012	-0.5435352	0.09844086	30.4570274	3.41E-08	3.86E-07
WHL22.1070	139.381686	-0.5435679	0.18934187	8.24073735	0.00409605	0.01907678
WHL22.7171	143.786467	-0.5436154	0.18881581	8.27878034	0.00401111	0.01874062
WHL22.1102	232.362365	-0.5440694	0.14917178	13.2921789	0.00026652	0.00168858
WHL22.2121	185.113957	-0.544097	0.17276616	9.88234191	0.00166872	0.0087364
WHL22.3467	230.583171	-0.5456068	0.14705016	13.7708157	0.00020652	0.00134384
WHL22.5546	113.035644	-0.545999	0.21033555	6.73619621	0.00944759	0.03931138
WHL22.5414	153.91694	-0.5461089	0.17860378	9.35561851	0.00222303	0.01124537
WHL22.2113	335.901253	-0.5463077	0.122467	19.9029928	8.15E-06	6.81E-05
WHL22.3540	337.603662	-0.5466345	0.12114781	20.3712431	6.38E-06	5.41E-05
WHL22.3656	273.655427	-0.547405	0.13526719	16.381656	5.18E-05	0.00037448
WHL22.5569	158.914593	-0.5479597	0.17619261	9.67702026	0.00186587	0.00963114
WHL22.2269	147.389107	-0.5486472	0.18352572	8.93966568	0.00279044	0.01371397
WHL22.4842	890.610901	-0.5511451	0.08001573	47.3866091	5.83E-12	9.80E-11
WHL22.5568	114.254686	-0.5511989	0.21011476	6.87669204	0.0087327	0.03690158
WHL22.2557	559.838302	-0.5515479	0.09664967	32.5590154	1.16E-08	1.40E-07
WHL22.4560	102.199767	-0.5522719	0.2192999	6.34556986	0.01176748	0.04751123
WHL22.6184	179.360648	-0.5534165	0.17028102	10.5482405	0.00116299	0.00633964
WHL22.2616	119.663306	-0.554205	0.20450882	7.34212443	0.00673572	0.02962263
WHL22.1981	371.384143	-0.5542235	0.11579805	22.9189501	1.69E-06	1.56E-05
WHL22.2656	588.111775	-0.5544039	0.09259303	35.8648878	2.11E-09	2.75E-08

WHL22.7232	1071.0015	-0.554484	0.06939437	63.8607066	1.34E-15	2.96E-14
WHL22.4617	128.2182	-0.5545823	0.19594748	8.01463668	0.00464008	0.0213464
WHL22.3422	690.108727	-0.556131	0.08716114	40.7049082	1.77E-10	2.54E-09
WHL22.2450	200.048203	-0.5562703	0.15732434	12.5080148	0.00040521	0.0024611
WHL22.7065	339.484255	-0.5563901	0.12084518	21.210864	4.11E-06	3.58E-05
WHL22.5857	144.217012	-0.5581397	0.18739125	8.86586773	0.00290552	0.01419875
WHL22.3773	258.581511	-0.5589965	0.14232372	15.4117997	8.64E-05	0.00060373
WHL22.3640	2708.97581	-0.5592074	0.04438063	158.776471	2.09E-36	1.08E-34
WHL22.5277	657.934696	-0.5598449	0.09133451	37.5375038	8.97E-10	1.21E-08
WHL22.3786	167.618091	-0.5600813	0.17433165	10.3150628	0.00131949	0.00710047
WHL22.7115	3430.37059	-0.5606868	0.04104754	186.466107	1.88E-42	1.17E-40
WHL22.1880	3161.99981	-0.5610862	0.04183745	179.81402	5.32E-41	3.10E-39
WHL22.5693	116.637127	-0.5613617	0.21156652	7.02322377	0.00804592	0.03445571
WHL22.5549	223.10459	-0.5616232	0.15023971	13.9744455	0.00018531	0.00121663
WHL22.5621	199.924693	-0.5633247	0.15763268	12.776551	0.00035099	0.0021658
WHL22.4680	153.762474	-0.5637975	0.17934912	9.88635501	0.00166509	0.00872359
WHL22.6420	238.964566	-0.5639151	0.14647003	14.8163389	0.0001185	0.00080763
WHL22.5869	130.529696	-0.5647339	0.19391287	8.48780429	0.00357535	0.01697482
WHL22.5208	189.498724	-0.5654522	0.16219643	12.1572502	0.00048897	0.00291321
WHL22.7116	181.068309	-0.5654844	0.16675103	11.4989129	0.00069637	0.00400106
WHL22.1878	259.758057	-0.5656292	0.13835459	16.7219506	4.33E-05	0.00031702
WHL22.7041	316.434303	-0.5667764	0.1254409	20.4257909	6.20E-06	5.27E-05
WHL22.8509	334.106444	-0.5674007	0.12169871	21.7523167	3.10E-06	2.76E-05
WHL22.5836	320.748975	-0.5677096	0.12488754	20.672685	5.45E-06	4.66E-05
WHL22.4212	133.031954	-0.5678432	0.19238077	8.7179232	0.00315097	0.0152359
WHL22.1731	148.760459	-0.5689065	0.1842207	9.53264294	0.00201849	0.01032815
WHL22.2936	849.019664	-0.5691538	0.07732104	54.2059808	1.81E-13	3.48E-12
WHL22.2871	798.408858	-0.5692544	0.08040895	50.1267326	1.44E-12	2.56E-11
WHL22.4733	208.424487	-0.5705076	0.1549089	13.5661483	0.0002303	0.00148152
WHL22.5892	313.939642	-0.5725827	0.12558934	20.799678	5.10E-06	4.38E-05
WHL22.3485	483.335438	-0.5727898	0.10241689	31.288318	2.22E-08	2.59E-07
WHL22.6750	291.995064	-0.5731384	0.13397624	18.2852244	1.90E-05	0.0001501
WHL22.4600	1295.42058	-0.5736642	0.06516036	77.4701141	1.35E-18	3.48E-17
WHL22.6238	106.798193	-0.5737255	0.2150866	7.11825989	0.00763027	0.03294483
WHL22.6871	279.183424	-0.5737636	0.13681459	17.5731951	2.76E-05	0.00021072
WHL22.4766	1246.59435	-0.574488	0.06442062	79.5469049	4.71E-19	1.25E-17
WHL22.5227	339.109008	-0.5765674	0.12266125	22.0958074	2.59E-06	2.33E-05
WHL22.4395	244.249768	-0.5768256	0.146238	15.5433598	8.06E-05	0.00056475
WHL22.2962	164.376549	-0.5776935	0.17301517	11.1570501	0.00083713	0.00471462
WHL22.1056	128.115499	-0.5781863	0.19616688	8.69259866	0.00319505	0.01539327
WHL22.3251	262.208191	-0.5788564	0.13789719	17.6287133	2.69E-05	0.00020508
WHL22.3852	206.567438	-0.5793882	0.15674869	13.6593555	0.00021915	0.00141597

WHL22.5025	579.880365	-0.5802892	0.09541478	36.974158	1.20E-09	1.60E-08
WHL22.5614	3200.77969	-0.580691	0.04124798	198.169345	5.24E-45	3.48E-43
WHL22.2650	3829.89068	-0.5812021	0.03818601	231.583691	2.69E-52	2.12E-50
WHL22.1028	483.504125	-0.5818984	0.10338952	31.6738813	1.82E-08	2.15E-07
WHL22.4269	129.195129	-0.5821546	0.19622075	8.80371604	0.00300618	0.01463218
WHL22.1640	3976.19323	-0.5822272	0.03761498	239.497746	5.06E-54	4.15E-52
WHL22.6527	728.847272	-0.5831975	0.08430628	47.8576767	4.58E-12	7.77E-11
WHL22.2599	116.728261	-0.5832177	0.20627541	7.99596645	0.00468817	0.02152715
WHL22.5650	2426.96584	-0.5833605	0.04750566	150.759341	1.18E-34	5.83E-33
WHL22.6576	307.955858	-0.5833729	0.12933315	20.339596	6.48E-06	5.50E-05
WHL22.4191	119.105813	-0.5838499	0.20552487	8.06803248	0.0045053	0.02077845
WHL22.5654	95.0459984	-0.5844435	0.22879351	6.52491082	0.01063739	0.04344932
WHL22.1982	139.537071	-0.5848178	0.19421523	9.04515322	0.00263392	0.01301008
WHL22.2015	118.174118	-0.5853737	0.20448687	8.19849084	0.00419252	0.01945204
WHL22.5861	94.0769178	-0.586193	0.23027924	6.47928047	0.01091392	0.04447981
WHL22.7133	120.732969	-0.5865711	0.20587223	8.10703064	0.00440939	0.02038093
WHL22.6568	135.06692	-0.5877586	0.19587052	8.98979512	0.00271491	0.01337414
WHL22.3762	835.06898	-0.5878243	0.07823083	56.4784541	5.68E-14	1.14E-12
WHL22.3069	119.373252	-0.5879662	0.22233797	6.92375744	0.00850581	0.03612999
WHL22.7019	167.265905	-0.5886211	0.1728592	11.5978249	0.00066029	0.00380717
WHL22.3513	317.13429	-0.588665	0.13236294	19.7334209	8.90E-06	7.40E-05
WHL22.6231	425.822147	-0.5892805	0.11055265	28.4040628	9.85E-08	1.05E-06
WHL22.4577	218.546793	-0.589556	0.15187938	15.0685212	0.00010368	0.00071188
WHL22.1360	296.364305	-0.5900867	0.13101531	20.2862326	6.67E-06	5.64E-05
WHL22.3221	276.209883	-0.5904557	0.13494022	19.1512226	1.21E-05	9.82E-05
WHL22.2619	113.52504	-0.5909369	0.2105789	7.87080891	0.00502392	0.02290407
WHL22.4466	199.634027	-0.5909985	0.1574938	14.0900136	0.00017427	0.00115028
WHL22.7612	171.751394	-0.5911002	0.17482698	11.4114254	0.00072994	0.0041727
WHL22.1629	254.583222	-0.5912125	0.14647204	16.2537244	5.54E-05	0.00039847
WHL22.6160	2483.1939	-0.5925257	0.04673117	160.74955	7.76E-37	4.08E-35
WHL22.1674	563.348099	-0.5929447	0.09613255	38.0396884	6.93E-10	9.41E-09
WHL22.5515	132.117083	-0.5935843	0.20000506	8.78385951	0.00303908	0.01475806
WHL22.6737	411.359408	-0.5945152	0.11388096	27.2322544	1.80E-07	1.88E-06
WHL22.1483	118.610243	-0.5951455	0.20587726	8.35351255	0.00384942	0.01811204
WHL22.5521	159.407253	-0.5951599	0.18059811	10.8437566	0.00099129	0.00548519
WHL22.2181	108.078158	-0.5952436	0.22057766	7.25968797	0.00705195	0.03076454
WHL22.2330	740.757307	-0.5954718	0.08424802	49.9506445	1.58E-12	2.79E-11
WHL22.2091	146.607099	-0.5956808	0.18642843	10.2020525	0.00140284	0.00749682
WHL22.3731	1156.73801	-0.5957283	0.06701756	79.033541	6.11E-19	1.61E-17
WHL22.6138	424.316331	-0.5960356	0.10913869	29.8366124	4.70E-08	5.20E-07
WHL22.3340	95.5573933	-0.5980624	0.2298574	6.76367555	0.00930319	0.03876551
WHL22.1960	194.529985	-0.5982226	0.16432549	13.2332853	0.00027502	0.00173723

WHL22.4663	178.33231	-0.5999357	0.16871652	12.6396122	0.00037766	0.0023129
WHL22.3175	340.789125	-0.6000906	0.12243823	24.0220324	9.52E-07	9.03E-06
WHL22.5978	248.470723	-0.600561	0.14211583	17.863319	2.37E-05	0.00018416
WHL22.3580	679.160649	-0.6011612	0.08671839	48.0723471	4.11E-12	7.00E-11
WHL22.4145	554.043662	-0.6014755	0.09688737	38.5351691	5.38E-10	7.36E-09
WHL22.3818	271.488056	-0.6015386	0.13589959	19.5995573	9.55E-06	7.89E-05
WHL22.3031	1225.97353	-0.6020693	0.06453887	87.0652047	1.05E-20	3.06E-19
WHL22.5976	1853.79585	-0.6027923	0.05371082	125.948795	3.16E-29	1.27E-27
WHL22.6110	171.455327	-0.6035362	0.1742249	11.9845722	0.00053643	0.00315748
WHL22.3573	169.037029	-0.604225	0.17369843	12.093471	0.00050599	0.00300117
WHL22.7053	226.789523	-0.6042776	0.14859232	16.5431067	4.76E-05	0.00034664
WHL22.5109	148.826101	-0.6059926	0.18763878	10.4094118	0.00125375	0.006784
WHL22.7041	107.71978	-0.606076	0.21498703	7.94830425	0.00481325	0.02207387
WHL22.6403	204.41521	-0.6063434	0.15606185	15.1035602	0.00010177	0.00069977
WHL22.2153	10808.168	-0.606519	0.02493616	590.596445	1.86E-130	3.95E-128
WHL22.1504	157.369704	-0.6067229	0.18228263	11.0595365	0.00088232	0.00494747
WHL22.1502	1006.74755	-0.606858	0.07200399	71.0401767	3.50E-17	8.44E-16
WHL22.5566	429.484468	-0.6073988	0.10869669	31.2348817	2.29E-08	2.65E-07
WHL22.6910	491.995767	-0.6082575	0.10081811	36.4222285	1.59E-09	2.10E-08
WHL22.7489	435.183261	-0.6084376	0.10779926	31.8679458	1.65E-08	1.96E-07
WHL22.8326	825.03838	-0.6086776	0.07832812	60.4174354	7.67E-15	1.61E-13
WHL22.7389	361.653711	-0.6104693	0.11907291	26.283553	2.95E-07	2.99E-06
WHL22.6687	299.808907	-0.6110992	0.12899961	22.4537615	2.15E-06	1.95E-05
WHL22.3486	1781.31326	-0.6116892	0.05694779	115.264229	6.89E-27	2.59E-25
WHL22.3804	109.010172	-0.6123822	0.22209749	7.56914311	0.0059376	0.02653394
WHL22.3976	289.270034	-0.6128469	0.13452423	20.7389184	5.26E-06	4.51E-05
WHL22.7335	673.358598	-0.6137452	0.08738728	49.3374979	2.16E-12	3.78E-11
WHL22.3896	380.903369	-0.6141256	0.11792264	27.1015665	1.93E-07	2.01E-06
WHL22.7534	153.305629	-0.6144702	0.18162287	11.4428856	0.00071768	0.00411064
WHL22.2244	599.078795	-0.6148492	0.09176473	44.9176531	2.05E-11	3.24E-10
WHL22.5918	225.383241	-0.6154191	0.15715616	15.285993	9.24E-05	0.00064042
WHL22.2903	112.958086	-0.6161931	0.21120295	8.50909765	0.00353375	0.0168045
WHL22.2619	312.295604	-0.6164491	0.1262829	23.8442275	1.04E-06	9.84E-06
WHL22.7086	102.436289	-0.6169416	0.22607585	7.42523723	0.00643153	0.02849832
WHL22.1182	261.75501	-0.6169777	0.14573567	17.8719187	2.36E-05	0.00018343
WHL22.1143	641.465954	-0.6177665	0.08861087	48.6314721	3.09E-12	5.33E-11
WHL22.1454	624.849469	-0.6183849	0.09297122	44.2099748	2.95E-11	4.56E-10
WHL22.2650	132.576569	-0.6183857	0.1932361	10.2467856	0.00136923	0.00734461
WHL22.3276	270.458539	-0.6188258	0.14351801	18.5421807	1.66E-05	0.00013237
WHL22.5928	105.58208	-0.619019	0.21791053	8.06745055	0.00450675	0.0207786
WHL22.2997	114.52761	-0.6190838	0.2076815	8.89242386	0.00286356	0.0140077
WHL22.4408	665.124747	-0.6198903	0.08711761	50.6579484	1.10E-12	1.97E-11

WHL22.5020	112.060931	-0.619972	0.21245012	8.51019606	0.00353162	0.0167998
WHL22.7521	276.519826	-0.6210915	0.1390819	19.9154586	8.09E-06	6.77E-05
WHL22.1811	183.974044	-0.6211731	0.16492318	14.1899977	0.00016525	0.00109567
WHL22.2879	20730.9965	-0.6213021	0.02027259	936.275556	1.28E-205	5.51E-203
WHL22.1596	127.823168	-0.6222587	0.1976758	9.91102301	0.00164292	0.00861974
WHL22.3746	110.906784	-0.6233489	0.21151688	8.68836997	0.00320247	0.01541891
WHL22.7691	195.867356	-0.6238816	0.16060029	15.0906212	0.00010247	0.00070425
WHL22.2234	126.457166	-0.6242969	0.19885509	9.85715408	0.00169173	0.00884106
WHL22.7419	1871.71021	-0.6244892	0.05314799	138.07604	7.01E-32	3.15E-30
WHL22.4529	655.224032	-0.6247297	0.08988442	48.2932059	3.67E-12	6.28E-11
WHL22.3984	117.846771	-0.6250881	0.20596777	9.21062074	0.00240615	0.01201847
WHL22.3728	714.560129	-0.6263694	0.0844259	55.0661359	1.17E-13	2.28E-12
WHL22.6106	275.564388	-0.6263763	0.13537022	21.4161664	3.70E-06	3.25E-05
WHL22.2694	162.827414	-0.6263797	0.17530792	12.769586	0.0003523	0.0021721
WHL22.4227	123.133821	-0.6265622	0.20247742	9.57255355	0.00197508	0.01012012
WHL22.2560	92.7006435	-0.6285378	0.23397807	7.20858996	0.00725555	0.03152158
WHL22.5516	308.354459	-0.6293837	0.13057023	23.2162535	1.45E-06	1.34E-05
WHL22.8148	140.662645	-0.6294726	0.18847156	11.1572023	0.00083706	0.00471462
WHL22.1841	226.33594	-0.6300091	0.14975348	17.6986214	2.59E-05	0.00019861
WHL22.2703	94.7891717	-0.630458	0.22811718	7.64380521	0.00569676	0.02559794
WHL22.1067	117.601511	-0.6306357	0.20481879	9.48744256	0.00206883	0.01056363
WHL22.1792	164.970537	-0.6311189	0.17333659	13.2662737	0.00027022	0.00170986
WHL22.5856	124.733175	-0.6316289	0.20202848	9.76612607	0.00177757	0.00922725
WHL22.6344	110.955976	-0.632455	0.2176303	8.4220102	0.00370706	0.01749826
WHL22.5936	179.355468	-0.6331646	0.17014658	13.8334489	0.00019975	0.00130383
WHL22.2719	363.240435	-0.6334538	0.11778235	28.9373996	7.48E-08	8.14E-07
WHL22.4704	598.890888	-0.6335159	0.09323181	46.170957	1.08E-11	1.76E-10
WHL22.6152	157.017525	-0.6336257	0.18762332	11.3568709	0.00075169	0.00428538
WHL22.6640	355.0007	-0.6365648	0.12207806	27.1695137	1.86E-07	1.94E-06
WHL22.3053	166.837761	-0.6373433	0.17371944	13.4609389	0.00024358	0.00155943
WHL22.7116	1562.70804	-0.6375923	0.05894388	116.973944	2.91E-27	1.11E-25
WHL22.2146	1764.81188	-0.6377777	0.05435137	137.732369	8.34E-32	3.72E-30
WHL22.6186	1199.06602	-0.6385355	0.06659237	91.9348347	8.96E-22	2.72E-20
WHL22.3769	172.057354	-0.6388724	0.17184017	13.8193112	0.00020126	0.00131251
WHL22.5477	311.18514	-0.6391898	0.12718266	25.268788	4.99E-07	4.91E-06
WHL22.3441	476.658527	-0.6392336	0.10313634	38.4297654	5.68E-10	7.77E-09
WHL22.4572	11338.6294	-0.6392682	0.02470023	668.424434	2.20E-147	6.59E-145
WHL22.2305	507.994127	-0.6394223	0.10109592	40.0009307	2.54E-10	3.59E-09
WHL22.1729	219.445002	-0.6395317	0.15230063	17.6308451	2.68E-05	0.00020496
WHL22.7522	220.44219	-0.6396539	0.1514854	17.831464	2.41E-05	0.00018668
WHL22.2198	185.351827	-0.6400132	0.16434107	15.1719139	9.82E-05	0.0006771
WHL22.2910	697.885713	-0.640238	0.08578148	55.7211675	8.35E-14	1.65E-12

WHL22.4596	151.527431	-0.6405169	0.1882457	11.5443294	0.00067956	0.00390908
WHL22.6747	244.972952	-0.6408433	0.14263803	20.1975034	6.98E-06	5.89E-05
WHL22.7025	762.22735	-0.6410739	0.08493444	56.9220618	4.53E-14	9.19E-13
WHL22.2375	153.993023	-0.6419002	0.1812846	12.5353187	0.00039933	0.00242942
WHL22.4808	164.638132	-0.6436675	0.17518352	13.500656	0.00023848	0.00153145
WHL22.4439	144.638547	-0.6438281	0.18597324	11.9878375	0.00053549	0.00315322
WHL22.4599	1315.89471	-0.6443913	0.0646112	99.4188142	2.04E-23	6.65E-22
WHL22.5318	748.15292	-0.6451891	0.08462093	58.1086543	2.48E-14	5.11E-13
WHL22.5644	1060.69597	-0.6458398	0.07281395	78.6002987	7.60E-19	2.00E-17
WHL22.6752	181.569513	-0.647253	0.1659434	15.2207922	9.56E-05	0.00066073
WHL22.5247	678.811704	-0.6484865	0.08919321	52.8273842	3.64E-13	6.83E-12
WHL22.6333	266.392323	-0.6486131	0.13665876	22.5435612	2.05E-06	1.87E-05
WHL22.7596	395.238943	-0.6489135	0.11316581	32.894107	9.73E-09	1.18E-07
WHL22.5367	406.867049	-0.6490638	0.11505042	31.7921354	1.72E-08	2.03E-07
WHL22.1028	84.9761353	-0.6495445	0.24887	6.78630707	0.00918597	0.03842978
WHL22.4568	85.9639283	-0.6499239	0.24661878	6.92198879	0.00851422	0.03615528
WHL22.5208	1944.18511	-0.6501172	0.05271414	152.075678	6.10E-35	3.07E-33
WHL22.6807	103.683186	-0.6505609	0.22432858	8.38848699	0.00377605	0.01779532
WHL22.5068	257.663414	-0.650992	0.13874847	22.0314788	2.68E-06	2.41E-05
WHL22.6350	263.832317	-0.6513735	0.13767988	22.3956904	2.22E-06	2.01E-05
WHL22.5560	336.880931	-0.6525391	0.12252369	28.3751826	9.99E-08	1.07E-06
WHL22.3482	240.314085	-0.6540886	0.14593429	20.0873953	7.40E-06	6.22E-05
WHL22.7376	74.5509396	-0.6541443	0.25865438	6.39626296	0.01143608	0.0463122
WHL22.4236	845.44255	-0.6547735	0.07920411	68.3282244	1.38E-16	3.23E-15
WHL22.5123	603.526627	-0.6557321	0.09202479	50.7919712	1.03E-12	1.85E-11
WHL22.4874	1350.72569	-0.6561001	0.06179574	112.770133	2.42E-26	8.80E-25
WHL22.4022	799.715193	-0.6569001	0.08141069	65.0951245	7.14E-16	1.60E-14
WHL22.5392	138.802322	-0.6572065	0.18926169	12.0650987	0.00051375	0.00304227
WHL22.2818	252.836814	-0.657836	0.14048131	21.9417901	2.81E-06	2.52E-05
WHL22.1670	170.19127	-0.6587313	0.17261708	14.5614969	0.00013566	0.0009152
WHL22.1149	205.999246	-0.6590495	0.15670127	17.6906305	2.60E-05	0.00019924
WHL22.7044	1279.14384	-0.6592952	0.06381196	106.772748	4.99E-25	1.72E-23
WHL22.3006	170.819665	-0.6604378	0.17295126	14.5763835	0.00013459	0.00090967
WHL22.7312	159.068061	-0.6612289	0.18836814	12.2569691	0.00046352	0.00278304
WHL22.3316	340.988289	-0.6622944	0.12350107	28.7491881	8.24E-08	8.91E-07
WHL22.7089	364.826264	-0.6628244	0.12005784	30.4621198	3.40E-08	3.86E-07
WHL22.1089	91.8341734	-0.6628449	0.24766462	7.10326164	0.00769438	0.03319233
WHL22.5466	352.897929	-0.6639727	0.12076015	30.2296497	3.84E-08	4.31E-07
WHL22.1192	83.4688434	-0.6646657	0.24304224	7.48564158	0.00621929	0.02764966
WHL22.4681	345.415713	-0.6650089	0.12163464	29.8945318	4.56E-08	5.07E-07
WHL22.6917	157.223481	-0.6651399	0.18037605	13.5891513	0.0002275	0.00146798
WHL22.3245	262.114498	-0.6652426	0.14104873	22.2301313	2.42E-06	2.18E-05

WHL22.3070	214.510141	-0.6654619	0.15241932	19.074174	1.26E-05	0.00010186
WHL22.1918	119.107341	-0.6661093	0.20457544	10.6065144	0.0011269	0.00616122
WHL22.1744	111.074228	-0.6674683	0.21094427	10.0201362	0.00154838	0.00818894
WHL22.3625	183.156756	-0.667743	0.16842275	15.7025082	7.41E-05	0.0005209
WHL22.3945	137.218484	-0.6682323	0.19054886	12.3043244	0.00045191	0.0027211
WHL22.1804	76.0541413	-0.6702219	0.26158892	6.54241445	0.01053323	0.04313189
WHL22.7171	289.199862	-0.6708127	0.1335079	25.2426531	5.06E-07	4.97E-06
WHL22.2596	134.992619	-0.6716603	0.19187295	12.2626713	0.00046211	0.00277796
WHL22.8975	73.0022444	-0.6719829	0.26038927	6.66373858	0.00983943	0.04069958
WHL22.3976	77.9217951	-0.6720508	0.25846214	6.73919628	0.00943171	0.03926759
WHL22.3656	1921.17313	-0.6728854	0.05461914	151.629125	7.64E-35	3.83E-33
WHL22.2743	499.879578	-0.6732575	0.10184455	43.7011351	3.83E-11	5.84E-10
WHL22.5321	350.532895	-0.6733271	0.12133994	30.79088	2.87E-08	3.29E-07
WHL22.5177	116.569828	-0.6737314	0.20648707	10.651958	0.00109954	0.00602738
WHL22.3379	287.613148	-0.6737482	0.13264028	25.8106842	3.77E-07	3.76E-06
WHL22.5367	1071.4493	-0.6744632	0.07018687	92.3440848	7.28E-22	2.22E-20
WHL22.5692	143.20279	-0.6758914	0.19054379	12.5641025	0.00039323	0.00239526
WHL22.3985	343.341455	-0.6762087	0.12048019	31.5270495	1.97E-08	2.31E-07
WHL22.1526	69.6935775	-0.6767573	0.26663849	6.44615028	0.0111193	0.04520392
WHL22.6707	226.78585	-0.6769281	0.15400093	19.2853359	1.13E-05	9.19E-05
WHL22.5515	90.4648624	-0.6777995	0.23481674	8.33426183	0.00389043	0.01827568
WHL22.7612	97.3544678	-0.6780452	0.22875537	8.77658015	0.00305123	0.01480728
WHL22.5473	3484.93746	-0.678209	0.04528452	223.596705	1.49E-50	1.11E-48
WHL22.6147	625.055623	-0.6782364	0.09184518	54.5220766	1.54E-13	2.98E-12
WHL22.1437	212.390108	-0.6784933	0.15378349	19.4754484	1.02E-05	8.36E-05
WHL22.4388	1098.21716	-0.6787534	0.06826921	98.8997594	2.66E-23	8.59E-22
WHL22.5240	164.205102	-0.6789503	0.17358678	15.3123417	9.11E-05	0.00063335
WHL22.1473	200.479021	-0.6791613	0.16036396	17.925731	2.30E-05	0.00017869
WHL22.4765	115.54211	-0.6799662	0.20831264	10.6556561	0.00109735	0.00601758
WHL22.5227	316.59706	-0.68009	0.12830759	28.0845341	1.16E-07	1.23E-06
WHL22.1494	212.052213	-0.6809679	0.15426714	19.4908387	1.01E-05	8.30E-05
WHL22.2494	251.003194	-0.6810427	0.14311229	22.6413062	1.95E-06	1.78E-05
WHL22.4711	203.432022	-0.684408	0.15806828	18.747687	1.49E-05	0.00011949
WHL22.6276	685.211071	-0.6844716	0.08625652	62.9998757	2.07E-15	4.54E-14
WHL22.2297	608.863629	-0.6858057	0.09428859	52.8646128	3.57E-13	6.72E-12
WHL22.5216	20362.7635	-0.6864823	0.02081394	1083.35701	1.37E-237	6.70E-235
WHL22.3480	74.8886219	-0.6878324	0.26178696	6.88855914	0.00867492	0.03669965
WHL22.5060	333.820607	-0.6890966	0.1242159	30.7749996	2.90E-08	3.31E-07
WHL22.7470	457.829026	-0.6897805	0.10983073	39.3861867	3.48E-10	4.86E-09
WHL22.1621	165.252147	-0.6899698	0.17863983	14.8919551	0.00011385	0.00077806
WHL22.7486	164.124799	-0.6905078	0.18152346	14.4261732	0.00014576	0.00097574
WHL22.3626	113.077076	-0.6909304	0.21785182	10.0199509	0.00154854	0.00818894

WHL22.3956	78.1006118	-0.6912334	0.25573189	7.29447667	0.00691669	0.03030956
WHL22.2898	572.892688	-0.6913484	0.09392679	54.2114673	1.80E-13	3.48E-12
WHL22.3377	113.605336	-0.6930136	0.20939737	10.9595237	0.00093124	0.00520387
WHL22.4318	184.654302	-0.6943769	0.16491385	17.7356942	2.54E-05	0.00019509
WHL22.7542	940.858565	-0.69493	0.07452199	86.9712173	1.10E-20	3.20E-19
WHL22.4229	489.202161	-0.6954662	0.10368005	44.9820491	1.99E-11	3.14E-10
WHL22.3649	66.6079008	-0.6956507	0.27238997	6.52718322	0.01062381	0.04344219
WHL22.1012	217.572478	-0.6957529	0.15587468	19.8973905	8.17E-06	6.83E-05
WHL22.5631	1168.78779	-0.6959035	0.06637614	109.96998	9.95E-26	3.52E-24
WHL22.5230	383.168183	-0.6968404	0.11773953	35.0032515	3.29E-09	4.22E-08
WHL22.1339	519.612379	-0.6981402	0.09978508	48.9565284	2.62E-12	4.55E-11
WHL22.2464	129.302192	-0.7018117	0.19592772	12.8415576	0.00033901	0.00209541
WHL22.7212	539.231646	-0.7023754	0.10620965	43.5821228	4.07E-11	6.17E-10
WHL22.6521	504.855911	-0.7026031	0.10059405	48.8038946	2.83E-12	4.90E-11
WHL22.1600	1082.22101	-0.7029231	0.07189166	95.5136903	1.47E-22	4.65E-21
WHL22.5805	306.532877	-0.7049683	0.13103096	28.9250515	7.52E-08	8.19E-07
WHL22.6332	245.165759	-0.7051889	0.14336699	24.2062993	8.65E-07	8.22E-06
WHL22.4807	75.9087527	-0.7066969	0.26151614	7.28107064	0.0069685	0.03050017
WHL22.1008	1358.67952	-0.7080867	0.0625137	128.299086	9.65E-30	3.96E-28
WHL22.6140	640.411698	-0.7094529	0.08984133	62.3743784	2.84E-15	6.16E-14
WHL22.4765	121.27635	-0.7095614	0.20716483	11.7132566	0.00062056	0.00359081
WHL22.3109	2607.19365	-0.7108711	0.04580041	240.842604	2.58E-54	2.14E-52
WHL22.5429	112.249665	-0.7118247	0.2100927	11.4900876	0.00069968	0.00401382
WHL22.5443	174.471617	-0.7118951	0.17389911	16.7329093	4.30E-05	0.00031567
WHL22.7547	267.722776	-0.7144174	0.13803778	26.7919318	2.27E-07	2.33E-06
WHL22.1456	1241.69226	-0.7160548	0.06674614	115.010001	7.83E-27	2.90E-25
WHL22.7016	187.119673	-0.7168902	0.17338893	17.0227091	3.69E-05	0.00027454
WHL22.5523	60.634798	-0.7172946	0.28575382	6.30613465	0.01203209	0.04843188
WHL22.4989	240.655369	-0.7174568	0.14384246	24.9014104	6.03E-07	5.85E-06
WHL22.7507	60.1180886	-0.7174874	0.28726263	6.24148271	0.0124792	0.04987601
WHL22.1274	802.917329	-0.717488	0.08011806	80.2307847	3.33E-19	8.96E-18
WHL22.6186	123.056252	-0.71772	0.20064962	12.8074345	0.00034524	0.00213218
WHL22.8326	472.932251	-0.718743	0.11098555	41.8220691	1.00E-10	1.48E-09
WHL22.3426	389.992418	-0.7187954	0.11825142	36.8953378	1.25E-09	1.66E-08
WHL22.3466	233.788195	-0.7197682	0.14778234	23.7232852	1.11E-06	1.04E-05
WHL22.2791	76.7706681	-0.720304	0.26486067	7.35259586	0.0066966	0.02945942
WHL22.5216	624.71986	-0.7207134	0.09203426	61.3093703	4.88E-15	1.04E-13
WHL22.1347	1099.32401	-0.7210777	0.06831295	111.481138	4.64E-26	1.67E-24
WHL22.6848	858.041834	-0.7215763	0.07863433	84.196295	4.48E-20	1.26E-18
WHL22.4980	101.807578	-0.7226217	0.23182336	9.66378695	0.00187936	0.00968714
WHL22.2619	1322.6622	-0.7236835	0.06640833	118.575415	1.30E-27	4.97E-26
WHL22.5597	1089.22146	-0.7239169	0.06893377	110.328595	8.30E-26	2.94E-24

WHL22.6037	88.4706788	-0.7241885	0.23682154	9.35850206	0.00221953	0.01123544
WHL22.9378	348.137246	-0.725176	0.12369049	34.3437632	4.62E-09	5.85E-08
WHL22.2445	128.938416	-0.7256759	0.20680406	12.2576277	0.00046336	0.00278304
WHL22.6085	7232.60809	-0.7270754	0.02939104	610.922642	7.05E-135	1.70E-132
WHL22.4526	153.156267	-0.7288293	0.1801054	16.3928103	5.15E-05	0.00037246
WHL22.7484	583.065282	-0.7294622	0.09330384	61.1640087	5.25E-15	1.12E-13
WHL22.2073	142.723606	-0.7301152	0.19301244	14.2764276	0.00015783	0.00104933
WHL22.3991	198.980135	-0.7309935	0.15940656	21.0369984	4.50E-06	3.91E-05
WHL22.3161	129.289043	-0.7311494	0.20003565	13.3434778	0.00025932	0.00164871
WHL22.7171	366.956328	-0.7321837	0.11765883	38.7453217	4.83E-10	6.64E-09
WHL22.2952	58.5520433	-0.7332425	0.29145498	6.33397464	0.01184466	0.04779537
WHL22.3146	158.451316	-0.7339025	0.1806566	16.4901803	4.89E-05	0.00035574
WHL22.5784	872.454988	-0.7360316	0.0770197	91.35863	1.20E-21	3.63E-20
WHL22.5837	211.694994	-0.7360949	0.15953604	21.2449154	4.04E-06	3.52E-05
WHL22.1691	1453.95008	-0.7364561	0.06087745	146.321476	1.10E-33	5.21E-32
WHL22.4027	79.0579307	-0.736653	0.26907259	7.41246558	0.00647735	0.02865807
WHL22.4436	76.3088461	-0.7366996	0.27177484	7.27723163	0.00698341	0.03052406
WHL22.1416	88.9985302	-0.7373572	0.24238089	9.22894853	0.00238218	0.01192717
WHL22.1054	61.3741611	-0.7381417	0.28660335	6.62888554	0.0100338	0.0413405
WHL22.1174	492.3951	-0.738512	0.10128022	53.210805	3.00E-13	5.68E-12
WHL22.2898	220.193431	-0.7424996	0.15496986	22.930307	1.68E-06	1.55E-05
WHL22.7559	2445.6367	-0.7429078	0.04734154	246.179927	1.77E-55	1.48E-53
WHL22.1712	724.310382	-0.7431198	0.08383787	78.6206969	7.53E-19	1.98E-17
WHL22.4229	449.795912	-0.7437567	0.10630849	48.9768848	2.59E-12	4.51E-11
WHL22.7014	299.744324	-0.7441879	0.13587619	29.9335236	4.47E-08	4.98E-07
WHL22.6047	179.341603	-0.744588	0.17238938	18.6180979	1.60E-05	0.00012762
WHL22.2677	97.3981792	-0.7455725	0.22673787	10.8178688	0.00100525	0.00555613
WHL22.1103	604.890171	-0.7463433	0.09157747	66.4681499	3.56E-16	8.06E-15
WHL22.7561	121.596625	-0.7466132	0.20957485	12.6549562	0.00037457	0.00229591
WHL22.4216	110.793726	-0.7469884	0.21241469	12.3793848	0.0004341	0.00262571
WHL22.1362	184.647735	-0.7470096	0.16727621	19.9324767	8.02E-06	6.72E-05
WHL22.7081	241.481552	-0.7476136	0.14476864	26.6822929	2.40E-07	2.46E-06
WHL22.7025	74.4420918	-0.7490386	0.25789665	8.44534212	0.0036598	0.017303
WHL22.4204	163.061148	-0.7496275	0.17795689	17.7346417	2.54E-05	0.00019509
WHL22.8203	126.280297	-0.7507882	0.2004451	14.0280804	0.0001801	0.00118666
WHL22.1089	370.594351	-0.7515233	0.11631788	41.7827888	1.02E-10	1.51E-09
WHL22.1540	128.305916	-0.7520443	0.19746015	14.5150213	0.00013905	0.00093633
WHL22.5383	106.984726	-0.7535714	0.21947192	11.7746549	0.00060043	0.0034908
WHL22.3033	86.6251131	-0.7552478	0.24148257	9.77974003	0.00176445	0.00916891
WHL22.2232	68.6335829	-0.756593	0.27209708	7.72513142	0.00544574	0.0245602
WHL22.5914	198.541747	-0.756714	0.16560582	20.8259319	5.03E-06	4.33E-05
WHL22.1339	66.1191629	-0.7574866	0.28763729	6.87969515	0.00871804	0.03685024

WHL22.1850	108.232131	-0.7582905	0.21841917	12.0370718	0.00052153	0.00307966
WHL22.5179	3397.41898	-0.7601545	0.0405086	351.960911	1.59E-78	1.74E-76
WHL22.1250	96.6240118	-0.7601973	0.22752239	11.1702828	0.00083118	0.00469297
WHL22.6269	475.67344	-0.7612047	0.10349826	54.1278669	1.88E-13	3.62E-12
WHL22.3644	96.4086577	-0.7614267	0.22956761	10.9956972	0.00091324	0.00510717
WHL22.7384	97.6467171	-0.7615575	0.22591881	11.3734375	0.00074502	0.00425228
WHL22.2462	224.781776	-0.761597	0.15048937	25.6211266	4.15E-07	4.12E-06
WHL22.3933	164.857959	-0.7638323	0.18071155	17.8207652	2.43E-05	0.00018763
WHL22.7317	60.7756796	-0.7657507	0.29187729	6.86263035	0.00880169	0.03712035
WHL22.6186	157.929375	-0.7660513	0.17895174	18.331293	1.86E-05	0.00014698
WHL22.6596	81.449123	-0.768164	0.25256111	9.23100921	0.0023795	0.01192189
WHL22.1790	500.924611	-0.7682282	0.10152548	57.2786941	3.78E-14	7.72E-13
WHL22.5869	222.542956	-0.768701	0.15484782	24.6063735	7.03E-07	6.79E-06
WHL22.4874	374.674905	-0.7688127	0.11805694	42.4040049	7.42E-11	1.11E-09
WHL22.5328	244.686519	-0.7700076	0.14614466	27.7434429	1.39E-07	1.46E-06
WHL22.1633	142.475257	-0.7703348	0.18766287	16.8614891	4.02E-05	0.00029656
WHL22.6417	67.1627712	-0.7705221	0.27326063	7.95456897	0.00479661	0.02200446
WHL22.3687	59.3907322	-0.7733661	0.29387263	6.91072973	0.008568	0.0363416
WHL22.1762	55.0444778	-0.7766634	0.30343349	6.54520823	0.0105167	0.04308106
WHL22.4935	135.804135	-0.7783147	0.19580313	15.7825225	7.11E-05	0.00050077
WHL22.3426	410.37002	-0.7795241	0.11104084	49.3233448	2.17E-12	3.81E-11
WHL22.3315	205.261239	-0.7805364	0.15854281	24.2334772	8.53E-07	8.11E-06
WHL22.5901	113.967931	-0.7819624	0.21849976	12.7557772	0.00035491	0.00218602
WHL22.4482	111.577025	-0.7821065	0.21311767	13.4680042	0.00024267	0.00155425
WHL22.3434	106.670289	-0.7823914	0.2189976	12.7552855	0.000355	0.00218602
WHL22.2386	59.5907676	-0.7823935	0.2963384	6.94287789	0.00841536	0.0357665
WHL22.6798	68.0920446	-0.7845095	0.28143377	7.71855227	0.00546562	0.02463473
WHL22.6470	5964.50216	-0.7845744	0.03200411	599.955099	1.71E-132	3.93E-130
WHL22.1198	142.743004	-0.7860636	0.18838369	17.4201116	3.00E-05	0.00022685
WHL22.6171	168.240983	-0.7866478	0.17338771	20.5943152	5.68E-06	4.85E-05
WHL22.5430	164.571639	-0.7874644	0.17482678	20.3043092	6.61E-06	5.59E-05
WHL22.1293	65.0795764	-0.7882013	0.27728983	8.08517118	0.00446289	0.02060228
WHL22.7342	75.6470052	-0.7882678	0.26069005	9.12842139	0.00251669	0.01251948
WHL22.1916	506.246874	-0.791814	0.10108697	61.377254	4.71E-15	1.01E-13
WHL22.5674	94.5010931	-0.7919593	0.23290358	11.5575238	0.00067476	0.00388448
WHL22.1561	402.861795	-0.7920771	0.11584202	46.7023186	8.26E-12	1.37E-10
WHL22.4508	69.5147413	-0.7922668	0.2765494	8.16984299	0.00425926	0.01971805
WHL22.2719	3051.85809	-0.7923018	0.04288539	341.102236	3.67E-76	3.91E-74
WHL22.5411	400.681146	-0.7928234	0.11522591	47.3154957	6.04E-12	1.01E-10
WHL22.5980	55.2115317	-0.794193	0.30058709	6.9857709	0.00821603	0.03506354
WHL22.7380	142.993274	-0.7945353	0.19286188	16.9397686	3.86E-05	0.00028536
WHL22.3931	54.1334271	-0.794897	0.30500766	6.79196381	0.00915691	0.03834098

WHL22.6082	1528.85622	-0.7949813	0.05911169	180.877998	3.12E-41	1.84E-39
WHL22.2394	139.804049	-0.7957136	0.19142972	17.2756844	3.23E-05	0.00024301
WHL22.1640	54.1897194	-0.7960252	0.30683871	6.71953752	0.00953624	0.0396241
WHL22.1196	216.306954	-0.7969255	0.15621571	25.9974489	3.42E-07	3.43E-06
WHL22.5761	212.388816	-0.7982382	0.15465412	26.6543476	2.43E-07	2.49E-06
WHL22.5390	200.114181	-0.7984567	0.16116264	24.5336425	7.30E-07	7.03E-06
WHL22.2609	405.315635	-0.7991126	0.11147533	51.4419447	7.37E-13	1.34E-11
WHL22.1670	228.113402	-0.7992751	0.15475407	26.6146399	2.48E-07	2.54E-06
WHL22.6971	76.392721	-0.8001983	0.26698266	8.92575335	0.00281177	0.01379722
WHL22.5385	429.042157	-0.8002164	0.10900811	53.9300997	2.08E-13	4.00E-12
WHL22.5279	52.8050346	-0.8010963	0.31319689	6.52068315	0.0106627	0.04352167
WHL22.5506	972.686954	-0.8014217	0.07270282	121.598238	2.83E-28	1.11E-26
WHL22.7395	93.1604752	-0.8028899	0.23724747	11.4251158	0.00072458	0.00414691
WHL22.7039	6998.61571	-0.8044199	0.03040957	698.008402	8.11E-154	2.48E-151
WHL22.6281	107.506749	-0.8047611	0.2158023	13.920173	0.00019074	0.00124892
WHL22.4674	121.38595	-0.8053464	0.2027494	15.7961877	7.05E-05	0.00049764
WHL22.2159	68.7705782	-0.8061356	0.27982817	8.25496184	0.00406408	0.01896397
WHL22.5817	150.17329	-0.8064081	0.18233503	19.5833445	9.63E-06	7.95E-05
WHL22.2213	192.26469	-0.8071678	0.16210951	24.8103625	6.33E-07	6.11E-06
WHL22.4892	83.7010297	-0.8102548	0.25058004	10.4233506	0.00124432	0.00674045
WHL22.3259	105.310517	-0.8114947	0.21756844	13.9282227	0.00018993	0.00124524
WHL22.7525	86.977562	-0.813307	0.23923373	11.5719689	0.00066953	0.00385593
WHL22.7060	84.535484	-0.8133577	0.24497652	11.0211987	0.00090076	0.00504315
WHL22.4352	252.83303	-0.8143609	0.1440282	31.9530567	1.58E-08	1.88E-07
WHL22.7221	427.813699	-0.8154878	0.11262894	52.3757374	4.58E-13	8.52E-12
WHL22.4623	1042.16094	-0.816186	0.07030315	134.879109	3.51E-31	1.52E-29
WHL22.6524	348.831732	-0.8168638	0.12041187	46.0662589	1.14E-11	1.85E-10
WHL22.7705	116.208969	-0.8188354	0.21522774	14.4243012	0.00014591	0.00097626
WHL22.1091	82.7862311	-0.8196404	0.24781472	10.9354691	0.00094341	0.00525786
WHL22.1539	435.877963	-0.8196813	0.10841369	57.2009418	3.93E-14	8.02E-13
WHL22.3125	212.767694	-0.8205133	0.16011842	26.2067865	3.07E-07	3.10E-06
WHL22.7547	67.3841722	-0.8211449	0.27278451	9.06686543	0.00260283	0.01288251
WHL22.3353	116.415708	-0.8218011	0.20825226	15.5811015	7.90E-05	0.00055412
WHL22.6424	228.451843	-0.8222675	0.14829136	30.781416	2.89E-08	3.30E-07
WHL22.7720	407.621772	-0.8227829	0.1159751	50.2650933	1.34E-12	2.39E-11
WHL22.1670	64.1692136	-0.8239868	0.2878286	8.15987457	0.00428273	0.01982047
WHL22.5810	163.896545	-0.8249672	0.17950953	21.091935	4.38E-06	3.81E-05
WHL22.6290	263.154845	-0.8280411	0.13820145	35.9416009	2.03E-09	2.66E-08
WHL22.5686	93.9526886	-0.8285082	0.23579048	12.3203884	0.00044804	0.00270333
WHL22.4922	302.817585	-0.8286768	0.12902661	41.2936183	1.31E-10	1.91E-09
WHL22.1322	98.8445522	-0.8287512	0.2347499	12.4072884	0.00042766	0.00258996
WHL22.3688	542.794132	-0.8292935	0.09830302	71.1802624	3.26E-17	7.88E-16

WHL22.2454	173.752918	-0.8314107	0.17097653	23.6604971	1.15E-06	1.08E-05
WHL22.2913	187.253286	-0.8315471	0.16833134	24.3719709	7.94E-07	7.59E-06
WHL22.5034	1434.50257	-0.8334662	0.06120913	185.413326	3.19E-42	1.95E-40
WHL22.3487	91.8553757	-0.8335541	0.23795979	12.2495951	0.00046536	0.00279063
WHL22.4525	464.604228	-0.8340512	0.10529153	62.7850346	2.31E-15	5.04E-14
WHL22.2276	140.676469	-0.8342876	0.19850063	17.5879559	2.74E-05	0.0002092
WHL22.1438	610.094794	-0.8344679	0.0912673	83.6814182	5.81E-20	1.61E-18
WHL22.2218	145.583959	-0.8344814	0.1967349	17.8969505	2.33E-05	0.00018122
WHL22.3376	172.105274	-0.8355517	0.17584032	22.5431363	2.05E-06	1.87E-05
WHL22.5627	5947.1599	-0.8363631	0.032405	664.689406	1.43E-146	4.19E-144
WHL22.6154	73.2663216	-0.8365582	0.26154611	10.2394433	0.00137469	0.00736782
WHL22.2252	219.092548	-0.837011	0.15144515	30.5816115	3.20E-08	3.63E-07
WHL22.4147	49.7608936	-0.8371552	0.32048902	6.81682006	0.00903032	0.03794079
WHL22.5365	322.542176	-0.8374088	0.12502659	44.9127133	2.06E-11	3.24E-10
WHL22.5696	255.571892	-0.8381467	0.1409539	35.3894491	2.70E-09	3.49E-08
WHL22.3315	266.096276	-0.8408484	0.13746978	37.4586792	9.34E-10	1.25E-08
WHL22.3357	120.172063	-0.8412667	0.20465484	16.9134961	3.91E-05	0.00028918
WHL22.3947	1086.87269	-0.842622	0.06957526	146.726166	9.01E-34	4.29E-32
WHL22.3561	725.882965	-0.844312	0.08382195	101.560215	6.93E-24	2.28E-22
WHL22.3468	261.047221	-0.8443322	0.14675688	33.0087905	9.17E-09	1.12E-07
WHL22.1124	154.023508	-0.846052	0.18749798	20.3044089	6.60E-06	5.59E-05
WHL22.2634	179.535269	-0.84638	0.16704778	25.7056831	3.98E-07	3.95E-06
WHL22.4984	48.8778937	-0.8467242	0.32106513	6.95561054	0.00835568	0.03554371
WHL22.6053	1828.19787	-0.8469482	0.05457194	240.818802	2.61E-54	2.15E-52
WHL22.6047	564.721638	-0.8484096	0.09561874	78.7779248	6.95E-19	1.83E-17
WHL22.1887	74.3593946	-0.8485088	0.26425216	10.2884003	0.00133869	0.00719589
WHL22.2653	216.263054	-0.8502286	0.15321657	30.8194284	2.83E-08	3.25E-07
WHL22.9963	96.7829239	-0.850531	0.22913667	13.7807602	0.00020543	0.00133734
WHL22.7556	47.9076292	-0.8516991	0.32567009	6.83356428	0.00894606	0.03765141
WHL22.3097	45.2039499	-0.852496	0.33584606	6.43478922	0.01119064	0.04544361
WHL22.6444	276.893247	-0.8529385	0.13601415	39.3482066	3.55E-10	4.94E-09
WHL22.4970	298.692236	-0.8533841	0.13589763	39.3607645	3.52E-10	4.92E-09
WHL22.2863	54.6180843	-0.8537614	0.32168084	6.96194954	0.00832613	0.03544353
WHL22.6110	634.47382	-0.8547299	0.19231326	19.3850605	1.07E-05	8.74E-05
WHL22.7069	582.920742	-0.8550381	0.09573179	79.7546956	4.24E-19	1.13E-17
WHL22.4718	873.262896	-0.8553471	0.0776531	121.368129	3.17E-28	1.24E-26
WHL22.9168	45.9539148	-0.8566144	0.3326192	6.6263777	0.01004794	0.04136935
WHL22.4984	52.308185	-0.8572064	0.31171817	7.55582086	0.00598165	0.02672267
WHL22.6352	45.4993478	-0.8597708	0.3360208	6.53307922	0.01058865	0.04333465
WHL22.1437	87.8231607	-0.8603198	0.24934834	11.837179	0.0005806	0.00338355
WHL22.7471	68.3025543	-0.8605189	0.28420963	9.09483739	0.00256332	0.01273419
WHL22.7612	895.570225	-0.8605712	0.07802068	121.603438	2.82E-28	1.11E-26

WHL22.4852	301.682401	-0.8612257	0.1306056	43.5047988	4.23E-11	6.40E-10
WHL22.2709	87.6295826	-0.8626408	0.24747102	12.0998605	0.00050426	0.00299211
WHL22.2869	145.80552	-0.8634508	0.19517824	19.4860854	1.01E-05	8.32E-05
WHL22.4229	115.703977	-0.8645366	0.21135621	16.7224217	4.33E-05	0.00031702
WHL22.6125	494.106423	-0.8651445	0.10535522	67.3595012	2.26E-16	5.17E-15
WHL22.3770	47.7942839	-0.8657784	0.3334204	6.71115477	0.00958117	0.03976577
WHL22.2592	172.974437	-0.8663983	0.1705619	25.8367919	3.72E-07	3.71E-06
WHL22.5654	316.138414	-0.8670585	0.12667772	46.8993815	7.47E-12	1.24E-10
WHL22.1462	148.131547	-0.8670802	0.18421889	22.1816189	2.48E-06	2.24E-05
WHL22.6375	65.7113893	-0.8692312	0.28215421	9.46278578	0.00209682	0.01067686
WHL22.7486	93.3488713	-0.870898	0.23205891	14.1006462	0.00017328	0.00114432
WHL22.4775	349.325615	-0.8716416	0.12270723	50.4547771	1.22E-12	2.18E-11
WHL22.4727	580.45965	-0.8718498	0.09390894	86.2777351	1.56E-20	4.47E-19
WHL22.2862	5715.18715	-0.8723125	0.03261103	714.156047	2.50E-157	7.97E-155
WHL22.5442	42.836647	-0.872647	0.34560091	6.3646103	0.01164187	0.04706764
WHL22.4350	4766.35124	-0.8760895	0.03489338	629.660876	5.92E-139	1.47E-136
WHL22.2095	61.1943803	-0.8765594	0.29284106	8.92867687	0.00280728	0.01378749
WHL22.4704	58.8959742	-0.8788516	0.29177231	9.08250109	0.00258067	0.01280738
WHL22.6170	336.718816	-0.8793416	0.12263438	51.4792163	7.24E-13	1.32E-11
WHL22.6192	383.755221	-0.880511	0.11761319	56.0361312	7.12E-14	1.41E-12
WHL22.7238	117.221347	-0.8807717	0.20898724	17.765481	2.50E-05	0.00019235
WHL22.5634	469.525643	-0.8813663	0.10440049	71.340245	3.01E-17	7.33E-16
WHL22.3976	42.50236	-0.8829339	0.35041253	6.32970653	0.0118732	0.04788421
WHL22.5239	84.3190037	-0.8836735	0.2459018	12.9139674	0.00032614	0.00202047
WHL22.2827	156.995602	-0.8837767	0.17889799	24.43906	7.67E-07	7.36E-06
WHL22.8507	75.6469938	-0.8839156	0.26029787	11.5246783	0.00068678	0.00394907
WHL22.7565	262.873293	-0.8839645	0.13870413	40.6664585	1.81E-10	2.59E-09
WHL22.6448	257.476766	-0.884276	0.14292102	38.2707641	6.16E-10	8.42E-09
WHL22.5181	864.797247	-0.8854938	0.08232025	115.463852	6.23E-27	2.34E-25
WHL22.4476	3715.26117	-0.8858968	0.03943539	504.078344	1.23E-111	2.23E-109
WHL22.7711	82.5081004	-0.8868636	0.24780144	12.8185753	0.00034319	0.00212041
WHL22.6207	86.5191127	-0.8891057	0.2427613	13.4164299	0.00024943	0.00159271
WHL22.3854	107.175652	-0.8904646	0.21646268	16.9497229	3.84E-05	0.00028415
WHL22.4849	200.711967	-0.8937267	0.16005158	31.1986873	2.33E-08	2.69E-07
WHL22.3489	61.6635228	-0.8956709	0.28770415	9.69131531	0.00185141	0.00956996
WHL22.6725	42.8798504	-0.8973236	0.35614537	6.28297824	0.01219031	0.04890782
WHL22.7526	88.8324138	-0.897376	0.24187037	13.7540811	0.00020837	0.00135467
WHL22.2378	3134.7142	-0.8977862	0.04200758	456.606848	2.63E-101	4.02E-99
WHL22.4009	75.4277805	-0.8993503	0.25780947	12.1870859	0.00048121	0.00287398
WHL22.5936	307.865193	-0.9020789	0.1336721	45.4667207	1.55E-11	2.48E-10
WHL22.3931	55.3666899	-0.9021178	0.30707542	8.60324215	0.00335565	0.01605114
WHL22.4031	206.49432	-0.902718	0.17078199	27.7460278	1.38E-07	1.46E-06

WHL22.2741	73.9652252	-0.9028126	0.26906783	11.2079216	0.00081449	0.00460582
WHL22.1464	200.046917	-0.9035103	0.16214847	31.0366827	2.53E-08	2.92E-07
WHL22.1983	110.738939	-0.9046419	0.21465963	17.7704397	2.49E-05	0.00019195
WHL22.4543	96.7373276	-0.9046718	0.23044903	15.4096829	8.65E-05	0.00060412
WHL22.4989	363.308689	-0.9048911	0.11911795	57.7564775	2.97E-14	6.09E-13
WHL22.6069	53.4085456	-0.904915	0.30880914	8.58304593	0.00339307	0.01619848
WHL22.4694	2478.09958	-0.905071	0.04694848	371.599205	8.39E-83	1.01E-80
WHL22.3983	195.299643	-0.9056736	0.16130587	31.5588714	1.93E-08	2.27E-07
WHL22.4989	481.706148	-0.9062348	0.10621545	72.7425372	1.48E-17	3.66E-16
WHL22.3578	44.3051446	-0.9065183	0.3394143	7.1325546	0.00756968	0.03272758
WHL22.6147	1114.94237	-0.9075583	0.0690873	172.613923	1.99E-39	1.09E-37
WHL22.7503	265.387227	-0.9083498	0.14248997	40.5952361	1.87E-10	2.68E-09
WHL22.6787	298.534794	-0.9101335	0.13091141	48.3833057	3.51E-12	6.01E-11
WHL22.1395	75.9260857	-0.911003	0.2571256	12.5726764	0.00039143	0.00238529
WHL22.5347	92.0763863	-0.9113435	0.23476189	15.0810733	0.00010299	0.00070749
WHL22.5353	754.668397	-0.9128635	0.08384326	118.574666	1.30E-27	4.97E-26
WHL22.3548	105.504909	-0.9138712	0.21976148	17.3039221	3.19E-05	0.00023979
WHL22.6584	166.332485	-0.9147521	0.18288624	24.925899	5.96E-07	5.78E-06
WHL22.7363	71.8191429	-0.9148852	0.26459769	11.971506	0.0005402	0.00317588
WHL22.3951	194.726178	-0.9167281	0.16154941	32.2384423	1.36E-08	1.63E-07
WHL22.5481	273.546717	-0.9182949	0.13604935	45.6237783	1.43E-11	2.30E-10
WHL22.6449	158.407303	-0.9187877	0.17824795	26.6122334	2.49E-07	2.54E-06
WHL22.3077	2722.36268	-0.9191266	0.04485006	419.926409	2.53E-93	3.47E-91
WHL22.4131	229.599334	-0.9223854	0.14942141	38.1410242	6.58E-10	8.95E-09
WHL22.7007	442.15868	-0.9225288	0.1116495	68.1901619	1.48E-16	3.45E-15
WHL22.1983	4396.40643	-0.9237759	0.03620873	650.189	2.03E-143	5.53E-141
WHL22.1791	152.683811	-0.9238992	0.184308	25.1284009	5.36E-07	5.25E-06
WHL22.7058	286.849554	-0.9241352	0.13705189	45.429983	1.58E-11	2.52E-10
WHL22.2015	125.588833	-0.924204	0.20748112	19.7949831	8.62E-06	7.19E-05
WHL22.7524	73.9916718	-0.9244883	0.26223625	12.435165	0.00042133	0.00255475
WHL22.1182	116.46731	-0.925135	0.20901177	19.6113115	9.49E-06	7.84E-05
WHL22.4066	82.0242877	-0.9262595	0.24754843	14.0250975	0.00018039	0.00118801
WHL22.3743	179.476618	-0.9271453	0.1685585	30.2935475	3.71E-08	4.18E-07
WHL22.4350	357.409716	-0.9275739	0.1193978	60.4336678	7.61E-15	1.60E-13
WHL22.3534	208.105454	-0.9341104	0.15732308	35.2811805	2.85E-09	3.67E-08
WHL22.4335	180.983524	-0.9348199	0.17506159	28.4257712	9.74E-08	1.04E-06
WHL22.3836	81.4440022	-0.935811	0.24842392	14.2140098	0.00016315	0.00108227
WHL22.6294	1209.40564	-0.9361681	0.06594629	201.66619	9.04E-46	6.23E-44
WHL22.1004	55.2800722	-0.9365339	0.30202358	9.62729509	0.00191707	0.00985729
WHL22.6110	49.9870761	-0.9391333	0.31707485	8.78530732	0.00303666	0.01475612
WHL22.4145	159.757717	-0.9421786	0.1806389	27.2059335	1.83E-07	1.91E-06
WHL22.6539	102.235516	-0.9422253	0.22942244	16.8242871	4.10E-05	0.00030173

WHL22.5900	167.410431	-0.9449912	0.17560163	28.9775901	7.32E-08	7.99E-07
WHL22.1056	70.5817176	-0.945445	0.27223677	12.0374248	0.00052143	0.00307966
WHL22.6437	263.884375	-0.9469483	0.1388895	46.5512875	8.93E-12	1.46E-10
WHL22.5920	75.0840126	-0.9491146	0.25920565	13.4289999	0.00024776	0.00158345
WHL22.2784	207.845129	-0.9507073	0.16468951	33.2122735	8.26E-09	1.02E-07
WHL22.4750	103.254345	-0.951023	0.22365646	18.0794479	2.12E-05	0.00016562
WHL22.5363	54.9293887	-0.9514076	0.30271353	9.89413446	0.00165806	0.00868989
WHL22.1910	4108.68455	-0.9519087	0.03887214	598.12917	4.27E-132	9.50E-130
WHL22.6357	284.743877	-0.9522965	0.13420626	50.4089224	1.25E-12	2.23E-11
WHL22.6542	167.03494	-0.9552892	0.18043884	27.9672577	1.23E-07	1.31E-06
WHL22.2262	158.696088	-0.9574853	0.18621927	26.3680735	2.82E-07	2.87E-06
WHL22.5573	3926.10389	-0.9575494	0.03816347	628.964095	8.40E-139	2.05E-136
WHL22.2897	77.5188716	-0.964006	0.26328255	13.3608515	0.00025693	0.00163492
WHL22.4149	184.655242	-0.9640704	0.1666311	33.5092666	7.09E-09	8.78E-08
WHL22.3788	114.31533	-0.96544	0.21782507	19.5842199	9.63E-06	7.95E-05
WHL22.7007	1602.32574	-0.9708943	0.05782768	282.007846	2.74E-63	2.60E-61
WHL22.5964	5153.29358	-0.9713494	0.03383988	822.667106	6.37E-181	2.23E-178
WHL22.6944	652.891639	-0.9743949	0.08891664	120.248546	5.58E-28	2.16E-26
WHL22.7721	41.6827035	-0.9749325	0.34856693	7.83559161	0.00512274	0.02326838
WHL22.4440	762.249217	-0.9760335	0.08589651	128.957941	6.93E-30	2.86E-28
WHL22.3394	96.369947	-0.9780303	0.2344159	17.3788355	3.06E-05	0.00023136
WHL22.5689	79.2599011	-0.979777	0.25480502	14.7900766	0.00012017	0.0008182
WHL22.3897	139.286375	-0.9807044	0.19147866	26.2671128	2.97E-07	3.01E-06
WHL22.2585	46.3837324	-0.9814181	0.3381471	8.38656896	0.00378004	0.01780839
WHL22.5595	173.819807	-0.9815256	0.17329726	32.0854978	1.48E-08	1.76E-07
WHL22.1335	155.278345	-0.9822971	0.18454636	28.3133251	1.03E-07	1.10E-06
WHL22.2421	79.2097814	-0.9826527	0.25804766	14.4740585	0.0001421	0.00095447
WHL22.6587	281.821752	-0.9832312	0.1366862	51.7588916	6.28E-13	1.15E-11
WHL22.4671	887.092388	-0.9847533	0.07701214	163.650287	1.80E-37	9.59E-36
WHL22.6006	243.342552	-0.9887893	0.14651091	45.5718029	1.47E-11	2.36E-10
WHL22.4787	741.194407	-0.9888293	0.08559644	133.434577	7.26E-31	3.12E-29
WHL22.5335	180.822953	-0.9914672	0.17089494	33.6521752	6.59E-09	8.21E-08
WHL22.1811	68.4571904	-0.9916873	0.27294482	13.212842	0.00027804	0.00175326
WHL22.5790	35.82947	-0.9918318	0.37830195	6.86806453	0.00877496	0.03703479
WHL22.4764	147.773722	-0.9934759	0.1857511	28.6518701	8.66E-08	9.35E-07
WHL22.3704	249.011696	-0.9943528	0.15002723	43.8142766	3.61E-11	5.54E-10
WHL22.1865	71.8867492	-0.9948247	0.27408013	13.1150367	0.00029294	0.00183773
WHL22.6541	3404.28689	-0.9984711	0.04075604	599.797343	1.85E-132	4.18E-130
WHL22.4618	202.193187	-0.9986718	0.16026888	38.8573504	4.56E-10	6.32E-09
WHL22.2615	387.449503	-0.9991807	0.11618482	74.0241226	7.72E-18	1.95E-16
WHL22.4013	2273.85213	-1.0004572	0.04974617	404.215478	6.66E-90	8.65E-88
WHL22.4788	97.9857875	-1.0005738	0.23660139	17.8049784	2.45E-05	0.00018886

WHL22.7282	3514.37264	-1.0006011	0.04068584	604.047773	2.20E-133	5.14E-131
WHL22.5061	297.364784	-1.0010502	0.13354776	56.1952456	6.56E-14	1.30E-12
WHL22.5518	37.9356659	-1.0019373	0.36638721	7.48048873	0.00623711	0.02770373
WHL22.2221	41.6532756	-1.0024243	0.34986391	8.21660593	0.00415088	0.0192954
WHL22.3654	47.5627553	-1.0046316	0.32876371	9.33644551	0.00224641	0.01134409
WHL22.1492	94.9434436	-1.0051539	0.23103908	18.9643405	1.33E-05	0.00010748
WHL22.3479	153.485443	-1.0057383	0.18651557	29.0480615	7.06E-08	7.72E-07
WHL22.2945	531.93006	-1.0073927	0.09829739	105.20174	1.10E-24	3.74E-23
WHL22.4908	76.7646875	-1.0083783	0.26111401	14.8976216	0.00011351	0.00077609
WHL22.4554	1396.80016	-1.0094322	0.0651685	239.42176	5.26E-54	4.29E-52
WHL22.6971	145.111927	-1.0099811	0.18702471	29.2193077	6.46E-08	7.09E-07
WHL22.2396	473.30306	-1.0112575	0.1049208	93.0047512	5.22E-22	1.61E-20
WHL22.1615	420.813858	-1.0118705	0.11290229	80.3303075	3.17E-19	8.53E-18
WHL22.6859	140.976024	-1.0129776	0.18990173	28.507649	9.33E-08	1.00E-06
WHL22.7219	57.1410102	-1.0144084	0.29827308	11.5839892	0.00066522	0.0038341
WHL22.3577	51.8240586	-1.014932	0.31347765	10.4933642	0.00119804	0.00651379
WHL22.6580	573.604228	-1.0162675	0.09478022	115.158204	7.27E-27	2.71E-25
WHL22.3278	86.5975922	-1.0207158	0.24592668	17.2187145	3.33E-05	0.0002499
WHL22.1547	92.4687998	-1.0207371	0.24108829	17.8855443	2.35E-05	0.00018222
WHL22.4990	59.5083627	-1.0215847	0.29532132	11.9579473	0.00054415	0.00319779
WHL22.6269	54.6924831	-1.0243479	0.30424512	11.3579675	0.00075125	0.00428452
WHL22.7551	31.1094724	-1.0250027	0.40455303	6.43484488	0.01119029	0.04544361
WHL22.7061	62.0013551	-1.0265474	0.28728227	12.7802625	0.0003503	0.00216247
WHL22.7892	118.691128	-1.0270127	0.20949741	24.042492	9.42E-07	8.94E-06
WHL22.5430	64.4480839	-1.0284927	0.28214397	13.3029938	0.00026498	0.00168177
WHL22.1420	145.626974	-1.0287656	0.1881746	29.9270477	4.49E-08	4.99E-07
WHL22.1503	86.4517914	-1.0289016	0.24324802	17.9185648	2.31E-05	0.00017927
WHL22.6936	511.831232	-1.0296623	0.10086251	104.352582	1.69E-24	5.69E-23
WHL22.8036	106.31014	-1.030339	0.2202146	21.9173307	2.85E-06	2.55E-05
WHL22.4969	1339.89392	-1.0316019	0.06300459	268.332347	2.62E-60	2.42E-58
WHL22.3552	282.949336	-1.0344052	0.14273478	52.3380808	4.67E-13	8.67E-12
WHL22.1156	52.7146453	-1.0356383	0.31028273	11.16662	0.00083282	0.00469994
WHL22.4618	279.739399	-1.0375795	0.13826873	56.3229052	6.15E-14	1.23E-12
WHL22.6877	70.9740599	-1.0379012	0.2679567	15.0284373	0.0001059	0.00072682
WHL22.1011	48.557492	-1.0384904	0.32539302	10.1868738	0.00141444	0.00754779
WHL22.1138	31.9629546	-1.0390023	0.39793271	6.82893689	0.00896926	0.03772745
WHL22.1954	103.815854	-1.0390269	0.2236834	21.5872639	3.38E-06	2.99E-05
WHL22.3379	54.752875	-1.0391848	0.30932604	11.2719325	0.00078688	0.00447207
WHL22.2164	51.3378148	-1.0394133	0.34143062	9.07399823	0.0025927	0.01284535
WHL22.2198	32.4263662	-1.0401627	0.40393001	6.60614488	0.01016274	0.04180137
WHL22.5033	5327.5515	-1.0402759	0.03528858	865.419351	3.23E-190	1.22E-187
WHL22.7666	44.9338065	-1.0411721	0.34014753	9.3559265	0.00222266	0.01124537

WHL22.6221	30.6587085	-1.0418221	0.40817779	6.5215216	0.01065768	0.04352009
WHL22.6660	2542.23984	-1.0445678	0.04859177	461.133565	2.72E-102	4.29E-100
WHL22.4513	46.2372732	-1.0453575	0.33416958	9.78776925	0.00175676	0.00913542
WHL22.6835	180.493962	-1.0467563	0.17135417	37.3206843	1.00E-09	1.34E-08
WHL22.4735	42.0569621	-1.0473756	0.36873322	7.94200495	0.00483003	0.02213905
WHL22.7274	706.351057	-1.0484104	0.08615738	148.26846	4.14E-34	1.99E-32
WHL22.3359	312.984448	-1.0495869	0.1326478	62.5508496	2.60E-15	5.65E-14
WHL22.9714	176.187626	-1.0506751	0.17167079	37.5077393	9.11E-10	1.22E-08
WHL22.3578	70.7768648	-1.0519452	0.2699876	15.193061	9.71E-05	0.00067006
WHL22.4066	40.6909584	-1.0535146	0.36325574	8.3543409	0.00384767	0.01810959
WHL22.6432	188.828144	-1.0537931	0.17292192	37.0119039	1.17E-09	1.57E-08
WHL22.6718	644.234481	-1.0544279	0.08967615	138.497283	5.67E-32	2.57E-30
WHL22.3492	1025.48921	-1.0569596	0.07498908	198.374934	4.73E-45	3.15E-43
WHL22.1464	41.8049051	-1.0579924	0.35262218	9.00122713	0.00269798	0.0132952
WHL22.6108	223.909225	-1.059461	0.156199	45.952023	1.21E-11	1.96E-10
WHL22.1713	48.12728	-1.0621965	0.32997869	10.3487793	0.0012956	0.00698474
WHL22.7474	41.7062966	-1.0626931	0.38066818	7.59374216	0.00585712	0.0262222
WHL22.6469	238.158103	-1.0661757	0.1467342	52.9064125	3.50E-13	6.59E-12
WHL22.6746	114.196318	-1.0685853	0.21358477	25.0480093	5.59E-07	5.45E-06
WHL22.3396	381.946943	-1.0690219	0.11916621	80.46763	2.96E-19	8.00E-18
WHL22.9704	62.5885416	-1.0690552	0.2861056	13.9819225	0.00018458	0.00121234
WHL22.3950	143.683954	-1.0695692	0.19545964	29.8693051	4.62E-08	5.12E-07
WHL22.5914	523.041245	-1.071535	0.09995207	115.108703	7.45E-27	2.77E-25
WHL22.5347	160.029871	-1.0768721	0.18486561	33.8756248	5.88E-09	7.35E-08
WHL22.9238	55.1780894	-1.0807067	0.30686505	12.4006231	0.00042919	0.00259815
WHL22.2608	437.092439	-1.0813069	0.10905559	98.4834805	3.28E-23	1.06E-21
WHL22.2585	59.327868	-1.0843622	0.301091	12.9294076	0.00032346	0.00200729
WHL22.1713	90.2114395	-1.0888194	0.23799092	20.9820734	4.64E-06	4.01E-05
WHL22.6984	205.820506	-1.0904911	0.16144461	45.6212669	1.43E-11	2.30E-10
WHL22.3241	631.938611	-1.0960773	0.09184195	142.577331	7.27E-33	3.38E-31
WHL22.2996	325.094299	-1.0979886	0.12810132	73.5148066	9.99E-18	2.50E-16
WHL22.5663	910.375431	-1.0985471	0.07744969	201.259529	1.11E-45	7.61E-44
WHL22.9366	26.6941911	-1.0991734	0.43780265	6.32090211	0.01193229	0.04808186
WHL22.2615	61.8878697	-1.1015357	0.28825119	14.6257299	0.00013111	0.00088902
WHL22.3495	523.990534	-1.1043827	0.10140066	118.689231	1.22E-27	4.72E-26
WHL22.4916	5663.65458	-1.1055532	0.03305935	1115.29744	1.56E-244	9.18E-242
WHL22.1764	253.409685	-1.1058849	0.14346099	59.5227287	1.21E-14	2.52E-13
WHL22.1190	60.7987342	-1.105959	0.29057641	14.5129325	0.0001392	0.00093694
WHL22.6970	98.9163433	-1.1067934	0.22722967	23.7869659	1.08E-06	1.01E-05
WHL22.2831	3464.51747	-1.1099078	0.04127605	721.949276	5.04E-159	1.65E-156
WHL22.3269	1620.2492	-1.1100192	0.05824154	363.375885	5.18E-81	6.04E-79
WHL22.6216	4645.99211	-1.1130913	0.03651955	926.401669	1.79E-203	7.50E-201

WHL22.2364	32.6389742	-1.1147695	0.40565552	7.50042515	0.00616844	0.02743829
WHL22.3744	46.4441617	-1.1148515	0.34741875	10.1890442	0.00141278	0.00754165
WHL22.3154	95.4024645	-1.1160103	0.2319638	23.2010542	1.46E-06	1.35E-05
WHL22.4534	74.8410654	-1.1162136	0.26456907	17.8043205	2.45E-05	0.00018886
WHL22.1071	421.027734	-1.1165101	0.11179093	99.9060922	1.60E-23	5.22E-22
WHL22.6075	236.407334	-1.1166906	0.14946644	55.8804926	7.70E-14	1.53E-12
WHL22.5364	88.1525557	-1.1173635	0.24385429	21.0140868	4.56E-06	3.95E-05
WHL22.4664	893.082725	-1.1203992	0.0780411	206.236078	9.10E-47	6.42E-45
WHL22.1071	64.8635494	-1.1247556	0.28224173	15.9060854	6.66E-05	0.00047139
WHL22.4281	263.874596	-1.1266326	0.14637411	59.114293	1.49E-14	3.09E-13
WHL22.7243	80.5866808	-1.126665	0.25558896	19.4399849	1.04E-05	8.50E-05
WHL22.5669	204.75404	-1.1271916	0.16449475	46.8815815	7.54E-12	1.25E-10
WHL22.1686	129.143942	-1.128182	0.19939404	32.0974629	1.47E-08	1.75E-07
WHL22.5564	73.4231332	-1.1290369	0.26573388	18.0823855	2.12E-05	0.00016545
WHL22.7749	947.397778	-1.1295654	0.07776578	210.75925	9.38E-48	6.78E-46
WHL22.4534	42.3823466	-1.1296535	0.3652978	9.44062098	0.00212232	0.01078801
WHL22.5118	257.318111	-1.1310185	0.14404936	61.6903765	4.02E-15	8.66E-14
WHL22.3976	9783.35573	-1.1328166	0.0264683	1822.34414	0	0
WHL22.5954	196.799564	-1.1336376	0.16472561	47.3874613	5.83E-12	9.80E-11
WHL22.6160	115.818173	-1.1337784	0.2274073	24.633527	6.93E-07	6.70E-06
WHL22.5977	152.799922	-1.133887	0.18429782	37.9285004	7.34E-10	9.94E-09
WHL22.6563	64.6418021	-1.1344796	0.2829047	16.1084599	5.98E-05	0.00042755
WHL22.7381	122.182074	-1.1346816	0.20497	30.7321511	2.96E-08	3.38E-07
WHL22.5015	38.555241	-1.1389688	0.36773056	9.59094171	0.0019554	0.01002978
WHL22.7159	40.5197333	-1.1417175	0.36074703	9.99580889	0.00156897	0.0082791
WHL22.9230	38.1145787	-1.1424967	0.36692401	9.71754973	0.00182517	0.00944429
WHL22.4989	33.622643	-1.144375	0.41563888	7.41439684	0.0064704	0.02863596
WHL22.7588	46.7173872	-1.1444083	0.34543023	10.8751382	0.00097464	0.00540116
WHL22.7646	29.6421756	-1.1455921	0.41615968	7.59872351	0.00584096	0.02616581
WHL22.2303	254.160105	-1.145651	0.14650938	61.1334515	5.33E-15	1.13E-13
WHL22.1050	62.0413951	-1.146153	0.29293062	15.2860025	9.24E-05	0.00064042
WHL22.7562	366.193762	-1.1467517	0.12333223	86.3866221	1.48E-20	4.24E-19
WHL22.5791	56.280079	-1.1471123	0.30330699	14.3261927	0.00015371	0.00102474
WHL22.5927	30.6500998	-1.1476779	0.41031183	7.83555345	0.00512285	0.02326838
WHL22.6068	41.1888959	-1.1480477	0.35373329	10.5591827	0.00115612	0.00630854
WHL22.5772	102.598042	-1.1495612	0.22523082	26.0981342	3.24E-07	3.26E-06
WHL22.6619	31.0459868	-1.1507607	0.41065494	7.84868513	0.00508577	0.02311427
WHL22.5643	31.0184489	-1.1511801	0.41139387	7.83164935	0.00513392	0.02331147
WHL22.4932	548.068446	-1.1525312	0.09805162	138.429237	5.87E-32	2.65E-30
WHL22.4065	65.755058	-1.1526126	0.28683592	16.1082593	5.98E-05	0.00042755
WHL22.3435	42.3164706	-1.1578154	0.37650242	9.27275043	0.00232588	0.01168913
WHL22.5473	45.3433301	-1.1627039	0.34619123	11.2255866	0.00080677	0.00457099

WHL22.7517	326.630235	-1.1629698	0.12822853	82.3458966	1.14E-19	3.13E-18
WHL22.7478	89.3685478	-1.1644982	0.24074193	23.4532262	1.28E-06	1.19E-05
WHL22.7654	1000.41183	-1.1669185	0.07285713	257.016575	7.67E-58	6.70E-56
WHL22.8899	213.558594	-1.167647	0.15573907	56.374189	5.99E-14	1.20E-12
WHL22.7555	237.400464	-1.1714153	0.15387136	57.852654	2.83E-14	5.81E-13
WHL22.4195	96.4245148	-1.1718221	0.23797501	24.2012572	8.68E-07	8.24E-06
WHL22.6925	50.1789639	-1.1720122	0.33031431	12.521452	0.00040231	0.0024465
WHL22.4639	43.3380243	-1.1723114	0.35039672	11.166102	0.00083305	0.00469994
WHL22.5669	614.019316	-1.1724616	0.09312238	158.79824	2.07E-36	1.07E-34
WHL22.7372	36.0531437	-1.1731123	0.38478427	9.26417201	0.0023368	0.01173999
WHL22.4174	432.334277	-1.1758097	0.11445845	105.412204	9.92E-25	3.38E-23
WHL22.3897	23.5776103	-1.1759634	0.46631038	6.37777601	0.01155581	0.04674548
WHL22.3697	39.6649148	-1.1759854	0.37194193	9.9212207	0.00163384	0.00858131
WHL22.6062	61.81371	-1.179386	0.28823295	16.7963354	4.16E-05	0.0003056
WHL22.7526	29.3434554	-1.1798038	0.44738735	6.76973693	0.00927165	0.03865601
WHL22.1166	49.3988204	-1.1820284	0.32554398	13.1955338	0.00028062	0.00176725
WHL22.2585	37.0896738	-1.1827542	0.3865012	9.27991892	0.0023168	0.01164746
WHL22.1088	519.44912	-1.1835934	0.10371746	130.200089	3.70E-30	1.55E-28
WHL22.2120	160.485932	-1.1844178	0.1794319	43.703759	3.82E-11	5.84E-10
WHL22.6448	199.327887	-1.1860983	0.1676082	49.9925569	1.54E-12	2.74E-11
WHL22.6544	39.5797859	-1.1868088	0.37520266	9.9369491	0.00161994	0.00851744
WHL22.5442	275.998979	-1.1873758	0.14139968	70.5116692	4.58E-17	1.10E-15
WHL22.6602	327.589728	-1.1882591	0.13269302	79.9984854	3.75E-19	1.00E-17
WHL22.6538	147.789037	-1.1883443	0.18810593	39.9976907	2.54E-10	3.59E-09
WHL22.7725	23.5521038	-1.1895141	0.46727582	6.49824273	0.01079812	0.04404455
WHL22.4390	85.7354687	-1.1905731	0.24560635	23.5714383	1.20E-06	1.12E-05
WHL22.5920	183.033795	-1.193436	0.16925796	49.8290429	1.68E-12	2.97E-11
WHL22.2872	315.024534	-1.1957545	0.12890191	86.2759092	1.57E-20	4.47E-19
WHL22.7239	35.275819	-1.1973212	0.38666271	9.57480084	0.00197266	0.01011127
WHL22.2452	997.455371	-1.1975921	0.07358947	265.247696	1.23E-59	1.11E-57
WHL22.2232	26.7988996	-1.2065882	0.46333062	6.62987907	0.01002821	0.04132905
WHL22.3324	749.869038	-1.2087927	0.08643795	195.574271	1.93E-44	1.27E-42
WHL22.5949	30.4271299	-1.2112155	0.4195401	8.29783766	0.00396923	0.01856861
WHL22.7562	153.9973	-1.2112161	0.18376641	43.5751767	4.08E-11	6.19E-10
WHL22.1481	54.4089637	-1.2151507	0.31599854	14.7414285	0.00012331	0.0008392
WHL22.6751	400.50727	-1.2169684	0.11667971	108.880629	1.72E-25	6.05E-24
WHL22.2827	42.6220672	-1.2194701	0.348218	12.300337	0.00045288	0.0027258
WHL22.5288	37.7421678	-1.2195049	0.37024728	10.8819289	0.00097107	0.0053875
WHL22.4558	111.771526	-1.2244603	0.21829566	31.5036119	1.99E-08	2.33E-07
WHL22.6751	1875.70482	-1.2245081	0.056803	463.664451	7.66E-103	1.22E-100
WHL22.5923	33.724453	-1.2249886	0.39213073	9.77993092	0.00176427	0.00916891
WHL22.9214	2056.86105	-1.2277097	0.05175204	563.440963	1.50E-124	3.10E-122

WHL22.2232	72.8574064	-1.2281655	0.26680599	21.2572995	4.02E-06	3.50E-05
WHL22.5716	29.3112342	-1.2320549	0.42378779	8.4500898	0.00365025	0.01726901
WHL22.6365	927.607559	-1.2320597	0.07630496	261.201241	9.39E-59	8.41E-57
WHL22.2462	103.221574	-1.2328486	0.2275613	29.3782078	5.95E-08	6.56E-07
WHL22.5537	245.979703	-1.2336339	0.14776921	69.811727	6.52E-17	1.56E-15
WHL22.6416	525.127743	-1.2377242	0.10115093	150.03364	1.70E-34	8.34E-33
WHL22.1323	155.325709	-1.2380044	0.18857839	43.0531092	5.33E-11	8.00E-10
WHL22.2917	45.1004054	-1.2407874	0.34023749	13.3453838	0.00025906	0.00164774
WHL22.2247	34.2410897	-1.2411551	0.41373003	8.81708532	0.00298423	0.01453018
WHL22.4361	164.266376	-1.2420165	0.18847517	43.2230134	4.88E-11	7.36E-10
WHL22.6375	1766.30553	-1.2421991	0.05581641	495.945286	7.25E-110	1.28E-107
WHL22.2927	1551.74597	-1.2437035	0.05986538	431.990566	5.99E-96	8.38E-94
WHL22.1174	90.8695434	-1.2545008	0.24216204	26.8760054	2.17E-07	2.24E-06
WHL22.2595	142.294946	-1.2554365	0.19282695	42.48874	7.11E-11	1.06E-09
WHL22.3110	70.9571438	-1.2569726	0.2706882	21.6406455	3.29E-06	2.91E-05
WHL22.8561	228.592561	-1.2624742	0.15197504	69.2089193	8.86E-17	2.10E-15
WHL22.7526	46.6898759	-1.2633321	0.33386154	14.3716763	0.00015004	0.00100119
WHL22.7145	97.4766057	-1.2671185	0.23929225	27.9600102	1.24E-07	1.31E-06
WHL22.7355	70.4090264	-1.2671602	0.27356184	21.5090458	3.52E-06	3.10E-05
WHL22.5136	45.4533704	-1.2672707	0.33741487	14.1629251	0.00016764	0.00111053
WHL22.6943	429.811644	-1.2682279	0.11162503	129.396742	5.55E-30	2.30E-28
WHL22.5036	134.184654	-1.2686061	0.1975067	41.3966002	1.24E-10	1.81E-09
WHL22.5659	21.9875445	-1.2693974	0.48826923	6.78135813	0.00921148	0.03847069
WHL22.9714	172.207097	-1.2709469	0.17407958	53.5031075	2.58E-13	4.94E-12
WHL22.1481	101.107053	-1.2746515	0.22805154	31.3335101	2.17E-08	2.53E-07
WHL22.3114	960.28516	-1.2748585	0.07663268	276.869411	3.61E-62	3.38E-60
WHL22.6009	114.185695	-1.2757123	0.22467165	32.09416	1.47E-08	1.75E-07
WHL22.6751	290.876881	-1.2779114	0.13898393	84.5252788	3.79E-20	1.07E-18
WHL22.5975	166.481348	-1.2784445	0.1825512	49.0295886	2.52E-12	4.40E-11
WHL22.5558	120.060233	-1.2804939	0.20835822	37.9194998	7.37E-10	9.97E-09
WHL22.6903	65.2171201	-1.2805219	0.29018771	19.4149429	1.05E-05	8.61E-05
WHL22.5964	78.8616429	-1.2816882	0.26199915	23.9357891	9.96E-07	9.41E-06
WHL22.6416	276.972172	-1.2818802	0.14017456	83.771001	5.56E-20	1.55E-18
WHL22.4386	1600.57625	-1.2831057	0.0584132	483.497848	3.70E-107	6.32E-105
WHL22.4521	63.5566355	-1.2866418	0.28931711	19.8151871	8.53E-06	7.12E-05
WHL22.5120	22.366271	-1.2887726	0.48717935	6.99009807	0.00819619	0.0349971
WHL22.3616	473.942976	-1.2907182	0.10573504	149.512913	2.22E-34	1.07E-32
WHL22.4783	152.101521	-1.2925471	0.18807689	47.3209492	6.03E-12	1.01E-10
WHL22.1805	24.1844973	-1.2931604	0.46443618	7.7811609	0.00527939	0.02389805
WHL22.1196	38.7129619	-1.3003223	0.37154528	12.2529624	0.00046452	0.00278788
WHL22.1323	42.9847477	-1.301961	0.3571047	13.2909901	0.00026668	0.00168893
WHL22.7508	50.3390199	-1.3022016	0.3258827	15.982422	6.39E-05	0.00045472

WHL22.3921	32.9537569	-1.3030775	0.41046458	9.99222155	0.00157203	0.00828929
WHL22.3110	41.1613396	-1.3035165	0.36177239	12.9666373	0.00031709	0.00197269
WHL22.1703	53.2792003	-1.3040243	0.31445725	17.2445304	3.29E-05	0.00024678
WHL22.1644	1134.65909	-1.3057302	0.06924324	356.461092	1.66E-79	1.86E-77
WHL22.5933	60.9850585	-1.3068936	0.29858363	19.1458955	1.21E-05	9.84E-05
WHL22.4712	23.9948809	-1.3088734	0.46881408	7.79850696	0.00522894	0.02369163
WHL22.3417	74.4382455	-1.310453	0.26629503	24.2987302	8.25E-07	7.86E-06
WHL22.6353	85.2128466	-1.3105377	0.24837891	27.9477856	1.25E-07	1.32E-06
WHL22.5851	331.99386	-1.3106457	0.12610147	108.435181	2.16E-25	7.52E-24
WHL22.5403	39.5680436	-1.3131189	0.36483237	12.9886427	0.00031339	0.00195268
WHL22.2092	60.8730173	-1.3149826	0.29423252	20.0475624	7.55E-06	6.35E-05
WHL22.2595	34.7358215	-1.3176796	0.39370097	11.2034995	0.00081643	0.00461358
WHL22.7288	22.0503262	-1.3194788	0.48534042	7.42459371	0.00643384	0.02849991
WHL22.6630	593.307492	-1.3230368	0.09610862	189.908355	3.33E-43	2.12E-41
WHL22.3421	50.0055749	-1.3275151	0.32533765	16.6921569	4.40E-05	0.00032172
WHL22.3998	27.2970771	-1.3328024	0.43814694	9.28421358	0.00231137	0.01163213
WHL22.6481	172.205543	-1.3350938	0.17527778	58.2433984	2.32E-14	4.79E-13
WHL22.7187	211.610872	-1.3385996	0.16360773	66.8932526	2.87E-16	6.51E-15
WHL22.1071	117.695228	-1.3415712	0.21205628	40.1806087	2.32E-10	3.29E-09
WHL22.5442	326.971583	-1.3418813	0.12727429	111.614678	4.34E-26	1.56E-24
WHL22.2958	23.7660472	-1.3419602	0.47258631	8.06455562	0.00451395	0.02080529
WHL22.4359	52.1786224	-1.3463534	0.32193385	17.4961665	2.88E-05	0.00021886
WHL22.4712	20.7309141	-1.3466092	0.50696364	7.08650084	0.00776667	0.03345504
WHL22.9517	246.209363	-1.3495357	0.14740561	84.1148602	4.67E-20	1.31E-18
WHL22.3550	21.7181421	-1.3526467	0.5177896	6.63324089	0.0100093	0.0412859
WHL22.7670	535.479232	-1.3541765	0.10084474	180.847443	3.17E-41	1.86E-39
WHL22.5235	19.913152	-1.3600615	0.53650205	6.32607055	0.01189756	0.04795613
WHL22.3202	151.379079	-1.3613716	0.1897898	51.5536353	6.97E-13	1.27E-11
WHL22.6114	26.0335667	-1.3648428	0.45636854	8.92630003	0.00281093	0.01379722
WHL22.7239	152.185398	-1.3653829	0.19240338	50.3528385	1.28E-12	2.29E-11
WHL22.6901	242.019204	-1.3668568	0.15348514	79.2863008	5.37E-19	1.43E-17
WHL22.7536	23.9251242	-1.3670458	0.4723688	8.36910468	0.00381654	0.01797457
WHL22.5391	236.538653	-1.3676144	0.15076219	82.5857054	1.01E-19	2.79E-18
WHL22.5558	502.187201	-1.3702984	0.10323542	176.901444	2.30E-40	1.31E-38
WHL22.5016	184.418486	-1.370528	0.17463419	61.5870691	4.24E-15	9.10E-14
WHL22.6749	36.3209966	-1.3723787	0.38537964	12.7087546	0.00036395	0.00223733
WHL22.1436	19.7514831	-1.3730114	0.53003989	6.6313354	0.01002001	0.04131848
WHL22.6702	143.661877	-1.3797184	0.2009706	47.0024368	7.09E-12	1.18E-10
WHL22.3837	304.681682	-1.381056	0.13579616	103.540843	2.55E-24	8.53E-23
WHL22.5594	31.065372	-1.3833328	0.41633381	11.0429227	0.00089026	0.0049882
WHL22.5025	40.744575	-1.3843074	0.37851337	13.1956082	0.00028061	0.00176725
WHL22.1790	72.5437718	-1.3846784	0.27368214	25.6479503	4.10E-07	4.06E-06

WHL22.6209	94.0197823	-1.3853013	0.24402148	32.1999222	1.39E-08	1.67E-07
WHL22.5558	122.855227	-1.3855017	0.20767474	44.7430479	2.25E-11	3.51E-10
WHL22.6079	717.700105	-1.385545	0.08657462	257.180274	7.07E-58	6.21E-56
WHL22.5558	21.8696024	-1.386956	0.5049176	7.46413507	0.00629403	0.02793962
WHL22.5981	221.339673	-1.3891468	0.16026305	75.1169079	4.44E-18	1.13E-16
WHL22.6542	757.943428	-1.3918368	0.08543939	266.088383	8.08E-60	7.37E-58
WHL22.6383	98.7796303	-1.3927066	0.23120012	36.4745994	1.55E-09	2.04E-08
WHL22.2736	32.4804583	-1.3930834	0.40948442	11.5551711	0.00067561	0.00388787
WHL22.7035	98.0438915	-1.3932858	0.23258946	36.052246	1.92E-09	2.51E-08
WHL22.6902	67.9552528	-1.3951331	0.28054176	24.8279501	6.27E-07	6.06E-06
WHL22.3758	24.2666276	-1.3971328	0.47379579	8.70439587	0.00317444	0.01530401
WHL22.1968	40.5878209	-1.3978976	0.3604838	15.114496	0.00010118	0.00069681
WHL22.5041	78.9317543	-1.4034098	0.26086943	29.0382351	7.10E-08	7.76E-07
WHL22.2282	24.8788857	-1.4044813	0.46239265	9.25710683	0.00234583	0.01177326
WHL22.5328	34.2141144	-1.4048704	0.39388324	12.7681404	0.00035257	0.00217287
WHL22.4816	70.6444684	-1.4090704	0.29515274	22.4722403	2.13E-06	1.93E-05
WHL22.4472	39.835464	-1.4119221	0.39641736	12.3451911	0.00044212	0.00266984
WHL22.7445	114.739384	-1.4131673	0.22868933	37.9272959	7.34E-10	9.94E-09
WHL22.4348	27.5263497	-1.4150945	0.44010216	10.3826135	0.00127208	0.00687304
WHL22.6544	61.0287135	-1.4162029	0.29753151	22.7146042	1.88E-06	1.72E-05
WHL22.1207	89.9803692	-1.4172756	0.2438476	33.9265511	5.72E-09	7.18E-08
WHL22.2871	145.03396	-1.4179333	0.19527917	52.8139482	3.67E-13	6.87E-12
WHL22.4618	1326.64546	-1.4203476	0.06575985	467.192408	1.31E-103	2.11E-101
WHL22.2241	102.922277	-1.4229899	0.2281218	39.0845059	4.06E-10	5.65E-09
WHL22.1805	70.1757915	-1.4232042	0.27555137	26.8166001	2.24E-07	2.30E-06
WHL22.6932	102.989453	-1.4233621	0.22834248	39.0192741	4.20E-10	5.83E-09
WHL22.3933	1352.3924	-1.4268329	0.06579207	470.55205	2.43E-104	4.01E-102
WHL22.5215	507.524815	-1.4289005	0.10644239	180.378146	4.01E-41	2.34E-39
WHL22.5328	280.341085	-1.4312605	0.14501419	97.2913831	5.98E-23	1.91E-21
WHL22.3725	23.9681754	-1.4338141	0.49269211	8.31646785	0.00392872	0.01841619
WHL22.6469	665.009784	-1.4357076	0.09308309	238.153806	9.94E-54	8.02E-52
WHL22.3359	17.245394	-1.4371347	0.55394101	6.76469595	0.00929788	0.03875435
WHL22.6902	34.8155642	-1.4440727	0.39044311	13.7570338	0.00020804	0.00135314
WHL22.3471	223.012097	-1.445044	0.16148638	80.0195995	3.71E-19	9.93E-18
WHL22.1610	10023.5616	-1.4451575	0.02761346	2712.05282	0	0
WHL22.5355	45.8855823	-1.4478447	0.35004139	17.0380037	3.66E-05	0.00027247
WHL22.1808	102.173003	-1.4479612	0.22948991	39.9955831	2.55E-10	3.59E-09
WHL22.3061	51.8362203	-1.4514183	0.32722492	19.6623422	9.24E-06	7.66E-05
WHL22.3668	184.537957	-1.4566787	0.17525056	69.1686304	9.04E-17	2.14E-15
WHL22.7243	23.2869124	-1.457401	0.50889083	7.97351065	0.00474668	0.02178901
WHL22.1145	17.1161558	-1.4576673	0.57587488	6.29218232	0.01212716	0.04870774
WHL22.5356	391.694583	-1.4582411	0.12044813	146.845226	8.48E-34	4.06E-32

WHL22.5169	1074.7768	-1.4593402	0.07295076	400.999549	3.34E-89	4.30E-87
WHL22.7206	466.2383	-1.4659659	0.108963	181.685201	2.08E-41	1.23E-39
WHL22.3346	21.1389978	-1.4663054	0.5094722	8.28755109	0.00399178	0.01866815
WHL22.3077	93.5196164	-1.4672718	0.24579491	35.6386199	2.38E-09	3.08E-08
WHL22.9980	52.9518456	-1.4677339	0.31839152	21.353682	3.82E-06	3.35E-05
WHL22.3970	28.4568559	-1.4687665	0.43627973	11.3531915	0.00075318	0.00429221
WHL22.6416	24.9608894	-1.4689651	0.46383898	10.0839454	0.00149567	0.0079437
WHL22.6879	142.842144	-1.4712466	0.19351489	58.1439778	2.44E-14	5.03E-13
WHL22.6577	23.7212134	-1.4754221	0.47533838	9.671743	0.00187124	0.00965545
WHL22.7521	129.993102	-1.4755668	0.2067741	51.0955339	8.80E-13	1.59E-11
WHL22.3560	93.7050915	-1.4776595	0.24348162	36.8997998	1.24E-09	1.66E-08
WHL22.1060	1147.29333	-1.4779049	0.06972685	450.973486	4.43E-100	6.70E-98
WHL22.4009	17.2788445	-1.4790558	0.56640668	6.77474946	0.00924565	0.03856951
WHL22.6748	935.484802	-1.4841448	0.07685308	374.582433	1.88E-83	2.28E-81
WHL22.2378	511.155794	-1.4858137	0.10427786	203.821041	3.06E-46	2.15E-44
WHL22.3697	126.24794	-1.486587	0.21739472	46.5759897	8.81E-12	1.45E-10
WHL22.7026	270.352416	-1.4876306	0.14220676	109.954481	1.00E-25	3.54E-24
WHL22.7365	179.90442	-1.4898312	0.17668051	71.2808495	3.10E-17	7.53E-16
WHL22.7136	41.3286696	-1.4912138	0.36033105	17.2302148	3.31E-05	0.00024852
WHL22.7532	25.7649328	-1.49166	0.46274726	10.3728204	0.00127884	0.00690452
WHL22.7176	42.1380681	-1.4950512	0.36336027	16.9397017	3.86E-05	0.00028536
WHL22.2619	46.8996693	-1.4971429	0.33765799	19.7906584	8.64E-06	7.20E-05
WHL22.2926	30.6687832	-1.4976145	0.42559416	12.3606101	0.00043849	0.00265115
WHL22.6149	267.171751	-1.5006771	0.14222377	112.001756	3.57E-26	1.29E-24
WHL22.7882	27.5159346	-1.5023437	0.44736752	11.2662429	0.00078929	0.00448406
WHL22.5955	18.0204415	-1.508903	0.54592725	7.67022332	0.00561395	0.02524902
WHL22.2872	130.700494	-1.5106261	0.20641307	53.741074	2.29E-13	4.39E-12
WHL22.7691	70.7295424	-1.5162834	0.28079887	29.2259438	6.44E-08	7.07E-07
WHL22.4884	18.7740129	-1.518563	0.54389949	7.74898068	0.00537429	0.02428271
WHL22.1841	255.528875	-1.5217025	0.14979834	103.376922	2.77E-24	9.24E-23
WHL22.2136	15.8243714	-1.5326501	0.5887265	6.78008171	0.00921807	0.03848727
WHL22.7666	44.2504203	-1.5352738	0.34877395	19.5052233	1.00E-05	8.26E-05
WHL22.7390	123.101565	-1.5369946	0.21092927	53.3854866	2.74E-13	5.22E-12
WHL22.5982	66.8279783	-1.5372278	0.28881038	28.3920413	9.91E-08	1.06E-06
WHL22.6775	148.455862	-1.5401369	0.19800697	60.4948454	7.38E-15	1.55E-13
WHL22.4789	113.662767	-1.540991	0.2209098	48.8634551	2.74E-12	4.76E-11
WHL22.5096	24.1276683	-1.5431062	0.47754192	10.4408006	0.00123262	0.00667953
WHL22.1006	211.957983	-1.5500004	0.16581962	87.4392191	8.69E-21	2.55E-19
WHL22.4535	69.415823	-1.5513579	0.27858042	31.2456837	2.27E-08	2.64E-07
WHL22.5193	24.2915286	-1.5521788	0.47796955	10.5588111	0.00115636	0.00630854
WHL22.1079	19.5883403	-1.5642246	0.54128428	8.24976406	0.00407573	0.01900649
WHL22.6072	21.3050628	-1.5654005	0.50432279	9.68346409	0.00185934	0.00960754

WHL22.1006	151.169577	-1.567411	0.19022403	68.3447235	1.37E-16	3.20E-15
WHL22.1481	57.2960766	-1.5683575	0.30750827	26.2008963	3.08E-07	3.11E-06
WHL22.6211	41.5309039	-1.5714949	0.36229281	18.9225288	1.36E-05	0.00010969
WHL22.4608	30.4637483	-1.5723789	0.42527747	13.7201784	0.00021216	0.00137568
WHL22.1625	43.0924038	-1.572585	0.36223353	18.8598993	1.41E-05	0.00011316
WHL22.6901	590.248374	-1.5762605	0.10068187	245.364054	2.66E-55	2.22E-53
WHL22.3467	100.745119	-1.5796603	0.23234473	46.5613836	8.88E-12	1.46E-10
WHL22.5964	33.3485558	-1.5829422	0.43255276	13.0724941	0.00029966	0.00187354
WHL22.1788	29.3807492	-1.5857107	0.43075147	13.6444292	0.0002209	0.00142601
WHL22.6775	16.9341186	-1.5862722	0.57492265	7.59201449	0.00586274	0.02623145
WHL22.3744	449.967445	-1.588876	0.11294813	198.654763	4.11E-45	2.75E-43
WHL22.3433	39.430705	-1.5903559	0.38318949	17.131237	3.49E-05	0.00026034
WHL22.3020	354.254861	-1.5906343	0.12492767	163.190052	2.27E-37	1.20E-35
WHL22.4452	84.7310426	-1.5938338	0.25402582	39.6443246	3.05E-10	4.28E-09
WHL22.6563	27.4933911	-1.5961141	0.47067798	11.2509823	0.00079581	0.00451584
WHL22.6522	318.746664	-1.5975618	0.13419809	142.270561	8.49E-33	3.92E-31
WHL22.6616	15.768381	-1.5982233	0.58837624	7.40726527	0.0064961	0.02870642
WHL22.7045	36.8731799	-1.5985311	0.38383099	17.4928786	2.88E-05	0.00021913
WHL22.3347	15.2571333	-1.5997893	0.59744072	7.23796463	0.00713779	0.03104672
WHL22.3336	14.8217154	-1.6015341	0.61548577	6.75623878	0.00934205	0.03890532
WHL22.3848	55.4419897	-1.6020623	0.31455944	26.1280584	3.20E-07	3.22E-06
WHL22.2913	330.839641	-1.608776	0.12919813	156.171678	7.77E-36	3.99E-34
WHL22.1901	41.9450378	-1.60916	0.37143865	18.7131755	1.52E-05	0.00012161
WHL22.1788	72.8960035	-1.6115605	0.27684124	34.0541029	5.36E-09	6.75E-08
WHL22.3495	77.6182222	-1.6116423	0.28028306	32.8392633	1.00E-08	1.22E-07
WHL22.8094	14.8253266	-1.6198603	0.62480869	6.64270772	0.00995625	0.04111329
WHL22.2361	27.424437	-1.6230832	0.4511278	12.9924258	0.00031275	0.00195039
WHL22.1185	222.676164	-1.6242927	0.15753936	107.110919	4.21E-25	1.45E-23
WHL22.6630	49.0235198	-1.6247464	0.33934346	22.9844886	1.63E-06	1.51E-05
WHL22.1207	279.822198	-1.6248186	0.14085877	134.006775	5.44E-31	2.34E-29
WHL22.4000	175.345356	-1.6267785	0.17803587	84.0708984	4.77E-20	1.33E-18
WHL22.4030	273.155446	-1.6303415	0.14453836	127.857886	1.21E-29	4.93E-28
WHL22.2136	30.6682855	-1.6349452	0.42561145	14.8269344	0.00011784	0.00080348
WHL22.5661	114.332506	-1.6374668	0.22009591	55.7520465	8.22E-14	1.63E-12
WHL22.4050	67.6909221	-1.6419368	0.2994914	29.8710117	4.62E-08	5.12E-07
WHL22.4697	31.0856026	-1.6450413	0.42372627	15.13771	9.99E-05	0.00068916
WHL22.6819	797.292331	-1.6476506	0.08382987	389.144149	1.27E-86	1.59E-84
WHL22.2615	287.262655	-1.6493058	0.14545158	128.608569	8.26E-30	3.40E-28
WHL22.7532	279.287887	-1.6568066	0.14045541	140.38728	2.19E-32	1.00E-30
WHL22.6418	78.2111117	-1.6597672	0.26543609	39.4339281	3.39E-10	4.74E-09
WHL22.1236	1826.87941	-1.6629054	0.05659464	867.470585	1.16E-190	4.47E-188
WHL22.5441	2971.48758	-1.6722042	0.04538164	1360.48953	8.10E-298	5.40E-295

WHL22.3502	99.393078	-1.6751037	0.23888727	49.4961258	1.99E-12	3.51E-11
WHL22.8498	12.3785456	-1.676516	0.67273859	6.24759692	0.01243619	0.04974476
WHL22.1569	53.3394095	-1.678883	0.3269807	26.4679143	2.68E-07	2.73E-06
WHL22.1207	328.484463	-1.679238	0.13322563	159.606737	1.38E-36	7.18E-35
WHL22.9369	74.7298781	-1.6831251	0.2755981	37.5111183	9.09E-10	1.22E-08
WHL22.6817	15.138404	-1.6837912	0.60121181	7.92644366	0.00487175	0.02228896
WHL22.3502	157.227696	-1.685883	0.2046963	67.2397129	2.40E-16	5.47E-15
WHL22.2392	35.7625315	-1.6883997	0.41157509	16.6610128	4.47E-05	0.00032656
WHL22.4282	21.1546645	-1.6903398	0.51337618	10.9284916	0.00094697	0.00527517
WHL22.6005	58.1085564	-1.6911044	0.31628113	28.6308182	8.76E-08	9.42E-07
WHL22.1061	18.8649945	-1.6924382	0.54149503	9.85138967	0.00169704	0.00885934
WHL22.4282	13.0318498	-1.6984695	0.66167635	6.53050467	0.01060399	0.04338532
WHL22.5557	24.782602	-1.7010508	0.47795047	12.7472585	0.00035653	0.0021945
WHL22.5222	216.802595	-1.7029844	0.16415605	108.135	2.51E-25	8.73E-24
WHL22.5705	105.779731	-1.7049054	0.23375032	53.444209	2.66E-13	5.08E-12
WHL22.1061	12.9339485	-1.706176	0.66194289	6.68219964	0.00973804	0.04031427
WHL22.4681	40.4738487	-1.7069305	0.38139087	19.9679419	7.88E-06	6.60E-05
WHL22.5557	93.7876739	-1.7073417	0.24417593	49.3084576	2.19E-12	3.83E-11
WHL22.6206	75.5907157	-1.7129517	0.27032585	40.5734355	1.89E-10	2.71E-09
WHL22.2151	39.3938228	-1.7155819	0.37551573	21.0715281	4.42E-06	3.84E-05
WHL22.1647	16.0708743	-1.7169867	0.5868939	8.63087771	0.00330512	0.01584042
WHL22.2784	25.3118254	-1.7185682	0.46845836	13.5786388	0.00022877	0.00147428
WHL22.2898	182.317857	-1.7190148	0.17879333	92.9165627	5.45E-22	1.68E-20
WHL22.3837	36.8515363	-1.721804	0.39023728	19.6365736	9.37E-06	7.76E-05
WHL22.3539	12.275515	-1.7254457	0.68191179	6.34552644	0.01176777	0.04751123
WHL22.2409	55.6720595	-1.7260444	0.31738184	29.8337139	4.71E-08	5.20E-07
WHL22.6026	17.13379	-1.7315332	0.56898693	9.32835716	0.00225635	0.01137862
WHL22.4081	13.9918306	-1.7329421	0.62676224	7.72217784	0.00545466	0.02459286
WHL22.1172	36.7540474	-1.7349498	0.39426261	19.4981081	1.01E-05	8.28E-05
WHL22.5123	15.0954741	-1.7375603	0.61723638	7.91001529	0.00491619	0.02248274
WHL22.2157	88.2602917	-1.7382286	0.25258558	47.7777607	4.77E-12	8.08E-11
WHL22.6445	30.3972409	-1.7382605	0.4536465	14.3880005	0.00014875	0.000993
WHL22.2455	19.6652359	-1.7426075	0.53027472	10.9113769	0.00095575	0.00531457
WHL22.3837	47.9369123	-1.7463199	0.34202678	26.2965951	2.93E-07	2.97E-06
WHL22.6943	58.1615451	-1.7472685	0.30887898	32.3507778	1.29E-08	1.54E-07
WHL22.4350	124.781186	-1.7483152	0.2116116	68.9860322	9.92E-17	2.33E-15
WHL22.3018	25.6519125	-1.7501269	0.47279923	13.7293813	0.00021113	0.00137078
WHL22.6295	286.358221	-1.7508422	0.14283312	151.259418	9.20E-35	4.58E-33
WHL22.6397	23.742019	-1.7513293	0.50795243	11.7481396	0.00060904	0.00353528
WHL22.2809	176.578614	-1.7583966	0.18384779	91.8419727	9.39E-22	2.85E-20
WHL22.7587	165.279321	-1.7602757	0.18757281	88.6536092	4.70E-21	1.39E-19
WHL22.2528	1843.78277	-1.7613946	0.05912966	887.474316	5.19E-195	2.06E-192

WHL22.2435	205.642271	-1.7636527	0.16889143	109.701725	1.14E-25	4.01E-24
WHL22.3359	12.4288261	-1.7639944	0.6714753	6.96764715	0.00829966	0.03535663
WHL22.4038	111.9908	-1.7665881	0.22445413	62.5647525	2.58E-15	5.62E-14
WHL22.4397	18.5619928	-1.766992	0.55840283	9.98929729	0.00157453	0.00829948
WHL22.2136	16.5283608	-1.7694592	0.58153558	9.34135822	0.00224039	0.01132151
WHL22.4350	73.3267601	-1.7705122	0.28653427	38.260068	6.19E-10	8.45E-09
WHL22.3548	56.5663304	-1.7707578	0.32431864	29.8486068	4.67E-08	5.18E-07
WHL22.5661	20.604401	-1.77396	0.53304583	11.0647755	0.00087983	0.0049354
WHL22.3876	4211.52308	-1.7802614	0.03898119	2088.46976	0	0
WHL22.3897	970.058378	-1.7803464	0.07707787	538.466377	4.07E-119	7.85E-117
WHL22.5041	68.4069569	-1.7837298	0.29330243	37.1383023	1.10E-09	1.47E-08
WHL22.6006	20.090478	-1.7881003	0.52558594	11.7188745	0.00061869	0.0035814
WHL22.5091	343.750976	-1.7940164	0.12951007	193.713584	4.92E-44	3.19E-42
WHL22.7273	161.992458	-1.796023	0.18702016	93.2428043	4.63E-22	1.43E-20
WHL22.1420	11.9416172	-1.80193	0.68653563	6.97597379	0.00826113	0.03523339
WHL22.7176	60.4205284	-1.8028504	0.30804136	34.5574785	4.14E-09	5.27E-08
WHL22.5135	24.5721074	-1.8061144	0.48011683	14.3193565	0.00015427	0.00102754
WHL22.5952	28.6027972	-1.8092173	0.44495854	16.7346546	4.30E-05	0.00031554
WHL22.2886	14.0036204	-1.8164471	0.64535219	7.92957793	0.00486331	0.02226176
WHL22.6845	16.054734	-1.8171257	0.61804348	8.5175485	0.00351738	0.01674218
WHL22.3803	248.036279	-1.8215119	0.15236207	144.411479	2.89E-33	1.36E-31
WHL22.1011	17.1106267	-1.8224767	0.58004236	9.88045142	0.00167044	0.00874226
WHL22.5558	33.5627434	-1.8239063	0.41326596	19.741643	8.86E-06	7.38E-05
WHL22.4816	18.5586129	-1.8305156	0.57028557	10.2190881	0.00138995	0.00743872
WHL22.5866	87.87984	-1.8318683	0.25778265	50.9091318	9.67E-13	1.74E-11
WHL22.4353	37.8396282	-1.8344292	0.38796204	22.5950301	2.00E-06	1.82E-05
WHL22.4250	23.2775979	-1.8493932	0.52522068	12.0572254	0.00051592	0.00305145
WHL22.9717	24.6288138	-1.8528387	0.48161382	14.9581492	0.00010992	0.00075229
WHL22.2409	52.4988745	-1.8529166	0.33743608	30.2895343	3.72E-08	4.19E-07
WHL22.3293	168.850267	-1.8547356	0.18475716	101.941973	5.72E-24	1.89E-22
WHL22.3748	15.8099648	-1.8553456	0.59735494	9.79732713	0.00174766	0.00909773
WHL22.2771	46.4687959	-1.8562489	0.35131231	28.2312285	1.08E-07	1.15E-06
WHL22.5010	31.0753644	-1.8597894	0.44043577	17.8063841	2.45E-05	0.00018886
WHL22.2247	442.099985	-1.8622841	0.11442242	268.036278	3.04E-60	2.79E-58
WHL22.2375	18.6960177	-1.8636123	0.56097164	11.0486417	0.00088752	0.00497473
WHL22.5879	15.8659099	-1.8723973	0.59667311	9.98384974	0.00157919	0.00831511
WHL22.6226	506.4713	-1.8725045	0.11650299	257.373518	6.41E-58	5.67E-56
WHL22.1935	15.6963825	-1.8831687	0.6165603	9.26293743	0.00233838	0.01174388
WHL22.6053	211.559311	-1.8852142	0.17115934	121.916341	2.41E-28	9.50E-27
WHL22.6949	62.8734748	-1.8941104	0.30098241	40.1813888	2.31E-10	3.29E-09
WHL22.1300	15.1965034	-1.8999243	0.61117404	9.81207968	0.00173369	0.00903145
WHL22.2092	16.7596108	-1.9051892	0.5860499	10.6955069	0.00107396	0.00590035

WHL22.1007	114.740777	-1.9098769	0.22370806	73.9638087	7.96E-18	2.00E-16
WHL22.3655	245.550868	-1.9115094	0.1540356	156.006098	8.44E-36	4.32E-34
WHL22.4272	695.731029	-1.9130938	0.09227173	434.947806	1.36E-96	1.94E-94
WHL22.8481	12.8646731	-1.9230841	0.66982938	8.32100422	0.00391892	0.01838013
WHL22.6416	814.271167	-1.9238964	0.08554899	511.628073	2.81E-113	5.15E-111
WHL22.2409	11.5724518	-1.9320308	0.70800907	7.53926255	0.00603687	0.02696116
WHL22.4124	62.8312494	-1.9389591	0.30217969	41.8358843	9.93E-11	1.47E-09
WHL22.7062	120.287674	-1.9392495	0.22135322	77.6972132	1.20E-18	3.11E-17
WHL22.6320	11.5902254	-1.9404317	0.71406747	7.48248411	0.00623021	0.02768142
WHL22.9518	109.940398	-1.941426	0.22861839	73.2762465	1.13E-17	2.81E-16
WHL22.1906	32.5163956	-1.948492	0.45040292	18.4242573	1.77E-05	0.00014029
WHL22.1576	13.6454478	-1.9497689	0.65692095	8.84015613	0.00294674	0.01438103
WHL22.4943	35.2242655	-1.9553937	0.40342678	23.8933627	1.02E-06	9.61E-06
WHL22.5652	19.2661431	-1.9579558	0.56513218	12.0322317	0.00052288	0.00308643
WHL22.6521	20.1952269	-1.9587931	0.54027988	13.2210836	0.00027682	0.00174782
WHL22.2037	16.7613917	-1.965355	0.58605174	11.4093951	0.00073074	0.00417564
WHL22.7883	69.8744732	-1.9665222	0.28883639	47.0578386	6.89E-12	1.15E-10
WHL22.4085	13.4942638	-1.9670519	0.6795791	8.21219486	0.00416098	0.01933012
WHL22.6050	273.713039	-1.9680297	0.14573318	185.328464	3.33E-42	2.03E-40
WHL22.1429	20.1913861	-1.9684921	0.53944364	13.4427116	0.00024596	0.0015726
WHL22.7229	51.3592584	-1.9688614	0.33506942	35.1095485	3.12E-09	4.00E-08
WHL22.3492	68.2457292	-1.9698427	0.29212471	46.1831868	1.08E-11	1.75E-10
WHL22.5767	19.591502	-1.9743503	0.54385998	13.3914883	0.00025277	0.00161122
WHL22.5952	14.3782083	-1.9743913	0.65070936	9.24646443	0.00235951	0.01182572
WHL22.2560	50.9363107	-1.9744165	0.51650556	13.5711725	0.00022969	0.0014795
WHL22.7161	19.6200299	-1.9767899	0.56409326	12.1407621	0.00049332	0.00293431
WHL22.6323	1278.19175	-1.9782515	0.06961549	815.723941	2.06E-179	7.03E-177
WHL22.1491	98.7416549	-1.992243	0.24316851	68.2328018	1.45E-16	3.38E-15
WHL22.2374	22.5247948	-1.9983942	0.5054905	15.928027	6.58E-05	0.00046684
WHL22.7273	109.068902	-1.9997149	0.23526329	73.0978154	1.23E-17	3.06E-16
WHL22.2868	27.2365876	-2.0119727	0.46488928	18.9884579	1.32E-05	0.00010625
WHL22.2374	14.5611097	-2.027123	0.64405072	9.91563706	0.0016388	0.00860431
WHL22.4283	23.4557032	-2.0271521	0.50092873	16.6433045	4.51E-05	0.00032929
WHL22.5813	25.8216671	-2.027739	0.47765403	18.2908904	1.90E-05	0.00014973
WHL22.7398	74.9199334	-2.0523379	0.2850232	52.5251717	4.25E-13	7.92E-12
WHL22.5705	22.0138471	-2.0581475	0.51838102	16.0561428	6.15E-05	0.00043842
WHL22.3891	758.546154	-2.0603891	0.09386145	484.3976	2.36E-107	4.08E-105
WHL22.7431	44.6580323	-2.0734339	0.39038197	28.0106997	1.21E-07	1.28E-06
WHL22.6676	44.6069649	-2.0734921	0.36987133	31.8408299	1.67E-08	1.98E-07
WHL22.4452	537.704026	-2.0811653	0.10577944	394.202782	1.01E-87	1.29E-85
WHL22.5557	12.1861127	-2.0857389	0.69584688	9.19901792	0.00242145	0.01208667
WHL22.1367	163.986772	-2.0910499	0.18987417	123.866366	9.01E-29	3.58E-27

WHL22.6018	71.0664189	-2.1011068	0.29520308	51.3168683	7.86E-13	1.43E-11
WHL22.4557	49.6459874	-2.1045722	0.34490523	38.0552723	6.88E-10	9.35E-09
WHL22.2100	28.8560447	-2.104593	0.46893285	20.1560932	7.14E-06	6.01E-05
WHL22.5041	71.9165433	-2.1127504	0.29524276	51.8105364	6.11E-13	1.13E-11
WHL22.3743	11.0963892	-2.131182	0.75053804	7.96525756	0.00476837	0.02188174
WHL22.7031	24.9709261	-2.1368169	0.49273258	19.120308	1.23E-05	9.96E-05
WHL22.6521	130.930964	-2.1527009	0.21502488	102.488796	4.34E-24	1.44E-22
WHL22.3346	25.0660718	-2.1563431	0.52100729	16.8097372	4.13E-05	0.0003036
WHL22.2870	62.5857848	-2.1658314	0.3140424	48.4235255	3.43E-12	5.90E-11
WHL22.2149	18.5780154	-2.1668714	0.57168687	14.6184797	0.00013162	0.00089203
WHL22.2421	368.613766	-2.1672395	0.12941858	286.130143	3.47E-64	3.33E-62
WHL22.5809	71.7225687	-2.181718	0.29326018	56.4984081	5.62E-14	1.13E-12
WHL22.2246	17.6184739	-2.1856302	0.61724748	12.2168197	0.00047361	0.0028343
WHL22.1253	67.1392932	-2.1861303	0.29991806	54.438672	1.60E-13	3.11E-12
WHL22.9959	1297.44665	-2.1866048	0.07072881	970.181792	5.44E-213	2.42E-210
WHL22.1564	31.8142226	-2.188029	0.44089097	25.0314424	5.64E-07	5.49E-06
WHL22.5559	297.381223	-2.1952069	0.14708213	226.289942	3.84E-51	2.97E-49
WHL22.3849	29.1567016	-2.1992816	0.45833327	23.4753027	1.27E-06	1.18E-05
WHL22.6020	19.1740936	-2.2023117	0.55878441	15.9485599	6.51E-05	0.00046203
WHL22.6356	14.0045089	-2.2031805	0.65783893	11.4930041	0.00069859	0.00401223
WHL22.5086	17.1509928	-2.204593	0.59344348	14.1157467	0.0001719	0.00113619
WHL22.2135	27.4600654	-2.2072682	0.509791	18.1828525	2.01E-05	0.00015762
WHL22.2763	72.4548992	-2.223001	0.29837524	56.250629	6.38E-14	1.27E-12
WHL22.6844	209.688604	-2.2272608	0.17327737	168.69522	1.43E-38	7.70E-37
WHL22.2763	219.518064	-2.2306692	0.170234	175.044448	5.85E-40	3.29E-38
WHL22.6167	20.2700634	-2.2397306	0.55161794	16.859762	4.02E-05	0.00029659
WHL22.1119	128.790146	-2.2524771	0.22230661	104.836572	1.33E-24	4.47E-23
WHL22.1754	40.3366603	-2.2553816	0.3945353	33.3312388	7.77E-09	9.58E-08
WHL22.3942	33.3774216	-2.2569449	0.42694667	28.7662357	8.17E-08	8.85E-07
WHL22.7628	24.9260075	-2.2704173	0.50148298	20.9127837	4.81E-06	4.15E-05
WHL22.4592	601.989397	-2.2807633	0.10175343	516.04153	3.07E-114	5.79E-112
WHL22.8311	12.64371	-2.2847739	0.75090544	8.86670669	0.00290419	0.01419695
WHL22.9979	51.5889828	-2.2861409	0.34863222	44.0675244	3.17E-11	4.89E-10
WHL22.1543	149.527472	-2.3001472	0.20389678	130.971622	2.51E-30	1.06E-28
WHL22.7311	31.5048865	-2.3018714	0.45018345	26.6860923	2.39E-07	2.46E-06
WHL22.2045	15.441032	-2.3018729	0.64017437	13.2157907	0.0002776	0.00175201
WHL22.6126	1860.94308	-2.3078921	0.05928087	1549.02722	0	0
WHL22.4559	16.8980757	-2.3224847	0.66166132	11.7274305	0.00061586	0.00356638
WHL22.2776	63.1005458	-2.3308788	0.320383	54.2945206	1.73E-13	3.34E-12
WHL22.1063	11.8353342	-2.3401702	0.72884322	10.5228989	0.00117904	0.00641764
WHL22.1194	3372.98749	-2.3712512	0.0455055	2761.29275	0	0
WHL22.2298	127.039772	-2.3725305	0.22468592	114.73724	8.98E-27	3.32E-25

WHL22.1182	77.4447851	-2.3877886	0.28539596	72.3835142	1.77E-17	4.36E-16
WHL22.3721	27.2470039	-2.4078067	0.48147265	25.9551275	3.49E-07	3.50E-06
WHL22.5735	12.7833487	-2.409824	0.70712646	12.0114107	0.00052876	0.00311706
WHL22.6944	24.065429	-2.4209263	0.5179586	22.4346154	2.17E-06	1.97E-05
WHL22.5786	16.0019329	-2.4228462	0.62974644	15.2769125	9.28E-05	0.0006429
WHL22.6200	12.6091763	-2.4493582	0.71376544	12.1987954	0.0004782	0.00285832
WHL22.2895	14.0780598	-2.4519296	0.68645931	13.0993673	0.0002954	0.00185079
WHL22.6944	286.451288	-2.4570201	0.16097511	235.559821	3.66E-53	2.92E-51
WHL22.9020	37.5573666	-2.4609365	0.41455992	36.4685371	1.55E-09	2.05E-08
WHL22.4348	16.6392255	-2.4789824	0.62344341	16.4051084	5.11E-05	0.00037042
WHL22.7518	22.5032289	-2.4885988	0.53453967	22.5411586	2.06E-06	1.87E-05
WHL22.6660	51.3522865	-2.4913916	0.35347574	51.7396056	6.34E-13	1.16E-11
WHL22.2297	123.751313	-2.5322582	0.23351737	121.690375	2.70E-28	1.06E-26
WHL22.5806	226.650121	-2.5368813	0.17137353	227.649488	1.94E-51	1.51E-49
WHL22.6786	45.4559634	-2.5432534	0.38019603	46.5842291	8.78E-12	1.45E-10
WHL22.2176	625.035392	-2.5608374	0.10379899	632.726028	1.28E-139	3.23E-137
WHL22.4631	32.7929723	-2.5613724	0.47407223	29.3566188	6.02E-08	6.62E-07
WHL22.4771	11.9466542	-2.5664156	0.75240901	11.9029343	0.00056046	0.00328312
WHL22.3788	18.9730687	-2.5723368	0.59079416	19.8431259	8.41E-06	7.02E-05
WHL22.6842	472.340063	-2.5947236	0.12561887	436.475019	6.33E-97	9.11E-95
WHL22.5216	117.289684	-2.60738	0.23864362	124.942056	5.24E-29	2.10E-27
WHL22.3661	19.5492719	-2.6169615	0.59800396	19.6332807	9.38E-06	7.76E-05
WHL22.8502	15.0370671	-2.6174045	0.67016886	15.8223715	6.96E-05	0.00049175
WHL22.6036	11.9642319	-2.6469366	0.75797589	12.6552916	0.0003745	0.00229591
WHL22.5081	39.1630977	-2.650152	0.42098147	41.127509	1.43E-10	2.06E-09
WHL22.5989	86.5651256	-2.6574936	0.27987458	94.6268914	2.30E-22	7.20E-21
WHL22.6115	12.0494361	-2.6911313	0.75106665	13.5447923	0.00023294	0.00149782
WHL22.4557	58.038941	-2.6961516	0.34150472	65.748794	5.12E-16	1.16E-14
WHL22.3743	604.043703	-2.7033445	0.10835537	650.553034	1.69E-143	4.69E-141
WHL22.2322	69.2742483	-2.7042251	0.31656506	76.4984428	2.20E-18	5.68E-17
WHL22.2394	121.26658	-2.7100448	0.36371621	51.5977226	6.81E-13	1.25E-11
WHL22.5806	72.7373263	-2.7257163	0.30769524	82.7363483	9.38E-20	2.59E-18
WHL22.7186	59.3187065	-2.7355238	0.3479632	64.4544855	9.88E-16	2.20E-14
WHL22.5214	15.9361221	-2.7505485	0.67221933	17.3529344	3.10E-05	0.00023429
WHL22.5642	41.8651558	-2.7556268	0.40633745	48.7149077	2.96E-12	5.12E-11
WHL22.3491	146.031586	-2.7610941	0.22905264	149.901893	1.82E-34	8.88E-33
WHL22.3512	72.1822273	-2.7625537	0.32028352	77.2639745	1.50E-18	3.86E-17
WHL22.5614	13.9363208	-2.770151	0.70935932	15.9510526	6.50E-05	0.00046187
WHL22.5848	30.6157894	-2.8168117	0.49277883	34.1281776	5.16E-09	6.51E-08
WHL22.3512	65.0579092	-2.8189777	0.33370022	75.0878819	4.50E-18	1.15E-16
WHL22.7314	167.031093	-2.8338699	0.20563451	202.207417	6.89E-46	4.77E-44
WHL22.1456	120.154953	-2.8504123	0.24657695	141.241369	1.42E-32	6.54E-31

WHL22.4631	15.3450932	-2.8892709	0.69846158	18.1255527	2.07E-05	0.000162
WHL22.6944	23.4929815	-2.9317747	0.55836375	29.5284246	5.51E-08	6.07E-07
WHL22.1063	13.8872608	-2.9335096	0.72071972	17.7995012	2.45E-05	0.00018924
WHL22.5723	13.9046843	-2.934129	0.72050017	17.7936663	2.46E-05	0.00018972
WHL22.2796	17.3024896	-2.9539369	0.64994345	22.1259096	2.55E-06	2.30E-05
WHL22.7327	107.62443	-2.9598026	0.27020512	126.233089	2.73E-29	1.11E-27
WHL22.6216	36.6682041	-2.9802301	0.45025265	47.0613368	6.88E-12	1.15E-10
WHL22.3256	16.3337608	-2.9963033	0.67430245	21.2396975	4.05E-06	3.53E-05
WHL22.4618	111.179705	-3.02759	0.26807782	135.293866	2.85E-31	1.24E-29
WHL22.5980	163329.268	-3.0472141	0.01441573	39886.5642	0	0
WHL22.5766	13.4776421	-3.1043215	0.7787686	16.678615	4.43E-05	0.0003237
WHL22.3255	19.9217832	-3.1276206	0.6330685	26.1416078	3.17E-07	3.20E-06
WHL22.4329	3341.37807	-3.1905173	0.05021517	4340.63906	0	0
WHL22.5628	21.7294257	-3.2213274	0.62679753	27.9516591	1.24E-07	1.31E-06
WHL22.3256	13.6479969	-3.2796796	0.79315065	18.2989052	1.89E-05	0.00014926
WHL22.2322	11.0958763	-3.3125248	0.86249784	16.166077	5.80E-05	0.00041565
WHL22.5028	70.7086334	-3.3542836	0.34226669	107.625477	3.25E-25	1.12E-23
WHL22.1504	26.286849	-3.3604177	0.56300946	39.771847	2.85E-10	4.02E-09
WHL22.2353	31.6093429	-3.5352898	0.5394055	48.0560238	4.14E-12	7.05E-11
WHL22.1177	77.1733386	-3.537125	0.33723711	126.603888	2.27E-29	9.20E-28
WHL22.4056	218.232635	-3.5889187	0.20383795	356.6945	1.48E-79	1.67E-77
WHL22.6106	1376.73576	-3.5918056	0.08174719	2208.92471	0	0
WHL22.1968	14.5570261	-3.6374665	0.80228757	23.4813626	1.26E-06	1.17E-05
WHL22.1253	102.030565	-3.7087013	0.40936108	78.0588728	1.00E-18	2.60E-17
WHL22.7445	12.7413988	-3.8839366	0.91767386	20.1096413	7.31E-06	6.16E-05
WHL22.3599	38.2599471	-3.9376426	0.51625522	71.3056931	3.06E-17	7.45E-16
WHL22.2017	36.8798661	-4.0091534	0.53533885	69.3143063	8.40E-17	1.99E-15
WHL22.6414	29.920992	-4.1628222	0.61484592	57.715961	3.03E-14	6.21E-13
WHL22.1319	1958.14859	-4.2735982	0.07899931	3699.5893	0	0
WHL22.2963	12.2230649	-4.4255049	1.02426543	24.3820008	7.90E-07	7.57E-06
WHL22.1495	12.9530824	-4.5718015	1.0184742	27.6703465	1.44E-07	1.51E-06
WHL22.7506	15.5693996	-4.8513463	0.99372814	35.2232869	2.94E-09	3.78E-08
WHL22.1264	30.6253547	-5.3374145	1.27817519	13.6966218	0.00021484	0.0013912

	baseMean	log2FoldCha	lfcSE	stat	pvalue	padj
WHL22.6988	38.3798103	6.07528892	0.95946529	51.2176611	8.27E-13	4.28E-10
WHL22.2246	926.257299	4.1587385	0.83454883	17.6047349	2.72E-05	0.00142799
WHL22.9950	132.853886	3.90406097	0.39202028	92.5803245	6.46E-22	2.00E-18
WHL22.3562	4957.54839	3.72555365	0.37226958	76.5499624	2.15E-18	3.33E-15
WHL22.6993	2319.8656	3.0920489	0.33153977	71.3107154	3.05E-17	3.44E-14
WHL22.4125	244.030646	3.06519076	0.32349697	83.7697489	5.56E-20	1.15E-16
WHL22.2753	550.489496	3.06438293	0.35835695	61.2324794	5.07E-15	4.49E-12
WHL22.4333	77.046223	3.01953363	0.42641358	46.5650567	8.86E-12	3.14E-09
WHL22.6886	232.715628	2.93871737	0.40882007	43.554736	4.12E-11	1.28E-08
WHL22.1041	54.5972815	2.83574335	0.49726083	30.2531365	3.79E-08	5.80E-06
WHL22.7098	76.257435	2.82780257	0.53055905	23.7976913	1.07E-06	0.00010377
WHL22.2429	1139.18927	2.63293674	0.37536862	40.2850408	2.19E-10	5.44E-08
WHL22.2429	335.889994	2.62711297	0.40812612	33.8106139	6.07E-09	1.16E-06
WHL22.9950	41.6267897	2.60597241	0.51670477	24.3793238	7.91E-07	8.10E-05
WHL22.2360	50.9279568	2.58125629	0.47175368	29.1848906	6.58E-08	9.37E-06
WHL22.1739	108.138851	2.5642377	0.55260798	16.7252554	4.32E-05	0.00207537
WHL22.1943	4970.52081	2.54117969	0.34454974	45.7416889	1.35E-11	4.52E-09
WHL22.2048	3103.88197	2.54035587	0.24688968	95.0543193	1.85E-22	1.15E-18
WHL22.2247	863.781253	2.46402984	0.41992452	27.5137621	1.56E-07	1.97E-05
WHL22.5899	823.884224	2.43276861	0.35105929	41.0014873	1.52E-10	4.28E-08
WHL22.5900	1390.11864	2.4297831	0.3501575	40.7762905	1.71E-10	4.60E-08
WHL22.2360	221.973399	2.42197386	0.35903542	40.3571382	2.12E-10	5.35E-08
WHL22.5084	3585.39906	2.413894	0.25213016	82.6593373	9.75E-20	1.73E-16
WHL22.7603	134.10826	2.39989432	0.33186375	49.3711367	2.12E-12	1.01E-09
WHL22.5140	240.548871	2.3677766	0.3243941	48.7377896	2.93E-12	1.21E-09
WHL22.7058	210.939544	2.3649185	0.32805249	48.7468407	2.91E-12	1.21E-09
WHL22.6085	74.34196	2.35106862	0.40687728	31.4925841	2.00E-08	3.26E-06
WHL22.2243	1444.88387	2.33070832	0.31247263	49.4565779	2.03E-12	1.01E-09
WHL22.1234	894.770796	2.33002264	0.27801422	63.7860681	1.39E-15	1.43E-12
WHL22.2177	79.1429182	2.30980552	0.49336998	19.4188128	1.05E-05	0.0006706
WHL22.2105	159.588305	2.29572781	0.36710688	35.4409186	2.63E-09	5.68E-07
WHL22.6123	207.578928	2.2614815	0.34377334	40.5480668	1.92E-10	5.06E-08
WHL22.2667	1295.90849	2.20161748	0.29229648	51.2120963	8.29E-13	4.28E-10
WHL22.5906	2347.80218	2.18025448	0.33209163	37.7919158	7.87E-10	1.88E-07
WHL22.4287	93.4731595	2.16770402	0.49586079	16.2687162	5.50E-05	0.00249408
WHL22.5125	2475.25268	2.13607174	0.35066378	32.1179697	1.45E-08	2.46E-06
WHL22.1155	35141.3135	2.12291915	0.29526101	46.2228049	1.06E-11	3.63E-09
WHL22.1940	701.946606	2.12062019	0.33559744	35.6489251	2.36E-09	5.32E-07
WHL22.1751	38.6408589	2.10005917	0.54861295	13.8923793	0.00019358	0.00660951

WHL22.5761	2599.0765	2.09840088	0.28600588	48.7711544	2.88E-12	1.21E-09
WHL22.6441	291.710184	2.09743808	0.28293124	51.7598981	6.27E-13	3.53E-10

WHL22.1078	183.41502	2.09061288	0.42555741	20.7780623	5.16E-06	0.00038312
WHL22.6411	324.038408	2.08124786	0.32376052	37.7185496	8.17E-10	1.88E-07
WHL22.7205	506.987601	2.07837957	0.35747771	29.4747122	5.67E-08	8.26E-06
WHL22.1155	36072.6917	2.07230478	0.30111236	42.2989741	7.83E-11	2.26E-08
WHL22.2359	397.016895	2.06861475	0.37252994	26.7643246	2.30E-07	2.85E-05
WHL22.4333	115.515057	2.06546931	0.37968849	27.2990593	1.74E-07	2.18E-05
WHL22.4188	40406.4723	2.06335594	0.29926319	42.523387	6.98E-11	2.06E-08
WHL22.5867	15031.7227	2.06266354	0.28006511	49.2656918	2.24E-12	1.03E-09
WHL22.6991	21648.9326	2.02720528	0.28124554	47.1742108	6.49E-12	2.44E-09
WHL22.1156	133.933179	2.02260842	0.38863463	25.08348	5.49E-07	5.92E-05
WHL22.7421	61.0317509	2.0074191	0.40736852	23.5125913	1.24E-06	0.00011822
WHL22.7104	121.09384	2.00640998	0.36381709	28.6135825	8.84E-08	1.20E-05
WHL22.2432	5428.91883	1.98424793	0.26345092	52.270746	4.84E-13	2.85E-10
WHL22.7603	54.5359335	1.97713218	0.42323796	21.1367592	4.28E-06	0.00032921
WHL22.5087	909.707006	1.96990344	0.27500089	47.5695705	5.31E-12	2.06E-09
WHL22.7289	74.9215599	1.96218237	0.44004547	18.2917832	1.90E-05	0.00108748
WHL22.2462	400.004944	1.95289133	0.28644815	43.8643166	3.52E-11	1.12E-08
WHL22.6096	765.045677	1.94217384	0.3790738	22.6469094	1.95E-06	0.00017234
WHL22.1718	65.5869092	1.9355604	0.44060718	18.1121517	2.08E-05	0.00116901
WHL22.4085	58.4680173	1.9277456	0.4201689	20.3442114	6.47E-06	0.00045554
WHL22.4375	1992.84599	1.9233784	0.36810164	23.2592764	1.42E-06	0.00013292
WHL22.7561	1696.14745	1.9206651	0.24852984	55.9147934	7.57E-14	5.23E-11
WHL22.1161	44.1119759	1.92016609	0.52578159	12.4694713	0.00041366	0.0114695
WHL22.3452	88.2080552	1.91749225	0.47966655	13.7415404	0.00020976	0.00698873
WHL22.7252	48.0364066	1.90361848	0.44363044	17.9969211	2.21E-05	0.00120807
WHL22.3995	74.1122495	1.90045844	0.48072189	13.7580292	0.00020793	0.00694632
WHL22.6281	98.9772933	1.89752632	0.39265772	22.5793733	2.02E-06	0.00017724
WHL22.2277	570.823111	1.89199222	0.32957964	29.8583567	4.65E-08	7.03E-06
WHL22.5036	185.836078	1.88136139	0.31925777	33.0285555	9.08E-09	1.63E-06
WHL22.6197	112.201674	1.87592173	0.41540137	18.4184445	1.77E-05	0.00103673
WHL22.8883	331.103597	1.87344056	0.34953375	25.9318709	3.54E-07	4.10E-05
WHL22.2418	241.656035	1.87227875	0.31361261	33.8500446	5.95E-09	1.15E-06
WHL22.4966	154.210201	1.86953144	0.33948387	28.7853736	8.09E-08	1.13E-05
WHL22.1926	7768.28147	1.86475272	0.29944553	35.2479984	2.90E-09	6.10E-07
WHL22.6285	42.7261453	1.85216225	0.48323787	14.4718872	0.00014227	0.00509612
WHL22.4506	154.061614	1.8501499	0.33673939	28.6244949	8.79E-08	1.20E-05
WHL22.2767	10450.5571	1.83244053	0.29435795	35.4201561	2.66E-09	5.68E-07
WHL22.7028	71.8945408	1.82664415	0.40670409	19.1826078	1.19E-05	0.00073615
WHL22.4040	1097.82646	1.81653269	0.27450802	40.8546061	1.64E-10	4.52E-08
WHL22.4675	175.740124	1.80889968	0.31954572	30.4086681	3.50E-08	5.49E-06
WHL22.1295	166.569446	1.80238135	0.32569982	29.2003684	6.53E-08	9.37E-06
WHL22.1227	2066.04986	1.79775809	0.35844068	21.9577874	2.79E-06	0.00023029

WHL22.1269	37.2192309	1.7955943	0.50829484	11.9027254	0.00056052	0.01459468
WHL22.7399	37.6809618	1.7833047	0.48113439	13.4305291	0.00024756	0.0078674
WHL22.4188	334.39123	1.76323155	0.30180527	32.3262466	1.30E-08	2.24E-06
WHL22.6401	241.780336	1.75916501	0.30159418	32.6922764	1.08E-08	1.88E-06
WHL22.1712	95.1020386	1.75899361	0.38327894	20.1787496	7.05E-06	0.00049388
WHL22.1247	194.693856	1.75506782	0.30968934	30.6230955	3.13E-08	4.98E-06
WHL22.5030	802.293405	1.74936294	0.28574231	34.9546081	3.37E-09	6.86E-07
WHL22.5677	80.4497846	1.74417354	0.46308529	12.5827939	0.00038931	0.01099253
WHL22.3859	427.751822	1.73601828	0.2758404	37.7485549	8.05E-10	1.88E-07
WHL22.6281	143.963496	1.73393179	0.40723951	16.3133991	5.37E-05	0.00245516
WHL22.1718	76.9459206	1.72987071	0.38701659	19.1582025	1.20E-05	0.00074191
WHL22.4333	1124.68736	1.7259895	0.26361025	40.4148622	2.05E-10	5.30E-08
WHL22.5726	928.380027	1.72349472	0.2906313	32.7414785	1.05E-08	1.86E-06
WHL22.5037	97.5866911	1.72276091	0.39287465	17.9167574	2.31E-05	0.00125451
WHL22.4509	1362.17561	1.71632549	0.3117074	27.6726089	1.44E-07	1.86E-05
WHL22.5240	58.2988277	1.70627998	0.52783857	8.94238955	0.00278628	0.04797291
WHL22.2806	68.5140166	1.685017	0.40872134	16.1673394	5.80E-05	0.00258514
WHL22.9502	117.253632	1.67888016	0.33352204	24.6172673	6.99E-07	7.22E-05
WHL22.7425	78.9610728	1.67733966	0.38156771	18.6212622	1.59E-05	0.00095
WHL22.5723	869.763834	1.67438318	0.28224828	33.0407845	9.02E-09	1.63E-06
WHL22.4802	128.422067	1.66945601	0.33109746	24.7245014	6.61E-07	6.89E-05
WHL22.5901	107.884623	1.6675605	0.36855837	19.496556	1.01E-05	0.00065056
WHL22.7014	155.821657	1.66533075	0.36028851	19.853531	8.36E-06	0.00056013
WHL22.4547	129.488801	1.66489451	0.36033479	20.0900297	7.39E-06	0.00050871
WHL22.3684	693.250971	1.6575669	0.27770673	33.6285194	6.67E-09	1.25E-06
WHL22.5342	71.5061079	1.65594084	0.42029901	14.7831841	0.00012061	0.00452258
WHL22.2502	68625.6904	1.64656251	0.30065806	27.5552204	1.53E-07	1.95E-05
WHL22.1079	113.185811	1.64474671	0.47757373	10.2700491	0.00135207	0.02840268
WHL22.5207	457.793161	1.64321325	0.33703365	21.6845918	3.21E-06	0.00025369
WHL22.1622	892.707173	1.6395284	0.36983178	17.2587887	3.26E-05	0.00161598
WHL22.3410	248.762462	1.61151676	0.30931804	25.751564	3.88E-07	4.38E-05
WHL22.4502	83.9315301	1.60867789	0.44497404	11.881652	0.0005669	0.01472291
WHL22.1280	192.902148	1.60858862	0.34747702	20.1046648	7.33E-06	0.00050765
WHL22.4612	49.8130128	1.60101269	0.47730306	10.6101928	0.00112466	0.02445444
WHL22.9990	429.309676	1.59993971	0.37019957	16.4620282	4.96E-05	0.00232139
WHL22.5046	91.4821632	1.59760897	0.36840204	18.2589368	1.93E-05	0.00109884
WHL22.4530	876.22421	1.59737431	0.26941321	33.3491286	7.70E-09	1.42E-06
WHL22.3254	106.27903	1.59524132	0.36265312	18.4862561	1.71E-05	0.00100523
WHL22.6045	1963.12834	1.59401199	0.31156192	24.0393428	9.44E-07	9.36E-05
WHL22.4227	20094.4032	1.58989975	0.32519231	21.5182284	3.50E-06	0.0002732
WHL22.1816	181.153	1.58955125	0.3095181	25.4762018	4.48E-07	4.95E-05
WHL22.7104	75.2595303	1.58876731	0.44370679	11.7255772	0.00061647	0.01556114

WHL22.6150	53.4135142	1.58561636	0.4707219	10.5431737	0.00116618	0.02516963
WHL22.5520	297.908495	1.58414519	0.32807175	21.8396294	2.96E-06	0.000238
WHL22.5536	62.4948959	1.58390765	0.40775828	14.6185698	0.00013161	0.00483277
WHL22.7673	109.263412	1.57990873	0.38341616	16.1019086	6.00E-05	0.00265057
WHL22.3401	82.1448631	1.57823193	0.40684284	14.7594974	0.00012213	0.0045593
WHL22.4936	97.6501588	1.56945731	0.36743985	17.4513553	2.95E-05	0.00150945
WHL22.5247	183.874059	1.56937667	0.30184279	26.1587516	3.14E-07	3.71E-05
WHL22.3925	95.0033054	1.56697841	0.49233492	8.96446288	0.00275282	0.04758494
WHL22.1316	178.749834	1.56223436	0.33302216	20.8310576	5.02E-06	0.0003768
WHL22.4389	778.601868	1.55621049	0.37617706	14.9844642	0.0001084	0.00415947
WHL22.4940	404.7237	1.55171399	0.34427247	18.5433215	1.66E-05	0.00098022
WHL22.2225	1446.45962	1.55051315	0.40218053	12.6016824	0.0003854	0.01093054
WHL22.5170	51.9464219	1.54935984	0.4841344	10.0516279	0.00152213	0.03081355
WHL22.3981	42.748697	1.54887167	0.44599592	11.8550213	0.00057506	0.01478694
WHL22.1493	203.636331	1.54788451	0.3426618	19.109737	1.23E-05	0.00075722
WHL22.4896	93.0897893	1.54346858	0.44104176	11.0046144	0.00090885	0.02087676
WHL22.4788	122.77937	1.53500717	0.37029596	16.4652383	4.96E-05	0.00232139
WHL22.4506	64.5449658	1.53003575	0.47110521	9.56536873	0.00198282	0.03745089
WHL22.6988	301.956077	1.52995368	0.28436701	27.8751276	1.29E-07	1.72E-05
WHL22.4705	253.901746	1.52757804	0.30018163	24.7683409	6.47E-07	6.80E-05
WHL22.1293	144.855839	1.52527191	0.4361833	10.6503721	0.00110049	0.02410432
WHL22.6664	120.564436	1.52213651	0.33844473	19.5415975	9.84E-06	0.00063873
WHL22.1502	733.667061	1.5210921	0.28874297	26.1699792	3.13E-07	3.71E-05
WHL22.5021	347.053643	1.51908415	0.30910354	22.8072983	1.79E-06	0.00016084
WHL22.2555	13584.8777	1.51514892	0.26086692	31.9568845	1.58E-08	2.64E-06
WHL22.1262	4463.6744	1.51161428	0.2994336	23.5853268	1.19E-06	0.00011481
WHL22.2660	579.080003	1.50944078	0.36574017	15.1681939	9.83E-05	0.00385728
WHL22.7741	438.107895	1.50923162	0.3122487	21.9094792	2.86E-06	0.00023305
WHL22.6082	15019.018	1.50864645	0.32549432	19.4033234	1.06E-05	0.0006726
WHL22.2211	3720.96734	1.5020322	0.24814673	35.025275	3.25E-09	6.72E-07
WHL22.5674	2832.93697	1.49287902	0.32907121	18.697129	1.53E-05	0.00091735
WHL22.6594	55.4249835	1.48869867	0.43724519	11.1386649	0.00084547	0.01980855
WHL22.7559	13722.5352	1.48718693	0.31821527	19.8860868	8.22E-06	0.00055366
WHL22.3174	783.403428	1.48612077	0.36761724	14.4201751	0.00014623	0.00517812
WHL22.5247	423.356571	1.48228845	0.26785289	29.576367	5.38E-08	7.93E-06
WHL22.5901	164.163771	1.48045335	0.35368287	16.4025086	5.12E-05	0.00237748
WHL22.6884	67.9077155	1.47480552	0.40192807	13.0632773	0.00030114	0.0090302
WHL22.6375	3632.28996	1.47469266	0.38231801	12.7475894	0.00035647	0.01027458
WHL22.6757	231.951346	1.46857298	0.38471076	13.1315935	0.00029036	0.008842
WHL22.7360	1613.74998	1.46525927	0.3626961	14.4531903	0.00014369	0.00511738
WHL22.1622	286.826988	1.46362055	0.41017341	11.0975482	0.00086442	0.02013837
WHL22.2706	129.176641	1.46249363	0.32439714	19.7654615	8.76E-06	0.00058339

WHL22.5674	222.582306	1.46170713	0.35504725	15.6884351	7.47E-05	0.00311642
WHL22.7557	102.30229	1.45988593	0.36268384	15.6359926	7.68E-05	0.00317341
WHL22.4389	1526.99523	1.45491088	0.38048297	12.6716587	0.00037124	0.01060173
WHL22.4229	3962.04384	1.45459499	0.25798343	30.3166711	3.67E-08	5.69E-06
WHL22.3119	510.399407	1.45332756	0.28487181	25.261638	5.01E-07	5.44E-05
WHL22.2815	86.4343426	1.45257171	0.39626002	12.8806741	0.00033199	0.00975557
WHL22.7322	370.227832	1.45257007	0.38179651	12.8935941	0.00032971	0.00973104
WHL22.2421	16072.3647	1.44952617	0.30406651	21.0420517	4.49E-06	0.00034375
WHL22.7421	1192.51504	1.44914199	0.28305902	24.7661443	6.47E-07	6.80E-05
WHL22.6546	88.9575951	1.44706128	0.41498486	11.2299045	0.0008049	0.0192585
WHL22.2000	141.179063	1.4468656	0.41220597	11.1652586	0.00083343	0.01963955
WHL22.6997	1927.79177	1.42919506	0.24883411	31.7031086	1.80E-08	2.97E-06
WHL22.2925	995.943752	1.41749182	0.27366653	25.5863543	4.23E-07	4.72E-05
WHL22.7561	16349.415	1.41069457	0.30417028	19.9321491	8.02E-06	0.00054642
WHL22.4373	470.244585	1.41045033	0.34125592	15.6351536	7.68E-05	0.00317341
WHL22.6503	263.322428	1.41012129	0.3036787	20.6732472	5.45E-06	0.00039713
WHL22.6004	2291.26253	1.40434004	0.28155752	23.4993952	1.25E-06	0.00011822
WHL22.4796	163.524138	1.40069742	0.32356191	18.1120345	2.08E-05	0.00116901
WHL22.6431	95.1902623	1.39704199	0.36224171	14.4352977	0.00014506	0.00515142
WHL22.6426	517.870359	1.39238155	0.40923213	9.87648036	0.00167405	0.03303847
WHL22.6278	350.372613	1.38813306	0.31988711	17.7198342	2.56E-05	0.00135563
WHL22.6216	114.630258	1.3849705	0.3490365	15.1936307	9.70E-05	0.00385446
WHL22.5203	47.9792939	1.37756978	0.42505628	10.3511697	0.00129393	0.02736677
WHL22.2475	322.338187	1.37517296	0.34472594	14.8848833	0.00011428	0.00434456
WHL22.3591	118.450016	1.37476515	0.36849743	13.2072573	0.00027887	0.00866236
WHL22.3984	113.059135	1.37349449	0.39165312	11.4784036	0.0007041	0.01724617
WHL22.5002	846.927606	1.3721342	0.30895962	18.4011995	1.79E-05	0.00104124
WHL22.1599	151.855092	1.3660003	0.32291039	17.4436846	2.96E-05	0.00150945
WHL22.2706	102.2997	1.36273395	0.34185602	15.5212171	8.16E-05	0.0033048
WHL22.4282	272.8501	1.36037358	0.29894932	19.8998026	8.16E-06	0.00055271
WHL22.3617	260.237198	1.34853492	0.34241077	14.4955426	0.00014049	0.00505945
WHL22.6028	220.883432	1.34832104	0.33519923	15.3020886	9.16E-05	0.00365482
WHL22.7180	1664.01804	1.34729742	0.27947344	22.0827469	2.61E-06	0.00022018
WHL22.1990	2150.80503	1.34485097	0.3705276	11.5925303	0.00066217	0.01651301
WHL22.6397	2847.2107	1.34096785	0.27618627	22.4027953	2.21E-06	0.00019026
WHL22.6469	123.888397	1.34035214	0.37277505	12.1536385	0.00048992	0.01311467
WHL22.4979	57.1381026	1.33978887	0.44102337	9.01229154	0.0026817	0.04705452
WHL22.2027	23590.5721	1.33628089	0.24110623	29.6434991	5.19E-08	7.75E-06
WHL22.4465	845.12741	1.33183064	0.30658273	17.6722544	2.62E-05	0.00138405
WHL22.5400	126.046939	1.32625282	0.32522189	16.2470625	5.56E-05	0.00249657
WHL22.4344	2870.64421	1.32616388	0.35766019	12.2205336	0.00047266	0.01270759
WHL22.4392	842.283012	1.3233818	0.26500079	24.0184067	9.54E-07	9.39E-05

WHL22.2926	222.841908	1.317212	0.33275964	14.8311334	0.00011758	0.00444288
WHL22.7681	342.108251	1.31403317	0.29314315	19.3757079	1.07E-05	0.00067891
WHL22.6035	109.706156	1.30790859	0.34137448	14.2817667	0.00015738	0.00551015
WHL22.2355	59.1365344	1.30670915	0.41925665	9.50539482	0.00204869	0.03835562
WHL22.3511	496.998075	1.30524209	0.3034064	17.5312647	2.83E-05	0.00146561
WHL22.7040	296.420955	1.30512919	0.28916436	19.6907806	9.10E-06	0.00059701
WHL22.4777	67.107618	1.30475122	0.42448933	9.05845186	0.00261483	0.04609991
WHL22.2999	116.034197	1.30469829	0.33467081	14.8063229	0.00011914	0.00448804
WHL22.6787	2778.29603	1.3021628	0.25332518	25.4605567	4.52E-07	4.95E-05
WHL22.6890	325.140073	1.29011371	0.30644907	16.963506	3.81E-05	0.00183765
WHL22.3948	536.055557	1.28860588	0.28687886	19.3255902	1.10E-05	0.00068646
WHL22.2556	92.5370177	1.28808554	0.34571653	13.6337413	0.00022216	0.00736172
WHL22.2142	64.5918888	1.28655845	0.39340903	10.4165189	0.00124893	0.02659665
WHL22.5225	457.393342	1.2847673	0.27705604	20.7760984	5.16E-06	0.00038312
WHL22.5098	186.178359	1.28444937	0.31067794	16.5976834	4.62E-05	0.00220267
WHL22.3267	363.486625	1.28197526	0.31642509	15.5148419	8.19E-05	0.0033048
WHL22.1925	10403.5858	1.28054705	0.2974578	17.3739288	3.07E-05	0.00154051
WHL22.2085	105.866482	1.27956396	0.38659702	10.4682619	0.00121443	0.02604089
WHL22.5650	6773.08527	1.27611183	0.29337387	17.8019365	2.45E-05	0.00130956
WHL22.3393	149.58081	1.27480836	0.34233103	13.2789233	0.00026841	0.00838172
WHL22.5811	1512.16478	1.27333984	0.33352447	13.3551894	0.00025771	0.00814806
WHL22.7478	554.841633	1.26474139	0.26663092	21.8193772	3.00E-06	0.000238
WHL22.5811	5772.47757	1.24854039	0.31970667	14.0868119	0.00017456	0.00604341
WHL22.4796	68.9199599	1.24315489	0.38633162	10.1839775	0.00141666	0.02944091
WHL22.4373	923.720614	1.24249489	0.36789395	10.1243938	0.0014632	0.029975
WHL22.5741	448.971646	1.24167702	0.29004712	17.5919343	2.74E-05	0.00143157
WHL22.7419	69.5687402	1.24049771	0.39723314	9.47408043	0.00208395	0.03870288
WHL22.6171	2815.44931	1.23906315	0.30078622	15.9375112	6.55E-05	0.00282589
WHL22.1493	792.732157	1.23862819	0.30506998	15.5207301	8.16E-05	0.0033048
WHL22.9711	1760.59003	1.23619529	0.28229583	18.2544267	1.93E-05	0.00109884
WHL22.5242	117.136246	1.23518597	0.35569947	11.60454	0.00065791	0.0164398
WHL22.3751	1675.90165	1.23066472	0.30669076	15.0927252	0.00010236	0.00398935
WHL22.4653	515.114848	1.22611955	0.2700738	19.99043	7.78E-06	0.00053295
WHL22.3392	533.641161	1.22562469	0.28074919	18.3696607	1.82E-05	0.00105367
WHL22.4579	161.984814	1.22355673	0.37840651	9.6734745	0.00186947	0.03614706
WHL22.9646	244.213945	1.21975223	0.30903785	15.1749036	9.80E-05	0.0038558
WHL22.7308	104.483621	1.21907267	0.34171361	12.5061671	0.00040561	0.01134795
WHL22.2957	733.869743	1.21842739	0.2958405	16.1296802	5.91E-05	0.00262761
WHL22.9646	127.013221	1.21832493	0.33381058	12.9537413	0.00031928	0.0095354
WHL22.7104	393.009815	1.21792851	0.28006231	18.3418156	1.85E-05	0.00106421
WHL22.6748	288.156925	1.21690121	0.28924875	17.2286517	3.31E-05	0.00162991
WHL22.1543	3092.99876	1.21448987	0.25342243	22.2189826	2.43E-06	0.0002065

WHL22.3222	304.510316	1.21073104	0.32551424	13.0698754	0.00030008	0.00902726
WHL22.3945	157.552641	1.20912557	0.3288991	13.101211	0.0002951	0.00894262
WHL22.4900	189.505272	1.20674796	0.35034922	11.2001029	0.00081793	0.01942031
WHL22.1730	480.383457	1.20555019	0.28080322	17.8281323	2.42E-05	0.00129725
WHL22.4989	821.587869	1.2027547	0.33198995	12.1394309	0.00049367	0.01313235
WHL22.6576	1842.30361	1.19810531	0.32663479	12.4112295	0.00042676	0.0117019
WHL22.5225	761.73205	1.19783812	0.28055838	17.5070881	2.86E-05	0.00147818
WHL22.4394	295.033531	1.19675396	0.31160847	14.1054719	0.00017284	0.00600051
WHL22.2088	9531.79408	1.19413195	0.25679511	20.8620275	4.94E-06	0.0003753
WHL22.5325	390.37973	1.19379627	0.2807111	17.5343743	2.82E-05	0.00146561
WHL22.1741	1030.19341	1.19178755	0.29129481	15.9318195	6.57E-05	0.00282589
WHL22.7602	25491.125	1.19175322	0.34221433	10.9862846	0.00091789	0.02098945
WHL22.3596	358.935801	1.18952836	0.33147224	12.0550542	0.00051652	0.01367899
WHL22.7483	297.647212	1.18911456	0.28868421	16.5454793	4.75E-05	0.00224687
WHL22.6585	958.937612	1.18818391	0.33093646	11.9099674	0.00055834	0.01456866
WHL22.4523	149.014586	1.18800496	0.34061233	11.6890131	0.0006287	0.01577356
WHL22.7191	288.423961	1.18536553	0.3002479	15.0296387	0.00010584	0.00409916
WHL22.4718	952.730781	1.18313512	0.28715716	16.2199088	5.64E-05	0.00252347
WHL22.3706	3187.62799	1.17952404	0.3084896	13.6771525	0.00021708	0.00721309
WHL22.5466	935.951332	1.17766372	0.30078147	14.5176382	0.00013885	0.00504481
WHL22.4395	1223.2164	1.17725724	0.28434543	16.3763807	5.19E-05	0.00239256
WHL22.1850	718.788726	1.17509382	0.34743147	10.4427548	0.00123131	0.02631193
WHL22.1918	137.178255	1.17442229	0.34293201	11.3065724	0.00077233	0.01865942
WHL22.6052	4872.25845	1.17092549	0.24687549	21.8440894	2.96E-06	0.000238
WHL22.5199	37914.8966	1.16918903	0.24168803	22.750653	1.84E-06	0.00016446
WHL22.4088	544.91405	1.16860435	0.27091227	18.074134	2.12E-05	0.00117559
WHL22.1474	246.526313	1.16637168	0.33166476	11.8398476	0.00057977	0.01487705
WHL22.7625	2654.39724	1.16204308	0.28027588	16.4220372	5.07E-05	0.00236196
WHL22.4911	649.07616	1.16138381	0.27446313	17.3362545	3.13E-05	0.00156502
WHL22.4008	633.232491	1.15702472	0.27485384	17.1357692	3.48E-05	0.00169811
WHL22.1125	345.311617	1.15635602	0.28612523	15.8549118	6.84E-05	0.00293291
WHL22.4376	161.98302	1.15516947	0.32184475	12.6781439	0.00036995	0.01058942
WHL22.3844	2278.64536	1.15431822	0.24525906	21.5790737	3.40E-06	0.00026634
WHL22.5302	104.243241	1.15131702	0.36733466	9.47243479	0.00208582	0.03870288
WHL22.7591	4338.70938	1.14932452	0.2652333	18.0851294	2.11E-05	0.00117407
WHL22.4232	2941.50447	1.1478105	0.29597716	14.2057838	0.00016387	0.00570493
WHL22.1119	3781.40801	1.14629351	0.34060853	10.280911	0.00134414	0.0282839
WHL22.7324	183.376939	1.14477059	0.30644572	13.6261982	0.00022305	0.00736172
WHL22.6341	133.259878	1.1439754	0.37110916	8.96845134	0.00274681	0.04754749
WHL22.6546	299.073614	1.14354084	0.33279624	11.1301893	0.00084934	0.01986172
WHL22.4393	440.242312	1.14217127	0.28460921	15.590567	7.86E-05	0.00322761
WHL22.4162	287.225259	1.1420009	0.30242879	13.7645411	0.00020721	0.00694632

WHL22.1011	135.576985	1.14029969	0.34473305	10.5407584	0.0011677	0.02516963
WHL22.5909	757.455173	1.13965672	0.25944071	18.8086967	1.45E-05	0.00087795
WHL22.2592	152.043343	1.1395921	0.35076786	10.0648774	0.00151123	0.03075556
WHL22.6546	151.911878	1.13865148	0.32568029	11.8733157	0.00056944	0.0147341
WHL22.1483	168.072215	1.13671521	0.31817093	12.4817706	0.00041094	0.01143242
WHL22.5025	1740.80646	1.13670134	0.29803252	13.7650109	0.00020716	0.00694632
WHL22.5466	1753.5801	1.12556362	0.30605345	12.7223751	0.00036131	0.01036582
WHL22.7482	676.815403	1.12524614	0.30060927	13.3728073	0.0002553	0.00809252
WHL22.4414	1907.79896	1.12449713	0.2969476	13.5871713	0.00022774	0.00744838
WHL22.6830	1121.56245	1.12398938	0.31228445	12.1440097	0.00049246	0.01313235
WHL22.3407	920.770159	1.12394168	0.25253184	19.3478949	1.09E-05	0.00068192
WHL22.1943	789.66577	1.12178978	0.29828041	13.4662199	0.0002429	0.00777778
WHL22.2234	273.448832	1.12163035	0.28461185	15.1859604	9.74E-05	0.0038558
WHL22.5499	138.824753	1.12152214	0.31571432	12.4121483	0.00042655	0.0117019
WHL22.1583	215.624031	1.12076457	0.34338033	10.1729972	0.00142512	0.02944091
WHL22.3898	217.233049	1.1159296	0.2909168	14.457568	0.00014335	0.00511738
WHL22.6432	80.0163819	1.10967041	0.36724354	9.00526438	0.00269203	0.04712574
WHL22.4612	485.884352	1.10839992	0.30791908	12.3312182	0.00044545	0.01213374
WHL22.4731	100.831845	1.104503	0.34237408	10.2276015	0.00138354	0.02896563
WHL22.3121	1139.83064	1.10206727	0.33882213	9.72471924	0.00181806	0.03531826
WHL22.2525	148.699968	1.09547315	0.34008581	9.99446358	0.00157012	0.03143782
WHL22.4913	95.6333437	1.09528085	0.34873297	9.70489018	0.00183778	0.03564551
WHL22.6259	1490.10507	1.0939304	0.28762724	13.8217624	0.00020099	0.00680636
WHL22.1743	554.412254	1.09014534	0.34844962	8.99294142	0.00271024	0.04724439
WHL22.4227	332.146598	1.08612754	0.28812399	13.8611922	0.00019682	0.00668929
WHL22.1926	2335.58637	1.08587808	0.34102577	9.26326538	0.00233796	0.04224002
WHL22.3059	310.328052	1.08340981	0.28028946	14.615932	0.0001318	0.00483277
WHL22.3806	141.684134	1.07809108	0.33110854	10.3272046	0.00131084	0.0276301
WHL22.4989	923.357793	1.07523369	0.32992309	9.87023667	0.00167974	0.03309807
WHL22.1745	142.612	1.07019799	0.32041626	10.9298596	0.00094627	0.02159858
WHL22.2402	126.438266	1.07010305	0.34602025	9.25869491	0.0023438	0.04226835
WHL22.2178	865.703229	1.06942065	0.2656388	15.7652863	7.17E-05	0.00304358
WHL22.4765	399.308103	1.06711713	0.30201144	11.9997855	0.00053207	0.01397126
WHL22.2429	205.207714	1.06711024	0.31959604	10.8028844	0.00101342	0.02291348
WHL22.3180	9983.28536	1.06461257	0.28321623	13.4929734	0.00023946	0.0077087
WHL22.4938	548.700052	1.0603202	0.26506714	15.6679897	7.55E-05	0.00313972
WHL22.2146	4853.90075	1.05930587	0.33133482	9.40355087	0.00216566	0.03982365
WHL22.5490	371.622337	1.05509544	0.30912631	11.1594796	0.00083603	0.01963955
WHL22.5248	1817.26268	1.04866367	0.32404092	9.74533091	0.00179779	0.03508942
WHL22.4725	3854.39014	1.04796892	0.25625074	16.2525289	5.54E-05	0.00249657
WHL22.5175	262.849885	1.04759005	0.28579287	13.1708254	0.00028434	0.00874893
WHL22.7697	1601.47078	1.04462191	0.28193606	13.1848467	0.00028222	0.00874465

WHL22.5534	247.033794	1.0435088	0.28947446	12.7243905	0.00036092	0.01036582
WHL22.1310	614.492407	1.04101043	0.30232635	11.3111303	0.00077044	0.01865003
WHL22.1788	165.815205	1.04053729	0.31328699	10.7969179	0.00101669	0.02291348
WHL22.7803	590.421284	1.03729322	0.30346476	11.1580689	0.00083667	0.01963955
WHL22.2408	439.19387	1.02495961	0.27775716	13.2861654	0.00026737	0.00838172
WHL22.9711	282.589643	1.02311486	0.31449404	10.1646445	0.0014316	0.02947374
WHL22.6214	2287.48885	1.02217647	0.26313601	14.6444778	0.00012981	0.00480275
WHL22.6322	169.528734	1.01985648	0.31881926	10.0493464	0.00152402	0.03081355
WHL22.6382	127.609657	1.01382493	0.32409548	9.63513084	0.00190891	0.03673755
WHL22.4022	5813.23626	1.01263802	0.27739737	12.799115	0.00034678	0.01006565
WHL22.6009	138.347407	1.00883632	0.32878088	9.18154414	0.00244468	0.04365897
WHL22.6866	528.438963	1.00766975	0.27495292	13.0907709	0.00029675	0.00894884
WHL22.6124	477.49723	1.00663829	0.26829236	13.7867499	0.00020478	0.00691549
WHL22.5633	544.365161	1.00643069	0.27402289	13.1647969	0.00028526	0.00874893
WHL22.4614	580.279949	1.0057407	0.29596082	11.1194745	0.00085426	0.01993917
WHL22.5036	592.405314	1.00129945	0.26969323	13.4554797	0.00024429	0.00778342
WHL22.2314	899.288587	0.99852056	0.28469116	11.8568341	0.0005745	0.01478694
WHL22.6914	166.53894	0.99763855	0.31011839	10.1876245	0.00141386	0.02944091
WHL22.2081	681.474553	0.99594441	0.28378083	11.9130525	0.00055742	0.01456866
WHL22.6888	294.963609	0.99005723	0.31811917	9.27047931	0.00232877	0.04224002
WHL22.7317	217.023065	0.98882779	0.29901133	10.7052151	0.00106834	0.02378363
WHL22.2749	983.688969	0.98736971	0.25663002	14.4909408	0.00014084	0.00505945
WHL22.7045	655.471088	0.98047097	0.28451625	11.4911236	0.00069929	0.0172307
WHL22.2976	344.953948	0.96934603	0.28093779	11.6647345	0.00063696	0.01594846
WHL22.1371	140.088984	0.96789233	0.31253462	9.46907468	0.00208965	0.03870288
WHL22.2925	10476.5045	0.96222577	0.27528213	11.765691	0.00060332	0.01532525
WHL22.1022	475.834761	0.96082248	0.27156582	12.2572878	0.00046344	0.01251401
WHL22.4027	266.746955	0.96009435	0.30721237	9.46700617	0.00209201	0.03870288
WHL22.5468	843.666777	0.95817425	0.27034638	12.2740038	0.00045931	0.01247413
WHL22.2971	2444.9646	0.95784648	0.25341929	13.9660213	0.00018614	0.00639079
WHL22.6866	256.602081	0.9529927	0.30839076	9.2567059	0.00234635	0.04226835
WHL22.2449	3913.27901	0.95225265	0.27291613	11.7616036	0.00060465	0.01532525
WHL22.6702	302.434687	0.95085753	0.29072721	10.4538492	0.00122394	0.02619953
WHL22.4675	174.223075	0.94528963	0.30291113	9.60781466	0.00193751	0.03688711
WHL22.2612	3387.90861	0.9446622	0.27942912	11.0031141	0.00090959	0.02087676
WHL22.4794	1785.01946	0.94197928	0.29654704	9.62238126	0.0019222	0.03677938
WHL22.3283	165.140312	0.94026272	0.30381368	9.45817521	0.0021021	0.03871239
WHL22.2563	480.847039	0.93602704	0.26968772	11.8319227	0.00058224	0.01490963
WHL22.7683	6281.55185	0.9359862	0.26583478	12.0232851	0.0005254	0.01383884
WHL22.4922	1447.397	0.93467917	0.27798425	10.9253624	0.00094857	0.02161127
WHL22.7652	1282.32321	0.92984361	0.2511473	13.4616692	0.00024349	0.00777778
WHL22.2291	1121.91152	0.92818515	0.25677337	12.804734	0.00034574	0.01005902

WHL22.5520	25482.544	0.92677166	0.27833724	10.6622377	0.00109345	0.02407144
WHL22.5133	482.969551	0.92656249	0.26776603	11.7623444	0.00060441	0.01532525
WHL22.3727	663.942299	0.9218122	0.26288256	12.0724912	0.00051171	0.01358066
WHL22.1806	1160.66746	0.92179638	0.24905162	13.4773372	0.00024146	0.00775306
WHL22.4452	1390.08298	0.91860556	0.28179498	10.2572783	0.00136146	0.02855158
WHL22.2612	2845.13044	0.91652891	0.28985409	9.57192518	0.00197575	0.03745089
WHL22.7423	939.428281	0.91407395	0.30015358	8.87761297	0.00288689	0.0495569
WHL22.1308	4259.60024	0.91366731	0.25689637	12.3457502	0.00044199	0.01209281
WHL22.7431	2750.44358	0.91097338	0.26508878	11.4833618	0.00070222	0.01723429
WHL22.3109	20356.8808	0.90320833	0.24054373	13.859506	0.000197	0.00668929
WHL22.4152	4348.74587	0.90107161	0.24296131	13.5230928	0.00023565	0.00762557
WHL22.7698	531.809009	0.90030211	0.28754418	9.51796907	0.0020347	0.03815133
WHL22.6874	642.775971	0.89909095	0.26194226	11.5795876	0.0006668	0.01659495
WHL22.6176	718.615844	0.89712678	0.26005084	11.6960523	0.00062633	0.01574587
WHL22.5343	617.278191	0.89449429	0.27373971	10.4354438	0.0012362	0.02637081
WHL22.6530	1593.88011	0.89358119	0.25071855	12.4797032	0.0004114	0.01143242
WHL22.1691	1043.94797	0.88922959	0.27028848	10.5486262	0.00116274	0.02515019
WHL22.5589	843.393448	0.88465722	0.25468232	11.8786225	0.00056782	0.01472291
WHL22.6028	454.714682	0.8834198	0.29219125	8.87349932	0.0028934	0.0496
WHL22.7045	452.051673	0.88326359	0.2860732	9.28796953	0.00230664	0.04198011
WHL22.4016	4986.88019	0.8830658	0.25911319	11.3316058	0.00076199	0.01855423
WHL22.5253	943.255678	0.88034378	0.25362371	11.858966	0.00057384	0.01478694
WHL22.5534	295.502178	0.87635428	0.28494937	9.28892675	0.00230543	0.04198011
WHL22.3731	532.788612	0.86685408	0.28498456	9.03796847	0.00264429	0.04655308
WHL22.4237	952.945793	0.86516025	0.25526475	11.3011976	0.00077457	0.01867711
WHL22.2231	649.182403	0.86494022	0.2621665	10.7043099	0.00106886	0.02378363
WHL22.1850	988.223106	0.85936643	0.26707382	10.1212207	0.00146572	0.0299771
WHL22.2456	5313.07148	0.84336512	0.27275731	9.26398853	0.00233704	0.04224002
WHL22.6305	2621.76743	0.84005417	0.2606431	10.1690869	0.00142815	0.02945173
WHL22.6476	611.884415	0.82985893	0.26541566	9.61485117	0.0019301	0.03680257
WHL22.2486	1182.87315	0.82256036	0.26114145	9.72970697	0.00181313	0.03527784
WHL22.7106	687.912323	0.82207316	0.26786877	9.27671105	0.00232086	0.042177
WHL22.4758	413.298405	0.81631089	0.26843476	9.13492953	0.00250775	0.04459264
WHL22.4217	1405.39682	0.81535157	0.26052352	9.60299166	0.00194261	0.03692739
WHL22.7044	1652.95661	0.81314088	0.25604405	9.90605834	0.00164736	0.03261554
WHL22.4805	4089.4807	0.81094142	0.25958691	9.54926051	0.0020003	0.03763304
WHL22.8179	6569.95771	0.79603288	0.26030614	9.13963965	0.0025013	0.04454189
WHL22.3476	2045.68233	0.78743218	0.24736131	9.99542465	0.0015693	0.03143782
WHL22.7477	5489.86928	0.78477137	0.24554338	10.0650327	0.0015111	0.03075556
WHL22.5433	1636.53627	0.77445978	0.2500997	9.45919782	0.00210093	0.03871239
WHL22.4438	1404.34035	0.74981545	0.24922368	8.94200106	0.00278687	0.04797291
WHL22.4916	7690.12734	-0.7569781	0.23990592	9.84052029	0.00170709	0.03353043

WHL22.2862	8894.09931	-0.7665098	0.24647431	9.52597959	0.00202583	0.03804271
WHL22.3698	3187.34276	-0.7808714	0.24840139	9.73329647	0.0018096	0.03526437
WHL22.4388	538.624621	-0.7860149	0.2608442	8.9764844	0.00273476	0.04740511
WHL22.4408	1099.43677	-0.8050842	0.25254118	10.0208942	0.00154774	0.03124223
WHL22.1474	938.607692	-0.8094397	0.25452146	9.97184328	0.00158952	0.03172391
WHL22.5353	1176.30123	-0.8200327	0.27077687	8.9451783	0.00278203	0.04797291
WHL22.3038	936.71388	-0.8216077	0.25561444	10.1760473	0.00142277	0.02944091
WHL22.6333	508.838917	-0.8241237	0.27338679	8.92025905	0.00282025	0.04848005
WHL22.1458	736.102194	-0.826017	0.2634932	9.66277248	0.0018804	0.03628828
WHL22.3660	2782.17254	-0.8339919	0.24749259	11.1755888	0.00082881	0.01960347
WHL22.4554	1753.02232	-0.8382073	0.2572648	10.4077423	0.00125488	0.02667752
WHL22.2637	650.234145	-0.8458627	0.25589652	10.7891641	0.00102096	0.02296511
WHL22.3038	342.210705	-0.8458778	0.27307238	9.47368507	0.0020844	0.03870288
WHL22.4797	487.459447	-0.8467552	0.26870643	9.76965547	0.00177416	0.0347376
WHL22.1792	277.710043	-0.852599	0.28228468	8.99548366	0.00270648	0.04724439
WHL22.3057	442.816081	-0.8545598	0.26858708	9.99464941	0.00156996	0.03143782
WHL22.6944	766.440752	-0.8553945	0.27322744	9.56834633	0.00197961	0.03745089
WHL22.1790	716.333489	-0.8558741	0.26391527	10.3294062	0.00130927	0.0276301
WHL22.2794	1434.32263	-0.8614204	0.27579212	9.46664026	0.00209242	0.03870288
WHL22.6845	3673.56674	-0.8618125	0.25474059	11.2051877	0.00081569	0.01940434
WHL22.1089	446.839701	-0.8618493	0.26439717	10.4864672	0.00120252	0.02583023
WHL22.4058	381.90315	-0.8628113	0.26967549	10.1008437	0.00148201	0.03026044
WHL22.1299	523.50219	-0.8643369	0.26168971	10.7636115	0.00103515	0.02320013
WHL22.4536	458.304973	-0.8704179	0.26833861	10.3646249	0.00128453	0.02721447
WHL22.2354	245.096553	-0.8710598	0.28883211	8.98795343	0.00271765	0.04725319
WHL22.1764	443.986575	-0.8724544	0.2659034	10.6182363	0.00111978	0.02439109
WHL22.2895	11776.6681	-0.8727624	0.24417966	12.5532946	0.00039551	0.01111549
WHL22.3676	3996.56836	-0.8730853	0.24490357	12.4977914	0.00040743	0.01137326
WHL22.4272	1019.27853	-0.8744526	0.27223962	10.0534752	0.00152061	0.03081355
WHL22.6524	410.598817	-0.878112	0.27332653	10.1551574	0.00143898	0.0295277
WHL22.3492	2086.477	-0.8797964	0.24359705	12.8521782	0.00033709	0.00987672
WHL22.3426	490.372738	-0.8859572	0.29106143	8.98746821	0.00271837	0.04725319
WHL22.3729	311.469979	-0.8864638	0.27918168	9.93144734	0.00162479	0.03222018
WHL22.7025	1268.578	-0.8870934	0.25870552	11.5204377	0.00068835	0.01702881
WHL22.5199	462.151961	-0.8893725	0.28649794	9.38216107	0.00219107	0.0401718
WHL22.7058	522.937692	-0.8952744	0.29122983	9.16014439	0.00247343	0.04410892
WHL22.5784	936.410368	-0.8991051	0.25703468	12.0235976	0.00052531	0.01383884
WHL22.3359	548.514527	-0.9003882	0.27260537	10.6872814	0.00107875	0.02391767
WHL22.6795	199.890433	-0.9021732	0.29894401	8.99914896	0.00270105	0.04721701
WHL22.2871	242.049135	-0.9042872	0.29529339	9.204298	0.00241448	0.04318183
WHL22.3660	1428.77295	-0.9043588	0.24657304	13.247257	0.00027298	0.00850076
WHL22.3121	672.659458	-0.9117222	0.27145843	11.0200696	0.00090131	0.02080223

WHL22.5837	317.994782	-0.9125363	0.27729948	10.6723062	0.00108751	0.0239975
WHL22.7086	275.678361	-0.9129733	0.29069814	9.67838109	0.00186449	0.03610698
WHL22.7039	8358.78054	-0.9159358	0.25649142	12.4381138	0.00042066	0.01161173
WHL22.2913	336.760919	-0.9199165	0.30061931	9.12604792	0.00251995	0.04474545
WHL22.7019	1447.17078	-0.9224142	0.24805057	13.5972546	0.00022652	0.00744681
WHL22.8406	503.670439	-0.9310619	0.27941728	10.8252445	0.00100125	0.02272811
WHL22.6253	370.814711	-0.9342249	0.28190263	10.7966931	0.00101682	0.02291348
WHL22.1494	284.109644	-0.9345555	0.28364599	10.6712165	0.00108816	0.0239975
WHL22.2872	492.433095	-0.9421797	0.27957856	11.0756709	0.00087468	0.02032322
WHL22.6879	231.854835	-0.9456376	0.30142617	9.61721242	0.00192762	0.03680257
WHL22.6619	657.934906	-0.9488681	0.26406341	12.6582607	0.00037391	0.01065342
WHL22.2898	200.831429	-0.9493318	0.29709577	10.0525577	0.00152137	0.03081355
WHL22.7596	349.495902	-0.9500041	0.28774632	10.6317494	0.00111163	0.02425613
WHL22.3354	933.370912	-0.9505656	0.26226937	12.8435123	0.00033865	0.00989916
WHL22.5173	194.30322	-0.9631251	0.30826264	9.56873045	0.0019792	0.03745089
WHL22.4600	1920.82745	-0.9671382	0.25917464	13.5819797	0.00022837	0.00744838
WHL22.5177	143.368162	-0.9674781	0.31805606	9.12025916	0.00252794	0.04482304
WHL22.5181	1122.84803	-0.96918	0.2859919	11.0689373	0.00087786	0.02033681
WHL22.5677	730.763404	-0.9738648	0.31520937	9.02589773	0.00266181	0.04679503
WHL22.3221	340.588766	-0.9773913	0.30479025	9.93380455	0.00162271	0.03222018
WHL22.5659	238.073617	-0.9859144	0.30961516	9.85142926	0.001697	0.03338508
WHL22.1395	237.764014	-0.9865316	0.30783266	10.0056635	0.0015606	0.03139939
WHL22.9036	694.808962	-0.9883105	0.27198123	12.8797032	0.00033216	0.00975557
WHL22.1511	254.518093	-0.9899536	0.30545167	10.2132064	0.00139439	0.02914336
WHL22.4764	290.32717	-0.9926811	0.28950284	11.4923523	0.00069883	0.0172307
WHL22.7517	303.562528	-0.9963792	0.27683486	12.7570404	0.00035467	0.01024662
WHL22.5060	496.839264	-1.0010868	0.27859146	12.5783253	0.00039025	0.01099253
WHL22.6936	1225.60316	-1.0020296	0.2707522	13.2784093	0.00026848	0.00838172
WHL22.6630	1019.36717	-1.0034689	0.25631271	15.0028779	0.00010735	0.00413187
WHL22.6807	197.578493	-1.0048497	0.31974942	9.56312022	0.00198525	0.03745089
WHL22.9029	278.634401	-1.0127105	0.31687101	9.80360247	0.0017417	0.03415613
WHL22.5669	285.35627	-1.0147624	0.29274091	11.7180031	0.00061898	0.01559285
WHL22.1339	1032.88852	-1.0187586	0.28005491	12.7665302	0.00035288	0.01021859
WHL22.4249	116.000801	-1.0187894	0.32996445	9.39250843	0.00217874	0.04000488
WHL22.5328	482.520958	-1.0189225	0.2947257	11.5298128	0.00068489	0.01697703
WHL22.1791	472.017351	-1.0214421	0.28307578	12.6528073	0.000375	0.01066004
WHL22.6216	6271.09172	-1.0295407	0.29880783	11.2335452	0.00080332	0.0192585
WHL22.2276	252.798069	-1.0303066	0.30389901	11.1614755	0.00083513	0.01963955
WHL22.6282	279.347203	-1.0354882	0.28094676	13.3472775	0.0002588	0.00816169
WHL22.6803	138.593213	-1.0412239	0.32315103	10.1728348	0.00142525	0.02944091
WHL22.5392	213.830001	-1.0433661	0.31809294	10.3910818	0.00126625	0.02687321
WHL22.1731	114.705796	-1.0478182	0.34088872	9.2314919	0.00237888	0.04266832

WHL22.6624	242.24679	-1.0491984	0.29902036	12.0214867	0.00052591	0.01383884
WHL22.4389	170.674336	-1.0521921	0.30865	11.3975519	0.00073541	0.01797765
WHL22.4852	486.873476	-1.0572518	0.31611491	10.5970296	0.00113269	0.02454304
WHL22.6522	656.765754	-1.0596266	0.26345327	15.799914	7.04E-05	0.00300899
WHL22.5806	167.188041	-1.0600844	0.31313168	11.2224811	0.00080812	0.01929843
WHL22.1460	1301.8748	-1.0613323	0.25786683	16.5030381	4.86E-05	0.00228899
WHL22.5566	1011.52225	-1.066039	0.25481957	17.0982741	3.55E-05	0.00172517
WHL22.3625	229.171408	-1.0682079	0.29408105	12.9287386	0.00032358	0.00961726
WHL22.5215	766.657089	-1.0687196	0.29557273	12.5121957	0.0004043	0.01133698
WHL22.5222	655.498003	-1.0737644	0.29250344	12.9299138	0.00032337	0.00961726
WHL22.6278	103.156681	-1.0743078	0.35222271	9.07684851	0.00258866	0.04570345
WHL22.3202	277.053923	-1.0745839	0.29508839	12.9172179	0.00032557	0.00965348
WHL22.6445	414.462299	-1.0754829	0.27000334	15.5491194	8.04E-05	0.00327744
WHL22.3557	378.393023	-1.0781909	0.28875138	13.5561895	0.00023153	0.00751189
WHL22.3259	100.871989	-1.0804601	0.35594143	9.01061182	0.00268417	0.04705452
WHL22.6893	96.3869863	-1.0827027	0.34676761	9.62166839	0.00192295	0.03677938
WHL22.5362	314.402032	-1.096126	0.32420017	10.8697051	0.0009775	0.02222963
WHL22.3897	115.520186	-1.0986603	0.33397187	10.6498836	0.00110078	0.02410432
WHL22.4637	462.822269	-1.1020224	0.26720028	16.6424667	4.51E-05	0.00215958
WHL22.6473	1602.55169	-1.1022594	0.27988565	14.8880754	0.00011408	0.00434456
WHL22.3496	392.389684	-1.1048565	0.27309286	16.0571196	6.15E-05	0.00268217
WHL22.5389	122.984183	-1.1080736	0.32798958	11.213159	0.00081219	0.01935832
WHL22.5061	406.21033	-1.1128762	0.30170462	13.0601948	0.00030164	0.0090302
WHL22.4779	361.06279	-1.1268736	0.31045048	12.5812422	0.00038964	0.01099253
WHL22.3221	149.383361	-1.128527	0.33229447	11.1927397	0.00082118	0.01946024
WHL22.7720	632.011369	-1.1356413	0.29613666	14.0604122	0.00017703	0.00611176
WHL22.6315	1493.92669	-1.1387946	0.27878526	15.9996156	6.34E-05	0.00275518
WHL22.7666	107.055858	-1.1430606	0.36816407	9.26415554	0.00233682	0.04224002
WHL22.3468	446.833705	-1.1459058	0.2915319	14.9309768	0.00011152	0.00426586
WHL22.4156	105.476481	-1.1516417	0.36509254	9.66058751	0.00188263	0.03628828
WHL22.3976	8118.22497	-1.1568648	0.29367401	14.6505726	0.0001294	0.00480157
WHL22.6404	120.624999	-1.1570407	0.36524281	9.62529213	0.00191916	0.03677938
WHL22.4281	374.881856	-1.1579973	0.3125526	13.1257271	0.00029127	0.00884799
WHL22.5654	254.437172	-1.1583941	0.30964605	13.5027631	0.00023821	0.00768855
WHL22.2247	510.766157	-1.158587	0.32598935	11.8209814	0.00058567	0.01496658
WHL22.7204	97.9855023	-1.1604702	0.34212628	11.3258453	0.00076436	0.01857538
WHL22.6126	2044.88955	-1.1613938	0.30817132	13.3186387	0.00026278	0.00826626
WHL22.3644	181.473663	-1.1640549	0.31193934	13.5628862	0.0002307	0.00750478
WHL22.1826	178.351364	-1.1664302	0.31238576	13.5832844	0.00022821	0.00744838
WHL22.5537	324.647824	-1.1680888	0.27666045	17.4333045	2.98E-05	0.00151149
WHL22.5477	566.380364	-1.1751435	0.29631735	15.0176536	0.00010651	0.00411242
WHL22.8938	475.697022	-1.1759716	0.2725392	18.1105098	2.08E-05	0.00116901

WHL22.3668	241.546856	-1.1760742	0.31832353	13.1566295	0.0002865	0.00874893
WHL22.3221	974.927023	-1.1776784	0.30821116	13.7605638	0.00020765	0.00694632
WHL22.1007	111.726861	-1.1795413	0.36638776	9.97924269	0.00158315	0.03164764
WHL22.2381	133.673288	-1.1821714	0.35030289	11.0130343	0.00090473	0.02084252
WHL22.1633	206.938704	-1.1844838	0.3292739	12.4610092	0.00041554	0.01149586
WHL22.2898	249.619733	-1.1874666	0.34970647	10.8120157	0.00100843	0.02284924
WHL22.3097	79.7201362	-1.1919809	0.3888028	9.11252062	0.00253866	0.04494876
WHL22.9714	204.929166	-1.193421	0.33135233	12.4324117	0.00042195	0.01162135
WHL22.5721	253.018451	-1.1945434	0.37050195	9.54863437	0.00200098	0.03763304
WHL22.6216	222.058782	-1.2017674	0.33517563	12.2222749	0.00047222	0.01270759
WHL22.5636	127.162152	-1.2023625	0.35234615	11.2315719	0.00080418	0.0192585
WHL22.1916	944.003559	-1.2038861	0.26234055	20.418408	6.22E-06	0.00044072
WHL22.7526	67.3186101	-1.2112236	0.39013222	9.4794876	0.00207782	0.03870288
WHL22.1207	409.688051	-1.2177288	0.34950294	11.3121423	0.00077002	0.01865003
WHL22.1917	98.6272509	-1.2202015	0.34924076	11.9397858	0.00054948	0.01439795
WHL22.7239	260.176481	-1.22108	0.2917181	17.0617112	3.62E-05	0.00175184
WHL22.6844	193.844308	-1.2251719	0.37427797	9.89604607	0.00165634	0.03274117
WHL22.1561	362.597899	-1.2257045	0.32749276	13.1751417	0.00028369	0.00874893
WHL22.6825	242.976749	-1.2259382	0.28750668	17.7552125	2.51E-05	0.00133636
WHL22.5859	452.133546	-1.2269727	0.35689757	10.9956242	0.00091327	0.02092255
WHL22.7342	251.817485	-1.2293067	0.30188931	16.0856913	6.05E-05	0.00265134
WHL22.2394	166.634324	-1.236908	0.31722295	14.8382756	0.00011713	0.00443963
WHL22.6219	78.2589518	-1.2437523	0.36305535	11.5591782	0.00067416	0.01674448
WHL22.7546	74.4252458	-1.2573394	0.38176339	10.5987483	0.00113164	0.02454304
WHL22.7342	64.507065	-1.2575345	0.40831704	9.23344883	0.00237634	0.04266832
WHL22.3655	75.2373559	-1.2580004	0.37890787	10.7708811	0.00103109	0.02315105
WHL22.1045	63.4534697	-1.2611659	0.39167777	10.1744222	0.00142402	0.02944091
WHL22.1982	111.197579	-1.2616744	0.37549309	10.7487278	0.00104351	0.02334525
WHL22.2528	4421.35848	-1.2644326	0.30820372	15.6891564	7.47E-05	0.00311642
WHL22.7549	242.805778	-1.265444	0.39311083	9.32350011	0.00226233	0.04141709
WHL22.4352	623.341739	-1.2705891	0.27350717	20.8319511	5.01E-06	0.0003768
WHL22.6357	238.303404	-1.2742642	0.30984531	16.26273	5.51E-05	0.00249408
WHL22.7670	512.848173	-1.2748186	0.2715898	21.3440623	3.84E-06	0.00029731
WHL22.5772	113.549964	-1.2759999	0.40283609	9.30613749	0.00228387	0.04174977
WHL22.3417	107.471849	-1.2778251	0.40657376	9.29485312	0.00229799	0.04194585
WHL22.5821	175.217995	-1.279211	0.31687477	15.7748319	7.13E-05	0.00303867
WHL22.6602	375.098989	-1.279957	0.37094192	10.7143405	0.00106308	0.02374028
WHL22.4592	492.746364	-1.282301	0.37183664	10.6878771	0.0010784	0.02391767
WHL22.1001	140.063157	-1.2839102	0.32466072	15.3546779	8.91E-05	0.00357381
WHL22.6289	465.977055	-1.296952	0.27026041	22.3690981	2.25E-06	0.00019229
WHL22.9040	201.999311	-1.3004892	0.30192042	18.0397687	2.16E-05	0.00119169
WHL22.3065	424.948623	-1.3011137	0.31265047	16.3824746	5.18E-05	0.00239256

WHL22.1763	61.8141216	-1.3077069	0.41492683	9.6302429	0.00191399	0.03677834
WHL22.7282	3428.03809	-1.3106487	0.2874377	19.6311705	9.39E-06	0.00061268
WHL22.3466	293.499499	-1.3127004	0.28446979	20.6814326	5.42E-06	0.00039713
WHL22.4152	270.939566	-1.3132769	0.28848735	20.1345005	7.22E-06	0.0005026
WHL22.2959	90.4062814	-1.3158065	0.39271312	10.6792433	0.00108344	0.02397893
WHL22.7331	1161.6405	-1.3163226	0.36931786	11.2621682	0.00079103	0.01903689
WHL22.9714	140.833274	-1.3229538	0.36819205	12.2693782	0.00046045	0.01247413
WHL22.6984	309.310186	-1.3247937	0.30669491	17.8910793	2.34E-05	0.0012605
WHL22.6842	597.159606	-1.3258136	0.30961475	17.2525124	3.27E-05	0.00161598
WHL22.6018	72.4964635	-1.3258468	0.38261748	11.7616735	0.00060463	0.01532525
WHL22.1713	64.484446	-1.3296265	0.39782518	11.0403682	0.00089149	0.02061408
WHL22.3070	2600.99601	-1.3327519	0.30797311	17.4216599	2.99E-05	0.00151457
WHL22.6226	1359.15945	-1.3450708	0.3197534	16.333104	5.31E-05	0.00243876
WHL22.6050	331.976478	-1.3482961	0.29789427	19.702221	9.05E-06	0.0005966
WHL22.1910	4225.39953	-1.3496824	0.25163302	27.6674301	1.44E-07	1.86E-05
WHL22.3931	78.5429326	-1.3499152	0.41939586	9.75106854	0.00179219	0.03503524
WHL22.7399	86.6012672	-1.3571346	0.43100932	9.20445356	0.00241427	0.04318183
WHL22.5356	429.496763	-1.357397	0.34083771	14.6533888	0.0001292	0.00480157
WHL22.7365	171.466743	-1.3588088	0.31958737	17.4702989	2.92E-05	0.00150081
WHL22.5385	427.824196	-1.3590434	0.29195202	20.7601038	5.21E-06	0.00038404
WHL22.5856	40.8427928	-1.361888	0.45146124	8.97916921	0.00273075	0.0474018
WHL22.9517	253.836312	-1.365851	0.31967509	17.4074094	3.02E-05	0.00151977
WHL22.4436	53.547391	-1.370373	0.41847473	10.48668	0.00120238	0.02583023
WHL22.3645	50.1183319	-1.3734745	0.42695101	10.1573711	0.00143725	0.0295277
WHL22.4849	292.270725	-1.3796656	0.29778659	20.6422418	5.54E-06	0.00040125
WHL22.4932	51.8069595	-1.3815073	0.42063282	10.6522858	0.00109935	0.02410432
WHL22.7587	138.288037	-1.3911782	0.35930098	14.2885734	0.00015681	0.00550581
WHL22.1236	1526.98321	-1.3989384	0.30653524	19.4287391	1.04E-05	0.00067058
WHL22.7073	75.9184584	-1.4035886	0.40280859	11.7497016	0.00060853	0.01539208
WHL22.7045	124.079717	-1.4088395	0.39758009	11.4860985	0.00070119	0.01723429
WHL22.4558	130.518738	-1.4130973	0.39124828	12.1390806	0.00049376	0.01313235
WHL22.2409	52.9276375	-1.4174051	0.4425275	9.9523575	0.00160644	0.03200991
WHL22.3061	84.0036356	-1.4177932	0.36091538	15.1346914	0.00010011	0.00391395
WHL22.5364	154.005179	-1.4242687	0.35458755	15.3001415	9.17E-05	0.00365482
WHL22.5981	193.348901	-1.4245716	0.3164396	19.7169831	8.98E-06	0.00059518
WHL22.2563	45.363584	-1.4463919	0.43963397	10.645388	0.00110346	0.02412037
WHL22.7883	123.777655	-1.4722204	0.34295844	17.9001044	2.33E-05	0.00126001
WHL22.4452	88.7057688	-1.4756922	0.44062013	10.1979198	0.00140599	0.02933647
WHL22.6106	1184.82971	-1.4775161	0.32611965	18.8123249	1.44E-05	0.00087795
WHL22.5169	1027.84459	-1.4775233	0.30115449	22.5362737	2.06E-06	0.00017873
WHL22.5280	35.4457505	-1.4782208	0.48324337	9.24166256	0.0023657	0.04255514
WHL22.6223	48.1149902	-1.4804899	0.44010963	11.0736457	0.00087563	0.02032322

WHL22.7333	37.754451	-1.4839906	0.47631085	9.4703593	0.00208818	0.03870288
WHL22.2596	153.647316	-1.5011605	0.31672229	21.930912	2.83E-06	0.00023199
WHL22.6062	101.108154	-1.5046963	0.3850077	14.5127719	0.00013921	0.00504481
WHL22.2863	114.247127	-1.5101247	0.45428232	10.0119541	0.00155527	0.0313432
WHL22.5558	102.026617	-1.5130368	0.38599833	14.5598908	0.00013577	0.00496396
WHL22.6053	259.190247	-1.5133866	0.30888721	22.9619185	1.65E-06	0.0001517
WHL22.3241	1129.40621	-1.5235874	0.25409086	34.4652848	4.34E-09	8.67E-07
WHL22.3951	343.465753	-1.5286298	0.3102789	22.8952367	1.71E-06	0.00015477
WHL22.5430	39.8564317	-1.5301367	0.49626576	9.1070491	0.00254626	0.04501909
WHL22.5041	98.5128944	-1.5312675	0.39168629	14.3306931	0.00015334	0.00541467
WHL22.170.0	63.5924803	-1.5325612	0.39713337	14.5073524	0.00013961	0.00504481
WHL22.5933	97.60061	-1.5339455	0.36269693	17.2797658	3.23E-05	0.00160576
WHL22.3876	5075.41319	-1.5366012	0.33602934	18.7007598	1.53E-05	0.00091735
WHL22.4943	55.3608868	-1.5425341	0.48158167	9.46408497	0.00209534	0.03870288
WHL22.7381	142.388985	-1.5484426	0.31852885	23.0067298	1.61E-06	0.00014932
WHL22.9518	121.861774	-1.5488883	0.37989933	15.691435	7.46E-05	0.00311642
WHL22.2954	59.0219203	-1.5493546	0.43389503	12.2673141	0.00046096	0.01247413
WHL22.3278	119.018658	-1.5495008	0.33706075	20.4519345	6.11E-06	0.00043807
WHL22.1632	112.843243	-1.5504631	0.36134113	18.08958	2.11E-05	0.00117407
WHL22.2908	48.851077	-1.5683973	0.43336843	12.8217645	0.00034261	0.00999133
WHL22.7187	182.153064	-1.574168	0.30399859	26.0224432	3.37E-07	3.95E-05
WHL22.3306	60.1111441	-1.57593	0.44768946	12.337663	0.00044391	0.01211856
WHL22.3146	113.676469	-1.5791191	0.38098849	16.0887607	6.04E-05	0.00265134
WHL22.5014	60.9078229	-1.5792172	0.40323485	15.0865153	0.00010269	0.00398995
WHL22.2462	162.311389	-1.5814319	0.35926106	18.7637866	1.48E-05	0.00089448
WHL22.6746	66.251709	-1.5889415	0.39553767	15.7005257	7.42E-05	0.00311642
WHL22.7549	754.09058	-1.6026514	0.29301801	28.2049226	1.09E-07	1.47E-05
WHL22.4597	44.1218718	-1.6032568	0.45415724	12.1553381	0.00048948	0.01311467
WHL22.1060	1176.15749	-1.609863	0.33694348	20.4899017	5.99E-06	0.00043196
WHL22.3942	66.7415112	-1.6104299	0.39600827	16.0996725	6.01E-05	0.00265057
WHL22.7116	172.83493	-1.6200183	0.32480477	23.7947679	1.07E-06	0.00010377
WHL22.6575	81.8393488	-1.6204296	0.41766437	14.2337685	0.00016145	0.00563656
WHL22.1182	82.1740518	-1.626019	0.41338158	14.6281716	0.00013094	0.00483006
WHL22.1850	160.754045	-1.6269096	0.33034906	23.1512008	1.50E-06	0.00013955
WHL22.7390	109.399213	-1.6434755	0.34089917	22.5623008	2.03E-06	0.00017756
WHL22.1644	1511.39336	-1.6617802	0.33738102	21.8234907	2.99E-06	0.000238
WHL22.6006	59.5530816	-1.6724955	0.44189993	13.623816	0.00022333	0.00736172
WHL22.2886	62.768246	-1.6770052	0.4257109	14.7804363	0.00012078	0.00452258
WHL22.4382	174.201941	-1.6835969	0.31388945	27.7278187	1.40E-07	1.84E-05
WHL22.4050	136.677987	-1.6863771	0.33795278	24.0723042	9.28E-07	9.30E-05
WHL22.1456	46.6204299	-1.7059178	0.47077686	12.8933073	0.00032976	0.00973104
WHL22.7229	58.838286	-1.7059647	0.413159	16.5875189	4.65E-05	0.00220602

WHL22.1640	54.52078	-1.7144508	0.44442399	14.3065306	0.00015533	0.00546903
WHL22.3626	38.7062774	-1.7338828	0.50395362	11.3431741	0.00075726	0.0184753
WHL22.6749	47.3308012	-1.7354186	0.44071305	15.1766361	9.79E-05	0.0038558
WHL22.2763	108.497223	-1.7385467	0.38635262	19.354701	1.09E-05	0.00068192
WHL22.4283	39.9228562	-1.7423519	0.53118367	9.94721594	0.00161093	0.03204791
WHL22.2763	323.076599	-1.744304	0.33754576	24.9603975	5.85E-07	6.25E-05
WHL22.5642	50.4270475	-1.7470643	0.46442844	14.0085159	0.00018198	0.00626532
WHL22.4030	160.706085	-1.7532516	0.33365815	26.2185449	3.05E-07	3.70E-05
WHL22.5989	62.6196346	-1.7551062	0.46710273	13.1655736	0.00028514	0.00874893
WHL22.7532	846.296188	-1.7911052	0.38559085	18.5524261	1.65E-05	0.00098022
WHL22.4195	49.4430474	-1.7934332	0.48043107	13.1560286	0.0002866	0.00874893
WHL22.3324	604.379737	-1.8059713	0.2927348	35.4774167	2.58E-09	5.68E-07
WHL22.7062	144.356997	-1.818626	0.36680214	22.9137959	1.69E-06	0.00015441
WHL22.2653	383.243455	-1.865094	0.33084667	29.0711352	6.98E-08	9.83E-06
WHL22.5041	61.4997463	-1.866666	0.47317404	14.5181228	0.00013882	0.00504481
WHL22.9980	66.6874792	-1.8759574	0.39417737	22.0658457	2.63E-06	0.00022063
WHL22.1754	54.2978697	-1.8784922	0.45446364	16.2760508	5.48E-05	0.00249408
WHL22.4051	273.09837	-1.8838258	0.293503	39.3004386	3.63E-10	8.83E-08
WHL22.1119	95.4588448	-1.8868815	0.37874735	24.0677577	9.30E-07	9.30E-05
WHL22.1443	43.2137934	-1.9004303	0.47544391	15.6256039	7.72E-05	0.00317888
WHL22.2322	51.4694519	-1.916706	0.47388856	15.4466829	8.49E-05	0.00341502
WHL22.7206	1375.98336	-1.9296124	0.35374363	25.8600984	3.67E-07	4.17E-05
WHL22.1914	76.6705844	-1.9380457	0.44458988	18.0201732	2.19E-05	0.00119869
WHL22.9959	1769.62345	-1.9454473	0.25932513	52.3944306	4.54E-13	2.81E-10
WHL22.5558	130.998981	-1.9455679	0.33957333	31.4378568	2.06E-08	3.31E-06
WHL22.4557	34.7716047	-1.9684652	0.5399407	13.0948427	0.00029611	0.00894884
WHL22.4350	112.078711	-1.9866563	0.37604375	26.4461753	2.71E-07	3.33E-05
WHL22.6352	54.5955589	-1.9873396	0.43268582	20.4342727	6.17E-06	0.00043959
WHL22.5216	236.954326	-1.9903172	0.29444759	43.3208795	4.65E-11	1.40E-08
WHL22.5558	481.903232	-2.009252	0.28404561	46.7720832	7.97E-12	2.91E-09
WHL22.7239	34.6274466	-2.0651414	0.5104156	15.9685186	6.44E-05	0.00279102
WHL22.1253	140.842812	-2.1223049	0.49055293	15.748033	7.24E-05	0.00306099
WHL22.2017	39.2807964	-2.1293723	0.53288113	15.5829881	7.90E-05	0.00322988
WHL22.5559	434.931632	-2.1557373	0.30996828	44.029087	3.24E-11	1.06E-08
WHL22.6211	55.5111471	-2.1673427	0.49842266	17.2136857	3.34E-05	0.00163631
WHL22.9979	54.084678	-2.2254431	0.43256398	25.8903083	3.61E-07	4.15E-05
WHL22.1198	52.9424932	-2.3074405	0.46040342	24.25947	8.42E-07	8.55E-05
WHL22.9704	36.4360543	-2.313387	0.59143433	13.9581238	0.00018693	0.00639996
WHL22.4056	91.0777979	-2.3345687	0.39069663	33.9109138	5.77E-09	1.14E-06
WHL22.4350	39.2836827	-2.3374068	0.49412229	22.0502928	2.66E-06	0.00022093
WHL22.5441	7313.4443	-2.4166316	0.30211477	55.9092755	7.59E-14	5.23E-11
WHL22.4452	677.800201	-2.4329879	0.31599978	52.5656695	4.16E-13	2.71E-10

WHL22.7518	36.574982	-2.7556592	0.53002345	26.1620626	3.14E-07	3.71E-05
WHL22.1194	7595.67587	-2.7841148	0.27762181	86.7691671	1.22E-20	3.02E-17
WHL22.3512	143.676706	-2.8546763	0.34875281	61.9846616	3.46E-15	3.30E-12
WHL22.3512	177.809527	-2.9398175	0.35954339	59.7269108	1.09E-14	9.00E-12
WHL22.7327	272.256301	-3.0414204	0.3333363	73.2652252	1.13E-17	1.56E-14
WHL22.1319	4542.1093	-3.7567674	0.34057124	93.7085955	3.66E-22	1.51E-18
WHL22.9020	72.2094242	-3.8849739	0.49438507	58.3339406	2.21E-14	1.71E-11
WHL22.2771	232.075574	-4.0437582	0.43719896	72.1067833	2.04E-17	2.53E-14
WHL22.7506	45.6179498	-4.080341	0.58938447	47.9897035	4.28E-12	1.71E-09
WHL22.1264	80.2966845	-5.3691584	0.58053332	103.627334	2.44E-24	3.03E-20

	baseMean	log2FoldCha	lfcSE	stat	pvalue	padj
PMI_006405	135.317187	3.16624268	0.74154994	14.3132549	0.00015477	0.02878962
PMI_015900	824.293913	2.59609854	0.55239886	18.5212064	1.68E-05	0.00612169
PMI_027297	90.6423431	2.35384177	0.42176414	28.0160374	1.20E-07	9.86E-05
PMI_007921	65.3587779	2.34446587	0.45260344	24.4158414	7.76E-07	0.0004895
PMI_008244	46.2177392	2.24469784	0.52007726	16.6256648	4.55E-05	0.01244127
PMI_009465	37.3282886	2.04545853	0.53055456	14.7886639	0.00012026	0.02602031
PMI_022566	441.884739	1.95652143	0.28731557	42.3877307	7.49E-11	1.02E-07
PMI_026189	55.6214477	1.93041479	0.43488873	18.6961829	1.53E-05	0.00571176
PMI_002316	83.7796807	1.87264648	0.42586738	17.4616422	2.93E-05	0.00887202
PMI_001608	82.7182959	1.86824472	0.42037211	18.0820497	2.12E-05	0.00722701
PMI_007293	215.51231	1.83909529	0.33037176	28.0808229	1.16E-07	9.86E-05
PMI_008243	129.658224	1.82168998	0.33732165	27.34692	1.70E-07	0.00013275
PMI_009520	551.423348	1.80106575	0.2375553	54.0043835	2.00E-13	8.20E-10
PMI_010916	52.908258	1.80024227	0.43445039	16.4219522	5.07E-05	0.01362525
PMI_024682	814.839026	1.63570606	0.22041884	52.2142477	4.98E-13	1.36E-09
PMI_015901	288.572342	1.61583134	0.31368257	24.2350113	8.53E-07	0.00049928
PMI_027270	148.395213	1.55543268	0.3488166	18.303618	1.88E-05	0.00657018
PMI_012532	109.382138	1.50482245	0.34678392	17.9324956	2.29E-05	0.00750497
PMI_018775	436.648196	1.49945499	0.22033085	44.7524626	2.24E-11	3.67E-08
PMI_010829	105.935229	1.44450512	0.34892474	16.3645364	5.23E-05	0.01381777
PMI_004312	158.211359	1.39793325	0.27584669	25.1091297	5.42E-07	0.00037009
PMI_004903	266.716445	1.37246729	0.28396563	22.1332581	2.54E-06	0.00130322
PMI_000625	1535.48338	1.34763907	0.22298656	34.7778068	3.70E-09	4.33E-06
PMI_011811	142.932396	1.31046061	0.33628606	14.2739136	0.00015804	0.02878962
PMI_011810	242.195758	1.30219335	0.30408646	17.1780084	3.40E-05	0.00996446
PMI_012985	8646.29191	1.29092595	0.18048381	49.4855524	2.00E-12	4.10E-09
PMI_012986	4186.69655	1.27395659	0.19370736	41.7615996	1.03E-10	1.30E-07
PMI_012984	2703.17221	1.26137333	0.18948356	42.9018433	5.76E-11	8.58E-08
PMI_005791	725.523264	1.24822482	0.2353496	26.9353778	2.10E-07	0.00015678
PMI_011809	424.485471	1.18870885	0.24978567	21.7649239	3.08E-06	0.00153111
PMI_002028	1344.53396	1.17517372	0.21715136	28.2108364	1.09E-07	9.86E-05
PMI_018150	750.249438	1.15342145	0.22974687	24.2803152	8.33E-07	0.00049928
PMI_010356	283.137797	1.14485	0.2938307	14.3196617	0.00015425	0.02878962
PMI_015902	2461.93292	1.11367359	0.19017986	33.4222846	7.42E-09	7.85E-06
PMI_005790	1120.29883	1.08945884	0.22372512	22.8655032	1.74E-06	0.00091887
PMI_027023	227.030245	1.08811906	0.28176247	14.367088	0.00015041	0.02867379
PMI_025723	304.847204	1.05925086	0.27096127	14.6662134	0.00012833	0.02602031
PMI_020120	550.613349	1.04219249	0.21543128	22.9077399	1.70E-06	0.00091887
PMI_027203	413.919204	1.03862381	0.25493493	15.9941223	6.35E-05	0.01627702

PMI_004128	169.991012	1.03606143	0.27195431	14.2850783	0.00015711	0.02878962
PMI_026967	714.224474	1.02944901	0.25702927	15.3122175	9.11E-05	0.02134283

PMI_026236	604.609654	1.02382102	0.22891156	19.4251468	1.05E-05	0.00439808
PMI_013310	300.345877	1.01915223	0.26987578	13.7278932	0.00021129	0.03685265
PMI_019393	1798.14648	1.008739	0.23016296	18.4352356	1.76E-05	0.00626494
PMI_001907	4461.98933	0.99497542	0.23167562	17.6267858	2.69E-05	0.0084742
PMI_027911	277.233893	0.98584824	0.25410649	14.6807053	0.00012734	0.02602031
PMI_008179	340.566398	0.9454479	0.2457791	14.4344805	0.00014512	0.02799124
PMI_019834	491.810516	0.91249229	0.2345493	14.7489007	0.00012282	0.02602031
PMI_006619	231.927509	0.9084075	0.24680288	13.3733032	0.00025523	0.04143088
PMI_005662	1495.03432	0.90456686	0.2000783	20.025647	7.64E-06	0.00347986
PMI_023092	572.664694	0.86029999	0.21860367	15.2064624	9.64E-05	0.02204118
PMI_019863	480.968485	0.85904082	0.21653393	15.5276268	8.13E-05	0.01960365
PMI_027346	6465.31577	0.85888266	0.22880306	13.5424515	0.00023323	0.04025016
PMI_004960	3223.32864	0.84986076	0.22356792	13.959438	0.0001868	0.03328853
PMI_004473	1612.88152	-0.6875715	0.18778269	13.2764634	0.00026876	0.04317862
PMI_025997	1517.32446	-0.7162455	0.19712049	13.0215088	0.00030793	0.04674603
PMI_027118	377.721512	-0.8173727	0.22352826	13.2022092	0.00027962	0.04324867
PMI_017191	549.314927	-0.8176926	0.20736056	15.3711742	8.83E-05	0.02098691
PMI_025238	4277.15938	-0.8219359	0.21998444	13.5186346	0.00023621	0.04033959
PMI_020236	538.919836	-0.8378691	0.22630882	13.4348978	0.00024699	0.04090245
PMI_003425	1558.26599	-0.8385016	0.22489491	13.4708326	0.0002423	0.04082852
PMI_010719	2533.86693	-0.8424496	0.23006038	12.9239855	0.0003244	0.04879369
PMI_027638	5847.90979	-0.8634315	0.2324586	13.2230126	0.00027653	0.04317862
PMI_005425	4702.53641	-0.8754275	0.22372996	14.7692485	0.0001215	0.02602031
PMI_014330	11390.0978	-0.8856401	0.2363943	13.3943775	0.00025238	0.04137765
PMI_010248	11882.8656	-0.8905533	0.21275429	16.972297	3.79E-05	0.01053983
PMI_003594	748.527145	-0.894691	0.24158943	13.2263698	0.00027604	0.04317862
PMI_013803	612.869781	-0.9047749	0.2171813	17.01928	3.70E-05	0.01052073
PMI_004718	5856.29789	-0.9057259	0.23131346	14.6892284	0.00012677	0.02602031
PMI_005167	3865.26923	-0.9491819	0.23934245	14.9791224	0.00010871	0.02440872
PMI_002987	195.694364	-0.9878644	0.25684582	14.5889072	0.0001337	0.02621232
PMI_013364	4875.57232	-0.9938979	0.25542689	14.2223387	0.00016243	0.02926432
PMI_018014	498.48242	-0.9954441	0.21368443	21.3261467	3.87E-06	0.00186812
PMI_023290	1302.56241	-1.072766	0.21344838	24.5217124	7.35E-07	0.00048186
PMI_000506	126.40984	-1.1299014	0.29295225	14.6397389	0.00013014	0.02602031
PMI_024244	694.860794	-1.1303053	0.25948592	17.9589893	2.26E-05	0.00750497
PMI_009579	101.510796	-1.2224534	0.3242859	13.859324	0.00019702	0.03473215
PMI_010080	128.287957	-1.233674	0.31707052	14.6467868	0.00012966	0.02602031
PMI_015698	513.430941	-1.2358369	0.27534554	18.8678722	1.40E-05	0.00546007
PMI_005282	241.40392	-1.2413972	0.3288367	13.0735229	0.0002995	0.04589057
PMI_014623	192.935478	-1.2451185	0.29532808	17.0081955	3.72E-05	0.01052073
PMI_013721	111.949057	-1.2920525	0.30332597	17.817084	2.43E-05	0.00781784
PMI_005961	3507.84507	-1.3511862	0.22751125	33.35834	7.66E-09	7.85E-06

PMI_013015	162.232482	-1.3669374	0.34524122	14.5804711	0.0001343	0.02621232
PMI_028908	1994.12054	-1.4082132	0.19519694	50.018708	1.52E-12	3.57E-09
PMI_010000	109.290793	-1.4089697	0.31771377	19.1316704	1.22E-05	0.00487865
PMI_006353	7134.47194	-1.4180444	0.20580593	45.1950047	1.78E-11	3.25E-08
PMI_013438	235.751449	-1.5038394	0.30082993	23.3617111	1.34E-06	0.00075883
PMI_020033	228.839731	-1.551773	0.27557511	30.2699982	3.76E-08	3.63E-05
PMI_006238	68.7326571	-1.5897189	0.39555043	15.6008025	7.82E-05	0.0194309
PMI_006074	133.847089	-1.6092382	0.35600192	18.8259698	1.43E-05	0.00546007
PMI_002888	49.0021735	-1.6300859	0.41764878	14.9538937	0.00011017	0.02440872
PMI_008827	65.4221913	-1.6423678	0.39961537	16.1779786	5.77E-05	0.01500547
PMI_004367	182.016851	-1.6519306	0.35218641	19.8210763	8.50E-06	0.00366902
PMI_026821	61.6730536	-1.6997279	0.39859107	17.5286159	2.83E-05	0.0087548
PMI_017948	91.2671276	-1.7119263	0.3935328	17.4329099	2.98E-05	0.00887202
PMI_006968	48.2842796	-1.7215949	0.43032231	15.6699305	7.54E-05	0.01902164
PMI_006131	604.617011	-1.7578132	0.20723737	68.6363918	1.18E-16	1.94E-12
PMI_028002	68.9640937	-1.8501271	0.44750679	15.5344343	8.10E-05	0.01960365
PMI_005584	405.857096	-1.8804785	0.23293927	61.8344765	3.74E-15	2.76E-11
PMI_000104	227.106354	-1.9120459	0.35344287	25.9629446	3.48E-07	0.00024809
PMI_005586	56.6075196	-1.9441185	0.42422059	20.6295226	5.57E-06	0.00261056
PMI_006131	1099.61201	-1.953806	0.23937081	61.2405982	5.05E-15	2.76E-11
PMI_005524	40.5759398	-1.9968849	0.52550795	13.4573386	0.00024405	0.04082852
PMI_001568	43.5041285	-2.0220234	0.50622776	15.1981996	9.68E-05	0.02204118
PMI_005585	203.415092	-2.0830373	0.27830414	53.1563846	3.08E-13	1.01E-09
PMI_012768	48.510034	-2.1179875	0.47034158	19.3012135	1.12E-05	0.00457566
PMI_028351	37.0569994	-2.3696008	0.60220546	13.248622	0.00027278	0.04317862
PMI_004287	40.6698593	-3.2702228	0.68404049	19.8965876	8.17E-06	0.00362224

	baseMean	log2FoldCha	lfcSE	stat	pvalue	padj
PMI_017349	699.472506	5.30919265	0.43381019	108.725114	1.86E-25	2.57E-21
PMI_012632	742.556608	5.00845168	0.67334865	33.1698471	8.44E-09	4.08E-06
PMI_013396	30.1238144	4.96759149	0.92818454	25.7115291	3.96E-07	8.97E-05
PMI_027270	776.089316	4.70325454	0.48313306	68.6207307	1.19E-16	8.24E-13
PMI_000092	1024.91307	4.02020752	0.50975447	45.2361082	1.75E-11	5.10E-08
PMI_004039	32.9508073	3.37946733	0.64488414	25.3942699	4.67E-07	9.92E-05
PMI_016293	70.6941827	3.29062422	0.51524419	36.6454042	1.42E-09	1.03E-06
PMI_010266	59.0299515	3.23009671	0.66723368	19.0065706	1.30E-05	0.00114537
PMI_015901	328.386774	3.20919119	0.45118336	42.4486708	7.26E-11	1.25E-07
PMI_001624	229.935868	3.19333191	0.44407767	44.7711402	2.21E-11	5.10E-08
PMI_022566	214.672355	3.07818374	0.48117173	34.4254777	4.43E-09	2.78E-06
PMI_016746	54.4720187	3.06741103	0.88153115	12.0778127	0.00051025	0.01707685
PMI_012218	287.422138	3.05122836	0.46252243	36.7550132	1.34E-09	1.03E-06
PMI_008671	45.4767714	2.96628996	0.62361579	19.9156356	8.09E-06	0.00077586
PMI_026189	152.483744	2.95557614	0.44986224	38.2527792	6.21E-10	5.36E-07
PMI_028391	63.5360024	2.89135742	0.54745243	24.8008943	6.36E-07	0.000125
PMI_005829	341.75954	2.8473996	0.52891962	23.3345267	1.36E-06	0.00021694
PMI_012931	447.785828	2.83484035	0.42567014	38.4368131	5.66E-10	5.20E-07
PMI_004572	75.7075878	2.8111063	0.51946492	26.1628895	3.14E-07	7.88E-05
PMI_027296	305.855445	2.77178045	0.44825539	33.2575679	8.07E-09	4.08E-06
PMI_028942	301.740329	2.7564546	0.45609653	31.4912759	2.00E-08	7.68E-06
PMI_029013	36.7008246	2.74064277	0.59184868	20.0122894	7.69E-06	0.00074277
PMI_003565	69.8053769	2.7392697	0.59452575	17.6968469	2.59E-05	0.00187225
PMI_028309	35.409742	2.67048605	0.64647348	15.0453516	0.00010496	0.00550892
PMI_001608	138.851834	2.65252546	0.45287805	30.8422134	2.80E-08	9.91E-06
PMI_015040	143.494819	2.60819876	0.50826904	22.7009143	1.89E-06	0.00026465
PMI_024324	40.1446082	2.59593695	0.60722808	16.8841378	3.97E-05	0.00264958
PMI_022698	388.548729	2.55530618	0.40313112	36.1179098	1.86E-09	1.28E-06
PMI_017258	199.140833	2.53254511	0.42608047	32.0105602	1.53E-08	6.41E-06
PMI_024181	142.191452	2.51186277	0.49471596	22.4287661	2.18E-06	0.00029806
PMI_025390	231.23537	2.50591586	0.57842361	14.9105515	0.00011273	0.00580647
PMI_027204	38.2784183	2.50184173	0.57677828	17.6338546	2.68E-05	0.00192522
PMI_007048	56.7808779	2.49495862	0.58353209	16.288511	5.44E-05	0.00336698
PMI_003439	350.704866	2.45246269	0.40286724	33.637189	6.64E-09	3.67E-06
PMI_007293	98.4975289	2.43056433	0.45894556	26.0013382	3.41E-07	8.39E-05
PMI_025694	745.782735	2.40750056	0.39875161	32.8021196	1.02E-08	4.69E-06
PMI_000340	1283.85654	2.34277877	0.47558411	20.6329468	5.56E-06	0.0005862
PMI_011682	117.654918	2.34073128	0.45203055	24.779034	6.43E-07	0.000125
PMI_002739	66.4218006	2.32746573	0.55717892	15.448956	8.48E-05	0.00475642

PMI_021865	2810.75782	2.3253332	0.38170009	33.644182	6.62E-09	3.67E-06
PMI_027056	85.8838537	2.32233984	0.64490835	10.1785613	0.00142083	0.03434875

PMI_006106	263.476797	2.3202594	0.49496317	18.8757423	1.40E-05	0.00119619
PMI_024182	806.756648	2.30761102	0.41983818	26.9217263	2.12E-07	5.85E-05
PMI_010928	938.136205	2.28558431	0.50635648	16.9377248	3.86E-05	0.00260096
PMI_004878	70.2597209	2.28002106	0.49103554	20.2146284	6.92E-06	0.0007026
PMI_029440	144.445484	2.26726482	0.50980009	17.03435	3.67E-05	0.00249626
PMI_029094	59.5876419	2.26399118	0.64550371	10.2521678	0.00136524	0.03348116
PMI_006405	70.5358163	2.26246981	0.51990346	17.1598537	3.44E-05	0.00235988
PMI_020466	719.319737	2.24856891	0.41115958	26.9860793	2.05E-07	5.77E-05
PMI_015900	312.482299	2.23320145	0.41875362	25.9688488	3.47E-07	8.39E-05
PMI_021734	68.5178868	2.20599756	0.51778882	16.6619051	4.47E-05	0.00293625
PMI_022472	228.536792	2.20528137	0.55237315	13.0609081	0.00030152	0.01154262
PMI_009888	84.0853309	2.20526739	0.5381193	14.8820706	0.00011445	0.00585114
PMI_011453	709.03665	2.20506111	0.4081832	26.4888397	2.65E-07	7.04E-05
PMI_001888	57.8701646	2.20082593	0.55344699	14.3318451	0.00015325	0.00717108
PMI_021733	101.89589	2.16609276	0.50546281	16.5383187	4.77E-05	0.0029915
PMI_009681	1147.09556	2.15628852	0.40200475	26.1850726	3.10E-07	7.88E-05
PMI_012373	161.330188	2.13010843	0.42663794	23.279203	1.40E-06	0.00021978
PMI_021471	146.445699	2.12438455	0.52567536	14.003478	0.00018247	0.00823155
PMI_018112	304.189561	2.11173138	0.5133772	14.3411735	0.00015249	0.00715991
PMI_018310	372.221695	2.11067787	0.53153323	13.0588122	0.00030186	0.01154262
PMI_017105	823.533077	2.11020507	0.4092911	24.2145352	8.62E-07	0.0001531
PMI_000699	141.750508	2.10025618	0.51015938	14.7937396	0.00011993	0.00601648
PMI_004095	28.7726213	2.09456009	0.62141173	10.762172	0.00103596	0.02798504
PMI_024974	158.36819	2.09446755	0.53333592	13.2094159	0.00027855	0.01108084
PMI_010721	1183.12932	2.09375982	0.43746222	20.3984652	6.29E-06	0.00064309
PMI_011495	127.202731	2.09342915	0.46589176	18.4286565	1.76E-05	0.00141559
PMI_004877	283.790544	2.09053834	0.40936515	24.2071622	8.65E-07	0.0001531
PMI_027769	71.7232902	2.07957138	0.48665945	17.2298561	3.31E-05	0.00229736
PMI_002776	144.198491	2.05346374	0.49246976	15.5783618	7.92E-05	0.00451512
PMI_019393	2624.22252	2.0489482	0.39460485	24.726991	6.61E-07	0.00012664
PMI_005460	102.126001	2.04413453	0.59722136	9.57768181	0.00196957	0.04189204
PMI_019119	49.6333803	2.03759115	0.56986242	11.6868905	0.00062942	0.01986105
PMI_008877	69.6650141	2.0262355	0.48666331	16.426556	5.06E-05	0.00314456
PMI_010744	2435.81073	2.01183438	0.47013887	15.8747442	6.77E-05	0.00400943
PMI_027203	199.087339	2.00880532	0.43800457	19.4400506	1.04E-05	0.00094273
PMI_010916	41.9812055	2.00435594	0.56753698	11.8221703	0.0005853	0.01883316
PMI_021611	139.195392	1.98442346	0.43214966	19.8946195	8.18E-06	0.00077902
PMI_011591	222.514569	1.97866162	0.5350153	11.5127328	0.00069121	0.0212505
PMI_005282	221.169709	1.96447654	0.44824383	17.5851251	2.75E-05	0.00196495
PMI_024151	234.844268	1.96363192	0.43601791	18.718329	1.52E-05	0.00127535
PMI_007921	67.380893	1.96332362	0.50911071	13.7815576	0.00020534	0.00893615
PMI_005498	684.373866	1.95627327	0.45411217	16.5015683	4.86E-05	0.00303625

PMI_021655	13011.7211	1.94587149	0.40189866	21.4892123	3.56E-06	0.00042381
PMI_009323	50.1785287	1.94451845	0.51549598	13.6316678	0.0002224	0.00947543
PMI_013974	32.367814	1.94327569	0.61196528	9.38871093	0.00218326	0.04511635
PMI_029671	285.619119	1.94239273	0.50780389	12.5819574	0.00038949	0.01392876
PMI_027297	63.7617435	1.94184078	0.52066418	13.1099711	0.00029373	0.01135749
PMI_007523	380.824682	1.93162065	0.43498979	18.0130036	2.19E-05	0.00166407
PMI_017191	444.916333	1.92999315	0.51895484	11.6015843	0.00065896	0.02044098
PMI_003226	78.727815	1.92464696	0.55387394	10.5512014	0.00116113	0.03024185
PMI_000693	216.035086	1.91951474	0.46657556	15.2815346	9.26E-05	0.00504568
PMI_006279	273.651723	1.91853299	0.43047048	18.3586218	1.83E-05	0.00145171
PMI_027331	210.262925	1.9156632	0.42261028	19.2564997	1.14E-05	0.00101776
PMI_009999	293.57889	1.91433637	0.41225556	20.1681358	7.09E-06	0.00070945
PMI_007700	272.764513	1.89970769	0.42382837	18.6798997	1.55E-05	0.00128773
PMI_027891	112.537421	1.89399203	0.49036678	13.6138834	0.00022452	0.00953618
PMI_018448	146.931557	1.89246923	0.45925837	15.7352846	7.29E-05	0.00422544
PMI_028852	144.193375	1.89140691	0.54032842	10.4876698	0.00120174	0.03068497
PMI_020503	216.00206	1.88149521	0.49323303	12.8552391	0.00033654	0.01255551
PMI_016857	102.864411	1.88105921	0.47291136	14.7485655	0.00012284	0.00609963
PMI_018963	58.1173835	1.88051694	0.54779124	10.8444657	0.00099091	0.02697946
PMI_010944	141.33348	1.87727286	0.47001171	14.6302158	0.0001308	0.00635764
PMI_012809	81.4925485	1.87380016	0.5353398	10.9843973	0.00091882	0.0255714
PMI_007802	263.132402	1.8706609	0.51774244	11.1730215	0.00082995	0.02397937
PMI_009105	93.728067	1.87012684	0.53523204	10.799558	0.00101524	0.02753324
PMI_023403	87.1756198	1.86443241	0.47124278	14.8344549	0.00011737	0.00591312
PMI_011632	337.29202	1.86406388	0.42317806	18.0472975	2.15E-05	0.0016434
PMI_009478	39.8621185	1.85728546	0.58286713	9.44738237	0.00211451	0.0443111
PMI_001813	158.570225	1.85644681	0.46091313	14.9560398	0.00011005	0.00569586
PMI_002049	113.675125	1.85506357	0.48114212	13.742515	0.00020965	0.00907233
PMI_004166	467.605416	1.85287973	0.48591922	12.6830768	0.00036898	0.01340368
PMI_006036	581.313758	1.85179052	0.41936077	17.9815854	2.23E-05	0.00167338
PMI_002051	90.9044066	1.85155109	0.52026463	11.4687522	0.00070776	0.02166285
PMI_012906	148.461594	1.84449277	0.50811551	11.6812024	0.00063135	0.01986105
PMI_007365	817.476724	1.84176579	0.40397798	19.3196571	1.11E-05	0.00099104
PMI_010123	287.904286	1.83873964	0.45847522	14.5657986	0.00013535	0.00648735
PMI_009047	64.1167454	1.83756021	0.52890164	11.1721373	0.00083035	0.02397937
PMI_027722	616.619443	1.83180306	0.53141385	9.83780921	0.00170961	0.03793861
PMI_024489	131.948898	1.83146613	0.43739975	16.6356694	4.53E-05	0.00296224
PMI_011158	111.00566	1.82624505	0.5210761	10.8913561	0.00096614	0.02646152
PMI_027432	60.7748826	1.80720543	0.55791149	9.2745242	0.00232363	0.04696251
PMI_001925	245.263569	1.80611082	0.48807515	12.142569	0.00049284	0.01679788
PMI_022903	69.3284684	1.79625997	0.50413782	11.9136176	0.00055725	0.01813455
PMI_023497	985.068664	1.79622552	0.4108032	17.7363019	2.54E-05	0.00185323

PMI_018030	77.1633026	1.79584018	0.49877448	12.1548282	0.00048961	0.01672913
PMI_013654	267.880392	1.78678509	0.43546279	15.5963166	7.84E-05	0.00449101
PMI_000091	1133.95324	1.7848714	0.44321506	14.6203426	0.00013149	0.00636861
PMI_006329	255.092694	1.77942778	0.4103938	17.8048679	2.45E-05	0.00180281
PMI_008426	182.807241	1.77624701	0.44604723	14.7880601	0.00012029	0.00601648
PMI_002131	175.96586	1.77488651	0.52396661	9.97144887	0.00158986	0.03644032
PMI_008173	113.153062	1.77173621	0.50633683	11.0676265	0.00087848	0.02480705
PMI_010209	175.464881	1.77057757	0.52301775	9.94194371	0.00161555	0.0366191
PMI_014494	100.22998	1.76906943	0.45644642	14.3218189	0.00015407	0.00718502
PMI_009240	705.340188	1.76892107	0.39447315	18.9252948	1.36E-05	0.00118018
PMI_007568	879.087924	1.75466014	0.45197641	13.5357436	0.00023406	0.00982067
PMI_015808	139.117201	1.75448122	0.50980652	10.535841	0.00117082	0.03037959
PMI_004712	192.519811	1.75447487	0.46606659	12.9523907	0.00031951	0.01201788
PMI_016158	144.148471	1.75076211	0.48170537	12.0753816	0.00051092	0.01707685
PMI_011443	353.529913	1.74645376	0.49310097	10.9774453	0.00092227	0.02561586
PMI_014561	332.319231	1.74175178	0.40946055	17.0655369	3.61E-05	0.00246775
PMI_005351	165.602995	1.73962778	0.47681666	12.1003008	0.00050414	0.0170173
PMI_018283	135.319393	1.73337072	0.43337768	15.2695213	9.32E-05	0.00504568
PMI_016157	137.409708	1.73313728	0.44022766	14.6740572	0.00012779	0.00627778
PMI_008672	215.110545	1.73249325	0.46408258	12.7360737	0.00035867	0.01320288
PMI_016621	606.283015	1.72951321	0.44430442	13.7768224	0.00020586	0.00893615
PMI_003579	371.97345	1.72867081	0.48646424	11.1009581	0.00086283	0.02450938
PMI_012945	177.997109	1.72824491	0.50529644	10.3371978	0.00130376	0.03247823
PMI_026774	190.116267	1.72519755	0.43598473	14.7377229	0.00012355	0.00611282
PMI_015207	109.350939	1.72175083	0.51183967	10.2104061	0.0013965	0.03393899
PMI_026282	1856.57551	1.72094492	0.39210298	18.0799995	2.12E-05	0.00162438
PMI_017074	207.007454	1.71913166	0.48839884	11.1038741	0.00086148	0.02450938
PMI_018364	383.974082	1.71808989	0.40939362	16.5833643	4.66E-05	0.00296462
PMI_020304	48.1065804	1.7176928	0.52111554	10.4708595	0.00121272	0.03077284
PMI_016337	47.69547	1.71626661	0.52140112	10.4591246	0.00122045	0.0307991
PMI_011633	2733.41886	1.71293461	0.47112876	11.614201	0.0006545	0.02034851
PMI_016072	221.327672	1.70539901	0.4523157	13.1338354	0.00029001	0.01130877
PMI_000692	1727.18083	1.70443381	0.38196448	18.836468	1.42E-05	0.00121354
PMI_005028	217.76664	1.70319615	0.44180446	13.830135	0.0002001	0.00874112
PMI_027362	100.168265	1.70077484	0.49868708	11.2228017	0.00080798	0.02363011
PMI_023188	151.240722	1.69661277	0.4420738	13.950664	0.00018767	0.00838286
PMI_010356	189.710472	1.69432767	0.44609588	13.4630538	0.00024331	0.01005574
PMI_004870	598.028434	1.68689656	0.44394182	13.1602228	0.00028595	0.01121398
PMI_015726	60.8892846	1.6799843	0.51410467	10.138956	0.00145168	0.03466962
PMI_013982	634.669515	1.66622772	0.43997627	13.0631324	0.00030117	0.01154262
PMI_027187	54.5171271	1.66368908	0.52796902	9.38596564	0.00218653	0.04511635
PMI_019282	9485.06174	1.66273933	0.411828	15.0878252	0.00010262	0.0054069

PMI_010338	123.78347	1.6545769	0.48175827	10.9082596	0.00095736	0.02632561
PMI_014156	92.1933185	1.65036444	0.45595286	12.5967044	0.00038643	0.01385583
PMI_008492	152.155918	1.64794787	0.4703286	11.3500598	0.00075446	0.02259111
PMI_023924	302.076339	1.64685301	0.43571945	13.2871401	0.00026723	0.01081783
PMI_007506	70.8359311	1.64020916	0.51794417	9.34007781	0.00224196	0.04578109
PMI_004263	420.837415	1.6341997	0.42603259	13.7219165	0.00021197	0.0091437
PMI_027688	120.870121	1.63162587	0.47616645	10.9201191	0.00095125	0.02622713
PMI_006956	530.077741	1.63093282	0.41256227	14.6568232	0.00012897	0.0063123
PMI_003861	98.8122543	1.63074062	0.46080809	11.9459915	0.00054765	0.01791415
PMI_016779	118.715172	1.62845979	0.47684921	10.8700854	0.0009773	0.02671416
PMI_017888	118.800723	1.62669662	0.49500597	9.87690204	0.00167366	0.03744452
PMI_021431	79.8843697	1.62443287	0.47872774	10.9536283	0.00093421	0.02589511
PMI_001154	148.285464	1.62203488	0.48215924	10.3674107	0.00128259	0.03207412
PMI_021270	115.298698	1.61988408	0.46426185	11.4802999	0.00070338	0.0215765
PMI_005871	114.649601	1.61730594	0.45406886	12.0990206	0.00050448	0.0170173
PMI_026073	95.0124185	1.61407567	0.482725	10.5188868	0.00118161	0.03055903
PMI_013375	202.211057	1.61204711	0.42084619	13.9601058	0.00018673	0.00836895
PMI_003635	235.20577	1.60867775	0.4131817	14.4776133	0.00014184	0.00677472
PMI_021566	53.1975262	1.60814625	0.50794552	9.65402275	0.00188937	0.04071704
PMI_013594	605.800031	1.60315443	0.430945	12.8014425	0.00034635	0.01285227
PMI_012235	722.123528	1.60172548	0.44075772	12.0941143	0.00050581	0.0170173
PMI_013035	2332.78998	1.59981808	0.39580548	15.3743678	8.82E-05	0.00486875
PMI_014193	720.002594	1.59842911	0.43935307	12.128634	0.00049653	0.01688218
PMI_006943	92.4304956	1.59764583	0.4979837	9.57414037	0.00197337	0.04190836
PMI_001153	319.789004	1.59568244	0.40444891	14.8511693	0.00011634	0.00588242
PMI_013438	219.764389	1.59558594	0.43861329	12.4337999	0.00042163	0.01480973
PMI_010565	448.307765	1.59522034	0.40905082	14.3746278	0.00014981	0.00705782
PMI_017499	1624.28618	1.58633799	0.46854774	10.1557642	0.00143851	0.03456738
PMI_020083	131.987843	1.58286433	0.44465861	12.0909454	0.00050667	0.0170173
PMI_011242	211.037423	1.58216359	0.45324743	11.3220889	0.00076591	0.02278568
PMI_022684	294.818489	1.58040886	0.41858525	13.499271	0.00023866	0.0099529
PMI_014857	314.391614	1.57953433	0.47201132	10.1083407	0.001476	0.03494799
PMI_008891	253.869427	1.57694946	0.47403745	10.0083892	0.00155829	0.03597091
PMI_003535	1513.9517	1.57581881	0.40962456	13.8403602	0.00019902	0.00872128
PMI_004409	210.987202	1.57367578	0.4890795	9.29885531	0.00229297	0.04654731
PMI_005631	137.612997	1.57256834	0.4853665	9.62824223	0.00191608	0.04113461
PMI_013179	2739.58396	1.57000117	0.39013088	15.3303722	9.03E-05	0.0049636
PMI_015902	1013.84968	1.56831514	0.38562142	15.773957	7.14E-05	0.00419585
PMI_015516	141.406038	1.56286251	0.43069758	12.6837762	0.00036884	0.01340368
PMI_027383	379.538073	1.55884224	0.47022111	9.89744947	0.00165508	0.03714915
PMI_006591	135.639262	1.55860694	0.44971135	11.3682117	0.00074712	0.02246888
PMI_017971	315.461602	1.5582045	0.48179331	9.3544091	0.0022245	0.04563675

PMI_014560	479.856788	1.55672246	0.45771166	10.5034352	0.00119153	0.03065427
PMI_002782	2154.21092	1.55470951	0.39693226	14.4689746	0.00014249	0.00677518
PMI_018416	402.495363	1.55438192	0.40444445	14.0562149	0.00017743	0.00803015
PMI_004695	502.986634	1.55385885	0.42184242	12.7011978	0.00036542	0.01338005
PMI_005148	262.759633	1.54608906	0.43298583	11.9947082	0.00053352	0.01753497
PMI_018026	258.368592	1.5459654	0.46093195	10.3308633	0.00130824	0.03247823
PMI_019249	55.3250285	1.54456324	0.50152444	9.19916025	0.00242126	0.04850958
PMI_023862	104.697759	1.54016005	0.46219338	10.5958799	0.0011334	0.02968775
PMI_013338	66.4294448	1.53737549	0.49510687	9.27064487	0.00232856	0.04699328
PMI_023512	154.855191	1.53587385	0.42377695	12.655217	0.00037452	0.01349833
PMI_019997	170.206035	1.53576613	0.43256883	12.0294693	0.00052366	0.01725203
PMI_015528	979.647848	1.52890145	0.40415115	13.5075749	0.0002376	0.00993898
PMI_004055	193.183573	1.52513646	0.4714407	9.61610744	0.00192878	0.04120537
PMI_018218	118.351213	1.52001117	0.48032607	9.34137335	0.00224038	0.04578109
PMI_024989	151.569161	1.5187908	0.45869779	10.2988173	0.00133116	0.03287167
PMI_024140	262.196814	1.51512541	0.44686899	10.686992	0.00107891	0.02864439
PMI_028651	599.980628	1.51331241	0.44739133	10.4795413	0.00120704	0.03068497
PMI_006854	4940.86531	1.51115109	0.40355568	13.1717954	0.00028419	0.01120867
PMI_016494	105.894025	1.50993274	0.45280667	10.6919031	0.00107605	0.02864439
PMI_006795	91.9103332	1.50928927	0.47158125	9.79085384	0.00175382	0.03861201
PMI_013810	226.123569	1.50281061	0.44805964	10.5180231	0.00118216	0.03055903
PMI_025911	75.8667903	1.50198934	0.47157789	9.81253227	0.00173327	0.03822047
PMI_003154	373.808097	1.4993285	0.42261413	11.8674441	0.00057124	0.01846689
PMI_011266	1162.25705	1.49676239	0.41039299	12.4957586	0.00040788	0.01443675
PMI_029320	149.20396	1.48103943	0.43485245	11.132003	0.00084851	0.02440171
PMI_011293	175.440313	1.47752717	0.43087626	11.2559969	0.00079366	0.02340963
PMI_016787	198.720898	1.47750015	0.44966066	10.051296	0.00152241	0.03558098
PMI_014809	402.924071	1.47554784	0.40739328	12.5120677	0.00040433	0.01438504
PMI_018282	96.5727432	1.47552246	0.47263029	9.28872679	0.00230568	0.04666812
PMI_014515	84.499844	1.47337031	0.47637083	9.17529293	0.00245304	0.04907504
PMI_018340	525.617302	1.47223071	0.44824482	9.9016655	0.00165129	0.0371245
PMI_011155	86.3112358	1.47209776	0.47124598	9.37956274	0.00219418	0.04520663
PMI_007342	670.714863	1.4699407	0.45013723	9.74013931	0.00180287	0.03931572
PMI_002445	342.068741	1.46739878	0.43859316	10.4602645	0.0012197	0.0307991
PMI_010649	176.294616	1.46658971	0.45062078	9.97175088	0.0015896	0.03644032
PMI_004927	385.167479	1.46519771	0.45128902	9.69901225	0.00184367	0.04001577
PMI_020634	475.353716	1.45914927	0.40013523	12.7232689	0.00036113	0.01325823
PMI_020931	160.255752	1.45903148	0.4464723	10.1406367	0.00145036	0.03466962
PMI_005928	173.48321	1.45737732	0.42701002	11.2074444	0.0008147	0.02372594
PMI_013172	674.200281	1.44740307	0.45038946	9.44235278	0.00212031	0.0443111
PMI_010179	309.18295	1.4440619	0.42148363	11.1485229	0.00084099	0.02423585
PMI_007755	402.411482	1.44105445	0.4093007	11.8268834	0.00058382	0.01882944

PMI_008333	147.101852	1.4275453	0.42907488	10.7027824	0.00106975	0.02864439
PMI_004621	314.509275	1.42452364	0.43225374	10.2304746	0.00138139	0.03380979
PMI_020556	204.759763	1.42199084	0.44218243	9.77636129	0.0017677	0.03882911
PMI_011828	169.947245	1.4217569	0.44379933	9.75445404	0.00178889	0.03907248
PMI_001902	122.196396	1.42096531	0.44238068	9.96018319	0.00159962	0.03649789
PMI_020349	412.095864	1.41997811	0.39616323	12.3801007	0.00043393	0.01516461
PMI_020120	380.380329	1.41445736	0.40192817	11.9144657	0.000557	0.01813455
PMI_001354	493.526369	1.41396731	0.43940874	9.61659892	0.00192827	0.04120537
PMI_018930	221.27975	1.41364527	0.41809899	11.0096896	0.00090637	0.02542989
PMI_010720	5938.58394	1.40985207	0.40865737	11.1896947	0.00082253	0.02389989
PMI_004379	231.451828	1.40956347	0.43384516	10.0155388	0.00155225	0.03597091
PMI_000327	323.738181	1.40430202	0.41223091	11.1106431	0.00085834	0.02450938
PMI_009159	125.925306	1.40345733	0.44212307	9.71821222	0.00182451	0.03966224
PMI_019532	219.588091	1.40286289	0.44356505	9.42263859	0.00214323	0.04455593
PMI_018054	98.5823913	1.39545387	0.4509082	9.3054744	0.0022847	0.04651625
PMI_006894	923.979116	1.39491912	0.43435199	9.56445521	0.00198381	0.04206532
PMI_004800	160.334385	1.39351668	0.42332801	10.4867296	0.00120235	0.03068497
PMI_022597	295.073419	1.39229693	0.43572626	9.61369643	0.00193132	0.04120537
PMI_003082	498.582719	1.39194291	0.41060846	10.9357118	0.00094328	0.02609433
PMI_007543	169.642858	1.38887911	0.43141725	9.96017918	0.00159962	0.03649789
PMI_000390	206.746467	1.38312841	0.42572212	10.1256097	0.00146223	0.03480114
PMI_008287	325.482668	1.37377499	0.4112803	10.6989107	0.00107199	0.02864439
PMI_005792	150.577186	1.37014053	0.42961641	9.83498199	0.00171224	0.03793861
PMI_002688	2302.83531	1.36608269	0.38763265	11.9100138	0.00055833	0.01813455
PMI_018912	2136.73662	1.36289367	0.43177246	9.22975704	0.00238113	0.04791422
PMI_001270	10932.982	1.34898049	0.38121686	12.0425666	0.00051999	0.01721995
PMI_003106	240.863504	1.34740644	0.43081388	9.31186128	0.00227675	0.04642285
PMI_013111	308.948971	1.34301485	0.40227744	10.7909372	0.00101998	0.02760752
PMI_025115	12501.1446	1.33550859	0.40838159	10.0884591	0.00149201	0.03514621
PMI_009045	3027.48628	1.33482843	0.39057166	11.186077	0.00082413	0.02389989
PMI_013670	289.309078	1.33388522	0.40782528	10.3312566	0.00130796	0.03247823
PMI_005255	3096.39629	1.3328665	0.40684303	10.1539929	0.00143989	0.03456738
PMI_011432	379.446301	1.33148595	0.40333551	10.5019207	0.00119251	0.03065427
PMI_015481	359.394353	1.32474248	0.41318141	9.8509007	0.00169749	0.03774053
PMI_028952	235.765373	1.32402782	0.4112225	10.029843	0.00154024	0.03591469
PMI_004871	2706.78678	1.31437748	0.38736929	11.0631514	0.0008806	0.02480786
PMI_022028	288.177983	1.30877772	0.40803042	9.93695447	0.00161993	0.0366583
PMI_003102	244.705665	1.30244227	0.41667269	9.43531448	0.00212847	0.04438269
PMI_027346	3244.10317	1.30089472	0.39190239	10.5578818	0.00115694	0.03024185
PMI_001136	493.564819	1.29515208	0.4047878	9.81421991	0.00173168	0.03822047
PMI_000036	280.736538	1.29450504	0.4064257	9.82473851	0.0017218	0.03808935
PMI_007372	5447.40126	1.29005451	0.41094139	9.30108762	0.00229018	0.04654731

PMI_010069	658.516705	1.28980876	0.39314571	10.4029385	0.00125815	0.03157726
PMI_003787	375.221557	1.288508	0.40069187	10.0089643	0.0015578	0.03597091
PMI_026236	472.325451	1.26512811	0.4004383	9.65922825	0.00188403	0.04069971
PMI_027563	1149.11506	1.24547839	0.39625588	9.49404363	0.0020614	0.04351004
PMI_000840	940.495942	1.23641728	0.38348512	10.0984628	0.00148393	0.03501569
PMI_025688	1483.15101	1.23073389	0.39322597	9.42777961	0.00213723	0.0444982
PMI_017524	2816.37813	1.22575739	0.37950301	10.1195904	0.00146702	0.03485489
PMI_004907	1323.24815	1.21664818	0.38477494	9.69169315	0.00185103	0.04011241
PMI_005953	1751.37408	-1.1769689	0.38366593	9.13908749	0.00250206	0.04986961
PMI_015074	2061.70188	-1.1912319	0.38202535	9.44104762	0.00212182	0.0443111
PMI_007395	991.68878	-1.2419744	0.38899679	9.86573322	0.00168386	0.0375508
PMI_015620	670.984173	-1.2438596	0.39186963	9.76658399	0.00177712	0.03893875
PMI_025325	803.166224	-1.2581722	0.39321687	9.88794889	0.00166365	0.03728082
PMI_017898	368.573762	-1.2584185	0.40729523	9.22306192	0.00238986	0.04801974
PMI_005728	290.635099	-1.2621345	0.40679212	9.35401642	0.00222497	0.04563675
PMI_022064	435.687797	-1.2677478	0.39733291	9.86871361	0.00168113	0.03755068
PMI_001414	9910.04654	-1.2689674	0.39389597	9.93010779	0.00162597	0.03673468
PMI_008803	1935.36438	-1.2891836	0.39765241	10.0501531	0.00152335	0.03558098
PMI_008848	1599.36404	-1.2957705	0.39703469	10.1923213	0.00141027	0.0341532
PMI_001491	305.718543	-1.3018294	0.41559489	9.44554764	0.00211662	0.0443111
PMI_001719	805.365155	-1.3065019	0.39691109	10.4485762	0.00122744	0.03086263
PMI_001562	615.264092	-1.3080639	0.3942387	10.6289666	0.0011133	0.02932464
PMI_010370	1942.58095	-1.3125979	0.39195224	10.7547793	0.0010401	0.02804217
PMI_009176	1448.73072	-1.3313583	0.41006694	9.96918187	0.00159182	0.03644032
PMI_019243	171.49933	-1.3739686	0.42591134	10.0819665	0.00149727	0.03521018
PMI_022881	260.253257	-1.3837106	0.42650601	10.0510937	0.00152258	0.03558098
PMI_012718	162.271474	-1.3894493	0.43949127	9.64508156	0.00189859	0.0408227
PMI_013040	240.559777	-1.3917349	0.41136289	11.0833033	0.00087108	0.02469087
PMI_005473	866.242706	-1.3970082	0.40068633	11.5907479	0.00066281	0.0204959
PMI_024640	743.698825	-1.4036444	0.39110327	12.3857633	0.00043262	0.01515706
PMI_004527	2738.89455	-1.4054292	0.38737026	12.5966168	0.00038645	0.01385583
PMI_017506	160.92141	-1.4133485	0.43354197	10.3139005	0.00132032	0.03266252
PMI_006244	347.659245	-1.4137993	0.41959263	10.8160706	0.00100623	0.02734247
PMI_016546	451.042181	-1.4175529	0.41252675	11.2393865	0.0008008	0.02351956
PMI_020964	143.270503	-1.4301552	0.43968614	10.2153749	0.00139275	0.03393899
PMI_007067	92.4610969	-1.4347439	0.46713052	9.13796373	0.0025036	0.04986961
PMI_021006	133.829642	-1.4446444	0.44414739	10.2231807	0.00138686	0.03388368
PMI_010873	159.134927	-1.4515804	0.44517197	10.2127009	0.00139477	0.03393899
PMI_019513	261.913206	-1.4518489	0.41491306	11.7662045	0.00060316	0.01931786
PMI_001476	175.693233	-1.4546748	0.42396305	11.3921137	0.00073757	0.02227868
PMI_014623	188.295408	-1.454783	0.46788127	9.14344577	0.00249611	0.04986432
PMI_019837	85.2526663	-1.4559914	0.46715886	9.46015015	0.00209984	0.04418624

PMI_002440	269.120992	-1.4562868	0.41117649	12.0919493	0.0005064	0.0170173
PMI_000439	143.746831	-1.4612309	0.45173822	10.0183766	0.00154986	0.03597091
PMI_017073	139.785439	-1.4628533	0.4359138	10.9188967	0.00095188	0.02622713
PMI_012448	118.824665	-1.464143	0.44832228	10.3276537	0.00131052	0.03247823
PMI_005893	426.498669	-1.4668149	0.39690734	13.1478128	0.00028786	0.01125652
PMI_009365	153.841277	-1.4716823	0.43460144	11.0669997	0.00087878	0.02480705
PMI_022886	569.825652	-1.476971	0.43865804	10.4838319	0.00120424	0.03068497
PMI_011706	117.257495	-1.4782372	0.4462788	10.64055	0.00110635	0.02925675
PMI_002912	227.002592	-1.4964602	0.45346037	10.1540029	0.00143988	0.03456738
PMI_010288	321.412321	-1.4993998	0.4027699	13.3388208	0.00025997	0.01062353
PMI_004318	338.161976	-1.5027654	0.40749269	13.0205434	0.00030809	0.01170809
PMI_015842	153.815307	-1.5041394	0.4594042	10.0994999	0.0014831	0.03501569
PMI_019277	87.8175857	-1.510066	0.47312071	9.8505263	0.00169783	0.03774053
PMI_005919	263.826676	-1.5154609	0.45232449	10.454608	0.00122344	0.03081815
PMI_004472	185.064279	-1.5232598	0.44607252	11.0368531	0.00089318	0.02511101
PMI_016953	255.270051	-1.5285499	0.42352044	12.4737423	0.00041271	0.01457054
PMI_024066	342.15774	-1.5298861	0.41086159	13.2267567	0.00027598	0.01101052
PMI_015248	523.563703	-1.5399365	0.44900447	10.7320739	0.00105294	0.02833301
PMI_003373	278.088186	-1.5459909	0.40661406	13.8962342	0.00019319	0.0085472
PMI_018190	256.939925	-1.5503864	0.44678415	11.2182471	0.00080997	0.0236381
PMI_019847	172.752325	-1.5529476	0.43520956	12.1955218	0.00047904	0.01644955
PMI_002299	209.634851	-1.5602708	0.47185954	9.98473319	0.00157843	0.03631451
PMI_005789	389.563759	-1.561929	0.46299069	10.3412718	0.00130088	0.03247269
PMI_001707	503.445686	-1.5623904	0.39227053	15.2015959	9.66E-05	0.00516964
PMI_020403	260.517097	-1.5643618	0.42073738	13.1664414	0.00028501	0.01120867
PMI_023031	332.392203	-1.5654568	0.41775007	13.3207948	0.00026248	0.01068808
PMI_018806	765.270998	-1.5676905	0.39469564	15.0035805	0.00010731	0.0055897
PMI_014543	196.168755	-1.5716644	0.42331533	13.2456202	0.00027322	0.01093187
PMI_013479	78.4464488	-1.5828933	0.4904854	9.99119784	0.0015729	0.03624766
PMI_004477	239.929482	-1.5843379	0.42868894	12.9651427	0.00031734	0.01196891
PMI_028731	145.662792	-1.5993773	0.45606091	11.680373	0.00063163	0.01986105
PMI_006282	217.60302	-1.5994798	0.42918419	13.1959441	0.00028056	0.01112871
PMI_000388	77.3280335	-1.6003606	0.49209165	10.1340185	0.00145558	0.03470257
PMI_001339	387.930149	-1.6010351	0.41433954	14.1307099	0.00017054	0.00784697
PMI_013272	146.019345	-1.60247	0.45035396	12.0347685	0.00052217	0.01724421
PMI_006397	115.296948	-1.6027877	0.48967752	9.95212421	0.00160664	0.03654636
PMI_007327	235.263708	-1.6028393	0.46380723	10.9990382	0.00091159	0.0254729
PMI_005063	277.623136	-1.6063936	0.4767218	10.2884146	0.00133868	0.03299848
PMI_003983	782.368652	-1.6106416	0.39206199	16.045143	6.19E-05	0.00373254
PMI_005536	62.4091098	-1.6131054	0.50911507	9.72197479	0.00182078	0.03964356
PMI_005982	80.4222582	-1.6190504	0.48151111	11.0010696	0.00091059	0.0254729
PMI_002644	302.601884	-1.619724	0.4520031	12.0418577	0.00052019	0.01721995

PMI_015315	88.9235366	-1.6225247	0.48737071	10.5100692	0.00118726	0.03063348
PMI_016327	153.836353	-1.6281764	0.45207027	12.2448088	0.00046655	0.0161817
PMI_024881	1631.03458	-1.6315974	0.40184626	15.4548016	8.45E-05	0.00475642
PMI_005164	50.3794218	-1.6324777	0.52751618	9.29421528	0.00229879	0.04659683
PMI_003899	1515.45767	-1.6356917	0.44248661	12.3471918	0.00044165	0.01535653
PMI_000469	98.5718048	-1.6365079	0.46248255	12.0424762	0.00052002	0.01721995
PMI_013472	102.478661	-1.6409869	0.48656389	10.7185798	0.00106065	0.02848486
PMI_008129	110.787987	-1.6500145	0.47005014	11.6698069	0.00063523	0.01992877
PMI_021004	406.117224	-1.6516071	0.40379081	15.899531	6.68E-05	0.00397432
PMI_005981	158.779407	-1.6518296	0.44367418	13.2500158	0.00027258	0.01093187
PMI_025896	68.0516843	-1.6553339	0.50484006	10.3935506	0.00126456	0.03168061
PMI_024253	98.6282299	-1.6574776	0.51395736	9.48034341	0.00207685	0.04376924
PMI_002719	86.0362291	-1.6610057	0.50287631	10.2517657	0.00136554	0.03348116
PMI_000130	262.189898	-1.6656691	0.41893707	15.0094868	0.00010697	0.0055897
PMI_011881	79.8008645	-1.6692617	0.48378818	11.4463189	0.00071636	0.02187744
PMI_010027	156.273859	-1.6735635	0.4725198	11.6457419	0.0006435	0.02014247
PMI_011817	74.8322852	-1.677522	0.49331194	11.100797	0.00086291	0.02450938
PMI_021426	551.94191	-1.6799035	0.39295719	17.381545	3.06E-05	0.00213182
PMI_008056	209.614821	-1.6825681	0.47699575	11.3438312	0.00075699	0.02261794
PMI_007790	3094.11154	-1.684413	0.39559594	16.9917593	3.75E-05	0.00254037
PMI_004579	510.449457	-1.6858413	0.41683018	15.3067997	9.14E-05	0.00500597
PMI_004094	65.2497567	-1.6905414	0.49655977	11.246643	0.00079767	0.02347773
PMI_019762	407.789279	-1.6914557	0.42108721	15.225769	9.54E-05	0.00514376
PMI_001536	69.5005088	-1.6992847	0.49994829	11.1111456	0.0008581	0.02450938
PMI_001306	13688.0324	-1.7019559	0.38279372	18.6282784	1.59E-05	0.0013045
PMI_010542	41.5050122	-1.7029522	0.55431621	9.1994556	0.00242087	0.04850958
PMI_001512	211.544173	-1.7041864	0.42050942	15.6568889	7.59E-05	0.00438583
PMI_021201	64.2001209	-1.7062723	0.52782704	10.0170841	0.00155095	0.03597091
PMI_007072	180.406053	-1.7086456	0.46967628	12.2278549	0.00047081	0.01628587
PMI_026602	131.020314	-1.7086598	0.4479653	13.887495	0.00019409	0.00855961
PMI_016080	43.2527347	-1.7113468	0.55118993	9.36936222	0.00220642	0.04539115
PMI_008331	140.502452	-1.7183087	0.48295866	11.6155181	0.00065404	0.02034851
PMI_001966	1172.01341	-1.7203467	0.44479514	13.5407646	0.00023344	0.00982067
PMI_000574	120.282812	-1.7296957	0.47342665	12.5692673	0.00039214	0.01398742
PMI_001606	72.2078187	-1.7296976	0.49712773	11.7168304	0.00061937	0.01970008
PMI_002903	209.18315	-1.7307767	0.436465	14.8564307	0.00011601	0.00588242
PMI_005033	1343.08172	-1.7322	0.38230435	19.4259318	1.05E-05	0.00094352
PMI_016813	200.010252	-1.7488466	0.4498585	14.0754594	0.00017562	0.00800087
PMI_009175	1373.11162	-1.7549828	0.39362557	18.639517	1.58E-05	0.0013045
PMI_017091	321.402896	-1.7637443	0.44554582	14.4306079	0.00014542	0.00687456
PMI_000677	79.306324	-1.7816105	0.54721001	9.55736993	0.00199148	0.04216322
PMI_004478	59.5483826	-1.7905203	0.55547216	9.61754042	0.00192728	0.04120537

PMI_003423	65.1039427	-1.7957231	0.51406104	11.6228193	0.00065148	0.02034609
PMI_020966	331.783384	-1.7959124	0.40662873	18.4716836	1.72E-05	0.00139209
PMI_000136	237.984726	-1.8086918	0.47266436	13.2504132	0.00027252	0.01093187
PMI_004675	334.596624	-1.8152243	0.53036735	9.91533592	0.00163907	0.03690987
PMI_019116	222.393613	-1.8210514	0.43754609	16.1600588	5.82E-05	0.00357116
PMI_021528	276.309252	-1.8211762	0.42072085	17.7046278	2.58E-05	0.00187225
PMI_015515	72.2774635	-1.8279468	0.53368124	10.8526906	0.00098652	0.02691297
PMI_007078	88.4856858	-1.8291477	0.46940273	14.5900796	0.00013362	0.00644908
PMI_005827	148.413534	-1.8300955	0.51225462	11.4157345	0.00072825	0.02207455
PMI_016120	240.256806	-1.8307233	0.4181764	18.155898	2.04E-05	0.00156963
PMI_016926	48.6029653	-1.836936	0.57933826	9.40923399	0.00215895	0.04481534
PMI_014912	49.2803285	-1.8370168	0.5708094	9.67126029	0.00187173	0.0404974
PMI_012970	232.458722	-1.8390475	0.42280234	17.833227	2.41E-05	0.00178959
PMI_018959	38.6554081	-1.8405978	0.58674153	9.39314026	0.00217799	0.04511635
PMI_019055	636.758353	-1.843467	0.39008438	21.0424526	4.49E-06	0.00051128
PMI_011944	117.026316	-1.8448254	0.52082764	11.3092355	0.00077123	0.02289461
PMI_005659	251.694028	-1.8526236	0.41657123	18.6767882	1.55E-05	0.00128773
PMI_000862	983.740027	-1.8594218	0.50451709	11.2873712	0.00078036	0.0230666
PMI_008290	110.261603	-1.8604141	0.45441481	16.0705829	6.10E-05	0.00371095
PMI_016477	31.8422426	-1.8610027	0.60088847	9.38616648	0.00218629	0.04511635
PMI_001846	88.0599457	-1.8622548	0.56820127	9.44236283	0.0021203	0.0443111
PMI_012977	89.6603806	-1.8640467	0.4940171	13.4220499	0.00024868	0.01024726
PMI_004449	39.99922	-1.8680144	0.57661021	10.1621377	0.00143354	0.03456738
PMI_018225	101.63491	-1.8744733	0.56071897	9.77468874	0.00176931	0.03882911
PMI_014959	364.622132	-1.8822402	0.4382257	16.9166006	3.91E-05	0.0026173
PMI_003785	374.387163	-1.8847819	0.40231588	20.6699671	5.46E-06	0.00058057
PMI_003166	45.1653228	-1.8927536	0.58008763	10.0124546	0.00155485	0.03597091
PMI_013282	87.0192706	-1.8966748	0.48587333	14.4644935	0.00014283	0.00677518
PMI_019516	377.972813	-1.9004591	0.46313199	15.1618106	9.87E-05	0.00525933
PMI_018669	80.1475662	-1.9025059	0.52229734	12.2234838	0.00047192	0.01628587
PMI_000135	56.4250902	-1.9035488	0.52145524	12.8022509	0.0003462	0.01285227
PMI_002496	95.769946	-1.9066342	0.50295894	13.348756	0.00025859	0.01062353
PMI_014343	117.912878	-1.9266417	0.51888859	12.4430131	0.00041956	0.01477445
PMI_013124	36.8611075	-1.9332566	0.59501561	10.1094506	0.00147511	0.03494799
PMI_005260	54.5801897	-1.9405573	0.55535921	11.5882551	0.0006637	0.0204959
PMI_003317	136.902424	-1.9428021	0.44252317	18.2701412	1.92E-05	0.00150345
PMI_025848	77.499913	-1.9467963	0.48692885	15.3995569	8.70E-05	0.00482357
PMI_003130	80.9091775	-1.9507793	0.52775553	12.6666244	0.00037224	0.01345135
PMI_023728	78.3081889	-1.9508134	0.51148644	13.5644632	0.00023051	0.00976054
PMI_001347	141.138352	-1.9538898	0.4921322	14.2355873	0.00016129	0.00749651
PMI_003042	556.296409	-1.9554247	0.41421898	20.6127838	5.62E-06	0.00058792
PMI_020154	39.6362117	-1.9555241	0.59041788	10.4815051	0.00120575	0.03068497

PMI_025194	53.1509714	-1.9590482	0.5309773	13.1172637	0.00029259	0.0113483
PMI_008849	518.566304	-1.9635452	0.3936718	23.3261274	1.37E-06	0.00021694
PMI_009376	41.4397242	-1.9690279	0.56223216	11.8772353	0.00056824	0.01841318
PMI_009649	79.4212334	-1.9786327	0.57314019	10.6256658	0.00111529	0.02932464
PMI_026915	54.326111	-1.9799819	0.53448827	13.1679558	0.00028478	0.01120867
PMI_019244	102.294535	-1.9801039	0.49613227	14.7714491	0.00012136	0.0060478
PMI_011055	40.6092889	-1.9802678	0.58261623	11.118742	0.0008546	0.02450938
PMI_016562	230.967836	-1.9814907	0.45652917	17.1769088	3.41E-05	0.00235048
PMI_012746	445.645796	-1.9829658	0.41213501	21.4406303	3.65E-06	0.00043058
PMI_011941	54.2939071	-1.9830676	0.54223043	12.7379566	0.00035831	0.01320288
PMI_015721	224.07941	-1.9883516	0.55047454	10.5412171	0.00116742	0.0303484
PMI_007554	149.92213	-1.9885319	0.48164346	15.5320653	8.11E-05	0.00460801
PMI_017635	61.1630579	-1.9908866	0.52363997	13.9312087	0.00018962	0.00841661
PMI_008586	114.718681	-1.9968397	0.56993459	10.5519594	0.00116065	0.03024185
PMI_004452	147.911576	-2.003402	0.48897403	15.2175954	9.58E-05	0.00514597
PMI_021616	55.3080781	-2.0045778	0.53859267	13.2698131	0.00026971	0.01088636
PMI_023178	32.3294184	-2.0075908	0.6084846	10.6073096	0.00112641	0.02956089
PMI_013038	41.6776136	-2.0079471	0.5935009	10.9877794	0.00091715	0.0255714
PMI_011721	30.2148256	-2.0105476	0.6346932	9.53875473	0.00201178	0.04252778
PMI_001537	758.53182	-2.011735	0.4947871	14.1554376	0.00016831	0.0077704
PMI_001065	145.986434	-2.0270985	0.51981614	13.4876464	0.00024014	0.00996944
PMI_009181	119.810979	-2.0362037	0.48018632	16.6253453	4.55E-05	0.00296224
PMI_023033	66.3284696	-2.036635	0.50558116	15.5237045	8.15E-05	0.00460947
PMI_019436	1254.25032	-2.0386194	0.42453957	20.766592	5.19E-06	0.0005639
PMI_013413	59.4327421	-2.0443247	0.56237558	12.2064087	0.00047626	0.01639462
PMI_012747	30.2881906	-2.0460637	0.6177905	10.6901296	0.00107709	0.02864439
PMI_003907	122.474394	-2.0523145	0.45693892	19.0665428	1.26E-05	0.00111705
PMI_009849	70.0053495	-2.0554027	0.50781492	15.6230141	7.73E-05	0.00444649
PMI_027370	56.6144089	-2.0578195	0.58148859	11.3860255	0.00073999	0.02230301
PMI_003552	556.904702	-2.0604466	0.44279083	19.4448803	1.04E-05	0.00094273
PMI_008930	56.8554647	-2.0623921	0.58115497	11.5142108	0.00069066	0.0212505
PMI_024527	30.377883	-2.0653585	0.64831162	9.6527054	0.00189073	0.04071704
PMI_014819	159.897576	-2.0686824	0.43821057	20.9810502	4.64E-06	0.00052057
PMI_004453	745.290194	-2.069598	0.4290142	21.0325344	4.52E-06	0.00051128
PMI_002759	80.4364285	-2.0752001	0.54387994	13.0166563	0.00030873	0.01170809
PMI_004300	75.2909489	-2.0825071	0.51098077	15.7611426	7.19E-05	0.0042034
PMI_007836	73.269941	-2.0889025	0.58361793	11.3594858	0.00075064	0.02252561
PMI_010553	175.11406	-2.092717	0.45446448	19.4980044	1.01E-05	0.00093297
PMI_010838	72.446865	-2.0956124	0.55507097	12.9412084	0.00032143	0.01205702
PMI_000365	470.605257	-2.0957435	0.5052412	14.650353	0.00012941	0.0063123
PMI_013721	46.6143782	-2.0996615	0.55192634	13.9795176	0.00018481	0.00830996
PMI_013817	127.707129	-2.1069087	0.48176256	17.4769091	2.91E-05	0.00204819

PMI_005620	85.640172	-2.1115567	0.51051154	15.7725764	7.14E-05	0.00419585
PMI_008917	478.420634	-2.1130818	0.4029125	25.4494074	4.54E-07	9.84E-05
PMI_018319	67.7406668	-2.1138153	0.50859016	16.549692	4.74E-05	0.0029915
PMI_027299	290.977599	-2.1153351	0.42186744	23.3430338	1.36E-06	0.00021694
PMI_000263	59.351749	-2.1166106	0.62511053	9.95165977	0.00160704	0.03654636
PMI_008942	146.693638	-2.1239886	0.44338686	21.5596307	3.43E-06	0.000419
PMI_014503	48.9830195	-2.1242257	0.55066849	14.2257639	0.00016214	0.00751046
PMI_006699	70.9224849	-2.1250807	0.50977951	16.5862629	4.65E-05	0.00296462
PMI_001346	499.700785	-2.1262807	0.4220115	23.0866569	1.55E-06	0.00023752
PMI_022660	37.5536249	-2.1293593	0.64954026	9.75592529	0.00178746	0.03907248
PMI_018130	224.230459	-2.1379271	0.46051774	19.4590673	1.03E-05	0.00094273
PMI_012058	595.360456	-2.1386352	0.3978703	26.6927829	2.39E-07	6.46E-05
PMI_002497	33.9461583	-2.1411293	0.64481453	10.2792771	0.00134533	0.03310319
PMI_004844	62.5723035	-2.1456914	0.55914345	13.5444368	0.00023298	0.00982067
PMI_022122	76.4807781	-2.1470863	0.57220251	12.1869851	0.00048124	0.016484
PMI_020290	60.0869199	-2.1527732	0.54102019	14.8965715	0.00011357	0.00582792
PMI_000133	339.126256	-2.1548354	0.4769433	17.9962147	2.21E-05	0.00166964
PMI_001160	44.4247343	-2.1566462	0.57919532	13.1167421	0.00029267	0.0113483
PMI_000018	99.7441689	-2.1604605	0.54624467	13.8568884	0.00019727	0.00867244
PMI_007179	80.8345489	-2.1626648	0.55086404	13.6508056	0.00022015	0.00940838
PMI_008330	35.3847968	-2.163238	0.61693394	11.6890358	0.00062869	0.01986105
PMI_020183	40.2291507	-2.1639239	0.58676761	13.0489513	0.00030345	0.0115715
PMI_006078	43.2525561	-2.1654788	0.59047365	12.6767585	0.00037023	0.01341375
PMI_013014	40.9557502	-2.1655406	0.58150689	13.4848505	0.0002405	0.00996944
PMI_009636	34.1101875	-2.1658511	0.65321506	10.1459903	0.00144615	0.03465749
PMI_001757	140.794638	-2.1792264	0.46615738	20.1378977	7.21E-06	0.00071046
PMI_018180	51.3617686	-2.1870236	0.55179065	14.9538935	0.00011017	0.00569586
PMI_000134	30.9378535	-2.1905717	0.65599477	10.484806	0.0012036	0.03068497
PMI_017775	83.5255802	-2.1915277	0.59606116	11.4203577	0.00072644	0.02207455
PMI_023407	31.4839694	-2.2009965	0.62315562	12.0636164	0.00051415	0.01714345
PMI_004320	29.2336552	-2.2031661	0.65708513	10.6867761	0.00107904	0.02864439
PMI_020498	29.3650797	-2.2065264	0.64230827	11.3375514	0.00075955	0.02264554
PMI_013565	41.507704	-2.2081544	0.61621776	11.6930766	0.00062733	0.01986105
PMI_008214	459.089492	-2.213075	0.42733689	24.2168118	8.61E-07	0.0001531
PMI_000901	70.6465547	-2.2211444	0.50611575	18.2752268	1.91E-05	0.00150345
PMI_000819	85.3865969	-2.2220952	0.57097206	13.3105081	0.00026392	0.01071527
PMI_016399	43.3944856	-2.2303231	0.64702769	10.6778478	0.00108426	0.02872772
PMI_012307	70.5526495	-2.2418045	0.52985164	16.6182826	4.57E-05	0.00296224
PMI_021130	63.0308327	-2.2461757	0.64245209	10.195482	0.00140785	0.0341532
PMI_005551	219.114881	-2.2464846	0.60562139	10.8941306	0.00096469	0.02646152
PMI_022644	366.178573	-2.2531617	0.50437531	16.6817249	4.42E-05	0.00291963
PMI_020669	68.2588601	-2.254374	0.61913338	11.4132832	0.00072921	0.02207455

PMI_001538	136.207038	-2.2579054	0.64171533	9.60602807	0.0019394	0.04131394
PMI_015513	73.8095945	-2.2626531	0.60122748	11.740765	0.00061146	0.01949325
PMI_015944	1060.24589	-2.2688248	0.61933308	9.92484817	0.00163062	0.03677961
PMI_009179	34.7993873	-2.271833	0.63815946	11.7408807	0.00061142	0.01949325
PMI_002956	45.3501881	-2.2863607	0.57855264	14.8618691	0.00011568	0.00588242
PMI_019306	322.256934	-2.2865309	0.45155503	22.8187745	1.78E-06	0.00025334
PMI_013722	51.1752616	-2.2878046	0.59043675	13.6603249	0.00021903	0.00938987
PMI_009848	131.225605	-2.3000949	0.45854789	23.3337457	1.36E-06	0.00021694
PMI_029081	38.527234	-2.3188666	0.61641224	13.3376929	0.00026012	0.01062353
PMI_008953	191.884993	-2.3202323	0.52473254	16.7944692	4.17E-05	0.00276442
PMI_003129	327.928519	-2.3218521	0.59493707	11.9490393	0.00054676	0.01791415
PMI_005483	136.71643	-2.3225506	0.49307079	19.7940377	8.63E-06	0.00081549
PMI_002722	79.1963961	-2.3245853	0.52165957	18.2282628	1.96E-05	0.00152818
PMI_003037	189.469562	-2.3291137	0.62764996	10.6368223	0.00110858	0.02925973
PMI_017785	90.2825287	-2.3296723	0.54183228	16.5950728	4.63E-05	0.00296462
PMI_006998	102.268922	-2.348328	0.5421738	16.2174186	5.65E-05	0.00348012
PMI_021608	237.551269	-2.3572358	0.46589988	22.6874365	1.91E-06	0.00026465
PMI_001271	74.0368117	-2.361695	0.50850637	20.3980954	6.29E-06	0.00064309
PMI_010857	46.5618583	-2.3724075	0.6267994	12.889567	0.00033042	0.01236071
PMI_005418	62.7800255	-2.3745295	0.59793086	13.9448154	0.00018826	0.00838286
PMI_006936	31.182789	-2.3846881	0.72252691	9.3465739	0.00223403	0.04575447
PMI_009493	649.406525	-2.3882427	0.4832885	20.7917706	5.12E-06	0.00056095
PMI_004287	131.671105	-2.3982055	0.52142357	18.5166504	1.68E-05	0.00136762
PMI_002654	47.3943121	-2.3984407	0.60962489	14.0624652	0.00017684	0.00802983
PMI_009927	51.0151095	-2.4014415	0.5470736	18.3711089	1.82E-05	0.00145057
PMI_010837	434.817498	-2.4061316	0.45269166	24.6845577	6.75E-07	0.00012768
PMI_022925	1233.71981	-2.4101808	0.45786936	23.844178	1.04E-06	0.00018252
PMI_008399	68.0930113	-2.4174477	0.52774927	19.6172341	9.46E-06	0.00088845
PMI_000886	52.3092822	-2.4175402	0.71424452	9.25735039	0.00234552	0.04726653
PMI_022656	115.40224	-2.4204672	0.47896244	23.5886477	1.19E-06	0.00019967
PMI_018626	39.4852657	-2.4247843	0.59409274	16.0102115	6.30E-05	0.00376483
PMI_006164	94.6489182	-2.4265245	0.57405704	15.2710457	9.31E-05	0.00504568
PMI_019761	242.840634	-2.428042	0.45614772	25.4545722	4.53E-07	9.84E-05
PMI_005401	132.719297	-2.4304208	0.48216751	22.9703547	1.65E-06	0.00024607
PMI_003146	28.5430818	-2.4325454	0.72594296	10.057416	0.00151736	0.03558098
PMI_017291	68.2399787	-2.4410611	0.50666793	22.0653766	2.64E-06	0.00034977
PMI_026973	60.7971664	-2.4447882	0.54458432	18.9351009	1.35E-05	0.00118018
PMI_003026	44.3750175	-2.4455853	0.60855169	15.0948844	0.00010224	0.0054069
PMI_000360	227.633464	-2.4486377	0.5538933	16.13293	5.90E-05	0.00360665
PMI_007938	127.042246	-2.4522897	0.48827963	22.9234856	1.69E-06	0.00024756
PMI_007939	75.6355728	-2.4618635	0.59719482	15.0967475	0.00010214	0.0054069
PMI_029481	33.4010921	-2.4631659	0.70059566	11.2892564	0.00077957	0.0230666

PMI_016563	172.771501	-2.4666285	0.47280784	24.2724838	8.36E-07	0.0001531
PMI_001432	109.699299	-2.4802683	0.46878752	26.2431712	3.01E-07	7.84E-05
PMI_003441	65.6617196	-2.4830117	0.59861517	14.7131861	0.00012517	0.00617078
PMI_020625	1131.85682	-2.4914531	0.41462907	31.9097736	1.62E-08	6.56E-06
PMI_001539	110.116853	-2.4992655	0.63193695	12.4988329	0.00040721	0.01443675
PMI_018705	286.728768	-2.5031844	0.59698034	13.1045301	0.00029458	0.01135871
PMI_013796	69.7725324	-2.5087223	0.66251295	11.7838392	0.00059747	0.01918022
PMI_012332	44.3776096	-2.5197097	0.71439343	10.467131	0.00121517	0.03077843
PMI_019832	86.7854525	-2.5249063	0.61869092	13.6927154	0.00021529	0.00925805
PMI_020940	75.2080135	-2.5250343	0.52241862	21.6207832	3.32E-06	0.00040948
PMI_024838	744.836553	-2.5279372	0.47758029	23.7810646	1.08E-06	0.00018625
PMI_007866	74.4019837	-2.5289146	0.53019438	20.8701583	4.91E-06	0.00054276
PMI_014132	49.4374034	-2.5417761	0.73460299	9.94504614	0.00161283	0.03661757
PMI_014907	568.707887	-2.5516461	0.46841387	25.4406267	4.56E-07	9.84E-05
PMI_018410	75.679602	-2.5578017	0.51767843	22.9556364	1.66E-06	0.00024607
PMI_025817	60.5436574	-2.5625554	0.53403285	21.7727162	3.07E-06	0.00039231
PMI_000678	43.8909821	-2.5658053	0.69896436	11.4178868	0.0007274	0.02207455
PMI_001706	144.968375	-2.5664484	0.5459938	18.8852123	1.39E-05	0.00119619
PMI_015925	733.911174	-2.5776155	0.51154389	20.8778117	4.90E-06	0.00054276
PMI_000109	41.8003085	-2.5785897	0.6307591	15.43794	8.53E-05	0.00476485
PMI_018386	40.3537037	-2.5864123	0.59638811	17.9366742	2.28E-05	0.00170407
PMI_008881	55.2670116	-2.6058144	0.54715036	21.4875029	3.56E-06	0.00042381
PMI_003577	151.998916	-2.6085833	0.4637516	28.6865779	8.51E-08	2.67E-05
PMI_022570	35.5232862	-2.6100343	0.6328344	16.028494	6.24E-05	0.00374486
PMI_003192	34.0839005	-2.6214603	0.73208112	11.2259621	0.00080661	0.02363011
PMI_008946	75.3246516	-2.6248803	0.55540086	20.1755599	7.06E-06	0.00070945
PMI_026711	43.2354518	-2.6294042	0.68382162	12.7535372	0.00035534	0.01315031
PMI_000335	208.69412	-2.6370593	0.54520345	19.5416216	9.84E-06	0.00091807
PMI_005825	136.499942	-2.6416556	0.51916377	22.3682856	2.25E-06	0.0003039
PMI_007229	77.6053285	-2.647918	0.62187157	14.580862	0.00013427	0.00645812
PMI_016464	552.302672	-2.6585585	0.56481999	17.3888109	3.05E-05	0.00213182
PMI_011323	35.1724073	-2.6655429	0.69535683	12.6927311	0.00036708	0.01340368
PMI_009852	45.3089667	-2.684021	0.70543205	12.3743723	0.00043527	0.0151728
PMI_009924	92.2573087	-2.6867552	0.49233013	27.6607183	1.45E-07	4.25E-05
PMI_008847	1092.41048	-2.6942348	0.39181676	41.8435647	9.89E-11	1.38E-07
PMI_011416	209.149424	-2.6952796	0.43263915	35.4430548	2.63E-09	1.73E-06
PMI_003505	171.503882	-2.7086551	0.45706727	31.5811733	1.91E-08	7.54E-06
PMI_011648	1167.66393	-2.7267862	0.54688619	18.7269056	1.51E-05	0.00127535
PMI_009421	98.9729422	-2.7267965	0.58553025	17.7988654	2.46E-05	0.00180281
PMI_029489	32.3523121	-2.7369136	0.67882367	15.4068084	8.67E-05	0.00482357
PMI_013523	479.116504	-2.7393637	0.46910305	29.1310061	6.76E-08	2.17E-05
PMI_018235	58.0174357	-2.743391	0.61028512	17.5504079	2.80E-05	0.00198063

PMI_007103	104.146571	-2.7440674	0.67062289	12.970574	0.00031642	0.01196693
PMI_014082	38.4285116	-2.7625749	0.60577098	20.0907693	7.39E-06	0.00072302
PMI_006747	117.69398	-2.7723547	0.46881085	32.4334615	1.23E-08	5.49E-06
PMI_025224	86.5909709	-2.7807218	0.5690184	21.0311728	4.52E-06	0.00051128
PMI_002498	183.32602	-2.787731	0.60703901	16.5814724	4.66E-05	0.00296462
PMI_010657	45.8910381	-2.7900734	0.59607473	20.4470668	6.13E-06	0.00063627
PMI_012315	29.8054741	-2.79575	0.68095867	16.0429882	6.19E-05	0.00373254
PMI_023363	63.0687425	-2.7988241	0.58902834	20.0351994	7.60E-06	0.00073909
PMI_014540	96.9522119	-2.8014407	0.52752512	25.0552034	5.57E-07	0.0001131
PMI_012957	59.2846918	-2.8217242	0.54003338	25.9042177	3.59E-07	8.39E-05
PMI_000110	89.65811	-2.8316483	0.63056645	16.5403527	4.76E-05	0.0029915
PMI_010668	89.6424733	-2.8401807	0.49651694	30.3431962	3.62E-08	1.25E-05
PMI_014179	47.1202361	-2.8592073	0.60024521	21.7895299	3.04E-06	0.00039231
PMI_009851	45.1334496	-2.8619042	0.70776506	14.080755	0.00017513	0.00800087
PMI_009038	502.155172	-2.863993	0.40131437	45.0020503	1.97E-11	5.10E-08
PMI_011707	73.164276	-2.8763012	0.52768258	27.7598739	1.37E-07	4.12E-05
PMI_002889	32.8367287	-2.8773428	0.73787545	14.1027867	0.00017309	0.00793786
PMI_014083	44.2017304	-2.885115	0.58830318	23.0511526	1.58E-06	0.00023929
PMI_027951	47.7122482	-2.8903125	0.61774656	20.6660926	5.47E-06	0.00058057
PMI_014818	99.4956221	-2.9183782	0.4882175	33.1432169	8.56E-09	4.08E-06
PMI_008872	255.920021	-2.9254541	0.42793114	41.8290487	9.96E-11	1.38E-07
PMI_020560	122.355521	-2.927207	0.58090223	21.5288124	3.49E-06	0.00042205
PMI_016664	70.4675212	-2.9368986	0.52497959	29.3196895	6.14E-08	2.07E-05
PMI_012322	39.0260338	-2.9637336	0.69754376	15.7405613	7.26E-05	0.00422544
PMI_002305	50.6194958	-3.0129365	0.59948194	23.6699352	1.14E-06	0.00019488
PMI_003744	263.434305	-3.0156338	0.57794102	21.301978	3.92E-06	0.00045896
PMI_001510	174.28024	-3.0279669	0.45433903	39.770846	2.86E-10	2.91E-07
PMI_013094	39.0203466	-3.0378421	0.61682841	23.5763003	1.20E-06	0.00019967
PMI_007711	35.6917548	-3.0467704	0.64395663	21.657963	3.26E-06	0.00040523
PMI_009850	44.5685569	-3.0511049	0.63411712	21.7945088	3.03E-06	0.00039231
PMI_003904	68.0661413	-3.054293	0.58657549	25.7289609	3.93E-07	8.97E-05
PMI_015010	421.007649	-3.0590681	0.44587974	39.9612412	2.59E-10	2.91E-07
PMI_026476	102.473343	-3.0740715	0.54585849	28.1723044	1.11E-07	3.40E-05
PMI_022414	291.339097	-3.0841485	0.60959681	18.1603009	2.03E-05	0.00156963
PMI_027561	44.8687089	-3.0845871	0.60166858	25.3059358	4.89E-07	0.00010232
PMI_021839	291.800483	-3.0900469	0.41935578	47.9925824	4.28E-12	1.97E-08
PMI_022571	47.6168495	-3.114172	0.59547002	25.9050111	3.59E-07	8.39E-05
PMI_001310	316.587847	-3.1198354	0.58506373	21.7160662	3.16E-06	0.00040036
PMI_018226	41.4599566	-3.1216248	0.68959069	18.617972	1.60E-05	0.0013045
PMI_017128	41.9962493	-3.1278939	0.62140379	24.269994	8.37E-07	0.0001531
PMI_001308	635.01561	-3.1476081	0.57537904	22.6762789	1.92E-06	0.00026465
PMI_015009	122.309246	-3.1499983	0.58563615	22.8232738	1.78E-06	0.00025334

PMI_015924	190.749785	-3.1565348	0.5064018	33.2121755	8.26E-09	4.08E-06
PMI_021875	146.945129	-3.17024	0.46070724	42.7096744	6.35E-11	1.25E-07
PMI_000073	34.7877779	-3.1724749	0.66864171	21.6663931	3.24E-06	0.00040523
PMI_005014	52.1832127	-3.1822526	0.63036279	22.9010134	1.71E-06	0.00024784
PMI_008022	248.326323	-3.2454396	0.60364553	20.6805094	5.43E-06	0.00058057
PMI_010656	38.2120011	-3.2500954	0.68960033	20.1528248	7.15E-06	0.00071001
PMI_024954	64.5257479	-3.2566591	0.54411703	33.8944787	5.82E-09	3.49E-06
PMI_005471	29.2038068	-3.2609119	0.75442268	17.5569443	2.79E-05	0.00198063
PMI_014133	492.114867	-3.2757539	0.53187531	29.1398544	6.73E-08	2.17E-05
PMI_001413	236.820721	-3.3156377	0.6136466	21.8591405	2.93E-06	0.00038574
PMI_004143	34.8721334	-3.3516773	0.66689506	24.7871653	6.40E-07	0.000125
PMI_021342	428.372369	-3.3699306	0.60381193	23.1552091	1.49E-06	0.00023178
PMI_022413	219.683565	-3.3790913	0.61659311	21.2459941	4.04E-06	0.00046859
PMI_017323	91.4707746	-3.4793346	0.64668116	22.3538724	2.27E-06	0.0003039
PMI_004374	80.6722874	-3.4813658	0.53502378	39.7052668	2.95E-10	2.91E-07
PMI_020185	54.8393635	-3.6088622	0.67795599	25.1733333	5.24E-07	0.00010796
PMI_006810	303.07056	-3.8190327	0.54685358	36.7859907	1.32E-09	1.03E-06
PMI_020184	33.7517536	-3.8199575	0.72664281	27.341921	1.70E-07	4.90E-05
PMI_008871	72.0278509	-3.858261	0.58925226	40.0097485	2.53E-10	2.91E-07
PMI_017093	62.9447965	-4.3440946	0.7274741	31.1966861	2.33E-08	8.70E-06
PMI_008870	34.0982329	-4.4831804	0.80675987	32.1243077	1.45E-08	6.24E-06
PMI_027916	28.7392038	-4.5459525	0.84678395	30.9279257	2.68E-08	9.73E-06

APPENDIX II - PUBLISHED PAPERS

This work includes some data already published in the book paper "A Differential Transcriptomic Approach to Compare Target Genes of Homologous Transcription Factors in Echinoderm Species". Authors: Elijah K. Lowe, Claudia Cuomo, and Maria I. Arnone. Book: Dynamics of Mathematical Models in Biology, A. Rogato, V. Zazzu and M. Guarracino Eds. Springer 2016, Cham, CH. My role in this paper was to take care of all the biological part for the preparation of the RNA samples for the sequencing. I covered the activities of microinjection, culture and collection of the sea urchin and sea star perturbed embryos, the extraction of the RNA and the quality check.

The methods applied in this work have been described in a review manuscript (currently under review) entitled "Omics approaches to study gene regulatory networks for development". Authors: Elijah K. Lowe, Claudia Cuomo and Maria I. Arnone. Journal: Briefings in Functional Genomics. My role in this paper was to help to describe the RNA-Seq, ChIP-Seq and ATAC-Seq combinatorial method to reveal and analyze a GRN. I also provided a description of the wet lab approaches to validate a GRN.

The PDF of these papers are attached.

A Differential Transcriptomic Approach to Compare Target Genes of Homologous Transcription Factors in Echinoderm Species

Elijah K. Lowe, Claudia Cuomo, and Maria I. Arnone

Abstract Embryonic development is controlled by differential gene expression throughout developmental time. The ParaHox genes, *Cdx* and *Xlox* have been shown to be involved in the formation of the properly functioning gut in the sea urchin *Strongylocentrotus purpuratus* and the sea star *Patiria miniata*. Several genes involved in the gene regulatory network (GRN) are known, however, the network is still incomplete. With the current state of sequencing technology, we are now able to expand the network and gain further insight into the process of gut development on a more global scale. Through the use of high-throughput sequencing technology and knockdown experiments we have further characterized the effects of *Cdx* and *Xlox* on the GRN involved in gut development at different developmental stages. Additionally, we have conducted a cross-species comparison to identify genes that are more likely to be evolutionarily important for the development of the echinoderm gut. Within those genes we found a number of transcription factors that could potentially have important roles in the formation of the echinoderm gut. Using both RNA-seq and gene homology, we have set the foundation for further

Keywords Differential transcriptomics • Gene regulatory network

1 Introduction

The developmental program of an organism and its phenotypic features are encoded into its DNA. The binding of transcription factors to specific DNA, which controls the expression of genes and ultimately the development of the embryo, is known as a gene regulatory network (GRN). Evolutionary conservation has provided us

E.K. Lowe (✉)

Stazione Zoologica Anton Dohrn, Naples, Italy

Beacon Center for Evolution in Action, Michigan State University, East Lansing, MI 48823, USA

e-mail: elijahkariem.lowe@szn.it

C. Cuomo • M.I. Arnone

Stazione Zoologica Anton Dohrn, Naples, Italy

© Springer International Publishing Switzerland 2016

55

A. Rogato et al. (eds.), *Dynamics of Mathematical Models in Biology*,

DOI 10.1007/978-3-319-45723-9_5

with a good tool to study the origins of phenotypic features and their developmental programs. With the advances in sequencing technology and the continued drop in prices, it has become more common to sequence an organism's transcriptome. This has facilitated the ability to examine organism on a genomic scale, allowing the study of all genes expressed at a giving time point in development, as well as for wild type versus experimental conditions. With transcriptomics we are able to better understand the complicity of evolution and increasing studies are taking advantage of this fact [1, 2].

In bilateria, homeobox-containing genes are important for the patterning of the anterior–posterior axis and mediate much of the embryonic development, with one of the most studied families being the Hox genes [3, 4]. Another important family of homeobox genes is the ParaHox family—*Gsx*, *Pdx* (*Xlox* in echinoderms), and *Cdx*, which are thought to be the ancient sister group to Hox genes and to have emerged from the ProtoHox cluster [5]. The ParaHox genes have been shown to be involved in gut development in vertebrates [6, 7] and also in the echinoderms [8, 9]. It appeared from the examination of the sea urchins *Strongylocentrotus purpuratus* that echinoderm had lost some chordate-like features in their function of *Xlox* and *Cdx* [10]. However, through the use of another echinoderm, the bat star *Patiria miniata*, it was discovered that these features appear to only have been lost in echinoids, while being retained in asteroids [11]. This shows the necessity to continue to study new organisms in order to gain a more complete evolutionary picture. The embryonic guts of both *S. purpuratus* and *P. miniata* first form a tube like structure with no sections known as the archenteron, then later divide into three sections, the foregut, the midgut, and the hindgut, which become in the larva the

esophagus, the stomach, and the intestine, respectively.

Portions of the GRN for gut development in echinoderms have already been formed, but the network downstream of Xlox and Cdx has yet to be assembled. In *S. purpuratus*, Xlox morpholino antisense oligo (MASO) RNA-seq experiments have been conducted looking at known genes in the network [9], but have not been studied in-depth. Here we present the groundwork for reconstructing the GRN for gut development downstream of Xlox and Cdx in both *S. purpuratus* and *P. miniata*. Through the analysis of these MASO RNA-seq experiments we will identify direct and indirect targets of Xlox and Cdx in both species. Secondly, looking at the overlap in these two networks at homologous stages, and will better define the genes needed for the developing gut to form and properly section.

2 Results and Discussion

2.1 Gene Orthology

Prior to understanding or reconstructing the gut GRN for *S. purpuratus* and *P. miniata*, we must first understand the homology relationship between the two species. Proteomes for *S. purpuratus*, *P. miniata*, and *Xenopus tropicalis* were used

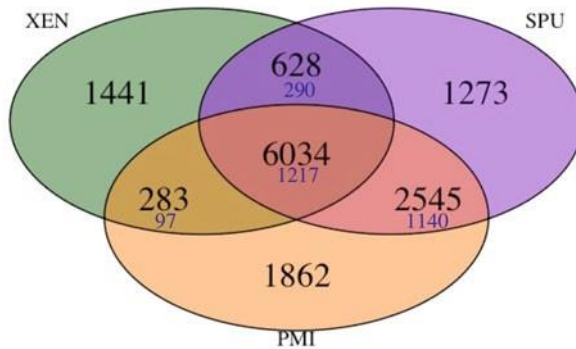


Fig. 1 Gene ortholog relationship between *S. purpuratus* (SPU), *P. miniata* (PMI), and *X. tropicalis* (XEN). Each circle represents one of the species and their overlap represents the orthologous groups that are in common. The numbers in the *larger black print* are the total number of orthologous groups and in the *smaller blue print* are the number of single copy orthologous groups

to construct orthologous groups and examine the gut GRN on an evolutionary scale. There were 29,805, 29,129, and 22,718 protein sequences in each proteome, respectively. Five sequences were removed from the *P. miniata*'s proteome during the filtering process, they were all eight base pairs or less in length. The three proteomes clustered into 14,066 homologous groups, being composed of 22,576 *S. purpuratus* proteins in 10,480 groups, 22,252 *P. miniata* proteins in 10,724 groups, and 20,813 *X. tropicalis* proteins in 8386 groups. Of these orthologous groups there were 6034 conserved amongst all three organisms, with 1217 (20 %) being single copy orthologs. The echinoderms had the largest number of orthologs as expected with 2545 orthologous groups and 45 % of the groups being single copy orthologs (Fig. 1).

2.2 *Differential Expression Analysis*

To identify genes downstream of *Xlox* and *Cdx* we analyzed both *S. purpuratus* and *P. miniata* embryos that were separately injected with MASO designed to block translation of *Xlox* or *Cdx* in each species. Time points for transcriptomic sequencing were selected based on QPCR expression trends from earlier studies [9, 11]; the midpoint of expression was chosen for each gene in their respective species. In *S. purpuratus* the time points selected are 48 hpf (late gastrula) and 72 hpf (pluteus larva) for *Xlox* and 66 hpf (prism) for *Cdx*. In *P. miniata* the time points are 66 hpf (late gastrula) for *Xlox* and 90 hpf (early bipinnaria larva) for *Cdx*, which are homologous stages to those of *S. purpuratus*. Looking at the morphology of the embryos, the sea urchin and the sea star late gastrula represent the stages when the gut is only an elongated tube without any constrictions, instead the sea urchin

Table 1 Homology of differential expressed transcripts

	Splox 48h	Splox 72h	Spcdx 66h	Pmlox 66h	Pmcdx 90h
Orthologous groups	183	1457	470	70	404
Proteins in core	97 (33 %)	929 (39 %)	289 (40 %)	39 (36 %)	270 (39 %)
SCO in all	16 (5 %)	145 (6 %)	39 (5 %)	5 (5 %)	34 (5 %)
SCO in echino	23 (8 %)	150 (6 %)	48 (7 %)	10 (9 %)	31 (4 %)
Total proteins	207 (70 %)	1659 (70 %)	529 (73 %)	78 (72 %)	450 (65 %)

In parenthesis is the number of differential expressed genes for the given MASO RNA-seq experiment. Orthologous groups refer to the number of groups the total number of proteins were clustered into, while “Total proteins” refers to the total number of proteins that were clustered into orthologous groups. Proteins in core are the number of proteins found in *S. purpuratus*, *P. miniata*, and *X. tropicalis*. SCO in all are the number of single copy orthologous found in *S. purpuratus*, *P. miniata*, and *X. tropicalis*, while SCO in echino are the number of single copy orthologs found in only *S. purpuratus* and *P. miniata*

prism and the sea star early bipinnaria larva have already a tripartite shaped gut. The pluteus larva is an extra time point we chose for the sea urchin in which the gut is now complete with its cardiac and pyloric sphincters visible.

Differential expressed transcripts were identified using DESeq2 with a threshold of $\log_2fc > \pm 0.5$ and adjusted p-value of < 0.05 . In *S. purpuratus*, as time progressed, the knockdowns had a larger effect of more transcripts. There were only a couple of hundreds (294) transcripts affected by the Sp-Lox MASO at 48 hpf, compared to 723 transcripts effected by Sp-Cdx at 66 h, and 2384 at 72 h. Fifty-seven percent (167) of transcripts affected by the Sp-Lox MASO at 48 hpf were also affected at 72 hpf, showing similarities in the GRN as gut transitions from a tube like structure to a trisectioned gut.

When examining the *P. miniata* Xlox MASO RNA-seq we did not find a large

number of transcripts to be differentially expressed at the late gastrula stage, with there being only 109 transcripts differentially expressed. However, when examining Pm-Cdx MASO RNA-seq at the early larva stage we observed many more genes being affected, 693, 450 (65 %) of which had a homologous relation to *S. purpuratus* and/or *X. tropicalis*.

Across all species at least 65 % of the transcripts were clustered into homologous groups, meaning that 30–35 % of the transcripts from each experiment were species specific or fell below our threshold (Table 1). Further analysis including phylogenetic trees is necessary to better understand the relationship of these two species, but is currently out of the scope of this paper.

2.3 Evolutionary Conserved Elements in *S. purpuratus* and *P. miniata* Gut GRNs

Through the use of our orthology analysis and our MASO differential expression analysis we are able to discover conserved components in the downstream networks of both *Xlox* and *Cdx* in *S. purpuratus* and *P. miniata*. In the Cdx MASO RNA-seq there was the largest overlap between the species, 129 transcripts were found

in both networks. Ninety-one out of these 129 genes were found in the “core” orthology group, meaning that at least one gene from *S. purpuratus*, *P. miniata*, and *X. tropicalis* was present in the orthologous group, and 11 (9 %) of those genes were identified as transcription factors that belong to the bzip, bHLH, C2H2, hmg, p53, and zf-C4 families. Late gastrula in *S. purpuratus* and *P. miniata* occurs at 48 hpf and 66 hpf, respectively, with 15 genes shared in their network, 67 % (10) of which were transcription factors. Although 48 hpf in *S. purpuratus* and 66 hpf in *P. miniata* are more morphologically similar, the overlaps in affected genes were stronger at 72 hpf in *S. purpuratus* and 66 hpf in *P. miniata*, with an additional 10 genes (25 in total) compared to the earlier stage, which also included the same group of transcription factors. Without the use of ChIP or other technologies such as ATAC-seq we are not able to determine the connectivity of these GRNs. Although we are not able to distinguish direct versus indirect targets in this study, identifying key components in the way of transcription factors is essential and will provide a foundation for future studies.

3 Conclusion

Here we present the foundation for studying the downstream GRN for gut development in *S. purpuratus* and *P. miniata* through the use of a MASO RNA-seq analysis. Seeing that RNA-seq can yield hundreds to thousands of potential genes we used the correlation between *S. purpuratus* and *P. miniata* to identify a subset

of genes to be examined in future studies. Moreover the genes identified in our study as transcription factors will be the starting points for ATAC-seq and ChIP analyses. This study provides evidence that a genome-wide approach to study GRNs in development and evolution is feasible in echinoderms.

4 Methods

All computational analyses were conducted on the high performance-computing cluster at Michigan State University. Scripts for all the performed analyses are readily available for use and can be found in the following github repository https://github.com/elijahlowe/paraHox_analysis. Snippets of code were generated with the help of biostar and seq-answer online forums [12, 13]. RNA-seq reads will be stored in EBI database.

4.1 *Animal Handling and Microinjection Procedures*

Adults *S. purpuratus* and *P. miniata* have been obtained from Patrick Leahy (Kerchoff Marine Laboratory, California Institute of Technology, Pasadena, CA, USA), housed in circulating seawater aquaria in the Stazione Zoologica Anton Dohrn of Naples and kept in large tanks of seawater at 15–16 °C.

Microinjection was performed as described in Annunziata and Arnone [9], for sea

urchin, and in Cheattle Jarvela and Hinman [14], for sea star. MASOs were obtained from Gene Tools (Corvallis) and injected at the following concentration: 150 μ M, for Sp-Lox and Sp-Cdx translation MASOs (sequences as reported in [8] and [9]); 700 μ M, for the Pm-Lox translation MASO (sequence 5⁰-CCAGGGTCATCATGTTTCATGTTGGT-3⁰), and for the Pm-Cdx splicing MASO (sequence 5⁰-TTGACCTGTAGTTGAAATATGAGAA-3⁰). For each experiment and for each MASO, 600 zygotes were injected in sea urchin and 50 zygotes in sea star and each experiment was repeated three times with different batches of embryos to obtain three independent biological replicas. As a negative control, the same number of eggs was injected with 100 μ M of the standard control morpholino (Gene Tools) and compared side-by-side with uninjected and MASO-injected embryos.

4.2 Embryos Collection, RNA Extraction, and Sequencing

Injected and uninjected sea urchin and sea star fertilized eggs have been allowed to develop until the desired stage at 15 °C in filtered seawater and then collected for the RNA extraction. The embryos have been collected in a tube and centrifuged at 3000 rpm for 2–3 min to remove all the seawater. RNA extraction has been carried out using the RNAqueous-Micro Kit (Ambion). Integrity and quantification of RNA has been checked before the sequencing using the Agilent Bioanalyzer 2100 with the RNA 6000 Pico kit for total eukaryote RNA. cDNA libraries have been prepared with 1 μ g of starting total RNA and using the Illumina TruSeq RNA

Sample Preparation Kit (Illumina), according to TruSeq protocol. Each library has been diluted to 2 nM and denaturated; 8 pM of each library has been loaded onto cBot (Illumina) for cluster generation with cBot Paired End Cluster Generation Kit (Illumina) and sequenced using the Illumina HiSeq 1500 with 100 bp paired-end reads in triplicate, obtaining 31–38 million reads for replicate. The sequencing service has been provided by the Laboratory of Molecular Medicine and Genomics (<http://www.labmedmolge.unisa.it>) at the University of Salerno, Italy.

4.3 *Quality Control, Mapping, and Differential Expression*

Reads were first trimmed using Trimmomatic (v0.33) with the scripts **trim_pm.qsub**, **trim_spcdx.qsub**, and **trim_splox.qsub** [15]. The parameters for trimming were chosen to efficiently remove erroneous reads while maximizing the information within the reads [16]. *S. purpuratus* reads were mapped to Genome sequence (V3.1) [17] and *P. miniata* reads were mapped to the genome sequence (V1.0) Scaffolds [18] using Bowtie2 (2.2.6) and Tophat (2.0.8b) [19, 20]. After mapping, reads were sorted using SamTools (v1.2) [21] and counts were extracted using

HTSeq (v0.6.1) [22]. The gff3 from Build 7 was used for generating exon-based transcript counts for *S. purpuratus* which is more informative seeing than DESeq2 does not use length-based count normalization [23, 24]. The following scripts were used **sp_cdx.qsub**, **sp_lox48.qsub**, and **sp_lox72.qsub** for *Sp*, while **pm_cdx.qsub** and **pm_lox.qsub** were used for *Pm*.

Differentially expressed genes were identified using DESeq2 [23], transcripts not meeting the threshold of 10 counts for at least one of the samples were removed. DESeq2 provides two methods of hypothesis testing: Wald test and likelihood ratio test (LRT). To account for the batch effect across different animals we used LRT, with the full model being batch C condition and the reduced model being batch. After, the differentially expressed genes using extracted information from Echinobase [18] for both species, which are in the **data/** directory, using **annot_sp.py** and **annot_pm.py** scripts.

4.4 Identification and Clustering of Orthologs

The proteomes for *S. purpuratus* (SPU_peptide sequence) and *P. miniata* (PMI_protein sequence) were downloaded from echinobase (<http://www.echinobase.org/Echinobase/SpDownloads> and <http://www.echinobase.org/Echinobase/PmDownload>) while *Xenopus tropicalis* proteome (release 83) was downloaded from Ensembl (ftp://ftp.ensembl.org/pub/release-83/fasta/xenopus_tropicalis/pep/) in fasta format [18, 25]. Orthology was determined using orthoMCL

235235
[26]. Sequences of the three proteomes were concatenated into one file and transformed into orthoMCL format, so an all-vs-all protein blast search was conducted using the blastp program in the BLASTC (v2.2.30) suite [27]. Prior to the blast search, sequences with stop codons and of a length shorter than 20 amino acids were removed. A protein blast (blastp) was performed using the concatenated fasta as the query and database. Blast results were then parsed, loaded into a MySQL database, and then proteins with at least 50 % similarity were clustered through the use of orthoMCL programs. The steps for orthoMCL are in the script ortho.qsub.

4.5 Transcription Factor Identification

Both the *S. purpuratus* and *P. miniata* proteomes were searched against the Pfam database [28] using HMMER/3.1b2 hmmscan [29]. These commands were executed using the following scripts `hmmes_pm_tf.qsub` and `hmmes_spur_tf.qsub`. The `grep` program was then used to search for the following term `homeobox, Pax, bzip, hmg, sox, hlh, PF00104.25 (nuclear receptor), t-box, mh2 (smad), b-box, f-box, fork_head, ets, phd-finger, zf-C2H2` within `-tblout` output. Additionally, Pfam ids were extracted from the DBD Transcription Factor prediction database [30] and

then grep against the `-tblout` output, combined filtered for redundancy. The list of Pfam ids can be found in the data directory in the github repository along with the TF we identified for *S. purpuratus* and *P. miniata*.

Acknowledgements This work was supported in part by Michigan State University through computational resources provided by the Institute for Cyber-Enabled Research and by MIUR (premiere PANTRAC to MIA). C.C. has been supported by a SZN PhD fellowship.

References

1. Wang, Z., Dai, M., Wang, Y., Cooper, K.L., et al.: Unique expression patterns of multiple key genes associated with the evolution of mammalian flight. *Proc. Biol. Sci.* **281**(1783), 20133133 (2014)
2. Lmanna, F., Kirschbaum, F., Waurick, I., Dieterich, C., Tiedemann, R.: Cross-tissue and cross-species analysis of gene expression in skeletal muscle and electric organ of African weakly-electric fish (Teleostei; Mormyridae). *BMC Genomics* **16**, 668 (2015). doi:[10.1186/s12864-015-1858-9](https://doi.org/10.1186/s12864-015-1858-9)
3. Finnerty, J.R.: The origins of axial patterning in the metazoa: how old is bilateral symmetry? *Int. J. Dev. Biol.* **47**(7–8), 523–529 (2003)
4. Mallo, M., Alonso, C.R.: The regulation of hox gene expression during animal. *Development* **140**(19), 3951–3963 (2013)
5. Brooke, N.M., Garcia-Fernandez, J., Holland, P.W.: The ParaHox gene cluster is an evolutionary sister of the Hox gene cluster. *Nature* **392**, 920–922 (1998)
6. Wright, C.V., Cho, K.W., Oliver, G., De Robertis, E.M.: Vertebrate homeodomain proteins:

7. Young, T., Deschamps, J.: Hox, Cdx, and anteroposterior patterning in the mouse embryo. *Curr. Top. Dev. Biol.* **88**, 235–255 (2009)
8. Cole, A.G., Rizzo, F., Martinez, P., Fernandez-Serra, M., Arnone, M.I.: Two ParaHox genes, SpLox and SpCdx, interact to partition the posterior endoderm in the formation of a functional gut. *Development* **136**, 541–549 (2009)
9. Annunziata, R., Arnone, M.I.: A dynamic regulatory network explains ParaHox gene control of gut patterning in the sea urchin. *Development* **141**(12), 2462–2472 (2014). doi:[10.1242/dev.105775](https://doi.org/10.1242/dev.105775)
10. Arnone, M.I., Rizzo, F., Annunziata, R., Cameron, R.A., Peterson, K.J., Martínez, P.: Genetic organization and embryonic expression of the ParaHox genes in the sea urchin *S. purpuratus*: insights into the relationship between clustering and collinearity. *Dev. Biol.* **300**, 63–73 (2006)
11. Annunziata, R., Martinez, P., Arnone, M.I.: Intact cluster and chordate-like expression of ParaHox genes in a sea star. *BMC Biol.* **11**, 68 (2013). <http://www.biomedcentral.com/1741-7007/11/68>
12. Parnell, L.D., Lindenbaum, P., Shameer, K., Dall’Olio, G.M., Swan, D.C., et al.: BioStar: an online question & answer resource for the bioinformatics community. *PLoS Comput. Biol.* **7**(10), e1002216(2011)
13. Li, J.W., Schmieder, R., Ward, R.M., Delenick, J., Olivares, E.C., Mittelman, D.: SEQanswers: an open access community for collaboratively decoding genomes. *Bioinformatics* **28**(9), 1272–1273 (2012)
14. Cheattle Jarvela, A.M., Hinman, V.: A method for microinjection of *Patiria miniata* zygotes. *J. Vis. Exp.* (91), e51913 (2014). doi:[10.3791/51913](https://doi.org/10.3791/51913)
15. Bolger, A.M., Lohse, M., Usadel, B.: Trimmomatic: a flexible trimmer for Illumina sequence data. *Bioinformatics* **30**, 2114–2120(2014)

16. MacManes, M.D.: On the optimal trimming of high-throughput mRNAseq data. *bioRxiv* (2014). doi:[10.1101/000422](https://doi.org/10.1101/000422)
17. Sodergren, E., Weinstock, G.M., Davidson, E.H., Cameron, R.A., Gibbs, R.A., Angerer, R.C., Coffman, J.A.: The genome of the sea urchin *Strongylocentrotus purpuratus*. *Science* **314**(5801), 941–952 (2006)
18. Cameron, R.A., Samanta, M., Yuan, A., He, D., Davidson, E.: SpBase: the sea urchin genome database and web site. *Nucleic Acids Res.* **37**, D750–D754 (2009)
19. Langmead, B., Salzberg, S.L.: Fast gapped-read alignment with Bowtie 2. *Nat. Methods* **9**(4), 357–359 (2012)
20. Kim, D., Pertea, G., Trapnell, C., Pimentel, H., Kelley, R., Salzberg, S.L.: TopHat2: accurate alignment of transcriptomes in the presence of insertions, deletions and gene fusions. *Genome Biol.* **14**(4), R36 (2013)
21. Li, H., Handsaker, B., Wysoker, A., Fennell, T., Ruan, J., Homer, N., Marth, G., Abecasis, G., Durbin, R., 1000 Genome Project Data Processing Subgroup: The Sequence alignment/map (SAM) format and SAMtools. *Bioinformatics* **25**, 2078–2079 (2009)
22. Anders, S., Pyl, P.T., Huber, W.: HTSeq — a Python framework to work with high-throughput sequencing data. *Bioinformatics* **31**, 166–169 (2014). doi:[10.1093/bioinformatics/btu638](https://doi.org/10.1093/bioinformatics/btu638)
23. Love, M.I., Huber, W., Anders, S.: Moderated estimation of fold change and dispersion for RNA-seq data with DESeq2. *Genome Biol.* **15**, 550 (2014). doi:[10.1186/s13059-014-0550-8](https://doi.org/10.1186/s13059-014-0550-8)
24. Zhao, S., Xi, L., Zhang, B.: Union exon based approach for RNA-seq gene quantification: to be or not to be? *PLOS One* (2015). doi:[10.1371/journal.pone.0141910](https://doi.org/10.1371/journal.pone.0141910)
25. Cunningham, F., Amode, M.R., Barrell, D., Beal, K., Billis, K., Brent, S., Carvalho-Silva, D., Clapham, P., Coates, G., Fitzgerald, S., Gil, L., Girón, C.G., Gordon, L., Hourlier, T., Hunt, S.E., Janacek, S.H., Johnson, N., Juettemann, T., Kähäri, A.K., Keenan, S., Martin, F.J., Maurel, T., McLaren, W., Murphy, D.N., Nag, R., Overduin, B., Parker, A., Patricio, M., Perry, E., Pignatelli, M., Riat, H.S., Sheppard, D., Taylor, K., Thormann, A., Vullo, A., Wilder, S.P., Zadissa, A., Aken, B.L., Birney, E., Harrow, J., Kinsella, R., Muffato, M., Ruffier, M., Searle, S.M.J., Spudich, G., Trevanion, S.J., Yates, A., Zerbino, D.R., Flicek, P.: Ensembl

2015. *Nucleic Acids Res.* **43**(Database issue), D662–D669 (2015). doi:[10.1093/nar/gku1010](https://doi.org/10.1093/nar/gku1010)
26. Fischer, S., Brunk, B.P., Chen, F., Gao, X., Harb, O.S., Iodice, J.B., Shanmugam, D., Roos, D.S., Stoeckert Jr., C.J.: Using OrthoMCL to assign proteins to OrthoMCL-DB groups or to cluster proteomes into new ortholog groups. *Curr. Protoc. Bioinformatics*. Chapter 6:Unit 6.12.1–19 (2011)
27. Camacho, C., Coulouris, G., Avagyan, V., Ma, N., Papadopoulos, J., Bealer, K., Madden, T.L.: BLASTC: architecture and applications. *BMC Bioinformatics* **10**, 421 (2008)
28. Finn, R.D.: Pfam: the protein families database. *Encyclopedia of Genetics, Genomics, Proteomics and Bioinformatics* (2012)
29. Durbin, R., Eddy, S.R., Krogh, A., Mitchison, G.: *Biological Sequence Analysis: Probabilistic Models of Proteins and Nucleic Acids*. Cambridge University Press (1998). ISBN 0-521-62971-3
30. Wilson, D., Charoensawan, V., Kummerfeld, S.K., Teichmann, S.A.: DBD - taxonomically broad transcription factor predictions: new content and functionality. *Nucleic Acids Res.* **36**, D88–D92 (2008). doi:[10.1093/nar/gkm964](https://doi.org/10.1093/nar/gkm964)

OXFORD
UNIVERSITY PRESS

Briefings in Functional Genomics

Omics approaches to study gene regulatory networks for development

Journal:	<i>Briefings in Functional Genomics</i>
Manuscript ID	
Manuscript Type:	Draft
Date Submitted by the Author:	Review Paper
Complete List of Authors:	n/a
	Lowe, Elijah; Stazione Zoologica Anton Dohrn, Biology and Evolution of
Keywords:	gene regulatory networks, data integration, next generation sequencing,

SCHOLARONE™
Manuscripts

1
2
3

Omics approaches to study gene regulatory networks for development

Elijah K. Lowe#, Claudia Cuomo and Maria I. Arnone*

Stazione Zoologica Anton Dohrn

Elijah K. Lowe, #Co-corresponding author

Email: elijahkariem.lowe@szn.it

Claudia Cuomo

Email: Claudia.cuomo@szn.it

Maria Ina Arnone, *Corresponding author

Email: miarnone@szn.it

Stazione Zoologica Anton Dohrn

Villa Comunale 80121 Napoli, Italy

Key words: Gene regulatory networks, data integration, next generation sequencing, echinoderm, embryo

Elijah Lowe PhD#, received his doctoral degree from Michigan State University in 2015.

Currently, he is a postdoctoral computational biology researcher.

Claudia Cuomo has graduated in Biology at University of Napoli Federico II in 2012. Currently she is a PhD student.

Maria I. Arnone PhD, received her doctoral degree in 1992 from University of Napoli Federico II.

Since 2000, she is a senior researcher, group leader at Stazione Zoologica Anton Dohrn working on evolutionary and developmental biology

Abstract

Gene regulatory networks (GRNs) describe the interactions for a developmental process at a given time and space. Historically, perturbation experiments represent one of the key methods for analyzing and reconstructing a GRN, and the GRN governing early development in the sea urchin embryo stands as one of the more deeply dissected so far. As technology progresses, so do the methods used to address different biological questions. Next-generation sequencing (NGS) has become a standard experimental technique for genome and transcriptome sequencing and studies of protein–DNA interactions and DNA accessibility. While several efforts have been made toward the integration of different omics approaches for the study of the regulatory genome in many animals, in a few cases, these are applied with the purpose of reconstructing and experimentally testing developmental GRNs. Here, we review emerging approaches integrating multiple NGS technologies for the prediction and validation of gene interactions within echinoderm GRNs. These approaches can be applied to both ‘model’ and ‘non-model’ organisms. Although a number of issues still need to be addressed, advances in NGS applications, such as assay for transposase-accessible chromatin sequencing, combined with the availability of embryos belonging to different species, all separated by various evolutionary distances and accessible to experimental regulatory biology, place echinoderms in an unprecedented position for the reconstruction and evolutionary comparison of developmental GRNs. We conclude that sequencing technologies and integrated omics approaches allow the examination of GRNs on a genome-wide scale only if biological perturbation and cis-regulatory analyses are experimentally accessible, as in the case of echinoderm embryos.

Introduction

The reconstruction of a gene regulatory network (GRN) for a given developmental process requires knowledge of the regulatory states that progressively establish the identity of the cell

population during development and gives them a specific function. A regulatory state is defined by the set of regulatory genes encoding transcription factors (TFs) and the signaling molecules active in a cell at a specific moment of animal development. To determine the complete structure of a GRN, all the elements of the system need to be identified and the regulatory interactions unraveled.

Echinoderms form five classes, and feature resolved phylogenetic relationships because of their excellent fossil records [1, 2]. Four of the five classes have various established protocols making them experimentally accessible to regulatory biology (reviewed by [3]), and placing them in a unique position to study the evolution of GRNs. A protocol published in 2008 [4] well describes the approach to experimentally determine the function of a specific regulatory element in the complexity of the sea urchin network. This method has been used to describe the so far most complete, among all living organisms, GRNs, accounting for the developmental process of a whole embryonic territory, the sea urchin endomesoderm specification network, and established the sea urchin as a well-suited organism for the study of GRNs [5]. The same method, moreover, can extensively be applied to other organisms as demonstrated in *Ciona intestinalis* [6, 7]. As an embryo develops, new genes are activated, while previously expressed genes may turn off leading to the formation of new tissue types, and because this happens in a modular fashion, GRNs can be reconstructed in a tissue-specific manner. The GRNs of neighboring tissues can then be linked to form a more complete and global network. In each set of events, the regulatory genes need to be analyzed in the temporal and spatial expression to characterize the regulatory state of the cells involved in the process. Approaches such as quantitative polymerase chain reaction, complementary DNA microarray and RNA-seq have been extensively adopted for the temporal studies, quantifying gene expression at a given stage, while in situ hybridization is commonly used to gain spatial information, showing where in the organism the gene is expressed. However, knowing the time and the location of expression is not enough to determine a gene's role in a network; for this, the knockout or knockdown of the gene is necessary to determine its function in

development and possible interactions. In echinoderms, the primary method for knockdowns is morpholino antisense oligonucleotide (MASO) and has been used numerous times to identify GRN interactions [8, 9]. MASO prevents the formation of a specific protein either blocking its translation or the spliceosome activity on the immature RNA. More recently, the CRISPR-Cas9 system [10, 11] has been developed, which borrows the prokaryotic immune mechanism using a Cas9 endonuclease and a guide RNA to recognize and cut a specific region of DNA creating an indel modification in the gene sequence. This technology is said to be more accurate and accounts for the nonspecific binding effects that occur in some MASO experiments [10, 12]. Although this technique is relatively new, two protocol papers have already been published using the CRISPR-Cas9 system in echinoderms [13, 14].

Since the arrival of Sanger sequencing [15] and more recently next-generation sequencing (NGS), genome and transcriptome sequencing has become increasingly ingrained into the different realms of biology, becoming less of a novelty and more of a standard experimental technique. NGS techniques consist of shearing or fragmenting DNA or RNA, and then after applying the proper chemistry to produce libraries, the samples are sequenced using various short-read technologies, with Illumina platforms being the most versatile and most frequently used because of their technology maturity and range of platforms that are applied to different biological niches [16]. The advances of sequence technologies have made sequencing a genome faster, easier and cheaper, new high-throughput biochemical and whole-genome approaches have made the study of GRNs more efficient. The first echinoderm genome—*Strongylocentrotus purpuratus*, the California purple sea urchin—was introduced in 2006 using Sanger sequencing [17], and was later annotated with RNA-seq data using an Illumina sequencing platform [18]. In addition to the genome itself, sequencing methods to determine protein–DNA interactions and DNA accessibility have also been developed, chromatin immunoprecipitation sequencing (ChIP-seq) and assay for transposase-accessible chromatin (ATAC-seq), respectively, and continue to contribute to efforts of understanding and reconstructing GRNs. The ability to generate putative GRNs with these in silico

techniques combined with the already well-established wet laboratory protocols and ‘testability’ of various echinoderm systems presents an ideal situation for the reconstruction of GRNs.

Many reviews have been written for NGS technologies, dealing with, e.g., which genome assembly method is best [19, 20], the best practices for transcriptomics [21], even the integration of different sequencing technologies, but none to our knowledge have been written with the purpose of reconstructing GRNs using omics technologies. In this review, echinoderm embryos and their genomes are used as examples to illustrate the state of the art of established omics and perturbation approaches to reconstruct GRNs for development, highlighting, more in detail, some of the advantages that ATAC-seq presents. Our goal is to outline the *in silico* and *in vivo* processes and technologies needed to reconstruct a GRN and to discuss some of the difficulties that may ensue.

Quality filtering

Before mapping or *de novo* assembly, quality control of the data is necessary to avoid misassembly and misleading results in downstream analysis and to reduce the time it takes to complete an analysis. The trimming of low-quality portions of reads, removing low-quality reads, adaptor removal and removal of over abundant or contaminated sequences (Figure 1), can be easily done with software such as Trimmomatic [22], TagCleaner [23] or FASTX [24] and FASTQC [25] for visualization. Another quality filtering step is the removal of microbial, viral metagenome, human or other contamination, which can lead to false conclusions when incorporated in the data. There are a number of methods developed for mapping sequences using tools such as BBDMap [26], FASTQ screen (Babraham Bioinformatics), other aligners to known contaminants using databases such as UniVec (<ftp://ftp.ncbi.nlm.nih.gov/pub/UniVec/>), artificial sequences (taxid:81077) on the National Center for Biotechnology Information (NCBI) or the EMVEC vector database from the European Bioinformatics Institute, and in cases when reads are long enough

(> 150 bp), software such as DeconSeq [27] can be used. This allows for the identification and removal of contaminated reads before assembly or mapping to the reference of interest. Alternatively, once assembled, a similar process can be performed using BLAST against known contaminations or bacterial genomes.

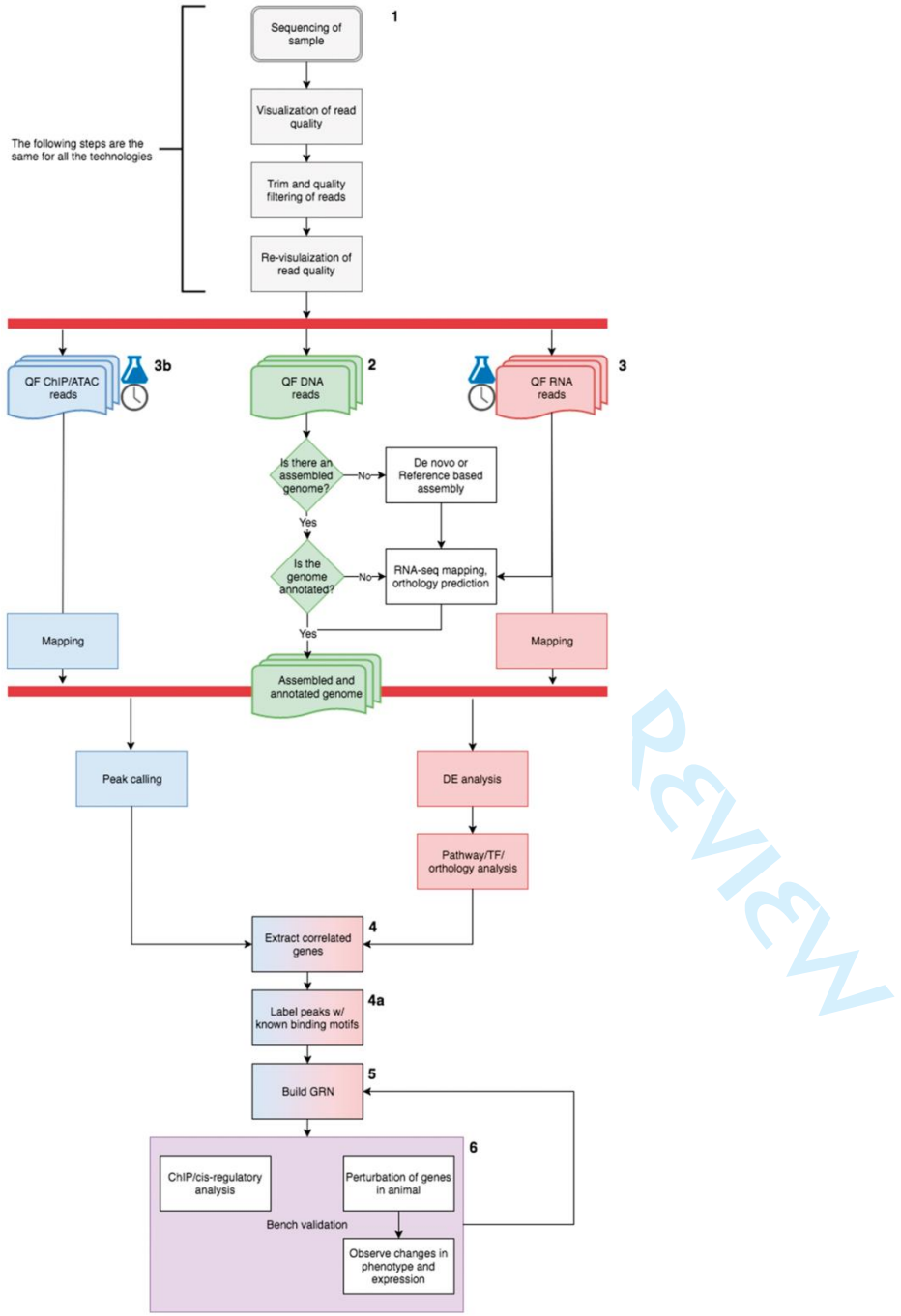


Figure 1 General scheme for constructing a GRNs from omics data. (A colour version of this figure is available online at: <https://academic.oup.com/bfg>.) 1. The first step is always to assess the quality of the data (grey boxes), which should be checked before and after each step.

2. Identify available omics data, and what else is needed for a comprehensive analysis. In cases such as human, mouse, chick, sea urchin, just to name a few, there are available genomes, which are major components of GRN analysis. For many 'non-model' organisms, there may not be a genome available, so the sequencing and assembly will have to be done before a GRN can be reconstructed.
3. Determine the time point (clock symbol) and method of comparison, whether it is perturbation, known-down or knockout (flask symbol). RNA-seq is also used to annotate the genome.
- 3b. ChIP-seq/ATAC-seq (peak data) read mapping and peak calling are also done in a time-specific manner and can also be tissue specific.
4. Identify the overlapping expression data and peak data for integration. It is best to focus on TF and specific tissues to reduce the information for better interpretation.
- 4a. After determining the overlapping data, peaks should then be label with binding motifs. These motifs are often called by their human or mouse ortholog, so this must be accounted for.
5. The network can be reconstructed using programs such as BioTapestry.
6. Confirmation of findings by bench validations.

Genome assembly and quality assessment

While differential expression (DE) can be performed without a genome, the reconstruction of GRNs cannot. A major component of reconstructing a GRN is identifying cis-regulatory models and promoter regions. Identifying these regions has proven to be difficult with a genome and is nearly impossible without a genome, even more so when analyzing multiple genes. Echinoderms have several genomes sequenced, the first of which was the purple sea urchin *S. purpuratus* [17]. This was a major step in the study of echinoderm development: >780 papers have been produced citing the *S. purpuratus* genome to date. In addition to the *S. purpuratus* genome, several other echinoderm genomes have been sequenced, covering four of the five classes of echinoderms, including but not limited to *Patiria miniata*, *Lytechinus variegatus*, *Eucidaris tribuloides*,

Parastichopus parvimensis and *Ophiothrix spiculata*, all of which can be found on EchinoBase, formerly known as SpBase [28]. Most recently, the sequences of both the Great Barrier Reef and Okinawa ‘species’ of *Acanthaster planci* were released (Table 1). However, not all of these genomes are well suited for the study GRNs because of genome fragmentation and/or missing data such as annotation (the genomes with annotation are listed in Table 2).

Resource	Link	Type of data
Echinobase	www.echinobase.org/	Genome browser, genomes, transcriptomes and ATAC-seq
The Davidson Laboratory	http://sugp.caltech.edu/endomes/	Perturbation and gene expression data, GRN and high-density time course data
Max Planck Institute for Molecular Genetics	http://owwww.molgen.mpg.de/~ag_seaurchin/	Expression data, EST database, Array Screens database and Genome database
Marine Genomics Unit	http://marinegenomics.oist.jp/	Genome, annotation, transcriptome and proteome for <i>A. planci</i> and several other marine organisms

Assembly (version)	Organism (class)	Number of	N50	Bases+gaps	Bases
--------------------	------------------	-----------	-----	------------	-------

		scaffolds	(kb)	(Mb)	(Mb)
<i>Strongylocentrotus purpuratus</i> (v4.2)	Sea urchin (Echinoidea)	32 008	401.6	936	816
<i>Patiria miniata</i> (v1.0)	Sea star (Asteroidea)	60 183	52	811	770
<i>Lytechinus variegatus</i> (v2.2)	Sea urchin (Echinoidea)	322 794	46.2	1061	1004
<i>Parastichopus parvimensis</i> (v1.0)	Sea cucumber (Holothuroidea)	21 559	89	873	760
<i>Acantaster planci</i> Okinawa (v1.0) ^a	Sea star (Asteroidea)	1765	1521	384	373 ^b
<i>Acantaster planci</i> Great barrier reef (v1.0) ^a	Sea star (Asteroidea)	3274	916	384	374 ^b

Table 2 Genome statistics ^a Note. Statistics generated using Quast. ^b Estimated using total base and N's per 1000 kb.

For echinoderm species without an assembled genome, *de novo* assembly is often required to produce a draft genome (Figure 1.2). There are many assemblers and new ones constantly being developed. Assemblathon 1 and Assemblathon 2 were competitions that examined which assemblers are best suited for genome assembly and which pipeline performs best using simulated data and genomes of several different species [19, 20, 29]. These competitions illustrate that not one assembler works best for all organisms and that several assemblers should be tested before committing to a draft genome, and for some species, a combination of several assemblers can produce a better assembly. Alternatively, a reference-based approach aligning to a closely related genome could provide improvement in contig—assembly overlapping DNA reads—and

scaffold—overlapping contigs with known gap size—lengths [30]. An alignment-assisted assembly is possible even with divergence, when factors such as translocation of genes and events such as gene copy number variation are accounted for, as it has been shown using human as a reference to improve a dog genome [31]. Post-assembly is necessary for the quality of the genome to be assessed. There are a number of tools to perform this step, such as Reapr [32] and Quast [33], which report contig distributions, N50, coverage, duplication and misassemblies using a reference genome or by mapping reads back to the assembled genome. Once assembled and checked for completeness, there are additional steps that can be performed if the genome was incomplete: additional sequencing at a higher depth that helps to recover previously unsequenced portions of the genome or using different sequencing technologies such as optical mapping, long-read technology (PacBio) or mate pair reads with large insert size for scaffolding highly fragmented genomes [16, 34]. This has been the case of the sea urchin *L. variegatus*, for which PacBio sequences were used to increase the contiguity of the genome and assemble previously missing portions of the genome. There have been attempts to improve a genome contiguity using RNA-seq data as well [35, 36]. Ideally, when additional sequencing is done, the same biological samples should be used to account for the biological variation within a species or population, which complicates assembly [37]. Although many draft genomes are not suited for NGS analysis, the continued effort to produce more genomes is needed because genotypic differences need to be seen in a functional context, and no one genome can give all of the answers to evolutionary or developmental questions [34].

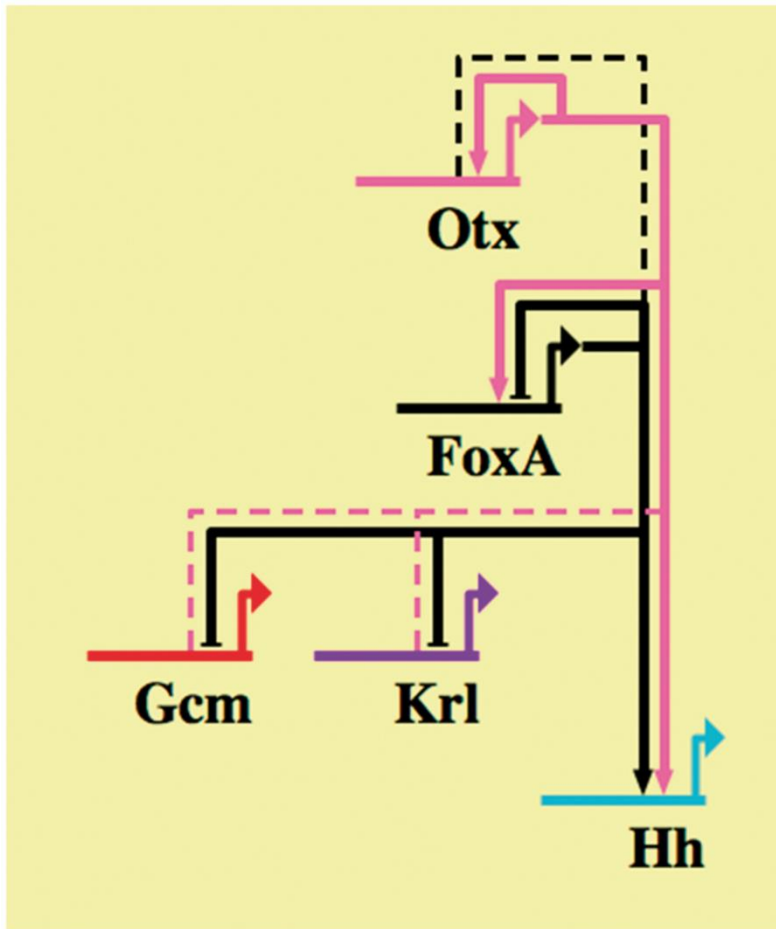


Figure 1 The *S. purpuratus* GRN module centered on the FoxA gene has been reconstructed using 24 and 48 h post-fertilization (hpf) ATAC-seq data and prior knowledge of the set of genes involved in this GRN. Genes were selected from the Davidson laboratory's Web site (Table 1), with the available time point being the 24–30 hpf interval. Next, using Homer [73] and the selected TFs, DNA-binding motifs were labeled, and the predicted interactions were drawn using BioTapestry [84]. In bold solid lines are the connections found in both ATAC-seq data and the Davidson laboratory's GRN. Dashed lines are putative connections found only in the ATAC-seq data set. Whether these newly identified connections are real, it awaits validation by functional analysis. (A colour version of this figure is available online at: <https://academic.oup.com/bfg>.)

Identifying differentially regulated genes and genes for downstream analysis

RNA-seq is typically used to determine the expression of genes at a given development time point [38], in a defined tissue or territory of the embryo and/or in a wild-type condition versus a treatment [39] (Figure 1.3). It reveals a multitude of information, and it is an important aspect in

the omics approach for reconstructing a GRN. Currently, there are other methods commonly being used for high-throughput RNA expression analysis—chiefly, microarrays and nanoString nCounter—in addition to RNA-seq. For small-scale analysis, where the genes of interest are known, both microarrays and nanoString can be sufficient, but there is a trade-off between the lower cost of microarrays analysis and less accuracy compared with RNA-seq, and while the accuracy of nanoString is more precise, the number of gene analyzed is smaller [16]. Materna et al. [40] analyzed 172 genes in early sea urchin development, ranging from TFs, signaling molecules to known markers. This analysis was done at high resolution using nanoString nCounter, and has proven to be an invaluable asset [41, 42], but is limited to 172 genes of tens of thousands. For a transcriptome-wide approach, RNA-seq has a number advantages, the number of genes covered, the fact that it is not needed to select target genes, the possibility of detecting splice variants and the number of downstream analyses that can be performed [16, 43]. Tu et al. [18] expanded the gene expression study in *S. purpuratus* by using one of the NGS Illumina platform, sequencing several transcriptomes covering 10 developmental stages. Additionally, these RNA-seq data were used for the genome annotation, which is a pivotal step for GRNs. Both the annotations and the expression data were made available through EchinoBase (Table 1).

For many echinoderms, as with many other ‘non-model’ organisms, not always there is a genome available. The absence of a genome limits the ability to reconstruct the GRN. However, some inferences can be made by identifying, through differential RNA-seq, TFs that are differentially expressed over time or across conditions. Additionally, identifying overlaps in previously dissected networks provides insight into what occurs in analogous networks of evolutionary close species, yielding to testable hypotheses. There are two options for transcriptome assembling, de novo assembly, using various overlap and graph-based methods, or aligning the RNA-seq reads to a closely related species if there is one available [44–46]. De novo assembly is not always straightforward, and several assemblers should be used as well as quality checked for chimeric sequences and other misassemblies metrics [37, 47, 48]. Alternatively, mapping the RNA-seq reads

to the genome of a reasonably distant species—15% divergence—can yield better results than de novo transcriptome assembly, allowing for better detection of splice variants and assembly more complete genome models [49]. However, this is not always an ideal situation because higher relative distance decreases mapping ability, and there is a decrease in orthology with increasing evolutionary distance [50]. Additionally, reference-based methods generally ignore variation from the reference sequence observed in the reads, and if the genome available for the species being studied—reference or relative species—is poorly assembled, then this can lead to misassembled or partially assembled transcripts. There have been pipelines designed to better address this by using denovo-assembled transcripts and aligning them to closely related species [51]. The combination of de novo assembly and mapping to a relative species is the best approach: the de novo assembly accounts for issues such as gene loss in the reference species, while the aligning to a reference genome aids in creating more complete gene models and reducing redundant gene models [46, 52].

As with any experiment, experimental design is important. With RNA-seq, the questions that can be answered heavily depend on the manipulations of the experimental system that can be performed, the availability of material and the sequencing budget. There are many echinoderm systems that have well-established perturbation protocols. However, in systems where perturbation may prove to be difficult or yet to be perfected, there are time courses and tissue-specific experiments that can be combined with RNA-seq, and in some cases are a better alternative than perturbations. There is still no golden standard for RNA sequencing and, on occasions, a trade-off between number of samples and sequencing depth is necessary, and this determines the type of analysis that can be done and the statistical power. When considering the biological variation in wild animals—which is the case for many, if not all, echinoderm species studied—compared with that of inbreed species, the variation among the RNA-seq samples is much larger [53]. Having only three replicates decreases the statistical power of the experiment

and makes it more difficult to identify a bad replicate [54]. However, DE analyses can still be performed but at a higher fold-change cutoff, with the caveat that not all differentially expressed genes will be identified. Ideally, for a standard pairwise DE analysis, when possible, six replicates have been recommended, increasing to 12 for co-expression analysis. Not only does the number of replicates determine the statistical power but it also dictates what DE software should be used. Taking biological variance into account, it has been shown that negative binomial models are best suited, with programs such as DESeq, EdgeR and limma perform the best [54, 55].

While several methods can be used to aid in the interpretation of the DE analysis, e.g. gene ontology/PANTHER/KEGG pathway, identifying TFs as candidate genes, or clustering analysis, they all have their advantages and disadvantages. With pathway analysis, genes are grouped based on known pathways and their biological process identified, which is the focus of many studies. However, caution must be taken because over evolutionary time pathways began to diverge. Additionally, the choice of database/software is important granted that of the ~3900 publication surveyed in 2015, 67% used software with outdated pathway database that only contain 26% of the biological processes and pathways currently identified [56]. Co-expression analysis allows genes to be grouped by expression patterns, leading to possible networks related to function but not actual GRNs [57]. However, the genes connected in these networks are typically numerous, producing complex networks, which limit their biological interpretation [58] and the generation of hypotheses that can be tested in the wet laboratory. To overcome the massive amount of data, partial knowledge of previously established GRNs is advisable [59]. In fact, while connections with a network may change, the genes involved are often the same [60–62]. Additionally, targeted approaches such as tissue-specific, or single-cell RNA-seq can be used to decrease the amount of data to be analyzed. In any case, although reducing the amount of genes to be analyzed can help reconstructing a GRN, the interconnectivity cannot be predicted with RNA-seq data only. Additional information, such as putative connections at transcription factor binding sites (TFBSs), is

needed.

Identifying potential binding sites and TF binding

Sequence conservation between species typically persists over evolutionary time because often there is a functional component to these sequences. In the post-genomic era, this attribute is used to identify regulatory modules. However, there are limits to this type of analysis: (i) the conserved sequence could be an unannotated protein-coding region in the genome; (ii) there has to be an assembled genome of a species whose sequence has not become too divergent; (iii) not all regulatory modules are found in these conserved blocks; and (iv) there is no temporal component to a simple conservation analysis, which indeed is an essential aspect of GRNs [63, 64]. Moreover, although knowing a cis-region in one species can likely point to an orthologous sequence in another, this is not always the case. Cis-modules diverge over time, functioning in one species while no longer functioning in another [65]. Alternatively, chromatin immunoprecipitation (ChIP) provides a detailed map of protein–DNA interactions, which is fundamental for chromatin modification and regulation of gene expression. The principle is based on the enrichment of DNA fragments to which a specific protein is bound [66]. ChIP, combined with NGS (ChIP-seq), provides a more accurate list of target binding sites (peaks) for TFs and a better identification of cis-regulatory modules (CRMs). The information obtained from ChIP-seq can be used to identify regions where a known protein binds, revealing not only the primary binding motif but also additional motifs that can imply additional functions [67]. The identification of these secondary or low-affinity binding sites has been proven important for understanding the evolution of GRN rewiring [68]. A major drawback of ChIP-seq is that the design of antibodies can be difficult, and many commercial antibodies have been shown not to be of ChIP quality. Additionally, the amount of biological material and the cost of reagents is a hindrance. Efforts by several groups to improve data quality, ensure the proper controls to assure data quality and reduce the amount of biological

material needed have been performed [69, 70]. However, cost still remains high.

More recently, ATAC-seq [71] has been developed to provide information about nucleosome position and nucleosome-free regions in the genome. This method uses a Tn5 transposase to simultaneously cut and ligate adapters for high-throughput sequencing at regions of increased accessibility. It is well known that DNA structure is manipulated throughout development, revealing portion of chromatin where TFs and other proteins bind to regulate gene expression. Therefore, ATAC-seq allows for the identification of potential protein–DNA binding regions (peaks) in a time-specific manner. The main advantages of ATAC-seq are the simple and fast protocol and the reduced amount of starting material (50 000 cells compared with millions for ChIP-seq) [72]. ATAC-seq ability to identify accessible chromatin regions combined with software such as Homer [73], which can annotate these regions with known TF-binding motifs and/or the nearby genes, provides prediction of potential interactions within a network that can be tested in the wet laboratory. ATAC-seq data are currently available for *S. purpuratus* via Echinobase.org and, separately, Hajdu et al. [74] have shown the utility of this technology studying histone modification in the sea urchin. Additionally, ATAC-seq data are being produced for *P. miniata* and *Paracentrotus lividus* (personal communications). To decrease the amount of information to a more manageable data set, tissue-specific ATAC-seq has been developed. This method creates the ability to identify tissue-specific chromatin accessibility and further reveal the inner connectivity of a network. The examination of binding motifs in both ATAC-seq and ChIP-seq can reveal tissue-specific binding [75], which is pertinent for determining which genes belong to a particular network and their connectivity. This also helps mitigate the fact that TFs are used in multiple tissues and different GRNs.

Integration of omics techniques to reconstruct GRNs

The true power comes with the ability to combine these NGS techniques, and the downside to this being that, although there is a plethora of software for each omics step, it is not the same for the integration of these technologies. There have been attempts to fill this gap; however, many of the tools developed are not for 'non-model' species [76], so for echinoderms, there is not always an easy solution. For example, Wang et al. [77] introduced BETA that integrates ChIP-seq with RNA-seq. However, BETA only recognizes Refseq IDs and official gene symbols; other gene identifiers must be converted with tools such as the DAVID gene ID conversion tool [77–79], but this depends on genome annotation or may not prove to be trivial and unusable by most echinoderm genomes. While limited to only a few tools, approaches using software such as Homer [73] or BEDTools [80] have proven sufficient in their ability to label peaks by their proximity to genes. This type of approach has been used for integration of RNA-seq with both ChIP-seq and ATAC-seq studies [62, 81], allowing inferences of regulatory interactions and the activation or repressive effects they cause. Taking advantage of the plethora of established GRNs in echinoderms, such as endomesoderm specification in sea urchins and sea stars [60, 61, 82, 83], it is possible to identify a set of regulatory genes involved in a given developmental process and then use ATAC-seq data to reconstruct the hypothetical GRN involving those genes, with the help of Homer, to label peaks, and BioTapestry [84, 85] to produce a visual representation of predicted interactions. An example of GRN reconstruction using ATAC-seq data is reported, as proof of principle, in Figure 2, where the GRN module around the sea urchin FoxA gene during gastrulation was analyzed. The ATAC-seq data not only allowed to uncover all gene interactions previously demonstrated by cis-regulatory and/or perturbation analyses (solid lines in Figure 2; data retrieved from the Davidson laboratory, see link in Table 1) but also to predict putative novel connections (dashed lines in Figure 2). This method (annotating ATAC-seq peaks with Homer) can be also used in conjunction with differential RNA-seq data, allowing to predict not only the interactions within the differentially expressed

gene set but also to determine the type of putative regulation that is occurring, as activation or repression. Alternatively, more naive methods that include data visualization can be used with tools such as IGV [86, 87], visPILG [88] and ChIPseeker [89], followed by scanning the sequence of the selected peaks for binding motifs of interest with programs such as JASPAR [90].

Validation of GRN by wet laboratory approaches

The key regulatory event driving expression of a given gene is the functional interaction between a trans-regulatory input, the TF, and one or more CRMs of the gene. For this reason, the most relevant form of validation of a predicted GRN is to analyze the cis-regulatory interactions occurring at each node of the system. In the era of the omics approaches, the increase of sequencing data allowed a deeper analysis of the gene regulatory regions leading to predict multiple TF-binding motifs for a single CRM. To analyze the actual capability of a TFBS to drive gene expression, the function of the cis-regulatory element containing it needs to be tested by cis-regulatory analysis. To this aim, CRM reporter gene constructs that contain wild-type and mutated forms of each predicted TFBS are created and tested in developing embryos by measuring both qualitative and quantitative changes in gene expression (for use of reporter gene constructs in sea urchin, see [91]). This kind of approach has been successfully exploited in sea urchin embryos since the late 90s [92–95] to study gene regulation during development, allowing the identification of many functional binding sites in regulatory region. However, as a network is composed by thousands of gene interactions, this analysis would require a huge effort to test each interaction individually. In 2010 [96], a much more efficient approach allowing the study of multiple CRMs in the same experiment has been developed, which makes this task now easily approachable in any embryo where transgenesis is feasible. The cis-regulatory analysis, however, does not prove the *in vivo* occupancy of a specific TF at the given CRM for which the previously mentioned ChIP approach can be used. The ultimate validation of a given GRN node is achieved by combining cis-

regulatory analysis of a given CRM and either a confirmation of actual binding of the given TF to a specific TFBS within the CRM by ChIP analysis or perturbation of the gene expression of the given TF in the presence of the given CRM reporter construct. If in the absence of the given TF, because of the specific perturbation, the expression of the given CRM reporter construct is abolished or strongly reduced, the regulatory interaction between the cis- and trans-elements can be considered functional and the given TF proven necessary for the regulation at the given node. In the systems where microinjection is feasible, such as the sea urchin embryo, this kind of validation can be easily achieved by co-injecting a vector containing the CRM for the cis-regulatory analysis and a morpholino specific for the putative TF regulating it. Although all the forms of validations mentioned above represent the most complete approach for a GRN analysis, this depth of knowledge is not easy to be reached for many organisms, as most often either gene direct interactions are difficult to be tested or to be demonstrated to be functional. So far, the sea urchin and the sea star embryos represent some of the few 'model' systems for which all abovementioned requirements are fulfilled, i.e. omics approaches are feasible, and predicted gene interactions can be validated with a complete set of wet laboratory approaches. This is because of the fact that most of the experimental methods required for the study of the GRN have been already established and are easily accessible in these echinoderms, from gene perturbation with morpholino oligonucleotide to cis-regulatory analysis with injection of reporter constructs, together with biochemical approaches such as ChIP. Examples of such in-depth analyses are the already mentioned GRN for endomesoderm development in the sea urchin embryo, which is constantly updated at the Davidson laboratory (Table 1), and the corresponding ones for the sea star embryo [60, 61], the GRN controlling sea urchin skeletogenic lineage [97] and the one for esophageal muscle development [42]. These in-depth studies also allow for powerful cross-species comparisons of GRNs aimed to understand the evolution and developmental mechanisms underlying body plan change (for a recent review, see [98]).

Conclusion

As the number of omics techniques increases and they become more efficient, so does the information we are able to obtain and the increased use of such techniques. Although these omics approaches provide new or better ways to address questions about gene regulation, it is the combination of the technologies that will give us a more complete picture and enable the reconstruction of more accurate GRNs. There have been efforts made for omics integration [77], but the lack of tools to integrate different omics data for 'non-model' organism creates black boxes of in-house scripts that decrease the reproducibility. In addition, naming conventions create additional issues for 'non-model' species, as gene IDs can differ between databases, and it has been shown that in some cases, excel converts gene names into dates or floating point numbers, leading to errors [99]. Although there are a number of issues that still need to be addressed, the integration of multiple NGS technologies for reconstruction of GRNs is possible even in 'non-model' species, with methods such as ATAC-seq providing a faster and simpler way to identify potential network connectivity. Moreover, within echinoderms, more genomes are being assembled, such as the two already mentioned *A. planci* genomes (Table 2) and the soon to be released *P. lividus* genome (personal communication). There are now options for both DNA and RNA sequencing, which focuses on more targeted approaches, which can address network questions more directly. Furthermore, experiments designed with the purpose of reconstructing a GRN need to account for the fact that genes are used in multiple tissue types and multiple networks. For this reason, tissue-specific experiments should be conducted when possible. Recently, there has been a technique developed to prepare libraries and sequence both DNA and RNA simultaneously by leveraging the enzymatic specificities of the Tn5 transposase and RNA ligase [100], which could prove to be useful for 'non-model' species without genomes. Although for these species there is more work involved in the downstream analysis after sequencing, the amount of information that can be produced and interpreted far outweighs the additional effort.

We are presented with methods for extensive and more informed generation of hypotheses, with systems that are well suited to investigate these hypotheses. In a recent study, Cary et al. [68] demonstrated this by studying multiple echinoderm—a sea urchin and a sea star—species to better understand the mechanism of GRN rewiring through the investigation of low-affinity TF-binding sites using RNA-seq, ChIP-seq and ATAC-seq. These omics approaches, combined with the rich history of echinoderm developmental GRNs and well-established perturbation and cis-regulatory protocols, give a bright outlook on the future for the reconstruction of echinoderm GRNs, potentially leading, with the extension to more species, also to insight into evolution of development.

Acknowledgements

The authors thank José Luis Gómez Skarmeta for access to unpublished ATAC-seq data.

Funding

This work was supported in part by Michigan State University through computational resources provided by the Institute for Cyber-Enabled Research and by MIUR (premiere PANTRAC to M.I.A.). C.C. has been supported by a SZN PhD fellowship.

References

- 1 Telford MJ, Lowe CJ, Cameron CB, et al. Phylogenomic analysis of echinoderm class relationships supports Asterozoa. *Proc Biol Sci* 2014;281:20140479.
- 2 O'Hara TD, Hugall AF, Thuy B, et al. Phylogenomic resolution of the class Ophiuroidea unlocks a global microfossil record. *Curr Biol* 2014;24:1874–9.
- 3 Arnone MI, Byrne M, Martinez P. Echinodermata. In: Wanninger A (ed). *Evolutionary Developmental Biology of Invertebrates*. Springer-Verlag, Wien, 2015. 1–58.
- 4 Materna SC, Oliveri P. A protocol for unraveling gene regulatory networks. *Nat Protoc* 2008;3:1876–87.
- 5 Davidson EH, Rast JP, Oliveri P, et al. A provisional regulatory gene network for specification of endomesoderm in the sea urchin embryo. *Dev Biol* 2002;246:162–90.
- 6 Imai KS, Stolfi A, Levine M, et al. Gene regulatory networks underlying the compartmentalization of the *Ciona* central nervous system. *Development* 2009;136:285–93.
- 7 Woznica A, Haeussler M, Starobinska E, et al. Initial deployment of the cardiogenic gene regulatory network in the basal chordate, *Ciona intestinalis*. *Dev Biol* 2012;368:127–39.
- 8 Hinman VF, Nguyen AT, Cameron RA, et al. Developmental gene regulatory network architecture across 500 million years of echinoderm evolution. *Proc Natl Acad Sci USA* 2003;100:13356–61.
- 9 Cole AG, Rizzo F, Martinez P, et al. Two ParaHox genes, SpLox and SpCdx, interact to partition the posterior endoderm in the formation of a functional gut. *Development* 2009;136:541–9.
- 10 Qi LS, Larson MH, Gilbert LA, et al. Repurposing CRISPR as an RNA-guided platform for sequence-specific control of gene expression. *Cell* 2013;152:1173–83.
- 11 Winnubst S (ed). *Stop making sense*. In: *Way Too Cool*. Columbia University Press, New York, 2015, 175–96.
- 12 Eisen JS, Smith JC. Controlling morpholino experiments: don't stop making antisense. *Development* 2008;135:1735–43.
- 13 Lin CY, Su YH. Genome editing in sea urchin embryos by using a CRISPR/Cas9 system. *Dev*

Biol 2016;409:420–8.

- 14 Oulhen N, Wessel GM. Albinism as a visual, in vivo guide for CRISPR/Cas9 functionality in the sea urchin embryo. *Mol Reprod Dev* 2016;83:1046–7.
- 15 Sanger F, Air GM, Barrell BG, et al. Nucleotide sequence of bacteriophage ϕ X174 DNA. *Nature* 1977;265:687–95.
- 16 Goodwin S, McPherson JD, McCombie WR. Coming of age: ten years of next-generation sequencing technologies. *Nat Rev Genet* 2016;17:333–51.
- 17 Sea Urchin Genome Sequencing Consortium, Sodergren E, Weinstock GM, et al. The genome of the sea urchin *Strongylocentrotus purpuratus*. *Science* 2006;314:941–52.
- 18 Tu Q, Cameron RA, Worley KC, et al. Gene structure in the sea urchin *Strongylocentrotus purpuratus* based on transcriptome analysis. *Genome Res* 2012;22:2079–87.
- 19 Earl D, Bradnam K, St John J, et al. Assemblathon 1: a competitive assessment of de novo short read assembly methods. *Genome Res* 2011;21:2224–41.
- 20 Bradnam KR, Fass JN, Alexandrov A, et al. Assemblathon 2: evaluating de novo methods of genome assembly in three vertebrate species. *Gigascience* 2013;2:10.
- 21 Conesa A, Madrigal P, Tarazona S, et al. A survey of best practices for RNA-seq data analysis. *Genome Biol* 2016;17:13.
- 22 Bolger AM, Lohse M, Usadel B. Trimmomatic: a flexible trimmer for Illumina sequence data. *Bioinformatics* 2014;30:2114–20.
- 23 Schmieder R, Robert S, Yan L, et al. TagCleaner: Identification and removal of tag sequences from genomic and metagenomic datasets. *BMC Bioinformatics* 2010;11:341.
- 24 Gordon A, Hannon GJ. Fastx-toolkit. FASTQ/A short-reads preprocessing tools (unpublished), 2010. http://hannonlab.cshl.edu/fastx_toolkit
- 25 Andrews S. FastQC: a quality control tool for high throughput sequence data, 2010. <http://www.bioinformatics.babraham.ac.uk/projects/fastqc/>
- 26 Bushnell B. BBMap short read aligner, 2016. <http://sourceforge.net/projects/bbmap>
- 27 Schmieder R, Edwards R. Fast identification and removal of sequence contamination from genomic and metagenomic datasets. *PLoS One* 2011;6:e17288.
- 28 Cameron RA, Samanta M, Yuan A, et al. SpBase: the sea urchin genome database and web site. *Nucleic Acids Res* 2009;37:D750–4.
- 29 Pop M. Genome assembly reborn: recent computational challenges. *Brief Bioinform* 2009;10:354–66.
- 30 Bao E, Jiang T, Girke T. AlignGraph: algorithm for secondary de novo genome assembly guided by closely related references. *Bioinformatics* 2014;30:i319–28.

- 31 Gnerre S, Lander ES, Lindblad-Toh K, et al. Assisted assembly: how to improve a de novo genome assembly by using related species. *Genome Biol* 2009;10:R88.
- 32 Hunt M, Kikuchi T, Sanders M, et al. REAPR: a universal tool for genome assembly evaluation. *Genome Biol* 2013;14:R47.
- 33 Gurevich A, Saveliev V, Vyahhi N, et al. QUAST: quality assessment tool for genome assemblies. *Bioinformatics* 2013;29:1072–5.
- 34 Werner T. Next generation sequencing in functional genomics. *Brief Bioinform* 2010;11:499–511.
- 35 Chen M, Hu Y, Liu J, et al. Improvement of genome assembly completeness and identification of novel full-length protein-coding genes by RNA-seq in the giant panda genome. *Sci Rep* 2015;5:18019.
- 36 Markelz RJC, Covington MF, Brock MT, et al. Using RNA-seq for genomic scaffold placement, correcting assemblies, and genetic map creation in a common *Brassica rapa* mapping population. *G3: Genes, Genomes, Genetics* 2016;7:doi:10.1101/076745.
- 37 da Fonseca RR, Albrechtsen A, Themudo GE, et al. Next-generation biology: sequencing and data analysis approaches for non-model organisms. *Mar Genomics* 2016; 30:3–13.
- 38 Dheilly NM, Haynes PA, Raftos DA, et al. Time course proteomic profiling of cellular responses to immunological challenge in the sea urchin, *Heliocidaris erythrogramma*. *Dev Comp Immunol* 2012;37:243–56.
- 39 Annunziata R, Arnone MI. A dynamic regulatory network explains ParaHox gene control of gut patterning in the sea urchin. *Development* 2014;141:2462–72.
- 40 Materna SC, Nam J, Davidson EH. High accuracy, high-resolution prevalence measurement for the majority of locally expressed regulatory genes in early sea urchin development. *Gene Expr Patterns* 2010;10:177–84.
- 41 Andrikou C, Iovene E, Rizzo F, et al. Myogenesis in the sea urchin embryo: the molecular fingerprint of the myoblast precursors. *Evodevo* 2013;4:33.
- 42 Andrikou C, Pai CY, Su YH, et al. Logics and properties of a genetic regulatory program that drives embryonic muscle development in an echinoderm. *Elife* 2015;4. doi:10.7554/elife.07343
- 43 Giorgi FM, Del Fabbro C, Licausi F. Comparative study of RNA-seq- and microarray-derived coexpression networks in *Arabidopsis thaliana*. *Bioinformatics* 2013;29:717–24.
- 44 Collins LJ, Biggs PJ, Voelckel C, et al. An approach to transcriptome analysis of non-model organisms using short-read sequences. *Genome Inform* 2008;21:3–14.
- 45 Kawahara-Miki R, Ryouka KM, Kenta W, et al. Expression Profiling without genome sequence information in a non-model species, Pandalid Shrimp (*Pandalus latirostris*), by next-generation sequencing. *PLoS One* 2011;6:e26043.

- 46 Ockendon NF, O'Connell LA, Bush SJ, et al. Optimization of next-generation sequencing transcriptome annotation for species lacking sequenced genomes. *Mol Ecol Resour* 2016;16:446–58.
- 47 Hayer K, Pizzaro A, Lahens NL, et al. Benchmark analysis of algorithms for determining and quantifying full-length mRNA splice forms from RNA-Seq data. *Bioinformatics* 2015; 31:3938–45. doi:10.1101/007088.
- 48 Yang Y, Smith SA. Optimizing de novo assembly of short-read RNA-seq data for phylogenomics. *BMC Genomics* 2013;14:328.
- 49 Hornett EA, Wheat CW. Quantitative RNA-Seq analysis in non-model species: assessing transcriptome assemblies as a scaffold and the utility of evolutionary divergent genomic reference species. *BMC Genomics* 2012;13:361.
- 50 Gibbons JG, Janson EM, Hittinger CT, et al. Benchmarking next-generation transcriptome sequencing for functional and evolutionary genomics. *Mol Biol Evol* 2009;26:2731–44.
- 51 Bao E, Jiang T, Girke T. BRANCH: boosting RNA-Seq assemblies with partial or related genomic sequences. *Bioinformatics* 2013;29:1250–9.
- 52 Martin JA, Zhong W. Next-generation transcriptome assembly. *Nat Rev Genet* 2011;12:671–82.
- 53 Todd EV, Black MA, Gemmell NJ. The power and promise of RNA-seq in ecology and evolution. *Mol Ecol* 2016;25:1224–41.
- 54 Gierliński M, Cole C, Schofield P, et al. Statistical models for RNA-seq data derived from a two-condition 48-replicate experiment. *Bioinformatics* 2015;31:3625–30.
- 55 Schurch NJ, Schofield P, Gierliński M, et al. How many biological replicates are needed in an RNA-seq experiment and which differential expression tool should you use? *RNA* 2016;22:839–51.
- 56 Wadi L, Meyer M, Weiser J, et al. Impact of outdated gene annotations on pathway enrichment analysis. *Nat Methods* 2016;13:705–6.
- 57 Ballouz S, Verleyen W, Gillis J. Guidance for RNA-seq co-expression network construction and analysis: safety in numbers. *Bioinformatics* 2015;31:2123–30.
- 58 Usadel B, Obayashi T, Mutwil M, et al. Co-expression tools for plant biology: opportunities for hypothesis generation and caveats. *Plant Cell Environ* 2009;32:1633–51.
- 59 Sahadevan S, Sudeep S, Asep G, et al. Pathway based analysis of genes and interactions influencing porcine testis samples from boars with divergent androstenone content in back fat. *PLoS One* 2014;9:e91077.
- 60 Hinman VF, Nguyen A, Davidson EH. Caught in the evolutionary act: precise cis-regulatory basis of difference in the organization of gene networks of sea stars and sea urchins. *Dev Biol* 2007;312:584–95.

- 61 Hinman VF, Davidson EH. Evolutionary plasticity of developmental gene regulatory network architecture. *Proc Natl Acad Sci USA* 2007;104:19404–9.
- 62 Lowe EK, Cuomo C, Arnone MIA. Differential transcriptomic approach to compare target genes of homologous transcription factors in echinoderm species. In: *Dynamics of Mathematical Models in Biology* . 2016, 55–63.
- 63 Emberly E, Rajewsky N, Siggia ED. Conservation of regulatory elements between two species of *Drosophila*. *BMC Bioinformatics* 2003;4:57.
- 64 King DC, Taylor J, Zhang Y, et al. Finding cis-regulatory elements using comparative genomics: some lessons from ENCODE data. *Genome Res* 2007;17:775–86.
- 65 Stolfi A, Lowe EK, Racioppi C, et al. Divergent mechanisms regulate conserved cardiopharyngeal development and gene expression in distantly related ascidians. *Elife* 2014;3:e03728.
- 66 Solomon MJ, Larsen PL, Alexander V. Mapping protein-DNA interactions in vivo with formaldehyde: evidence that histone H4 is retained on a highly transcribed gene. *Cell* 1988;53:937–47.
- 67 Cheatle Jarvela AM, Brubaker L, Vedenko A, et al. Modular evolution of DNA-binding preference of a Tbrain transcription factor provides a mechanism for modifying gene regulatory networks. *Mol Biol Evol* 2014;31:2672–88.
- 68 Cary G, Chaetle-Jarvela A, Francolini R, et al. Genome-wide use of high and low affinity Tbrain transcription factor binding sites during echinoderm development. *Proc Natl Acad Sci USA* 2017;114:5854–61.
- 69 Kidder BL, Gangqing H, Keji Z. ChIP-Seq: technical considerations for obtaining high-quality data. *Nat Immunol* 2011;12:918–22.
- 70 Gilfillan GD, Hughes T, Sheng Y, et al. Limitations and possibilities of low cell number ChIP-seq. *BMC Genomics* 2012;13:645.
- 71 Buenrostro JD, Giresi PG, Zaba LC, et al. Transposition of native chromatin for fast and sensitive epigenomic profiling of open chromatin, DNA-binding proteins and nucleosome position. *Nat Methods* 2013;10:1213–18.
- 72 Buenrostro JD, Giresi PG, Zaba LC, et al. Transposition of native chromatin for fast and sensitive mulitmodal analysis of chromatin architecture. *Biophys J* 2014;106:77a.
- 73 Heinz S, Sven H, Christopher B, et al. Simple combinations of lineage-determining transcription factors prime cis-regulatory elements required for macrophage and B cell identities. *Mol Cell* 2010;38:576–89.
- 74 Hajdu M, Calle J, Puno A, et al. Transcriptional and post-transcriptional regulation of histone variant H2A.Z during sea urchin development. *Dev Growth Differ* 2016;58:727–40.
- 75 Buenrostro JD, Wu B, Litzenburger UM, et al. Single-cell chromatin accessibility reveals

principles of regulatory variation. *Nature* 2015;523:486–90.

76 Wang LY, Wang P, Li MJ, et al. EpiRegNet: constructing epigenetic regulatory network from high throughput gene expression data for humans. *Epigenetics* 2011;6:1505–12.

77 Wang S, Sun H, Ma J, et al. Target analysis by integration of transcriptome and ChIP-seq data with BETA. *Nat Protoc* 2013;8:2502–15.

78 Huang DW, Sherman BT, Stephens R, et al. DAVID gene ID conversion tool. *Bioinformatics* 2008;2:428–30.

79 Huang DW, Sherman BT, Lempicki RA. Systematic and integrative analysis of large gene lists using DAVID bioinformatics resources. *Nat Protoc* 2009;4:44–57.

80 Quinlan AR. BEDTools: the swiss-army tool for genome feature analysis. *Curr Protoc Bioinformatics* 2014;47:11.12.1–34.

81 Ackermann AM, Wang Z, Schug J, et al. Integration of ATAC-seq and RNA-seq identifies human alpha cell and beta cell signature genes. *Mol Metab* 2016;5:233–44.

82 Hinman VF, Nguyen AT, Davidson EH. Expression and function of a starfish Otx ortholog, AmOtx: a conserved role for Otx proteins in endoderm development that predates divergence of the eleutherozoa. *Mech Dev* 2003;120:1165–76.

83 Su YH, Li E, Geiss GK, et al. A perturbation model of the gene regulatory network for oral and aboral ectoderm specification in the sea urchin embryo. *Dev Biol* 2009;329:410–21.

84 Longabaugh WJR. BioTapestry: a tool to visualize the dynamic properties of gene regulatory networks. *Methods Mol Biol* 2012;786:359–94.

85 Paquette SM, Leinonen K, Longabaugh WJR. BioTapestry now provides a web application and improved drawing and layout tools. *F1000Res* 2016;5:39.

86 Robinson JT, Thorvaldsdóttir H, Winckler W, et al. Integrative genomics viewer. *Nat Biotechnol* 2011;29:24–6.

87 Thorvaldsdottir H, Robinson JT, Mesirov JP. Integrative Genomics Viewer (IGV): high-performance genomics data visualization and exploration. *Brief Bioinform* 2012;14:178–92.

88 Scales M, Matthew S, Roland J, et al. visPIG—a web tool for producing multi-region, multi-track, multi-scale plots of genetic data. *PLoS One* 2014;9:e107497.

89 Yu G, Wang LG, He QY. ChIPseeker: an R/Bioconductor package for ChIP peak annotation, comparison and visualization. *Bioinformatics* 2015;31:2382–3.

90 Mathelier A, Fornes O, Arenillas DJ, et al. JASPAR 2016: a major expansion and update of the open-access database of transcription factor binding profiles. *Nucleic Acids Res* 2015;44:D110–15.

91 Arnone MI, Dmochowski IJ, Gache C. Using reporter genes to study cis-regulatory elements. *Methods Cell Biol* 2004;621–52.

- 92 Gan L, Klein WH. A positive cis-regulatory element with a bicoid target site lies within the sea urchin Spec2a enhancer. *Trends Genet* 1993;9:264.
- 93 Yuh CH, Davidson EH. Modular cis-regulatory organization of Endo16, a gut-specific gene of the sea urchin embryo. *Development* 1996;122:1069–82.
- 94 Kirchhamer CV, Yuh CH, Davidson EH. Modular cis-regulatory organization of developmentally expressed genes: two genes transcribed territorially in the sea urchin embryo, and additional examples. *Proc Natl Acad Sci USA* 1996;93:9322–8.
- 95 Arnone MI, Martin EL, Davidson EH. Cis-regulation downstream of cell type specification: a single compact element controls the complex expression of the Cylla gene in sea urchin embryos. *Development* 1998;125:1381–95.
- 96 Nam J, Dong P, Tarpine R, et al. Functional cis-regulatory genomics for systems biology. *Proc Natl Acad Sci USA* 2010;107:3930–5.
- 97 Oliveri P, Tu Q, Davidson EH. Global regulatory logic for specification of an embryonic cell lineage. *Proc Natl Acad Sci USA* 2008;105:5955–62.
- 98 Arnone MI, Andrikou C, Annunziata R. Echinoderm systems for gene regulatory studies in evolution and development. *Curr Opin Genet Dev* 2016;39:129–37.
- 99 Ziemann M, Eren Y, El-Osta A. Gene name errors are widespread in the scientific literature. *Genome Biol* 2016;17:177.
- 100 Reuter JA, Spacek DV, Pai RK, et al. Simul-seq: combined DNA and RNA sequencing for whole-genome and transcriptome profiling. *Nat Methods* 2016;13:953–8. doi:10.1038/nmeth.4028.

Acknowledgments

This work represents the outcome of a period of three years spent at the Stazione Zoologica Anton Dohrn of Naples, Italy, in the laboratory of Dr. Maria Ina Arnone, where I met wonderful people who deserve to be mentioned here. First of all, I want to thank my mentor Ina, who has been a perfect guide for my studies and a great example of determination and love for science. Thank you for giving me the opportunity to join your lab to pursue my PhD and to improve my professional skills, travelling a lot among several laboratories around the world. I want to thank Dr. Salvatore D'Aniello with whom I have done my first professional experience abroad in the laboratory of Observatoire Océanologique of Banyuls sur mer, and for his advice in my experiments. I want to thank my current lab mates Ylenia, Mena, Elijah, Danila, Jovana, Maria, and previous ones, Ivan, Rossella, Carmen, Evgenya, Hrsitiana, Monika: you have been my family and my support in these years. From you I have learnt to never give up and keep on fighting to reach the final goal. I will remember our funny days in the lab forever. I thank the marine animal service in the person of Davide Caramiello, for his kind and constant help in animal maintenance. I thank Luigi, for his support during hard days and for always encouraging to raise my head and go ahead. I also thank all the people I have met during these years, sometimes for a short periods, sometimes longer. All of you have left a memory in my life. I finally thank my parents and my family, who although still do not know what I exactly study, they still believe in what I do.